

# **Carcinogenesis, Prediction, and Palliative Treatment of Gastrointestinal Cancer**

Vincent T. Janmaat

## **Carcinogenesis, Prediction, and Palliative Treatment of Gastrointestinal Cancer**

**Copyright © 2020, V.T. Janmaat**

All rights reserved. No part of this thesis may be reproduced, stored or transmitted in any way or by any means without the prior permission of the author, or when applicable, of the publishers of the scientific papers.

<b>Cover</b>	Proefschriftmaken.nl
<b>Layout</b>	Renate Siebes   Proefschrift.nu
<b>Printing</b>	Proefschriftmaken.nl
<b>ISBN/EAN</b>	978-94-6380-972-6

The printing of this thesis has been financially supported by the Department of Gastroenterology and Hepatology, Erasmus University Medical Center, Rotterdam; Erasmus University Rotterdam; Nederlandse Vereniging voor Gastroenterologie; Sectie Experimentele Gastroenterologie van de Nederlandse Vereniging voor Gastroenterologie; Tramedico; Boston Scientific; Dr. Falk Pharma Benelux; Medicidesk Rabobank Rotterdam; Chipsoft; Sysmex Nederland; Pentax Medical.



# **Carcinogenesis, Prediction, and Palliative Treatment of Gastrointestinal Cancer**

**Carcinogenese, predictie en palliatieve behandeling  
van gastro-intestinale carcinomen**

## **Proefschrift**

ter verkrijging van de graad van doctor aan de  
Erasmus Universiteit Rotterdam  
op gezag van de rector magnificus  
Prof. dr. R.C.M.E. Engels  
en volgens besluit van het College voor Promoties.

De openbare verdediging zal plaatsvinden op  
dinsdag 27 oktober 2020 om 11:30 uur

door

**Vincent Theodoor Janmaat**

geboren te Woerden

## **Promotiecommissie**

### **Promotoren**

Prof. dr. M.P. Peppelenbosch

Prof. dr. M.J. Bruno

### **Overige leden**

Prof. dr. K.K. Krishnadath

Prof. dr. L.J.W. van der Laan

Prof. dr. W.N.M. Dinjens

### **Copromotoren**

Prof. dr. V.M.C.W. Spaander

Dr. G.M. Fuhler

# Table of contents

## Part 1: Introduction

<b>Chapter 1.1</b>	General introduction	<b>9</b>
<b>Chapter 1.2</b>	Outline of the thesis	<b>23</b>

## Part 2: *HOX* genes in (pre)malignant lesions of the gastrointestinal tract

<b>Chapter 2</b>	<i>HOXA13</i> in etiology and oncogenic potential of Barrett's esophagus	<b>31</b>
<b>Chapter 3</b>	Forced expression of <i>HOXA13</i> confers oncogenic hallmarks to esophageal keratinocytes	<b>123</b>
<b>Chapter 4</b>	<i>HOXA9</i> mediates and marks premalignant compartment size expansion in colonic adenomas	<b>153</b>

## Part 3: Predicting the development of malignant lesions

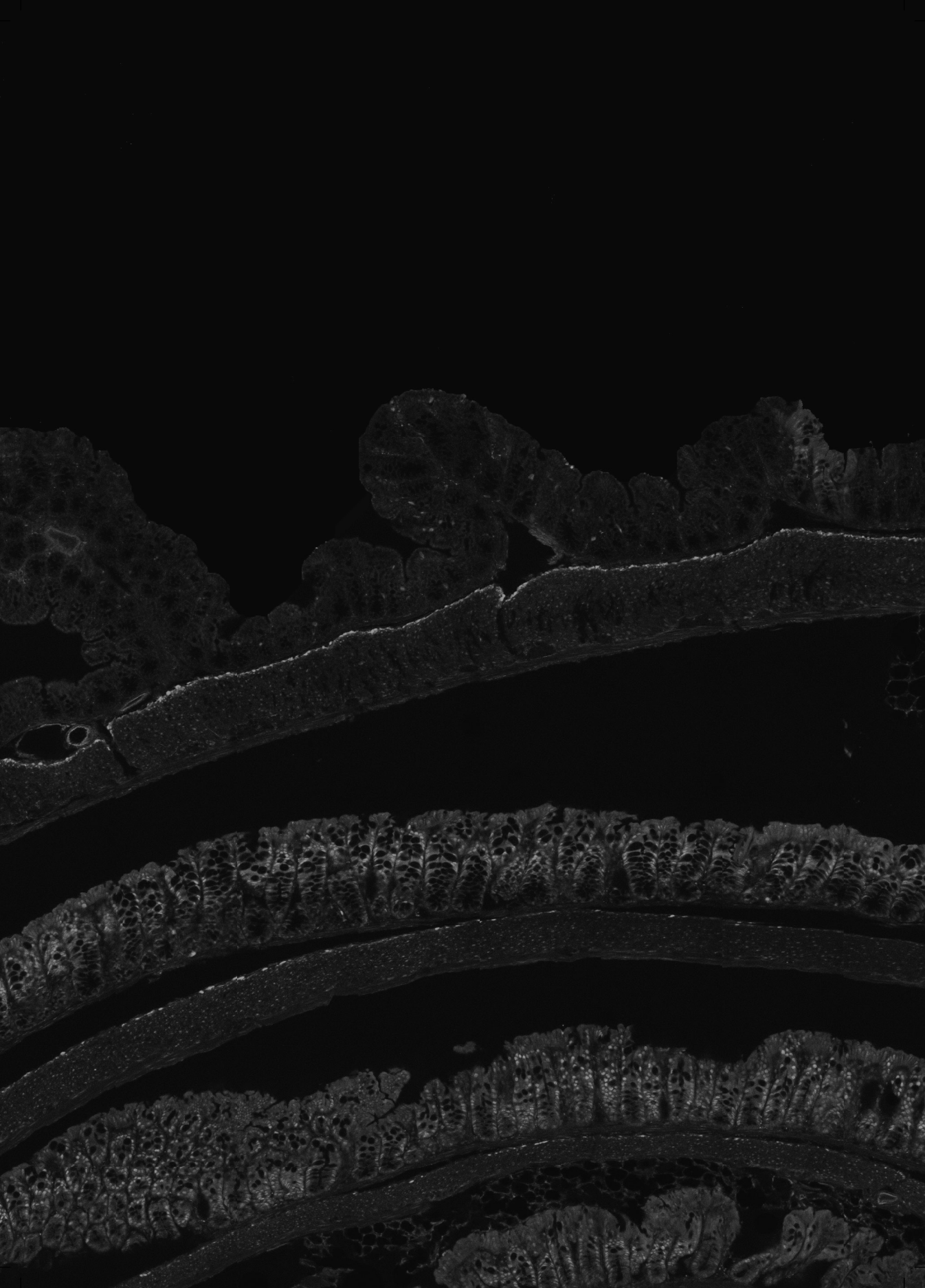
<b>Chapter 5</b>	Vitamin D receptor polymorphisms are associated with reduced esophageal vitamin D receptor expression and reduced esophageal adenocarcinoma risk	<b>185</b>
<b>Chapter 6.1</b>	Use of immunohistochemical biomarkers as independent predictor of neoplastic progression in Barrett's oesophagus surveillance: a systematic review and meta-analysis	<b>205</b>
<b>Chapter 6.2</b>	Letter to the editor in response to: Meta-analysis of biomarkers predicting risk of malignant progression in Barrett's oesophagus	<b>237</b>
<b>Chapter 7</b>	DNA integrity as biomarker in pancreatic cyst fluid	<b>241</b>
<b>Chapter 8</b>	Molecular profile of Barrett's esophagus and gastroesophageal reflux disease in the development of translational physiological and pharmacological studies	<b>251</b>

## Part 4: Palliative treatment of esophageal cancer

<b>Chapter 9</b>	Palliative chemotherapy and targeted therapies for esophageal and gastroesophageal junction cancer	<b>291</b>
<b>Chapter 10</b>	Cost-effectiveness of cetuximab for advanced esophageal squamous cell carcinoma	<b>357</b>

## Part 5: Summary, discussion, and appendices

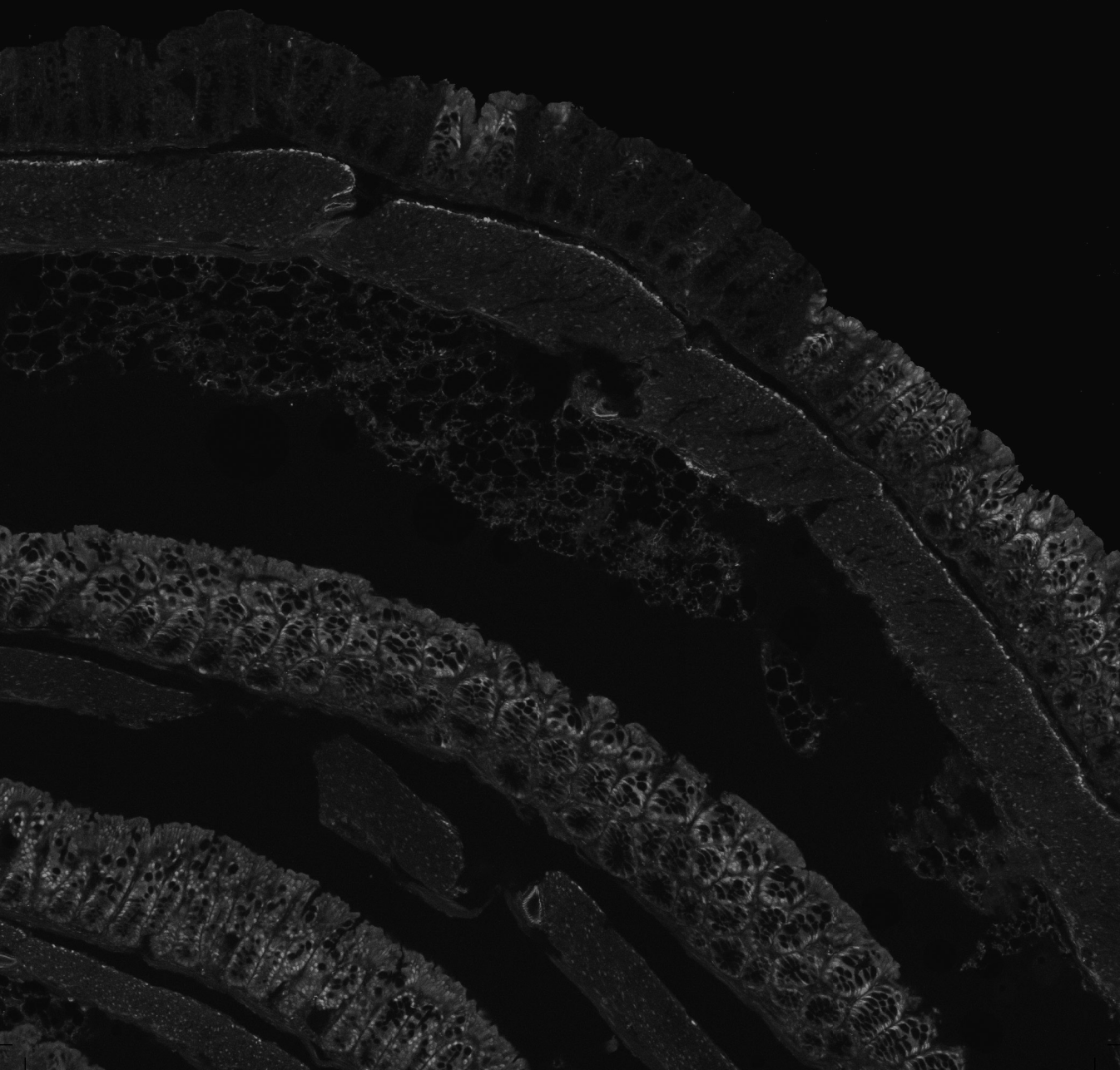
<b>Chapter 11</b>	Summary and general discussion	<b>373</b>
<b>Chapter 12</b>	Nederlandse samenvatting	<b>401</b>
<b>Chapter 13</b>	Appendices	<b>411</b>
	Dankwoord	<b>413</b>
	List of publications	<b>418</b>
	PhD portfolio	<b>420</b>
	Curriculum vitae	<b>424</b>



# Part 1

---

## General introduction





# Chapter 1.1

---

General introduction





## Gastrointestinal cancer

Gastrointestinal cancer is a type of disease characterized by increased cell growth combined with the ability of these cells to spread to or invade other parts of the body. Intestinal cancer is one of the leading causes of morbidity and mortality worldwide. In clinical practice, gastroenterologists are often confronted with premalignant tissues or cancer. As populations in Western countries age, the treatment options for cancer will become even more relevant. Therefore, it is important to understand the etiology of gastrointestinal cancer and identify novel avenues for the rational treatment of this disease.

### Barrett's esophagus and esophageal cancer

Esophageal cancer is the eighth most common cancer worldwide, with approximately 398,000 people diagnosed with squamous cell carcinoma (SCC) and 52,000 with esophageal adenocarcinoma (EAC) in 2012. This corresponds with incidence rates of 5.2 and 0.7 per 100,000 population, respectively (1). EACs develop from metaplastic Barrett's esophagus (BE) located in the lower esophagus and SCC develops from the squamous epithelium (2). Both histological types have dysplasia as their precursor. Recent epidemiological data indicate that 79% of SCCs worldwide occur in Southeastern and Central Asia, whereas 46% of people with EACs are diagnosed in Northern and Western Europe, North America, and Oceania. In general, the incidence of esophageal cancer is higher in men compared to women, especially in EACs, for which the male to female ratio is 4.4:1, compared to 2.7:1 for SCC (1). In the past decades, developed countries have seen an increase in the incidence of EAC, attributed to the higher prevalence of obesity (3). On the other hand, the decreasing incidence of SCC in these contexts correlates with the decline in smoking (4). By 2030, it is predicted that 1 in each 100 men in the Netherlands and the United Kingdom will be diagnosed with EAC during their lifetime (5). SCC remains most common in low- and middle-income countries, including in Africa and Eastern Asia (6). Almost half of people with esophageal carcinoma have distant disease at the time of diagnosis and treatment of this group is at present limited to palliative strategies only (7).

Endoscopic therapy may be an option for early esophageal cancers. Surgical resection is a potentially curative treatment for esophageal cancer, but it is only feasible in people who are fit for surgery, have locally resectable disease, and show no signs of distant metastases. Unfortunately, most people develop recurrent tumor growth within the first few years after surgery. Palliative care is the only option for metastatic disease, with a five-year survival rate of less than three percent (8). Palliative therapy aims to control tumor growth and increase survival without significantly decreasing quality of life.

BE is a premalignant condition of the distal esophagus. In BE, the pre-existent squamous epithelium is replaced by columnar epithelium which develops under the influence of

gastroesophageal reflux disease (GERD), and frequently contains goblet cells (9-11). The progression from BE to EAC is a gradual process, in which intestinal metaplasia (IM) evolves to low-grade dysplasia (LGD), high-grade dysplasia (HGD) and eventually EAC (12). In Western countries, the prevalence of BE has increased dramatically since the 1970s (13), which explains the increasing incidence of EAC. This increasing incidence makes it paramount to improve understanding of the etiology of this disease.

### **Colorectal cancer**

Colorectal cancer (CRC) is one of the leading contributors to cancer mortality worldwide (14, 15). In the United States CRC accounts for 8% of new cancer cases and also for 8% of deaths due to cancer in both males and females (14). In Europe CRC is the second most common cancer (15). The majority of CRCs are sporadic rather than familial (16). Environmental factors that are involved in the pathogenesis of CRC include obesity, smoking, diet, and low physical activity (17). In the past decades, there has been a decline in the incidence rate of CRC, probably due to changes in occurrence of risk factors and, more importantly, screening for premalignant lesions with colonoscopy (18). Increased use of colonoscopy since 2000 has led to a more rapid decline of CRC incidence because some premalignant lesions are resected, being mostly colonic adenomas (19). Colonic adenomas are premalignant epithelial tumors with a glandular origin or with glandular characteristics. Adenomas grow in different ways, namely tubular, villous, or tubulovillous (20). The villous type is found in larger polyps and has a higher potential of malignant transformation (21, 22). About thirty years ago Vogelstein et al. described the importance of premalignant lesions and their role in the adenoma-carcinoma sequence (23). The prevalence of these premalignant lesions is considered 25 percent at the age of 50 years and increases up to 50 percent at the age of 70 years (24-27). Obviously, not all adenomas will lead to colorectal carcinomas. Thus, most screened patients are overtreated by removal of the adenomas. In some screened patients colorectal cancer will develop even though adenomas were removed (28). Identifying the molecular aberrations in the removed adenomas might provide information on the malignant potential and could lead to better understanding of colorectal cancer development.

### **Pancreatic cancer**

Pancreatic cancer is a disease affecting roughly 40,000 people each year. Survival is very poor, of the 15 – 20% of patients whom are eligible for curative therapy by surgery, 5-year survival is below 20% (29-31). Pancreatic cancer has two types of precursor lesions, the pancreatic cystic neoplasms (PCN) and pancreatic intraepithelial neoplasias (PanIN). Pancreatic cystic neoplasms can be categorized into 4 types, with intraductal papillary mucinous neoplasms and mucinous cystic neoplasms showing a high malignant potential, whereas serous cystic adenomas and solid pseudopapillary neoplasms have a

more favorable prognosis (32, 33). Development of pancreatic cancer can be prevented by resection of the cysts with high-risk malignant potential. Unfortunately, current imaging and diagnostic techniques have difficulty distinguishing low-risk cysts from high-risk and transformed cysts, which in some cases leads to unnecessary surgery. Thus, better diagnostic tools are urgently needed.

## ***HOX* genes in the etiology of GI-tract cancers**

Given the large disease burden of GI-tract cancer and the limited understanding of its etiology, we decided to investigate its molecular etiology. In this thesis, we concentrated these efforts on *HOX* gene function in these pathologies, below we explain why.

### **Barrett's esophagus**

As stated above, premalignant metaplasia constitutes the precursor lesion for many gastrointestinal cancers. Ever since the opening lecture of Rudolph Virchow "on metaplasia" at the eighth International Medical Congress, in 1884 at Copenhagen, the field has been characterized by a lack of consensus on the definition, origin, and molecular biology of metaplasia.

The most striking feature of upper GI tract metaplasia is its aberrant morphology. BE appears to involve the acquisition of a posterior phenotype by anterior gut epithelium through a process of homeotic transformation. Misinterpretation of positional information is likely to be involved in the pathogenesis of this disease. The same holds true for other types of metaplasia and heterotopias such as gastric metaplasia, Paneth cell metaplasia and prepyloric metaplasia in the colon, the gastric inlet patch, and gastric heterotopia in the Meckels diverticulum, all of which were studied in this thesis.

In general, regulation of anterior to posterior patterning of specialized tissue is largely dependent on the concerted action of two evolutionary highly conserved gene systems, the Caudal-related Homeobox (*CDX*) transcription factor gene family and the genes of the Homeobox (*HOX*) cluster. The function of *CDX* genes has been studied extensively in the context of BE (34-39). In that context, *HOX* genes have barely been studied, but *HOX* genes have been linked to homeotic transformations in general (40).

*HOX* genes are grouped in the A, B, C, and D clusters. The 3' to 5' sequence of the *HOX* genes in a single *HOX* cluster, i.e. paralogues, corresponds to the sequence in which the paralogues act along bodies length axes. This property, termed collinearity, links clustering to function. *HOX* genes encode transcriptional regulatory proteins that control organogenesis, maintain tissue homeostasis and are key drivers of developmental processes (41, 42). In addition, *HOX* proteins have shown to be associated with worse prognosis for patients with gastric and esophageal squamous cell carcinoma (43, 44).

Previously, a *Hox* gene expression gradient was established along the murine embryonic gut (45). The presence of a rough *HOX* gradient along the adult human gut has been established by Yahagi et al. in 2004 (46). It is clear that ectopic expression of *Hox* genes in mice can interfere with intestinal organogenesis (47, 48). Furthermore, di Pietro et al. (49) explored the expression of mid cluster *HOXB* genes in human BE, normal esophagus, and other GI epithelia amongst which colon epithelium. They concluded that in BE the mid cluster *HOXB* gene expression resembled *HOXB* expression in the colon. The cluster with the highest potential for being implicated in BE seems to be cluster A (43, 44, 50). Additionally, it was found that conditions of GERD, mimicked *in vitro*, did not induce *HOXB* genes (49). These observations prompt further investigation into the role of *HOX* genes in the Barrett's process.

### **Barrett's esophagus model systems**

The process of conversion of normal squamous epithelium towards Barrett's metaplasia is difficult to monitor directly under clinical conditions. This has impeded the progress of the field. Thus, over the years, several experimental models have been published to investigate the mechanisms of BE pathogenesis. However, either the technical possibilities or the translational relevance of these models, or both, is limited. There is a continuing need for more and better model systems. In this thesis, several new model systems are described to facilitate the study of Barrett's esophagus etiology. These are a cell culture based, bile and acid exposure model, a stem cell differentiation based model, and an *ex vitro in vivo* model.

### **Squamous esophagus**

The disease etiology of esophageal squamous cell carcinoma (ESCC) is still poorly understood. However, a possible role for *HOX* genes in ESCC development is emerging. *HOXA13* overexpression has been detected in human ESCC tissue (51), and in other types of cancer like gastric cancer, cervical cancer, ovarian cancer and prostate carcinoma (52-55). High *HOXA13* protein expression is correlated with a shorter median survival time in ESCC patients (56) and poor clinicopathological characteristics of patients (57). The expression profile of *HOXA13*, *ANXA2* and *SOD2* was suggested as predictive marker of the postoperative outcome of patients with ESCC (58). Expression of *FGF2*, the normal morphogen of *HOXA13*, also correlates with poor survival of patients with ESCC (59). Much is still unclear on how *HOXA13* exerts these effects in ESCC.

### **Colon**

In acute myeloid leukemia (AML) a translocation encoding the *NUP98-HOXA9* oncogene results in overexpression of *HOXA9* (60). This *HOXA9* expression is the factor most strongly correlated with poor prognosis in AML (61). In addition to

hematopoietic malignancies, *HOXA9* has a pro-oncogenic effect in epithelial ovarian cancer, osteosarcoma, breast, and oral squamous cell cancer (62-65). Moreover, an upregulation of *HOXA9* has been described in CRC (66, 67). Upregulation of *HOXA9* in premalignant colonic tissues is unclear, as well as its potential function.

## Screening and surveillance

After being informed on the etiology of GI-tract cancers, it is important to develop high quality screening and surveillance tools to detect patients whom are at risk, and estimate their risk of progression to malignancy. These tools have the potential to prevent malignant disease and can theoretically prevent nearly all the disease burden in the population. The estimated incidence of EAC in patients with BE is around 0.12% to 0.38% per year (68-71). This relatively low annual risk reinforces the need for risk stratification tools to make BE surveillance more effective. BE length, male gender, smoking, and LGD are known risk factors for progression to HGD and EAC (68, 71-74). Two large population studies confirmed that patients with LGD have an approximately five times higher risk of progression compared to patients with non-dysplastic BE (68, 71). Thus, surveillance that is more intensive is recommended in BE patients with LGD (75, 76). However, the histological diagnosis of LGD is subject to a considerable inter- and intra-observer variation, because of sample error and overlap with features of non-neoplastic regenerative changes (77-80).

Because none of the current clinical and histologic criteria is able to accurately predict which patients are likely to progress to HGD or EAC, there is an increasing interest in (molecular) biomarkers. Many immunohistochemical (IHC) biomarkers have been studied in BE progression, mainly because they can be applied to standard histological samples. In clinical practice, IHC biomarkers are relatively easily applicable compared to other techniques. Currently, the addition of p53 IHC to the histological assessment is recommended in the guideline of the British Society of Gastroenterology as it may improve the diagnostic reproducibility of a histological diagnosis of LGD (75). The use of IHC biomarkers as independent predictor of neoplastic progression is not yet performed in routine clinical care, neither for p53, nor for other IHC biomarkers.

Current guidelines recommend endoscopic surveillance in BE patients to detect HGD or EAC at an early stage, with the aim to improve survival rates (75, 76). Several studies have shown that patients diagnosed with EAC during BE surveillance have earlier staged tumors and probably better survival compared to those diagnosed after the onset of symptoms (81-84).

## Palliative care for esophageal cancer

In daily practice, clinicians often offer palliative chemotherapy to control tumor growth, increase quality of life, and increase life expectancy. Clinicians have the option to choose from cytostatic therapies, which are directed against fast dividing cells in general, or from targeted therapies directed against specific molecules needed for carcinogenesis and tumor growth. The most extensively used agents for this disease are 5-fluorouracil (5-FU) and cisplatin, which are included in most combination chemotherapy regimens. However, the chemotherapy agents used in randomized controlled trials are very heterogeneous. Researchers have examined targeted therapies as palliative treatment for a decade (85). People treated with these anti-neoplastic agents generally experience fewer side effects compared to people treated with classic cytotoxic chemotherapies. Palliative chemotherapy and/or targeted therapies are widely accepted treatment options. However, with the exception of ramucirumab, evidence for the efficacy of palliative treatment for esophageal and gastroesophageal junction cancer is lacking. Due to the limited availability of relevant data, summarizing the available evidence could increase insight into whether chemotherapy and targeted therapies are justifiably being prescribed to people with advanced or metastatic esophageal or gastroesophageal junction (GEJ) cancer.

The use of biologicals in palliative oncology is expanding at a rapid pace. These new therapeutic agents may improve patients' survival and quality of life. However, the money spend on biologicals is expected to increase at a faster rate than the overall spending growth on pharmaceuticals and is projected to represent roughly one fifth of the total costs in 2017 (86). It would be beneficial for drug companies, policy makers, physicians, and patients alike when the cost-effectiveness of these biologicals would become apparent at an early stage of development. ESCC is a good example of a carcinoma for which biologicals are being studied in palliative phase II studies.

## References

1. Arnold M, Soerjomataram I, Ferlay J, Forman D. Global incidence of oesophageal cancer by histological subtype in 2012. *Gut*. 2015;64(3):381-7.
2. Enzinger PC, Mayer RJ. Esophageal cancer. *N Engl J Med*. 2003;349(23):2241-52.
3. Edgren G, Adami HO, Weiderpass E, Nyren O. A global assessment of the oesophageal adenocarcinoma epidemic. *Gut*. 2013;62(10):1406-14.
4. Cook MB, Chow WH, Devesa SS. Oesophageal cancer incidence in the United States by race, sex, and histologic type, 1977-2005. *Br J Cancer*. 2009;101(5):855-9.
5. Arnold M, Laversanne M, Brown LM, Devesa SS, Bray F. Predicting the Future Burden of Esophageal Cancer by Histological Subtype: International Trends in Incidence up to 2030. *Am J Gastroenterol*. 2017;112(8):1247-55.

6. Malhotra GK, Yanala U, Ravipati A, Follet M, Vijayakumar M, Are C. Global trends in esophageal cancer. *J Surg Oncol*. 2017;115(5):564-79.
7. Howlader N NA, Krapcho M, Garshell J, Miller D, Altekruse SE, Kosary CL, Yu M, Ruhl J, Tatalovich Z, Mariotto A, Lewis DR, Chen HS, Feuer EJ, Cronin KA (eds). SEER Cancer Statistics Review, 1975-2011. National Cancer Institute. Bethesda, MD, 2014.
8. Hur C, Miller M, Kong CY, Dowling EC, Nattinger KJ, Dunn M, et al. Trends in esophageal adenocarcinoma incidence and mortality. *Cancer*. 2013;119(6):1149-58.
9. American Gastroenterological A, Spechler SJ, Sharma P, Souza RF, Inadomi JM, Shaheen NJ. American Gastroenterological Association medical position statement on the management of Barrett's esophagus. *Gastroenterology*. 2011;140(3):1084-91.
10. Kastelein F, Spaander MC, Biermann K, Vucelic B, Kuipers EJ, Bruno MJ. Role of acid suppression in the development and progression of dysplasia in patients with Barrett's esophagus. *Digestive diseases*. 2011;29(5):499-506.
11. Winters C, Jr., Spurling TJ, Chobanian SJ, Curtis DJ, Esposito RL, Hacker JF, 3rd, et al. Barrett's esophagus. A prevalent, occult complication of gastroesophageal reflux disease. *Gastroenterology*. 1987;92(1):118-24.
12. Buttar NS, Wang KK. Mechanisms of disease: Carcinogenesis in Barrett's esophagus. *Nature clinical practice Gastroenterology & hepatology*. 2004;1(2):106-12.
13. Holmes RS, Vaughan TL. Epidemiology and pathogenesis of esophageal cancer. *Semin Radiat Oncol*. 2007;17(1):2-9.
14. Siegel RL, Miller KD, Jemal A. Cancer statistics, 2016. *CA Cancer J Clin*. 2016;66(1):7-30.
15. Ferlay J, Steliarova-Foucher E, Lortet-Tieulent J, Rosso S, Coebergh JW, Comber H, et al. Cancer incidence and mortality patterns in Europe: estimates for 40 countries in 2012. *Eur J Cancer*. 2013;49(6):1374-403.
16. Kharazmi E, Fallah M, Sundquist K, Hemminki K. Familial risk of early and late onset cancer: nationwide prospective cohort study. *Bmj*. 2012;345:e8076.
17. Johnson CM, Wei C, Ensor JE, Smolenski DJ, Amos CI, Levin B, et al. Meta-analyses of colorectal cancer risk factors. *Cancer Causes Control*. 2013;24(6):1207-22.
18. Edwards BK, Ward E, Kohler BA, Ehemann C, Zauber AG, Anderson RN, et al. Annual report to the nation on the status of cancer, 1975-2006, featuring colorectal cancer trends and impact of interventions (risk factors, screening, and treatment) to reduce future rates. *Cancer*. 2010;116(3):544-73.
19. Siegel RL, Ward EM, Jemal A. Trends in colorectal cancer incidence rates in the United States by tumor location and stage, 1992-2008. *Cancer Epidemiol Biomarkers Prev*. 2012;21(3):411-6.
20. Langner C. Serrated and non-serrated precursor lesions of colorectal cancer. *Dig Dis*. 2015;33(1):28-37.
21. Rossini FP, Arrigoni A, Pennanzio M. Treatment and follow-up of large bowel adenoma. *Tumori*. 1995;81(3 Suppl):38-44.
22. Muto T, Bussey HJ, Morson BC. The evolution of cancer of the colon and rectum. *Cancer*. 1975;36(6):2251-70.
23. Vogelstein B, Fearon ER, Hamilton SR, Kern SE, Preisinger AC, Leppert M, et al. Genetic alterations during colorectal-tumor development. *N Engl J Med*. 1988;319(9):525-32.
24. Williams AR, Balasooriya BA, Day DW. Polyps and cancer of the large bowel: a necropsy study in Liverpool. *Gut*. 1982;23(10):835-42.
25. Rex DK. Colonoscopy: a review of its yield for cancers and adenomas by indication. *Am J Gastroenterol*. 1995;90(3):353-65.

26. Rex DK, Lehman GA, Ulbright TM, Smith JJ, Pound DC, Hawes RH, et al. Colonic neoplasia in asymptomatic persons with negative fecal occult blood tests: influence of age, gender, and family history. *Am J Gastroenterol*. 1993;88(6):825-31.
27. Wang FW, Hsu PI, Chuang HY, Tu MS, Mar GY, King TM, et al. Prevalence and risk factors of asymptomatic colorectal polyps in taiwan. *Gastroenterol Res Pract*. 2014;2014:985205.
28. Iwatate M, Kitagawa T, Katayama Y, Tokutomi N, Ban S, Hattori S, et al. Post-colonoscopy colorectal cancer rate in the era of high-definition colonoscopy. *World J Gastroenterol*. 2017;23(42):7609-17.
29. Winter JM, Cameron JL, Campbell KA, Arnold MA, Chang DC, Coleman J, et al. 1423 pancreaticoduodenectomies for pancreatic cancer: A single-institution experience. *J Gastrointest Surg*. 2006;10(9):1199-210; discussion 210-1.
30. Ferrone CR, Brennan MF, Gonen M, Coit DG, Fong Y, Chung S, et al. Pancreatic adenocarcinoma: the actual 5-year survivors. *J Gastrointest Surg*. 2008;12(4):701-6.
31. Konstantinidis IT, Warshaw AL, Allen JN, Blaszkowsky LS, Castillo CF, Deshpande V, et al. Pancreatic ductal adenocarcinoma: is there a survival difference for R1 resections versus locally advanced unresectable tumors? What is a “true” R0 resection? *Ann Surg*. 2013;257(4):731-6.
32. Spinelli KS, Fromwiller TE, Daniel RA, Kiely JM, Nakeeb A, Komorowski RA, et al. Cystic pancreatic neoplasms: observe or operate. *Ann Surg*. 2004;239(5):651-7; discussion 7-9.
33. Fernandez-del Castillo C, Targarona J, Thayer SP, Rattner DW, Brugge WR, Warshaw AL. Incidental pancreatic cysts: clinicopathologic characteristics and comparison with symptomatic patients. *Arch Surg*. 2003;138(4):427-3; discussion 33-4.
34. Debruyne PR, Witek M, Gong L, Birbe R, Chervoneva I, Jin T, et al. Bile acids induce ectopic expression of intestinal guanylyl cyclase C Through nuclear factor-kappaB and Cdx2 in human esophageal cells. *Gastroenterology*. 2006;130(4):1191-206.
35. Eda A, Osawa H, Satoh K, Yanaka I, Kihira K, Ishino Y, et al. Aberrant expression of CDX2 in Barrett's epithelium and inflammatory esophageal mucosa. *Journal of Gastroenterology*. 2003;38(1):14-22.
36. Gao N, White P, Kaestner KH. Establishment of intestinal identity and epithelial-mesenchymal signaling by Cdx2. *Developmental cell*. 2009;16(4):588-99.
37. Liu T, Zhang X, So C-K, Wang S, Wang P, Yan L, et al. Regulation of Cdx2 expression by promoter methylation, and effects of Cdx2 transfection on morphology and gene expression of human esophageal epithelial cells. *Carcinogenesis*. 2007;28(2):488-96.
38. Mari L, Milano F, Parikh K, Straub D, Everts V, Hoebe KK, et al. A pSMAD/CDX2 complex is essential for the intestinalization of epithelial metaplasia. *Cell Rep*. 2014;7(4):1197-210.
39. Silberg DG, Sullivan J, Kang E, Swain GP, Moffett J, Sund NJ, et al. Cdx2 ectopic expression induces gastric intestinal metaplasia in transgenic mice. *Gastroenterology*. 2002;122(3):689-96.
40. Pearson JC, Lemons D, McGinnis W. Modulating Hox gene functions during animal body patterning. *Nat Rev Genet*. 2005;6(12):893-904.
41. Garcia-Fernàndez J, Garcia-Fernandez J. The genesis and evolution of homeobox gene clusters. *Nat Rev Genet*. 2005;6(12):881-92.
42. Stern CD, Charite J, Deschamps J, Duboule D, Durston AJ, Kmita M, et al. Head-tail patterning of the vertebrate embryo: one, two or many unresolved problems? *Int J Dev Biol*. 2006;50(1):3-15.
43. Gu ZD, Shen LY, Wang H, Chen XM, Li Y, Ning T, et al. HOXA13 promotes cancer cell growth and predicts poor survival of patients with esophageal squamous cell carcinoma. *Cancer Res*. 2009;69(12):4969-73.
44. Han Y, Tu WW, Wen YG, Li DP, Qiu GQ, Tang HM, et al. Identification and validation that up-expression of HOXA13 is a novel independent prognostic marker of a worse outcome in gastric cancer based on immunohistochemistry. *Med Oncol*. 2013;30(2):564.



45. Kawazoe Y, Sekimoto T, Araki M, Takagi K, Araki K, Yamamura K. Region-specific gastrointestinal Hox code during murine embryonal gut development. *Dev Growth Differ.* 2002;44(1):77-84.
46. Yahagi N, Kosaki R, Ito T, Mitsuhashi T, Shimada H, Tomita M, et al. Position-specific expression of Hox genes along the gastrointestinal tract. *Congenit Anom (Kyoto).* 2004;44(1):18-26.
47. Zacchetti G, Duboule D, Zakany J. Hox gene function in vertebrate gut morphogenesis: the case of the caecum. *Development.* 2007;134(22):3967-73.
48. Gao N, White P, Kaestner KH. Establishment of intestinal identity and epithelial-mesenchymal signaling by Cdx2. *Dev Cell.* 2009;16(4):588-99.
49. di Pietro M, Lao-Sirieix P, Boyle S, Cassidy A, Castillo D, Saadi A, et al. Evidence for a functional role of epigenetically regulated midcluster HOXB genes in the development of Barrett esophagus. *Proc Natl Acad Sci U S A.* 2012;109(23):9077-82.
50. Mallo M, Wellik DM, Deschamps J. Hox genes and regional patterning of the vertebrate body plan. *Dev Biol.* 2010;344(1):7-15.
51. Chen K-N, Gu Z-D, Ke Y, Li J-Y, Shi X-T, Xu G-W. Expression of 11 HOX Genes Is Deregulated in Esophageal Squamous Cell Carcinoma. *Clinical Cancer Research.* 2005;11(3):1044.
52. Liu C, Tian X, Zhang J, Jiang L. Long Non-coding RNA DLEU1 Promotes Proliferation and Invasion by Interacting With miR-381 and Enhancing HOXA13 Expression in Cervical Cancer. *Front Genet.* 2018;9:629.
53. Yu H, Xu Y, Zhang D, Liu G. Long noncoding RNA LUCAT1 promotes malignancy of ovarian cancer through regulation of miR-612/HOXA13 pathway. *Biochem Biophys Res Commun.* 2018;503(3):2095-100.
54. Han Y, Song C, Wang J, Tang H, Peng Z, Lu S. HOXA13 contributes to gastric carcinogenesis through DHRS2 interacting with MDM2 and confers 5-FU resistance by a p53-dependent pathway. *Mol Carcinog.* 2018;57(6):722-34.
55. Dong Y, Cai Y, Liu B, Jiao X, Li ZT, Guo DY, et al. HOXA13 is associated with unfavorable survival and acts as a novel oncogene in prostate carcinoma. *Future Oncol.* 2017;13(17):1505-16.
56. Gu Z-D, Shen L-Y, Wang H, Chen X-M, Li Y, Ning T, et al. HOXA13 Promotes Cancer Cell Growth and Predicts Poor Survival of Patients with Esophageal Squamous Cell Carcinoma. *Cancer Research.* 2009;69(12):4969.
57. Lin C, Wang Y, Wang Y, Zhang S, Yu L, Guo C, et al. Transcriptional and posttranscriptional regulation of HOXA13 by lncRNA HOTTIP facilitates tumorigenesis and metastasis in esophageal squamous carcinoma cells. *Oncogene.* 2017;36(38):5392-406.
58. Ma RL, Shen LY, Chen KN. Coexpression of ANXA2, SOD2 and HOXA13 predicts poor prognosis of esophageal squamous cell carcinoma. *Oncology Reports.* 2014;31(5):2157-64.
59. Barclay C, Li AW, Geldenhuys L, Baguma-Nibasheka M, Porter GA, Veugeliers PJ, et al. Basic fibroblast growth factor (FGF-2) overexpression is a risk factor for esophageal cancer recurrence and reduced survival, which is ameliorated by coexpression of the FGF-2 antisense gene. *Clin Cancer Res.* 2005;11(21):7683-91.
60. Nakamura T, Largaespada DA, Lee MP, Johnson LA, Ohyashiki K, Toyama K, et al. Fusion of the nucleoporin gene NUP98 to HOXA9 by the chromosome translocation t(7;11)(p15;p15) in human myeloid leukaemia. *Nat Genet.* 1996;12(2):154-8.
61. Golub TR, Slonim DK, Tamayo P, Huard C, Gaasenbeek M, Mesirov JP, et al. Molecular classification of cancer: class discovery and class prediction by gene expression monitoring. *Science.* 1999;286(5439):531-7.
62. Zhang ZF, Wang YJ, Fan SH, Du SX, Li XD, Wu DM, et al. MicroRNA-182 downregulates Wnt/beta-catenin signaling, inhibits proliferation, and promotes apoptosis in human osteosarcoma cells by targeting HOXA9. *Oncotarget.* 2017;8(60):101345-61.

63. Park SM, Choi EY, Bae M, Choi JK, Kim YJ. A long-range interactive DNA methylation marker panel for the promoters of HOXA9 and HOXA10 predicts survival in breast cancer patients. *Clin Epigenetics*. 2017;9:73.
64. Wang K, Jin J, Ma T, Zhai H. MiR-139-5p inhibits the tumorigenesis and progression of oral squamous carcinoma cells by targeting HOXA9. *J Cell Mol Med*. 2017;21(12):3730-40.
65. Ko SY, Barengo N, Ladanyi A, Lee JS, Marini F, Lengyel E, et al. HOXA9 promotes ovarian cancer growth by stimulating cancer-associated fibroblasts. *J Clin Invest*. 2012;122(10):3603-17.
66. Kanai M, Hamada J, Takada M, Asano T, Murakawa K, Takahashi Y, et al. Aberrant expressions of HOX genes in colorectal and hepatocellular carcinomas. *Oncol Rep*. 2010;23(3):843-51.
67. Segditsas S, Sieber O, Deheragoda M, East P, Rowan A, Jeffery R, et al. Putative direct and indirect Wnt targets identified through consistent gene expression changes in APC-mutant intestinal adenomas from humans and mice. *Hum Mol Genet*. 2008;17(24):3864-75.
68. Bhat S, Coleman HG, Yousef F, Johnston BT, McManus DT, Gavin AT, et al. Risk of malignant progression in Barrett's esophagus patients: results from a large population-based study. *J Natl Cancer Inst*. 2011;103(13):1049-57.
69. Desai TK, Krishnan K, Samala N, Singh J, Cluley J, Perla S, et al. The incidence of oesophageal adenocarcinoma in non-dysplastic Barrett's oesophagus: a meta-analysis. *Gut*. 2012;61(7):970-6.
70. Desai TK, Singh J, Samala N, Subbiah P. The incidence of esophageal adenocarcinoma in Barrett's esophagus has been overestimated. *The American journal of gastroenterology*. 2011;106(7):1364-5; author reply 5-6.
71. Hvid-Jensen F, Pedersen L, Drewes AM, Sorensen HT, Funch-Jensen P. Incidence of adenocarcinoma among patients with Barrett's esophagus. *N Engl J Med*. 2011;365(15):1375-83.
72. Yousef F, Cardwell C, Cantwell MM, Galway K, Johnston BT, Murray L. The incidence of esophageal cancer and high-grade dysplasia in Barrett's esophagus: a systematic review and meta-analysis. *American journal of epidemiology*. 2008;168(3):237-49.
73. Wani S, Falk G, Hall M, Gaddam S, Wang A, Gupta N, et al. Patients with nondysplastic Barrett's esophagus have low risks for developing dysplasia or esophageal adenocarcinoma. *Clin Gastroenterol Hepatol*. 2011;9(3):220-7; quiz e6.
74. Coleman HG, Bhat S, Johnston BT, McManus D, Gavin AT, Murray LJ. Tobacco smoking increases the risk of high-grade dysplasia and cancer among patients with Barrett's esophagus. *Gastroenterology*. 2012;142(2):233-40.
75. Fitzgerald RC, di Pietro M, Ragunath K, Ang Y, Kang JY, Watson P, et al. British Society of Gastroenterology guidelines on the diagnosis and management of Barrett's oesophagus. *Gut*. 2014;63(1):7-42.
76. Wang KK, Sampliner RE, Practice Parameters Committee of the American College of G. Updated guidelines 2008 for the diagnosis, surveillance and therapy of Barrett's esophagus. *The American journal of gastroenterology*. 2008;103(3):788-97.
77. Curvers WL, ten Kate FJ, Krishnadath KK, Visser M, Elzer B, Baak LC, et al. Low-grade dysplasia in Barrett's esophagus: overdiagnosed and underestimated. *The American journal of gastroenterology*. 2010;105(7):1523-30.
78. Kerkhof M, van Dekken H, Steyerberg EW, Meijer GA, Mulder AH, de Bruine A, et al. Grading of dysplasia in Barrett's oesophagus: substantial interobserver variation between general and gastrointestinal pathologists. *Histopathology*. 2007;50(7):920-7.
79. Cameron AJ, Carpenter HA. Barrett's esophagus, high-grade dysplasia, and early adenocarcinoma: a pathological study. *The American journal of gastroenterology*. 1997;92(4):586-91.

80. Levine DS, Haggitt RC, Blount PL, Rabinovitch PS, Rusch VW, Reid BJ. An endoscopic biopsy protocol can differentiate high-grade dysplasia from early adenocarcinoma in Barrett's esophagus. *Gastroenterology*. 1993;105(1):40-50.
81. Cooper GS, Kou TD, Chak A. Receipt of previous diagnoses and endoscopy and outcome from esophageal adenocarcinoma: a population-based study with temporal trends. *The American journal of gastroenterology*. 2009;104(6):1356-62.
82. Fountoulakis A, Zafirellis KD, Dolan K, Dexter SP, Martin IG, Sue-Ling HM. Effect of surveillance of Barrett's oesophagus on the clinical outcome of oesophageal cancer. *The British journal of surgery*. 2004;91(8):997-1003.
83. Kastelein F, van Olphen SH, Steyerberg EW, Spaander MC, Bruno MJ, ProBar-study group. Impact of surveillance for Barrett's oesophagus on tumour stage and survival of patients with neoplastic progression. *Gut*. 2016;65(4):548-54.
84. Rubenstein JH, Sonnenberg A, Davis J, McMahon L, Inadomi JM. Effect of a prior endoscopy on outcomes of esophageal adenocarcinoma among United States veterans. *Gastrointestinal endoscopy*. 2008;68(5):849-55.
85. Lorenzen S, Schuster T, Porschen R, Al-Batran SE, Hofheinz R, Thuss-Patience P, et al. Cetuximab plus cisplatin-5-fluorouracil versus cisplatin-5-fluorouracil alone in first-line metastatic squamous cell carcinoma of the esophagus: a randomized phase II study of the Arbeitsgemeinschaft Internistische Onkologie. *Ann Oncol*. 2009;20(10):1667-73.
86. S. Rickwood MK, M. Núñez-Gaviria, IMS Institute for Healthcare Informatics. The Global Use of Medicines: Outlook through 2017. <http://www.imshealth.com/2013>.



# Chapter 1.2

---

Outline of the thesis



The overall aim of this thesis is to increase our understanding of the etiology, the detection, and the palliative treatment of gastrointestinal (GI) cancers. This thesis is divided into five parts.

**Part 1** contains the introduction of this thesis. **Chapter 1.1** describes the general introduction on intestinal cancer, focusing on Barrett's esophagus and esophageal cancer, colorectal cancer, and pancreatic cancer. Additionally, it focuses on *HOX* genes in the etiology of gastrointestinal tract cancers, screening and surveillance, and palliative care. **Chapter 1.2** describes the outline of this thesis.

**Part 2** describes investigations into the involvement of *HOX* genes in the etiology of (pre)malignant lesions of the GI tract. In **Chapter 2** the involvement of *HOX* genes was studied in esophageal carcinogenesis. We show the adult gut is characterized by *HOX* collinearity. In BE, *HOX* expression is reprogrammed to a distal pattern in stem and differentiated cells, characterized by prominent *HOXA13* expression. Strikingly, *HOXA13* was found to be expressed in the adult physiological gastroesophageal junction. In a model of the cell of origin of BE, *HOXA13* confers a relative competitive advantage and a pro-oncogenic expression profile. In a BE model, *HOXA13* downregulates the epidermal differentiation complex, increases proliferation, and conveys phenotypical aspects of BE. We concluded, *HOXA13* helps explain the etiology, phenotype, and oncogenic potential of BE. **Chapter 3** studies the oncogenic hallmarks *HOXA13* confers to esophageal keratinocytes. In this context, it provides a proliferation advantage to keratinocytes, reduces sensitivity to chemical agents, regulates MHC class I expression, and differentiation status, and promotes cellular migration. **Chapter 4** focusses on the role of *HOXA9* in colonic adenomas. *HOXA9* levels are increased in colonic adenomas compared to location matched healthy tissue. It inhibits cellular migration, which appears to be mediated by decreased PAK activity. Strikingly, the pro-oncogenic phenotype of *HOXA9* alteration in hematologic malignancies was also found in this study as *HOXA9* stimulates cell growth. This phenotype appears to be mediated through increased IGF1, FLT3, PTGS2, p-4E-BP1, and p-ERK1/2. In conjunction, these data identify *HOX* as a pivotal mediator of the etiology and behavior of malignancies in the GI-tract.

**Part 3** focusses on predicting the development of malignant lesions. **Chapter 5** studies vitamin D receptor polymorphisms and shows these are associated with reduced esophageal vitamin D receptor expression and reduced esophageal adenocarcinoma risk. In **Chapter 6.1** the existing literature is systematically reviewed regarding the value of immunohistochemical biomarkers for predicting neoplastic progression in BE patients and a meta-analysis is performed for the biomarkers investigated multiple times in independent studies. Aberrant p53 expression in BE patients appeared to be associated with a significantly increased risk of neoplastic progression for both non-dysplastic and LGD BE patients. **Chapter 6.2** contains a letter to the editor in response to a review and meta-analysis in which studies were included without follow-up, which were used

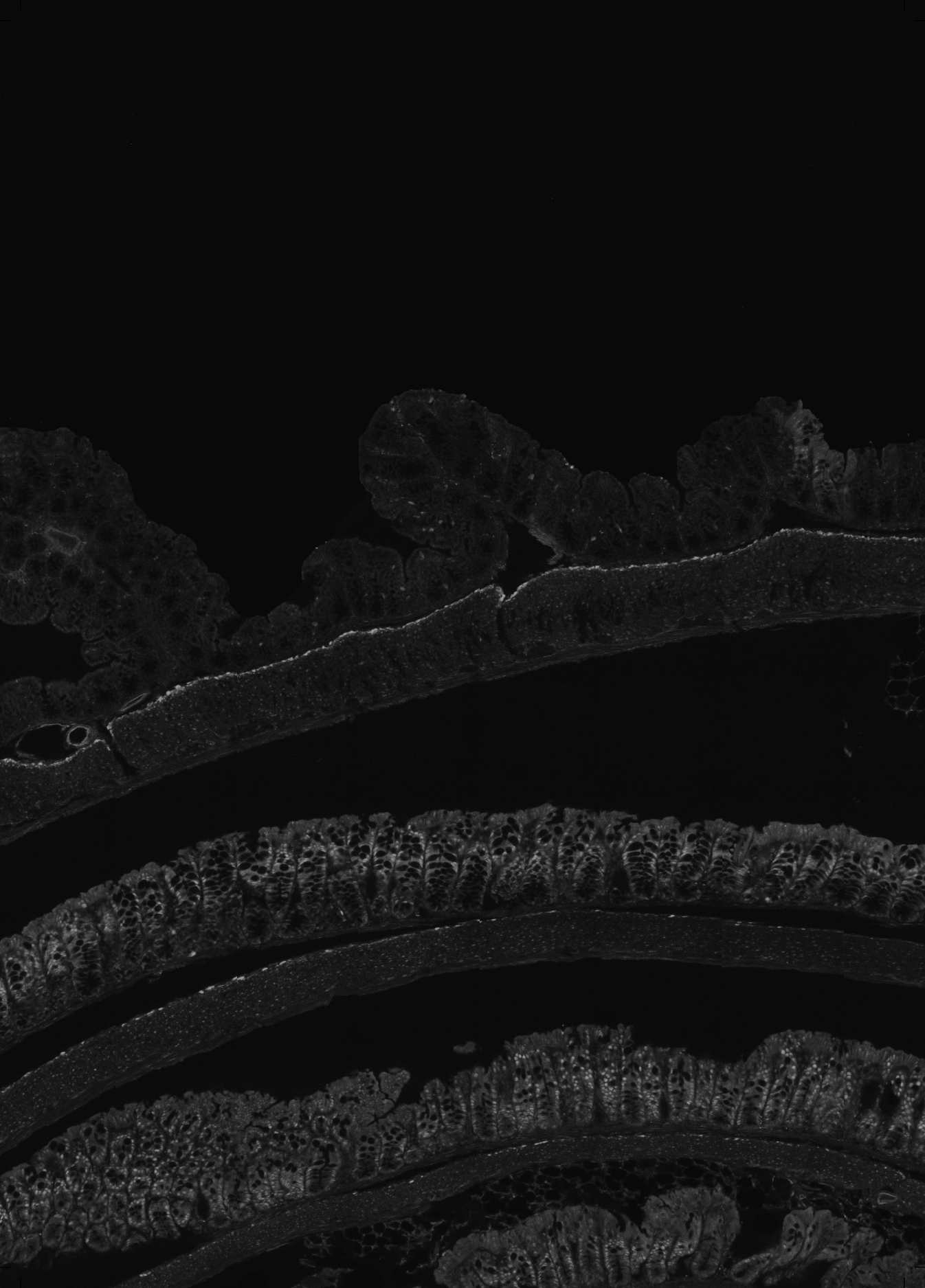
to assess the value of p53 as a biomarker. In **Chapter 7** we focus our attention on DNA-based molecular biomarkers, and investigate whether DNA integrity may serve as a basis to predict malignant transformation in premalignant lesions of the pancreas. **Chapter 8** optimized and established *in vitro* and *in vivo* BE models which aid in the investigation of the etiology of malignant lesions.

**Part 4** investigates palliative treatment of esophageal cancer. **Chapter 9** studies palliative chemotherapy and targeted therapies for esophageal and GEJ cancer. People who receive more chemotherapeutic or targeted therapeutic agents have an increased overall survival compared to people who receive less. With the exception of ramucirumab, it remains unclear which other individual agents cause the survival benefit. Although treatment-associated toxicities of grade 3 or more occurred more frequently, there is no evidence that palliative chemotherapy and/or targeted therapy decrease quality of life. **Chapter 10** investigates the cost-effectiveness of cetuximab for advanced esophageal squamous cell carcinoma, based on phase II trial data. It shows that the addition of cetuximab is not cost-effective. This also shows that phase II trial data can be used for cost-effectiveness assessments.

**Part 5** contains a summary and general discussion of the main findings of this thesis in **Chapter 11**. **Chapter 12** contains a Dutch summary and **Chapter 13** consists out of the appendices.



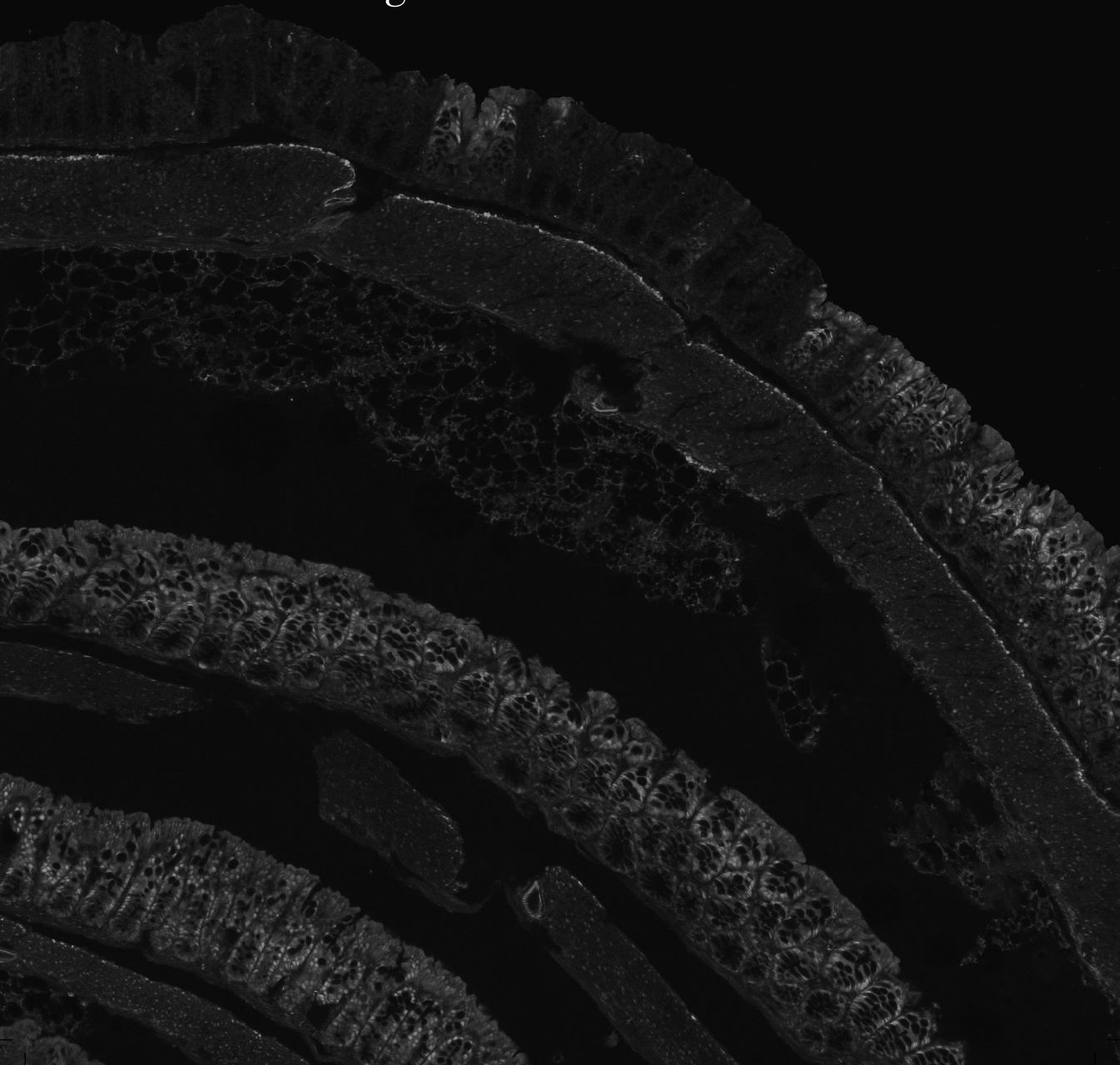




# Part 2

---

*HOX* genes in  
(pre)malignant lesions of  
the gastrointestinal tract





# Chapter 2

---

## *HOXA13* in etiology and oncogenic potential of Barrett's esophagus

Vincent T. Janmaat · Kateryna Nesteruk · Manon C.W. Spaander · Auke P. Verhaar ·  
Bingting Yu · Rodrigo A. Silva · Wayne A. Phillips · Marcin Magierowski ·  
Anouk van de Winkel · H. Scott Stadler · Tatiana Sandoval-Guzmán ·  
Luc J.W. van der Laan · Ernst J. Kuipers · Ron Smits · Marco J. Bruno ·  
Gweny M. Fuhler · Nicholas J. Clemons · Maikel P. Peppelenbosch

*In revision*

## Abstract

Barrett's esophagus in gastrointestinal reflux patients constitutes a columnar epithelium with distal characteristics, prone to progress to esophageal adenocarcinoma. *HOX* genes are known mediators of position-dependent morphology. Here we show *HOX* collinearity in the adult gut while Barrett's esophagus shows high *HOXA13* expression in stem cells and their progeny. *HOXA13* overexpression appears sufficient to explain both the phenotype (through downregulation of the epidermal differentiation complex) and the oncogenic potential of Barrett's esophagus. Intriguingly, employing a mouse model that contains a reporter coupled to the *HOXA13* promotor we identify single *HOXA13*-positive cells distally from the physiological esophagus, which is mirrored in human physiology, but increased in BE. Additionally, we observe that *HOXA13* expression confers a competitive advantage to cells. We thus propose that Barrett's esophagus and associated esophageal adenocarcinoma is the consequence of expansion of this gastro-esophageal *HOXA13*-expressing compartment following epithelial injury.

## Introduction

Barrett's esophagus (BE) and gastric intestinal metaplasia (IM) are important risk factors for adenocarcinoma of the esophagus and stomach. In the esophagus, the chronic inflammation associated with gastroesophageal reflux disease (GERD) is believed to lead to Barrett's esophagus (BE), a crypt-structured columnar epithelium with distal gastrointestinal (GI)-tract characteristics, located just above the gastroesophageal junction (GEJ). BE is a precursor lesion for esophageal adenocarcinoma (EAC) (1, 2), a disease which has shown a strong increase in incidence in the past decades. Analogously, *H. pylori*-infection can degenerate into atrophic gastritis and gastric IM, which in turn can progress into gastric cancer, the third leading cause of cancer-related death (3). Similarly, while absolute risk is low, heterotopic tissues in Meckel's diverticula and gastric inlet patches of the proximal esophagus represent relatively high-risk regions for adenocarcinoma comparatively to other sites of the ileum and proximal esophagus, respectively (4, 5). Therefore, a deeper understanding of the biology of BE and gastric IM is necessary for designing rational avenues for the prevention and treatment of GI cancers.

BE is characterized by the presence of cells with a caudal intestinal phenotype at a rostral location. Therefore, dysregulation of positional specification is likely involved in the etiology of BE. Regulation of rostral-caudal patterning of specialized tissue in embryology and adulthood is to a large extent dependent on the concerted action of two evolutionary highly conserved gene systems, the Caudal-related Homeobox (*CDX*) transcription factor gene family and the genes of the Homeobox (*HOX*) cluster. A substantial research effort has been invested in investigating the role of *CDX* genes in positional misspecification in BE (6). However, these efforts have not yielded convincing evidence that these genes are the principal mediators of the distal phenotype in this disease (7, 8). Intriguingly, however, a microarray-based gene expression study of BE suggested potential misregulation of the *HOX* gene family in BE (9). *HOX* genes are linked to morphological transformations and neoplasia (10, 11). Four clusters of *HOX* genes, *HOXA* to *HOXD*, have been defined. The 3' to 5' sequence of *HOX* gene paralogues corresponds to the sequence in which they act along the rostrocaudal axis. This property is termed collinearity and links clustering to function. Previously, a *Hox* expression gradient was found along the murine embryonic gut (12). Ectopic *Hox* expression in mice can alter intestinal differentiation (8). A *HOX* gradient along the adult human gut has also been reported (13), but that study involved pooling full thickness gut specimens, limiting data interpretation. Nevertheless, we feel that there is sufficient evidence to prompt exploring the function of *HOX* gene expression with respect to positional identity in physiology and pathology of the GI-tract in general and in BE in particular.

## Methods

### Collection of human material

All human tissues used in this study were obtained at the Erasmus University Medical Center, department of Gastroenterology & Hepatology. The use of these samples was approved by the Erasmus MC medical ethical committee (MEC-2015-208, MEC-2015-209, MEC-2015-199, MEC-2010-093; tissues were handled according to the FEDERA code of conduct and informed consent was obtained where necessary (14). Biopsy specimens to investigate *HOX* collinearity were obtained by double balloon enteroscopy. Nine biopsy specimens were obtained from each patient (n=3) at different locations along the GI-tract. Sequentially these locations were: esophagus, stomach, duodenum, jejunum, proximal ileum, distal ileum, ascending colon, descending colon and sigmoid/rectum (**Supplementary Figure S1a**). Included patients had unexplained symptoms, mostly anemia, while inflammatory bowel disease patients were excluded. All biopsies for RNA isolation were stored in RNA-later at -80°C. Squamous esophageal biopsies (n=13) originated 5 cm above the squamocolumnar junction (SCJ). Barrett's (BE) biopsies (n=13) originated caudal of the SCJ and cranial of the gastric folds (all patients were on PPI therapy), stomach biopsies (n=12) were from the corpus. All three types of biopsy specimens were derived from the same patients, (one stomach biopsy specimen was not obtained due to patient agitation during the gastroscopy). The squamous esophageal, BE, and stomach biopsies were taken in a paired fashion from 13 patients. Where the number of samples is indicated below, this indicates the number of individual patients. To determine the proximal colonic *HOXA13* border, biopsies were taken from the cecum at the appendix base, the ileocecal valve, 5 cm distal to the ileocecal valve, and from the transverse colon in each patient (n=5). Forceps biopsy specimens of EACs (n=12) were obtained. Pathological examination of simultaneously taken forceps biopsies around the study specimens had to be positive for EAC.

### Collection of archival pathology specimens

FFPE material was collected from gastric IM (from the antrum, angulus, and corpus, i.e. not from the cardia; n=12), the gastric inlet patch (n=5), CLE (from the proximal esophagus; n=14), and Meckel's diverticula (n=14). For RNAscope RNA-ISH, one FFPE specimen of each of these origins was used. Depending on the extent of metaplasia, remainder of tissues was used whole, macroscopically separated, or processed with the Photo-Activated Localization Microscopy with the Laser Caption Microdissection (PALM LCM) for mRNA isolation and subsequent qPCR. Nuclease-free membrane slides treated with UV light at 254 nm for 30 minutes were used to mount 10 µm sections, dried overnight at 56°C, deparaffinized, stained with hematoxylin and eosin, and dehydrated. AdhesiveCap microtubes obtained from Zeiss (Oberkochen, Germany) were used to collect the tissue of interest after cutting and pulsing of the PALM LCM.



Additionally, FFPE materials or fresh pinch biopsies were collected from the squamous esophagus of a patient without BE, the squamous esophagus of a BE patient, BE, EAC, stomach (the corpus), and the ileum. Colon was used as a positive control. FFPE materials that were collected only for RNA-ISH were pyloric metaplasia (from the colon; n=5), Paneth cell metaplasia (from the colon; n=5), fetal GEJ tissue (n=2 of 17 weeks, and n=1 of 20 weeks; this material originated from spontaneous abortions), and adult GEJ tissue consisting out of continuous strips of tissue containing squamous esophageal epithelium, GEJ, and oxyntic stomach epithelium (n=3). Two strips came from surgical specimens without evidence of BE, with a neuroendocrine tumor and decompensated achalasia (male of 71 and female of 56 years old). The third patient had surgery to remove an EAC (male of 63 years old). All tissues were obtained from the gastroenterology and pathology departments of the ErasmusMC according to the FEDERA code of conduct (14).

### Animal studies

For the *Hoxa13* mRNA expression analysis throughout the murine gastrointestinal (GI) tract, four *C57BL/6J* wildtype mice were used between three and five months of age. The GI-tract was divided into 1: esophagus; 2: stomach; 3: duodenum; 4: jejunum; 5: proximal ileum; 6: distal ileum; 7: cecum; 8: proximal colon; 9: distal colon, of which sections were opened and rinsed in PBS followed by storage in RNAlater at -80°C (**Supplementary Figure S1b**). For determining which cells express *Hoxa13* in the GI-tract, tissues from a *C57BL/6J-Hoxa13-GFP* heterozygous mutant mouse model were employed, in which GFP expression is driven by the endogenous mouse *Hoxa13* promotor through the creation of a fusion protein (15). These tissues were taken out and embedded in O.C.T. Compound bought from Qiagen Inc. (Hilden, Germany) and frozen at -80°C. Cryosections were made which were mounted in fluoroshield mounting medium with DAPI obtained from Abcam (Cambridge, UK). Subsequently, the GEJ and the distal GI-tract were analyzed directly for GFP expression using the Zeiss confocal laser scan microscope LSM 510. Additionally, immunohistochemistry staining was performed with anti-GFP antibody (#AB3080, Bio-Connect BV) (see below). These murine experiments were approved by the Ethical Committee for Animal Experiments of the Erasmus MC.

### Immunohistochemistry

For immunohistochemistry, slides were blocked in 10% of normal goat serum, antigens were retrieved by boiling samples in citrate buffer (pH6), and samples were incubated overnight at 4°C with primary antibody. Dilutions and manufactures of primary antibodies are presented in the **Supplementary Table S6**. After incubation with HRP-conjugated secondary antibody (Dako EnVision+System-HRR labeled Polymer Anti Mouse, Dako) endogenous peroxidase was blocked in 3% H<sub>2</sub>O<sub>2</sub> and antibody binding

was visualized by DAB staining. IHC analysis for HOXA13 was tried using antibodies ab106503 and ab26084, however these failed to show specificity and have since been discontinued by the companies offering them. H&E staining was performed. For H&E stainings de-parafinized 4 $\mu$ M slides were incubated during 3 min in hematoxylin solution, followed by tap water washes and 15sec of incubation with eosin. For PAS staining, de-parafinized slides were incubated with 0.5% Periodic Acid solution for 10 min, followed by two dH<sub>2</sub>O washes and incubation in Schiff's reagent (Sigma Aldrich) for 15 min and hematoxylin for 3 minutes.

### **RNA isolation**

RNA was isolated using the NucleoSpin RNA isolation kit (Macherey Nagel, Düren, Germany). Biopsies and animal tissues were homogenized by the TissueRuptor obtained from Qiagen Inc. RNA concentrations were measured using a Nanodrop spectrophotometer and samples were stored in RNA storage solution (Sodium Citrate pH 6.4), bought from Ambion (Foster City, USA) and kept at -80°C. RNA integrity was checked with 1% agarose gel-electrophoresis. FFPE material was deparaffinized with xylene and ethanol, lysed, digested with proteinase K, and RNA was isolated with the High Pure FFPE RNA isolation kit obtained from Roche (Basel, Switzerland). RNA isolation from de-differentiated KH2 mouse embryonic stem cells (mESCs) was done using a picopure RNA isolation kit (Thermo-Fisher Scientific, Waltham, USA). After RNA isolation all samples for RNA-Sequencing were tested on the Agilent 2100 Bioanalyzer to determine RNA integrity and quantity.

### **cDNA and qPCR**

cDNA was made from 1  $\mu$ g RNA using Primescript RT Master Mix according to manufacturer's instructions (Takara, Otsu, Japan), for 15 min at 37°C and 5 sec at 95°C, and stored at -20°C. qPCR was performed for 40 cycles in the iQ5 Real-Time PCR detection system that was obtained from BioRad Laboratories (Veenendaal, The Netherlands). For each reaction 10  $\mu$ l cDNA template, 12.5  $\mu$ l SYBR GreenER purchased from Invitrogen (Carlsbad, CA), and 2.5  $\mu$ l 10 pM/ $\mu$ l primer were used. Reactions were performed in duplicate. Primers used are shown in **Supplementary Table S4** and were ordered at Sigma-Aldrich (Darmstadt, Germany). qPCR data were analyzed with Microsoft Excel using the  $\Delta\Delta$ Ct method. Reference genes used for PCRs on human materials were *RP2*,  $\beta$ -*ACTIN*, and *GAPDH*. Reference genes used for PCRs on mice materials were *Eef2*, *Rpl37*, and *Leng8*. Differences in expression were analyzed with a two sided Student's *t*-test using Prism 5.01, obtained from GraphPad Software (San Diego, USA). Values from individual samples were excluded if they deviated more than 2SD from the mean. Correlations between *HOTTIP* expression in the squamous esophagus and BE, and correlations between *HOTTIP* and *HOXA13* expression levels in the squamous esophagus and BE were tested using nonparametric Spearman correlations.

This is depicted in graphs by connecting lines between datapoints, also indicating the paired nature of the specimens, i.e. they are derived from the same patient, used for this analysis.

### ***In situ* hybridization by RNAscope**

RNAscope was performed according to the instructions of the manufacturer of the probes and the reagent kit (VS Reagent Kit 320600; Advanced Cell Diagnostics), on proteinase K (0.1%, 10 min at 37°C) treated paraffin sections (5 µm). Subsequently, slides were hybridized with the RNA probe from RNAscopeVS Hs-*HOXA13*, (art. #ACDA 400226), or the control probe also from RNAscopeVS Hs-*PPIB* (art. #ACDA 313901)(16). *PPIB* (peptidylprolyl isomerase B) is a ubiquitously expressed gene. The RNAscope probe Hybridization in situ Multiplex was bought from Advanced Cell Diagnostics (Newark, USA). Pyloric metaplasia and Paneth cell metaplasia of the colon were quantified using FIJI, for which a macro was made (**Supplementary Macro S1**) (17). For illustrations of RNA-Scope slides in the paper, background grey signal reduction was performed using Photoshop.

### **Analysis of GSE datasets**

Expression profiles from clonogenic human gastro-intestinal stem cell cultures were obtained from Gene Expression Omnibus datasets GSE57584 (18) and GSE65013 (19). *In silico* analyses were performed using the NCBI Gene Expression Omnibus (GEO) database. Analyses in the GEO database were performed by using the GEO2R tool ([www.ncbi.nlm.nih.gov/geo/geo2r/](http://www.ncbi.nlm.nih.gov/geo/geo2r/)), R 3.2.3., Biobase 2.30.0, GEOquery 2.40.0, limma 3.26.8 (20). The results were represented as a <sup>2</sup>log-fold change (<sup>2</sup>log-FC). In Microsoft Excel, this <sup>2</sup>log-FC was converted to fold change (FC). For each <sup>2</sup>log-FC an empirical Bayes moderated t-statistic was calculated. *P*-values were corrected for multiple testing using the Benjamini & Hochberg false discovery rate method.

### **Analysis of single cell RNA seq datasets**

BE and ESMG Single Cell Experiment Matrix from supplementary Data files 6 ll three Experiment Matrixes have been mapped to hg38 standard human genome ('*TxDb.Hsapiens.UCSC.hg38.knownGene*' R-package), normalized as Reads Per Kilobase per Million mapped reads (RPKM). Genes expressed in less than in 0.5% cells were filtered out. Low-quality cells were excluded based on: (1) the number of expressed genes - for 10x Single-Cell sequence data, cells expressing less than 400 or more than 7000 genes, for smartSeq data cells expressing less than 1000 and more than 7000 were removed. Different numbers were chosen due to the different sequencing depth. (2) Boxplot representation of all cells – outliers, i.e. cells mapping higher or lower than 1.5x the first or third quartile were removed. (3) Based on % of reads - cells were removed if there

were more than 20% of reads mapping to mitochondrial or ribosomal genes. *HOXA13-related genes query*: *HOXA13*-positive cells from normal esophagus were selected with R. Genes that were expressed in at least 70% of these *HOXA13*-positive cells (20445) were analyzed for their expression in *HOXA13*-negative cells of normal esophagus as well as *HOXA13*-negative and positive cells in BE tissue. For *T-SNE* plot, 638 cells were included (388 cells from Barrett's tissue, 250 cells from normal esophagus) and plotted based on their location of origin (color) as well as *HOXA13* expression (open vs closed symbols).

### Cell culture

All cells were cultured with penicillin (100u/mL) and streptomycin (100u/mL) and were regularly STR-verified and checked for mycoplasma by handing in samples prepared according to instructions at GATC Biotech (Konstanz, Germany). Primary human esophageal epithelial cells transformed with hTERT (**EPC2-hTERT**) (gift of K.K. Krishnadath) (21), were cultured with Keratinocyte SFM medium, supplemented with bovine pituitary extract at 50 µg/ml and EGF at 1 ng/ml (Thermo-Fisher Scientific). **HET1A**, the primary immortalized human squamous esophageal cell line Het-1A was a gift of J.W.P.M. van Baal (University Utrecht, The Netherlands). These cells were grown in EPM2 medium obtained from AthenaES, (Baltimore, Maryland, USA). The primary immortalized human BE cell line (**BAR-T**) was a gift of dr. J.W.P.M. van Baal who had, in turn, received them from dr. R.F. Souza (University of Texas Southwestern Medical Center, USA). These cells were grown in supplemented keratinocyte basal medium (KBM2), bought from Lonza (Basel, Switzerland), according to the method of Jaiswal et al. (22). **KH2 mESCs** were a gift of J. Gribnau and maintained in DMEM with 10% FCS, Non-Essential Amino Acids, sodium pyruvate, LIF, and β-mercaptoethanol (embryonic stem cell medium; **Supplementary Table S5**). Dishes were coated with attachment factor protein solution (Thermo-Fisher Scientific). Irradiated mouse embryonic fibroblasts (**3T3-Swiss albino cells**) (gift of J.W.P.M. van Baal), cultured in DMEM with 10% FCS, and were used as feeder cells. **HEK293T** cells were cultured in DMEM with 10% FCS.

### Generation of EPC2-hTERT *HOXA13* overexpression model

The human *HOXA13* gene including its single intron was amplified using Q5 polymerase from gDNA using primers (AgeI HoxA13 F; GGTGGTACCGGTGCCACCATGACAGCCTCCGTGCTCCT, and XbaI HoxA13 R; ACCACCTCTAGATTAAGTAGTGGTTTTCAGTT) and cloned into pEN\_TmiRc3 using AgeI and XbaI restriction sites, a gift from Iain Fraser (Addgene (Cambridge, USA) #25748) (23). Subsequently, the *HOXA13* insert was transferred into pSLIK-Venus, using a Gateway reaction (24). pSLIK-Venus was a gift from Iain Fraser (Addgene #25734) (23). A similar plasmid but without the *HOXA13* insert

served as control. Both plasmids were sequenced by LGC Genomics (Teddington, UK). Next, plasmids were packaged into lentiviral particles following transfection in HEK293T cells with third generation packaging plasmids. The supernatant was collected and ultracentrifuged. EPC2-hTERT cells were transduced with the virus and Fluorescence-Activated Cell Sorted (FACS) for YFP (pSLIK-Venus) positive cells on the BD FACSCanto™ II that was bought from BD Biosciences (San Jose, USA). These cells were grown and analyzed as a cell pool. *HOXA13* was induced by the addition of 1.25 µg/ml doxycycline to the culture medium. Overexpression was determined by qPCR according to scientific standards (data not shown).

### **Generation of KH2 mouse embryonic stem cells *HOXA13* overexpression model**

The human *HOXA13* gene including its single intron was amplified using Q5 polymerase from gDNA using primers with an added N-terminal FLAG-tag sequence (GACTACAAAGACGATGACGACAAG) and Kozak sequence (GCCGCCACC; **Supplementary Table S5**). Next, this PCR product was ligated into EcoRI digested pgk-ATG-frt (Addgene #20734) using Gibson Cloning (New England BioLabs Inc., Ipswich, USA). pgk-ATG-frt was a gift from Rudolf Jaenisch (25). KH2 mESCs were passaged the day before the electroporation and four h before electroporation medium was replaced. Approximately  $1.5 \times 10^7$  KH2 cells were electroporated with 50 µg of pgk-ATG-frt-*HOXA13* and 25 µg of pCAGGS-FLPe-puro (Addgene #20733) (26). Cells were electroporated in 4 mm cuvettes, with two consecutive pulses (400V/250uF) using a Gene PulserXcell (Bio-Rad Laboratories). The next day 140 µg/ml Hygromycin B (Thermo-Fisher Scientific) was added for the selection of correctly targeted colonies. DNA from resistant colonies was isolated with the Kleargene XL blood DNA extraction kit (LGC, Teddington, UK) and analyzed by Q5 PCR using the following primers: PGK-F1 or PGK-F2 and T1E2-HygroR6 and T1E2-HygroR7 (**Supplementary Table S5**). Correctly-targeted clones were checked for proper *HOXA13* induction by the addition of 1.25 µg/ml doxycycline to the culture medium for 3 days. Overexpression was determined according to scientific standards (data not shown). Three *HOXA13* overexpression versus three control biological replicates were selected and used for experiments.

### **Differentiation of KH2 mouse embryonic stem cells**

An optimized version of the Ogaki protocol was used (27). Cells were plated on 50% confluent pre-cultured M15 cells, a mesoderm-derived feeder cell line (28) (gift of N. Hastie, University of Edinburgh, UK). Cells grew six days in differentiation medium consisting of ESC medium without LIF, with the addition of Activin-A, basic Fibroblast Growth Factor, CHIR, and Noggin (**Supplementary Table S5**). *HOXA13*-expression was induced on day four using doxycycline at 1.25 µg/ml. On day six, cells were analyzed by FACS by double staining with 0.8 µg PE Rat Anti-Mouse CD184 (CXCR4) and

2.0 µg Anti-CD324 Alexa Fluor® 488 (E-Cadherin) at 4°C for 45 min (**Supplementary Table S5**). The cells were analysed with a BD FACSCanto™ II (BD Biosciences, USA). Data were analyzed with BD FACSDiva v8.0.1 software, which was obtained from BD Biosciences, and processed using Microsoft Excel. Double-positive cells were sorted and cultured for another day with doxycycline at 1.25 µg/ml before harvesting and RNA isolation took place, using the picopure RNA isolation kit (Thermo-Fisher Scientific).

### **Generation of the BAR-T *HOXA13* knock-out model**

Functional *HOXA13* was removed from BAR-T cells using CRISPR/Cas9-mediated gene editing. A *HOXA13* sgRNA targeting exon 1 was cloned into pTLCV2, by ligating two annealed oligonucleotides, i.e. Guide1sgRNA F and R (**Supplementary Table S4**). TLCV2 was a gift from Adam Karpf (Addgene #87360) (29). Following sequence verification, the pTLCV2-*HOXA13*sgRNA plasmid was packaged into lentiviral particles by cotransfection into HEK293T cells with pSPAX2 and pMD2.G, gifts from Didier Trono (Addgene #12260 and #12259). The supernatant was harvested and ultracentrifuged after which BAR-T cells were transduced. Mixed populations of transduced cells were plated at very low confluence, single cell clones could subsequently be isolated using glass cloning cylinders and low melting point agarose from Sigma-Aldrich, followed by DNA isolation using the Kleargene kit, followed by sequence verification with primers TIL*HOXA13*R3 and Pre-*HOXA13*-FW2 flanking the sgRNA-site (**Supplementary Table S4**). Three cell lines in which both alleles were affected by unique out-of-frame deletions were selected along with three control cell lines (data not shown).

### **RNA-sequencing**

The EPC2-hTERT samples (n=8) were treated with the TruSeq Stranded mRNA Library Prep Kit. Sequencing took place according to the Illumina TruSeq v3 protocol on an Illumina HiSeq2500 sequencer. Sample preparation and sequencing was performed at the Erasmus MC. Reads of 50 base-pairs were generated and mapped against reference genome hg19 with Tophat (version 2.0.10). Expression was quantified using HTseq-count (0.6.1). Stranded libraries of the BAR-T (n=6), and both non-differentiated and differentiated KH2 mESCs (n=6 each) were prepared with the NEBNext RNA Ultra sample prep kit. Sequencing took place according to the Illumina NestSeq 500 protocol on an Illumina HiSeq2500 sequencer. Sample preparation and sequencing was performed at GenomeScan in Leiden, The Netherlands. Reads of 75 base-pairs were generated, mapped against reference genome hg19 or mm9 with Tophat (version 2.1.0), and quantified using HTSeq (version 0.6.1p1). Data were processed using R, version 3.2.5 (30), in combination with the module DeSeq2 (31). Generated FCs and *p* values adjusted for multiple testing, i.e. *q* values, were analyzed using Ingenuity Pathway Analysis (IPA) version 42012434, obtained from Qiagen Inc. (Hilden, Germany) (32).

We limited the number of genes analyzed to a maximum of 1000 by eliminating genes with a (relatively) low fold change if differentially expressed genes number was above 1000. The dataset cut-offs used were always a  $q$  value of 0.05, the fold change cut-off was set at: nondifferentiated KH2-mESCs, FC 2, 888 genes; differentiation of KH2-mESCs, FC 5, 924 genes; differentiated KH2-mESCs, FC not restricted, 665 genes; BAR-T, FC not restricted, 146 genes; EPC2-hTERT, FC 1.3, 990 genes. Activity scores are known in IPA as “z-scores” which represents the number of standard deviations from the mean of a normal distribution. For analysis and visualization of gene expression in the epidermal differentiation complex the raw counts from both models normalized to total reads were used. Genes for which one of both cell models had less than ten reads in the control or experimental samples were excluded. Overlap in multiple testing corrected differentially expressed genes in the BAR-T and EPC2-hTERT datasets was calculated as follows; the proportion of overexpressed genes in the EPC2-hTERT dataset was determined. Half of the differentially expressed genes in the BAR-T dataset would be expected to be regulated in the same direction if regulation would be random. This expected overlap if regulation was random, and the observed overlap, were used as input for an  $X^2$  test. Information included in **Supplementary Table S2 and S3** in the “known function” and “Detailed description” columns was obtained through non-systematic review and should not be considered as an exhaustive overview of the literature. Association of expression of molecules in the distal GI-tract with their regulation by *HOXA13* expression was reviewed using the human proteome atlas and depicted in **Supplementary Table S2** (33).

### Acid and bile exposure

For assessment of *HOXA13* mRNA expression upon acid/bile exposure, EPC2-hTERT and HET-1A cells were treated for 30 minutes with cell culture medium adjusted to a pH of 7.0 or 4.0 using HCl. Cells were subsequently washed using PBS and given standard medium. Acid experiments were performed four times in duplo. Cells were separately exposed to medium with a bile acid mixture in concentrations of 0, 200, (and 400 for EPC2-hTERT)  $\mu\text{mole/L}$  for 30 minutes at a pH of 7.0. The bile acid mixture consisted of 25% deoxycholic acid, 45% glycocholic acid and 30% taurochenodeoxycholic acid. Cells were subsequently washed using PBS and given normal medium. Bile experiments were performed twice in duplicate. After 24 h, the cells were harvested and RNA was isolated. Methods were derived from Bus et al. (34). To assess the effect of bile/acid on expansion of cells, EPC2-hTERT cells transduced with *HOXA13* or control vector as described above were seeded in 96-well plate with at least 2 wells per condition. Next day, medium was replaced with 100  $\mu\text{l}$  of bile/acid mixture in cell culture medium (50  $\mu\text{M}$  of sodium glycocholatenhydrate, 50  $\mu\text{M}$  taurochenodeoxycholic acid, pH=4.95). After incubation for 4 days, MTT test was performed as described below. Experiment was performed at least five times.

**BAR-T spatial distribution experiments**

These were performed with three biological replicate cell lines containing *HOXA13* knock-out and three control cell lines. 40,000 BAR-T cells were seeded in a 6 well plate and pictures were taken the second day after seeding. Per well three pictures were taken. These pictures were analyzed using FIJI, using the multipoint tool, an X and Y (pixel) coordinate table was generated (17). The distance between each cell and its three closest neighbors was quantified using Microsoft Excel and analyzed by two sided student's *t*-test. The experiment was performed in three independent cell lines and repeated three times.

**MTT assay**

For assessment of cell growth of EPC2 and BAR-T cells, we performed a 3-(4,5-dimethylthiazol-2-yl)-2,5-diphenyltetrazolium bromide (MTT) assay (35). We seeded 1000 cells per well in 96 well plates for each of the three wild-type and three *HOXA13* knock-out cell lines. Per condition at least 2 wells were used. On days one, three, five, and seven 10  $\mu$ l MTT at 5  $\mu$ g/ml was added and incubated for three h, the medium was removed, and the precipitate was dissolved in 100  $\mu$ l DMSO, which was incubated for five minutes under continuous shaking. For BAR-T cells, absorption was measured in a BioRad microplate reader Model 680 XR at 490 and 595 nm, the average absorption was used to process the data. For EPC2 cells it was measured with Tecan microplate reader Model Infinite 200 pro at 565 nm with reference wavelength 670 nm. The experiment was repeated three times and a two sided Student's *t*-test was used to test for statistical significance.

**3D culture EPC2-hTERT cells**

3D culturing of EPC2-hTERT cells was performed as previously described (36). 4000 EPC2-hTERT cells in culture medium were mixed 1:1 with ice-cold Matrigel basement membrane matrix (Corning BV), seeded in 50  $\mu$ l drops in a 24 well plate for cell suspension, and incubated at 37°C for 30 minutes. After solidification, 500  $\mu$ l of culturing medium supplemented with 0.6mM CaCl<sub>2</sub> was added. Y27632 (10  $\mu$ M) was included in medium only the first 24 h after seeding. Medium was refreshed and pictures were taken every three days. The morphology of spheroids (based on number of extrusions, or 'invadosomes') was counted on day 5. The area of the spheroids was measured with FIJI (17). For H&E staining and IHC analysis of involucrin (see above), spheroids were fixed in 4% formaldehyde for 7 min on day 11, washed with PBS, put in 2% agarose, and embedded in paraffin, then 4  $\mu$ m slices were sectioned. Quantification was based on the percentage of positive cells and the intensity of the staining (scores ranged from 0, 2 to 9).



### Organotypic air-liquid interface culture

Plate inserts (Sigma-Aldrich, Germany) were covered with bovine collagen I (Thermo Fisher Scientific, USA). The fibroblast (3T3-Swiss albino) feeder layer was embedded within a collagen matrix and was allowed to mature for 7 days, after which time BAR-T *HOXA13* knock-out and control epithelial cells were seeded on top and allowed to grow to confluence for an additional 3 days as described (37). Then the culture media level of the upper well was reduced, exposing the apical side of keratinocytes to the air, while maintaining liquid levels at the basolateral side. On day 15, cultures were harvested for histologic examination. 4  $\mu$ M paraffin-embedded sections were deparaffinized, and staining with hematoxylin and eosin, PAS staining and immunohistochemistry for involucrin were performed.

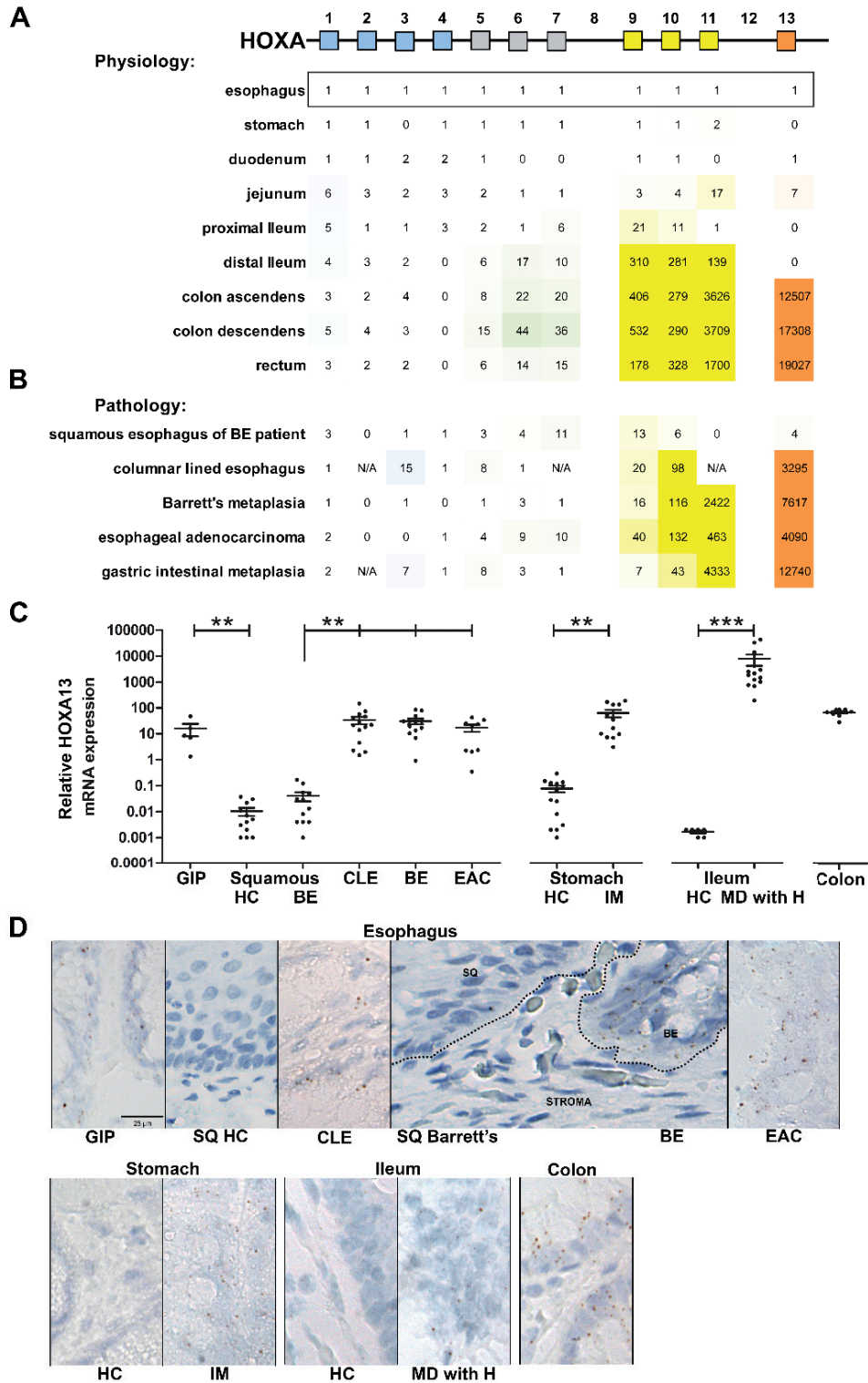
### Rat trachea *in vivo* tissue reconstitution model

500,000 parental BAR-T cells (derived from six independent clones) or *HOXA13* knock-out clones (three independent clones) in 30  $\mu$ l of medium were sealed in the lumen of devitalized and denuded rat tracheas and implanted under the dorsal skin of NOD SCID gamma mice as described by Croagh et al. (38). Mice were sacrificed after four or six weeks. Harvested rat tracheas were formalin fixed, decalcified, embedded in paraffin and sectioned. Staining with hematoxylin and eosin, alcian blue, PAS staining and immunohistochemistry using antibodies against human mitochondria, CK7, TFF3, CDX2, p63, CK5, and involucrin (a gift from Prof. Pritinder Kaur, Curtin University, Australia or #I9018-100UL from Sigma-Aldrich) were performed (**Supplementary Figure S6** and **Table S6**). These murine experiments were approved by the Peter MacCallum Cancer Centre Animal Experimentation Ethics Committee.

## Results

### *HOX* cluster gene expression in the gastrointestinal tract is collinear in men and mice

Investigating *HOX* gene mRNA expression in the murine and human gastrointestinal tract, we observed collinearity that is similar in adult humans and mice (**Figure 1A** for human *HOXA*, **Supplementary Figure S2** for all *HOX* genes and **Supplementary Figure S1** for graphical presentation of the studied *HOX* clusters and the locations of biopsies taken along the human (n=3) and mouse (n=4) GI tract). The highest *HOX* gene cluster expression was observed in the colon, except for the *HOXC* cluster. For individual paralogues, there is a higher expression of 5' *HOXA/B* genes in the distal GI-tract from *HOXA5/B5* onward. Of all *HOXA* paralogues, expression of *HOXA13* was highest and restricted to the colon (**Figure 1A**). *HOXA13* expression is regulated by lncRNA *HOTTIP*, which is located 5' to *HOXA13* (39). Accordingly, *HOTTIP* and



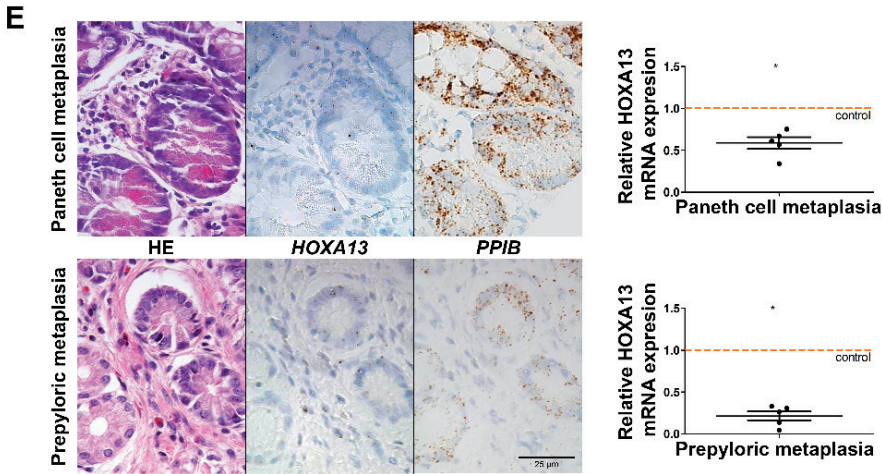


**Figure 1.** *HOXA* cluster gene expression shows collinearity along the adult gastrointestinal tract but is deregulated in BE, various metaplasias and esophageal adenocarcinoma. **(A)** *HOXA* cluster genes are collinearly expressed along the GI-tract of adult humans (n=3). Numbers represent fold changes of mRNA expression relative to the esophagus, which is indicated by a black rectangle. Thus, fold changes can be compared within each *HOXA* paralogue member but not between them. **(B)** *HOXA* cluster gene expression in the squamous esophagus of BE patients (n=13), columnar lined esophagus (CLE) (n=14), BE (n=13), EAC (n=12), and gastric IM (n=12) is characterized by an upregulation of 5' *HOXA* genes. Numbers represent fold changes of mRNA expression relative to the mRNA expression in the esophagus of healthy individuals. **(C)** *HOXA13* expression quantified by qPCR in BE, CLE, IM of the stomach, and heterotopias along the GI tract with their corresponding physiological epithelia. SQ Barrett's and BE are derived from the same person. Mean±SEM, \* $p<0.05$ ; \*\* $p<0.01$ ; \*\*\* $p<0.001$ . Gastric inlet patch (GIP; from proximal esophagus; n=5); squamous esophagus of a healthy control (HC) (from 5 cm proximal to the GEJ; n=12); squamous esophagus of BE patients (from 5 centimeter proximal to the GEJ; n=13); CLE (from below the GEJ and above the gastric folds in segments at least 2 centimeter in length; n=14); BE (from below the GEJ and above the gastric folds in segments at least 2 centimeter in length; n=13); EAC (n= 12); stomach (from the cardia; n=14); gastric IM (from the antrum, angulus, and corpus, i.e. not from the cardia; n=12); ileum (n=6); Meckel's diverticulum with gastric heterotopia (n=14), and; colon (from ascending, transverse, and sigmoid; n=9). SQ: squamous epithelium. **(D)** Deregulation of *HOXA13* expression in gastrointestinal tract pathology as evaluated with RNA *in situ* hybridization in clinical samples. *HOXA13* is upregulated in IM and heterotopia and downregulated in pyloric and Paneth cell metaplasia in the colon. One sample of each tissue type was analyzed; **(E)** Downregulation of *HOXA13* expression (corrected for *PPIB* expression) relative to adjacent non-metaplastic tissue, was observed for Paneth cell metaplasia (n=5; FC 0.59;  $p=0.0041$ ) and pyloric metaplasia (n=5; FC 0.22;  $p=0.0001$ ) (lower panels. Representative images of HE staining, *HOXA13* RNA-scope, and *PPIB* reference gene RNA-scope of Paneth cell metaplasia (from the colon) present in two glands to the bottom right (upper panels) and pyloric metaplasia (from the colon) in the top left two glands (middle panels) are shown.

*HOXA13* share a similar expression pattern (**Supplementary Figure S2**). For *HOXD*, all paralogue genes have increased expression in the distal colon, while *HOXC* expression is mainly localized in the proximal and ileal regions. Thus, *HOX* gene expression is linked to positional identity in the mammalian gut, and collinearity is particularly strong for the *HOXA/B* paralogues.

Subsequently, we addressed the question as to whether gastrointestinal *HOX* coding is already present at the gastrointestinal stem cell stage, or is established only upon the formation of differentiated derivatives. For this, we used publicly available data published by Wang et al. which contains the mRNA expression of human stem cells isolated from the GI-tract and either cultured as stem cells or differentiated in an air-liquid interface (ALI) (18). Analysis of this data shows that *HOX* gene expression patterns in stem cell and ALI cultures are similar. *HOXA* and *B* cluster genes have a significantly higher expression in the large intestine as compared to the small intestine, in particular 5' *HOXA* genes including *HOXA13* (**Figure 2A** for *HOXA* genes, for clusters *HOXB*, *C*, and *D* see **Supplementary Figure S3**). No clear regulation of the *HOXC* or *D* clusters is seen in this dataset, with exception of an upregulation of *HOXC10* in the large intestine. Hence, *HOX* coding is an inherent feature of the location-specific stem cell and is maintained in its derivatives.

### ***HOXA13* in BE, GI heterotopias and GI cancers**

As positional phenotype is linked to *HOX* status in physiology, we subsequently characterized *HOX* mRNA expression in several metaplastic tissues known to assume the morphological phenotype of other intestinal locations, as well as their sequelae. BE shows upregulation of *HOXA10*, *11*, and *13*, and *HOXB* *6*, *7*, *9*, and *13* mRNA by qPCR when compared to the normal squamous esophagus (**Figure 1B** and **Supplementary Figure S4**), which closely resembles colonic *HOXA* and *B* expression patterns. High 5' *HOXA* gene expression is also present in columnar-lined esophagus without goblet cells (CLE; a BE-related condition), esophageal adenocarcinoma (EAC), and IM of the stomach (**Figure 1B**). In accordance with a regulatory role for *HOTTIP* on *HOXA13* expression, we find that *HOTTIP* is also overexpressed in BE, and correlates with *HOXA13* expression patterns (**Supplementary Figure S5A, B, C**). *HOTAIR*, a lncRNA located in the *HOXC* cluster and associated with chromatin reprogramming in cancer progression (40) is upregulated as well (**Supplementary Figure S5D, E, F**) (39). We concluded that BE, EAC and various metaplasias with caudal histo-morphological characteristics have *HOXA* and *HOXB* expression patterns typical of the caudal GI-tract, with upregulation of *HOXA13* expression being the most prominent feature (**Figure 1C**). Heterotopias, namely the gastric inlet patch in the proximal esophagus and heterotopia of the Meckel's diverticulum, are tissues which have a physiological appearance, but are normally found in a different location. These heterotopias are also characterized by abundant *HOXA13* mRNA expression (**Figure 1C**). One of the existing hypotheses on the cell of origin of BE states that BE may arise from cells with progenitor properties that are able to give rise to a variety of cell types (41). To investigate whether aberrant *HOX* gene expression in BE is established at the level of the epithelium-specific stem cell, we interrogated the publically available data of Yamamoto et al. (18, 19). *HOX* gene expression patterns in squamous esophageal and BE stem cells as well as their respective ALI-differentiated derivatives were retrieved. *HOX* gene expression in

stem cell cultures from these locations is similar to their ALI differentiated counterparts (Figure 2B, Supplementary Figure S3). In BE stem cells, an upregulation of 5' *HOXA* genes (Figure 2B) as well as *HOXB6*, 7, 13, and *HOXC10* is seen (Supplementary

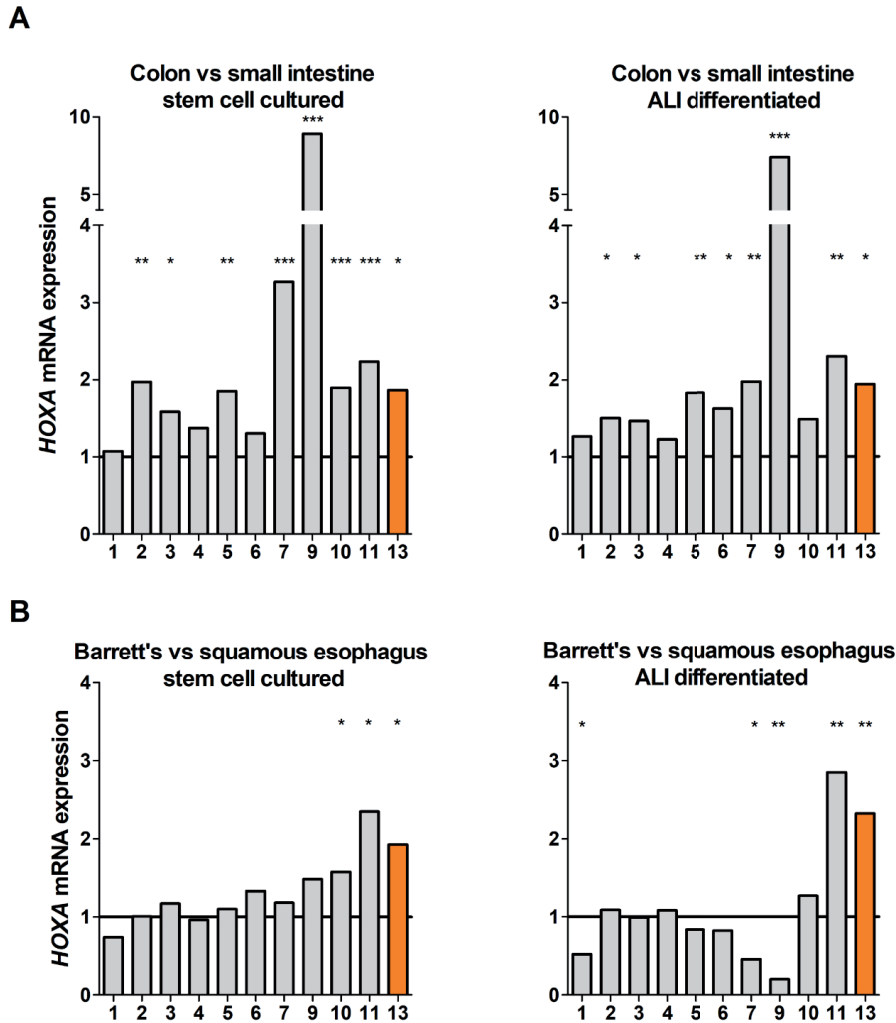


**Figure 2.** *HOXA* expression in stem cells of the GI-tract and in BE. (A) *HOXA* cluster genes, in particular 5' *HOXA* genes including *HOXA13*, have a higher expression in the large intestine (n=3 in technical duplicate) compared to the small intestine (n=3 in technical duplicate), in both stem cells (left panel) and differentiated cells (right panel). (B) 5' *HOXA* cluster gene expression in BE is higher compared to the squamous esophagus in stem cell and ALI differentiated cultures. n=12 (BE) versus n=2 (squamous esophagus) in technical duplicates are depicted for stem cell cultures and n=1 each for ALI differentiated samples in technical duplicates. Normalization was performed by setting mRNA expression to 1 for the small intestine (A) or squamous esophagus (B). \* $p < 0.05$ ; \*\* $p < 0.01$ ; \*\*\* $p < 0.001$ . This figure includes no estimate of variance as the empirical Bayes-moderated t-statistic was used which does not generate a standard error. Data were derived from publically available databases belonging to two studies (18, 19).

**Figure S3**), reaching levels similar to those observed in the colon. Thus, alternative *HOX* coding associated with BE is established at the epithelium-specific stem cell level and is maintained in derivatives of the stem cells involved.

According to the collinearity theory, a paralogue group 13 member is more likely to confer the distal characteristics seen in BE as compared to more anterior paralogue group members (42). Of the paralogue group 13 members, *HOXA13* and *HOXB13* are overexpressed in BE, with *HOXA13* showing much higher expression compared to *HOXB13* in BE, EAC, and IM of the stomach (**Supplementary Figure S4**). Therefore, while *HOX* genes such as *HOXA11*, *B6*, *B9*, and *B13* are also potentially interesting candidates, here we chose to focus on the *HOXA13* gene for further in-depth analysis of different metaplastic tissues. As immunohistochemistry for *HOXA13* was unsuccessful, (two anti-*HOXA13* antibodies were tested but lacked specificity) we resorted to *in situ* hybridization (ISH) for *HOXA13* to further confirm the observed atypical expression of this gene in different tissues (examples shown in **Figure 1D**). Metaplasia is found throughout the GI-tract. While BE and IM acquire a more distal phenotype, distally located colonic pyloric and Paneth cell metaplasia, related to inflammatory bowel disease, acquire a more rostral phenotype (43). Accordingly, downregulation of *HOXA13* expression (corrected for PPIB expression as a reference gene) relative to adjacent non-metaplastic tissue, was seen for these tissues (**Figure 1E**), again supporting a role for *HOXA13* in positional identity.

### Binary regulation of *HOXA13* expression

To study in more detail which cells in the healthy GI-tract express Hoxa13, we employed a murine model in which expression of a Hoxa13-GFP fusion protein is driven by the endogenous mouse *Hoxa13* promoter. Within the epithelial compartment, the proximal expression border is located at the transition from the distal to the proximal colon as can be seen from fluorescent images and images of anti-GFP IHC staining (**Figure 3A, B and Supplementary Figure S6 A-D** for bigger overview images). This proximal expression border seems to be crypt-clonal, with some crypts expressing Hoxa13 and others not (see arrows in **Figure 3B** and close-up in **Figure 3C**). Functional consequences of this clonality are unknown and, while beyond the scope of the present manuscript, present an interesting biological question. The distal Hoxa13-GFP expression is limited by the anal squamocolumnar junction (SCJ); **Supplementary Figure S6E**, please note this cannot be appreciated in **Figure 3A**, as this part was damaged for this mouse). To investigate whether these local gradients of Hoxa13 expression are also present in humans, *HOXA13* mRNA expression was assessed by qPCR in an additional set of biopsies taken from different colonic locations. Cecal biopsies are *HOXA13*-negative, while *HOXA13* expression increases from the ileocecal valve to the distal transverse colon, demonstrating a similar expression pattern as observed in the mouse (**Figure 3D**).



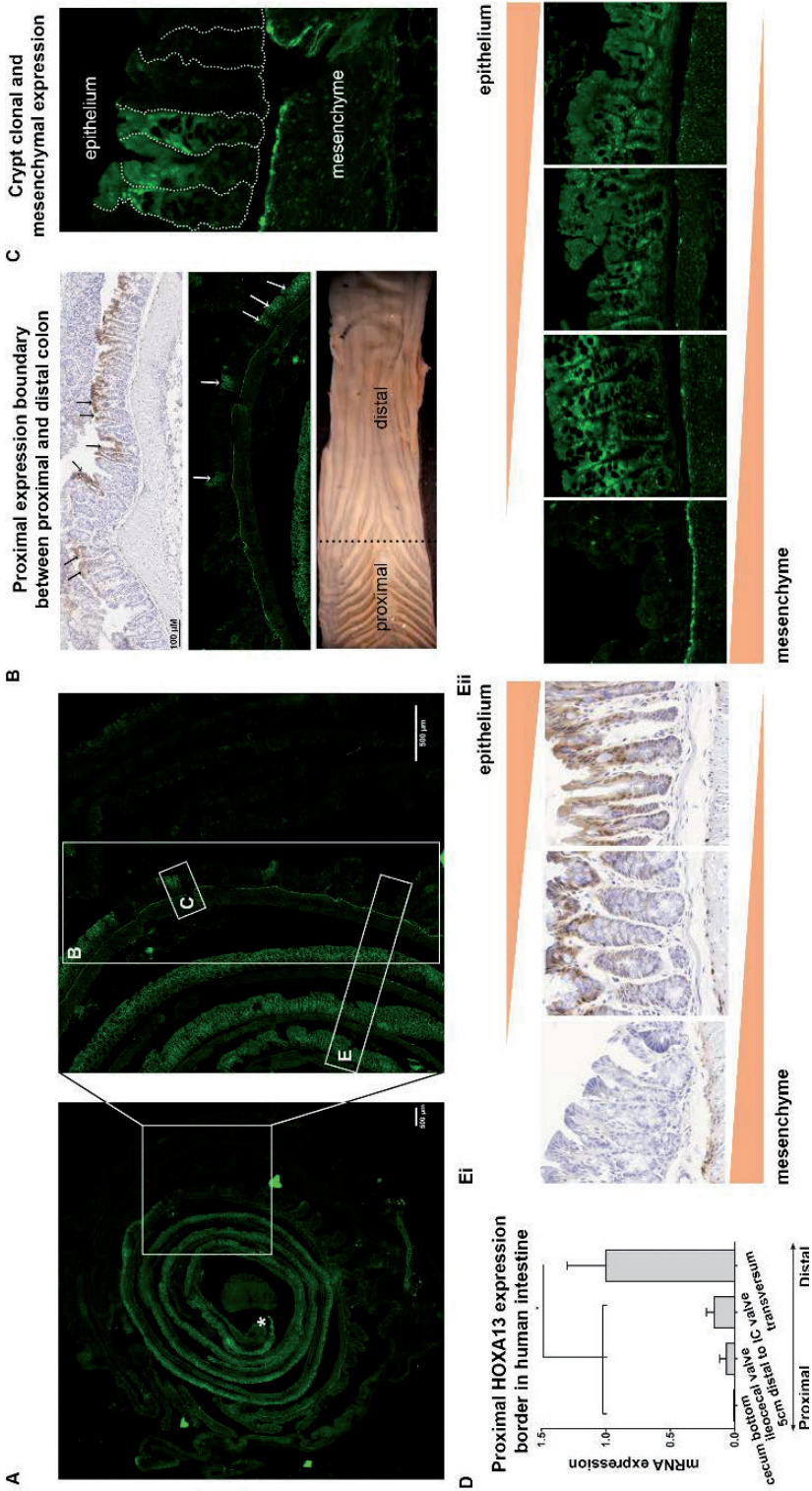


**Figure 3.** Murine and human *HOXA13* expression is subject to strict spatial control in colon. **(A)** A representative example of a “Swiss roll” configuration of the large intestine of the *Hoxa13*-GFP heterozygous mouse model. An asterisk indicates the most distal portion of the epithelium. Magnification of the insets are shown in panels B, C and E. **(B)** The proximal border of physiological *Hoxa13* expression in the adult mouse is patchy and located between the proximal and distal colon, indicated by a black dashed line in the bottom panel (macroscopic image of an opened mouse colon). Representative images of anti-GFP IHC and confocal microscopy are shown. Arrows indicate crypts that are positive for *Hoxa13* among *Hoxa13*-negative crypts. **(C)** The *Hoxa13* expression is crypt clonal. **(D)** In adult humans the cecum bottom is negative for *HOXA13* while positivity increases distally (n=5). Mean±SEM, \**p*<0.05. *HOXA13* mRNA levels were normalized to levels in the transverse colon. **(E)** *Hoxa13* expression is tightly regulated along the baso-luminal axis. Distally, *Hoxa13* is expressed along the entire baso-luminal axis of the colonic crypts, proximally only expression at the luminal side is seen. In addition, a mesenchymal expression is observed in the cells just beneath the epithelium, predominantly in the proximal colon. **(Ei)** anti-GFP IHC, **(Eii)** confocal images.

In addition to a *Hoxa13* gradient along the GI tract, epithelial *Hoxa13*-GFP expression is also tightly regulated along the baso-luminal axis of individual crypts. Proximally, only apical expression is seen, while distally *Hoxa13*-GFP is expressed along the entire baso-luminal axis of the crypts (**Figure 3E**). In addition, mesenchymal expression is observed in the cells just beneath the epithelium in the proximal colonic epithelium (**Figure 3E**). Within the cell, the strongest signal is co-localized with nuclei, as expected, but cytoplasmic staining is also seen which can be explained by ribosomal synthesis (**Figure 3E**).

We concluded that spatial regulation of *Hoxa13*/*HOXA13* expression is very precise, robust and colon-specific, raising questions as to the cellular origin of the *HOXA13* expression observed in BE.

### Individual *Hoxa13*/*HOXA13*-positive cells in the upper GI tract

No significant expression of *HOXA13* mRNA was seen in the squamous esophagus of BE patients by qPCR (**Figure 1C, D**), suggesting that GERD does not provoke *HOXA13* expression *per se*. Indeed, when two primary immortalized squamous esophageal cell lines (EPC2-hTERT and HET-1A) were exposed to either bile or acid, only minor effects on *HOXA13* expression were observed (two to fourfold from a low baseline expression; **Figure 4A, B**), more in agreement with cells having a relatively high *HOXA13* expression showing better survival of the treatment rather than upregulation of expression *per se*. This was confirmed by analysis of the publicly available single cell RNAseq database recently published by Owen et al. (44). Results at single cell level demonstrate the presence of a small population of *HOXA13*-positive cells in the normal squamous esophagus of BE patients (8%). In BE tissue, the percentage of these *HOXA13*-positive cells increase to 30%, but their individual *HOXA13* mRNA levels are not increased as compared to *HOXA13*-expressing cells of the normal esophagus (**Figure 4C, D**). Similarly, the number of *HOXA13*-positive cells, but not *HOXA13* expression *per cell*, is increased in IM of the stomach, early gastric cancer, and colorectal cancer



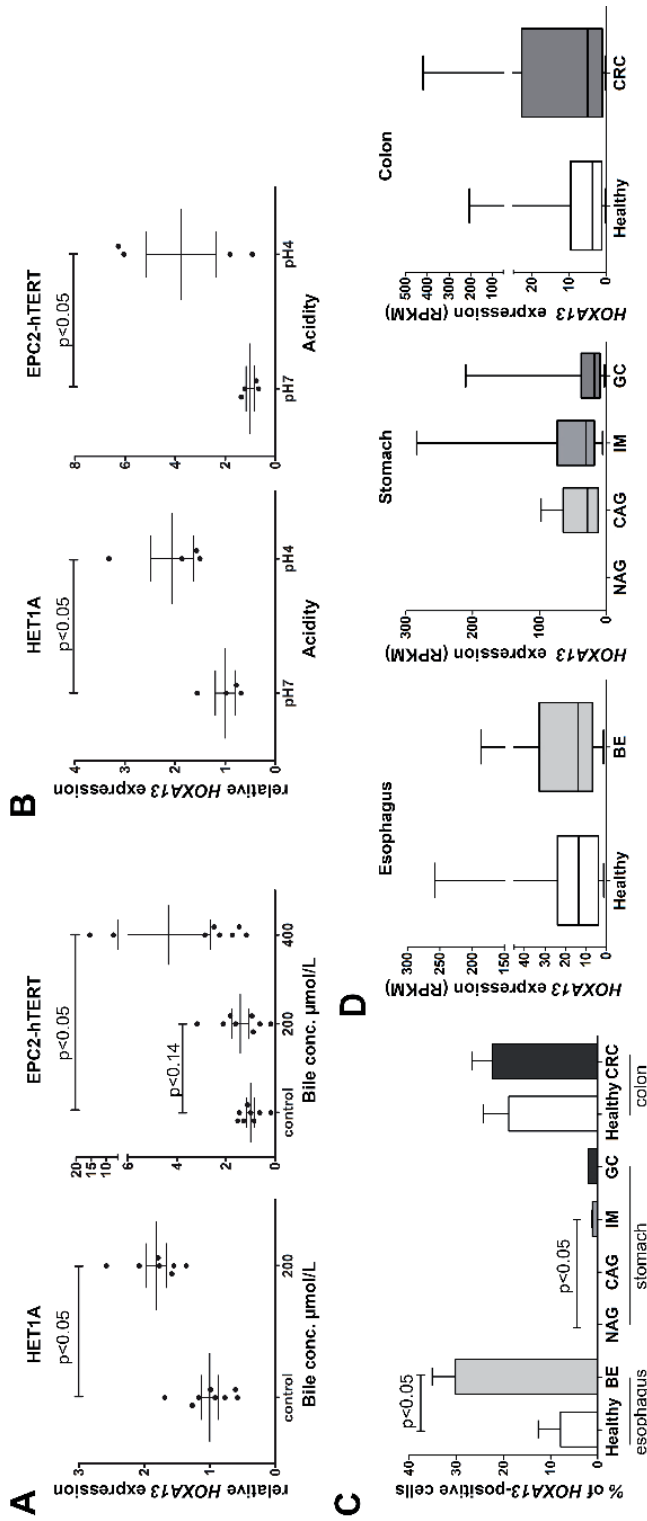


**Figure 4.** Exposure to bile (at pH 7) (A) or to acid (B), in two *in vitro* model systems of GERD, marginally induces the expression of *HOXA13* from low baseline expression levels in two primary immortalized squamous esophageal cell lines. Error bars represent the 95% CI of the mean. (C) The number of *HOXA13*-positive cells are increasing in BE and IM as compared to normal esophagus or stomach tissue. Healthy and BE esophageal samples are derived from the same patients. Mean $\pm$ SEM are shown. Graphs are based on the analysis of single cell RNA data seq ((44), GSE134520 (77), GSE81861 (78)). (D) *HOXA13* expression level per cell is unchanged. Expression level presented in *HOXA13*<sup>+</sup> cells only. BE - Barrett's esophagus, NAG - non-atrophic gastritis, CAG - chronic atrophic gastritis, IM - intestinal metaplasia of stomach, GC - early gastric cancer, and CRC - colorectal cancer. For GC, statistics are not presented as data per patient was not provided. Boxplots with median and whiskers representing min-max values.

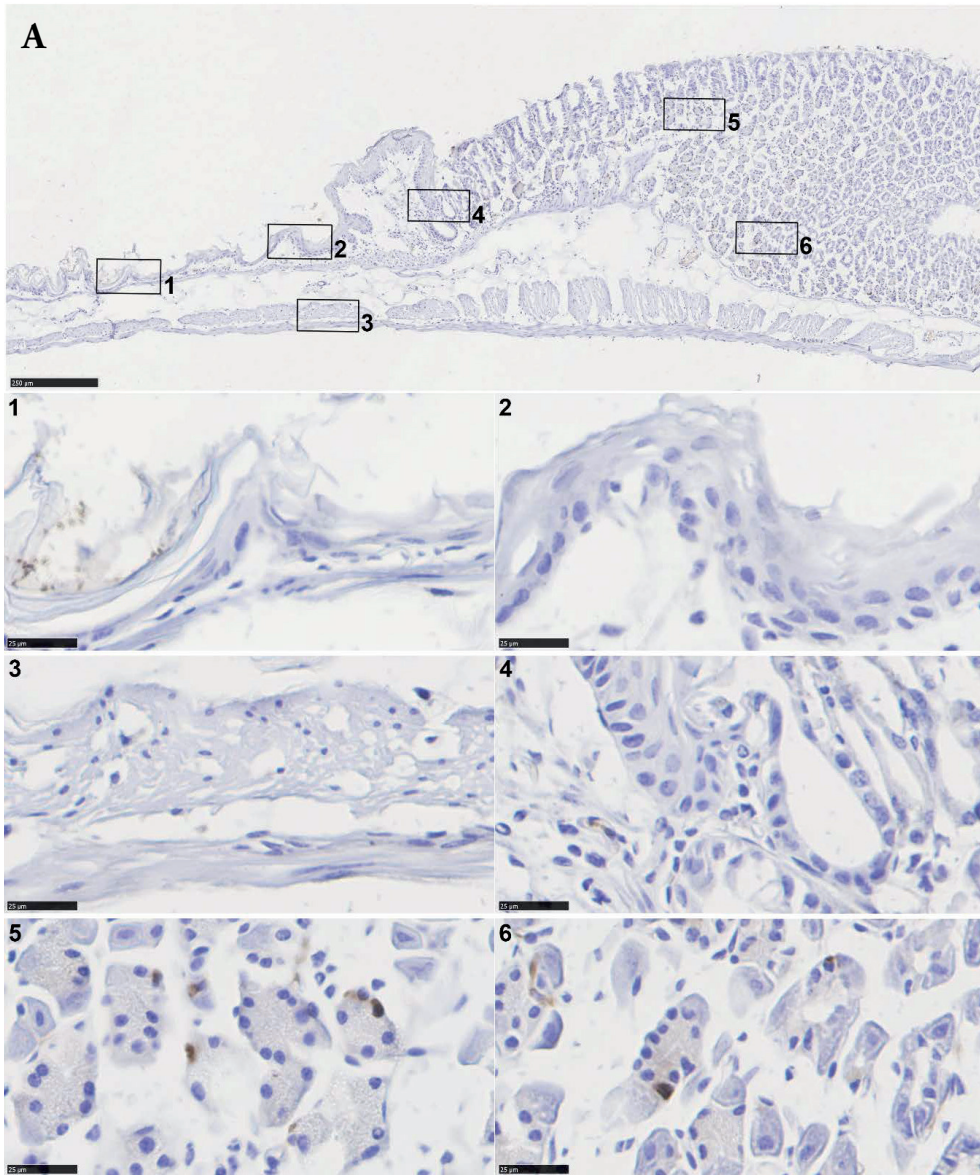


**Figure 5.** *HOXA13* expression in upper GI tract. (A) Representative example of anti-GFP IHC of a *Hoxa13*-GFP heterozygous mouse with GEJ (n=3). *Hoxa13* is expressed in single cells of stomach starting from GEJ (5-6) and absent in the esophagus and stroma (1-4).

(Figure 4C, D). Thus, we further investigated *Hoxa13* at cellular level in our samples. Although *Hoxa13* mRNA expression was detectable in only one of four mice in the upper GI-tract by q-PCR (Supplementary Figure S2), detailed inspection of specimens involved did identify single *Hoxa13*-positive cells in the stomach of *Hoxa13*-GFP mice

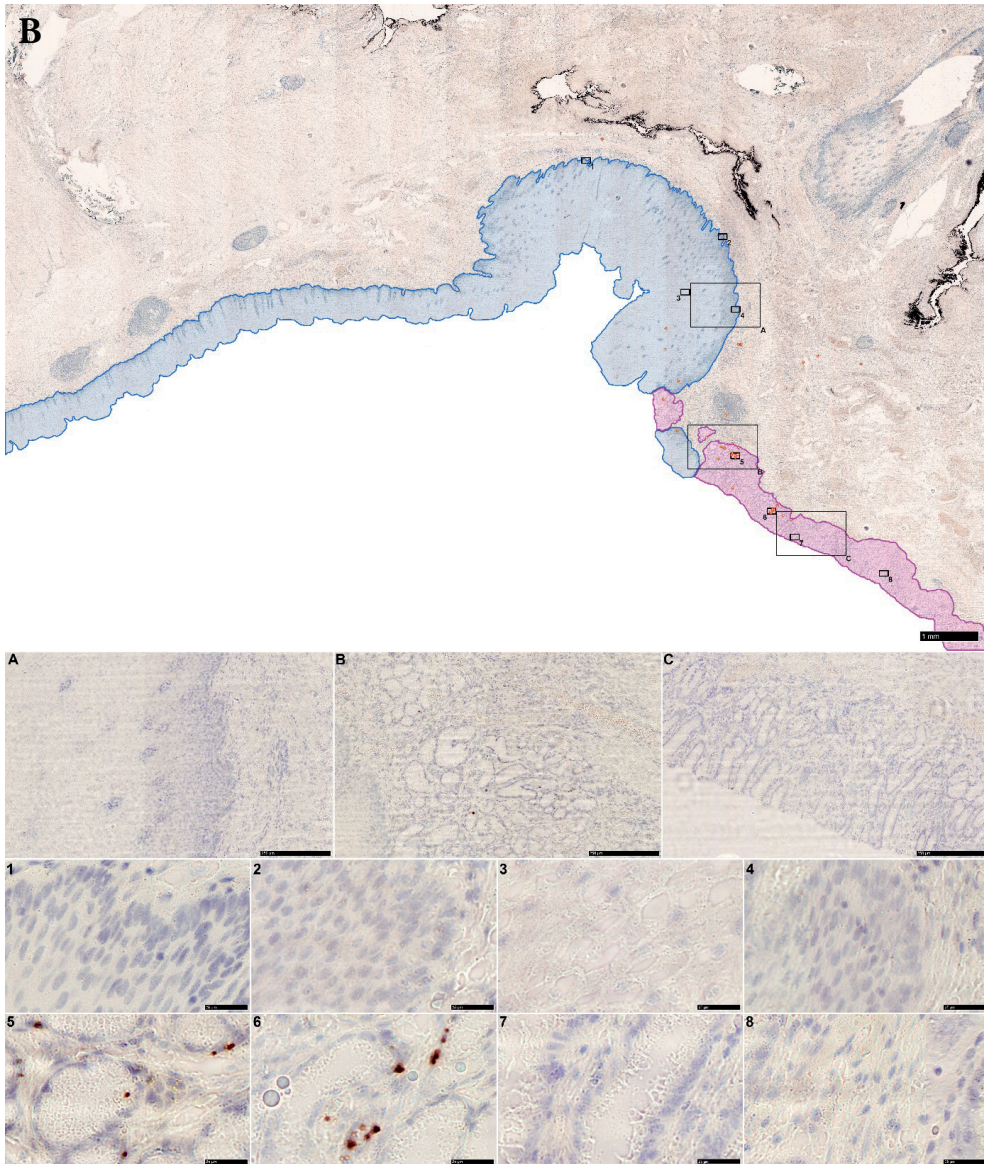


**Figure 5. Continued. (B)** *HOXA13* expression as measured by RNA ISH in a representative example of an adult human GEJ with magnification panel of: A – esophagus (blue), B – GEJ area, C – proximal stomach (pink). Orange circles indicate the positive signal in the overview image.

by immunohistochemistry. Such signal was present at the basolateral side along the stomach starting from the GEJ, but not seen in the squamous cells along the esophagus, nor the stroma (**Figure 5A** and **Supplementary Figure S7**). This is of particular interest as the GEJ has been suggested as a place of origin of BE (41). A littermate negative



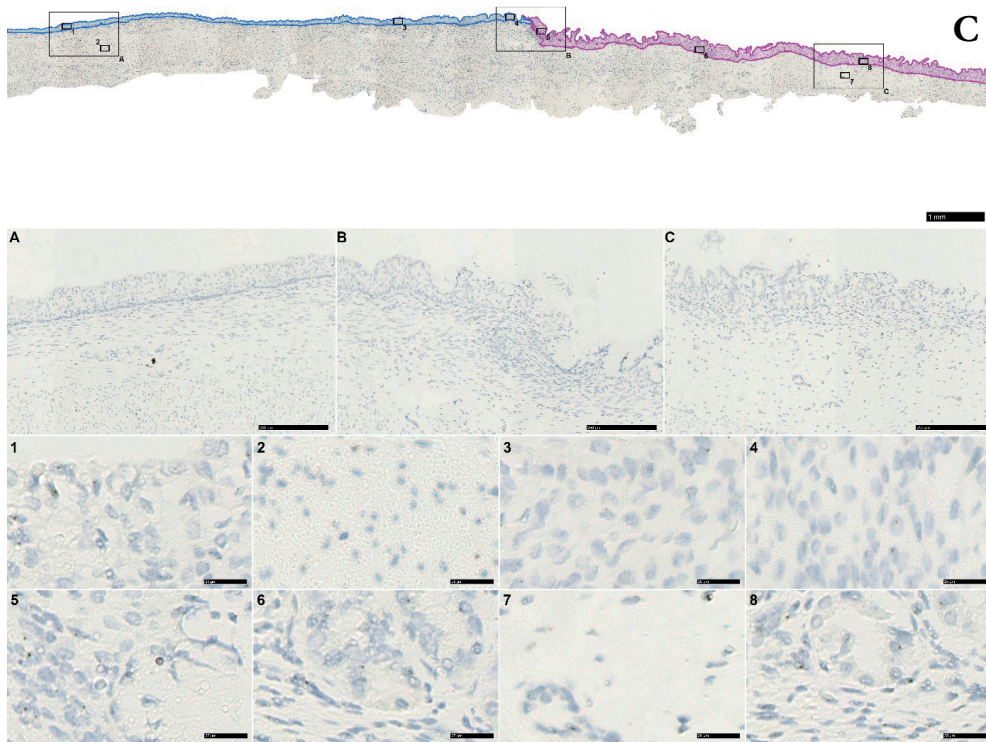


**Figure 5.** *Continued.* (C) Overview of a representative example of a 17-week old fetus GEJ: A) Gastric epithelium of the proximal stomach, B) GEJ area, C) Stratified esophageal epithelium of the distal esophagus.

for *Hoxa13*-GFP showed no positivity (**Supplementary Figure S6D**, **Supplementary Figure S7D**).

Subsequently, we employed ISH for *HOXA13* on surgical samples from the human GEJ of three adult patients to analyze the presence of *HOXA13*-expressing cells in the human upper GI tract. In all three specimens, the GE junction area contained a clear positive signal for *HOXA13* mRNA, some signal was seen in cells of the proximal stomach, while signal was even lower in the squamous epithelium and stroma (**Figure 5B** and **Supplementary Figure S8 A, B**). We also studied *HOXA13* expression in the GEJ of three spontaneously aborted human fetuses of 17-20 weeks of age, a gestation period characterized by transition of the esophageal epithelium from columnar to a squamous phenotype. We observed high and specific *HOXA13* expression at the gastric cardia, while more distal stomach and epithelium of esophagus were less positive (**Figure 5C**, **Supplementary Figure S8 C, D**). These data imply that *HOXA13*-positive cells are present in the human embryonic esophagus during the epithelial transition period, reduced in adult squamous esophagus, and increase again in BE. Thus, strikingly, the

epithelium of both the human and mouse adult upper GI tract, in particular the GEJ, is characterized by the presence of a subpopulation of *HOXA13*/*Hoxa13*-positive cells in an otherwise *HOXA13*-negative surrounding.

### ***HOXA13* affects differentiation potential and posteriorizes**

Having established that individual *HOXA13*-positive cells reside in the physiological upper GI tract and are enhanced in BE tissue, we next set out to investigate the potential role of this population of cells in the etiology of BE. To this end, we further analyzed the single cell RNA-seq (44) data set mentioned above. In this study, the GEJ was not sampled for analysis. However, the 4% of cells of the normal esophagus that express *HOXA13* exhibit transcriptional overlap with cells derived from BE tissue as seen from the t-Distributed Stochastic Neighbour Embedding (t-SNE) plot (**Figure 6A**). Gene expression analysis indicates that these cells are derived from esophageal submucosal glands (ESMG) (**Figure 6B** and **Supplementary File S1**) (44, 45). Specifically, and in contrast to the *HOXA13*-negative cell population, >70% of the *HOXA13*-positive cells from the normal squamous mucosa are positive for submucosal markers *LEFTY1* and *OLFM4*, designated ESGM markers, which have also been described as markers of BE progenitor cells (44). Additionally, *HOXA13*-positive cells express mucosal markers *TFF3*, *Lyz* and *SOX9*, as well as columnar and BE markers *TFF1*, *KRT7*, *VIL1*, *MUC5B*, *MUC3A*, *MUC13*, *MUC1*, *CEACAM5*, while being negative for keratinization marker *IVL* and basal epithelial cell marker *p63* (**Figure 6B** and **Supplementary File S1** for the list of genes enriched in *HOXA13*-positive cells). In BE, the percentage of cells positive for these columnar and ductal markers increase also in the *HOXA13*-negative population, suggesting either that upon differentiation some of these cells might lose *HOXA13* expression, or that there is more than one population giving rise to BE tissue. This would be in line with mouse data, as the murine esophagus lacks ESGMs and *Hoxa13*-positive cells. (Of note, we were unable to assess *HOXA13* presence in human submucosal glands of the esophagus, as no ESGMs were present in our sections as determined by expert pathologist).

The cell of origin with respect to formation of the BE segment should be able to generate a variety of differentiated cell types that exhibit colonic, gastric, pancreatic acinar or other phenotypes (46, 47). In chick embryos, *HOXA13* regulates regionalization after 1.5 days of development, showing the involvement of *HOXA13* in early differentiation, consistent with an effect of this gene on cellular phenotype in such pluripotent progenitor cells (48). In an effort to experimentally test the influence of *HOXA13* on cell fate, we generated *HOXA13*-inducible pluripotent mouse embryonic stem cells (mESCs). These pluripotent mESCs can be efficiently differentiated to multipotent definitive endoderm, as determined by membrane expression of CXCR4 and E-cadherin (**Figure 6C**). This was further confirmed by RNAseq, showing a strong upregulation of definitive endoderm markers such as *Sox17* and *Foxa1* in these differentiated cells, while pluripotency markers such as *Nanog* are downregulated (see **Supplementary Table S1**). Using

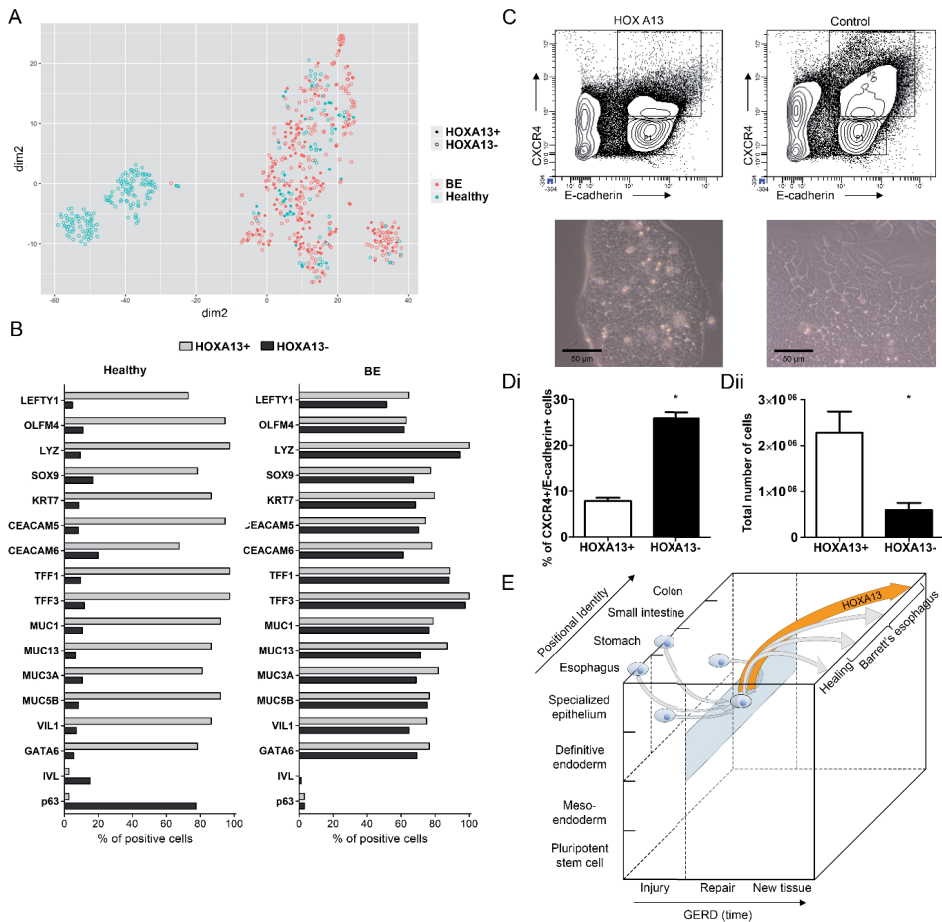


**Figure 6.** (A) *HOXA13*<sup>+</sup> cells of normal esophagus are clustering together with BE cells in *T-SNE* plot based on single cell RNA expression profiling (44). (B) Analysis of single cell RNA-seq data revealed that *HOXA13*<sup>+</sup> cells express submucosal glands markers, BE markers and have decreased expression of squamous markers (p63, IVL) in healthy esophagus in contrast to *HOXA13*<sup>-</sup> population. This difference is not observed in BE. (C) *HOXA13*-overexpressing definitive endoderm is relatively resistant to terminal differentiation. Mouse ESC cells with and without forced *HOXA13* expression were differentiated from pluripotent stem cells to definitive endoderm. The percentage of differentiated definitive endoderm cells, defined as CXCR4<sup>+</sup>/E-cadherin<sup>+</sup> cells, was analyzed by FACS analysis (upper panels). Lower panels (representative light microscopy images) show morphological differences in cultures of *HOXA13* overexpressing and wildtype mESCs after the differentiation protocol. Differentiation to definitive endoderm induces a flattening of cell layers, with larger and irregular shaped cells. (Di) Quantification of FACS analysis results indicates that the percentage of CXCR4<sup>+</sup>/E-cadherin<sup>+</sup> cells in cell cultures under differentiation conditions is decreased in *HOXA13*-overexpressing cell cultures under differentiation conditions. Mean±SEM, \*\*\**p*<0.001 (Dii). (E) Model of cellular identity in BE development. The X-axis represents time (hypothetical units) following exposure to GERD-inducing agents. Y-axis shows differentiation during embryology and pathology. Z-axis indicates the positional identity of GI-tract tissues. Several theories exist regarding the cell of origin of BE: they may be fully differentiated esophageal or stomach cells, or less differentiated cells within these organs (depicted by the 4 cells on the Y-Z plane). Irrespective of its location or differentiation state, this cell or origin might lose its correct positional identity or maintain its aberrant positional identity and resembles a definitive endoderm like cell. This is visualized by the blue rectangle harboring the cell with the thicker blue contour. *In toto*, for the model of cellular identity in BE, these data suggest that *HOXA13* expressing clones in the GEJ, depicted in orange, may outcompete clones with another positional identity, providing an explanation for the distal phenotype observed in BE.

ingenuity pathway analysis (IPA) to further analyze differentially expressed genes, a positive association was found with “differentiation of embryonic cells” ( $z=1.82$ ,  $p=6.38 \cdot 10^{-15}$ ). Intriguingly, when *HOXA13* expression was induced, cells differentiated less effectively towards definitive endoderm as determined by CXCR4<sup>+</sup>/E-cadherin<sup>+</sup> expression and morphological assessment (**Figure 6C and Di**). Consistent with a reduced unilinear differentiation, clones expressing *HOXA13* showed greater expansion (**Figure 6Dii**).

We next contrasted the transcriptome of non-differentiated, pluripotent *HOXA13*-overexpressing and control cultures to identify potential molecular mediators of the *HOXA13* effects observed. Results of IPA analysis of differential gene expression are broadly consistent with *HOXA13* conferring a pluripotent phenotype. Specifically, forced *HOXA13* expression results in upregulation of the “role of *Nanog* in mammalian embryonic cell pluripotency” category ( $z=1.34$ ,  $p=2.32 \cdot 10^{-3}$ ), an effect that involves *Sox2*, *Nanog*, *Tbx3*, *Hesx-1*, and *Dppa-1* amongst others (49, 50) (See **Table 1** for more details/results, fold changes, and  $q$  values with regard to this experiment). *HOXA13* expression also appears to downregulate Wnt signaling, possibly through BMP signaling (51). Wnt signaling is known to promote mesoendodermal differentiation (52), these results are consistent with *HOXA13*-mediated downregulation of Wnt signaling during axial elongation (53). Thus, the transcriptional profile provoked by *HOXA13* is consistent with maintaining a relatively pluripotent phenotype which in turn may increase compartment expansion.

*HOXA13* expression does not block endodermal differentiation of mESC cells completely, suggesting that a role for *HOXA13* in this compartment is still relevant. Definitive endoderm is a feature of the entire GI tract epithelium, and does not distinguish upper and lower GI epithelium *per se*. To investigate the role of *HOXA13* in this cell compartment and test our prediction that *HOXA13* expression would predispose endoderm to acquire distal phenotypes, we sorted CXCR4<sup>+</sup>/E-cadherin<sup>+</sup> cells of *HOXA13*-positive and negative cultures and contrasted their mRNA expression. *HOXA13* upregulates gene expression associated with determination of morphology in definitive endoderm cells. In IPA analysis, “actin cytoskeleton signaling” was most activated ( $z=3.00$ ,  $p=3.74 \cdot 10^{-2}$ ). “RhoA signaling”, which stimulates actin polymerization, ( $z=2.12$ ,  $p=1.12 \cdot 10^{-2}$ ) was also stimulated. *HOXA13* supports distal epithelial functions with upregulation of microvillus-associated genes, *Ezr* and *Vill*, keratins, *Krt19* and *Krt20*, tetraspan network genes, *Igf8*, and exocrine function associated genes such as *Gcnt3*, normally expressed in the distal GI-tract epithelium (33). In addition, more transcripts of “Cell proliferation of carcinoma cell line” ( $z=1.13$ ,  $p=1.5 \cdot 10^{-6}$ ) and “Neoplasia of cancer cells” ( $z=1.13$ ,  $p=2.22 \cdot 10^{-4}$ ) categories, such as *Egfr2* and *Nek2*, were detected. Thus, forced *HOXA13* expression during endodermal differentiation supports caudal epithelial functions and proliferative potential (see **Table 1** for fold changes and  $q$  values; see **Supplementary Table S2** for more relevant molecules).

Together, these data are in apparent agreement with *HOXA13*-expressing cells displaying a progenitor phenotype and having a competitive advantage, while simultaneously

**Table 1.** Fold changes and  $q$  values for the mRNAs mentioned in the results section of the main text pertaining to cell culture models analyzed by RNA-Seq

Gene name	Fold change	$q$ value (multiple testing corrected $p$ value)	Gene name	Fold change	$q$ value (multiple testing corrected $p$ value)
Forced <i>HOXA13</i> in mESC confers a relative competitive advantage in multipotent cell cultures through upregulation of <i>Nanog</i> signaling and downregulation of <i>Wnt</i> signaling			Forced <i>HOXA13</i> expression supports caudal epithelial functions and appears to promote proliferation in DE		
<i>Sox2</i>	1.43	0.01	<i>Sox17</i>	12.55	0.00
<i>Nanog</i>	1.47	0.00	<i>Lgr5</i>	5.39	0.00
<i>Tbx3</i>	3.53	0.00	<i>Nanog</i>	0.20	0.02
<i>Hesx-1</i>	20.56	0.00	<i>Ezr</i>	2.20	0.00
<i>Dppa-1</i>	64.95	0.00	<i>Vill</i>	2.58	0.048
<i>Igf2</i>	3.61	0.00	<i>Krt19</i>	2.34	0.00
<i>Wnt3</i>	0.43	0.00	<i>Krt20</i>	2.84	0.01
<i>Wnt4</i>	0.36	0.00	<i>Igsf8</i>	4.67	0.00
<i>Wnt6</i>	0.36	0.00	<i>Gcnt3</i>	3.51	0.00
<i>Wnt8a</i>	0.48	0.01	<i>Fgfr2</i>	2.81	0.00
<i>Sp8</i>	0.12	0.00	<i>Nek2</i>	2.35	0.01
<i>Lef1</i>	0.34	0.00	<i>HOXA13</i> downregulates the chromosome 1 epidermal differentiation complex, is pro-oncogenic, and conveys typical characteristics of the BE phenotype		
<i>Tbxt</i>	0.41	0.00	<i>ANXA9</i>	0.48	0.04
<i>Axin2</i>	0.55	0.04	<i>EVPL</i>	0.61	0.03
<i>Fgf8</i>	0.10	0.00	<i>SCEL</i>	0.52	0.01
<i>Cdx1</i>	2.47	0.00	<i>KLK7</i>	0.42	0.01
<i>Grhl3</i>	5.00	0.00	<i>EMP1</i>	0.56	0.03
<i>Vill</i>	1.87	0.00	<i>SERPINB13</i>	0.38	0.00
			<i>DLL1</i>	2.57	0.00
			<i>FURIN</i>	1.49	0.03
			<i>JAG1</i>	1.85	0.04

driving the acquisition of a more distal columnar phenotype once committed to differentiation (see **Figure 6E**).

### ***HOXA13* and the chromosome 1 epidermal differentiation complex**

Further support for a role of *HOXA13* in the loss of the squamous phenotype and the appearance of caudal columnar phenotypes in the esophagus comes from experiments in



which we investigated the effect of *HOXA13* directly on esophageal cell models. To this end, we used CRISPR-Cas9 technology to delete *HOXA13* from BAR-T, a primary monoclonal immortalized cell line derived from metaplastic tissue of a BE patient, with cells expressing both columnar and squamous markers (22). Three separate *HOXA13* knock-out clones were selected to circumvent potential off target effects. Reversely, we provoked lentivirus-mediated *HOXA13* expression in EPC2-hTERT, an immortalized squamous esophageal cell line. For these latter experiments we used a mixed cell population of lentivirally transduced cells as to avoid clonal artifacts influencing results. Transcriptomes in these two models (**Figure 7A**) were contrasted to their respective control lines. There was substantial overlap in the gene sets significantly affected by losing *HOXA13* in BAR-T compared with those significantly affected by gaining *HOXA13* in EPC2-hTERT, taking into account the direction of regulation ( $X^2$  test:  $p=4.74 \cdot 10^{-34}$ ) (see **Supplementary Table S3**). Investigation of this overlap across the two technically independently generated datasets limits the incidence of chance findings or single model system bias. Overlapping genes positively affected by *HOXA13* expression in esophageal cells are *IL7r*, *FAM196B*, *ADAMTS6*, *NRG1*, *LTBP1*, *JAG1*, *ELL2*, *SMAD7*, *C12ORF75*, *AXL*, *TIPARP*, *IKBIP*, *DUSP7*, and *GOLIM4*. Downregulated by *HOXA13* expression are *SERPINB13*, *MYO5C*, *KLK7*, *ANXA9*, *TMPRSS4*, *TTC9*, *MATN2*, *TNFAIP2*, *RAB27B*, *HCAR2*, *C6ORF132*, *EXPH5*, *MAP3K5*, and *FUCA1*. IPA analysis of the results predicts an increase in “(malignant) cell transformation” ( $z=2.00$ ,  $p=5.81 \cdot 10^{-3}$ ) and a decrease in “inflammation of an organ” ( $z=-2.59$ ,  $p=8.29 \cdot 10^{-3}$ ; gene function is described in **Supplementary Table S3**) in cells expressing *HOXA13*. Intriguingly, *HOXA13* downregulates the epidermal differentiation

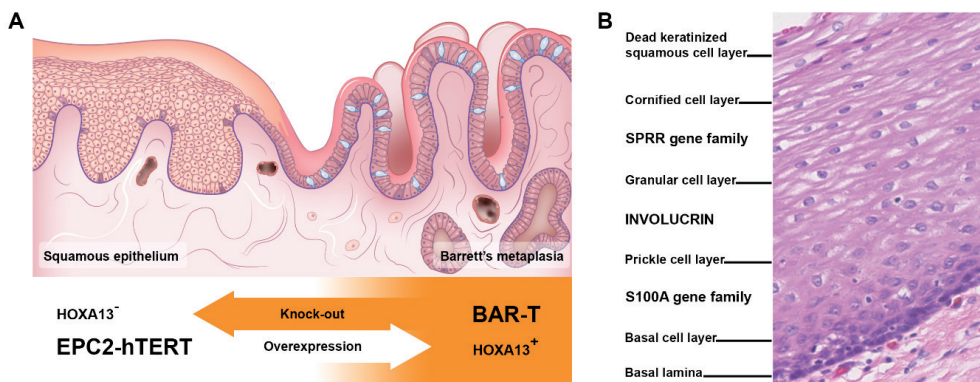


**Figure 7.** *HOXA13* counteracts squamous identity and increases growth of esophageal cells. **(A)** Two models were constructed to investigate the function of *HOXA13* at the GEJ. One model used EPC2-hTERT, a primary immortalized human squamous esophageal cell line, characterized by low *HOXA13* expression, in which *HOXA13* was transduced. The second model employed BAR-T, a primary immortalized human BE cell line, characterized by high *HOXA13* expression, in which *HOXA13* was knocked out. **(B)** H&E staining of the squamous esophagus of a patient without BE indicating the expected location of some of the products of the Ch1q21.3 epidermal differentiation complex along with other genes from the cornified envelope of the epidermis.

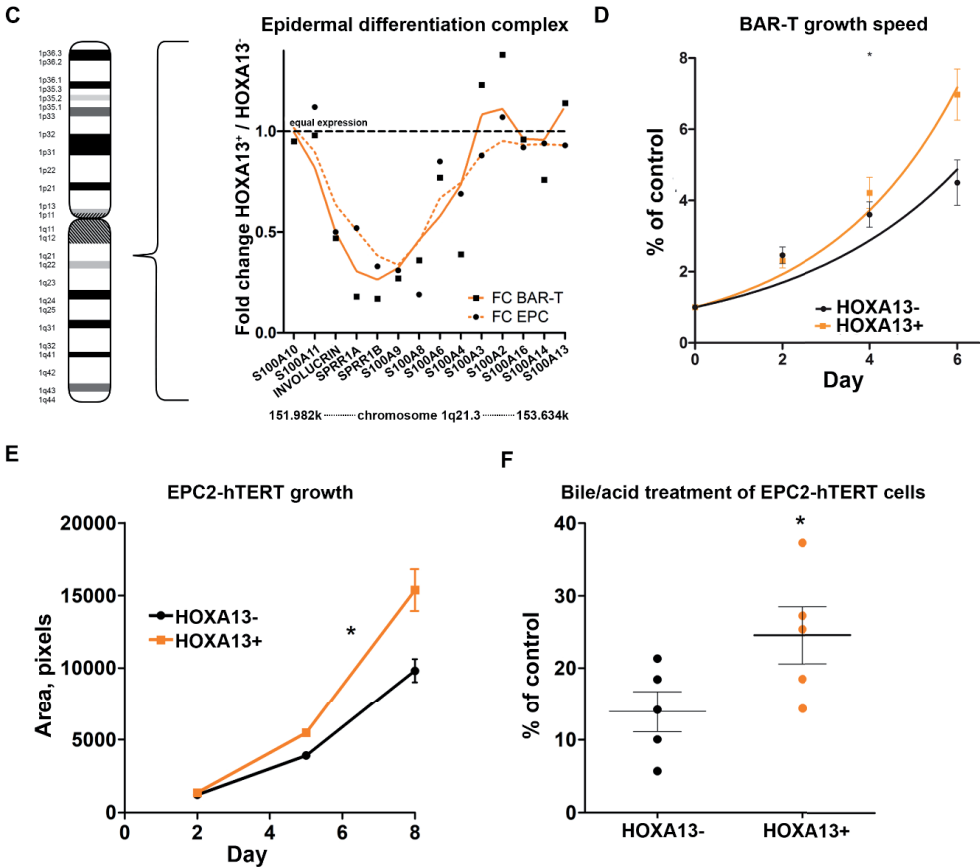


**Figure 7. Continued.** (C) *HOXA13* leads to a downregulation of genes in the Ch1q21.3 epidermal differentiation complex in both model systems. A cubic spline fit of *HOXA13* mRNA regulation is shown, with the BAR-T control transduced cell line presented compared to its *HOXA13* knock-out counterpart, and *HOXA13* overexpressing EPC2-hTERT cells presented compared to their parental line. (D) *HOXA13* knock-out in a BE cell line reduces the growth of the cell pool, as measured by MTT assay. Mean±SEM, \* $p<0.05$ ; \*\*\* $p<0.001$ . (E) *HOXA13* overexpression in a EPC2-hTERT cell line increases its growth in 3D culture (area of spheroids, Mean±SEM, \* $p<0.05$ ). (F) EPC2-hTERT cells with *HOXA13* overexpression are less sensitive to bile/acid exposure. MTT data presented as % of corresponding vehicle-treated controls. Mean±SEM, \* $p<0.05$ .

complex (EDC); **Figure 7B** and **C**). The EDC, located on chromosome 1q21.3, contains clustered multigene families of genes associated with cornified envelope formation in stratified squamous epithelia, such as the S100 and the small proline-rich region (SPRR) genes (54). Among the overlapping downregulated genes in both cell models, *ANXA9* is also associated with differentiating keratinocytes (55), and *EVPL*, *SCEL*, and *KLK7* are cornified envelope genes (56-58). *EMP1* and *SERPINB13* downregulation is associated with increased disease severity in gastric cancer (*EMP1*) and head and neck squamous cell carcinoma (SCC) (*SERPINB13*) (59, 60). See **Table 1** for fold changes and  $q$  values and **Supplementary Table S3** for more differentially expressed molecules related to

morphology. The downregulation of a gene region known to be essential for maintaining a squamous phenotype provides mechanistic support to the notion that altered *HOXA13* expression is cardinal for provoking the BE phenotype.

These experiments also provide mechanistic support for the notion that *HOXA13* expression may offer an explanation as to why BE is prone to progression to EAC. *HOXA13* mediates down-regulation of the EDC and many EDC and cornified envelope genes are progressively down-regulated in the BE to EAC cascade (56, 61). In BE, EAC, and esophageal SCC, loss of heterozygosity (LOH) of the EDC is common (62-64). Low EDC gene expression predicts chemotherapy non-response and LOH of the EDC is associated with reduced survival in curatively treated EAC patients (63, 65). In our experimental models, we observed *HOXA13*-mediated upregulation of genes associated with Notch signaling, specifically *DLL1*, *FURIN*, and *JAG1*. Notch signaling is associated with malignant transformation (66, 67). In IPA analysis "Non-melanoma solid tumor" ( $z=2.03$ ,  $p=9.28 \cdot 10^{-8}$ ) and "invasion of cells" ( $z=2.08$ ,  $p=2.47 \cdot 10^{-3}$ ) were shown to be activated by *HOXA13*, whereas *HOXA13* expression negatively influenced the "Apoptosis" ( $z=-1.52$ ,  $p=2.23 \cdot 10^{-3}$ ) and "killing of cells" ( $z=-2.03$ ,  $p=2.03 \cdot 10^{-3}$ ) categories. Many individual genes showed differential regulation in a pro-oncogenic direction (see **Supplementary Table S3**).

In conclusion, using *HOXA13* knock-out and overexpression in a Barrett's and a squamous cell line, we show that *HOXA13* downregulates the epithelial differentiation complex and other cornified envelope genes which normally function to maintain squamous epithelial morphology and act as tumor suppressor genes. Additionally, Notch signaling is overexpressed and many individual genes show differential regulation in a pro-oncogenic direction.

### ***HOXA13* supports columnar phenotype *in vitro* and *in vivo* and provides proliferative advantage in the presence of bile/acid**

Having established the transcriptional effect of *HOXA13* on BAR-T and EPC2-hTERT cells, we next investigated the functional consequences of *HOXA13* in these cells. As was seen for mESCs, *HOXA13* expression significantly enhances the growth-rate of esophageal cells. For BAR-T cells, a proliferative advantage of *HOXA13* expression was seen in 2D cultures (**Figure 7D**), while for EPC2-hTERT the positive effect of *HOXA13* expression on cell growth was more noticeable under 3D culture conditions (**Figure 7E**). Moreover, *HOXA13* expression decreases the sensitivity of keratinocytes to bile/acid exposure (**Figure 7F**), consistent with the notion that *HOXA13* confers cellular protection under GERD-like conditions.

To gain further insight into the role of *HOXA13* in cell morphology and organization, we made use of the fact that EPC2-hTERT cells can be differentiated in 3D spheroid cultures, and become organized in layers with a more flattened cytological aspect in the

middle of spheroids and high expression of keratinization markers such as involucrin, similar to esophageal stratified epithelium (see example in **Figure 8Ai** for differentiated morphology) (36). Upon overexpression of *HOXA13*, EPC2-hTERT spheroids increase in size while maintaining a less differentiated phenotype (undifferentiated morphology, **Figure 8A**). Quantification of these morphological states indicates that in control cultures, 80% of spheroids attain a stratified epithelial phenotype, while overexpression of *HOXA13* reduces this number to 28.6% ( $p < 0.05$ , **Figure 8Aii**). This was further confirmed by staining for involucrin as a marker of keratinization, showing a decreased expression in spheroids derived from *HOXA13*-overexpressing EPC-hTERT cells. Thus, in primary immortalized esophageal cells *HOXA13* overexpression reduces keratinization (**Figure 8Ai and Aiii**).

We further investigated the morphological role of *HOXA13* in the BE-derived BAR-T cell line. In 2D cultures, an altered spatial distribution in growth pattern was observed,

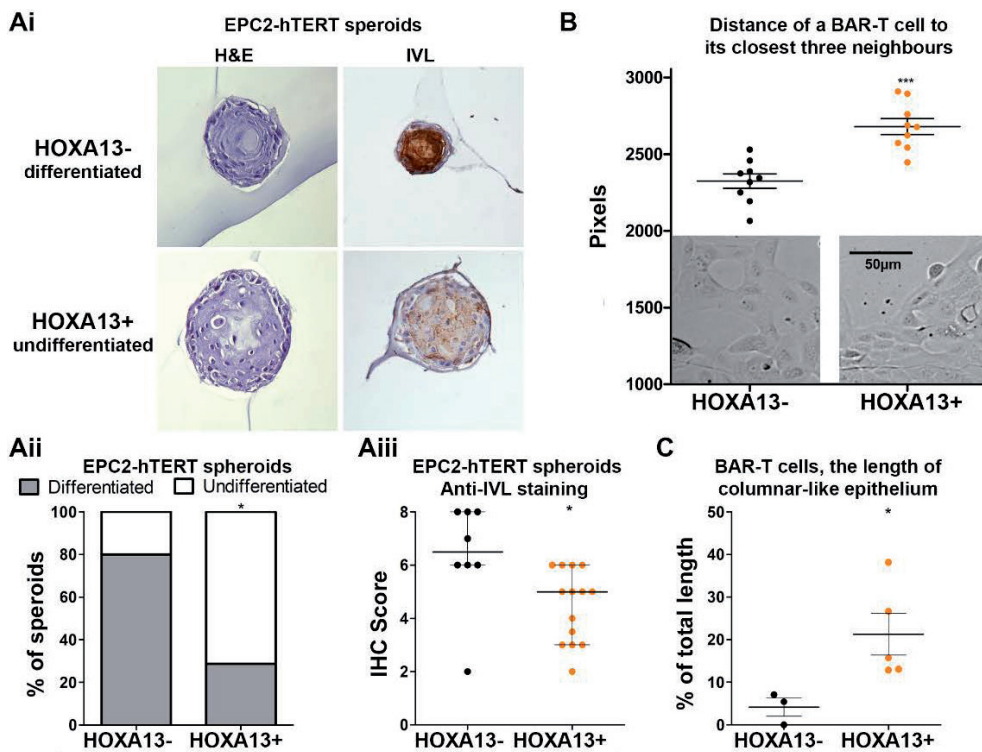


**Figure 8.** *HOXA13* supports intestinal-type columnar epithelial differentiation. (A) *HOXA13* overexpression impairs squamous differentiation of EPC2-hTERT spheroids as seen from the representative pictures (Ai) and quantitative assessment of morphologies based on H&E (Aii) or anti-involucrin (IVL) IHC (Aiii). Median with interquartile range, \* $p < 0.05$ . (B) *HOXA13* KO affects spatial distribution of BAR-T cells. Line at mean, \*\*\* $p < 0.001$ . (C) The length of columnar and mixed BAR-T epithelium decreases upon *HOXA13* KO in the rat trachea *in vivo* tissue reconstitution model. Mean±SEM, \* $p < 0.05$ .

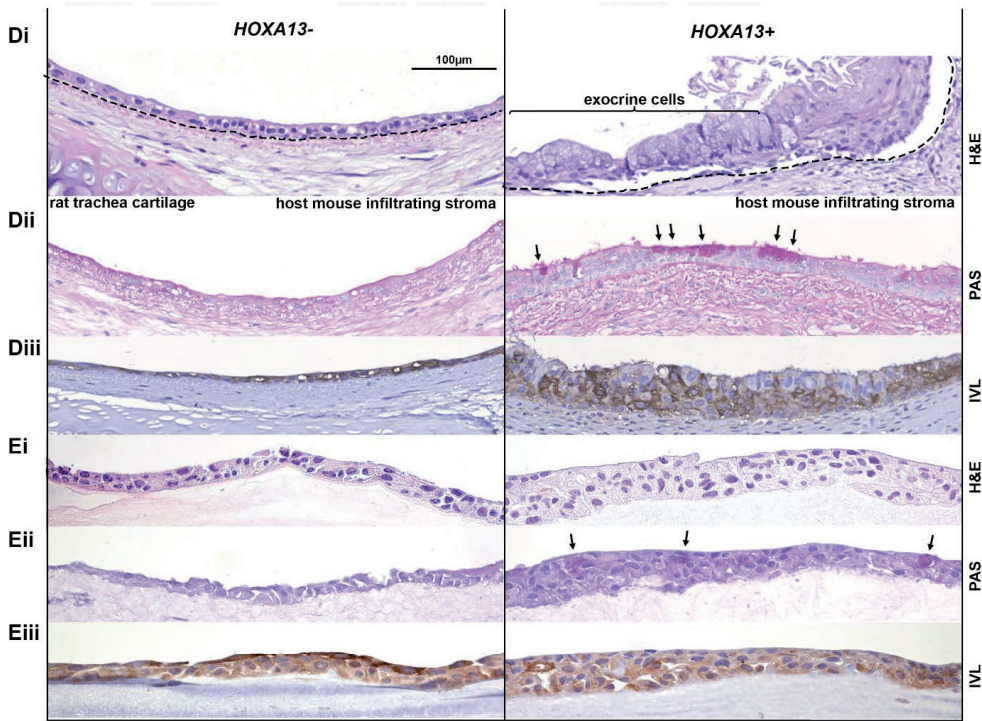


**Figure 8.** *Continued.* (D) Representative examples of H&E (Di), PAS staining (Dii), anti-IVL IHC (Diii) of BAR-T epithelium from the rat trachea *in vivo* tissue reconstitution model. H&E staining shows more layers of cells in *HOXA13*<sup>+</sup> wild type cells. PAS stains polysaccharide molecules, and positivity is indicative of goblet-like cells. The arrows point to PAS positivity, which is present in the right panel but not in the left panel, where the BAR-T *HOXA13*<sup>+</sup> cells are shown. IVL staining is strong in morphologically squamous cells in the left hand panel and weaker in the *HOXA13*<sup>+</sup> epithelium. (E) *HOXA13*<sup>-</sup> and *HOXA13*<sup>+</sup> representative pictures of H&E staining (Ei), PAS staining (Eii) and IVL IHC (Eiii) of the BAR-T organotypic cell culture system indicate that *HOXA13* KO reprograms the columnar epithelium phenotype towards squamous keratinized epithelium.

with cells growing more closely together in the absence of *HOXA13* suggesting effect on tissue morphology (Figure 8B). The BAR-T cell model also allows testing the effect of *HOXA13* on columnar *versus* squamous differentiation in *in vitro* and *in vivo* settings. A 3D *in vivo* tissue reconstitution model was employed in which BAR-T cells were grafted in the lumina of devitalized and denuded rat tracheas and implanted in NOD SCID mice. Under these conditions, parental non-transfected BAR-T cells produce both intestinal-type columnar epithelium and stratified squamous epithelium from the same clone. Hence this cell line has the potential to produce two types of morphologically distinct epithelia (22, 68) (Supplementary Figure S9 and Figure 8D). Thus the epithelium in the model finds itself on a tipping point between both morphologies. This characteristic makes the *in vivo* tissue reconstitution model ideally suited for studying the influence of modulators of morphology, i.e. to show if the modulator favors intestinal-type columnar epithelium or stratified squamous epithelium. Studying the effect of

*HOXA13* knock-out, two important observations were made. Firstly, *HOXA13* knock-out decreases the length of columnar-like epithelium which contains PAS positive cells and is negative for involucrin (**Figure 8C, D, E**). Thus, loss of *HOXA13* counteracts the proliferation of the intestinal-type columnar epithelium while the stratified squamous epithelial proliferation remains present. Secondly, *HOXA13* knock-out impairs epithelial proliferation in general, as inferred from the thickness of the epithelial layer (**Figure 8Di; Supplementary Figure S9B**). *In vitro* 2D organotypic ALI cultures of these cell lines confirm the *in vivo* findings, with *HOXA13* knockout reprogramming the BAR-T epithelial cells towards a squamous keratinized differentiated epithelium (**Figure 8E**). In conclusion, *HOXA13* supports intestinal-type columnar epithelial differentiation and proliferation of the Barrett's epithelium confirming the notion that *HOXA13* expression can mediate both a competitive advantage as well as a predisposition to the formation of columnar phenotypes.

## Discussion

In this study, we extensively characterized *HOX* gene expression and localization in mice and men, demonstrating a collinearity of these genes along the gastrointestinal tract. Following in depth analysis of one of these *HOX* genes, *HOXA13*, we observed single *HOXA13*-positive cells in the upper GI tract, which present rare exceptions to the *HOX* gene collinearity theory and are not reported before to our best knowledge. Specifically, in the normal physiology of the esophagus and proximal stomach, non-squamous structures such as the epithelium at the GEJ, glandular cells of ESMGs and glands of stomach contain single cells expressing *HOXA13*. The fact that these cells have not been described before may be a reflection of the fact that homogenization of tissues for qPCR masks this fraction, and that single cell analysis of the GI tract for this gene has not been performed before. We observe that GI pathology with distal phenotypes like intestinal metaplasia of the esophagus and stomach are characterized by an expansion of *HOXA13*-positive cells, while conversely, a relatively low expression of *HOXA13* is found in the phenotypically rostral Paneth cell metaplasia and pyloric metaplasia of the colon, compared to the surrounding physiological tissue.

It is clear that in normal physiology, *HOXA13* contributes to the distal phenotype of the caudal GI tract, begging the question as to the role and origin of the *HOXA13*-expressing compartment now observed in the upper GI tract. We demonstrate that esophageal *HOXA13*-positive cells express columnar and BE markers and show gene expression patterns overlapping with BE-derived cells. Functionally, *HOXA13* provides cells with several properties required for development of a BE segment. *HOXA13* maintains cells in a stem-like progenitor state, while conferring a proliferative advantage, and resistance to bile and acid exposure. Furthermore, in cells that are lineage committed, *HOXA13* supports



a phenotypically columnar phenotype, most likely partly driven by downregulation of the chromosome 1 epidermal differentiation complex. Thus, our data are consistent with the hypothesis that BE arises as a consequence of the expansion of resident HOXA13-positive cells under abrasive environments such as GERD. Several potential theories have been proposed as to the origin of BE: transdifferentiation of basal cells in the squamous epithelium, extension of a special population of cells from the gastroesophageal junction, repopulation of the esophagus after injury with cells derived from progenitors ESMGs or ducts, resident embryonic stem cells or circulating bone marrow cells (69). These potential sources of esophageal columnar epithelium are not mutually exclusive, and BE may have more than one precursor cell or location. Our study supports the previously proposed hypothesis that BE may originate from ESMGs and the GEJ as *HOXA13* is expressed in OLMF4<sup>+</sup>, LEFTY1<sup>+</sup> cells of ESMGs, recently suggested as a cell of BE origin (44). The fact that in addition to the GEJ, rare *HOXA13*<sup>+</sup> cells are found in the human esophagus and stomach, is consistent with the observation that after esophagogastrostomy BE can reoccur in patients, indicating that the involvement of the GEJ is not an absolute prerequisite for the development of BE (70). Furthermore, our data show that *HOXA13* is already present at stem cell level, supportive of the notion that BE may arise from a cell with stem-cell like characteristics. While *HOXA13* expression overlaps greatly with *KRT7*, a columnar cytokeratin seen in Barrett's, we did not observe direct transcriptional overlap with the previously described *KRT7*<sup>+</sup>*KR14*<sup>+</sup>*TP63*<sup>+</sup> cell of BE origin. However, *KRT7*<sup>+</sup>*KR14*<sup>+</sup>*TP63*<sup>+</sup> cells gave rise to BE-like epithelium only upon ectopic expression of *CDX2* (71). Lineage-tracing studies are needed to further confirm whether one or more types of cells of origin might exist for BE. While we focused on HOXA13 here, it is conceivable that other HOX paralogues are involved in BE pathophysiology, in particular caudal genes such as *HOXA10*, *11*, *B13*, and *C10* are interesting candidates for further investigation, in particular as disruption of collinearity was reported for cluster B in BE (9) and in duodenum of murine embryos (12).

BE is considered as the precursor lesion for EAC, a dangerous form of cancer of which the incidence has substantially increased in recent decades. Increased insight into the pathogenesis of BE may aid development of novel prevention and treatment strategies for EAC. HOXA13 is involved in ESCC (72) and other types of cancer (73-76). Here we show that expression of *HOXA13* also increases in EAC and colorectal cancer, provides proliferative advantage to the cells and activates cancer-related genes transcription like Notch signaling. Hence, we speculate that HOXA13 may play a role in BE progression towards EAC.

*In toto*, the present study identifies a previously unrecognized importance of regional patterning by *HOX* genes in the gut epithelium. In Barrett's esophagus, gastric IM, and heterotopia of the upper GI-tract, a colon-like *HOX* gene expression is present, especially characterized by *HOXA13* upregulation. Strikingly, single cells expressing the generally thought to be distally-restricted *HOXA13* gene are present in the physiological upper GI tract, in particular the GEJ, where it supports a columnar phenotype and

may confer a relative competitive advantage. Thus, *HOXA13* mediates BE phenotype and proliferative potential and hence appears a rational target for strategies aimed at counteracting EAC development.

## Acknowledgments

We would like to acknowledge H.F.B.M. Sleddens, H. Stoop, M.H.W. van Dullemen, P. Vasic, I.T.A. Edelijjn, M.J. van der Lee, P.J. Zwalua, W.W. van Dam, E. Zielhuis, and J. Knoop, Erasmus MC - University Medical Center Rotterdam, for their involvement in investigation, W.N.M. Dinjens for providing material, and F. McKeon, The Jackson Laboratory for Genomic Medicine, for conceptualization and providing resources. FAPESP n. 2016/01139-0; 2017/01046-5 for funding.

## Author contributions

Conceptualization, V.T.J., M.P.P., A.W., J.C., E.J.K., L.J.W.L., W.A.P., M.C.W.S., K.N. and R.S.; Methodology, V.T.J., G.M.F., M.P.P., R.A.S., N.C., R.S., K.N.; Formal Analysis, V.T.J., R.A.S.; Investigation, V.T.J., R.A.S., N.C., K.N.; Resources, M.C.W.S., H.S.S., E.M.T., T.S.G.; Writing – Original Draft, V.T.J., K.N. and A.P.V.; Writing – Review & Editing, V.T.J., M.P.P., M.C.W.S., A.P.V., A.W., G.M.F., R.A.S., R.S., M.J.B., N.C., W.A.P., J.C., E.J.K., L.J.W.L., H.S.S., E.M.T., T.S.G., J.C., M.M., E.J.K., L.J.W.L., K.N.; Funding Acquisition, M.C.W.S., M.P.P., M.J.B., V.T.J., W.A.P.; Visualization, V.T.J., N.C., A.P.V., K.N.; Supervision, M.P.P., M.J.B., M.C.W.S.

## References

1. Grotenhuis BA, van Hagen P, Wijnhoven BPL, Spaander MCW, Tilanus HW, van Lanschot JJB. Delay in diagnostic workup and treatment of esophageal cancer. *Journal of Gastrointestinal Surgery*. 2010;14(3):476-83.
2. Thrift AP, Whiteman DC. The incidence of esophageal adenocarcinoma continues to rise: analysis of period and birth cohort effects on recent trends. *Ann Oncol*. 2012;23(12):3155-62.
3. Ferlay J, Soerjomataram I, Dikshit R, Eser S, Mathers C, Rebelo M, et al. Cancer incidence and mortality worldwide: sources, methods and major patterns in GLOBOCAN 2012. *Int J Cancer*. 2015;136(5):E359-86.
4. Thirunavukarasu P, Sathiaiah M, Sukumar S, Bartels CJ, Zeh H, 3rd, Lee KK, et al. Meckel's diverticulum--a high-risk region for malignancy in the ileum. Insights from a population-based epidemiological study and implications in surgical management. *Ann Surg*. 2011;253(2):223-30.
5. Orosey M, Amin M, Cappell MS. A 14-Year Study of 398 Esophageal Adenocarcinomas Diagnosed Among 156,256 EGDs Performed at Two Large Hospitals: An Inlet Patch Is Proposed as a Significant Risk Factor for Proximal Esophageal Adenocarcinoma. *Dig Dis Sci*. 2017.



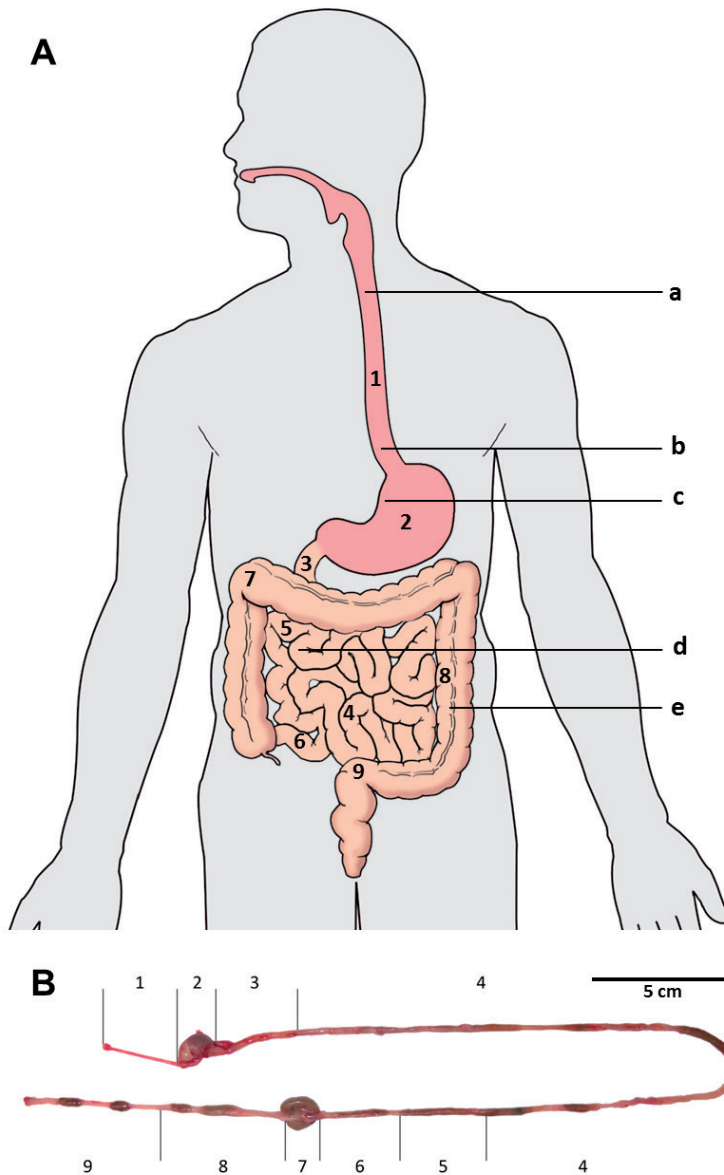
6. Barros R, Pereira D, Calle C, Camilo V, Cunha AI, David L, et al. Dynamics of SOX2 and CDX2 Expression in Barrett's Mucosa. *Dis Markers*. 2016;2016:1532791.
7. Mari L, Milano F, Parikh K, Straub D, Everts V, Hoebe KK, et al. A pSMAD/CDX2 complex is essential for the intestinalization of epithelial metaplasia. *Cell Rep*. 2014;7(4):1197-210.
8. Silberg DG, Sullivan J, Kang E, Swain GP, Moffett J, Sund NJ, et al. Cdx2 ectopic expression induces gastric intestinal metaplasia in transgenic mice. *Gastroenterology*. 2002;122(3):689-96.
9. Di Pietro M, Lao-Sirieix P, Boyle S, Cassidy A, Castillo D, Saadi A, et al. Evidence for a functional role of epigenetically regulated midcluster HOXB genes in the development of Barrett esophagus. *Proceedings of the National Academy of Sciences of the United States of America*. 2012;109(23):9077-82.
10. Pearson JC, Lemons D, McGinnis W. Modulating Hox gene functions during animal body patterning. *Nat Rev Genet*. 2005;6(12):893-904.
11. Shah N, Sukumar S. The Hox genes and their roles in oncogenesis. *Nature Reviews Cancer*. 2010;10(5):361-71.
12. Kawazoe Y, Sekimoto T, Araki M, Takagi K, Araki K, Yamamura K-i. Region-specific gastrointestinal Hox code during murine embryonal gut development. *Development, growth & differentiation*. 2002;44(1):77-84.
13. Yahagi N, Kosaki R, Ito T, Mitsuhashi T, Shimada H, Tomita M, et al. Position-specific expression of Hox genes along the gastrointestinal tract. *Congenital anomalies*. 2004;44(1):18-26.
14. FEDERA. Human Tissue and Medical Research: Code of conduct for responsible use (2011). 2011.
15. Perez WD, Weller CR, Shou S, Stadler HS. Survival of Hoxa13 homozygous mutants reveals a novel role in digit patterning and appendicular skeletal development. *Dev Dyn*. 2010;239(2):446-57.
16. Wang F, Flanagan J, Su N, Wang LC, Bui S, Nielson A, et al. RNAscope: a novel in situ RNA analysis platform for formalin-fixed, paraffin-embedded tissues. *J Mol Diagn*. 2012;14(1):22-9.
17. Schindelin J, Rueden CT, Hiner MC, Eliceiri KW. The ImageJ ecosystem: An open platform for biomedical image analysis. *Mol Reprod Dev*. 2015;82(7-8):518-29.
18. Wang X, Yamamoto Y, Wilson LH, Zhang T, Howitt BE, Farrow MA, et al. Cloning and variation of ground state intestinal stem cells. *Nature*. 2015;522(7555):173-8.
19. Yamamoto Y, Wang X, Bertrand D, Kern F, Zhang T, Duleba M, et al. Mutational spectrum of Barrett's stem cells suggests paths to initiation of a precancerous lesion. *Nature Communications*. 2016;7:10380.
20. Barrett T, Wilhite SE, Ledoux P, Evangelista C, Kim IF, Tomashevsky M, et al. NCBI GEO: archive for functional genomics data sets--update. *Nucleic Acids Res*. 2013;41(Database issue):D991-5.
21. Harada H, Nakagawa H, Oyama K, Takaoka M, Andl CD, Jacobmeier B, et al. Telomerase induces immortalization of human esophageal keratinocytes without p16INK4a inactivation. *Molecular cancer research : MCR*. 2003;1(10):729-38.
22. Jaiswal KR, Morales CP, Feagins LA, Gandia KG, Zhang X, Zhang HY, et al. Characterization of telomerase-immortalized, non-neoplastic, human Barrett's cell line (BAR-T). *Diseases of the esophagus : official journal of the International Society for Diseases of the Esophagus / I S D E*. 2007;20(3):256-64.
23. Shin KJ, Wall EA, Zavzavadjian JR, Santat LA, Liu J, Hwang JI, et al. A single lentiviral vector platform for microRNA-based conditional RNA interference and coordinated transgene expression. *Proc Natl Acad Sci U S A*. 2006;103(37):13759-64.
24. Katzen F. Gateway(™) recombinational cloning: a biological operating system. *Expert Opin Drug Discov*. 2007;2(4):571-89.
25. Beard C, Hochedlinger K, Plath K, Wutz A, Jaenisch R. Efficient method to generate single-copy transgenic mice by site-specific integration in embryonic stem cells. *Genesis*. 2006;44(1):23-8.

26. Heimeier RA, Das B, Buchholz DR, Fiorentino M, Shi YB. Studies on *Xenopus laevis* intestine reveal biological pathways underlying vertebrate gut adaptation from embryo to adult. *Genome Biol.* 2010;11(5):R55.
27. Ogaki S, Shiraki N, Kume K, Kume S. Wnt and Notch signals guide embryonic stem cell differentiation into the intestinal lineages. *Stem Cells.* 2013;31(6):1086-96.
28. Larsson SH, Charlier JP, Miyagawa K, Engelkamp D, Rassoulzadegan M, Ross A, et al. Subnuclear localization of WT1 in splicing or transcription factor domains is regulated by alternative splicing. *Cell.* 1995;81(3):391-401.
29. Sanjana NE, Shalem O, Zhang F. Improved vectors and genome-wide libraries for CRISPR screening. *Nat Methods.* 2014;11(8):783-4.
30. R Development Core Team. R: A language and environment for statistical computing. Vienna, Austria. 2008.
31. Love MI, Huber W, Anders S. Moderated estimation of fold change and dispersion for RNA-seq data with DESeq2. *Genome Biol.* 2014;15(12):550.
32. Krämer A, Green J, Pollard J, Jr., Tugendreich S. Causal analysis approaches in Ingenuity Pathway Analysis. *Bioinformatics.* 2014;30(4):523-30.
33. Uhlen M, Fagerberg L, Hallstrom BM, Lindskog C, Oksvold P, Mardinoglu A, et al. Proteomics. Tissue-based map of the human proteome. *Science.* 2015;347(6220):1260419.
34. Bus P, Siersema PD, Verbeek RE, van Baal JWPM. Upregulation of miRNA-143, -145, -192, and -194 in esophageal epithelial cells upon acidic bile salt stimulation. *Diseases of the esophagus : official journal of the International Society for Diseases of the Esophagus / I S D E.* 2013.
35. Queiroz KC, Milani R, Ruela-de-Sousa RR, Fuhler GM, Justo GZ, Zambuzzi WF, et al. Violacein induces death of resistant leukaemia cells via kinome reprogramming, endoplasmic reticulum stress and Golgi apparatus collapse. *PLoS One.* 2012;7(10):e45362.
36. Kasagi Y, Chandramouleeswaran PM, Whelan KA, Tanaka K, Giroux V, Sharma M, et al. The Esophageal Organoid System Reveals Functional Interplay Between Notch and Cytokines in Reactive Epithelial Changes. *Cell Mol Gastroenterol Hepatol.* 2018;5(3):333-52.
37. Kalabis J, Wong GS, Vega ME, Natsuizaka M, Robertson ES, Herlyn M, et al. Isolation and characterization of mouse and human esophageal epithelial cells in 3D organotypic culture. *Nature protocols.* 2012;7(2):235-46.
38. Croagh D, Cheng S, Tikoo A, Nandurkar S, Thomas RJ, Kaur P, et al. Reconstitution of stratified murine and human oesophageal epithelia in an in vivo transplant culture system. *Scand J Gastroenterol.* 2008;43(10):1158-68.
39. Wang KC, Yang YW, Liu B, Sanyal A, Corces-Zimmerman R, Chen Y, et al. A long noncoding RNA maintains active chromatin to coordinate homeotic gene expression. *Nature.* 2011;472(7341):120-4.
40. Gupta RA, Shah N, Wang KC, Kim J, Horlings HM, Wong DJ, et al. Long non-coding RNA HOTAIR reprograms chromatin state to promote cancer metastasis. *Nature.* 2010;464(7291):1071-6.
41. Que J, Garman KS, Souza RF, Spechler SJ. Pathogenesis and Cells of Origin of Barrett's Esophagus. *Gastroenterology.* 2019;157(2):349-64 e1.
42. Gaunt SJ. The significance of Hox gene collinearity. *Int J Dev Biol.* 2015;59(4-6):159-70.
43. Symonds DA. Paneth cell metaplasia in diseases of the colon and rectum. *Arch Pathol.* 1974;97(6):343-7.
44. Owen RP, White MJ, Severson DT, Braden B, Bailey A, Goldin R, et al. Single cell RNA-seq reveals profound transcriptional similarity between Barrett's oesophagus and oesophageal submucosal glands. *Nat Commun.* 2018;9(1):4261.

45. Krüger L, Gonzalez LM, Pridgen TA, McCall SJ, von Furstenberg RJ, Harnden I, et al. Ductular and proliferative response of esophageal submucosal glands in a porcine model of esophageal injury and repair. *Am J Physiol Gastrointest Liver Physiol.* 2017;313(3):G180-G91.
46. Rotterdam H. Pathology of the gastric cardia. *Verh Dtsch Ges Pathol.* 1999;83:37-42.
47. Johansson J, Hakansson HO, Mellblom L, Kempas A, Kjellen G, Brudin L, et al. Pancreatic acinar metaplasia in the distal oesophagus and the gastric cardia: prevalence, predictors and relation to GORD. *J Gastroenterol.* 2010;45(3):291-9.
48. Matsushita S, Ishii Y, Scotting PJ, Kuroiwa A, Yasugi S. Pre-gut endoderm of chick embryos is regionalized by 1.5 days of development. *Dev Dyn.* 2002;223(1):33-47.
49. Boyer LA, Lee TI, Cole MF, Johnstone SE, Levine SS, Zucker JP, et al. Core transcriptional regulatory circuitry in human embryonic stem cells. *Cell.* 2005;122(6):947-56.
50. Shin MR, Cui XS, Jun JH, Jeong YJ, Kim NH. Identification of mouse blastocyst genes that are downregulated by double-stranded RNA-mediated knockdown of Oct-4 expression. *Mol Reprod Dev.* 2005;70(4):390-6.
51. Voorneveld PW, Kodach LL, Jacobs RJ, van Noesel CJ, Peppelenbosch MP, Korkmaz KS, et al. The BMP pathway either enhances or inhibits the Wnt pathway depending on the SMAD4 and p53 status in CRC. *Br J Cancer.* 2015;112(1):122-30.
52. Bakre MM, Hoi A, Mong JC, Koh YY, Wong KY, Stanton LW. Generation of multipotential mesendodermal progenitors from mouse embryonic stem cells via sustained Wnt pathway activation. *J Biol Chem.* 2007;282(43):31703-12.
53. Denans N, Iimura T, Pourquie O. Hox genes control vertebrate body elongation by collinear Wnt repression. *Elife.* 2015;4.
54. Mischke D, Korge BP, Marenholz I, Volz A, Ziegler A. Genes encoding structural proteins of epidermal cornification and S100 calcium-binding proteins form a gene complex ("epidermal differentiation complex") on human chromosome 1q21. *J Invest Dermatol.* 1996;106(5):989-92.
55. Boczonadi V, Maatta A. Annexin A9 is a periplakin interacting partner in membrane-targeted cytoskeletal linker protein complexes. *FEBS Lett.* 2012;586(19):3090-6.
56. Dai Y, Wang Q, Gonzalez Lopez A, Anders M, Malferttheiner P, Vieth M, et al. Genome-Wide Analysis of Barrett's Adenocarcinoma. A First Step Towards Identifying Patients at Risk and Developing Therapeutic Paths. *Transl Oncol.* 2017;11(1):116-24.
57. Kalinin A, Marekov LN, Steinert PM. Assembly of the epidermal cornified cell envelope. *J Cell Sci.* 2001;114(Pt 17):3069-70.
58. Lundstrom A, Egelrud T. Stratum corneum chymotryptic enzyme: a proteinase which may be generally present in the stratum corneum and with a possible involvement in desquamation. *Acta Derm Venereol.* 1991;71(6):471-4.
59. Sun G, Zhao G, Lu Y, Wang Y, Yang C. Association of EMP1 with gastric carcinoma invasion, survival and prognosis. *Int J Oncol.* 2014;45(3):1091-8.
60. de Koning PJ, Bovenschen N, Leusink FK, Broekhuizen R, Quadir R, van Gemert JT, et al. Downregulation of SERPINB13 expression in head and neck squamous cell carcinomas associates with poor clinical outcome. *Int J Cancer.* 2009;125(7):1542-50.
61. Kimchi ET, Posner MC, Park JO, Darga TE, Kocherginsky M, Karrison T, et al. Progression of Barrett's metaplasia to adenocarcinoma is associated with the suppression of the transcriptional programs of epidermal differentiation. *Cancer Res.* 2005;65(8):3146-54.
62. Chaves P, Crespo M, Ribeiro C, Laranjeira C, Pereira AD, Suspiro A, et al. Chromosomal analysis of Barrett's cells: demonstration of instability and detection of the metaplastic lineage involved. *Mod Pathol.* 2007;20(7):788-96.

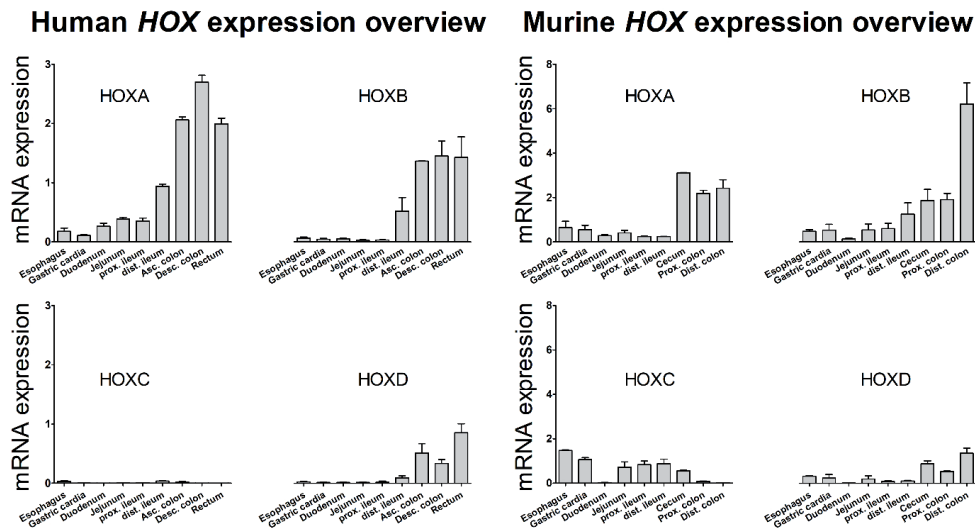
63. Maru DM, Luthra R, Correa AM, White-Cross J, Anandasabapathy S, Krishnan S, et al. Frequent loss of heterozygosity of chromosome 1q in esophageal adenocarcinoma: loss of chromosome 1q21.3 is associated with shorter overall survival. *Cancer*. 2009;115(7):1576-85.
64. Li J, Liu Z, Wang Y, Yu Z, Wang M, Zhan Q, et al. Allelic imbalance of chromosome 1q in esophageal squamous cell carcinomas from China: a novel region of allelic loss and significant association with differentiation. *Cancer Lett*. 2005;220(2):221-30.
65. Luthra MG, Ajani JA, Izzo J, Ensor J, Wu TT, Rashid A, et al. Decreased expression of gene cluster at chromosome 1q21 defines molecular subgroups of chemoradiotherapy response in esophageal cancers. *Clin Cancer Res*. 2007;13(3):912-9.
66. Quante M, Bhagat G, Abrams JA, Marache F, Good P, Lee MD, et al. Bile acid and inflammation activate gastric cardia stem cells in a mouse model of Barrett-like metaplasia. *Cancer Cell*. 2012;21(1):36-51.
67. Menke V, van Es JH, de Lau W, van den Born M, Kuipers EJ, Siersema PD, et al. Conversion of metaplastic Barrett's epithelium into post-mitotic goblet cells by gamma-secretase inhibition. *Dis Model Mech*. 2010;3(1-2):104-10.
68. Bajpai M, Liu J, Geng X, Souza RF, Amenta PS, Das KM. Repeated exposure to acid and bile selectively induces colonic phenotype expression in a heterogeneous Barrett's epithelial cell line. *Lab Invest*. 2008;88(6):643-51.
69. Nesteruk K, Spaander MCW, Leeuwenburgh I, Peppelenbosch MP, Fuhler GM. Achalasia and associated esophageal cancer risk: What lessons can we learn from the molecular analysis of Barrett's-associated adenocarcinoma? *Biochim Biophys Acta Rev Cancer*. 2019;1872(2):188291.
70. Hamilton SR, Yardley JH. Regenerative of cardiac type mucosa and acquisition of Barrett mucosa after esophagogastrostomy. *Gastroenterology*. 1977;72(4 Pt 1):669-75.
71. Jiang M, Li H, Zhang Y, Yang Y, Lu R, Liu K, et al. Transitional basal cells at the squamous-columnar junction generate Barrett's oesophagus. *Nature*. 2017;550(7677):529-33.
72. Gu ZD, Shen LY, Wang H, Chen XM, Li Y, Ning T, et al. HOXA13 promotes cancer cell growth and predicts poor survival of patients with esophageal squamous cell carcinoma. *Cancer Research*. 2009;69(12):4969-73.
73. Qin Z, Chen Z, Weng J, Li S, Rong Z, Zhou C. Elevated HOXA13 expression promotes the proliferation and metastasis of gastric cancer partly via activating Erk1/2. *Onco Targets Ther*. 2019;12:1803-13.
74. Deng Y, He R, Zhang R, Gan B, Zhang Y, Chen G, et al. The expression of HOXA13 in lung adenocarcinoma and its clinical significance: A study based on The Cancer Genome Atlas, Oncomine and reverse transcription-quantitative polymerase chain reaction. *Oncol Lett*. 2018;15(6):8556-72.
75. Quagliata L, Matter MS, Piscuoglio S, Arabi L, Ruiz C, Procino A, et al. Long noncoding RNA HOTTIP/HOXA13 expression is associated with disease progression and predicts outcome in hepatocellular carcinoma patients. *Hepatology*. 2014;59(3):911-23.
76. Dong Y, Cai Y, Liu B, Jiao X, Li ZT, Guo DY, et al. HOXA13 is associated with unfavorable survival and acts as a novel oncogene in prostate carcinoma. *Future Oncol*. 2017;13(17):1505-16.
77. Zhang P, Yang M, Zhang Y, Xiao S, Lai X, Tan A, et al. Dissecting the Single-Cell Transcriptome Network Underlying Gastric Premalignant Lesions and Early Gastric Cancer. *Cell Rep*. 2019;27(6):1934-47 e5.
78. Li H, Courtois ET, Sengupta D, Tan Y, Chen KH, Goh JLL, et al. Reference component analysis of single-cell transcriptomes elucidates cellular heterogeneity in human colorectal tumors. *Nat Genet*. 2017;49(5):708-18.

## Supplementary information



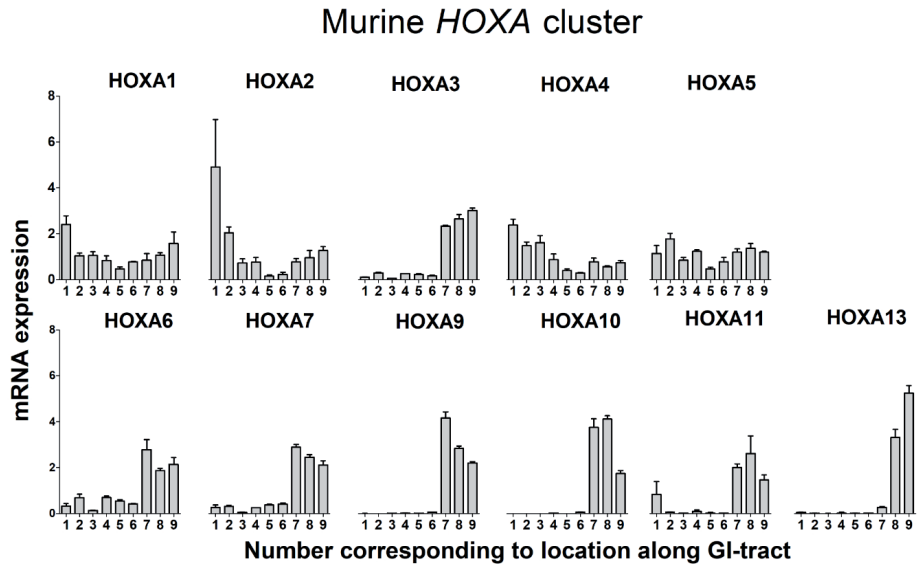
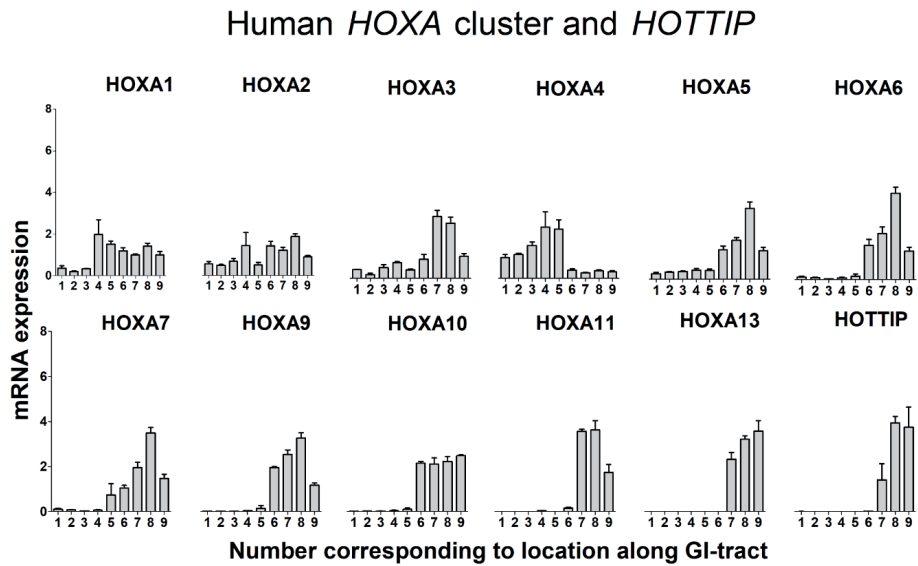
**Supplementary Figure S1.** Locations of forceps biopsies taken along the human GI-tract and sections of murine GI-tract analyzed. **(A)** Location of the forceps biopsies taken along the GI-tract are indicated by number in the schematic illustration of the GI-tract: 1) esophagus, 2) stomach, 3) duodenum, 4) jejunum, 5) proximal ileum, 6) distal ileum, 7) ascending colon, 8) descending colon and 9) sigmoid/rectum. Lesions studied: a) gastric inlet patch; b) CLE, BE, EAC; c) gastric IM; d) Meckel's diverticulum; e) pyloric and Paneth cell metaplasia (from the colon). **(B)** Sections of mouse GI-tract used: 1) esophagus, 2) stomach, 3) duodenum, 4) jejunum, 5) proximal ileum, 6) distal ileum, 7) cecum and proximal colon, 8) proximal colon and distal colon and 9) distal colon.

A



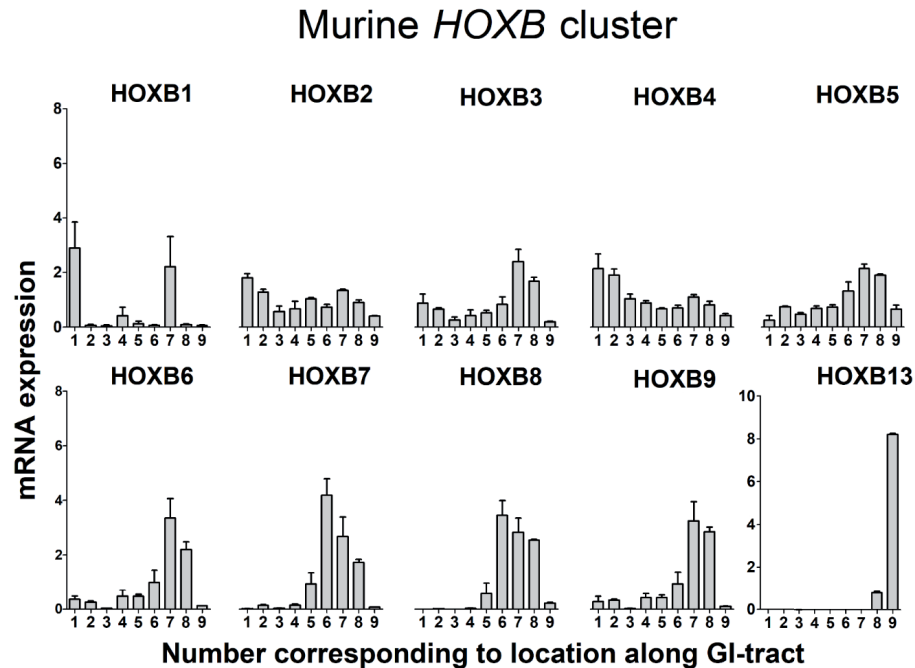
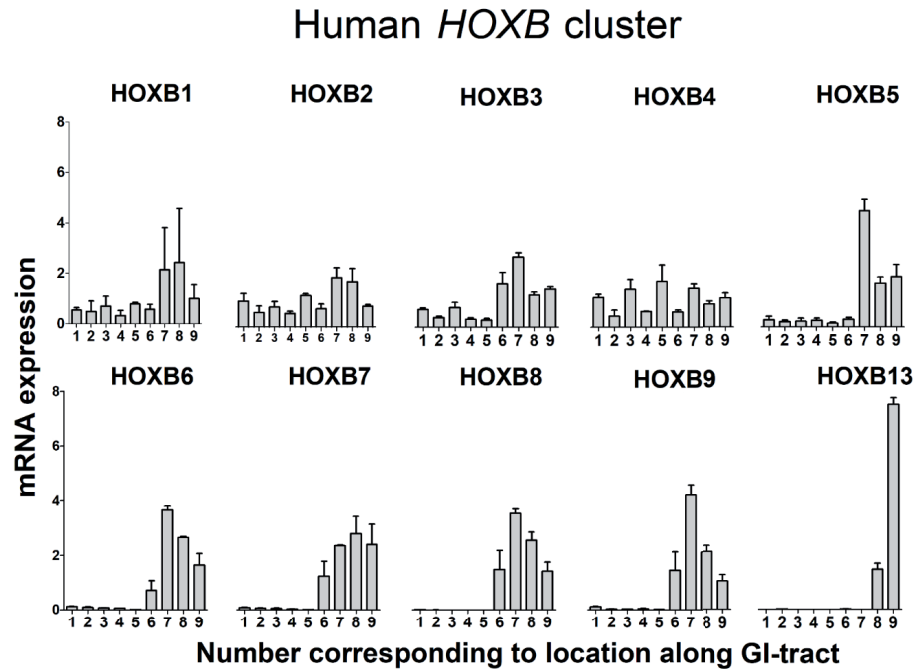
**Supplementary Figure S2.** *HOX* cluster gene expression along the adult human and mouse gut. **(A)** Overview of *HOX* cluster gene expression in the different epithelial regions along the human and mouse adult GI tract. The Y-axis represents the fold changes of mRNA expression relative to the average mRNA expression of all *HOX* genes of a given cluster. **(B - E)** Individual *HOX* gene expression of the *HOXA*, *B*, *C*, and *D* clusters is depicted. The Y-axis represents the fold changes of mRNA expression relative to the average mRNA expression of the depicted *HOX* gene. Individual mice are not shown. Error bars represent the standard error of the mean (SEM). Human data, n=3. Mouse data, n=4.

B



Supplementary Figure S2. *Continued.*

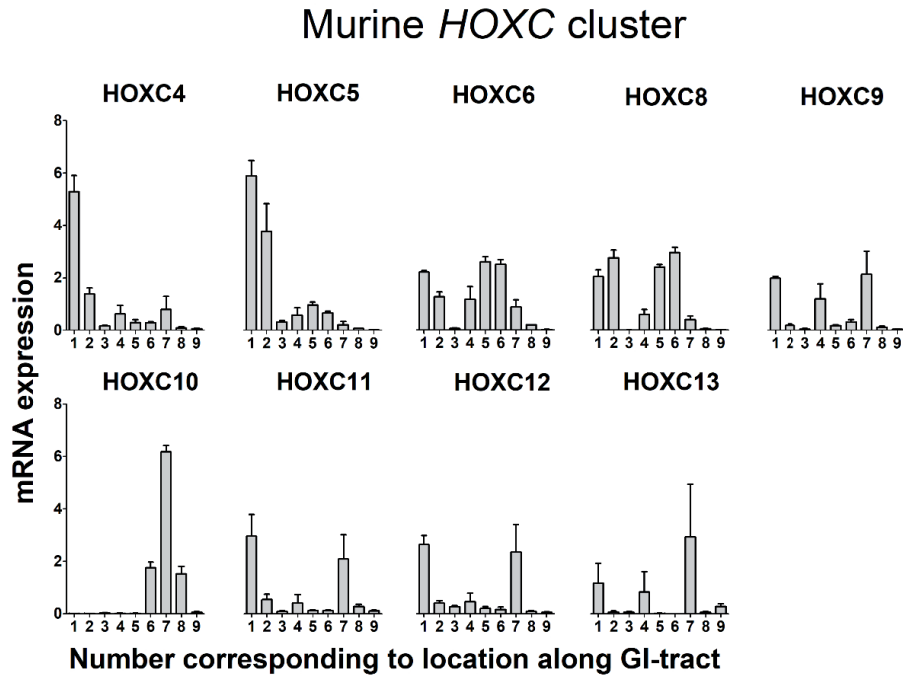
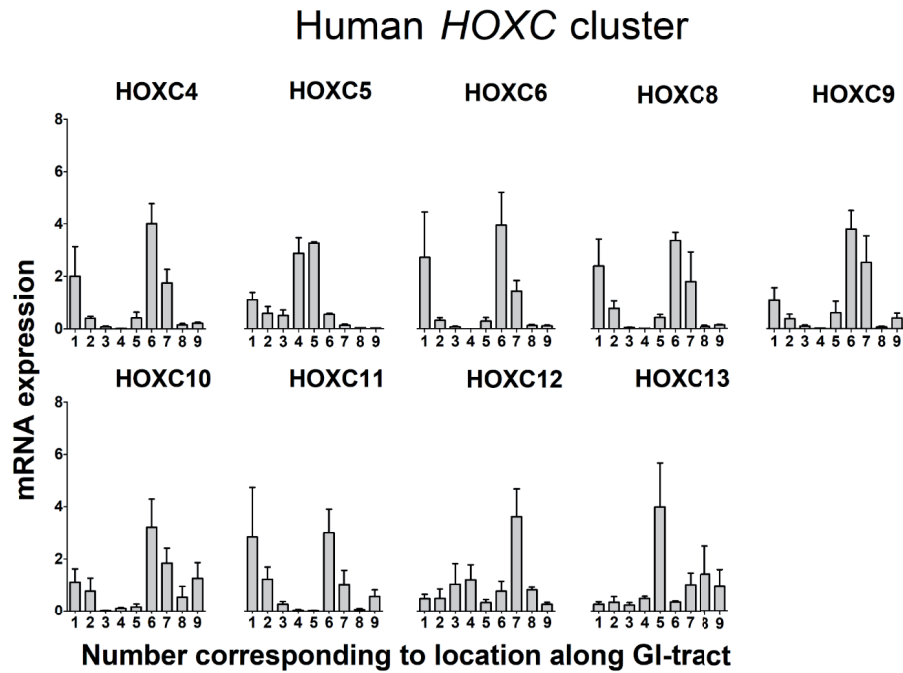
C



Supplementary Figure S2. *Continued.*

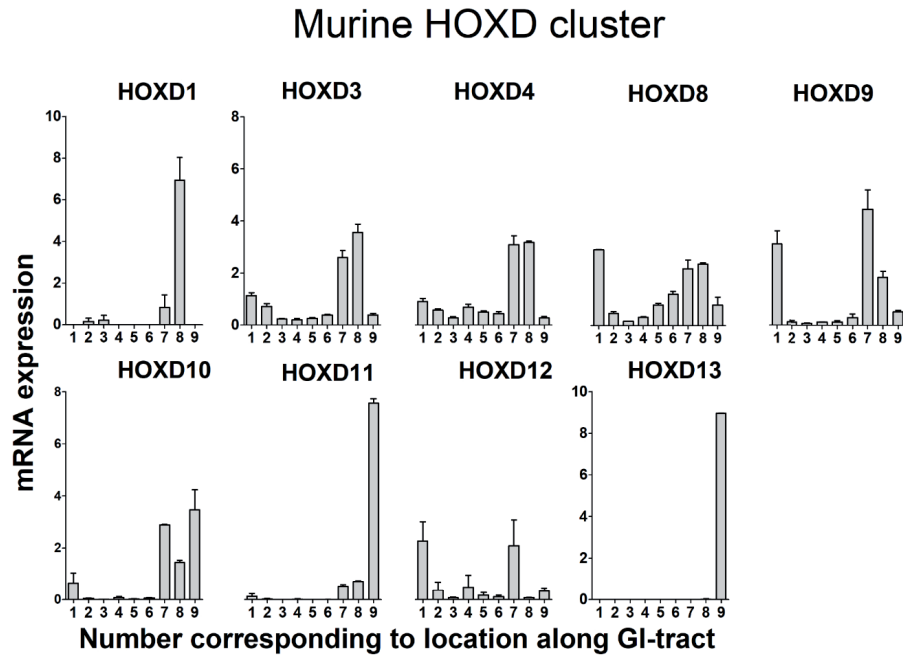
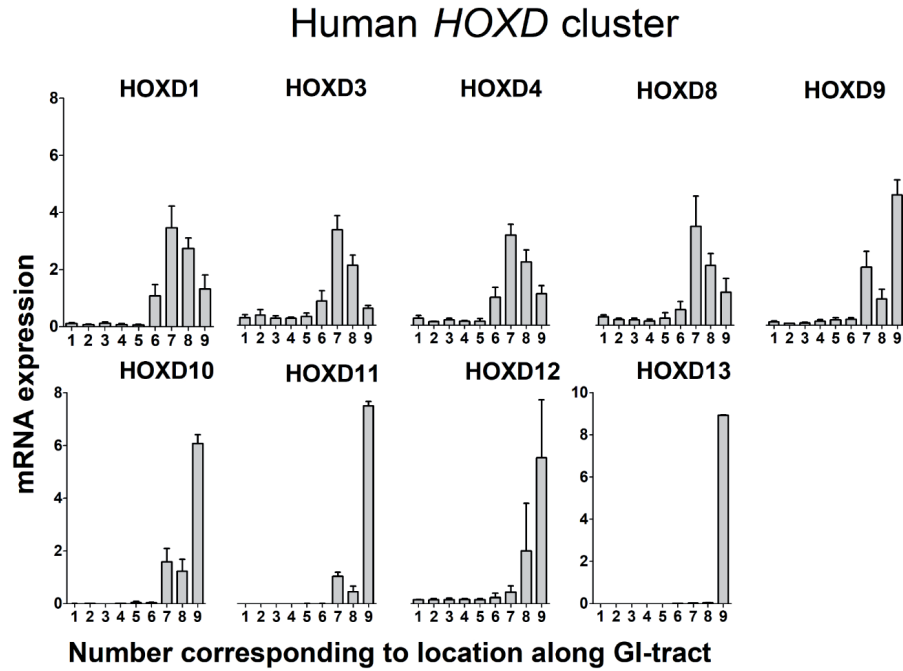


D

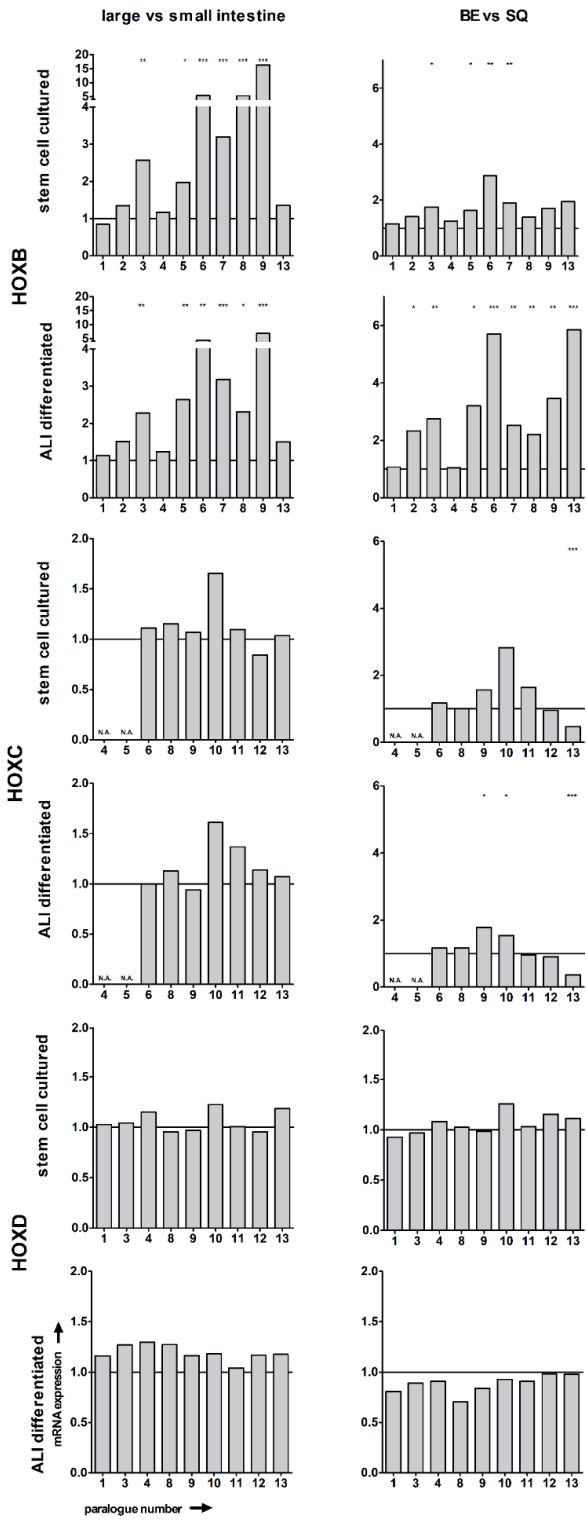


Supplementary Figure S2. *Continued.*

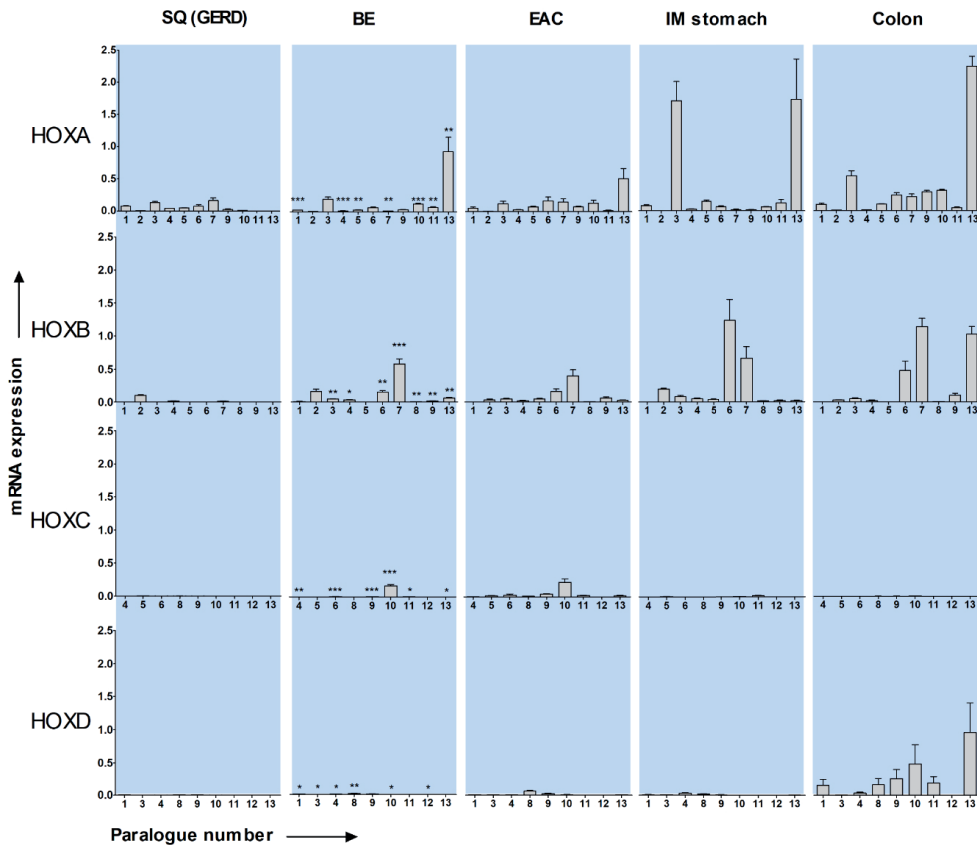
E



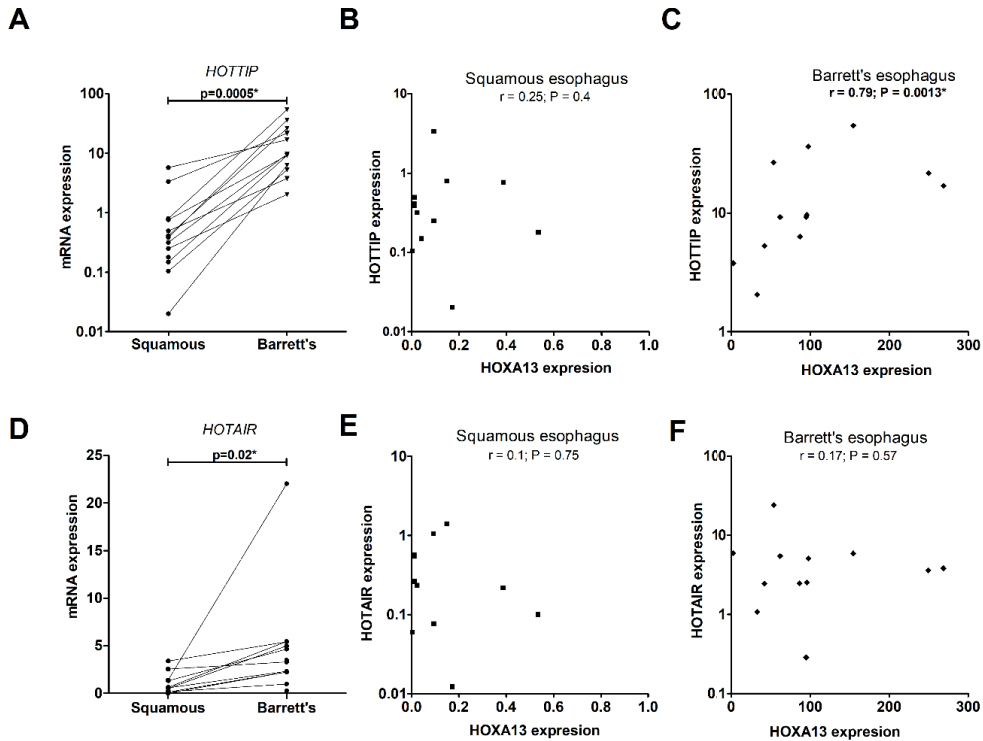
Supplementary Figure S2. *Continued.*



**Supplementary Figure S3.** *HOX* coding is established at the level of the stem cell. Public data of Wang et al. contains the mRNA expression of human stem cells isolated from the GI-tract and either cultured as stem cells or differentiated in an air-liquid interface (ALI). Right column: *HOXB*, *C*, and *D* cluster gene expression in the large (n=3 in technical duplicate) compared to the small intestine (n=3 in technical duplicate). Left panels: *HOXB*, *C*, and *D* cluster gene expression in Barret's esophagus (BE, n=12) vs squamous esophagus (n=2) in technical duplicates are depicted for stem cell cultures and n=1 each for ALI differentiated samples in technical duplicates. Normalization was performed by setting mRNA expression to 1 for the small intestine or squamous esophagus. *HOX* gene expression in stem cell and ALI cultures are similar, which is not seen in the dataset in general. *HOXB* cluster genes have a higher expression in the large versus the small intestine (left column). No clear regulation of the *HOXC* or *D* clusters is seen, with exception of an upregulation of *HOXC10* in the ascending colon. *HOXB* cluster genes are upregulated in BE stem cells vs squamous esophagus, including mid cluster and 5' *HOXB* genes. *HOXC10* is the most pronounced *HOXC* gene upregulated in BE stem cells. \* $p<0.05$ ; \*\* $p<0.01$ ; \*\*\* $p<0.001$ ; NA: not available.

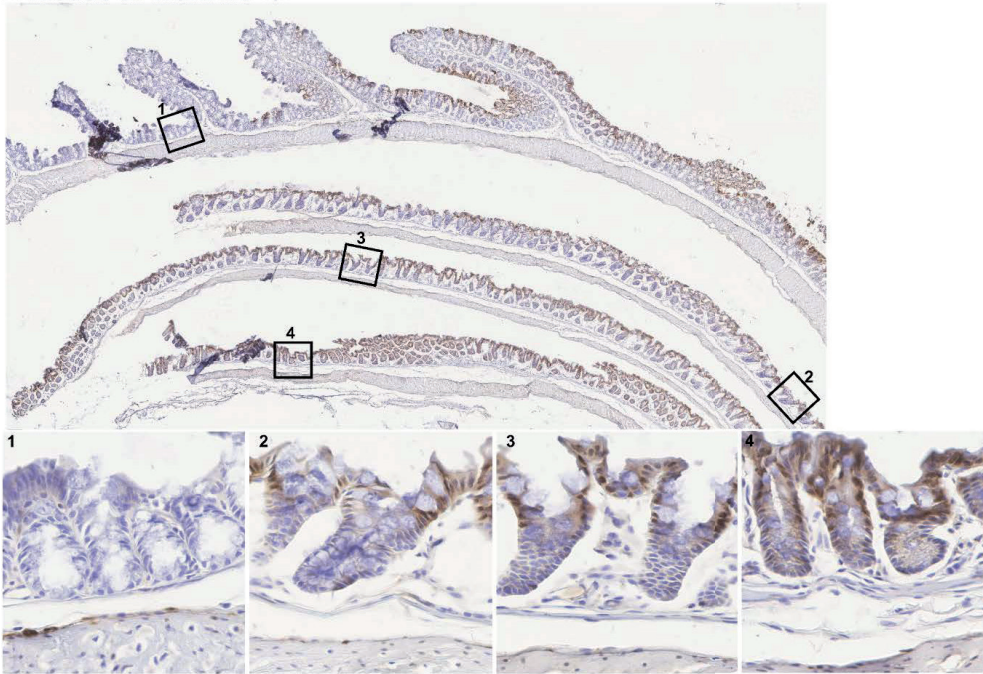


**Supplementary Figure S4.** *HOX* cluster gene expression in BE, esophageal adenocarcinoma and gastric IM, and colon. Comparison of the mRNA expression levels of the squamous esophagus from GERD patients (n=13), BE (n=13), EAC (n=9), IM of the stomach (n=12), and material from the colon (n=3). Expression in BE was compared to expression in the squamous esophagus of matched samples from the same patients (SQ (GERD)) by two sided Student's *t*-tests. \**p*<0.05; \*\**p*<0.01; \*\*\**p*<0.001. Y-axis values represent the fold change in mRNA expression in relation to the average mRNA expression of all *HOX* genes in all samples. Error bars represent the SEM.

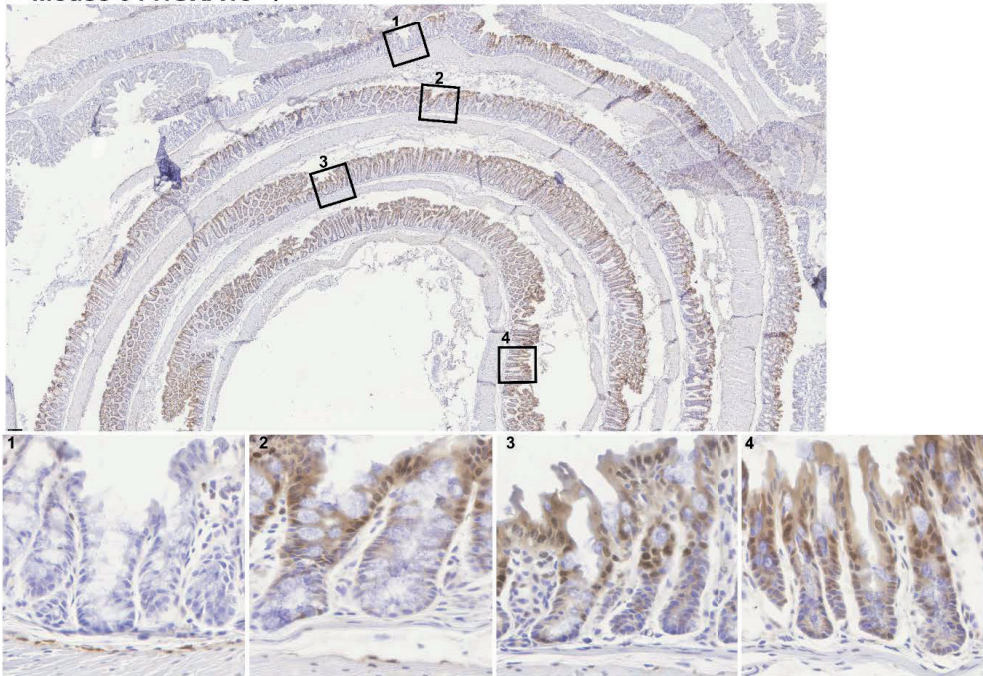


**Supplementary Figure S5.** Gene expression of lncRNA *HOTTIP* and lncRNA *HOTAIR*, in the normal squamous esophagus and BE tissue from BE patients. **(A)** *HOTTIP* expression, normalized to mean expression in the squamous esophagus, is overexpressed in BE as tested with a Wilcoxon signed rank test. Matched squamous esophageal and BE were taken from the same patient ( $n=13$ ). **(B, C)** Correlations between expression levels of *HOTTIP* and *HOTAIR* and *HOXA13* in squamous and BE tissues were tested with a non-parametric Spearman test. *HOTTIP* expression does not correlate with *HOXA13* in normal squamous esophagus **(B)**, but does correlate to *HOXA13* in BE tissue **(C)**. **(D)** *HOTAIR* is overexpressed in BE tissue (Wilcoxon signed rank test) and does not correlate with *HOXA13* expression **(E, F)**. \* $p<0.05$ ; \*\* $p<0.01$ ; \*\*\* $p<0.001$ . Error bars represent the SEM.

**A Mouse 02 HOXA13 +/-**



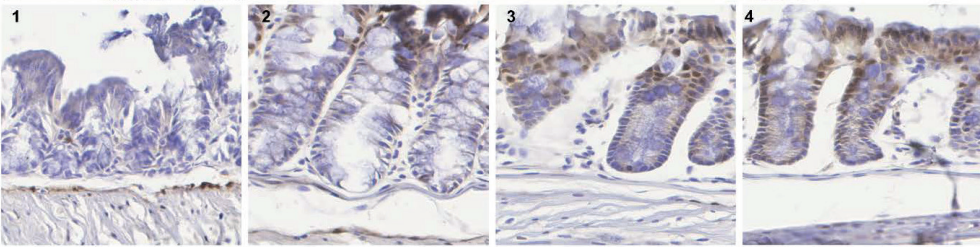
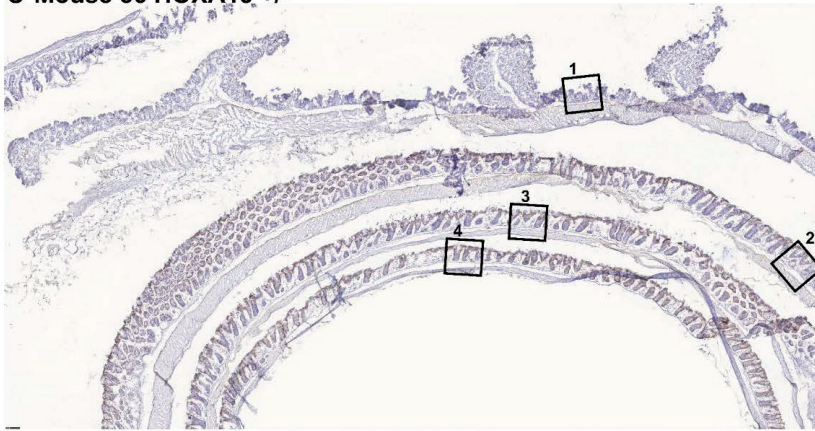
**B Mouse 04 HOXA13 +/-**



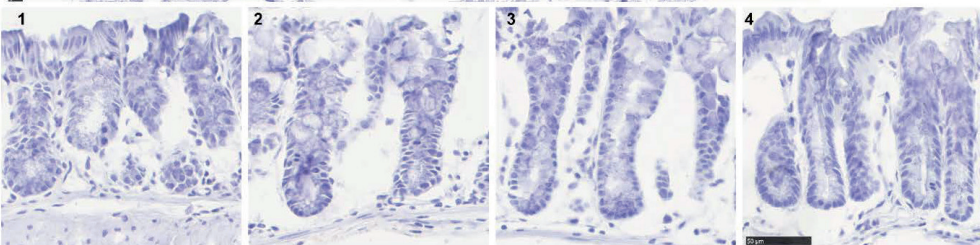
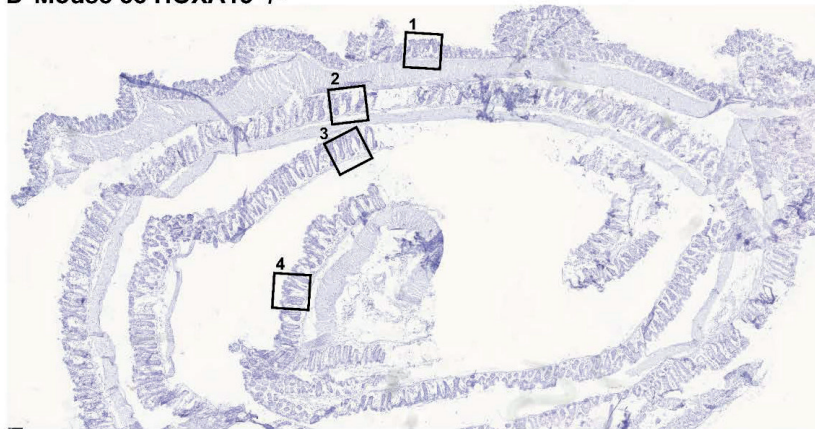
**Supplementary Figure S6.** Expression of Hoxa13 in murine GI tract. Anti-GFP IHC of Hoxa13-GFP mouse model was performed on swiss roles of bowels isolated from three Hoxa13<sup>+/-</sup> mice (A-C) and one Hoxa13<sup>-/-</sup> negative control mouse (D). Overall presentation of swill role and close ups of proximal (1) and distal (2-4) colon. (E) The distal Hoxa13 expression border is the anal SCJ (confocal images).



**C Mouse 56 HOXA13 +/-**

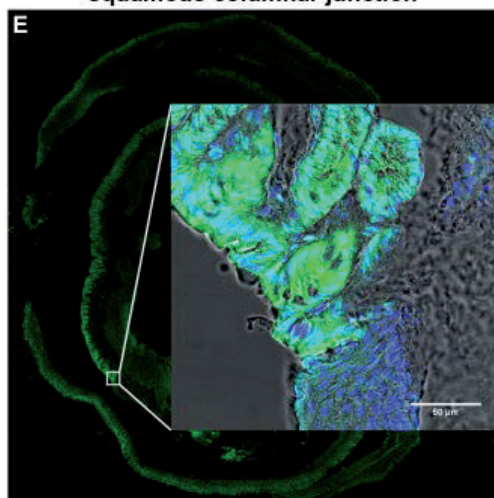


**D Mouse 55 HOXA13 -/-**



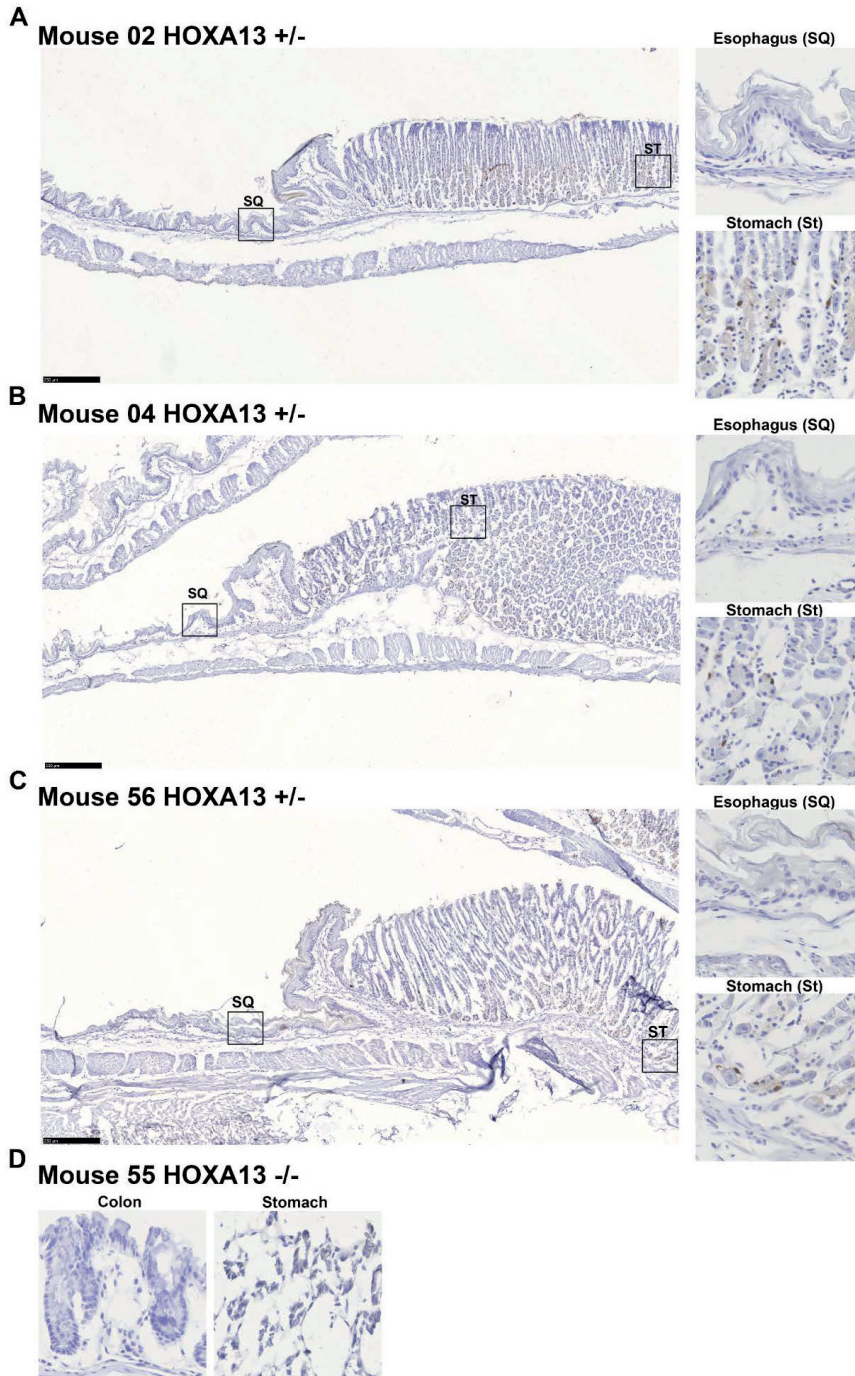
**Supplementary Figure S6. Continued.**

**Distal expression boundary at anal  
squamous columnar junction**



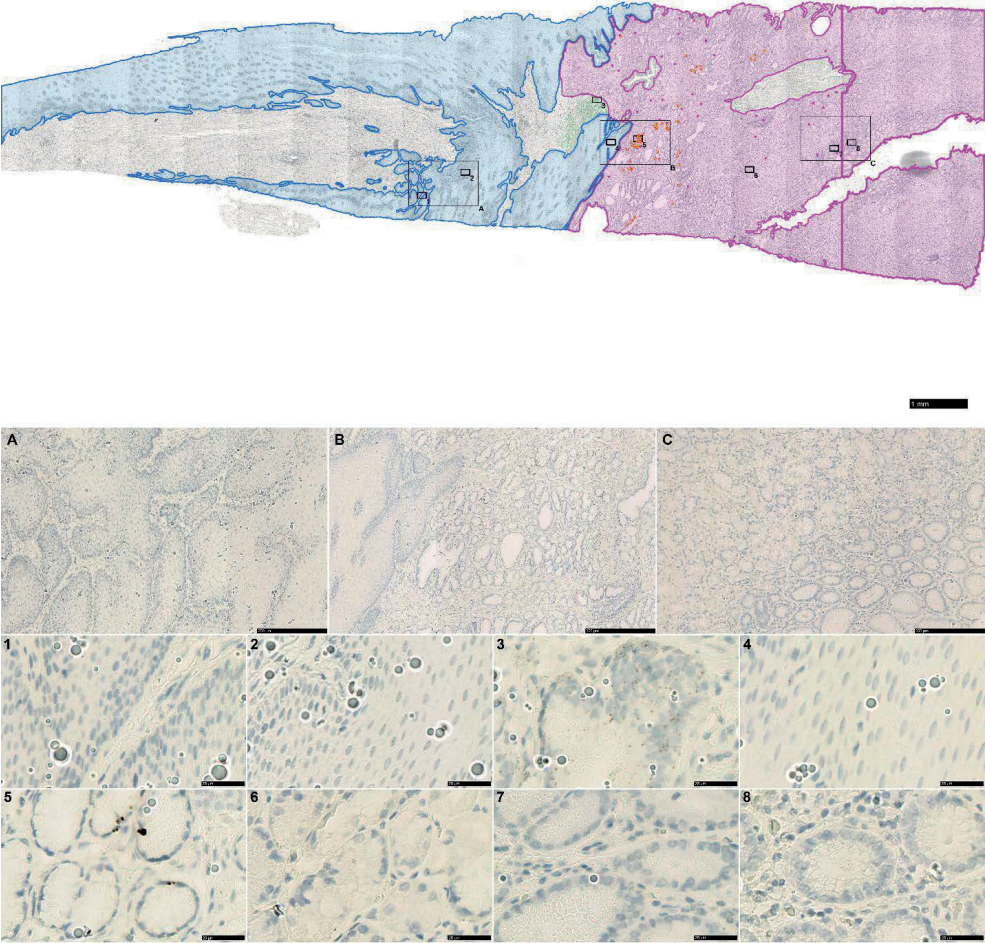
**Supplementary Figure S6.** *Continued.*





**Supplementary Figure S7.** Expression of Hoxa13 in murine upper GI tract. Anti-GFP IHC of Hoxa13-GFP mouse model was performed on upper gastrointestinal tract isolated from three *Hoxa13*<sup>+/-</sup> mice (A-C) and one *Hoxa13*<sup>-/-</sup> negative control mouse (D). Magnification of squamous esophagus and stomach indicated in the overview image are presented on the right.

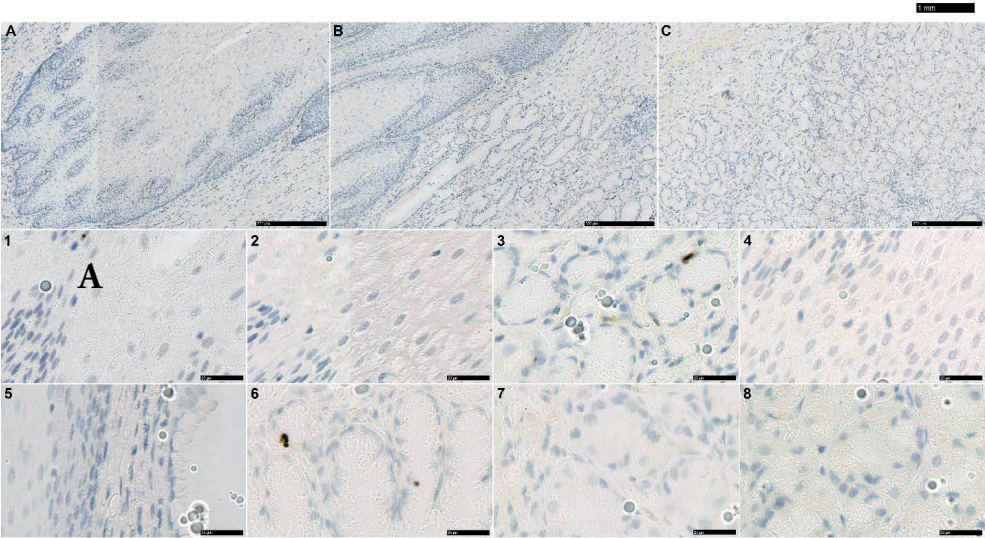
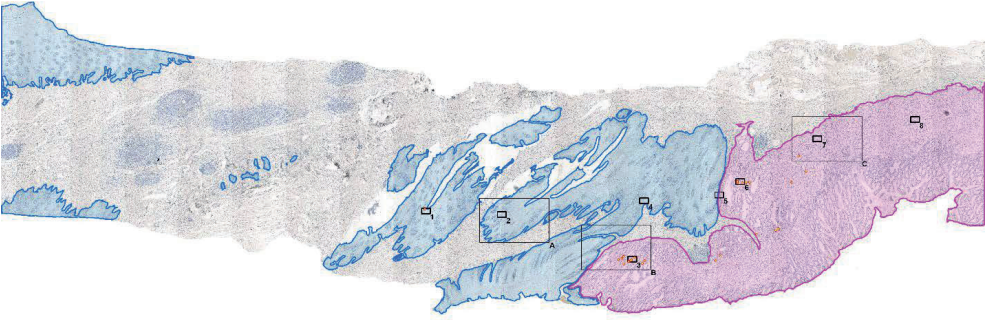
A



**Supplementary Figure S8.** (A, B) *HOXA13* expression as measured by RNA ISH in a representative example of an adult human GEJ with magnification panel of: A – esophagus, B – GEJ area, C – proximal stomach. (C, D) *HOXA13* expression as measured by RNA ISH in a representative example of a fetus human GEJ with magnification panel of: A – esophagus, B – GEJ area, C – proximal stomach.

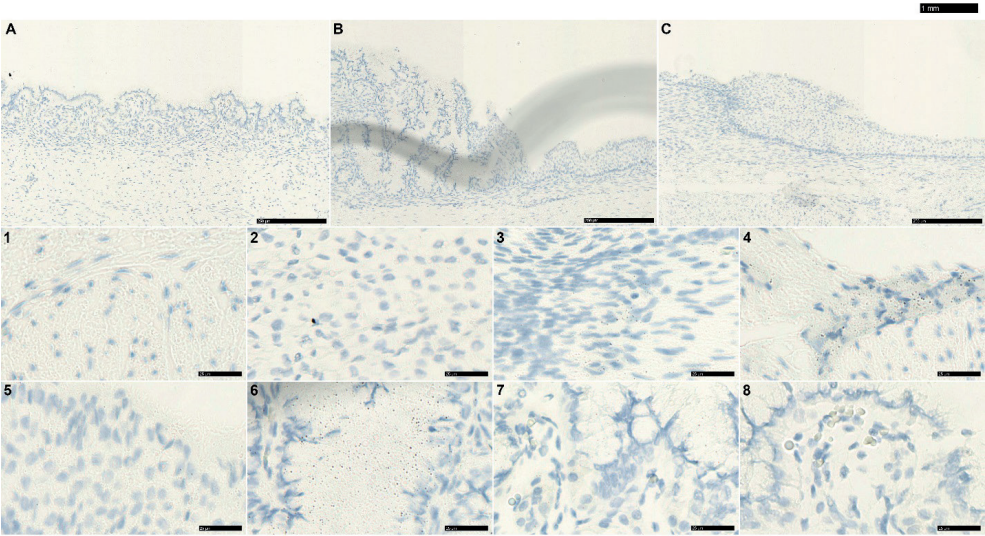
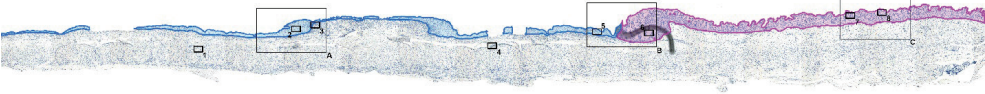


B



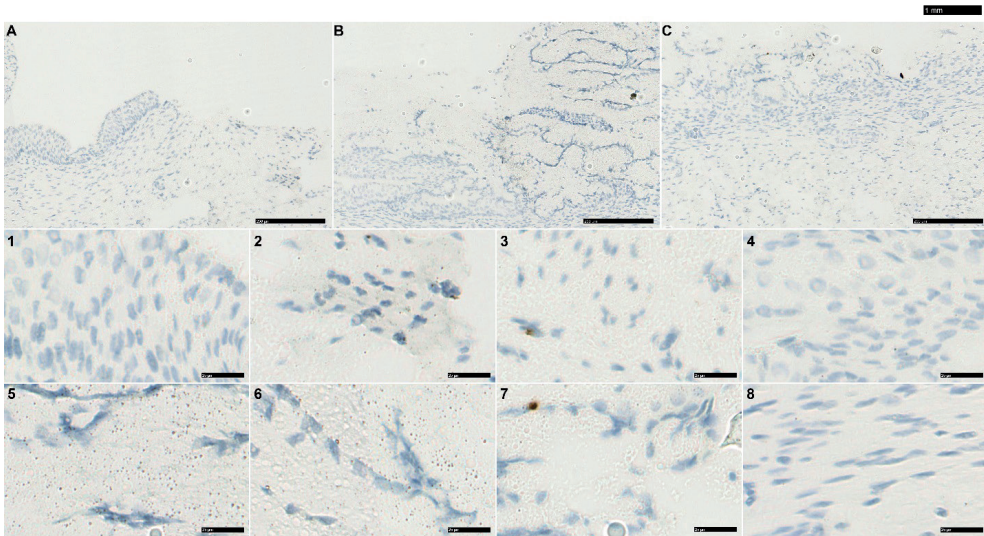
Supplementary Figure S8. *Continued.*

C



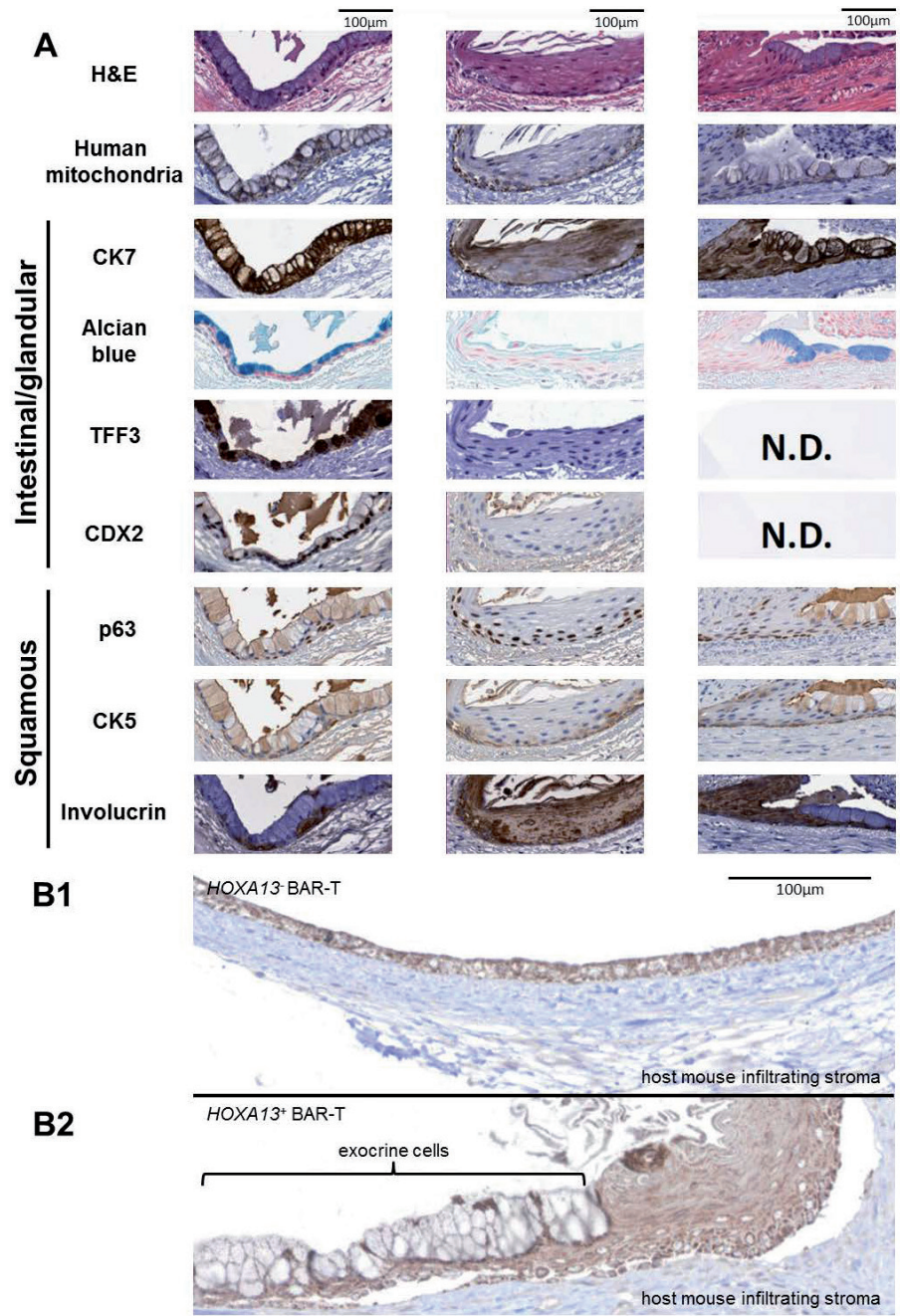
Supplementary Figure S8. *Continued.*

D

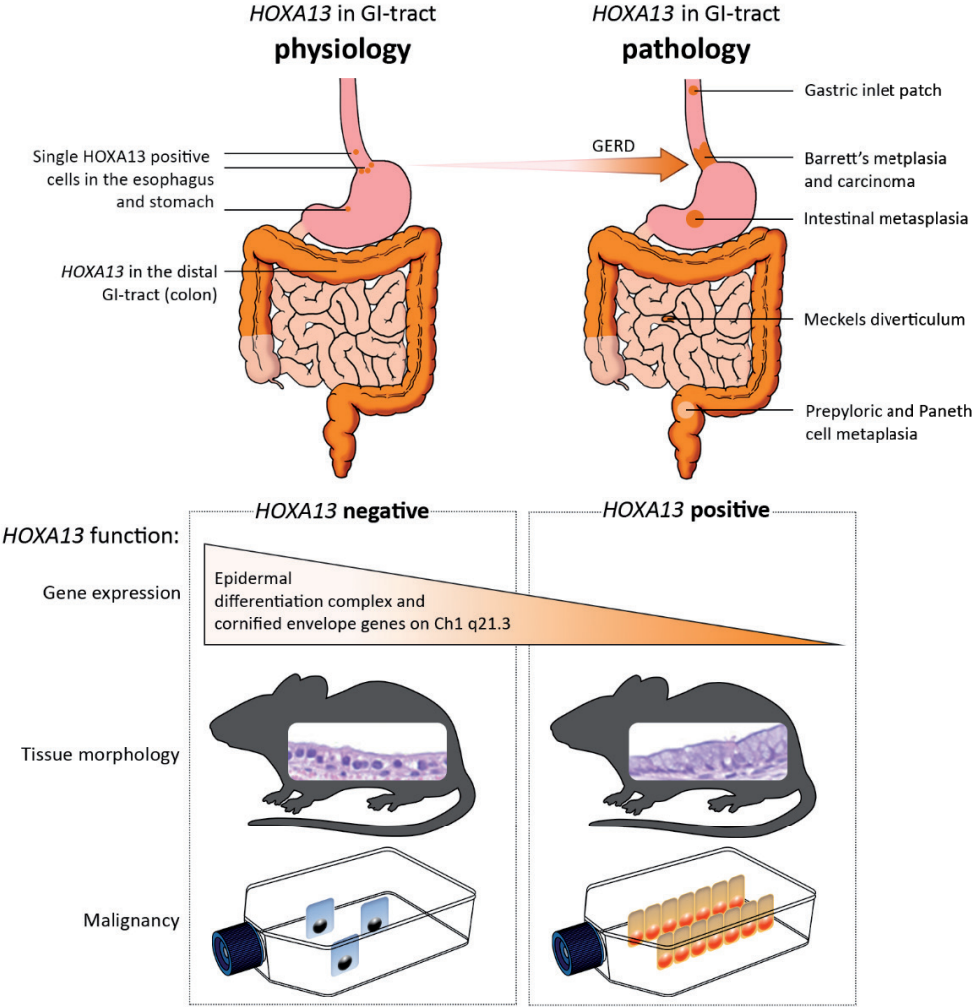


Supplementary Figure S8. *Continued.*





**Supplementary Figure S9.** Proof of the human origin of epithelium in the rat trachea *in vivo* tissue reconstitution model. **(A)** Staining of the *in vivo* tissue reconstitution model with intestinal/glandular and squamous markers shows that parental BAR-T cells form intestinal-type columnar epithelium (left), squamous epithelium (middle), and multi layered epithelium with mixed phenotype (right) from the same clone. Human origin of the epithelium was confirmed by staining for human mitochondria. **(B1)** *HOXA13* and **(B2)** *HOXA13*<sup>+</sup> representative examples of the BAR-T epithelium stained for human mitochondria.



Supplementary Figure S10. Summary figure.

**Supplementary Table S1.** Differentially regulated genes in definitive endoderm versus non-differentiated KH2 mESCs. Pluripotent mESC gene expression was compared to CXCR4<sup>+</sup>/E-cadherin<sup>+</sup> FACS selected definitive endoderm cell gene expression. Both samples did not express *HOXA13*. Common definitive endoderm or pluripotency markers are included.

	Fold change and <i>q</i> value of CXCR4 <sup>+</sup> /E-cadherin <sup>+</sup> vs non-differentiated mESCs cells		Reference
Definitive endoderm markers			
Sox17	12.55	0.00	[2-5]
Foxa1	4.30	0.00	[3, 5]
Gata4	6.86	0.00	[2]
Lgr5	5.39	0.00	[6]
Pax3	25.91	0.00	[3]
Bmp2	16.32	0.00	[4]
Tacstd2	17.55	0.00	[3]
Bmp4	4.73	0.00	[4]
Pluripotency markers			
Nanog	0.20	0.02	[4]
Tcl1	0.01	0.00	[7]
Dppa3	0.02	0.00	[8]



**Supplementary Table S2.** *HOXA13* induced differentially regulated genes in mouse definitive endoderm cells. Molecules associated with epithelial identity, the cytoskeleton (microvilli, keratins, and the tetraspan network), exocrine function, oncogenic molecules, and specific signaling pathways were included. All fold change and *q* values depicted pertain to the BAR-T dataset. Information in the “known function” and “Detailed description” columns was obtained through non-systematic review and should not be considered as an exhaustive overview of the literature. In the first column, molecules of which the direction of regulation by *HOXA13* is in line with their relative expression in the distal compared to the proximal GI-tract are indicated with an \*, the reverse with a †. If no clear relationship was present no symbol was added to the gene name.

Gene (colon expression relatively high *, low †	Fold Change and <i>q</i> value of <i>HOXA13</i> +/- CXCR4 <sup>+</sup> /E- cadherin <sup>+</sup> DE	Detailed description
Epithelial identity: EMT was downregulated ( <i>p</i> value 6.69E-6, z-score -3.184), i.e. the <i>HOXA13</i> overexpressing definitive endoderm cells have a more epithelial identity.		
Cdh1	1.99 0.10	E (epithelial)-cadherin, links the actin cytoskeleton to cell-cell adhesions, inactivation was found to be associated with EMT, leading to diffuse gastric cancer and lobular breast carcinomas [9].
Cdh2*	0.46 0.03	N (neuronal)-cadherin, was found to create cell-adhesion zippers [10].
Vim*	0.43 0.10	Vimentin, from the intermediate filaments type III gene family, was found to be a protein binding to actin associated with the actin core bundle of the brush border [11].
Bmp7†	3.49 0.00	Was found to decrease EMT in mouse kidney tubule cells [12].
Jag1	0.38 0.00	Jagged 1, is a ligand of the NOTCH pathway, this pathway was found to be associated with malignant transformation [13-15].
Mgat5*	4.31 0.00	Mannosyl (alpha-1,6-)-glycoprotein beta-1,6-N-acetylglucosaminyltransferase, was found to enhance EMT in mouse keratinocytes [16].
Prrx2*	0.40 0.03	Paired mesoderm homeobox protein 2, was found to promote EMT in breast cancer [17].
Scube3	0.31 0.00	Signal peptide, CUB domain and EGF like domain containing 3, was found to regulate EMT in lung cancer [18].
“Formation of epidermis” ( <i>p</i> value 3.68E-12, z-score 0.908) was upregulated, in line with the more epithelial character of <i>HOXA13</i> <sup>+</sup> cells.		
Pkp3	21.18 0.00	Plakophilin was found to be a desmosomal component [19]. Was found to mediate desmosome assembly and adherens junction maturation [20].
Dsc2	2.29 0.01	Desmocollin 2, desmosome component [21].
Emp1†	1.97 0.00	Epithelial membrane protein 1, was found to be associated with oncogenesis [22].
Ppl†	2.88 0.00	Periplakin, was found to be localized with ANXA9 in the epidermis [23].

Supplementary Table S2. *Continued.*

Gene (colon expression relatively high *, low †	Fold Change and <i>q</i> value of <i>HOXA13</i> +/- <i>CXCR4</i> +/E- cadherin+ DE	Detailed description
Evpl†	2.44 0.01	Envoplakin, cornified envelope gene, was found to be downregulated in ESCC [24].
An upregulation of “actin cytoskeleton signaling” ( <i>p</i> value 3.74E-2, <i>z</i> -score 3.000) was the most pronounced <i>z</i> -score in the pathway analysis of IPA, and directly related to its morphological phenotype [25]. In line with this is the activation of “ <b>integrin signaling</b> ” ( <i>p</i> value 1.34E-2, <i>z</i> -score 1.732).		
Microvilli:		
Clc5*	3.51 0.00	Chloride intracellular channel 5, was found to form a complex with EZR and PODXL (FC1.61, <i>q</i> =0.16). Was found to be associated with increased migration and invasion in a hepatocellular carcinoma (HCC) cell line together with CLIC5 [26].
Ezr*	2.20 0.00	Ezrin, cytovillin, or villin-2, a cytoplasmic membrane protein and protein-tyrosine kinase substrate in microvilli. It was found to be an intermediate between actin cytoskeleton and plasma membrane. Was found to maintain cell surface structure important for adhesion and migration [27]. In ESCC it was found to be associated with reduced survival [28-30].
Pls3	2.55 0.00	Plastin 3, was found to be a microvillus component [31]. Overexpression increases length and density of microvilli. Abundant Pls3 is associated with cisplatin and UV radiation resistance [32, 33].
Vav3*	2.53 0.03	Vav guanine nucleotide exchange factor 3 is associated with actin cytoskeletal rearrangements. Vav3 was found to be overexpressed in BE and EAC [34].
Vill*	2.58 0.048	Villin like, was found to be associated with and modifies actin filaments in microvilli [35].
“RhoA signaling” was activated ( <i>p</i> value 1.12E-2, <i>z</i> -score 2.12), although RhoA itself was not differentially regulated. Villi in RhoA KO mice are noticeably shorter and intestinal epithelial architecture was disorganized compared to that of WT mice [36].		
Atp8b1*	2.55 0.00	ATPase phospholipid transporting 8B1, was found to be expressed in differentiated enterocytes and where it was required for apical protein expression and microvillus formation [37, 38].
Eps8*	1.84 0.046	Epidermal growth factor receptor pathway substrate 8, was found to be required for intestinal cell apical morphology [39]. KO mice have a 25% reduction in intestinal microvilli length [40]. <i>Eps8L1</i> (FC2.98, <i>q</i> =0.02).
Myo5b*	2.18 0.03	Myosin5B mutations cause microvillus inclusion disease, and disrupt epithelial cell polarity. It is essential for microvillus function [41].
Keratins:		
Krt15†	2.50 0.054	Keratin 15, was found to be expressed in the esophagus and glandular prostate cells. Long-lived keratin 15+ esophageal progenitor cells were found to contribute to homeostasis and regeneration [42].

Supplementary Table S2. *Continued.*

Gene (colon expression relatively high *, low †	Fold Change and <i>q</i> value of <i>HOXA13</i> +/- CXCR4+/E- cadherin+ DE		Detailed description
KRT19*	2.34	0.00	Keratin 19, is a columnar keratin [14].
KRT20*	2.84	0.01	Keratin 20, is a more distal GI tract marker [43].
Krt81	4.01	0.00	Keratin 81, is a hair keratin. It was found to be expressed in normal and breast cancer cells and contributes to their invasiveness [44]. In PDAC patients receiving chemotherapy it was associated with a dismal prognosis [45]. It is associated with a malignant phenotype in hepatoblastoma patients [46].
Tetraspan network: by connecting several molecules, the tetraspan network may organize the positioning of cell surface proteins and play a role in signal transduction, cell adhesion, and motility [47].			
Cd9	2.03	0.04	Motility related protein-1 clustering was found to be accompanied by the formation of microvilli that protrude from either side of adjacent cell surfaces, thus forming structures like micro-villi zippers [48].
Cd82†	4.12	0.00	CD82 was found to be associated with favorable outcomes in cancer patients [49].
Igsf8	4.67	0.00	Immunoglobulin superfamily, member 8 links the tetraspanin web to the actin cytoskeleton through their direct association with ezrin-radixin-moesin proteins [50].
Exocrine function: molecules from the list “development of exocrine gland” ( <i>p</i> value 8.50E-7, z-score 0.914) in IPA:			
Dkk1*	0.36	0.03	Dickkopf WNT signaling pathway inhibitor 1, was found to decrease differentiation of mucous secretory cells in the mouse small intestine [51].
ErbB3	2.89	0.00	Human epidermal growth factor receptor 3 was found to limit the number of Paneth cells [52]. Paneth cell metaplasia in the distal colon occurs exclusively in mucosa affected by inflammatory bowel disease, even in the inactive phase [53]. This is in line with our observation that Paneth cell metaplasia in the colon is characterized by a decrease in <i>HOXA13</i> expression (see main text). As a decrease in <i>ErbB3</i> signaling which subsequently does not limit the number of Paneth cells could lead to an increased Paneth cell number. Physiological Paneth cell distribution is inverse to <i>HOXA13</i> expression, also in line with the observation in Paneth cell metaplasia.
Fgfr2	2.81	0.00	Fibroblast growth factor receptor 2, inhibition of Fgfr2b in rat in organ culture decreases development of pancreas exocrine cells [54].
Gcnt3*	3.51	0.00	Glucosaminyl (N-acetyl) transferase 3, mucin type, was found heavily expressed in colon, small intestine, trachea, and stomach, where mucin is produced [55].

**Supplementary Table S2.** *Continued.*

Gene (colon expression relatively high *, low †	Fold Change and <i>q</i> value of <i>HOXA13</i> +/- <i>CXCR4</i> +/E- cadherin+ DE	Detailed description
Ncoa2	1.92 0.00	Steroid receptor coactivator 2 was found critical for progesterone-dependent uterine function and mammary morphogenesis in the mouse [56].
Shh signaling:		
Ptch1*	2.26 0.02	Patched 1, its levels correlate with Hedgehog pathway activity [57]. It was found increased in BE, and may contribute to its etiology [58].
Smo	0.62 0.04	Smoothened, frizzled class receptor, was found to decrease SMO expression correlates with less Hedgehog pathway activity. Hedgehog pathway activity serves to induce the proximal tractus, especially the esophagus [59].
Wnt signaling:		
Dkk1	0.36 0.03	Dickkopf WNT signaling pathway inhibitor 1, see above.
Fzd7	2.10 0.03	Frizzled class receptor 7, deletion in mouse adult intestinal epithelium was found to lead to stem cell loss <i>in vivo</i> and organoid death <i>in vitro</i> [60].
Wnt2b	0.23 0.00	Wnt family member 2b.
Wnt3*	0.47 0.053	Wnt family member 3 was found to be necessary and sufficient to induce Paneth cell formation [61]. <i>Wnt3</i> is produced specifically by Paneth cells [62].
Wnt5a*	0.37 0.03	Wnt family member 5a, overexpression from 10.5 dpc until 18.5 dpc was found to result in drastic shortening of the small intestine, colon, cecum and stomach [63]. It inhibits proliferation of intestinal epithelial stem cells [64]. It up-regulates the expression of the tumor suppressor 15-PGDH and induces differentiation of colon cancer cells [65].
Wnt10a	3.21 0.00	Wnt family member 10A was found to promote an invasive and self-renewing phenotype in ESCC [66].
Sox signaling:		
Sox9*	2.55 0.00	SRY-box 9, was found to be correlated with ERBB3 in pancreatic ductal AC [67]. Sox9 induces Paneth cells which is not in line with the function of Erbb3 and Wnt3 [68]. SOX9 is essential in the development of embryonic CLE, but is switched off in post-natal life, and is re-expressed again in BE [69-72]. Sox9 was found to drive columnar differentiation of SQ [73].
Sox11*	0.60 0.00	SRY-box 11, knock out was found to cause hypoplasia of the lung, stomach, and pancreas [74].
Sox13	3.03 0.00	SRY-box 13, expressed in pancreas and liver, an autoantigen in primary biliary cirrhosis, Sox13 was found to inhibit canonical Wnt signaling in T cells [75].

Supplementary Table S2. *Continued.*

Gene (colon expression relatively high *, low †	Fold Change and <i>q</i> value of <i>HOXA13</i> +/- CXCR4*/E- cadherin* DE		Detailed description
Glypicans:			
Gpc1	2.41	0.00	Glypican 1, can be a biomarker for relapse of stage III CRC and may be involved in EMT activation, invasion, and migration of CRC [76]. It was found to be a marker of pancreatic cancer and <i>ex vivo</i> it appears to have an oncogenic role [77]. GPC1 is an independent prognostic factor in ESCC [78].
Gpc2	0.51	0.049	Glypican 2, a neuroblastoma oncoprotein and candidate immunotherapeutic target [79].
Gpc3	0.23	0.00	Glypican 3, is a fetal gut marker [80].
Gpc6	0.24	0.00	Glypican 6, was found to be hypermethylated in cancer and mRNA is down-regulated [81].
Interleukin:			
Il1rn	5.15	0.00	Interleukin 1 receptor antagonist, was found to be downregulated in BE and EAC [82] typical SQ marker, downregulated in ESCC [83].
Il5ra	3.06	0.00	Interleukin 5 receptor subunit $\alpha$ , heterozygous mutants were more frequent in atopic dermatitis of Koreans [84], which implicates il5ra in epithelial homeostasis.
Il22ra1	3.10	0.01	Interleukin 22 receptor subunit $\alpha$ 1, was found to mediate fucosylation promotes intestinal colonization resistance to <i>E. faecalis</i> [85]. It was found to have a higher expression in the colon compared to the cecum in line with the expression of HOXA13 in the colon with exception of the cecum [86].
Apoptosis/necrosis:			
Casp8*	2.30	0.00	Caspase 8, high Caspase-8 was found to be a negative markers of OS [87].
Cxcl1*	3.15	0.00	CXC motif chemokine ligand 1, was found important for mucosal barrier [88].
Ripk3	2.19	0.04	Receptor interacting serine/threonine kinase 3, a substrate of caspase 8 [89, 90]. The RIPK1-RIPK3 necrosome was found to promote pancreatic oncogenesis through upregulation of the chemokine CXCL1 (See below) [91]. Loss of RIPK3 appears to promote tumors in the colon [92].
BE/metaplasia specific, oncogenic molecules:			
Anxa1†	1.69	0.00	Annexin A1, was found to promote the proliferation of ESCC cells [93]. High expression is frequent in EAC and GEJ AC, correlates with more advanced pathologic T stage and the presence of distant metastasis, and is an independent prognostic factor for patient survival [94].

**Supplementary Table S2.** *Continued.*

Gene (colon expression relatively high *, low †	Fold Change and <i>q</i> value of <i>HOXA13</i> +/- <i>CXCR4</i> +/E- cadherin+ DE		Detailed description
Artn	2.21	0.04	Artemin, is hypoxia responsive and was found to promote oncogenicity and increased tumor initiating capacity in HCC [95].
Fgfr2	2.81	0.00	Fibroblast growth factor receptor 2, has been found to be highly expressed early in progression from BE to EAC [96].
Fgf13	2.37	0.02	Fibroblast growth factor 13, tumor suppression by TP53 was found to be involved in inhibiting <i>FGF13</i> [97].
Sparc	0.41	0.00	Secreted protein acidic and cysteine rich, expression correlates with matrix metalloproteinase 2 ( <i>MMP2</i> ; FC=0.25, <i>q</i> =0.00) expression in esophageal tumors, and high SPARC expression was found to be correlated significantly with lymph node metastasis and poor patient prognosis [98].
Oncogenic molecules:			
Atp2c2*	7.38	0.00	ATPase secretory pathway Ca <sup>2+</sup> transporting 2, the Orai1-Atp2c2 complex was found to be associated with constitutive store-independent Ca <sup>2+</sup> signaling which promotes tumorigenesis [99].
Cd55	4.79	0.00	Decay accelerating factor, was found to prohibit formation of the membrane attack complex indirectly [100].
Ezr*	2.20	0.00	Ezrin, was found to be associated with reduced survival in ESCC [28-30].
Nek2*	2.35	0.01	NIMA related kinase 2, was found to be overexpressed in a wide variety of human cancers implicating in various aspects of malignant transformation, including tumorigenesis, drug resistance and tumor progression. NEK2 inhibitors are being developed [101].
Nkd1*	0.22	0.00	Naked cuticle homolog 1, downregulation was found to promote HCC progression and promotes gastric cancer migration and invasion [102, 103]. <i>NKD1</i> expression is reduced in HCC and is associated with a poor prognosis [104].
Pim1*	2.61	0.00	Pim-1 proto-oncogene, serine/threonine kinase, was found to regulate glycolysis and promotes tumor progression in HCC [105]. Pim1 is a pro-survival kinases that is commonly amplified in cancer [106].
Slc2a1	2.01	0.01	Solute carrier family 2 member 1, was found to be a marker of HGD, EAC and gastric cancer [107, 108]. <i>Slc2a1</i> expression in CRC is independently associated with poor prognosis [109].
Spink6	15.13	0.00	Serine peptidase inhibitor, Kazal type 6, in nasopharyngeal carcinoma was found to promote metastasis [110].

**Supplementary Table S3.** *HOXA13*-induced differentially regulated genes in the BAR-T dataset. Multiple testing corrected significantly differentially regulated genes in the same direction in both the BAR-T and EPC2-hTERT dataset (n=28); molecules which have been associated with morphological characteristics in literature; molecules, not described in the main text, which are associated in literature with oncogenic characteristics are described in more detail. All FC and *q* values shown pertain to the BAR-T dataset. Information in the “known function” and “Detailed description” columns was obtained through non-systematic review and should not be considered as an exhaustive overview of the literature.

Gene	Fold Change and <i>q</i> of <i>HOXA13</i> <sup>+</sup> vs <i>HOXA13</i> <sup>-</sup> BAR-T cells		Known function	Detailed description
All multiple testing corrected, significantly regulated genes, in the same direction in both the BAR-T and EPC2-hTERT datasets.				
IL7R	3.07	0.00	immunity	Interleukin 7 receptor, blockade of the IL-7/IL-7R signaling pathway was found to render T cell-deficient mice more sensitive to chemically-induced intestinal epithelial cell damage and subsequent colitis [111].
FAM196B	2.32	0.02	cancer	Family with sequence similarity 196 member B, was found to promote proliferation of gastric cancer cells through the AKT signaling pathway [112].
ADAMTS6	2.13	0.03	cancer	ADAM metalloproteinase with thrombospondin type 1 motif 6, is upregulated in breast cancer where it was found to suppress tumor progression via the ERK signaling pathway [113, 114].
NRG1	2.07	0.02	cancer	Neuregulin 1, ligand of ERBB3, paracrine NRG1/ERBB3 signaling was found to promote CRC cell progression, and high NRG1 expression is associated with poor prognosis in CRC [115].
LTBP1	1.94	0.02	cancer	Latent transforming growth factor $\beta$ binding protein 1, its expression increases with glioma progression [116].
JAG1	1.85	0.04	morphology	Jagged 1, is a ligand of the NOTCH pathway, this pathway was found to be associated with malignant transformation [13-15].
ELL2	1.82	0.02	cancer	Elongation factor for RNA polymerase 2, was found to be part of the super elongation complex and in combination with <i>HOXA9</i> and <i>10</i> associated with leukemia. ELL2 regulates DNA non-homologous end joining repair in prostate cancer cells [117].
SMAD7	1.80	0.05	cancer/ immunity	SMAD family member 7, is a TGF $\beta$ type 1 receptor antagonist. It was found to block TGF $\beta$ 1 and activating from binding to the receptor, which prevents access to SMAD2 [118].
C12orf75	1.78	0.03	cancer	Chromosome 12 open reading frame 75, is overexpressed in CRC, and upregulates the Wnt pathway [119].

**Supplementary Table S3.** *Continued.*

Gene	Fold Change and <i>q</i> of <i>HOXA13</i> vs <i>HOXA13</i> BAR-T cells		Known function	Detailed description
AXL	1.70	0.04	immune regulation, cancer	AXL receptor tyrosine kinase, was found to be a negative predictor of survival in EAC and ESCC [120]. AXL also contributes to a reduction in inflammation (Dransfield and Farnworth, 2016).
TIPARP	1.57	0.00	cancer	TCDD inducible poly(ADP-ribose) polymerase, was found to be overexpressed in meningioma and its locus was associated with ovarian cancer in a GWAS [121, 122].
IKBIP	1.56	0.02	cancer	Inhibitor of nuclear factor kappa-B kinase-interacting protein, was found to be a TP53 target gene with pro-apoptotic function [123].
DUSP7	1.52	0.04	cancer	Dual specificity phosphatase 7, was found to be overexpressed in myeloid leukemia and other malignancies [124].
GOLIM4	1.47	0.04	morphology	Golgi integral membrane protein 4, was found to be essential for podocyte cytoskeleton [125]. It mediates endosome exit [126].
FUCA1	0.69	0.02	cancer	$\alpha$ -L-fucosidase 1, loss-of-function mutations are found in several cancers, its expression is reduced in CRC, and low expression is associated with poorer prognosis in several cancers [127]. Has high expression in the distal vs the proximal GI-tract [128].
MAP3K5	0.63	0.04	immune regulation, cancer	Mitogen-activated protein kinase kinase kinase 5, also called apoptosis signal-regulating kinase 1. Knockdown of <i>MAP3K5</i> blocked dextran sulfate sodium induced tight junction disruption and subsequent barrier dysfunction [129].
EXPH5	0.56	0.04	morphology	Exophilin 5, mutations result in a skin fragility phenotype [130].
C6orf132	0.56	0.03	unknown	Chromosome 6 open reading frame 132.
HCAR2	0.50	0.05	cancer/ immunity	Hydroxycarboxylic acid receptor 2, is a G-protein-coupled receptor for the bacterial fermentation product butyrate and was found to function as a tumor suppressor in colon [131, 132].
RAB27B	0.50	0.03	cancer	RAB27B, member RAS oncogene family, decreased expression was found to correlate with metastasis and poor prognosis in CRC [133]. However, it prevented cancer invasion and proliferation in pancreatic ductal AC cells [134].



Supplementary Table S3. Continued.

Gene	Fold Change and <i>q</i> of <i>HOXA13</i> vs <i>HOXA13</i> BAR-T cells		Known function	Detailed description
TNFAIP2	0.49	0.03	cancer	TNF $\alpha$ induced protein 2, downregulation was found to suppress proliferation and metastasis in ESCC through activation of the Wnt/ $\beta$ -catenin signaling pathway [135].
MATN2	0.49	0.04	cancer	Matrilin 2, was identified as a tumor suppressor in HCC [136].
TTC9	0.48	0.02	cancer	Tetratricopeptide repeat domain 9, up-regulation is coupled with progesterone-mediated growth inhibition and induction of focal adhesion [137].
TMPRSS4	0.48	0.02	cancer	Transmembrane serine protease 4, overexpression appears a poor prognostic factor for solid tumors [138].
ANXA9	0.48	0.04	morphology	Annexin A9, and periplakin ( <i>PPL</i> ; FC0.57, $q=0.21$ , $p=0.01$ ) co-localize in the epidermis, <i>ANXA9</i> was found upregulated in differentiating keratinocytes [23].
KLK7	0.42	0.01	morphology	Kallikrein related peptidase 7, also called stratum corneum chymotryptic enzyme is a proteinase generally present in the stratum corneum [139].
MYO5C	0.42	0.01	morphology	Myosin VC, is involved in actin mediated membrane trafficking. <i>Myo5c</i> appears to mediate apical exocytosis of secretory vesicles [140, 141].
SERPINB13	0.38	0.00	cancer	Serpin family B member 13, was found downregulated in many types of cancer, its expression in head and neck SCC associates with poor clinical outcome (de Koning et al., 2009; Shiiba et al., 2010).
Morphology associated genes from the BAR-T dataset.				
MCAM	3.47	0.00	morphology	Melanoma cell adhesion molecule, it mediates the extension of microvilli in mouse melanoma cell lines [142]. When subjects with fatal asthma are compared to controls it is located at the brush border of airway epithelium of the subjects [143].
SHROOM4	2.54	0.00	morphology	Shroom family member 4, was found to be regulator of cyto-skeletal architecture [144]. In <i>Xenopus</i> , cells expressing Shroom family of protein members tend to be elongated, this is associated with microtubule bundles arranged along the apico-basal axis [145].
NIPAL4	2.05	0.00	morphology	NIPA like domain containing 4, also called Ichthyin, is mutated in ichthyosis. In <i>Nipal4</i> knock-out mice, the number of stratum corneum layers was from 10 to 20, indicative of hyperkeratosis [146].

**Supplementary Table S3.** *Continued.*

Gene	Fold Change and $q$ of <i>HOXA13</i> vs <i>HOXA13</i> BAR-T cells		Known function	Detailed description
TMOD2	1.74	0.02	morphology	Tropomodulin 2, is a neuronal-specific actin-regulatory protein, was found to cap the pointed end of actin filaments preventing both elongation and depolymerization [147].
EXPH5	0.56	0.04	morphology	Exophilin 5, see above.
FBLN1	0.52	0.02	morphology	Fibulin-1, is a secreted extracellular matrix glycoprotein [148, 149].
MPP7	0.51	0.02	morphology	Membrane palmitoylated protein 7, forms a complex with the polarity protein <i>DLG1</i> and was found to facilitate epithelial cell polarity and tight junction formation [150]. It is overexpressed in metaplasia [151, 152].
SPTBN2	0.47	0.02	morphology	Spectrin $\beta$ , non-erythrocytic 2, is a components of a cell's membrane-cytoskeleton [153].
MUC5AC	0.37	0.00	morphology	Mucin 5AC, oligomeric mucus/gel-forming, is a gastric mucin [128].
ITGB7	0.34	0.00	morphology	Integrin subunit $\beta$ 7, affects multiple myeloma-cell adhesion and migration [154].

Cancer associated genes from the BAR-T dataset.

DLL1	2.57	0.00	pro-oncogenic	Notch signaling was found to be associated with malignant transformation at the GEJ [14, 155]
MAF	2.39	0.00	pro-oncogenic	MAF bZIP transcription factor, also called c-MAF, was found to be a mediator of bone metastasis in breast cancer [156]. Overexpressing c-Maf enhanced cholangiocarcinoma growth in mice [157].
FAM196B	2.32	0.02	pro-oncogenic	Family with sequence similarity 196 member B, see above.
EPGN	2.23	0.03	pro-oncogenic	Epithelial mitogen, was found to be an activator of <i>ErbB1</i> and can act as a mitogen [158].
FBXO2	2.19	0.02	pro-oncogenic	F-box protein 2, the overexpression of which was found to induce EMT in gastric cancer cells, and is associated with more lymph node metastasis and shorter overall survival [159].
ADAMTS6	2.13	0.03	pro-oncogenic	ADAM metallopeptidase with thrombospondin type 1 motif 6, see above.
BCL11B	2.12	0.01	pro-oncogenic	B cell CLL/lymphoma 11B, its impairment was found to promote tumor development in mouse and human intestine [160]. On the other hand, it was identified as a potential oncogene in AML [161].

Supplementary Table S3. *Continued.*

Gene	Fold Change and $q$ of <i>HOXA13</i> <sup>*</sup> vs <i>HOXA13</i> <sup>-</sup> BAR-T cells		Known function	Detailed description
NRG1	2.07	0.02	pro-oncogenic	Neuregulin 1, see above.
NDRG1	2.05	0.00	anti-oncogenic	N-myc downstream regulated 1, was found to be a potent, iron-regulated growth and metastasis suppressor that was found to be negatively correlated with cancer progression in a number of tumors [162].
TGFBI	2.03	0.02	pro-oncogenic	Transforming growth factor $\beta$ induced, was found to promote the growth of GI-tract tumors, specifically ESCC and gastric cancer [163].
IL1B	2.00	0.00	pro-oncogenic	Interleukin 1 $\beta$ , was found to be sufficient to induce esophagitis, BE, and EAC in a mouse model (Quante et al., 2012). <i>MMP9</i> (FC2.06, $p=0.001$ , $q=0.051$ ) could upregulate Il1 $\beta$ in the mouse (Fang et al., 2017).
LAMC2	1.94	0.00	pro-oncogenic	Laminin subunit $\gamma$ 2, in ESCC and CRC <i>LAMC2</i> is upregulated and was found to be associated with worse survival [164, 165].
CD274	1.90	0.03	pro-oncogenic	CD274 molecule, also called programmed cell death 1 ligand 1, and programmed cell death 1 ligand 2 ( <i>PDCD1LG2</i> ; FC=1.99, $q=0.053$ , $p=0.00$ ) were both upregulated.
GRB10	1.87	0.00	pro-oncogenic	Growth factor receptor bound protein 10, is upregulated in CRC vs peritumor tissue [166]. Overexpression in CRC was found to be associated with decreased survival [167].
ELL2	1.82	0.02	pro-oncogenic	Elongation factor for RNA polymerase II 2, see above.
SMAD7	1.80	0.05	unknown	SMAD family member 7, see above
C12orf75	1.78	0.03	pro-oncogenic	Chromosome 12 open reading frame 75, see above.
ITGA5	1.77	0.00	pro-oncogenic	Integrin subunit $\alpha$ 5, overexpression of the ITGA5 is correlated with an increased risk of perineural invasion in CRC [168]. ITGA5 was found to modulate apoptosis, adhesion, migration, and facilitates cancer cell invasion through enhanced contractile forces [169, 170].
AXL	1.70	0.04	pro-oncogenic	AXL receptor tyrosine kinase, see above.
DUSP7	1.52	0.04	pro-oncogenic	Dual specificity phosphatase 7, see above.

**Supplementary Table S3.** *Continued.*

Gene	Fold Change and <i>q</i> of <i>HOXA13</i> vs <i>HOXA13</i> BAR-T cells		Known function	Detailed description
LPCAT1	1.50	0.02	pro- oncogenic	Lysophosphatidylcholine acyltransferase 1, its expression was higher in CRC vs normal mucosa. A CRC cell line with overexpression, SW480, were found to significantly increase their growth rate [171].
FURIN	1.49	0.03	pro- oncogenic	Notch signaling was found to be associated with malignant transformation at the GEJ [14, 155].
MAP3K5	0.63	0.04	unknown	Mitogen-activated protein kinase kinase kinase 5, see above.
CTSD	0.53	0.03	unknown	Cathepsin D, can either induce apoptosis in presence of cytotoxic factors, but in certain studies an inhibitory role in apoptosis was also reviewed [172].
APOBEC3B	0.50	0.02	anti- oncogenic	Apolipoprotein B mRNA editing enzyme catalytic subunit 3B, was found to be an enzymatic source of mutations in various cancer types [173].
HCAR2	0.50	0.05	pro- oncogenic	Hydroxycarboxylic acid receptor 2, see above.
RAB27B	0.50	0.03	anti- oncogenic	RAB27B, member RAS oncogene family, see above.
PHLPP1	0.49	0.02	pro- oncogenic	PH domain and leucine rich repeat protein phosphatase 1, is an important regulator of Akt serine-threonine kinases and protein kinase C isoforms. It may act as a tumor suppressor in several types of cancer due to its ability to block growth factor-induced signaling in cancer cells [174, 175].
TNFAIP2	0.49	0.03	anti- oncogenic	TNF $\alpha$ induced protein 2, see above.
TMPRSS4	0.48	0.02	anti- oncogenic	Transmembrane serine protease 4, see above.
RTKN2	0.47	0.02	anti- oncogenic	Rhotekin 2, was found to be increase proliferation and reduces apoptosis in pancreatic cancer, CRC, and HCC [176-178].
LTBP3	0.37	0.00	pro- oncogenic	Latent-transforming growth factor $\beta$ -binding protein 3, promotes early metastatic events [179, 180].

**Supplementary Table S4.** All primers used in this study

Primer name	Sequence (5' to 3')
huHOXA1 L	TCTTCTCCAGCGCAGACTTT
huHOXA1 R	TTGACCCAGGTAGCCGTACT
huHOXA2 L	CCAAGAAAACCGCACTTCTG
huHOXA2 R	CATCGGCGATTTCAGG
huHOXA3 L	ATGCAAAAAGCGACCTACTACG
huHOXA3 R	TACGGCTGCTGATTGGCATTA
huHOXA4 L	GAAGAAGATCCATGTCAGCG
huHOXA4 R	GGAACTCCTTCTCCAGCTCC
huHOXA5 L	GCGCAAGCTGCACATAAGTC
huHOXA5 R	GAACTCCTTCTCCAGCTCCA
huHOXA6 L	AAAGCACTCCATGACGAAGG
huHOXA6 R	CATGGCTCCCATACACAGC
huHOXA7 L	CAATTTCGCGATCTACCCCT
huHOXA7 R	GGAACTCCTTCTCCAGCTCC
huHOXA9 L	AATGCTGAGAATGAGAGCGG
huHOXA9 R	GTATAGGGGCACCGCTTTTT
huHOXA10 L	CCGGAGAAGGATTCCCTG
huHOXA10 R	CAGTGTCTGGTGCTTCGTGT
huHOXA11 L	ACACTGAGGACAAGGCCG
huHOXA11 R	GAAGAAGAACTCCCGTTCCA
huHOXA13 L	CCTCTGGAAGTCCACTCTGC
huHOXA13 R	GCACCTTGGTATAAGGCACG
huHOXB1 L	AGGAGACGGAGGCTATTTTCA
huHOXB1 R	GTCTGCTCGTTCCCATAAGGG
huHOXB2 L	CGCCAGGATTCACCTTTCCTT
huHOXB2 R	CCCTGTAGGCTAGGGGAGAG
huHOXB3 L	ATATTCACATCGAGCCCCAG
huHOXB3 R	CGTCATGAATGGGATCTGC
huHOXB4 L	CTTCTCCAGCTCCAAGACCT
huHOXB4 R	CTGGATGCGCAAAGTTCAC
huHOXB5 L	GGAACTCCTTTTCCAGCTCC
huHOXB5 R	GGAAGCTTCACATCAGCCAT
huHOXB6 L	GGGGACATGGACAAAATGAG
huHOXB6 R	GTGAGAACTGAGGAGCGGAC
huHOXB7 L	CTTTCTCCAGCTCCAGGGTC

**Supplementary Table S4.** *Continued.*

Primer name	Sequence (5' to 3')
huHOXB7 R	AACTTCCGGATCTACCCCTG
huHOXB8 L	GAACTCCTTCTCCAGCTCCA
huHOXB8 R	ACACAGCTCTTCCCCTGGAT
huHOXB9 L	TCCAGCGTCTGGTATTTGGT
huHOXB9 R	GAAGCGAGGACAAAGAGAGG
huHOXB13 L	GCTGTACGGAATGCGTTTCT
huHOXC4 L	GAGGTCTGGGGGTTGAGC
huHOXC4 R	GGAGCTGAGACAGGCTCG
huHOXC5 L	GAGTCTGGTAGCGCGTGAAC
huHOXC5 R	CCACAGATTTACCCGTGGAT
huHOXC6 L	GATCATAGGCGGTGGAATTG
huHOXC6 R	GGCACAGAATGAGGGAAGAC
huHOXC8 L	CAAGGTCTGATACCGGCTGT
huHOXC8 R	ATCAAACTCGTCTCCCAGC
huHOXC9 L	GTACTTGGTGTAGGGGCAGC
huHOXC9 R	ACAAAGAGGAGAAGGCCGAC
huHOXC10 L	ACCTCTTCTTCCTTCCGCTC
huHOXC10 R	GACACCTCGGATAACGAAGC
huHOXC11 L	ATAAGGGCAGCGCTTCTTG
huHOXC11 R	GAACACAAATCCCAGCTCGT
huHOXC12 L	GCAACTTCGAATAGGGCTTG
huHOXC12 R	AGCTTGGTATCGCCGTTG
huHOXC13 L	GCTGCACCTTAGTGTAGGGC
huHOXC13 R	CCACCTCTGGAAGTCTCCCT
huHOXD1 L	TTCTGTCAGTTGCTTGGTGC
huHOXD1 R	GGATGAAAGTGAAGAGGAATGC
huHOXD3 L	CACCTCCAATGTCTGCTGAA
huHOXD3 R	CAAAATTCAAGAAAACACACACA
huHOXD4 L	AGTTCTAGGACTTGCTGCCG
huHOXD4 R	CTACCCCTGGATGAAGAAGG
huHOXD8 L	TCTTCCTCTTCGTCTACCAGG
huHOXD8 R	TAATATTGGCGAGGACCCAG
huHOXD9 L	CTTTCTCCAGCTCAAGCGTC
huHOXD9 R	CAGCAGCAACTTGACCCAA
huHOXD10 L	TTCTGCCACTCTTTGCAGTG

**Supplementary Table S4.** *Continued.*

Primer name	Sequence (5' to 3')
huHOXD10 R	CTGAGGTCTCCGTGTCCAGT
huHOXD11 L	AAAGAAAACTCGCGTTCCA
huHOXD11 R	CGAGAAGAGCAGCAGCG
huHOXD12 L	GCTGCTTCGTGTAGGGTTTC
huHOXD12 R	TGAACATGACAGTGCAGGC
huHOXD13 L	CCTCTTCGGTAGACGCACAT
huHOXD13 R	CAGGTGTACTGCACCAAGGA
huRP2 L	AAGCTGAGGATGCTCAAAGG
huRP2 R	CCCATTAAACTCCAAGGCAA
huβ-ACTIN L	GCACAGAGCCTCGCCTT
huβ-ACTIN R	GTTGTGACGACGAGCG
huGAPDH L	AAGGTCGGAGTCAACGATT
huGAPDH R	ACCAGAGTTAAAAGCAGCCCT
moHoxA1 L	AAAAGAAACCTCCCAAAACA
moHoxA1 R	AGCTCTGTGAGCTGCTTGGT
moHoxA2 L	GATGAAGGAGAAGAAGGCGG
moHoxA2 R	TGCCATCAGCTATTTCAGG
moHoxA3 L	GCTGCCTGGTCATTCAAAGT
moHoxA3 R	GTCTCCAGTTCCAGGTGCTC
moHoxA4 L	ACCTTGATGGTAGGTGTGGC
moHoxA4 R	ACGCTGTGCCCCAGTATAAG
moHoxA5 L	CTCAGCCCCAGATCTACCC
moHoxA5 R	CAGGGTCTGGTAGCGAGTGT
moHoxA6 L	CCCTGTTTACCCCTGGATG
moHoxA6 R	GTCTGGTAGCGCGTGTAGGT
moHoxA7 L	AAGCCAGTTTCCGCATCTAC
moHoxA7 R	CTTCTCCAGTTCCAGCGTCT
moHoxA9 L	ACAATGCCGAGAATGAGAGC
moHoxA9 R	GTAAGGGCATCGCTTCTTCC
moHoxA10 L	CTCCAGCCCCTTCAGAAAAC
moHoxA10 R	TCTTTGCTGTGAGCCAGTTG
moHoxA11 L	AGGCTCCAGCCTACTGGAAT
moHoxA11 R	CCTTTTCCAAGTCGCAATGT
moHoxA13 L	GCTGCCCTACGGCTACTTC
moHoxA13 R	GCGGTGTCCATGTACTTGTC

**Supplementary Table S4.** *Continued.*

Primer name	Sequence (5' to 3')
moHoxB1 F	GGTGAAGTTTGTGCGGAGAC
moHoxB1 R	TTCGACTGGATGAAGGTCAA
moHoxB2 F	GAACCAGACTTTGACCTGCC
moHoxB2 R	GAGCTGGAGAAGGAGTTCCA
moHoxB3 F	ATCTGTTTGGTGAGGGTGGA
moHoxB3 R	CCGCACCTACCAGTACCACT
moHoxB4 F	GACCTGCTGGCGAGTGTAG
moHoxB4 R	CTGGATGCGCAAAGTTCAC
moHoxB5 F	CTGGTAGCGAGTATAGGCGG
moHoxB5 R	AGGGGCAGACTCCACAGATA
moHoxB6 F	TCCTATTTTCGTGAACTCCACCT
moHoxB6 R	GCATAGCCAGACGAGTAGAGC
moHoxB7 F	GAGCAGAGGGACTCGGACTT
moHoxB7 R	GTCTGGTAGCGCGTGTAGGT
moHoxB8 F	CCTGCGCCCCAATTATTATGA
moHoxB8 R	AACTCCTGGATTTGCGAAGGG
moHoxB9 F	TCCAGCGTCTGGTATTTGGT
moHoxB9 R	GAAGCGAGGACAAAGAGAGG
moHoxB13 F	TGCCCCCTTGCTATAGGGAAT
moHoxB13 R	ATTCTGGAAAGCAGCGTTTG
moHoxC4 F	CTACCCTGAGCGTCAGTATAGC
moHoxC4 R	CGCAGAGCGACTGTGATTTCT
moHoxC5 F	TTCTCGAGTTCCAGGGTCTG
moHoxC5 R	ATTTACCCGTGGATGACCAA
moHoxC6 F	CAGGGTCTGGTACCGAGAGTA
moHoxC6 R	TCCAGATTTACCCCTGGATG
moHoxC8 F	CAAGGTCTGATACCGGCTGT
moHoxC8 R	ATCAGAACTCGTCTCCCAGC
moHoxC9 F	ACTCGCTCATCTCTCACGACA
moHoxC9 R	GGACGGAATCGCTACAGTC
moHoxC10 F	ACCTCTTCTTCCTTCCGCTC
moHoxC10 R	ACTCCAGTCCAGACACCTCG
moHoxC11 F	TCCAACCTCTATCTGCCAGT
moHoxC11 R	CAAGACGAGTAGCTGTTCCGA
moHoxC12 F	AATACGGCTTGCGCTTCTT



**Supplementary Table S4.** *Continued.*

Primer name	Sequence (5' to 3')
moHoxC12 R	GACCCTGGCTCTCTGGTTTC
moHoxC13 F	GGGCTATGGTTACCCATTG
moHoxC13 R	CTGGAGGACAGGTCGTCAC
moHoxD1 F	CAGCACTTTCGAGTGGATGA
moHoxD1 R	GCTCTGTCAGTTGCTTG
moHoxD3 F	ACCAGCTGAGCACTCGTGTA
moHoxD3 R	AGAACAGCTGTGCCACTTCA
moHoxD4 F	CTCCCTGGGCTGAGACTGT
moHoxD4 R	CCCTGGGAACCACTGTTCT
moHoxD8 F	GTAATATTGGCGAGGACCCA
moHoxD8 R	CTACCAGGAGCTTGTGGTC
moHoxD9 F	GCTGAAGGAGGAGGAGAAGC
moHoxD9 R	GTGTAGGGACAGCGCTTTT
moHoxD10 F	TCTCCTGCACTTCGGGAC
moHoxD10 R	GGAGCCCACTAAAGTCTCCC
moHoxD11 F	GAAAAAGCGCTGTCCCTACA
moHoxD11 R	AGGTTGAGCATCCGAGAGAG
moHoxD12 F	TGCTTTGTGTAGGGTTTCTCT
moHoxD12 R	CTTCACTGCCCCGACGGTA
moHoxD13 F	TGGTGTAAGGCACCCTTTTC
moHoxD13 R	CCCATTTTTTGAAATCATCC
Eef2 F	GCTTCCCTGTTACCTCTGA
Eef2 R	CGGATGTTGGCTTTCTTGTC
Rpl37 F	GTCGGATGAGGCACCTAAAG
Rpl37 R	GAAGAACTGGATGCTGCGAC
Leng8 F	GGTTGTCTTGAAGCTGCCTT
Leng8 R	GACCTTGGGGTGTAGGGAAT
HOT TIP F	CCTAAAGCCACGCTTCTTTG
HOT TIP R	TGCAGGCTGGAGATCCTACT
HOTAIR F	GGTAGAAAAAGCAACCACGAAGC
HOTAIR R	ACATAAACCTCTGTCTGTGAGTGCC
MEIS1 F	GGGCATGGATGGAGTAGGC
MEIS1 R	GGGTACTGATGCGAGTGCAG
AgeI HoxA13 F	GGTGGTACCGGTGCCACCATGACAGCCTCCGTGCTCCT
XbaI HoxA13 R	ACCACCTCTAGATTAAGTAGTGGTTTTTCAGTT

**Supplementary Table S4.** *Continued.*

Primer name	Sequence (5' to 3')
HOXA13gibson F	ctccgcgccccgaagccgccaccatggactacaaagacgatgacgacaagATGACAGCCTCCGTGCTC
HOXA13gibson R	cgaagcggccatgaaTTAACTAGTGGTTTTTCAGTTTGTTGATG
HOXA13colonyPCR F	CCTCTGGAAGTCCACTCTGC
HOXA13colonyPCR R	GCACCTTGGTATAAGGCACG
pBS31-TetO-F	CCATCCACGCTGTTTTGAC
MF13-R	AGCGGATAACAATTTACACAGGA
T1E2 HygroR6	TGTATTGACCGATTCCTTGC
T1E2 HygroR7	AGGACATTGTTGGAGCCGAA
PGK-F1	AACAGCTATGACCATG
PGK-F2	GGGCCTTTCGACCTGCATCCATC
Guide1sgRNA F	CACCGTTTCTCTACGACAACGGCGG
Guide1sgRNA R	AAACCCGCCGTTGTCTAGAGAAAC
px330-F	GATACAAGGCTGTTAGAGAG
TILHOXA13R3	CGAGCAGGGGCTGCATTG
Pre HOXA13 FW2	GCTTTGCATACGCCGTGG
Rat HoxA13 1 F	GGGCTATGACAGCCTCCGT
Rat HoxA13 1 R	ATGTTCTTGTTGAGCTCGTCGG
Rat HoxA13 2 F	GTCGTCTCCCATCCTTCAGA
Rat HoxA13 2 R	TATCCTCCTCCGTTTGTCTT
Rat HoxA13 3 F	CTGGAACGGCCAAATGTACT
Rat HoxA13 3 R	CCTCCGTTTGTCTTGGTAA
Rat Hmbs F	TCCTGGCTTTACCATTGGAG
Rat Hmbs R	TGAATTCCAGGTGAGGGAAC
Rat Hprt F	AGGCCAGACTTTGTTGGATT
Rat Hprt R	GCTTTTCCACTTTCGCTGAT
Rat Sdha F	TCCTTCCCCTGTGCATTACAA
Rat Sdha R	CGTACAGACCAGGCACAATCTG
Rat Mapk6 F	TAAAGCCATTGACATGTGGG
Rat Mapk6 R	TCGTGCACAACAGGGATAGA
Rat Rps18 F	AAGTTTCAGCACATCCTGCGAGTA
Rat Rps18 R	TTGGTGAGGTCAATGTCTGCTTTC
HOXA7methF	GACTGCGCCTACCTGAAGAC
HOXA7methR	CAACAGCCCCCTTTATCAGA
HOXA9methF	TGTAGGTCCCCACAGCTACC
HOXA9methR	AATCCTGATTGCCAGCTGAT

**Supplementary Table S4.** *Continued.*

Primer name	Sequence (5' to 3')
HOXA10methF	GGTGTCTCGTCCCTAGTCA
HOXA10methR	CAGACAGGCAGACACAAGGA
HOXA11methF	TCGAAAACTGGTCGAAAGC
HOXA11methR	CAATCTGGCCCACTGCTACT
HOXA13methF	AGTACATTTGGCCGTTCCAG
HOXA13methR	CTTCTACCACCAGGGCTACG
HOTTIPmethF	CTTCGAGCGTTTGAAGGAAG
HOTTIPmethR	GTCGCGTTGTGCATTAAGAA

**Supplementary Table S5.** Mouse ESC culture medium and differentiation medium components

Details of used products to culture mESCs.			
Product	Product details		Manufacturer
Dulbecco's Modified Eagle Medium (DMEM)	DMEM 4.5 g/L Glucose with L-Glutamine	82%	Lonza
Foetal Bovine Serum (FBS)		15%	Biowest (Nuaillé, France)
Penicillin/Streptomycin	10,000 Units/mL Penicillin, 10,000 µg/mL Streptomycin	1%	Thermo-Fisher Scientific
MEM Non-Essential Amino Acids		1%	Thermo-Fisher Scientific
Leukaemia Inhibitory Factor (LIF)		0.01%	Department of Developmental Biology, Erasmus MC
2-Mercaptoethanol / β-Mercaptoethanol	55 mM in DPBS	0.1%	Thermo-Fisher Scientific
Sodium Pyruvate	100 mM	1%	Thermo-Fisher Scientific
Details of the components used to differentiate the mESCs to definitive endoderm cells.			
Product	Product details		Manufacturer
Activin A	50 ng/mL		Thermo-Fisher Scientific
(Recombinant Human β-Fibroblast Growth Factor, 154 a.a.)	50 ng/mL		PeproTech EC Ltd. (London, UK)
CHIR	5 µM		Cayman Chemical (Ann Arbor, USA)

**Supplementary Table S6.** All antibodies used in this study

Details of antibodies.				
Antibody	Concentration	Manufacturer	Product #	RRID
PE rat anti-mouse (clone 2B11) CD184 (CXCR4)	1:250	BD Pharmingen	551966	AB_394305
Alexa Fluor 488 rat anti-mouse (clone DECMA-1) anti-CD324 (E-Cadherin)	1:250	Thermo-Fisher Scientific	53-3249-80	AB_10671270
Anti-human mitochondria (clone 113-1)	1:500	Merck Millipore, Billerica, USA	MAB1273	AB_94052
Mouse anti-human monoclonal (clone OV-TL 12/30) CK7	1:100	Dako Cytomation, Glostrup, Denmark	M7018	AB_2134589
Mouse anti-human monoclonal (clone 415909) TFF3	1:50	R&D Systems, Minneapolis, USA	MAB4407	AB_2271768
Rabbit anti-human monoclonal (clone EPR2764Y) CDX2	1:100	Cell Marque, Rocklin, CA	235R-14	AB_1516797
Mouse anti-human monoclonal (clone DAK-p63) P63	1:100	Dako Cytomation, Glostrup, Denmark	M7317	NA
Rabbit anti-human monoclonal (clone EP1601Y) CK5	1:100	Cell Marque, Rocklin, CA	305R-16	AB_1159468
Rabbit anti-human Involucrin	1:100	gift from A/Prof. Pritinder Kaur, Curtin University, Australia	NA	NA
Mouse anti-human Involucrin	1:500	Sigma-Aldrich, Sigma-Aldrich, St. Louis, Missouri, USA	#I9018	AB_477129
Rabbit polyclonal anti-GFP	1:100	Merck Millipore, Billerica, USA	#AB3080	AB_91337

## Supplementary Macro and other data files

**Supplementary Macro S1:** Related to the methods. Macro used to quantify *HOXA13*-ISH in FIJI

```
//setTool("freehand");
run("Cut");
run("Internal Clipboard");
selectWindow("Clipboard");
run("Colour Deconvolution", "vectors=[H&E DAB]");
selectWindow("Clipboard-(Colour_2)");
close();
selectWindow("Clipboard-(Colour_1)");
close();
selectWindow("Colour Deconvolution");
close();
selectWindow("Clipboard");
close();
selectWindow("Clipboard-(Colour_3)");
run("Measure");
run("Duplicate...", " ");
selectWindow("Clipboard-(Colour_3)");
setAutoThreshold("Default");
//run("Threshold...");
setThreshold(0, 10);
//setThreshold(0, 10);
run("Convert to Mask");
run("Measure");
close();
selectWindow("Clipboard-(Colour_3)-1");
setThreshold(3, 150);
//setThreshold(3, 150);
run("Convert to Mask");
run("Measure");
close();
String.copyResults();
IJ.deleteRows(0, 4);
```

**Supplementary File S1.** Contains mRNA expression determined by single cell RNA-Seq. The expression is depicted as present or not present in *HOXA13*-positive and negative cell fractions in both the healthy esophagus and BE. This data file can be obtained through communication with the authors.

## Supplementary information related references

1. Wang, X., et al., Cloning and variation of ground state intestinal stem cells. *Nature*, 2015. 522(7555): p. 173-8.
2. Li, F., et al., Combined Activin A/LiCl/Noggin treatment improves production of mouse embryonic stem cell-derived definitive endoderm cells. *Journal of Cellular Biochemistry*, 2011. 112(4): p. 1022-1034.
3. Sherwood, R.I., et al., Prospective isolation and global gene expression analysis of definitive and visceral endoderm. *Dev Biol*, 2007. 304(2): p. 541-55.
4. Teo, A.K., et al., Activin and BMP4 synergistically promote formation of definitive endoderm in human embryonic stem cells. *Stem Cells*, 2012. 30(4): p. 631-42.
5. Wang, P., et al., A molecular signature for purified definitive endoderm guides differentiation and isolation of endoderm from mouse and human embryonic stem cells. *Stem Cells Dev*, 2012. 21(12): p. 2273-87.
6. Tsai, Y.H., et al., LGR4 and LGR5 Function Redundantly During Human Endoderm Differentiation. *Cell Mol Gastroenterol Hepatol*, 2016. 2(5): p. 648-662 e8.
7. Ivanova, N., et al., Dissecting self-renewal in stem cells with RNA interference. *Nature*, 2006. 442(7102): p. 533-8.
8. Waghray, A., et al., Tbx3 Controls Dppa3 Levels and Exit from Pluripotency toward Mesoderm. *Stem Cell Reports*, 2015. 5(1): p. 97-110.
9. Polyak, K. and R.A. Weinberg, Transitions between epithelial and mesenchymal states: acquisition of malignant and stem cell traits. *Nat Rev Cancer*, 2009. 9(4): p. 265-73.
10. Shapiro, L., et al., Structural basis of cell-cell adhesion by cadherins. *Nature*, 1995. 374(6520): p. 327-37.
11. Friederich, E., et al., Villin function in the organization of the actin cytoskeleton. Correlation of in vivo effects to its biochemical activities in vitro. *J Biol Chem*, 1999. 274(38): p. 26751-60.
12. Zeisberg, M., et al., BMP-7 counteracts TGF-beta1-induced epithelial-to-mesenchymal transition and reverses chronic renal injury. *Nat Med*, 2003. 9(7): p. 964-8.
13. Danahay, H., et al., Notch2 is required for inflammatory cytokine-driven goblet cell metaplasia in the lung. *Cell Rep*, 2015. 10(2): p. 239-52.
14. Quante, M., et al., Bile acid and inflammation activate gastric cardia stem cells in a mouse model of Barrett-like metaplasia. *Cancer Cell*, 2012. 21(1): p. 36-51.
15. Menke, V., et al., Conversion of metaplastic Barrett's epithelium into post-mitotic goblet cells by gamma-secretase inhibition. *Disease models & mechanisms*, 2010. 3(1-2): p. 104-10.
16. Terao, M., et al., Enhanced epithelial-mesenchymal transition-like phenotype in N-acetylglucosaminyltransferase V transgenic mouse skin promotes wound healing. *J Biol Chem*, 2011. 286(32): p. 28303-11.
17. Lv, Z.D., et al., Silencing of Prrx2 Inhibits the Invasion and Metastasis of Breast Cancer both In Vitro and In Vivo by Reversing Epithelial-Mesenchymal Transition. *Cell Physiol Biochem*, 2017. 42(5): p. 1847-1856.
18. Wu, Y.Y., et al., SCUBE3 is an endogenous TGF-beta receptor ligand and regulates the epithelial-mesenchymal transition in lung cancer. *Oncogene*, 2011. 30(34): p. 3682-93.
19. Bonné, S., et al., Defining desmosomal plakophilin-3 interactions. *The Journal of Cell Biology*, 2003. 161(2): p. 403-416.
20. Todorovic, V., et al., Plakophilin 3 mediates Rap1-dependent desmosome assembly and adherens junction maturation. *Molecular Biology of the Cell*, 2014. 25(23): p. 3749-3764.

21. Harrison, O.J., et al., Structural basis of adhesive binding by desmocollins and desmogleins. *Proc Natl Acad Sci U S A*, 2016. 113(26): p. 7160-5.
22. Wang, Y.W., et al., EMP1, EMP2, and EMP3 as novel therapeutic targets in human cancer. *Biochim Biophys Acta*, 2017. 1868(1): p. 199-211.
23. Boczonadi, V. and A. Maatta, Annexin A9 is a periplakin interacting partner in membrane-targeted cytoskeletal linker protein complexes. *FEBS Lett*, 2012. 586(19): p. 3090-6.
24. Otsubo, T., et al., Aberrant DNA hypermethylation reduces the expression of the desmosome-related molecule periplakin in esophageal squamous cell carcinoma. *Cancer Med*, 2015. 4(3): p. 415-25.
25. Heller, E. and E. Fuchs, Tissue patterning and cellular mechanics. *J Cell Biol*, 2015. 211(2): p. 219-31.
26. Flores-Tellez, T.N., et al., Co-Expression of Ezrin-CLIC5-Podocalyxin Is Associated with Migration and Invasiveness in Hepatocellular Carcinoma. *PLoS One*, 2015. 10(7): p. e0131605.
27. Viswanatha, R., A. Bretscher, and D. Garbett, Dynamics of ezrin and EBP50 in regulating microvilli on the apical aspect of epithelial cells. *Biochem Soc Trans*, 2014. 42(1): p. 189-94.
28. Cao, H.H., et al., A three-protein signature and clinical outcome in esophageal squamous cell carcinoma. *Oncotarget*, 2015. 6(7): p. 5435-48.
29. Tanaka, H., et al., Adherens junctions associated protein 1 serves as a predictor of recurrence of squamous cell carcinoma of the esophagus. *Int J Oncol*, 2015. 47(5): p. 1811-8.
30. Shen, Z.Y., et al., Upregulated expression of Ezrin and invasive phenotype in malignantly transformed esophageal epithelial cells. *World J Gastroenterol*, 2003. 9(6): p. 1182-6.
31. Schwebach, C.L., et al., The Roles of Actin-Binding Domains 1 and 2 in the Calcium-Dependent Regulation of Actin Filament Bundling by Human Plastins. *J Mol Biol*, 2017. 429(16): p. 2490-2508.
32. Hisano, T., et al., Increased expression of T-plastin gene in cisplatin-resistant human cancer cells: identification by mRNA differential display. *FEBS Lett*, 1996. 397(1): p. 101-7.
33. Higuchi, Y., et al., Search for genes involved in UV-resistance in human cells by mRNA differential display: increased transcriptional expression of nucleophosmin and T-plastin genes in association with the resistance. *Biochem Biophys Res Commun*, 1998. 248(3): p. 597-602.
34. Duggan, S.P., et al., The characterization of an intestine-like genomic signature maintained during Barrett's-associated adenocarcinogenesis reveals an NR5A2-mediated promotion of cancer cell survival. *Sci Rep*, 2016. 6: p. 32638.
35. Khurana, S. and S.P. George, Regulation of cell structure and function by actin-binding proteins: villin's perspective. *FEBS Lett*, 2008. 582(14): p. 2128-39.
36. Liu, M., et al., RHOA GTPase Controls YAP-Mediated EREG Signaling in Small Intestinal Stem Cell Maintenance. *Stem Cell Reports*, 2017. 9(6): p. 1961-1975.
37. Bruurs, L.J., et al., ATP8B1-mediated spatial organization of Cdc42 signaling maintains singularity during enterocyte polarization. *J Cell Biol*, 2015. 210(7): p. 1055-63.
38. Verhulst, P.M., et al., A flippase-independent function of ATP8B1, the protein affected in familial intrahepatic cholestasis type 1, is required for apical protein expression and microvillus formation in polarized epithelial cells. *Hepatology*, 2010. 51(6): p. 2049-60.
39. Croce, A., et al., A novel actin barbed-end-capping activity in EPS-8 regulates apical morphogenesis in intestinal cells of *Caenorhabditis elegans*. *Nat Cell Biol*, 2004. 6(12): p. 1173-9.
40. Tocchetti, A., et al., Loss of the actin remodeler Eps8 causes intestinal defects and improved metabolic status in mice. *PLoS One*, 2010. 5(3): p. e9468.
41. Muller, T., et al., MYO5B mutations cause microvillus inclusion disease and disrupt epithelial cell polarity. *Nat Genet*, 2008. 40(10): p. 1163-5.

42. Giroux, V., et al., Long-lived keratin 15+ esophageal progenitor cells contribute to homeostasis and regeneration. *J Clin Invest*, 2017. 127(6): p. 2378-2391.
43. Shearer, C., et al., Cytokeratin 7 and 20 expression in intestinal metaplasia of the distal oesophagus: relationship to gastro-oesophageal reflux disease. *Histopathology*, 2005. 47(3): p. 268-75.
44. Nanashima, N., et al., Hair keratin KRT81 is expressed in normal and breast cancer cells and contributes to their invasiveness. *Oncol Rep*, 2017. 37(5): p. 2964-2970.
45. Muckenhuber, A., et al., Pancreatic Ductal Adenocarcinoma Subtyping Using the Biomarkers Hepatocyte Nuclear Factor-1A and Cytokeratin-81 Correlates with Outcome and Treatment Response. *Clin Cancer Res*, 2018. 24(2): p. 351-359.
46. Liu, S., et al., Identification of differentially expressed genes, lncRNAs and miRNAs which are associated with tumor malignant phenotypes in hepatoblastoma patients. *Oncotarget*, 2017. 8(57): p. 97554-97564.
47. Rubinstein, E., et al., CD9, CD63, CD81, and CD82 are components of a surface tetraspan network connected to HLA-DR and VLA integrins. *Eur J Immunol*, 1996. 26(11): p. 2657-65.
48. Singethan, K., et al., CD9 clustering and formation of microvilli zippers between contacting cells regulates virus-induced cell fusion. *Traffic*, 2008. 9(6): p. 924-35.
49. Zhu, J., et al., Prognostic role of CD82/KAI1 in multiple human malignant neoplasms: a meta-analysis of 31 studies. *Onco Targets Ther*, 2017. 10: p. 5805-5816.
50. Sala-Valdes, M., et al., EWI-2 and EWI-F link the tetraspanin web to the actin cytoskeleton through their direct association with ezrin-radixin-moesin proteins. *J Biol Chem*, 2006. 281(28): p. 19665-75.
51. Pinto, D., et al., Canonical Wnt signals are essential for homeostasis of the intestinal epithelium. *Genes Dev*, 2003. 17(14): p. 1709-13.
52. Almohazey, D., et al., The ErbB3 receptor tyrosine kinase negatively regulates Paneth cells by PI3K-dependent suppression of Atoh1. *Cell Death Differ*, 2017. 24(5): p. 855-865.
53. Tanaka, M., et al., Spatial distribution and histogenesis of colorectal Paneth cell metaplasia in idiopathic inflammatory bowel disease. *J Gastroenterol Hepatol*, 2001. 16(12): p. 1353-9.
54. Miralles, F., et al., Signaling through fibroblast growth factor receptor 2b plays a key role in the development of the exocrine pancreas. *Proceedings of the National Academy of Sciences of the United States of America*, 1999. 96(11): p. 6267-6272.
55. Yeh, J.C., E. Ong, and M. Fukuda, Molecular cloning and expression of a novel beta-1, 6-N-acetylglucosaminyltransferase that forms core 2, core 4, and I branches. *J Biol Chem*, 1999. 274(5): p. 3215-21.
56. Mukherjee, A., et al., Steroid receptor coactivator 2 is critical for progesterone-dependent uterine function and mammary morphogenesis in the mouse. *Mol Cell Biol*, 2006. 26(17): p. 6571-83.
57. Charytoniuk, D., et al., Intrastriatal sonic hedgehog injection increases Patched transcript levels in the adult rat subventricular zone. *Eur J Neurosci*, 2002. 16(12): p. 2351-7.
58. Wang, D.H., et al., Aberrant epithelial-mesenchymal Hedgehog signaling characterizes Barrett's metaplasia. *Gastroenterology*, 2010. 138(5): p. 1810-22.
59. Ramalho-Santos, M., D.A. Melton, and A.P. McMahon, Hedgehog signals regulate multiple aspects of gastrointestinal development. *Development*, 2000. 127(12): p. 2763-72.
60. Flanagan, D.J., et al., Frizzled7 functions as a Wnt receptor in intestinal epithelial Lgr5(+) stem cells. *Stem Cell Reports*, 2015. 4(5): p. 759-67.
61. Farin, H.F., J.H. Van Es, and H. Clevers, Redundant sources of Wnt regulate intestinal stem cells and promote formation of Paneth cells. *Gastroenterology*, 2012. 143(6): p. 1518-1529 e7.
62. Farin, H.F., et al., Visualization of a short-range Wnt gradient in the intestinal stem-cell niche. *Nature*, 2016. 530(7590): p. 340-3.



63. Bakker, E.R., et al., Induced Wnt5a expression perturbs embryonic outgrowth and intestinal elongation, but is well-tolerated in adult mice. *Dev Biol*, 2012. 369(1): p. 91-100.
64. Miyoshi, H., et al., Wnt5a potentiates TGF-beta signaling to promote colonic crypt regeneration after tissue injury. *Science*, 2012. 338(6103): p. 108-13.
65. Mehdaoui, L.M., et al., Non-canonical WNT5A signaling up-regulates the expression of the tumor suppressor 15-PGDH and induces differentiation of colon cancer cells. *Mol Oncol*, 2016. 10(9): p. 1415-1429.
66. Long, A., et al., WNT10A promotes an invasive and self-renewing phenotype in esophageal squamous cell carcinoma. *Carcinogenesis*, 2015. 36(5): p. 598-606.
67. Grimont, A., et al., SOX9 regulates ERBB signalling in pancreatic cancer development. *Gut*, 2015. 64(11): p. 1790-9.
68. Mori-Akiyama, Y., et al., SOX9 is required for the differentiation of paneth cells in the intestinal epithelium. *Gastroenterology*, 2007. 133(2): p. 539-46.
69. Herfs, M., P. Hubert, and P. Delvenne, Epithelial metaplasia: adult stem cell reprogramming and (pre)neoplastic transformation mediated by inflammation? *Trends Mol Med*, 2009. 15(6): p. 245-53.
70. Que, J., et al., Morphogenesis of the trachea and esophagus: current players and new roles for noggin and Bmps. *Differentiation*, 2006. 74(7): p. 422-37.
71. Zhang, X., M. Westerhoff, and J. Hart, Expression of SOX9 and CDX2 in nongoblet columnar-lined esophagus predicts the detection of Barrett's esophagus during follow-up. *Mod Pathol*, 2015. 28(5): p. 654-61.
72. Minacapelli, C.D., et al., Barrett's metaplasia develops from cellular reprogramming of esophageal squamous epithelium due to gastroesophageal reflux. *Am J Physiol Gastrointest Liver Physiol*, 2017. 312(6): p. G615-G622.
73. Clemons, N.J., et al., Sox9 drives columnar differentiation of esophageal squamous epithelium: a possible role in the pathogenesis of Barrett's esophagus. *Am J Physiol Gastrointest Liver Physiol*, 2012. 303(12): p. G1335-46.
74. Sock, E., et al., Gene targeting reveals a widespread role for the high-mobility-group transcription factor Sox11 in tissue remodeling. *Mol Cell Biol*, 2004. 24(15): p. 6635-44.
75. Lefebvre, V., The SoxD transcription factors--Sox5, Sox6, and Sox13--are key cell fate modulators. *Int J Biochem Cell Biol*, 2010. 42(3): p. 429-32.
76. Li, J., et al., The clinical significance of circulating GPC1 positive exosomes and its regulative miRNAs in colon cancer patients. *Oncotarget*, 2017. 8(60): p. 101189-101202.
77. Tanaka, M., et al., EVI1 modulates oncogenic role of GPC1 in pancreatic carcinogenesis. *Oncotarget*, 2017. 8(59): p. 99552-99566.
78. Hara, H., et al., Overexpression of glypican-1 implicates poor prognosis and their chemoresistance in oesophageal squamous cell carcinoma. *Br J Cancer*, 2016. 115(1): p. 66-75.
79. Bosse, K.R., et al., Identification of GPC2 as an Oncoprotein and Candidate Immunotherapeutic Target in High-Risk Neuroblastoma. *Cancer Cell*, 2017. 32(3): p. 295-309 e12.
80. Filmus, J., J.G. Church, and R.N. Buick, Isolation of a cDNA corresponding to a developmentally regulated transcript in rat intestine. *Mol Cell Biol*, 1988. 8(10): p. 4243-9.
81. Farkas, S.A., et al., DNA methylation changes in genes frequently mutated in sporadic colorectal cancer and in the DNA repair and Wnt/beta-catenin signaling pathway genes. *Epigenomics*, 2014. 6(2): p. 179-91.
82. Dai, Y., et al., Genome-Wide Analysis of Barrett's Adenocarcinoma. A First Step Towards Identifying Patients at Risk and Developing Therapeutic Paths. *Transl Oncol*, 2017. 11(1): p. 116-124.

83. Li, Y., et al., Immune signature profiling identified predictive and prognostic factors for esophageal squamous cell carcinoma. *Oncoimmunology*, 2017. 6(11): p. e1356147.
84. Yoon, N.Y., et al., Simultaneous detection of barrier- and immune-related gene variations in patients with atopic dermatitis by reverse blot hybridization assay. *Clin Exp Dermatol*, 2018. 43(4): p. 430-6.
85. Pham, T.A., et al., Epithelial IL-22RA1-mediated fucosylation promotes intestinal colonization resistance to an opportunistic pathogen. *Cell Host Microbe*, 2014. 16(4): p. 504-16.
86. Morrison, P.J., et al., Differential Requirements for IL-17A and IL-22 in Cecal versus Colonic Inflammation Induced by *Helicobacter hepaticus*. *Am J Pathol*, 2015. 185(12): p. 3290-303.
87. Yao, Q., et al., Synergistic role of Caspase-8 and Caspase-3 expressions: Prognostic and predictive biomarkers in colorectal cancer. *Cancer Biomark*, 2018. 21(4): p. 899-908.
88. Shea-Donohue, T., et al., Mice deficient in the CXCR2 ligand, CXCL1 (KC/GRO-alpha), exhibit increased susceptibility to dextran sodium sulfate (DSS)-induced colitis. *Innate Immun*, 2008. 14(2): p. 117-24.
89. Lin, Y., et al., Cleavage of the death domain kinase RIP by caspase-8 prompts TNF-induced apoptosis. *Genes Dev*, 1999. 13(19): p. 2514-26.
90. Feng, S., et al., Cleavage of RIP3 inactivates its caspase-independent apoptosis pathway by removal of kinase domain. *Cell Signal*, 2007. 19(10): p. 2056-67.
91. Seifert, L., et al., The necrosome promotes pancreatic oncogenesis via CXCL1 and Mincle-induced immune suppression. *Nature*, 2016. 532(7598): p. 245-9.
92. Moriwaki, K., S. Balaji, and F.K. Chan, Border Security: The Role of RIPK3 in Epithelium Homeostasis. *Front Cell Dev Biol*, 2016. 4: p. 70.
93. Han, G., et al., Effect of Annexin A1 gene on the proliferation and invasion of esophageal squamous cell carcinoma cells and its regulatory mechanisms. *Int J Mol Med*, 2017. 39(2): p. 357-363.
94. Wang, K.L., et al., Expression of annexin A1 in esophageal and esophagogastric junction adenocarcinomas: association with poor outcome. *Clin Cancer Res*, 2006. 12(15): p. 4598-604.
95. Zhang, M., et al., Artemin is hypoxia responsive and promotes oncogenicity and increased tumor initiating capacity in hepatocellular carcinoma. *Oncotarget*, 2016. 7(3): p. 3267-82.
96. Paterson, A.L., et al., Characterization of the timing and prevalence of receptor tyrosine kinase expression changes in oesophageal carcinogenesis. *J Pathol*, 2013. 230(1): p. 118-28.
97. Manfredi, J.J., Tumor suppression by p53 involves inhibiting an enabler, FGF13. *Proceedings of the National Academy of Sciences of the United States of America*, 2017. 114(4): p. 632-633.
98. Yamashita, K., et al., Clinical significance of secreted protein acidic and rich in cysteine in esophageal carcinoma and its relation to carcinoma progression. *Cancer*, 2003. 97(10): p. 2412-9.
99. Feng, M., et al., Store-independent activation of Orai1 by SPCA2 in mammary tumors. *Cell*, 2010. 143(1): p. 84-98.
100. Andoh, A., et al., Intestinal trefoil factor induces decay-accelerating factor expression and enhances the protective activities against complement activation in intestinal epithelial cells. *J Immunol*, 2001. 167(7): p. 3887-93.
101. Fang, Y. and X. Zhang, Targeting NEK2 as a promising therapeutic approach for cancer treatment. *Cell Cycle*, 2016. 15(7): p. 895-907.
102. Hu, S., et al., miR-532 promoted gastric cancer migration and invasion by targeting NKD1. *Life Sci*, 2017. 177: p. 15-19.
103. Wang, C., et al., Long non-coding RNA HNF1A-AS1 promotes hepatocellular carcinoma cell proliferation by repressing NKD1 and P21 expression. *Biomed Pharmacother*, 2017. 89: p. 926-932.
104. Zhang, S., J. Li, and X. Wang, NKD1 correlates with a poor prognosis and inhibits cell proliferation by inducing p53 expression in hepatocellular carcinoma. *Tumour Biol*, 2016. 37(10): p. 14059-14067.

105. Leung, C.O.-n., et al., PIM1 regulates glycolysis and promotes tumor progression in hepatocellular carcinoma. *Oncotarget*, 2015. 6(13): p. 10880-10892.
106. Warfel, N.A. and A.S. Kraft, PIM kinase (and Akt) biology and signaling in tumors. *Pharmacology & therapeutics*, 2015. 151: p. 41-49.
107. Younes, M., et al., Relationship between dysplasia, p53 protein accumulation, DNA ploidy, and Glut1 overexpression in Barrett metaplasia. *Scand J Gastroenterol*, 2000. 35(2): p. 131-7.
108. Berlth, F., et al., Both GLUT-1 and GLUT-14 are Independent Prognostic Factors in Gastric Adenocarcinoma. *Ann Surg Oncol*, 2015. 22 Suppl 3: p. S822-31.
109. Shen, Y.M., et al., Overexpression of GLUT1 in colorectal cancer is independently associated with poor prognosis. *Int J Biol Markers*, 2011. 26(3): p. 166-72.
110. Zheng, L.S., et al., SPINK6 Promotes Metastasis of Nasopharyngeal Carcinoma via Binding and Activation of Epithelial Growth Factor Receptor. *Cancer Res*, 2017. 77(2): p. 579-589.
111. Shalapour, S., et al., Interleukin-7 links T lymphocyte and intestinal epithelial cell homeostasis. *PLoS One*, 2012. 7(2): p. e31939.
112. Zhang, J., et al., FAM196B acts as oncogene and promotes proliferation of gastric cancer cells through AKT signaling pathway. *Cell Mol Biol (Noisy-le-grand)*, 2017. 63(9): p. 18-23.
113. Porter, S., et al., Dysregulated expression of adamalysin-thrombospondin genes in human breast carcinoma. *Clin Cancer Res*, 2004. 10(7): p. 2429-40.
114. Xie, Y., et al., ADAMTS6 suppresses tumor progression via the ERK signaling pathway and serves as a prognostic marker in human breast cancer. *Oncotarget*, 2016. 7(38): p. 61273-61283.
115. De Boeck, A., et al., Bone marrow-derived mesenchymal stem cells promote colorectal cancer progression through paracrine neuregulin 1/HER3 signalling. *Gut*, 2013. 62(4): p. 550-60.
116. Tritzler, I., et al., Modulation of TGF-beta activity by latent TGF-beta-binding protein 1 in human malignant glioma cells. *Int J Cancer*, 2009. 125(3): p. 530-40.
117. Zang, Y., et al., ELL2 regulates DNA non-homologous end joining (NHEJ) repair in prostate cancer cells. *Cancer Lett*, 2018. 415: p. 198-207.
118. Liu, X., et al., Smad7 but not Smad6 cooperates with oncogenic ras to cause malignant conversion in a mouse model for squamous cell carcinoma. *Cancer Res*, 2003. 63(22): p. 7760-8.
119. Najafi, H., et al., Alternative splicing of the OCC-1 gene generates three splice variants and a novel exonic microRNA, which regulate the Wnt signaling pathway. *Rna*, 2017. 23(1): p. 70-85.
120. Zhang, S., et al., The prognostic role of Gas6/Axl axis in solid malignancies: a meta-analysis and literature review. *Onco Targets Ther*, 2018. 11: p. 509-519.
121. Talari, N.K., et al., Overexpression of aryl hydrocarbon receptor (AHR) signalling pathway in human meningioma. *J Neurooncol*, 2018. 137(2): p. 241-8.
122. Goode, E.L., et al., A genome-wide association study identifies susceptibility loci for ovarian cancer at 2q31 and 8q24. *Nat Genet*, 2010. 42(10): p. 874-9.
123. Hofer-Warbinek, R., et al., A highly conserved proapoptotic gene, IKIP, located next to the APAF1 gene locus, is regulated by p53. *Cell Death Differ*, 2004. 11(12): p. 1317-25.
124. Lountos, G.T., et al., Structure of human dual-specificity phosphatase 7, a potential cancer drug target. *Acta Crystallogr F Struct Biol Commun*, 2015. 71(Pt 6): p. 650-6.
125. Lu, Y., et al., Genome-wide identification of genes essential for podocyte cytoskeletons based on single-cell RNA sequencing. *Kidney Int*, 2017. 92(5): p. 1119-1129.
126. Natarajan, R. and A.D. Linstedt, A cycling cis-Golgi protein mediates endosome-to-Golgi traffic. *Mol Biol Cell*, 2004. 15(11): p. 4798-806.
127. Ezawa, I., et al., Novel p53 target gene FUCA1 encodes a fucosidase and regulates growth and survival of cancer cells. *Cancer Sci*, 2016. 107(6): p. 734-45.

128. Uhlen, M., et al., Proteomics. Tissue-based map of the human proteome. *Science*, 2015. 347(6220): p. 1260419.
129. Samak, G., et al., Calcium/Ask1/MKK7/JNK2/c-Src signalling cascade mediates disruption of intestinal epithelial tight junctions by dextran sulfate sodium. *Biochem J*, 2015. 465(3): p. 503-15.
130. Malchin, N., et al., A novel homozygous deletion in EXPH5 causes a skin fragility phenotype. *Clin Exp Dermatol*, 2016. 41(8): p. 915-918.
131. Thangaraju, M., et al., GPR109A is a G-protein-coupled receptor for the bacterial fermentation product butyrate and functions as a tumor suppressor in colon. *Cancer Res*, 2009. 69(7): p. 2826-32.
132. Singh, N., et al., Activation of Gpr109a, receptor for niacin and the commensal metabolite butyrate, suppresses colonic inflammation and carcinogenesis. *Immunity*, 2014. 40(1): p. 128-39.
133. Dong, W., et al., Decreased expression of Rab27A and Rab27B correlates with metastasis and poor prognosis in colorectal cancer. *Discov Med*, 2015. 20(112): p. 357-67.
134. Li, J., et al., Effects of Rab27A and Rab27B on Invasion, Proliferation, Apoptosis, and Chemoresistance in Human Pancreatic Cancer Cells. *Pancreas*, 2017. 46(9): p. 1173-1179.
135. Xie, Y. and B. Wang, Downregulation of TNFAIP2 suppresses proliferation and metastasis in esophageal squamous cell carcinoma through activation of the Wnt/beta-catenin signaling pathway. *Oncol Rep*, 2017. 37(5): p. 2920-2928.
136. Fullar, A., et al., Lack of Matrilin-2 favors liver tumor development via Erk1/2 and GSK-3beta pathways in vivo. *PLoS One*, 2014. 9(4): p. e93469.
137. Cao, S., J.K. Iyer, and V. Lin, Identification of tetratricopeptide repeat domain 9, a hormonally regulated protein. *Biochem Biophys Res Commun*, 2006. 345(1): p. 310-7.
138. Zeng, P., et al., TMPRSS4 as an emerging potential poor prognostic factor for solid tumors: A systematic review and meta-analysis. *Oncotarget*, 2016. 7(46): p. 76327-76336.
139. Lundstrom, A. and T. Egelrud, Stratum corneum chymotryptic enzyme: a proteinase which may be generally present in the stratum corneum and with a possible involvement in desquamation. *Acta Derm Venereol*, 1991. 71(6): p. 471-4.
140. Marchelletta, R.R., et al., The class V myosin motor, myosin 5c, localizes to mature secretory vesicles and facilitates exocytosis in lacrimal acini. *Am J Physiol Cell Physiol*, 2008. 295(1): p. C13-28.
141. Sladewski, T.E., E.B. Kremmentsova, and K.M. Trybus, Myosin Vc Is Specialized for Transport on a Secretory Superhighway. *Curr Biol*, 2016. 26(16): p. 2202-7.
142. Okumura, S., et al., Involvement of gicerin in the extension of microvilli. *Exp Cell Res*, 2001. 271(2): p. 269-76.
143. Simon, G.C., et al., Up-regulation of MUC18 in airway epithelial cells by IL-13: implications in bacterial adherence. *Am J Respir Cell Mol Biol*, 2011. 44(5): p. 606-13.
144. Yoder, M. and J.D. Hildebrand, Shroom4 (Kiaa1202) is an actin-associated protein implicated in cytoskeletal organization. *Cell Motil Cytoskeleton*, 2007. 64(1): p. 49-63.
145. Lee, C., M.P. Le, and J.B. Wallingford, The shroom family proteins play broad roles in the morphogenesis of thickened epithelial sheets. *Dev Dyn*, 2009. 238(6): p. 1480-91.
146. Honda, Y., et al., Decreased Skin Barrier Lipid Acylceramide and Differentiation-Dependent Gene Expression in Ichthyosis Gene Nipal4 Knockout Mice. *J Invest Dermatol*, 2017. 2018. 138(4): p. 741-9.
147. Arslan, B., et al., Characterizing interaction forces between actin and proteins of the tropomodulin family reveals the presence of the N-terminal actin-binding site in leiomodlin. *Arch Biochem Biophys*, 2018. 638: p. 18-26.
148. Timpl, R., et al., Fibulins: a versatile family of extracellular matrix proteins. *Nat Rev Mol Cell Biol*, 2003. 4(6): p. 479-89.

149. Balbona, K., et al., Fibulin binds to itself and to the carboxyl-terminal heparin-binding region of fibronectin. *J Biol Chem*, 1992. 267(28): p. 20120-5.
150. Stucke, V.M., et al., The MAGUK protein MPP7 binds to the polarity protein hDlg1 and facilitates epithelial tight junction formation. *Mol Biol Cell*, 2007. 18(5): p. 1744-55.
151. Botelho, N.K., et al., Gene expression alterations in formalin-fixed, paraffin-embedded Barrett esophagus and esophageal adenocarcinoma tissues. *Cancer Biol Ther*, 2010. 10(2): p. 172-9.
152. Shimizu, T., et al., Characterization of progressive metaplasia in the gastric corpus mucosa of Mongolian gerbils infected with *Helicobacter pylori*. *J Pathol*, 2016. 239(4): p. 399-410.
153. Naydenov, N.G. and A.I. Ivanov, Adducins regulate remodeling of apical junctions in human epithelial cells. *Mol Biol Cell*, 2010. 21(20): p. 3506-17.
154. Neri, P., et al., Integrin beta7-mediated regulation of multiple myeloma cell adhesion, migration, and invasion. *Blood*, 2011. 117(23): p. 6202-13.
155. Menke, V., et al., Conversion of metaplastic Barrett's epithelium into post-mitotic goblet cells by gamma-secretase inhibition. *Dis Model Mech*, 2010. 3(1-2): p. 104-10.
156. Pavlovic, M., et al., Enhanced MAF Oncogene Expression and Breast Cancer Bone Metastasis. *J Natl Cancer Inst*, 2015. 107(12): p. djv256.
157. Yang, H., et al., Deregulated methionine adenosyltransferase alpha1, c-Myc, and Maf proteins together promote cholangiocarcinoma growth in mice and humans(double dagger). *Hepatology*, 2016. 64(2): p. 439-55.
158. Kochupurakkal, B.S., et al., Epigen, the last ligand of ErbB receptors, reveals intricate relationships between affinity and mitogenicity. *J Biol Chem*, 2005. 280(9): p. 8503-12.
159. Sun, X., et al., FBXO2, a novel marker for metastasis in human gastric cancer. *Biochem Biophys Res Commun*, 2018. 495(3): p. 2158-2164.
160. Sakamaki, A., et al., Bcl11b SWI/SNF-complex subunit modulates intestinal adenoma and regeneration after gamma-irradiation through Wnt/beta-catenin pathway. *Carcinogenesis*, 2015. 36(6): p. 622-31.
161. Abbas, S., et al., Integrated genome-wide genotyping and gene expression profiling reveals BCL11B as a putative oncogene in acute myeloid leukemia with 14q32 aberrations. *Haematologica*, 2014. 99(5): p. 848-57.
162. Bae, D.H., et al., The role of NDRG1 in the pathology and potential treatment of human cancers. *J Clin Pathol*, 2013. 66(11): p. 911-7.
163. Yokobori, T. and M. Nishiyama, TGF-beta Signaling in Gastrointestinal Cancers: Progress in Basic and Clinical Research. *J Clin Med*, 2017. 6(1).
164. Huang, D., et al., Overexpression of LAMC2 predicts poor prognosis in colorectal cancer patients and promotes cancer cell proliferation, migration, and invasion. *Tumour Biol*, 2017. 39(6): p. 1010428317705849.
165. Shou, J.Z., et al., Overexpression of CDC25B and LAMC2 mRNA and protein in esophageal squamous cell carcinomas and premalignant lesions in subjects from a high-risk population in China. *Cancer Epidemiol Biomarkers Prev*, 2008. 17(6): p. 1424-35.
166. Zhang, T., et al., A Deregulated PI3K-AKT Signaling Pathway in Patients with Colorectal Cancer. *J Gastrointest Cancer*, 2019. 50(1): p. 35-41.
167. Qi, L. and Y. Ding, Screening and regulatory network analysis of survival-related genes of patients with colorectal cancer. *Sci China Life Sci*, 2014. 57(5): p. 526-31.
168. Viana Lde, S., et al., Relationship between the expression of the extracellular matrix genes SPARC, SPP1, FN1, ITGA5 and ITGAV and clinicopathological parameters of tumor progression and colorectal cancer dissemination. *Oncology*, 2013. 84(2): p. 81-91.

169. Mierke, C.T., et al., Integrin  $\alpha 5 \beta 1$  facilitates cancer cell invasion through enhanced contractile forces. *J Cell Sci*, 2011. 124(Pt 3): p. 369-83.
170. Desgrosellier, J.S. and D.A. Cheresh, Integrins in cancer: biological implications and therapeutic opportunities. *Nat Rev Cancer*, 2010. 10(1): p. 9-22.
171. Mansilla, F., et al., Lysophosphatidylcholine acyltransferase 1 (LPCAT1) overexpression in human colorectal cancer. *J Mol Med (Berl)*, 2009. 87(1): p. 85-97.
172. Minarowska, A., et al., Regulatory role of cathepsin D in apoptosis. *Folia Histochem Cytobiol*, 2007. 45(3): p. 159-63.
173. Zou, J., et al., APOBEC3B, a molecular driver of mutagenesis in human cancers. *Cell Biosci*, 2017. 7: p. 29.
174. Brognard, J. and A.C. Newton, PHLiPPing the switch on Akt and protein kinase C signaling. *Trends Endocrinol Metab*, 2008. 19(6): p. 223-30.
175. Gao, T., F. Furnari, and A.C. Newton, PHLPP: a phosphatase that directly dephosphorylates Akt, promotes apoptosis, and suppresses tumor growth. *Mol Cell*, 2005. 18(1): p. 13-24.
176. Pang, X., et al., Knockdown of Rhotekin 2 expression suppresses proliferation and induces apoptosis in colon cancer cells. *Oncol Lett*, 2017. 14(6): p. 8028-8034.
177. Liao, Y.X., et al., Silencing of RTKN2 by siRNA suppresses proliferation, and induces G1 arrest and apoptosis in human bladder cancer cells. *Mol Med Rep*, 2016. 13(6): p. 4872-8.
178. Wei, W., H. Chen, and S. Liu, Knockdown of Rhotekin 2 expression suppresses proliferation and invasion and induces apoptosis in hepatocellular carcinoma cells. *Mol Med Rep*, 2016. 13(6): p. 4865-71.
179. Deryugina, E.I., et al., LTBP3 promotes early metastatic events during cancer cell dissemination. *Oncogene*, 2018. 37(14): p. 1815-29.
180. Hou, Z., et al., HBx-related long non-coding RNA MALAT1 promotes cell metastasis via up-regulating LTBP3 in hepatocellular carcinoma. *Am J Cancer Res*, 2017. 7(4): p. 845-856.







# Chapter 3

---

## Forced expression of *HOXA13* confers oncogenic hallmarks to esophageal keratinocytes

Vincent T. Janmaat\* · Kateryna Nesteruk\* · Hui Liu · Timo L.M. Ten Hagen ·  
Maikel P. Peppelenbosch · Gwenny M. Fuhler

\* These authors contributed equally

*Biochim Biophys Acta Mol Basis Dis.* 2020;1866(8):165776

## Abstract

*HOXA13* overexpression has been detected in human ESCC tissue and high *HOXA13* protein expression is correlated with a shorter median survival time in ESCC patients. Although aberrant expression of *HOXA13* in ESCC has thus been established, little is known regarding the functional consequences thereof. The present study aimed to examine to what extent aberrant *HOXA13* might drive carcinogenesis in esophageal keratinocytes. To this end, we overexpressed *HOXA13* in a non-transformed human esophageal cell line EPC2-hTERT, performed gene expression profiling to identify key processes and functions, and performed functional experiments. We found that *HOXA13* expression confers oncogenic hallmarks to esophageal keratinocytes. It provides proliferation advantage to keratinocytes, reduces sensitivity to chemical agents, regulates MHC class I expression and differentiation status and promote cellular migration. Our data indicate a crucial role of *HOXA13* at early stages of esophageal carcinogenesis.

## Introduction

Esophageal cancer is the 8th most common cancer worldwide and the 6th cause of cancer related death (1-3). Moreover, the prevalence of esophageal cancer has been growing; it rose by 44% from 1990 and reached 455,800 new cases per year in 2012. Approximately 85% of patients have a histological subtype called esophageal squamous cell carcinoma (ESCC), which is especially frequent in Eastern Asia, particularly in China (2, 4). Contributing to ESCC development are environmental factors (alcohol consumption and tobacco use, a diet low in fruits and vegetables, ingestion of very hot food and beverages, etc.), genetic factors (e.g. aldehyde dehydrogenase (ALDH2) deficiency) and predisposing diseases (achalasia, tylosis) (3, 5). ESCC arises from dysplastic precursor lesions: patches of squamous epithelial cells exhibiting nuclear atypia and abnormal maturation, but which do not invade through the basement membrane until disease progression to invasive carcinoma occurs (6). ESCC is usually diagnosed at an advanced stage and prognosis is poor, with only 15% to 25% of patients diagnosed with ESCC surviving for 5 years after diagnosis (7).

While some studies have investigated the molecular pathways underlying ESCC development, disease etiology is still poorly understood. However, a possible role for *HOX* genes in ESCC development is now emerging. *HOX* genes are a highly conserved family of transcription factors which play a crucial role in the development of an embryo along the anterior-posterior axis (8, 9). In humans, 39 *HOX* genes are expressed with temporal and spatial collinearity (10, 11) which persists in adult tissues such as the skeleton and digestive system (12). For example, The *HOX13* paralogues (*HOXA13*, *HOXB13*, and *HOXD13*) show high expression in the hindgut region and weak expression in the foregut including the esophagus (13). As carcinogenesis can be seen as an aberrant form of organogenesis, these transcription factors may also regulate carcinogenic pathways (14-19). Both tumor-promoting and tumor-suppressing properties have been ascribed to *HOX* genes (20). *HOXA13* overexpression has been detected in human ESCC tissue (21), and in other types of cancer like gastric cancer, cervical cancer, ovarian cancer and prostate carcinoma (22-25). High *HOXA13* protein expression is correlated with a shorter median survival time in ESCC patients (26) and poor clinicopathological characteristics of patients (27). The expression profile of *HOXA13*, *ANXA2* and *SOD2* was suggested as predictive marker of the postoperative outcome of patients with ESCC (28). Expression of *FGF2*, the normal morphogen of *HOXA13*, also correlates with poor survival of patients with ESCC (29).

Although aberrant expression of *HOXA13* in ESCC has thus been established, little is known regarding the functional consequences thereof. One study investigated the molecular targets of *HOXA13* in a cancer cell model of ESCC by CHIP-DSL and identified 1938 gene promoters. The targeted genes mostly regulate cell proliferation, survival, and migration (30) and functional assays confirmed that knockdown of

*HOXA13* decreased tumor growth *in vivo* and colony formation of ESCC cell lines *in vitro* (26). Similarly, elevated *HOXA13* expression promoted the proliferation and metastasis of gastric cancer partly via activating Erk1/2 (31) while downregulation of *HOXA13* sensitizes human ESCC to chemotherapy (32).

Although *HOXA13* seems to play a prognostic role when esophageal cancer has already been established, it remains unknown if there is a causal relationship between *HOXA13* and ESCC and whether this factor can drive neoplastic transformation. Advancement of high-throughput genomic technologies has led to a better understanding of the molecular basis of ESCC development (33, 34). ESCC and even its precursor lesion are highly mutated and heterogeneous diseases, but early events of ESCC are not completely clear. The present study aimed to examine to what extent aberrant *HOXA13* might drive oncogenic hallmarks in esophageal keratinocytes. To this end, we overexpressed *HOXA13* in a non-transformed human esophageal cell line, performed gene expression profiling to identify key processes and functions, and employed functional experiments to study the role of *HOXA13* in keratinocytes.

## Methods

### Cell lines

EPC2-hTERT cells (35) are normal hTERT immortalized human esophageal keratinocytes. Cells were routinely cultured in keratinocyte–serum-free medium (KSFM) without calcium chloride ( $\text{CaCl}_2$ ) (17005042, Gibco), supplemented with 50  $\mu\text{g}/\text{ml}$  bovine pituitary extract (BPE) (129-5, Cell Applications), 1 ng/ml human recombinant epidermal growth factor (EGF) (E9644-.2 Sigma) and Penicillin-Streptomycin (100u/ml, Gibco). Cell line identity was confirmed with short tandem repeats (STR) analysis by DSMZ and cells were routinely checked for Mycoplasma infection (Eurofins, Ebersberg, Germany).

### Generation of EPC2-hTERT *HOXA13* overexpression model

Amplification of the human *HOXA13* gene including its single intron was performed with Q5 polymerase using primers (AgeI HoxA13 F; GTGGTACCGGTGCCACCATGACAGCCTCCGTGCTCCT, and XbaI HoxA13 R; ACCACCTCTAGATTAAGTAGTGGTTTTCAGTT). The gene was cloned into pEN\_TmiRc3 using AgeI and XbaI restriction sites, a gift from Iain Fraser (Addgene #25748, Cambridge, USA) (36). Subsequently, two plasmids with and without the *HOXA13* insert were prepared. The *HOXA13* insert was transferred into pSLIK-Venus, using a Gateway reaction (37). pSLIK-Venus was a gift from Iain Fraser (Addgene #25734) (36). Both plasmids were sequenced by LGC Genomics (Teddington, UK).

Next, they were packaged into lentiviral particles following transfection in HEK293T cells with third generation packaging plasmids. The supernatant was collected and ultracentrifuged. EPC2-hTERT cells were transduced with the virus and YFP (pSLIK-Venus) positive cells were sorted by Fluorescence-Activated Cell Sorting (FACS; BD FACSCanto™ II, BD Biosciences, San Jose, CA). These cells were grown and analyzed as a heterogeneous cell pool. Cells transduced with control vector are hereafter called ‘control’, while cells transduced with the *HOXA13*-containing plasmid are denoted as *HOXA13*<sup>+</sup> cells. While *HOXA13* gene expression was supranormally induced by 1.25 µg/ml doxycycline in the culture medium, ‘leakage’ of the vector caused *HOXA13* overexpression even in absence of doxycycline (**Supplementary Figure S1A**) (38, 39). Doxycyclin itself affected growth of EPC2-hTERT cells (**Supplementary Figure S1B**). For this reason, doxycycline was not added to functional assays with longer timepoints.

### RNA isolation

RNA was isolated using the NucleoSpin RNA isolation kit (Macherey Nagel, Düren, Germany). RNA concentrations were measured using a Nanodrop spectrophotometer and samples were stored in RNA storage solution (Sodium Citrate pH 6.4), obtained from Ambion (Foster City, USA) and kept at -80°C. RNA integrity and quantity were determined by the Agilent 2100 Bioanalyzer.

### RNA-Seq

The EPC2-hTERT samples were prepared with the TruSeq Stranded mRNA Library Prep Kit. Sequencing took place according to the Illumina TruSeq v3 protocol on an Illumina HiSeq2500 sequencer. 50 base-pairs reads were generated and mapped against reference genome hg19 with Tophat (version 2.0.10). Expression was quantified using HTseq-count (0.6.1). Data were processed using R. version 3.2.5, (40) module DeSeq2 (41). Generated fold changes (FCs) and *p* values were analyzed using ingenuity pathway analysis (IPA) (QIAGEN Inc., <https://www.qiagenbioinformatics.com/products/ingenuitypathway-analysis>) (42).

Only differentially expressed genes with a *p* value <0.05 in RNA-Seq were used as input data. In IPA analysis, *p* value (calculated using a Right-Tailed Fisher’s Exact Test) reflects the likelihood that the association or overlap between a set of significant molecules from the experiment and a given process/pathway/transcription neighborhood is due to random chance. The smaller the *p* value, the less likely that the association is random. The *p* value does not consider the directional effect of one molecule on another or the direction of change of molecules in the dataset. Z-scores, a statistical measure of correlation between relationship direction and gene expression were considered significant when > 2 or < -2. Z-score takes into account the directional effect of one molecule on another molecule or on a process and the direction of change of molecules

in the dataset. Canonical pathway analysis identified the pathways most significant to the data set, based the ratio of the number of proteins from the data set that map to a pathway divided by the total number of proteins assigned to this canonical pathway.

### **FACS**

EPC2-hTERT cells were stained with 5  $\mu$ l of Anti-human HLA-ABC (APC) antibody per 50  $\mu$ l (Clone W6/32, eBioscience, #17-9983-41) in 2% mouse serum, for 15 minutes at room temperature. Cells were analyzed on a FACSCanto II flow cytometer (BD Biosciences, San Jose, CA) and analyzed with FlowJo v10 (FLOWJO, LLC).

### **MTT assay**

MTT assays were performed as previously described (43). Transduced EPC2-hTERT cells were seeded in a 96-wells plate, 1000 cells/well. After 24 h, 3, 5 and 7 days 10  $\mu$ l of 5 mg/mL MTT reagent (Sigma-Aldrich Chemie BV) was added to 100  $\mu$ l of culturing medium. After 3h of incubation at 37°C, medium was replaced by dimethyl sulfoxide (DMSO; Sigma-Aldrich). OD was measured in a Model 680 XR microplate reader (Bio-Rad, USA). This experiment was repeated three times.

### **Cell adhesion test**

EPC2-hTERT cells were in seeded in 96 well plate (20,000 cells per well). After 60 mins, 90 mins, 2 h, 3 h, 4 h, 6 h unattached cells were removed from the wells and counted by hemocytometer with Trypan Blue (Sigma-Aldrich Chemie BV). This experiment was repeated four times.

### **3D culture EPC2-hTERT cells**

3D culturing of EPC2-hTERT cells was performed as previously described (44). 4000 EPC2-hTERT cells were seeded in 50  $\mu$ L drop of ice-cold 1:1 mixture of Matrigel basement membrane matrix (Corning BV) with culture medium in a 24 well plate for cell suspension, and incubated at 37°C for 30 minutes. After solidification, 500  $\mu$ L of medium was added supplemented with 0.6 mM  $\text{CaCl}_2$ . Y27632 (10  $\mu$ M) was included in medium only first 24 h after seeding. Medium was refreshed every 2-3 days. Pictures were made every three days. Morphological assessment was performed on day 12. Differentiated spheroids were characterized by at least three layers of prolonged cells and a nuclei-free mass in the middle, undifferentiated spheroids had round nuclei and lacked the cell-free area in the center. The area of the spheroids was measured with FIJI (45) on photographs taken on day 2, 5 and 8 of culture.

### Histology and immunohistochemistry of 3D culture

EPC2-hTERT spheroids were fixed in 4% formaldehyde for 7 mins on day 11, washed with PBS, put in 2% agarose, and embedded in paraffin. Then 4  $\mu$ m slices were sectioned for H&E and immunohistochemistry staining.

For IHC, slides were deparaffinized and rehydrated followed by sodium citrate antigen retrieval (microwaved for 15 min at 200 Watt). Then they were blocked with Goat serum diluted 1:10 in PBS and incubated overnight at 4°C with anti-IVL (mouse monoclonal anti-IVL I9018, 1:500; Sigma-Aldrich) or anti-CK19 (rabbit monoclonal anti-cytokeratin-19 EP72, 1:100, BSB 5382, ITK Diagnostic). After this, secondary antibodies (Dako EnVision+System-HRR labeled Polymer Anti Mouse, Dako) were applied for 30 mins at RT. Next, slides were counterstained with hematoxylin for 10s, dehydrated, and mounted with Pertex. Stained objects were captured and imaged with Axiovert 40 CFL Zeiss microscope (20x objective), Leica DFC400 digital camera and Leica Application Suite software (Leica Microsystems). Quantification was based on the percentage of positive cells and intensity of the staining (scores ranged from 0, 2 to 9).

### 2D migration assays

2D migration assays were performed as previously described (46). Sterile coverslips placed in an Attofluor incubation chamber were coated with gelatin (1 mg/ml) and incubated for 1 h at 37°C, prior to cell seeding. A removable circular sterile migration barrier was inserted into the chamber, which prevents cell growth in the center of the coverslip.  $2.5 \times 10^5$  EPC2 *HOXA13* overexpression and control cells were seeded around this barrier and the rings were incubated at 37°C for 24 h. A confluent monolayer grew in the periphery and a cell-free area was present in the center of the coverslip. After removing the migration barrier, time-lapse imaging was conducted at 37°C under humidified 5% CO<sub>2</sub> airflow for 24 h on an Axiovert 100M inverted microscope, equipped with an AxioCam MRC digital camera, using a 10X/0.30 Plan-Neofluar objective (Carl Zeiss B.V., Sliedrecht, Netherlands). ‘Total migration’ is the net track movement of cells in 24 h, ‘effective migration’ is the directional movement of cells to the cell-free center of the coverslip. Migration efficiency was determined as the percentage of directional movement over the total track distance. Velocity was defined as distance per hour. For each cell line, at least three independent migration assays were performed, data of one representative experiment are depicted.

### 3D-migration using cell dispersion assay

The procedure was performed as described before (47). Cytodex-3 microcarrier beads (Sigma–Aldrich) were mixed with  $5 \times 10^5$  EPC2-hTERT *HOXA13* overexpression and control cell suspensions, which constitutes a density of 40 cells per bead. These suspensions were incubated at 37°C for 6 h with gentle mixing. The bead suspension

was transferred to a 25 cm<sup>2</sup> tissue culture flask and incubated for 48 h to ensure complete coating of beads and to remove unattached cells. Coated beads were embedded in 1.6 mg/ml collagen gel (collagen: modified Eagle's medium: 7.5% w/v NaHCO<sub>3</sub> in the ratio 11:8:1) in a 24-well plate such that each well had approximately 150 beads. Plates were incubated at 37°C for 2 h for the beads to settle in the gel and the polymerized gels were covered with 500 µl DMEM, 10% FBS, 1% p/s. Cell dispersion was measured as the maximum migrated distance from the surface of the bead into the collagen gel. All measurements were performed using AxioVision 4.5 software and assays were performed twice with ten beads per group. Two-way analysis of variance was performed to calculate *p* values.

### **Phosphoprotein profiling**

EPC2 control and *HOXA13* transduced cells were seeded in a 6 well plate. When they reached 80-90% of confluency, total proteins were extracted in 300 µl Laemmli Buffer (SDS 4%, glycerol 20%, Tris-Cl (pH 6.8) 120 mM, bromophenol blue 0.02% (w/v) and DTT 0.1 M) and the protein concentrations were measured using RC DC Protein Assay (Bio Rad). Western blotting was performed as described before (47, 48). Briefly, proteins were resolved by SDS-PAGE and blotted onto Immobilon FL PVDF membranes (Millipore, Bedford, MA, USA). Membranes were blocked in Odyssey Blocking Buffer (Thermo Fisher Scientific) and incubated overnight at 4°C with primary antibody (See **Supplementary Table S1** for details), followed by the appropriate Alexa-linked secondary antibodies, at 1:5000 dilution, in Odyssey Blocking Buffer for 1 h. The fluorescent bands were detected using fluorescent Odyssey Imaging System and densitometric analysis was performed with Image Studio Lite Ver.5.2 (49). All blots were reprobed for Actin to control for equal loading and normalized results are represented as ratios of protein of interest over Actin levels per lane. Three independent experiments were performed, run together on one blot, and heat maps of the phospho-protein profile in the 6 samples were constructed with CIMminer (Genomics and Bioinformatics Group, Laboratory of Molecular Pharmacology, Center for Cancer Research, National Cancer Institute) (50). For some samples, more than one western blot was run for particular phospho-proteins – in this case the mean for that particular sample was used for heatmap preparation.

### **Drug sensitivity assay**

10,000 EPC2 cells per well were seeded in 96 well plate. Next day, 10 µl of chemical compounds were added to 90 µl of cell culture medium and added to cells (see **Supplementary Table S2** for the information on compounds and range of its serial dilution). The final concentration of solvents (DMSO, Ethanol or dH<sub>2</sub>O) was 1%. Appropriate controls for solvents were made. After incubation for 72 h, MTT test was performed as described above. Each concentration was tested in quadruplicates, and



experiments were performed at least three times for each drug (**Supplementary Table S2**).

### Statistics

A two-way analysis of variance (ANOVA) was used to test for significant differences at each time point in the MTT assay, measurement of area of spheroids, and for 3D migration assay (Graphpad Prism 5; GraphPad Software Inc., USA). For the comparison of the level of MHC class I, IHC score, Western Blot data, and for the 2D migration assay a *t*-test or Mann-Whitney test was used based on the result of normality test (either a Komogorov-Smirnov test, the D'Agostino, Pearson omnibus normality test or the Shapiro-Wilk normality test). *P* values <0.05 were considered to be statistically significant. Statistical analyses of proportions were performed with “N-1” Chi-squared test using MedCalc for Windows, version 18.11.3 (MedCalc Software, Ostend, Belgium) [https://www.medcalc.org/calc/comparison\\_of\\_proportions.php](https://www.medcalc.org/calc/comparison_of_proportions.php).

## Results

### HOXA13 alters keratinocyte gene expression profiles

In order to investigate the tumor-initiating role of *HOXA13* in ESCC, we overexpressed this transcription factor in the primary immortalized esophageal squamous epithelial cell line EPC2-hTERT, which has low endogenous levels of *HOXA13*, and determined the ensuing molecular consequences by RNAseq profiling. A log2FC of 5.24 confirmed successful overexpression of *HOXA13* ( $p < 3.14 \times 10^{-215}$ ). This affected 2995 genes: 1745 (58.3%) were downregulated and 1250 upregulated ( $p < 0.05$ ) (log2 fold change (FC) ranging from -5.28 to 4.97). The top 20 of *HOXA13*-induced differentially expressed genes and functions of their products are reported in **Table 1**. Upregulation of *ANPEP*, *MAGEA11*, *LCPI*, *CSAG1*, *CSAG1*, *ZNF486*, *MAGEA12*, *GPC4*, *CYP24A1*, *LRRC38* was observed, while *UBR1*, *PSMB8*, *UBR1*, *PSMB8*, *EPSTI1*, *SAMD9L*, *APOL6*, *TLR3*, *GBP1*, *SLC12A7*, *HS6ST2*, *SFRP1* are down-regulated. Subsequently, *in silico* functional enrichment analysis was performed for all differentially expressed genes. Canonical pathway analysis indicates that *HOXA13* influenced both metabolic and signaling pathways. The top canonical pathways affected include Antigen Presentation Pathway, Molecular Mechanisms Of Cancer, Epithelial Adherent Junction Signaling and 14-3-3 protein-Mediated Signaling. An extended list of pathways based on Z-scores > 2 and < -2 is shown in **Figure 1A and B**. A clear indication of altered cytoskeletal rearrangement was seen, as evidenced by the signaling by Rho family GTPases, Rac GTPase signaling and its downstream PAK signaling. IPA prediction indicates that altered transcriptome upon *HOXA13* expression would affect the following molecular and cellular categorical functions: Cell Death And Survival, Cellular Movement,

Cellular Assembly And Organization, Cellular Function And Maintenance, Cellular Development. On organismal level *HOXA13* overexpression affects Physiological System Development, Organismal Survival, Organismal Development, and Cardiovascular Development and Function.

Functional analysis identified the toxic functions and diseases that were most significant to the data set. The top three Disease and Disorders categories identified were Cancer ( $p$  value

**Table 1.** Top *HOXA13*-induced differentially expressed genes

Gene	log2FoldChange	$p$ value	Protein function, biological processes
<i>HOXA13</i>	5.46	3.14E-215	
<i>ANPEP</i>	4.97	2.35E-255	membrane alanyl aminopeptidase
<i>MAGEA11</i>	2.55	3.91E-39	part of the androgen receptor signaling pathway, linked to cancer development
<i>LCPI</i>	2.38	3.37E-60	actin binding, actin filament network formation, cell migration
<i>CSAG1</i>	2.13	1.11E-26	unknown, tumor antigen
<i>ZNF486</i>	2.11	6.81E-37	DNA binding, regulation of transcription
<i>MAGEA12</i>	2.10	1.40E-26	protein binding, tumor antigen
<i>GPC4</i>	1.94	6.34E-22	transmembrane receptor, cell proliferation and differentiation
<i>CYP24A1</i>	1.82	3.75E-20	mitochondrial monooxygenase
<i>LRRC38</i>	1.81	6.58E-26	potassium channel regulator, ion transport
<i>UBR1</i>	-3.06	3.14E-293	ubiquitin-protein ligase activity, protein catabolic process
<i>PSMB8</i>	-3.11	3.00E-138	antigen presentation, interferon signaling, protein ubiquitination
<i>EPSTI1</i>	-3.15	2.04E-59	unknown
<i>SAMD9L</i>	-3.72	1.21E-123	protein binding, proliferation, cell division, differentiation
<i>APOL6</i>	-3.86	4.44E-161	lipid binding, lipid transport; lipoprotein metabolic process
<i>TLR3</i>	-3.94	2.06E-110	transmembrane receptor, pathogen recognition and activation of innate immunity
<i>GBP1</i>	-4.16	5.79E-135	guanylate binding, cell response to interferon
<i>SLC12A7</i>	-4.60	1.95E-150	electroneutral potassium-chloride cotransporter, cell volume homeostasis
<i>HS6ST2</i>	-4.64	1.03E-150	heparan sulfate 6-O-sulfotransferase, glycosaminoglycan biosynthesis
<i>SFRP1</i>	-5.28	2.40E-263	cysteine endopeptidase, soluble modulators of Wnt signaling

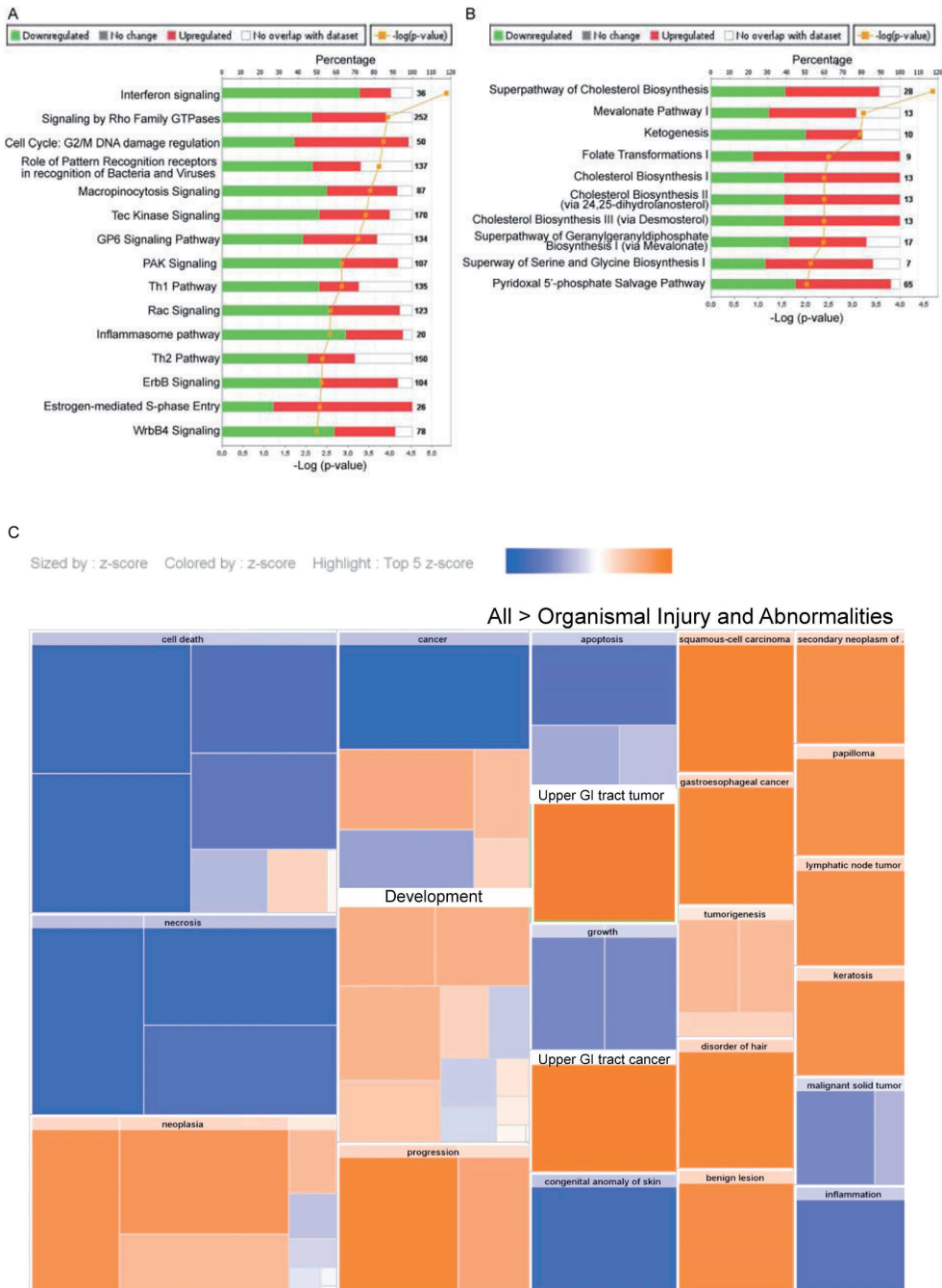


**Figure 1.** *In silico* functional enrichment analysis: signaling (A) and metabolic (B) canonical pathways regulated by *HOXA13*. Z-score > 2 or < -2. (C) Organismal injury and abnormalities caused by *HOXA13* overexpression. Downregulated processes by *HOXA13* are shown in blue, upregulated processes in orange. General cancerous processes are decreased ('cancer'), while "upper GI tract tumor", "upper GI tract cancer", "squamous cell carcinoma" are increased.

= 7.98E-08 – 1.22E-83, #Molecules = 2739), Organismal Injury And Abnormalities ( $p$  value = 8.08E-08 – 1.22E-83, #Molecules = 2768) and Gastrointestinal Disease ( $p$  value = 8.08E-08 – 7.69E-08 – 9.19E-68, #Molecules = 2533). Z-score for cancerous processes in general was negative (Z-score = -2.507) indicating inhibition of such processes, however, for such categories as Upper Gastrointestinal Tract Tumor, Upper Gastrointestinal Tract Cancer and Squamous-cell Carcinoma, Z-scores were positive (Z-score = 2.451, Z-score = 2.236, Z-score = and 2.157 respectively) indicating activation of these processes (**Table 2, Figure 2**). Upstream regulator analysis for the 2995 genes involved in the preceding processes was used to identify the potential upstream transcriptional regulators that can explain the observed gene expression changes our dataset (42). *TP53* (log2FC = 0.032, activation Z-score = -1.723,  $p=295E-35$ ), *TGFB1* (log2FC = 0.156, activation Z-score = 1.456,  $p=5.88E-33$ ), *TNF- $\alpha$*  (log2FC = 0.155, activation Z-score = -2.773,  $p=3.78E-32$ ), *IFNL1* (activation Z-score = -6.991,  $p=1.93E-30$ ) and *OSM* (activation Z-score = -2.167) were indicated as the most significant regulators, of which *TP53* (51), *TGFB1* (52) and *TNF- $\alpha$*  (53) have previously been implicated in ESCC pathogenesis. In total, these results suggest a specificity of *HOXA13* for gastrointestinal tumorigenesis and squamous cells carcinomas in particular.

**Table 2.** IPA predicted toxic functions and diseases caused by *HOXA13* overexpression

Categories	$p$ value	Predicted activation state	Activation Z-score	#Molecules
Cancer	1.80E-76	Decreased	-2.5	2690
Necrosis of tumor	1.83E-08	Decreased	-2.4	135
Cell death of tumor cells	4.35E-08	Decreased	-2.4	131
Necrosis of tumor	1.83E-08	Decreased	-2.4	135
Upper gastrointestinal tract tumor	2.20E-18	Increased	2.5	754
Upper gastrointestinal tract cancer	4.12E-17	Increased	2.2	599
Squamous-cell carcinoma	2.95E-14	Increased	2.2	805
Gastroesophageal cancer	6.94E-13	Increased	2.0	483

### ***HOXA13* influences oncogenic cellular phosphoprofile**

Next, we investigated to what extent *HOXA13*-induced transcriptomic changes are translated to altered signal transduction patterns. To this end, we performed phosphoprotein profiling to quantify the expression and activation status of several important signal transduction pathways and targeted some of these pathways with molecular inhibitors. A distinctly altered phosphoprofile was seen upon *HOXA13* overexpression, as evidenced by the clustering of control and overexpressing samples (**Figure 2A, Supplementary Figure S2** for individual western blot examples and

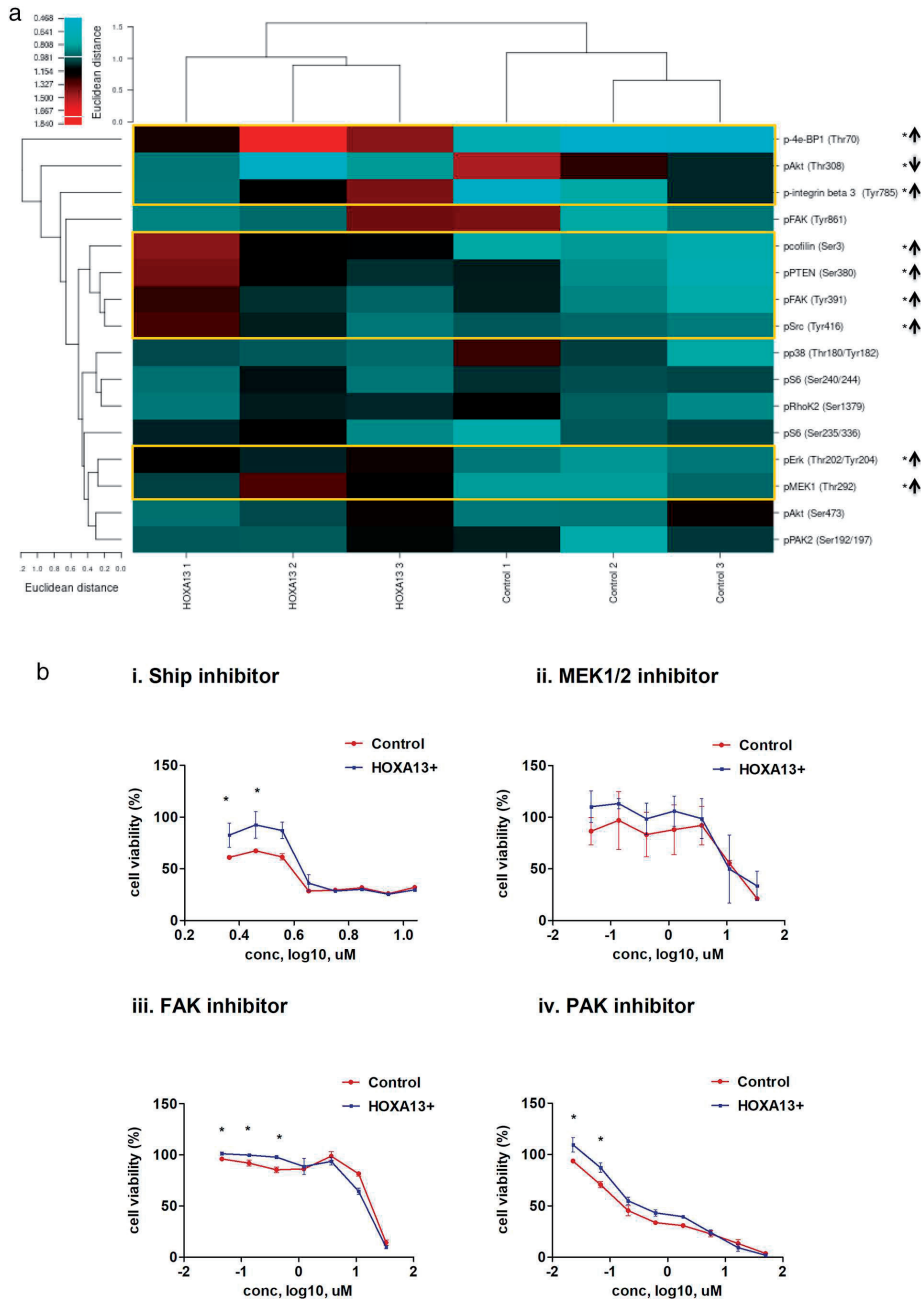


**Figure 2.** Phosphorylation events are modulated by *HOXA13*. **(A)** *HOXA13* influences cellular phosphoprofile as determined by western blot analysis. Heat map of the phospho-protein profile is shown. Increased phosphorylation is depicted in red, conversely decreased phosphorylation is depicted in blue. Magnitude of the phosphorylation differences is indicated by the scale bar in the top left corner. Statistical significance in phosphorylation status of individual proteins as calculated in Figure S2 is indicated on the right side of the figure with an asterisk \* $p < 0.05$ . **(B)** *HOXA13* overexpression causes different sensitivity of keratinocytes to protein activity inhibitors (Ship, MEK, FAK and PAK). Representative figures are shown. \* $p < 0.05$ .

quantification). *HOXA13* overexpressing cells showed inactivation of the tumor suppressor lipid phosphatase PTEN as evidenced by increased inhibitory phosphorylation at Ser380. PTEN is known to inactivate the Akt survival pathway, which was consistent with a non-significant increase in Akt phosphorylation at Ser473, although surprisingly, phosphorylation at Thr308 was decreased. However, *HOXA13* overexpressing cells were significantly less sensitive to inhibition of Akt by treatment of cells with a SHIP2 lipid phosphatase inhibitor (54) (**Figure 2B-i**), suggesting overall enhanced Akt activity levels in these cells.

Significant activation of mitogen-activated growth signaling was also observed through enhanced activation of ERK1/2 (as evidenced by phosphorylation at Thr202/Tyr204) and its target substrate MEK1 (at Thr292). As MEK1 phosphorylation at Thr292 itself inhibits functionality of this protein, we also investigated cell growth in the presence of a MEK1/2 inhibitor (**Figure 2B-ii**). Overexpression of *HOXA13* did not make cells more sensitive to targeting of MEK1, suggesting that activation of ERK1/2 upon *HOXA13* overexpression exerts its effects via other targets. Indeed, a significant upregulation of the ERK2 substrate 4e-BP1 (Thr70) in *HOXA13* overexpressing cells was seen, which is known to enhance mRNA translation.

In light of the effects seen on cytoskeletal regulation on mRNA level in our sequencing efforts, we also investigated several phospho-proteins involved in actin modulation and adhesion. In particular adhesive properties appeared to be affected by *HOXA13* overexpression, as evidenced by significantly enhanced phosphorylation of Integrin- $\beta$ 3 (Tyr 785) and focal adhesion kinase (FAK, Tyr391). While inhibition of FAK affected control cells more than *HOXA13*-overexpressing cells at low concentrations, higher concentrations indicated enhanced sensitivity upon *HOXA13* overexpression, suggesting that the effect of FAK activity present in the cell may be dichotomous (**Figure 2B-iii**). *HOXA13*-overexpressing EPC2-hTERT cells were more resistant to inhibition of PAK, a target of the cytoskeletal GTPases Rac and CDC42 (**Figure 2B-iv**). While we did not observe a clear difference in phosphorylation of PAK1, PAK2 phosphorylation could not be visualized. Taken together, these data suggest that oncogenic signaling is activated upon *HOXA13* overexpression, with, in particular, ERK-induced translational control and cytoskeletal signaling playing important roles.

### ***HOXA13* downregulates MHC class I in keratinocytes**

Having demonstrated that *HOXA13* overexpression induces numerous molecular changes associated with tumorigenesis, we next investigated to what extent these changes translate to cellular consequences. Functional enrichment analysis predicted that the antigen presentation pathway is affected (**Figure 3A**), with *HOXA13* regulating expression of genes associated with the major histocompatibility complex (MHC) class I: HLA-A (FC=0.22), HLA-B (FC=0.21), HLA-C (FC=0.57), B2M (FC=0.55) and

TAP1 (FC=0.63) (**Figure 3B**). To validate this on protein level, EPC2-hTERT cells were stained with antibodies against MHC class I and analyzed by FACS. Confirming RNA sequencing data, *HOXA13* overexpression decreases MHC class I protein expression on EPC2-hTERT cells (FC=0.17,  $p=0.0286$ ) (**Figure 3C**). This suggests activation of immune escape mechanisms upon *HOXA13* expression in esophageal keratinocytes.

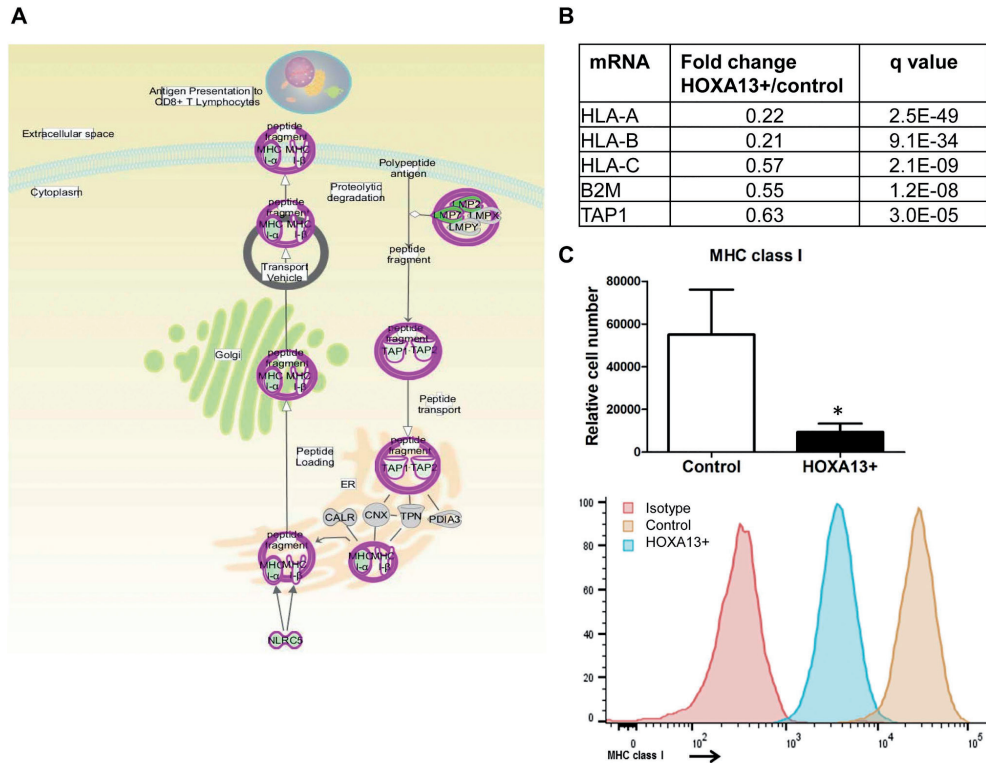


**Figure 3.** *HOXA13* downregulates MHC class I and affects the antigen presentation pathway. **(A)** Illustration of the antigen presentation pathway. Molecules with a decreased expression upon *HOXA13* overexpression are indicated in green. IPA analysis based on RNAseq data. **(B)** RNA expression data of genes associated with MHC class I as determined by RNAseq. **(C)** *HOXA13* decreases expression protein expression of MHC class I. Quantification of FACS data is shown in upper panel ( $p<0.05$ ), representative example is shown in lower panel.

### *HOXA13* overexpression provides a proliferative advantage to esophageal keratinocytes and decreases paclitaxel-induced cell death

Next, we investigated cellular proliferation potential of EPC2-hTERT cells, as a hallmark of tumorigenesis. As shown in **Figure 4A**, induction of *HOXA13* in esophageal keratinocytes does not affect 2D growth as determined by MTT assay. However, in line with RNA analysis predicted decrease in cell death upon *HOXA13* overexpression

(Table 2), we observed a decreased sensitivity of *HOXA13* overexpressing keratinocytes to paclitaxel, a chemotherapeutic agent targeting the cytoskeleton and used for ESCC treatment (Figure 4B).

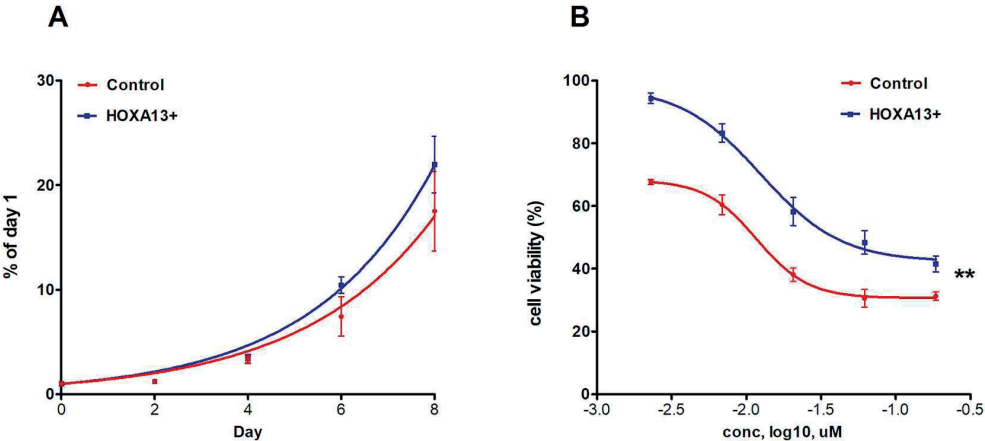


**Figure 4.** *HOXA13* confers resistance to drug-induced cell death. *HOXA13* overexpression does not affect 2D growth of esophageal cells (MTT data) (A) but makes them more resistant to paclitaxel-induced death (B). MTT was performed after 3 days of paclitaxel treatment (0.002–0.19 $\mu$ M). Data are presented as % of vehicle-treated corresponding control. Mean $\pm$ SEM, \* $p$ <0.05.

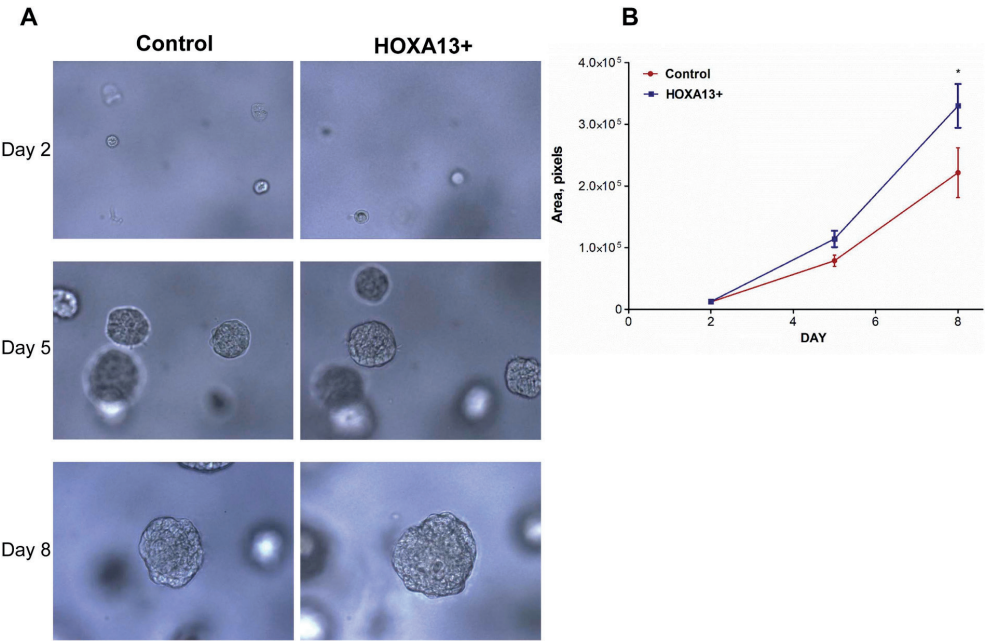


**Figure 5.** *HOXA13* promotes growth of EPC2-hTERT spheroids. (A) Representative illustrations of EPC spheroids after 2-8 days in 3D culture. (B) Area of spheroids measured on day 2, 5 and 8, Mean $\pm$ SEM, \* $p$ <0.05.



To gain further insight into the role of *HOXA13* in cell growth, we cultured EPC2-hTERT spheroids in 3D cultures, allowing assessment of growth of individual colonies in a more physiological setting. We found that spheroids derived from EPC2-hTERT cells with *HOXA13* overexpression are 1.5 times bigger in size upon 8 days of culture ( $p < 0.05$ ) (**Figure 5A,B**), indicating a proliferative advantage of cells upon overexpression of *HOXA13*.

### ***HOXA13* overexpression changes the morphology and differentiation status of EPC- derived spheroids**

EPC2 spheroids are characterized by a proliferation-differentiation gradient with Ki-67 staining seen in the basaloid cell layer and more differentiated cells toward the center of these structures (44). As shown in **Figure 6A**, upon one week of culturing, EPC2-hTERT spheroids become organized in layers with a more flattened cytological aspect

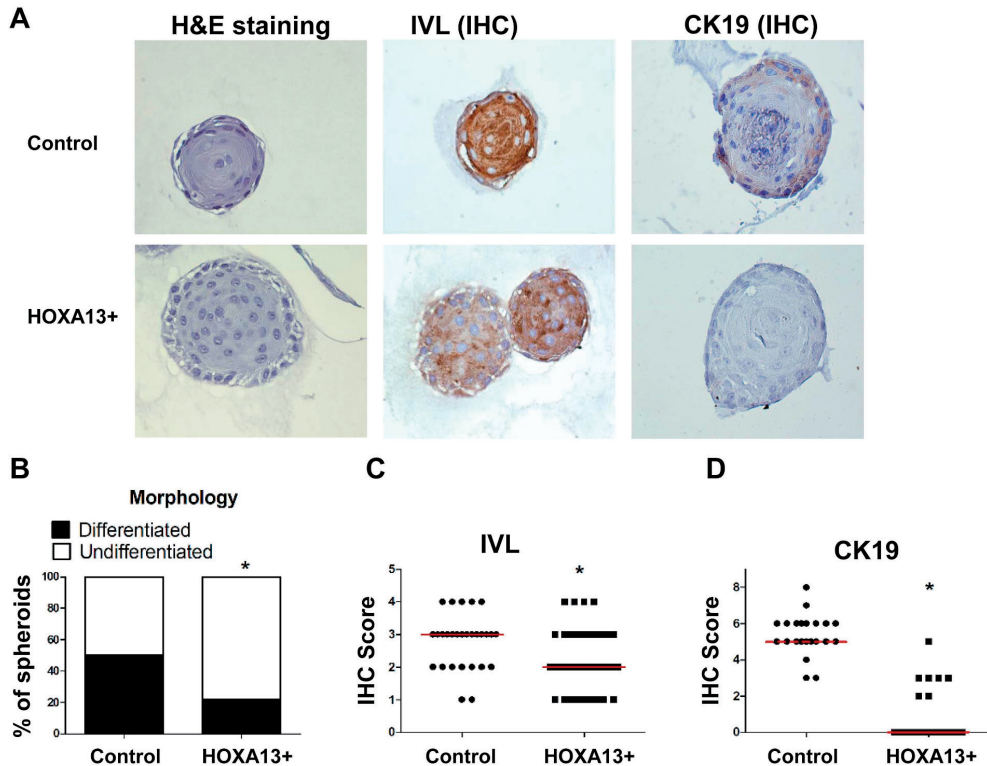


**Figure 6.** *HOXA13* overexpression influences spheroid morphology and differentiation status. (A) Representative pictures of H&E, anti-involucrin (IVL) and anti-cytokeratin-19 (CK19) staining of EPC2-hTERT spheroids. (B) Spheroids with a more differentiated aspect are more frequently observed for control EPC2-hTERT spheroids compared to *HOXA13*-overexpressing EPC2-hTERT spheroids (\* $p < 0.05$ ). (C) EPC2-hTERT spheroids with *HOXA13* overexpression express less involucrin (IVL) and D) cytoke-  
 ratin 19 (CK19) (Median with range, \* $p < 0.05$ ).

in the middle of spheroids, reminiscent of differentiated stratified epithelium. Upon overexpression of *HOXA13*, not only do spheroids become bigger (notice the increased number of nuclei, consistent with a proliferative advantage), they also are kept in a less differentiated state. Quantification of morphology indicates that 50% of spheroids obtain a differentiated morphology in control cells vs 22% upon forced *HOXA13* expression ( $p < 0.05$ , **Figure 6A, lower panel**). We also investigated the expression of involucrin and cytokeratin 19 as a markers of differentiation and keratinization. Intensity of both stainings was significantly lower in *HOXA13* overexpressing EPC2-hTERT spheroids (IVL: median IHC score for control = 3, N=28, for *HOXA13*<sup>+</sup> cells = 2, N=43,  $p < 0.05$ , CK19: IHC score for control = 5, N=22, for *HOXA13*<sup>+</sup> cells = 0, N=22,  $p < 0.05$ ) (**Figure 6B**). Thus, these results indicate that *HOXA13* overexpression prevents the differentiation of keratinocytes, which is consistent with the effect of *HOXA13* seen on cellular assembly and organization as well as on cellular development in IPA analyses.

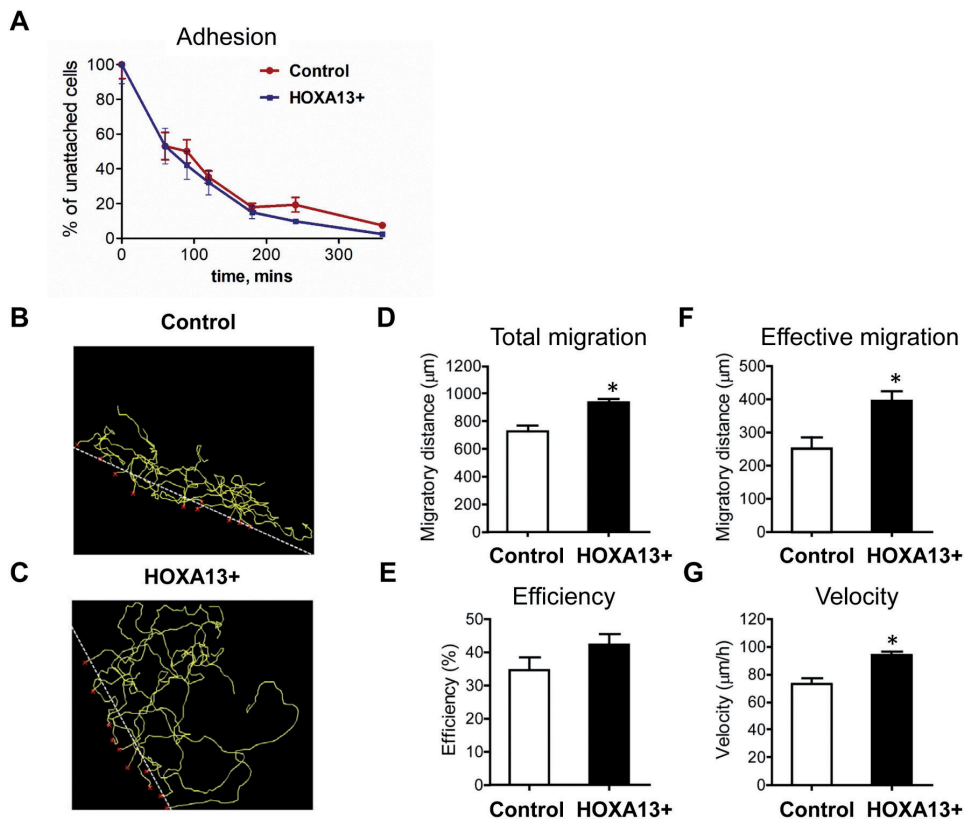


**Figure 7.** *HOXA13* does not influence adhesion of EPC2-hTERT cells, but affects cellular migration. (A) Adhesive properties of keratinocytes per se are not affected by *HOXA13* overexpression. (B-G) *HOXA13* promotes cellular migration in 2D migration assay as determined by: (D) total migration (E) efficiency, (F) effective migration and (G) velocity of migration. Mean±SEM, \*\* $p < 0.01$ . Representative pictures of Individual cell tracking show cell migration in 24 h time-lapse microscopy of control cells (B) and *HOXA13*-overexpressing cells (C).

### HOXA13 promotes cellular migration

IPA analysis, as well as phosphoprotein profiling, indicated a direct effect of *HOXA13* on cytoskeletal rearrangement and cellular adhesion. Therefore, we first tested the adhesive strength of EPC2 cells upon replating, but no difference in time to adhesion was seen between wild type and overexpressing cells (**Figure 7A**). More advanced adhesive properties are also required for migration and invasion of cells. Therefore, we investigated a migratory ability of these cells using 2D ring-barrier assays to track individual cell movement. Indeed, *HOXA13* significantly increases total migration, effective migration and velocity of EPC2 cells in 2D migration assay (**Figure 7**) ( $p < 0.01$ ). Furthermore, a pronounced increase in migratory distance of keratinocytes was seen in 3D cultures upon *HOXA13* overexpression, indicating that *HOXA13* enhances invasive potential of esophageal keratinocytes ( $p = 0.0038$ ) (**Figure 8**).

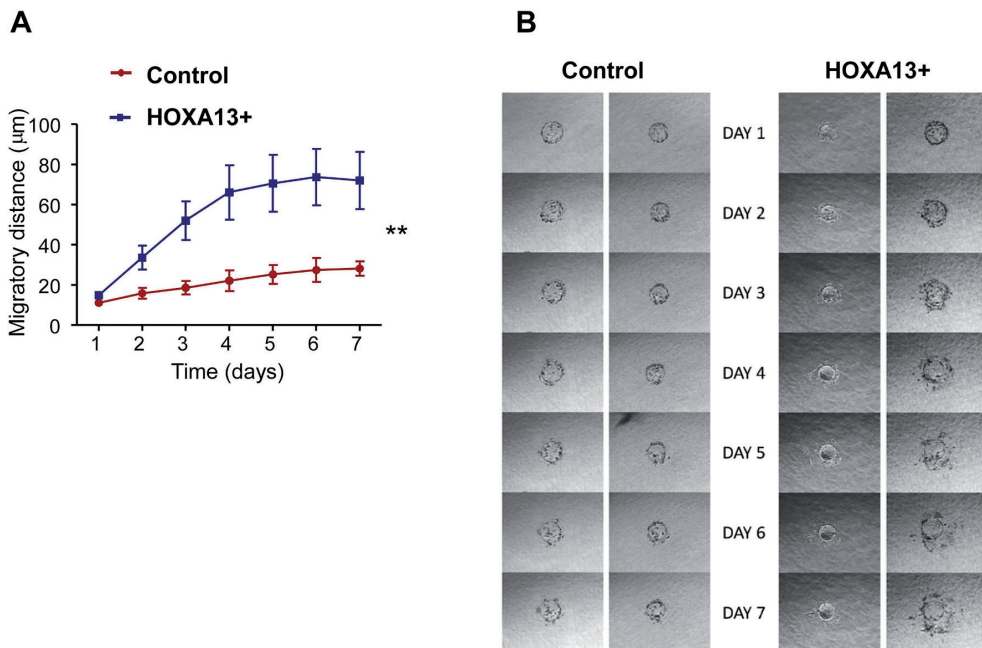


**Figure 8.** *HOXA13* promotes cellular migration in 3D migration assay. **(A)** Migratory distances of cell invading collagen matrix were measured for *HOXA13*-overexpressing cells and control cells over 7 days, Mean $\pm$ SEM, \*\* $p < 0.01$ . **(B)** Representative photographs of cells migrating in collagen matrix from microcarrier beads in 7 days.

## Discussion

A better understanding of the molecular mechanisms behind ESCC development might reveal new targets for its treatment and early diagnosis. Homeobox genes were shown to be responsible not only for proper embryonic development and differentiation of stem

cells but they are also associated with cancer development (55). One of these genes, transcriptional factor *HOXA13*, has previously been investigated in human ESCC tissue and in cancerous cell lines (26, 56). However, its role was not reported for early stages of ESCC or for squamous dysplasia. In this study, we overexpressed *HOXA13* in primary immortalized esophageal keratinocytes and compared them to wild type keratinocytes in terms of hallmarks of cancer to investigate *HOXA13* as a driver of esophageal carcinogenesis. Initiation of cancer implies the cellular acquisition of several oncogenic characteristics, including selective growth and proliferative advantage, altered stress response favoring overall survival, vascularization, invasion and metastasis, metabolic rewiring, an abetting microenvironment, and immune modulation (57, 58). Furthermore, cancerous cells are characterized by some level of dedifferentiation and heterogeneity (59).

First of all, we found that *HOXA13* downregulates MHC class I in keratinocytes and affects an antigen presentation pathway. Downregulation of MHC class I and escape from immune response is associated with the clinical course of ESCC (60). Our results indicate that *HOXA13* expression may drive the immune escape of neoantigen-bearing transformed keratinocytes.

Second, we observe that overexpression of *HOXA13* provides a proliferative advantage to keratinocytes and decreases their sensitivity to paclitaxel-induced cell death. Upon overexpression of *HOXA13*, cells showed increased resistance to paclitaxel treatment and formed bigger spheroids in 3D culture. These data are in line with clinical data previously obtained (32) showing that downregulation of *HOXA13* sensitizes human ESCC to chemotherapy and with experiments done on cancerous cell lines showing that HOTTIP/*HOXA13* enhances ESCC cell proliferation *in vitro* and *in vivo* (56). However, while these earlier publications suggest that *HOXA13* plays a role in the maintenance of tumor cell characteristics, our data suggest that overexpression of this gene can drive tumorigenesis. Nevertheless, thus far, no activating *HOXA13* mutations have been reported for ESCC, suggesting alternative mechanisms for its over-expression in this tumor type. IPA analysis of our dataset revealed TGF- $\beta$ 1 and TP53 as the most significant regulators of signaling pathways affected by *HOXA13* overexpression. Mutation of TP53 is an early and most common event in esophageal carcinogenesis and is typical also for squamous dysplasia and other types of esophageal cancer (34). TGF- $\beta$ 1 also plays an important role in pathogenesis of ESCC (61) as it regulates epithelial-to-mesenchymal transition (EMT) of ESCC. As *HOXA13* was reported to induce the EMT cascade (56), it is conceivable that *in vivo*, TGF- $\beta$ 1 drives this effect.

Losing epithelial traits (dedifferentiation) is an important step during tumorigenesis which at early stages is required for local migration/invasion and at later stages contributes to macroscopic metastases (62). Moreover, differentiation status of ESCC is associated with clinical outcome (63, 64). The prognosis of patients with keratinizing ESCC has

been reported to be significantly better than that of patients with non-keratinizing tumors (63). In the present study, RNA expression data, morphology data on EPC2 spheroids and anti-IVL staining all indicate that *HOXA13* limits the differentiation of keratinocytes. Concomitantly, we observed that *HOXA13* promotes cellular migration, which is in line with data from cancerous cell lines (56). Our study further suggests that Integrin- $\beta$ 3, FAK, PAK, GTPases Rac, and CDC42 are likely candidates to be involved and mediate this effect.

We acknowledge several limitations to our study. Tumors are heterogeneous, and *HOXA13* may not play a similar role in all patients developing ESCC. Here, we employed a heterogeneous pool of EPC2-hTERT cells, but while cell lines are by nature heterogeneous, this does not fully reflect the heterogeneity of patients. Future studies are needed to confirm *HOXA13* overexpression in esophageal premalignant lesions. Second, while our studies implicate a role for *HOXA13* in driving oncogenic hallmarks, and previous publications have clearly shown the overexpression of *HOXA13* in malignant tissues, the driving mechanisms for this overexpression remain to be elucidated.

*In toto*, we show here that *HOXA13* expression confers oncogenic hallmarks to esophageal keratinocytes. It provides proliferation advantage to keratinocytes, reduces sensitivity to chemical agents, regulates MHC class I expression and differentiation status and promote cellular migration. Our data indicate a crucial role of *HOXA13* at early stages of esophageal carcinogenesis.

## References

1. Pennathur A, Gibson MK, Jobe BA, Luketich JD. Oesophageal carcinoma. *Lancet*. 2013;381(9864):400-12.
2. Kamangar F, Dores GM, Anderson WF. Patterns of cancer incidence, mortality, and prevalence across five continents: defining priorities to reduce cancer disparities in different geographic regions of the world. *J Clin Oncol*. 2006;24(14):2137-50.
3. Ferlay J, Soerjomataram I, Dikshit R, Eser S, Mathers C, Rebelo M, et al. Cancer incidence and mortality worldwide: sources, methods and major patterns in GLOBOCAN 2012. *Int J Cancer*. 2015;136(5):E359-86.
4. Pickens A, Orringer MB. Geographical distribution and racial disparity in esophageal cancer. *Ann Thorac Surg*. 2003;76(4):S1367-9.
5. Domper Arnal MJ, Ferrandez Arenas A, Lanás Arbeloa A. Esophageal cancer: Risk factors, screening and endoscopic treatment in Western and Eastern countries. *World J Gastroenterol*. 2015;21(26):7933-43.
6. Taylor PR, Abnet CC, Dawsey SM. Squamous dysplasia--the precursor lesion for esophageal squamous cell carcinoma. *Cancer Epidemiol Biomarkers Prev*. 2013;22(4):540-52.
7. Pennathur A, Farkas A, Krasinskas AM, Ferson PE, Gooding WE, Gibson MK, et al. Esophagectomy for T1 esophageal cancer: outcomes in 100 patients and implications for endoscopic therapy. *Ann Thorac Surg*. 2009;87(4):1048-54; discussion 54-5.

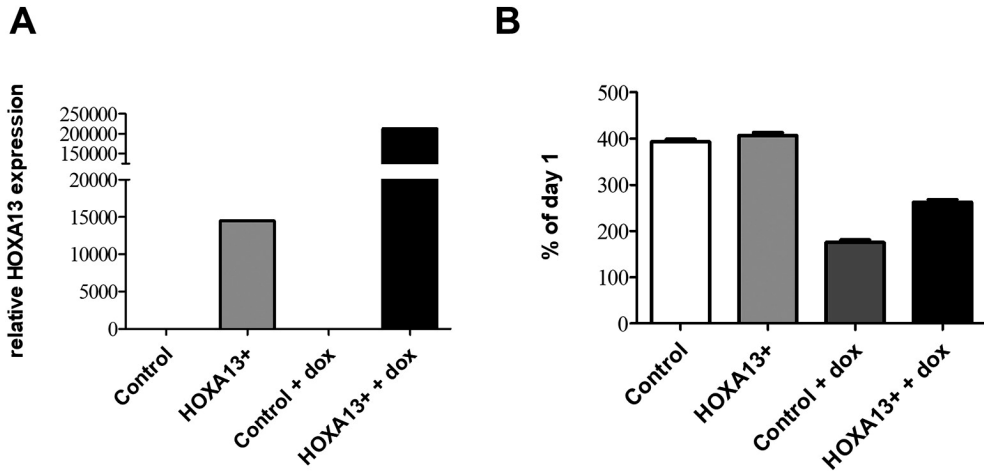
8. Copeland NG, Jenkins NA, Court DL. Recombineering: a powerful new tool for mouse functional genomics. *Nat Rev Genet.* 2001;2(10):769-79.
9. Knosp WM, Scott V, Bachinger HP, Stadler HS. HOXA13 regulates the expression of bone morphogenetic proteins 2 and 7 to control distal limb morphogenesis. *Development.* 2004;131(18):4581-92.
10. Lewis EB. A gene complex controlling segmentation in *Drosophila*. *Nature.* 1978;276(5688):565-70.
11. Noordermeer D, Leleu M, Splinter E, Rougemont J, De Laat W, Duboule D. The dynamic architecture of Hox gene clusters. *Science.* 2011;334(6053):222-5.
12. Mallo M, Wellik DM, Deschamps J. Hox genes and regional patterning of the vertebrate body plan. *Dev Biol.* 2010;344(1):7-15.
13. Yahagi N, Kosaki R, Ito T, Mitsuhashi T, Shimada H, Tomita M, et al. Position-specific expression of Hox genes along the gastrointestinal tract. *Congenit Anom (Kyoto).* 2004;44(1):18-26.
14. McGinnis W, Krumlauf R. Homeobox genes and axial patterning. *Cell.* 1992;68(2):283-302.
15. Pearson JC, Lemons D, McGinnis W. Modulating Hox gene functions during animal body patterning. *Nat Rev Genet.* 2005;6(12):893-904.
16. Hueber SD, Rauch J, Djordjevic MA, Gunter H, Weiller GF, Frickey T. Analysis of central Hox protein types across bilaterian clades: on the diversification of central Hox proteins from an Antennapedia/Hox7-like protein. *Dev Biol.* 2013;383(2):175-85.
17. Abate-Shen C. Deregulated homeobox gene expression in cancer: cause or consequence? *Nat Rev Cancer.* 2002;2(10):777-85.
18. Reya T, Clevers H. Wnt signalling in stem cells and cancer. *Nature.* 2005;434(7035):843-50.
19. Taipale J, Beachy PA. The Hedgehog and Wnt signalling pathways in cancer. *Nature.* 2001;411(6835):349-54.
20. Joo MK, Park JJ, Chun HJ. Impact of homeobox genes in gastrointestinal cancer. *World Journal of Gastroenterology.* 2016;22(37):8247-56.
21. Chen K-N, Gu Z-D, Ke Y, Li J-Y, Shi X-T, Xu G-W. Expression of 11 HOX Genes Is Deregulated in Esophageal Squamous Cell Carcinoma. *Clinical Cancer Research.* 2005;11(3):1044.
22. Liu C, Tian X, Zhang J, Jiang L. Long Non-coding RNA DLEU1 Promotes Proliferation and Invasion by Interacting With miR-381 and Enhancing HOXA13 Expression in Cervical Cancer. *Front Genet.* 2018;9:629.
23. Yu H, Xu Y, Zhang D, Liu G. Long noncoding RNA LUCAT1 promotes malignancy of ovarian cancer through regulation of miR-612/HOXA13 pathway. *Biochem Biophys Res Commun.* 2018;503(3):2095-100.
24. Han Y, Song C, Wang J, Tang H, Peng Z, Lu S. HOXA13 contributes to gastric carcinogenesis through DHRS2 interacting with MDM2 and confers 5-FU resistance by a p53-dependent pathway. *Mol Carcinog.* 2018;57(6):722-34.
25. Dong Y, Cai Y, Liu B, Jiao X, Li ZT, Guo DY, et al. HOXA13 is associated with unfavorable survival and acts as a novel oncogene in prostate carcinoma. *Future Oncol.* 2017;13(17):1505-16.
26. Gu Z-D, Shen L-Y, Wang H, Chen X-M, Li Y, Ning T, et al. HOXA13 Promotes Cancer Cell Growth and Predicts Poor Survival of Patients with Esophageal Squamous Cell Carcinoma. *Cancer Research.* 2009;69(12):4969.
27. Lin C, Wang Y, Wang Y, Zhang S, Yu L, Guo C, et al. Transcriptional and posttranscriptional regulation of HOXA13 by lncRNA HOTTIP facilitates tumorigenesis and metastasis in esophageal squamous carcinoma cells. *Oncogene.* 2017;36(38):5392-406.
28. Ma RL, Shen LY, Chen KN. Coexpression of ANXA2, SOD2 and HOXA13 predicts poor prognosis of esophageal squamous cell carcinoma. *Oncology Reports.* 2014;31(5):2157-64.

29. Barclay C, Li AW, Geldenhuys L, Baguma-Nibasheka M, Porter GA, Veugelers PJ, et al. Basic fibroblast growth factor (FGF-2) overexpression is a risk factor for esophageal cancer recurrence and reduced survival, which is ameliorated by coexpression of the FGF-2 antisense gene. *Clin Cancer Res.* 2005;11(21):7683-91.
30. Shen LY, Chen KN. Exploration of target genes of HOXA13 in esophageal squamous cell carcinoma cell line. *Cancer Lett.* 2011;312(1):18-23.
31. Qin Z, Chen Z, Weng J, Li S, Rong Z, Zhou C. Elevated HOXA13 expression promotes the proliferation and metastasis of gastric cancer partly via activating Erk1/2. *Onco Targets Ther.* 2019;12:1803-13.
32. Shi Q, Shen L, Dong B, Fu H, Kang X, Dai L, et al. Downregulation of HOXA13 sensitizes human esophageal squamous cell carcinoma to chemotherapy. *Thorac Cancer.* 2018;9(7):836-46.
33. Contino G, Vaughan TL, Whiteman D, Fitzgerald RC. The Evolving Genomic Landscape of Barrett's Esophagus and Esophageal Adenocarcinoma. *Gastroenterology.* 2017;153(3):657-73 e1.
34. Chen X-X, Zhong Q, Liu Y, Yan S-M, Chen Z-H, Jin S-Z, et al. Genomic comparison of esophageal squamous cell carcinoma and its precursor lesions by multi-region whole-exome sequencing. *Nature Communications.* 2017;8(1):524.
35. Harada H, Nakagawa H, Oyama K, Takaoka M, Andl CD, Jacobmeier B, et al. Telomerase induces immortalization of human esophageal keratinocytes without p16INK4a inactivation. *Mol Cancer Res.* 2003;1(10):729-38.
36. Shin KJ, Wall EA, Zavzavadjian JR, Santat LA, Liu J, Hwang JJ, et al. A single lentiviral vector platform for microRNA-based conditional RNA interference and coordinated transgene expression. *Proc Natl Acad Sci U S A.* 2006;103(37):13759-64.
37. Katzen F. Gateway((R)) recombinational cloning: a biological operating system. *Expert Opin Drug Discov.* 2007;2(4):571-89.
38. Merten OW, Hebben M, Bovolenta C. Production of lentiviral vectors. *Mol Ther Methods Clin Dev.* 2016;3:16017.
39. Kubo S, Mitani K. A new hybrid system capable of efficient lentiviral vector production and stable gene transfer mediated by a single helper-dependent adenoviral vector. *J Virol.* 2003;77(5):2964-71.
40. R Development Core Team. R: A language and environment for statistical computing. Vienna, Austria. 2008.
41. Love MI, Huber W, Anders S. Moderated estimation of fold change and dispersion for RNA-seq data with DESeq2. *Genome Biol.* 2014;15(12):550.
42. Krämer A, Green J, Pollard J, Jr., Tugendreich S. Causal analysis approaches in Ingenuity Pathway Analysis. *Bioinformatics.* 2014;30(4):523-30.
43. Queiroz KC, Milani R, Ruela-de-Sousa RR, Fuhler GM, Justo GZ, Zambuzzi WF, et al. Violacein induces death of resistant leukaemia cells via kinome reprogramming, endoplasmic reticulum stress and Golgi apparatus collapse. *PLoS One.* 2012;7(10):e45362.
44. Kasagi Y, Chandramouleeswaran PM, Whelan KA, Tanaka K, Giroux V, Sharma M, et al. The Esophageal Organoid System Reveals Functional Interplay Between Notch and Cytokines in Reactive Epithelial Changes. *Cell Mol Gastroenterol Hepatol.* 2018;5(3):333-52.
45. Schindelin J, Arganda-Carreras I, Frise E, Kaynig V, Longair M, Pietzsch T, et al. Fiji: an open-source platform for biological-image analysis. *Nat Methods.* 2012;9(7):676-82.
46. Das AM, Eggermont AM, ten Hagen TL. A ring barrier-based migration assay to assess cell migration in vitro. *Nat Protoc.* 2015;10(6):904-15.
47. Somasundaram R, Fernandes S, Deuring JJ, de Haar C, Kuipers EJ, Vogelaar L, et al. Analysis of SHIP1 expression and activity in Crohn's disease patients. *PLoS One.* 2017;12(8):e0182308.

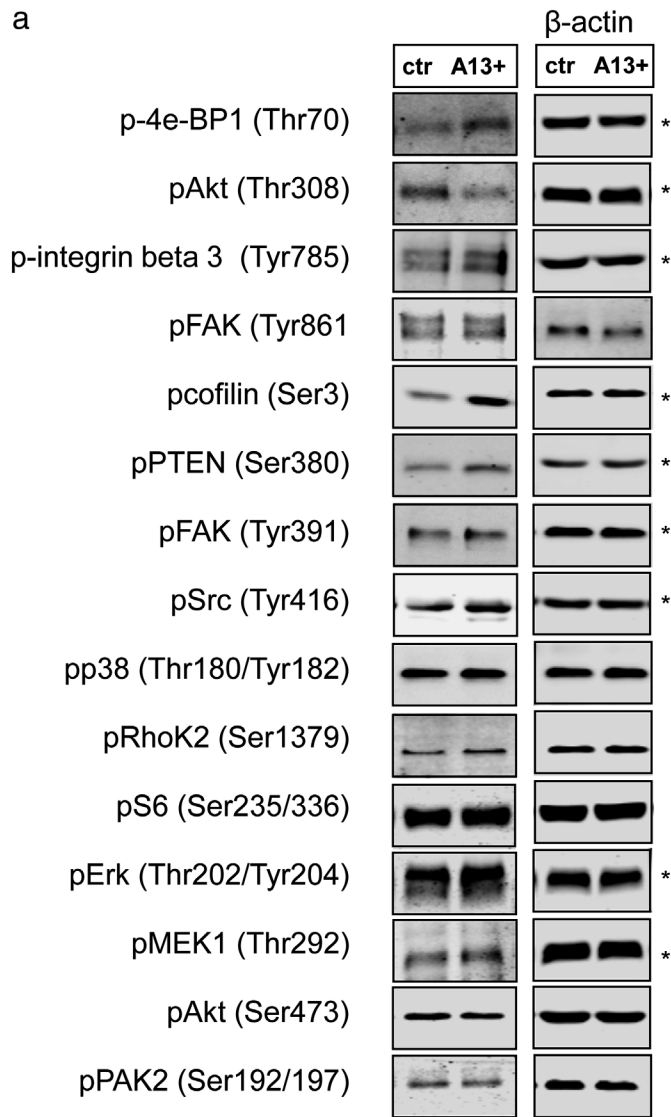
48. de Sousa RR, Queiroz KC, Souza AC, Gurgueira SA, Augusto AC, Miranda MA, et al. Phosphoprotein levels, MAPK activities and NFkappaB expression are affected by fisetin. *J Enzyme Inhib Med Chem*. 2007;22(4):439-44.
49. Schindelin J, Rueden CT, Hiner MC, Eliceiri KW. The ImageJ ecosystem: An open platform for biomedical image analysis. *Mol Reprod Dev*. 2015;82(7-8):518-29.
50. Myers TG, Anderson NL, Waltham M, Li G, Buolamwini JK, Scudiero DA, et al. A protein expression database for the molecular pharmacology of cancer. *Electrophoresis*. 1997;18(3-4):647-53.
51. Shimada H. p53 molecular approach to diagnosis and treatment of esophageal squamous cell carcinoma. *Ann Gastroenterol Surg*. 2018;2(4):266-73.
52. Jin G, Deng Y, Miao R, Hu Z, Zhou Y, Tan Y, et al. TGFB1 and TGFB2 functional polymorphisms and risk of esophageal squamous cell carcinoma: a case-control analysis in a Chinese population. *J Cancer Res Clin Oncol*. 2008;134(3):345-51.
53. Tu Y, Tan F, Zhou J, Pan J. Pristimerin targeting NF-kappaB pathway inhibits proliferation, migration, and invasion in esophageal squamous cell carcinoma cells. *Cell Biochem Funct*. 2018;36(4):228-40.
54. Fuhler GM, Brooks R, Toms B, Iyer S, Gengo EA, Park MY, et al. Therapeutic potential of SH2 domain-containing inositol-5'-phosphatase 1 (SHIP1) and SHIP2 inhibition in cancer. *Mol Med*. 2012;18:65-75.
55. Bhatlekar S, Fields JZ, Boman BM. Role of HOX Genes in Stem Cell Differentiation and Cancer. *Stem Cells Int*. 2018;2018:3569493.
56. Lin C, Wang Y, Wang Y, Zhang S, Yu L, Guo C, et al. Transcriptional and posttranscriptional regulation of HOXA13 by lncRNA HOTTIP facilitates tumorigenesis and metastasis in esophageal squamous carcinoma cells. *Oncogene*. 2017;36:5392.
57. Fouad YA, Aanei C. Revisiting the hallmarks of cancer. *Am J Cancer Res*. 2017;7(5):1016-36.
58. Hanahan D, Weinberg Robert A. Hallmarks of Cancer: The Next Generation. *Cell*. 2011;144(5):646-74.
59. Friedmann-Morvinski D, Verma IM. Dedifferentiation and reprogramming: origins of cancer stem cells. *EMBO Rep*. 2014;15(3):244-53.
60. Liu Q, Hao C, Su P, Shi J. Down-regulation of HLA class I antigen-processing machinery components in esophageal squamous cell carcinomas: association with disease progression. *Scand J Gastroenterol*. 2009;44(8):960-9.
61. Pang L, Li Q, Wei C, Zou H, Li S, Cao W, et al. TGF-beta1/Smad signaling pathway regulates epithelial-to-mesenchymal transition in esophageal squamous cell carcinoma: in vitro and clinical analyses of cell lines and nomadic Kazakh patients from northwest Xinjiang, China. *PLoS One*. 2014;9(12):e112300.
62. Pattabiraman DR, Weinberg RA. Targeting the Epithelial-to-Mesenchymal Transition: The Case for Differentiation-Based Therapy. *Cold Spring Harb Symp Quant Biol*. 2016;81:11-9.
63. Ohbu M, Saegusa M, Okayasu I. Apoptosis and cellular proliferation in oesophageal squamous cell carcinomas: differences between keratinizing and nonkeratinizing types. *Virchows Arch*. 1995;427(3):271-6.
64. Nozoe T, Oyama T, Takenoyama M, Hanagiri T, Sugio K, Yasumoto K. Significance of immunohistochemical expression of p27 and involucrin as the marker of cellular differentiation of squamous cell carcinoma of the esophagus. *Oncology*. 2006;71(5-6):402-10.
65. Hornbeck PV, Zhang B, Murray B, Kornhauser JM, Latham V, Skrzypek E. PhosphoSitePlus, 2014: mutations, PTMs and recalibrations. *Nucleic Acids Res*. 2015;43(Database issue):D512-20.
66. Fuhler GM, Brooks R, Toms B, Iyer S, Gengo EA, Park MY, et al. Therapeutic potential of SH2 domain-containing inositol-5'-phosphatase 1 (SHIP1) and SHIP2 inhibition in cancer. *Mol Med*. 2012;18(1):65-75.



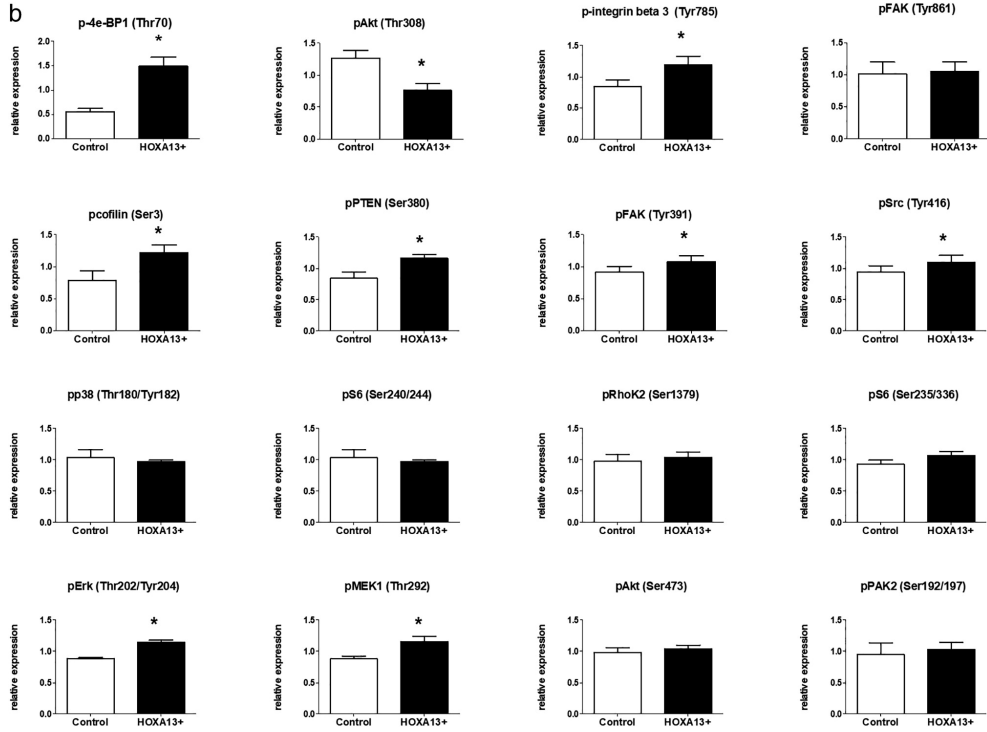
## Supplementary information



**Supplementary Figure S1.** (A) *HOXA13* is overexpressed in EPC2-hTERT *HOXA13*-transduced cells even without doxycycline (dox) treatment in contrast to control EPC2-hTERT cells (empty vector transduced). qPCR data are calculated relatively to corresponding control with or without dox treatment. (B) Effect of doxycycline on growth of EPC2-hTERT cells with and without *HOXA13* overexpression (MTT). Mean±SEM, \* $p<0.05$ .



**Supplementary Figure S2.** *HOXA13* influences cellular phosphoprofile as determined by western blot analysis. Three independent experiments were performed to obtain lysates of *HOXA13*<sup>+</sup> and control cells. These lysates were subsequently blotted a minimum of 1 time, results in an N of at least 3 for control and *HOXA13*<sup>+</sup> cells. (A) Representative examples of control and *HOXA13*<sup>+</sup> cell lysates are shown for the presence of indicated phopho-proteins. (B) Quantification of western blots.



Supplementary Figure S2. *Continued.*

**Supplementary Table S1.** List of primary antibodies used for phosphoprotein profiling (65)

#	Antibody	Company	Cat #	Species	Dilution	Result of phosphorylation on protein activity
1	pErk (Thr202/Tyr204)	CST	4696	mouse	1:1000	+
2	pS6 (Ser235/336)	CST	4856	rabbit	1:1000	+
3	pS6 (Ser240/244)	CST	5364	rabbit	1:1000	+
4	pAkt (Thr308)	Signal way	11055-2	rabbit	1:1000	+
5	pAkt (Ser473)	CST	4060S	rabbit	1:1000	+
6	p-4e-BP1 (Thr70)	CST	9455	rabbit	1:1000	-
7	pp38 (Thr180/Tyr182)	CST	4511	rabbit	1:1000	+
8	pFAK (Tyr391)	Invitrogen	44-625G	rabbit	1:1000	+
9	pFAK (Tyr861)	ITK	21076-1	rabbit	1:1000	+
10	pcofilin (Ser3)	Signal Way	11139	rabbit	1:1000	-
11	pRhoK2 (Ser1379)	Signal Way	13005	rabbit	1:1000	-
12	pSrc (Tyr416)	CST	2113	rabbit	1:1000	+
13	p-integrin beta 3 (Tyr785)	Signal way	11060-1	rabbit	1:1000	-
14	pPAK2 (Ser192/197)	CST	2605	rabbit	1:1000	-
15	pMEK1 (Thr292)	Merck	07-348	rabbit	1:1000	-
16	pPTEN (Ser380)	CST	9551	rabbit	1:1000	-
17	$\beta$ -actin	SCBT - Santa Cruz Biotechnology	477778	mouse	1:1000	N/A

**Supplementary Table S2.** List of chemicals for drug sensitivity test

Compound	Target	Manufacturer	Solvent	Concentration range
1 Paclitaxel	Tubulin	Sigma-Aldrich, 7191-1MG	DMSO	0.002-0.2 uM
2 FAK inhibitor 14	FAK	Sigma-Aldrich, SML0837-10MG	H <sub>2</sub> O	0.05-33 uM
3 FRAX1036	PAK-1	Selleckchem, S7989	Etanol	0.02-50 uM
4 U0126-EtOH	MEK1/2	MedChemExpress, HY-12031	DMSO	0.05-33 uM
5 2PIQ	SHIP2	Synthesized (66)	DMSO	2.3-11 uM





# Chapter 4

---

*HOXA9* mediates and marks  
premalignant compartment size  
expansion in colonic adenomas

Vincent T. Janmaat · Hui Liu · Rodrigo A. da Silva · Pieter H.A. Wisse ·  
Manon C.W. Spaander · Timo L.M. Ten Hagen · Ron Smits · Marco J. Bruno ·  
Gwenny M. Fuhler · Maikel P. Peppelenbosch

*Carcinogenesis*. 2019;40(12):1514-24

## Abstract

The transformation of normal colonic epithelium to colorectal cancer (CRC) involves a relatively ordered progression, and understanding the molecular alterations involved may aid rational design of strategies aimed at preventing or counteracting disease. *HOXA9* is an oncogene in leukemia and has been implicated in CRC pathology, although its role in disease etiology remains obscure at best. We observe that *HOXA9* expression is increased in colonic adenomas compared to location-matched healthy colon epithelium. Its forced expression results in dramatic genetic and signaling changes, with increased expression of growth factors *IGF1* and *FLT3*, super-activity of the AKT survival pathway and a concomitant increase in compartment size. Furthermore, a reduced mRNA expression of the epithelial to mesenchymal transition marker N-cadherin as well as reduced activity of the actin cytoskeletal mediator PAK was seen, which is in apparent agreement with an observed reduced migratory response in *HOXA9* overexpressing cells. Thus *HOXA9* appears closely linked with adenoma growth while impairing migration and metastasis and hence is both a marker and driver of premalignant polyp growth.



## Introduction

Colorectal cancer (CRC) is the second most common cancer in men and the third in women (1). Its incidence has slightly risen in The Netherlands over the past decades while prognosis improved (2). In Europe, high CRC prevalence has resulted in the initiation of many national CRC screening programs (3). These programs are continuously evaluated and improved (4, 5). In Europe, incidence rates are declining, probably due to changes in life style and more intensive screening. However, CRC is still the second leading cause of cancer death in Europe (6). Obviously, better understanding of the molecular pathways that mediate progression from normal colonic epithelium to invasive carcinoma would aid efforts aimed at improving prevention and treatment of CRC.

Better definition of molecular markers that relate to the natural history of early CRC would prove exceedingly useful. About thirty years ago Vogelstein et al. described the importance of premalignant lesions and their role in the adenoma-carcinoma sequence (7). The prevalence of these premalignant lesions is considered to be 25 percent at the age of 50 years and increases up to 50 percent at the age of 70 (8-11). It is fair to say that the mechanisms that drive growth of premalignant lesions remain poorly understood. Also stratifying early lesions into those that are truly benign to those that are at risk to undergo micrometastasis is not yet possible. Identifying the molecular determinants involved defines a major question in contemporary preclinical cancer research.

Molecular pathways that underlie carcinogenesis are often aberrations of normal cellular physiology. Carcinogenesis can be seen as an aberrant form of organogenesis (12-14). Homeobox genes, which include the *HOX* gene clusters, regulate important pathways with relation to both embryogenesis and carcinogenesis (15). The evolutionary well-conserved mammalian *HOX* genes encode for transcription factors regulating the formation of tissues, structures and organs along the longitudinal body axis during embryology (15-17). Thus far, 39 *HOX* genes have been identified in humans, which are organized in four clusters (*A* to *D*) on separate chromosomes (7, 17, 12, and 2 respectively). During embryogenesis the different *HOX* clusters are expressed with temporal and spatial collinearity (18). The nested pattern of *HOX* genes along the length of the human body's axis is most clearly observed in segmented structures like the vertebrae, branchial arches and limbs (19-21). However, position specific expression of *HOX* genes is also present in discrete organs, including the human gut (22, 23). However, the specific functionality of expression of single *HOX* genes in gastrointestinal pathophysiology remains to be established.

As *HOX* genes are important regulators of tissue growth and differentiation, it is conceivable that they also play a role in malignant transformation. This has led to an increasing interest in *HOX* expression patterns in different forms of cancer (24-30). Interestingly, when screening for the expression of *HOX* family members in

gastrointestinal pathophysiology we observed markedly high expression of *HOXA9* in esophageal adenomas as compared normal esophagus (unpublished data). *HOXA9* overexpression as a result of the *NUP98-HOXA9* translocation-derived fusion gene is seen in patients with the premalignant Myelodysplastic Syndrome as well as overt myeloid leukemia (31). In MDS, in particular patients with refractory anemia with excess of blasts in transformation (REAB-t) show *HOXA9* fusion genes (32). In line with the fact that the *NUP98/HOXA9* fusion transcript has been shown to induce hematopoietic hyperproliferation (33) this suggests that it drives the transformation process of MDL to AML. *HOXA9* overexpression was also shown to be the strongest factor associated with poor prognosis in AML (34). In addition to hematopoietic malignancies, *HOXA9* has a pro-oncogenic effect in epithelial ovarian cancer, osteosarcoma, breast, and oral squamous cell cancer (35-37). Moreover, an upregulation of *HOXA9* has been described in CRC (38-41). However, it is as yet unclear whether this upregulation of *HOXA9* is already present in premalignant colonic tissues. Furthermore, to what extent aberrant *HOXA9* expression may drive oncogenic hallmarks is unknown. The above-mentioned considerations prompted us to compare *HOXA9* expression between adenoma tissue and location matched healthy colon epithelium and to investigate the role of *HOXA9* in oncological transformation of colonic epithelial cells. We observe that *HOXA9* is overexpressed in colonic adenomas and drives compartment expansion but concomitantly counteracts metastasis. Thus, *HOXA9* expression emerges as a molecular determinant for pre-micrometastatic colonic adenomas and may be a marker for benign polyp growth in the colon.

## Materials and methods

### Sample collection and preparation

Participants were recruited at the Havenziekenhuis (Rotterdam, The Netherlands) in the context of the nationwide screening for CRC. Asymptomatic patients, aged between 55 and 75 years, with a positive immunologic fecal occult blood test (iFOBT) were referred to this hospital for colonoscopy. If during colonoscopy a premalignant lesion was found, biopsies were taken; one from the center of the premalignant lesion and another from healthy mucosa located in the vicinity of the lesion. Biopsies were immediately stored in *RNAlater*<sup>TM</sup> (Qiagen, Germany) at 4°C and stored at -80°C within 24 h until RNA was extracted. After the biopsy was taken the remainder of the colonic polyp was resected and examined by a pathologist. Only biopsies from lesions classified as tubular adenoma with low grade dysplasia were included for further examination. Thus, only early stages in the adenoma-carcinoma sequence were studied (7). The biopsies were collected as part of the 'biobank for premalignant colonic lesions' and material collection was approved by the medical ethical committee of both the Erasmus Medical Center (Rotterdam, The

Netherlands; MEC-2015-199) and the Havenziekenhuis. Written informed consent was obtained from all participants.

### Transduction

A GeneArt bacterial plasmid (Thermo Fisher Scientific, Waltham, Massachusetts, USA) containing the *HOXA9* gene and a kanamycin resistance gene were used for the construction of the lentiviral vector. Firstly, the *HOXA9* gene was cloned into the pEN\_TmiRc3 plasmid, which was a kind gift from Iain Fraser (California Institute of Technology, California, USA). Subsequently, the *HOXA9* insert was transferred into a pSLIK-Hygro plasmid, also received from Iain Fraser (plasmid #25737; Addgene, USA), using a Gateway reaction. The same procedure was followed to create a control plasmid, lacking the *HOXA9* insert. All created plasmids were sequenced by LGC Genomics (LGC Genomics GmbH; Germany) and were confirmed to be sequence correct. The pSLIK-Hygro plasmid was transiently transfected in HEK293T cells together with three packaging plasmids (VSV-G, MD, and REV). After two days the medium was harvested and viral particles were collected by ultracentrifugation. Caco-2 cells were transduced with the concentrated virus, after one day the transduced cells were selected by adding hygromycin B (Thermo Fisher Scientific, The Netherlands) (400 µg/mL) for a period of one week. Expression of *HOXA9* was confirmed after stimulation doxycycline hyclate by qRT-PCR (see **Supplementary Figure S1**).

### Cell culture

The monthly short tandem repeat identity-verified (verification commercially performed by the molecular pathology department of the Erasmus MC) and American Type Culture Collection (ATCC, Manassas, VA)-obtained mycoplasma-free (monthly commercially checked by GATC Biotech, Konstanz, Germany) human human CRC cell line Caco-2 was cultured at 37°C in a 5% CO<sub>2</sub> incubator using Dulbecco's modified Eagle's medium (DMEM; Lonza, Basel, Switzerland) containing 10% fetal calf serum (FCS; Sigma-Aldrich) and 1% Penicillin/Streptomycin (antibiotics) (P/S; Gibco, USA). The cells were routinely confirmed to be mycoplasma free using the LookOut Mycoplasma PCR Detection Kit (Sigma-Aldrich). Before performing experiments, *HOXA9* expression in transduced Caco-2 cells was induced by culturing in the presence of 0.5 ng/mL doxycycline hyclate (Sigma-Aldrich) and 200 µg/mL hygromycin B for up to three days.

### RNA isolation, cDNA synthesis and PCR Array/qRT-PCR

Total RNA was extracted with the NucleoSpin® RNA kit (Machery-Nagel, Germany). For cDNA preparation the reverse transcription system from TAKARA (TAKARA BIO INC) was used according to the manufactures manual. A cDNA concentration of 10 ng/µl for patient material and 30 ng/µl for Caco-2 cells was used for qPCR. The

commercially available RT<sup>2</sup> Profiler<sup>TM</sup> PCR Array (PAHS-033ZC-2; Qiagen, Germany) was used. This array focuses on genes important in human cancer (See **Figure 2B**). Gene expression in *HOXA9* overexpressing cells were expressed as compared to control cells by  $\Delta\Delta$ CT method, using *ACTB*, *B2M*, *GAPDH*, *HPRT1*, and *RPLPO* represented on the plate as housekeeping controls. In addition, potential interesting candidates as derived from the array as well as *HOXA9* targets identified in literature but not present in the array were tested separately (for primers and conditions, see **Table S1**) in three independent experiments. Quantitative PCR was performed with SYBR Green (Applied Biosystems, USA) in an IQ5 PCR machine (Bio-Rad, Hercules, California, USA). To establish a loading control, *TPT1*, *UBC*, and *GAPDH* were used as reference genes (42). The  $\Delta\Delta$ CT method was used to calculate expression values.

### **(Phospho)protein profiling**

Caco-2 control and *HOXA9* transduced cell lines were seeded in a Petri dish (60 cm) at 500,000 cells/dish and treated with 0.5 ng/mL doxycycline hyclate. After 72 h, proteins were extracted in 500  $\mu$ l Laemmli Buffer (SDS 4%, glycerol 20%, Tris-Cl (pH 6.8) 120 mM, bromophenol blue 0.02% (w/v) and DTT 0.1 M) and the protein concentrations were determined using a commercial kit (RC DC Protein Assay – Bio Rad). Western blotting was performed as described (43, 44). In short, 40  $\mu$ g protein was resolved by SDS-PAGE and blotted onto Immobilon FL PVDF membranes (Millipore, Bedford, MA, USA). Membranes were blocked in Odyssey Blocking Buffer (PBS) and incubated overnight at 4°C with appropriate primary antibody (See **Table S2** for details), followed by the appropriate Alexa-linked secondary antibodies, at 1:5000 dilution, in Odyssey Blocking Buffer for 1 h. The fluorescent bands were detected using fluorescent Odyssey Imaging System and densitometric analysis was performed with ImageJ (45). All blots were reprobated for Actin to control for equal loading and normalized results are represented as ratios of protein of interest over Actin levels per lane. Three independent experiments were performed, run together on one blot, and heat maps of the phospho-protein profile (46) in the 6 samples were constructed with CIMminer (Genomics and Bioinformatics Group, Laboratory of Molecular Pharmacology, Center for Cancer Research, National Cancer Institute) (47).

### **Cell count and 3-(4,5-dimethylthiazol-2-yl)-2,5-diphenyltetrazolium bromide assay**

For these experiments  $4 \cdot 10^5$  cells of the *HOXA9* transduced and control transduced cell lines were seeded and cultured for six days in separate T75 Cellstar culture flasks. After six days of culturing the number of cells in both flasks was measured using a Cellometer<sup>TM</sup> Auto T4 cell counter (Nexcelom Bioscience LLC, USA). After six days of stimulation, the total number of *HOXA9* overexpressing cells in the T75 flask was calculated relative to the number of cells in the control cell line. This experiment was repeated four times. MTT assays were performed as previously described (48). Transduced Caco-2 cells were

seeded in a 96-wells plate, each well containing 1000 cells. After 24, 48, 72 and 96 h cell metabolic activity and viable cells were detected by firstly adding 10  $\mu$ l 5 mg/ $\mu$ l MTT to 100  $\mu$ l DMEM, followed by three h incubation at 37°C and replacing the DMEM by dimethyl sulfoxide (DMSO; Sigma-Aldrich). Intensity of color was measured in a Model 680 XR microplate reader (Bio-Rad, USA). This experiment was repeated eight times.

### 3D spheroid-based cell expansion assay

Cytodex-3 microcarrier beads (Sigma-Aldrich) were mixed with  $5 \times 10^5$  Caco-2 *HOXA9* overexpression and control cell suspensions, at a density of 40 cells per bead and incubated at 37°C for 6 h with gentle mixing. The suspension was transferred to 25 cm<sup>2</sup> flasks and incubated for 48 h. Coated beads were embedded in 1.6 mg/ml collagen gel (collagen: modified Eagle's medium: 7.5% w/v NaHCO<sub>3</sub> in the ratio 11:8:1), put in plates, incubated at 37°C for 2 h to polymerize and covered with 500  $\mu$ l DMEM, 10% FBS, 1% P/S, 5 ng/ml doxycycline. Spheroid growth was measured by quantifying the cell layer extending from the surface of the bead. Ten coated beads were photographed every 24 h with a 10 $\times$  objective. All measurements were performed using AxioVision 4.5 software and assays were performed three times independently. Data was statistically analyzed by two-way ANOVA.

### Migration assay

Migration assays were performed as described (49). Briefly, a barrier is inserted in a culture chamber, this prevents cells from entering a defined area occupied by the barrier. Cells were seeded around this barrier to form a monolayer, the barrier is removed, and migration into the defined cell-free area is measured.

### cBioportal query

We performed a query on the 15<sup>th</sup> of April 2018 on <http://www.cbioportal.org> (50, 51). We selected all 8 studies from the category “bowel” including a total of 3473 cases. This included four published studies (52-55), and “colorectal adenocarcinoma (TGCA, Provisional)”, “Colorectal adenocarcinoma (TCGA, PanCancer Atlas)”, “Rectum adenocarcinoma (TGCA, PanCancer Atlas)”, and “Targeted sequencing of 1134 samples from metastatic colorectal cancer samples (MSK, Cancer Cell 2018)”.

### Statistics

Relative expression of potential target genes was calculated comparing the transduced cell line overexpressing *HOXA9* to the control cell line. The one-sample *t*-test was used to test for statistical significance. The Komogorov-Smirnov test, the D'Agostino and Pearson omnibus normality test and the Shapiro-Wilk normality test were used for each

target gene to see if the results came from a Gaussian distribution. If this assumption was violated the relative expression of the target gene was displayed using the median and the interquartile range. In those cases the Wilcoxon Signed-Rank Test was used to test for difference in expression. The Student's *t*-test was used to test for statistical significance in phospho-protein profile. To test for significance of the observed difference in cell number after six days of stimulation the paired *t*-test was used (Graphpad Prism 5; GraphPad Software Inc., USA). A two-way analysis of variance (ANOVA) was used to test for significant difference at each time point in the MTT assay. *P* values <0.05 were considered to be statistically significant. Given that the biological significance of a given fold-change is likely to depend on the gene and on the experimental context no fixed fold change cut-off was employed in this study.

## Results

### *HOXA9* is overexpressed in colonic adenomas

*HOX* genes have been linked to cancer development and especially *HOXA9* is interesting in this respect as it functions as an oncogene in various hematological malignancies (56). It has been reported that *HOXA9* contributes to self-renewal and overpopulation of cancer stem cells in CRC (57). Thus, we decided to investigate whether *HOXA9* mRNA expression is deregulated in colonic premalignant tissue. To this end we collected 27 biopsies from colonic adenomas and location-matched healthy tissue and determined *HOXA9* expression by qPCR. A direct comparison between the paired adenoma and healthy tissues demonstrates significantly increased *HOXA9* mRNA expression levels in the adenoma samples (fold change (FC) 1.95;  $p < 1.0 \cdot 10^{-4}$ ; **Figure 1**).

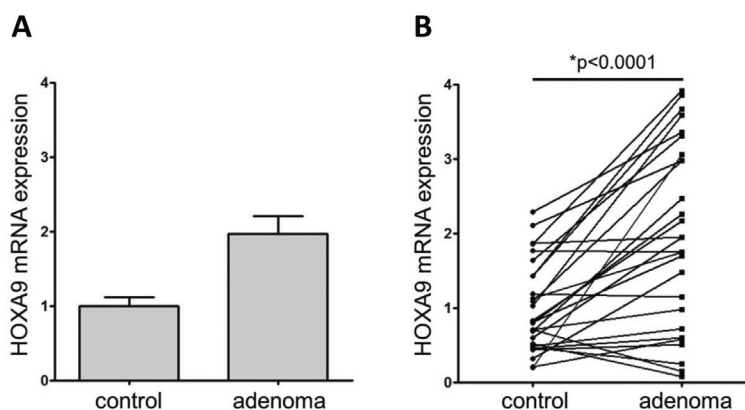


**Figure 1.** mRNA expression of *HOXA9* in colonic adenoma tissue and matched healthy control tissue. Paired tissue samples were taken and analyzed for *HOXA9* expression by RT-qPCR. In the left panel (A) mean expression levels with standard error of the mean (SEM) are depicted. In the right panel (B) the pairs are linked and the result of a paired sample *t*-test is shown ( $p < 0.0001$ ).

Of note, five patients did not adhere to this trend of upregulated *HOXA9* in their adenomatous tissue, however, no differences in clinical parameters (age, gender, ethnicity or type of polyp) could be detected and no follow-up data was available to assess long term consequences of differences in *HOXA9* between patient groups. We concluded that pre-malignant colonic polyps are characterized by an abundance of *HOXA9* expression as compared to healthy colonic tissue.

### ***HOXA9* overexpression substantially alters the oncogenic mRNA profile**

Having shown that *HOXA9* upregulation is an early event during colonic carcinogenesis, we next investigated the molecular consequences of this upregulation by overexpressing *HOXA9* in the CRC model cell lines. Transduction of such cells with an inducible *HOXA9* lentiviral vector results in a  $\approx 30$ -70 fold increase in *HOXA9* mRNA expression upon doxycycline induction, when compared to cells transduced with a control plasmid (**Supplementary Figure S1**). Next, the effect of *HOXA9* overexpression on potential target genes was examined. To identify potentially interesting *HOXA9* targets, we employed the Cancer Pathway Finder RT<sup>2</sup> Profiler PCR Array (**Figure 2A**). Intriguingly, analysis of the differentially expressed genes showed that the most drastically downregulated gene was *CCL2*, which encodes for the chemokine MCP-1, and is a well-known mediator of tumor metastasis. Indeed, high levels of *CCL2* are associated with poor outcome in CRC patients due to high incidence of metastasis (58, 59). Thus, this result implies that *HOXA9* expression might be specific to pre-metastatic lesions.

Other downregulated genes included the metabolism genes *ACLY* and *ACSL4* and the apoptosis genes *CASP2* and *CASP7*. Among the most prominently upregulated genes were the cell cycle genes *CCND2*, *CCND3*, *SKP2* and *MKI67* and the growth factor *FGF2*, suggesting that *HOXA9* overexpression provokes a proliferative phenotype. Another highly upregulated gene is the insulin growth factor binding protein 7 (*IGFBP7*). This gene is part of the category of IGF1 signaling modulating genes, and while often considered tumor suppressive, has also been shown to be upregulated in some cancers, and may have growth stimulatory effects in CRC (60-62). *HOXA9* overexpression led to overexpression of the HMG-box gene *SOX10*. This gene is best known for its role in neural crest differentiation during embryogenesis, but its ectopic expression in tumors has also been shown to confer tumor aggressiveness in some tumor types (63-66), although a tumor suppressive role has also been reported (67). In conjunction, these results are best interpreted as indicating that *HOXA9* expression may stimulate adenoma growth and is responsible for compartment expansion but concomitantly would be associated with non-metaplastic behavior.

Taken together, this exploratory analysis suggests a decreased migratory phenotype, with reduced apoptosis, and increased proliferation markers. Next, we expanded on these findings by designing qPCR primers for a range of target genes not included

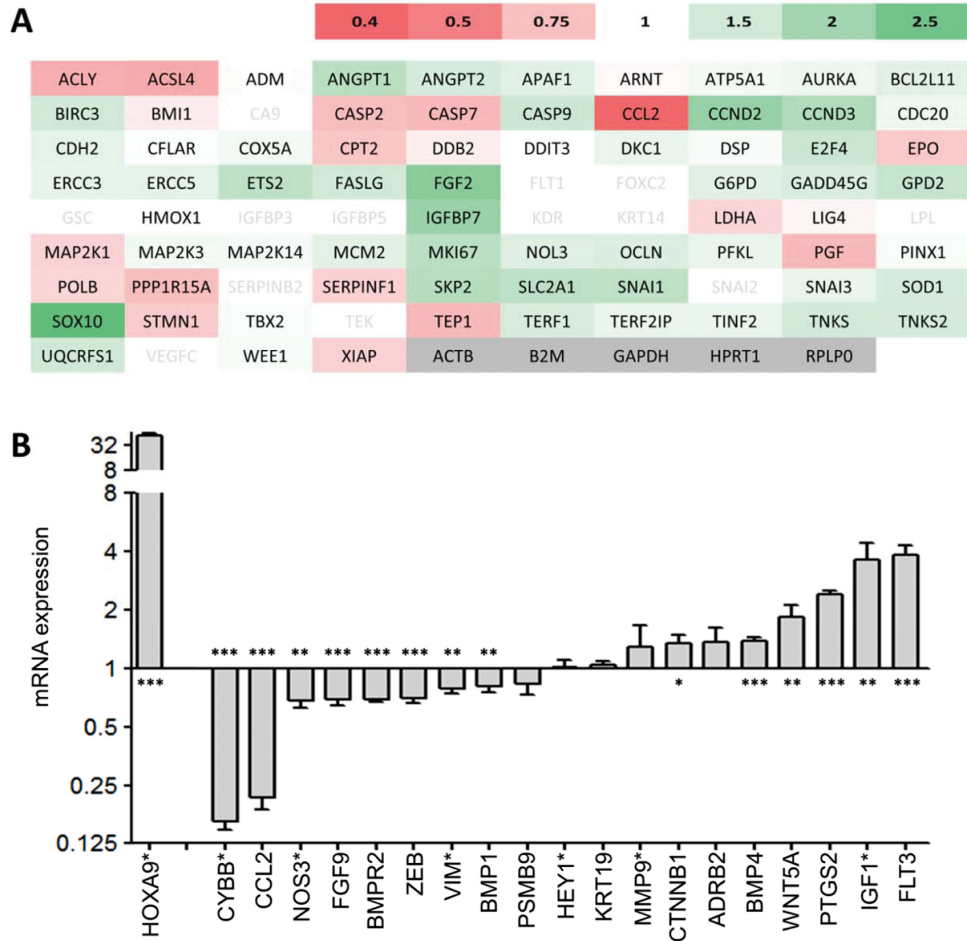


**Figure 2.** Effect of *HOXA9* overexpression on target genes. **(A)** The RT<sup>2</sup> Profiler™ PCR Array was used to detect differential expression profiles between *HOXA9* overexpressing cells and control cells. Depicted are the mRNA levels quantified in a single experiment. mRNAs in red are downregulated upon *HOXA9* overexpression compared to a control transduced Caco-2 cell line, conversely, mRNAs in green are upregulated. See scale bar in the right upper corner for the magnitude of the fold changes. **(B)** The overexpression of *HOXA9* is depicted in this panel. RT-qPCR was performed on 25 mRNA targets identified to be modulated by *HOXA9* in literature (Table S2). Of these, 6 were not detectable by qPCR, the expression of the remainder of mRNAs (19) are shown as a fold change compared to control cells. Expression data of mRNAs that did not meet the assumption of Gaussian distribution, according to both the Komogorov-Smirnov test, the D'Agostino and Pearson omnibus normality test, and the Shapiro-Wilk normality test were indicated with an \* next to their name on the X-axis. Expression data of mRNAs that did not meet assumption of Gaussian distribution are presented as medians ±IQR. \* $p<0.05$ , \*\* $p<0.01$ , \*\*\* $p<0.001$ . For the genes that did meet the assumption of Gaussian distribution, results presented as means ± SEM.



in the array, but with specific connection to *HOXA9* as identified in literature search including all tissues and model systems (see **Supplementary Table S1**; (68-72). In addition, we also verified the main interesting finding of the Cancer Pathway Finder array, *CCL2* expression using alternative primers. The statistically significantly regulated genes with the highest upregulation were *FLT3* (mean FC=3.8), *IGF1* (mean FC=2.8), *PTGS2* (mean FC=2.4) and *WNT5a* (mean FC=1.8). *FLT3*, *IGF1* and *WNT5a* are all associated with compartment expansion (**Figure 2B**). *FLT3* is a tyrosine kinase receptor, *IGF* is a growth factor which stimulates phosphorylation dependent kinase cascades via the *IGF*-receptor, and *WNT5a* activates intracellular signaling through ligation to the *Ror2*/*Frizzled* receptors. Overexpression of *PTGS2* (better known as *COX2*) has been associated with adenomatous changes and its inhibition is well-established to counteract colorectal polyp formation (73, 74). The genes with the highest relative downregulation were *CYBB* (mean FC=0.2), encoding for the NADPH oxidase complex protein *NOX2*, and *CCL2* (mean FC=0.2). Interestingly, a switch in expression from *NOX1* to *NOX2* induced a migratory invasive phenotype in colorectal cancer cells (75), which, together with the decreased *CCL2* expression, suggests that *HOXA9* overexpression decreases CRC migratory behavior. Genes associated with epithelial to mesenchymal transition (EMT) (*BMP1*, *BMPR2*, *KRT19*, *VIM* and *ZEB*) measured in this study showed little to no difference in expression as a result of *HOXA9* overexpression. Overall, a picture emerges that *HOXA9* is associated with polyp formation but also counteracts malignant progression.

### Changes in cellular phosphoprofile support a role for *HOXA9* in polyp growth but not malignant expansion

As *HOXA9* overexpression modulates genetic transcription patterns towards an early proliferative phenotypes, we next sought to determine to what extent *HOXA9* induced changes are translated to altered signal transduction patterns. We performed extensive (phospho) protein profiling to quantify the expression and activation status of several important signal transduction molecules (**Supplementary Table S2**). Analysis of constitutive expression of signaling molecules did not reveal significantly discriminative patterns between *HOXA9* overexpressing and mock transduced cell pools (**Supplementary Figure S2A, B**). However, a distinct phosphoprofile upon *HOXA9* overexpression was seen, as evidenced by the clustering of control and overexpression samples (**Figure 3**).

The most discriminate findings were a clustering of downregulated p-S6 (FC=0.50,  $p < 1.0 \cdot 10^{-4}$ ) and p-PDK1 (FC=0.45,  $p = 5.9 \cdot 10^{-3}$ ) upon *HOXA9* overexpression (see **Figure 4** for individual analyses). Canonical signaling dictates that activity of PDK1 results in phosphorylation of the Thr308 residue of AKT, a survival protein, while phosphorylation of this protein on its Ser473 residue is dependent on the mammalian target of rapamycin (mTOR) when in association with Rictor in the so called mTORC2 complex (**Figure 5A**). Fully activated AKT in turn is known to activate the mTOR/Raptor

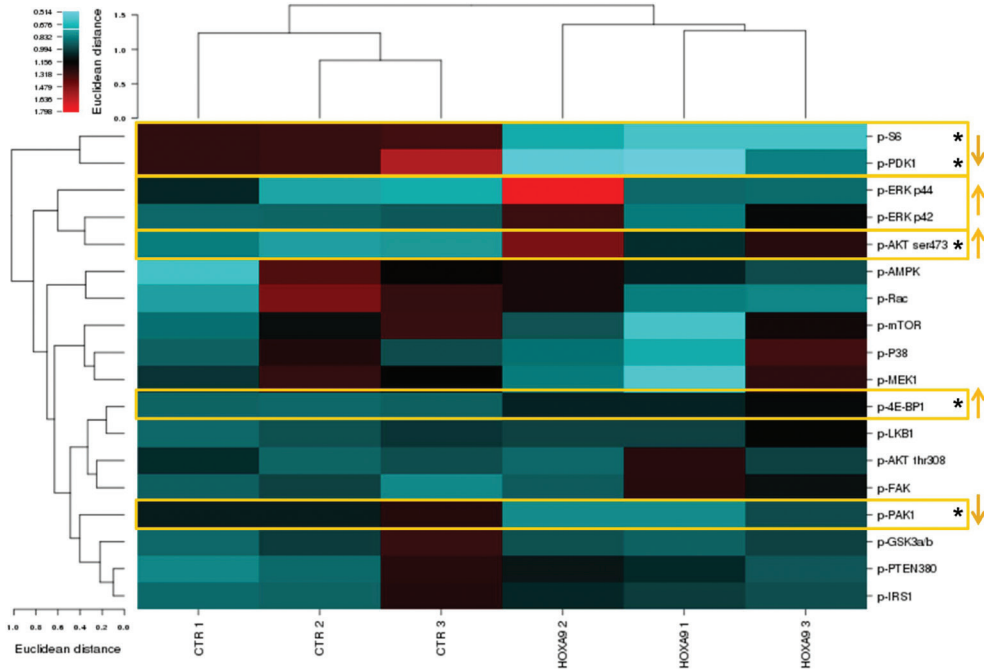


**Figure 3.** *HOXA9* influences cellular phosphoprofile. Heat maps of the phospho-protein profile constructed with CIMminer. Increased phosphorylation is depicted in red, conversely decreased phosphorylation is depicted in blue. See scale bar in the top left corner for magnitude of the phosphorylation. Euclidian distance between the samples is depicted on top. For the phosphorylation status of the various signaling proteins Euclidian distance is depicted to the left. Statistical significance was indicated on the right side of the figure with an asterisks \* $p < 0.05$ , \*\* $p < 0.01$ , \*\*\* $p < 0.001$ . Orange boxes and arrows are placed over molecules or molecule pairs to clarify the direction of regulation visually.

complex (mTORC1), which results in phosphorylation both the ribosomal S6 kinase and the translation factor 4E-BP regulating cell size and protein synthesis, respectively (76). However, our results indicate an uncoupling with canonical mTOR signaling in cells overexpressing *HOXA9*: 1) the decreased PDK activity was not accompanied by reduced AKT-thr308 phosphorylation, but corresponded closely to decreased S6 phosphorylation. 2) While there was a trend towards lower mTOR phosphorylation, this was not significant, suggesting that the phosphorylation of S6 upon *HOXA9* is not a direct effect of reduced mTOR signaling. 3) 4E-BP phosphorylation was significantly increased ( $FC=1.21$ ,  $p=2.0 \cdot 10^{-3}$ ), rather than decreased in *HOXA9* overexpressing cells. Uncoupling between mTOR and its downstream targets is not unprecedented, as a direct activation of S6 via PDK1 has also been described (77, 78), and 4E-BP1 signaling can be independent of mTOR activity in CRC (79). However, this begs the question as to what activates 4E-BP; if not mTOR. Based on our dataset, it is tempting to speculate that AKT activity ( $FC=1.6$ ,  $p=2.12 \cdot 10^{-2}$ ) may bypass mTOR in the phosphorylation of 4E-BP (**Figure 5B**). Adding a further layer of complexity, it was previously shown

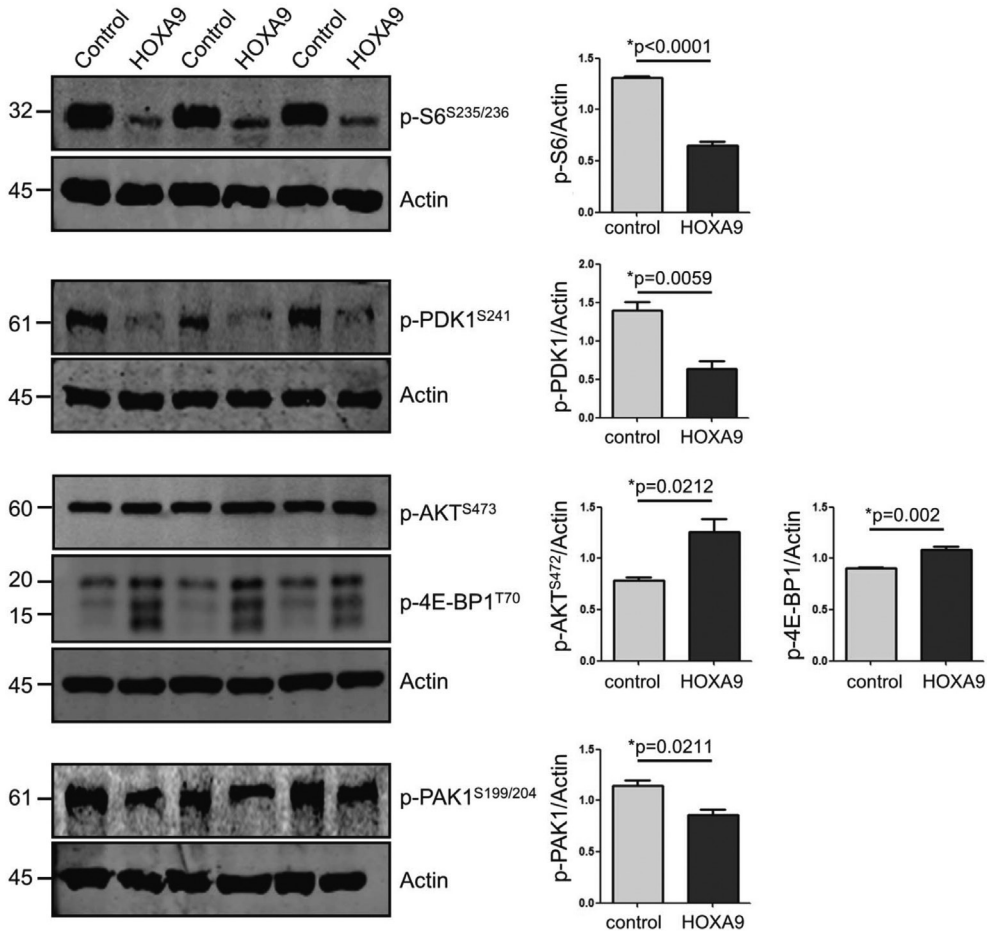


**Figure 4.** *HOXA9* induces differential protein expression. (A) Western blots of the five proteins for which the phosphorylation status was significantly altered by *HOXA9*, their names are depicted on the right, and the size of the band is indicated on the left. The *HOXA9* status of the samples is depicted on top. (B) The results of densitometric analysis of the fluorescence bands are depicted expressed in normalized densitometry values (AU, arbitrary units). Blots were reprobed for actin for loading control. Additionally, their corresponding *p* values are depicted above the panels.

that knockdown of Rictor promotes AKT phosphorylation, and it is conceivable that *HOXA9* modulates part of the mTORC2 complex rather than mTOR *per se* (80).

Another interesting feature revealed by the phosphoproteomics was a significantly downregulation of PAK activity ( $FC=0.75$ ,  $p=2.1 \cdot 10^{-2}$ ), a protein involved in cytoskeletal rearrangement and migration. The direct upstream activator of PAK is the GTPase RAC1 (81). While we did not observe any significant changes in activity of RAC1 as measured by its phosphorylation, there was a trend towards reduced RAC1 phosphorylation levels in *HOXA9*-overexpressing cells. It should be noted that the role of phosphorylation for

RAC1 activity has been questioned, and its activity is best measured by demonstrating its GTP-loading. However, we have also previously shown that PAK activity can be mediated through AMPK-tubero sclerosis complex (TSC), independent of mTOR and RAC1 (82). *In toto* support these observations the notion that *HOXA9* expression supports benign but not malignant compartment expansion.

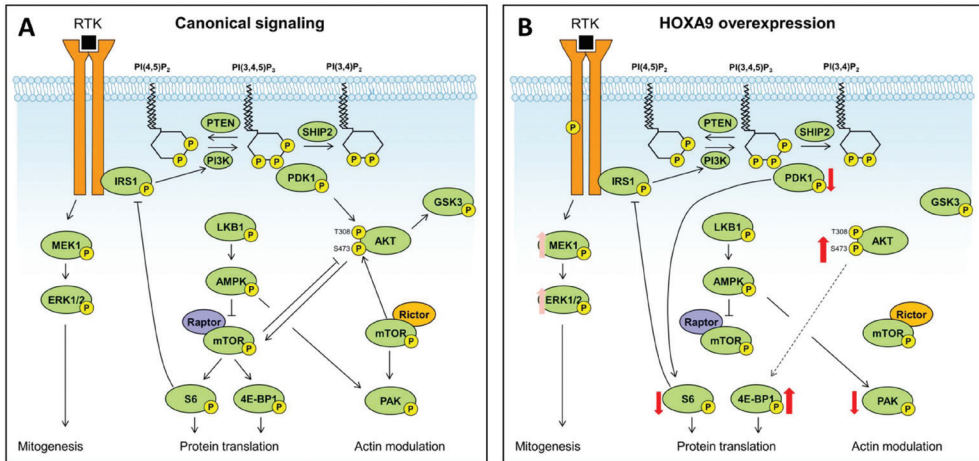


**Figure 5.** *HOXA9* influences mitogenesis, protein translation, and actin modulation. (A) Canonical signaling pathways of phosphoproteins. (B) Altered signaling upon *HOXA9* overexpression. Red arrows indicate statistically significant directional regulation, pink arrows depict a trend in regulation.

### ***HOXA9* overexpression stimulates adenoma growth**

Taken together our mRNA and protein analyses of forced *HOXA9* expression indicates that this gene provokes increased growth-factor (*IGF1*, *FLT3*, *WNT5a*) action, enhances survival (pAKT) signaling and protein synthesis (phosphorylation of p-4E-BP1 which relieves its suppressive action on the translation-initiation factor eIF4E, resulting in increased translational activity (83). We next sought to validate whether these molecular consequences of *HOXA9* overexpression translate into cellular phenotypic changes. Therefore, we compared the cell pool growth of both the *HOXA9* overexpressing and control cell lines. Starting with equal cell numbers, 70% more cells were seen after 6 days of culture in cell cultures of *HOXA9* overexpressing cells as compared to controls ( $p < 4.0 \cdot 10^{-3}$ ; **Figure 6A**), suggesting that *HOXA9* confers a growth advantage to cells. To confirm this, the cell pool size was measured daily for four consecutive days. **Figure 6B** shows that *HOXA9* overexpressing cells have a significantly increased growth rate compared to control cell cultures (day two,  $p < 0.05$ , day three,  $p < 1.0 \cdot 10^{-3}$ , and day four,  $p < 1.0 \cdot 10^{-3}$ ; **Figure 6B**). We further confirmed these data by culturing cells in a 3D spheroid-based model, which again indicated that *HOXA9* overexpressing cells grow

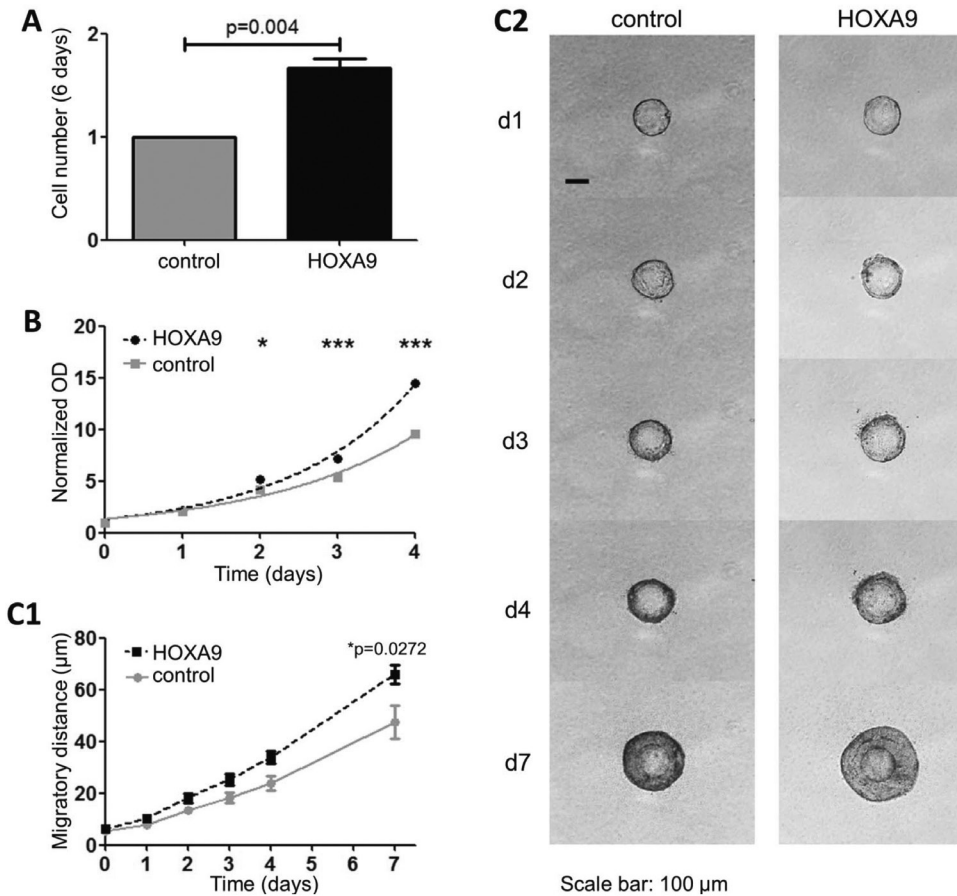


**Figure 6.** *HOXA9* overexpression results in increased growth of the cell pool. (A) Cell count after six days stimulation with doxycycline. Amount of control cells after six days is the reference value. (B) MTT assay measuring viable cells in *HOXA9* and control transduced Caco-2 cells. Results are represented as mean  $\pm$  SEM of three independent experiments.  $*p<0.05$ ,  $***p<0.001$  compared with control by Student's *t*-test. (C1) 3D-migration assay, quantified results of one representative experiment (out of three) with data of ten coated beads. (C2) Photographs of control and *HOXA9* overexpressing cells on beads in gelatin at days 1, 2, 3, 4, and 7. "d"=day. Data was statistically analyzed by two-way ANOVA.

faster in 3D as compared to control cells. ( $p=0.0272$ ; **Figure 6C1** for quantified results and **C2** for illustrations of cells on the beads). Hence increased *HOXA9* expression may be directly related to the compartment size expansion that characterizes the adenomatous epithelium.

### ***HOXA9* overexpression inhibits cellular migration suggesting that its expression is specific for the adenoma stage in CRC progression**

The reduced expression of chemokines (*CCL2*) and cytoskeletal modulators (pPAK) suggests that motility of cells might be affected upon overexpression of *HOXA9* (84, 85).

Therefore, we investigated migratory ability of these cells using 2D ring-barrier assays which, unlike conventional scratch assays, are not influenced by proliferative capacity of cell cultures but use time-lapse microscopy to track individual cell movement. Results show that *HOXA9* overexpression leads to a significant reduction in individual cell migration, compromising the total and effective migration after three days, as well as in the efficiency and speed of cellular migration (**Figure 7**).

Tubular adenoma is the precursor to full blown CRC but is considered to have no metastatic potential. The present study shows that *HOXA9* is highly expressed in colonic tubular adenomas and this expression can drive compartment expansion in a preclinical model. However, forced expression of *HOXA9* also counteracts *CCL2* and metastasis. In conjunction, these findings suggest that *HOXA9* is a defining molecular marker of specifically the tubular adenoma stage in CRC development. This would fit a recent report that showed that in full blown CRC, tumors are characterized by increased *HOXA9* expression but that such expression does not correlate with clinical outcome (41). Here we show that this increase is particularly manifest at the adenoma stage, but our mechanistic studies also reveal that for successful metastasis, *HOXA9* expression is inhibitory. Thus, increased *HOXA9* expression has a specific pro-oncogenic functionality only at early stage of the CRC process and can be considered a marker of these early stages.

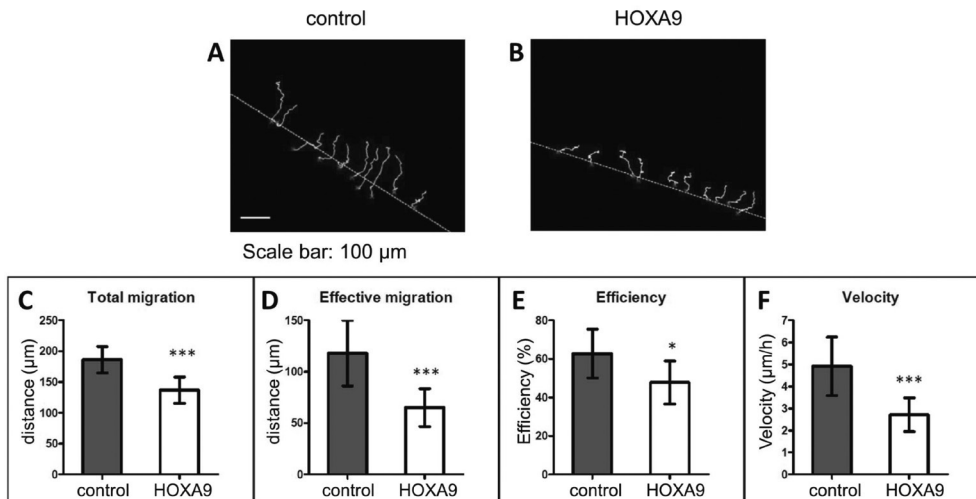


**Figure 7.** *HOXA9* overexpression inhibits cellular migration. Individual cells were tracked in time laps microscopy of cellular migration for control cells (A) and *HOXA9* overexpressing cells (B). A minimum of 10 cells were traced for each condition per experiment, and total migration (C), effective migration (D), efficiency (E) and velocity (F) of migration were calculated. Results are represented as mean  $\pm$  standard error of the mean (SEM) of three independent experiments.

## Discussion

CRC remains a major health problem. Better definition of molecular markers that relate to the natural history of early CRC would prove exceedingly useful. In this study we compared *HOXA9* expression between adenoma tissue and location matched healthy colon epithelium and we subsequently decided to investigate the role of *HOXA9* in oncological transformation of colonic epithelial cells. We observe that *HOXA9* is overexpressed in colonic adenomas and drives compartment expansion but concomitantly counteracts metastasis. Thus, *HOXA9* expression emerges as a molecular determinant for pre-micrometastatic colonic adenomas and may support benign polyp growth in the colon.

### Potential mechanisms mediating increased *HOXA9* expression in adenoma

Based on the data from the publically available cBioPortal (**Supplementary Figure S3**), gene amplification appears not to be involved in the increase of *HOXA9* levels in CRC (50) (not shown). Given that gene amplifications are rare in colonic adenomas this is in line with our findings. Also chromosomal translocation, which can drive altered *HOXA9* expression in hematological malignancies, does not appear an important factor in this respect (not shown). Furthermore, *HOXA9* was not found to be differentially methylated in CRC (86). Bhatlekar et al. found that *HOXA4* and *HOXA9* are up-regulated in CRC stem cells (57). Their data indicates that *HOXA9* aids self-renewal and overpopulation of stem cells in CRC. Multiple reports have described *HOXA9* as a pro-oncogenic factor in other solid tumors (87). Hence, increased *HOXA9* expression may well be driven by selection of clones that have a competitive advantage because of relatively high *HOXA9* expression and the resulting outcompeting of cells not having such high expression. In line with this train of thought is that  $\beta$ -catenin signaling, activated upon WNT5A ligation to its receptor, is required for *HoxA9*-mediated transformation in the hematopoietic system (88). Additionally, colonic adenomas are almost universally characterized by high levels of  $\beta$ -catenin signaling (89). However further experimentation is obviously necessary to substantiate this notion.

## Conclusion

In conclusion, *HOXA9* is overexpressed in colonic adenomas. It inhibits cellular migration which appears to be mediated by effects on PAK activity. Strikingly, the pro-oncogenic phenotype of *HOXA9* alteration in hematologic malignancies was also found in this study as *HOXA9* stimulates cell growth. This phenotype appears to be mediated through increased *IGF1*, *FLT3*, *PTGS2* and p-AKT and p-4E-BP1. This is the first mechanistic study into the effect of *HOXA9* in a premalignant lesion.

## Funding

MPP is grateful to the Dutch Society for the Replacement of Animal Testing (dsRAT) for the financial support of his work. The authors would like to thank the FAPESP (2016/08888-9; 2016/01139-0) for financial support for RdS.

## Acknowledgements

We would like to acknowledge M.H.W. van Dullemen for experimentation.

## References

1. Ferlay J, Shin HR, Bray F, Forman D, Mathers C, Parkin DM. Estimates of worldwide burden of cancer in 2008: GLOBOCAN 2008. *Int J Cancer*. 2010;127(12):2893-917.
2. Brouwer NPM, Bos A, Lemmens V, Tanis PJ, Hugén N, Nagtegaal ID, et al. An overview of 25 years of incidence, treatment and outcome of colorectal cancer patients. *Int J Cancer*. 2018;143(11):2758-66.
3. Elferink MAG, Toes-Zoutendijk E, Vink GR, Lansdorp-Vogelaar I, Meijer GA, Dekker E, et al. [National population screening for colorectal carcinoma in the Netherlands: results of the first years since the implementation in 2014] Landelijk bevolkingsonderzoek naar colorectaal carcinoom. *Ned Tijdschr Geneeskd*. 2018;162:D2283.
4. Toes-Zoutendijk E, van Leerdam ME, Dekker E, van Hees F, Penning C, Nagtegaal I, et al. Real-Time Monitoring of Results During First Year of Dutch Colorectal Cancer Screening Program and Optimization by Altering Fecal Immunochemical Test Cut-Off Levels. *Gastroenterology*. 2017;152(4):767-75 e2.
5. Greuter MJE, de Klerk CM, Meijer GA, Dekker E, Coupe VMH. Screening for Colorectal Cancer With Fecal Immunochemical Testing With and Without Postpolypectomy Surveillance Colonoscopy: A Cost-Effectiveness Analysis. *Ann Intern Med*. 2017;167(8):544-54.
6. Edwards BK, Ward E, Kohler BA, Ehemann C, Zauberg AG, Anderson RN, et al. Annual report to the nation on the status of cancer, 1975-2006, featuring colorectal cancer trends and impact of interventions (risk factors, screening, and treatment) to reduce future rates. *Cancer*. 2010;116(3):544-73.
7. Vogelstein B, Fearon ER, Hamilton SR, Kern SE, Preisinger AC, Leppert M, et al. Genetic alterations during colorectal-tumor development. *N Engl J Med*. 1988;319(9):525-32.
8. Williams AR, Balasooriya BA, Day DW. Polyps and cancer of the large bowel: a necropsy study in Liverpool. *Gut*. 1982;23(10):835-42.
9. Rex DK. Colonoscopy: a review of its yield for cancers and adenomas by indication. *Am J Gastroenterol*. 1995;90(3):353-65.
10. Rex DK, Lehman GA, Ulbright TM, Smith JJ, Pound DC, Hawes RH, et al. Colonic neoplasia in asymptomatic persons with negative fecal occult blood tests: influence of age, gender, and family history. *Am J Gastroenterol*. 1993;88(6):825-31.
11. Wang FW, Hsu PI, Chuang HY, Tu MS, Mar GY, King TM, et al. Prevalence and risk factors of asymptomatic colorectal polyps in taiwan. *Gastroenterol Res Pract*. 2014;2014:985205.



12. Abate-Shen C. Deregulated homeobox gene expression in cancer: cause or consequence? *Nat Rev Cancer*. 2002;2(10):777-85.
13. Reya T, Clevers H. Wnt signalling in stem cells and cancer. *Nature*. 2005;434(7035):843-50.
14. Taipale J, Beachy PA. The Hedgehog and Wnt signalling pathways in cancer. *Nature*. 2001;411(6835):349-54.
15. McGinnis W, Krumlauf R. Homeobox genes and axial patterning. *Cell*. 1992;68(2):283-302.
16. Pearson JC, Lemons D, McGinnis W. Modulating Hox gene functions during animal body patterning. *Nat Rev Genet*. 2005;6(12):893-904.
17. Hueber SD, Rauch J, Djordjevic MA, Gunter H, Weiller GF, Frickey T. Analysis of central Hox protein types across bilaterian clades: on the diversification of central Hox proteins from an Antennapedia/Hox7-like protein. *Dev Biol*. 2013;383(2):175-85.
18. Lewis EB. A gene complex controlling segmentation in *Drosophila*. *Nature*. 1978;276(5688):565-70.
19. Hunt P, Whiting J, Nonchev S, Sham MH, Marshall H, Graham A, et al. The branchial Hox code and its implications for gene regulation, patterning of the nervous system and head evolution. *Dev Suppl*. 1991;Suppl 2:63-77.
20. Pollock RA, Jay G, Biebrich CJ. Altering the boundaries of Hox3.1 expression: evidence for antipodal gene regulation. *Cell*. 1992;71(6):911-23.
21. Yokouchi Y, Sasaki H, Kuroiwa A. Homeobox gene expression correlated with the bifurcation process of limb cartilage development. *Nature*. 1991;353(6343):443-5.
22. Yahagi N, Kosaki R, Ito T, Mitsunashi T, Shimada H, Tomita M, et al. Position-specific expression of Hox genes along the gastrointestinal tract. *Congenit Anom (Kyoto)*. 2004;44(1):18-26.
23. Beck F. Homeobox genes in gut development. *Gut*. 2002;51(3):450-4.
24. Abe M, Hamada J, Takahashi O, Takahashi Y, Tada M, Miyamoto M, et al. Disordered expression of HOX genes in human non-small cell lung cancer. *Oncol Rep*. 2006;15(4):797-802.
25. Cantile M, Pettinato G, Procino A, Feliciello I, Cindolo L, Cillo C. In vivo expression of the whole HOX gene network in human breast cancer. *Eur J Cancer*. 2003;39(2):257-64.
26. Miller GJ, Miller HL, van Bokhoven A, Lambert JR, Werahera PN, Schirripa O, et al. Aberrant HOXC expression accompanies the malignant phenotype in human prostate. *Cancer Res*. 2003;63(18):5879-88.
27. Liu YJ, Zhu Y, Yuan HX, Zhang JP, Guo JM, Lin ZM. Overexpression of HOXC11 homeobox gene in clear cell renal cell carcinoma induces cellular proliferation and is associated with poor prognosis. *Tumour Biol*. 2015;36(4):2821-9.
28. Cantile M, Scognamiglio G, Anniciello A, Farina M, Gentilcore G, Santonastaso C, et al. Increased HOXC13 expression in metastatic melanoma progression. *J Transl Med*. 2012;10:91.
29. Cantile M, Scognamiglio G, La Sala L, La Mantia E, Scaramuzza V, Valentino E, et al. Aberrant expression of posterior HOX genes in well differentiated histotypes of thyroid cancers. *Int J Mol Sci*. 2013;14(11):21727-40.
30. Cheng W, Liu J, Yoshida H, Rosen D, Naora H. Lineage infidelity of epithelial ovarian cancers is controlled by HOX genes that specify regional identity in the reproductive tract. *Nat Med*. 2005;11(5):531-7.
31. Nakamura T, Largaespada DA, Lee MP, Johnson LA, Ohyashiki K, Toyama K, et al. Fusion of the nucleoporin gene NUP98 to HOXA9 by the chromosome translocation t(7;11)(p15;p15) in human myeloid leukaemia. *Nat Genet*. 1996;12(2):154-8.
32. Heinrichs S, Berman JN, Ortiz TM, Kornblau SM, Neuberg DS, Estey EH, et al. CD34+ cell selection is required to assess HOXA9 expression levels in patients with myelodysplastic syndrome. *Br J Haematol*. 2005;130(1):83-6.

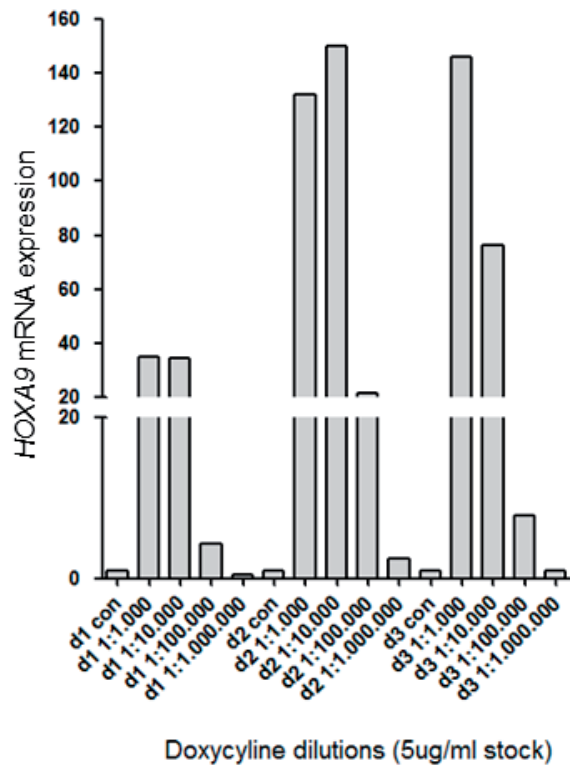
33. Baril C, Gavory G, Bidla G, Knaevelsrud H, Sauvageau G, Therrien M. Human NUP98-HOXA9 promotes hyperplastic growth of hematopoietic tissues in *Drosophila*. *Dev Biol.* 2017;421(1):16-26.
34. Golub TR, Slonim DK, Tamayo P, Huard C, Gaasenbeek M, Mesirov JP, et al. Molecular classification of cancer: class discovery and class prediction by gene expression monitoring. *Science.* 1999;286(5439):531-7.
35. Zhang ZF, Wang YJ, Fan SH, Du SX, Li XD, Wu DM, et al. MicroRNA-182 downregulates Wnt/beta-catenin signaling, inhibits proliferation, and promotes apoptosis in human osteosarcoma cells by targeting HOXA9. *Oncotarget.* 2017;8(60):101345-61.
36. Park SM, Choi EY, Bae M, Choi JK, Kim YJ. A long-range interactive DNA methylation marker panel for the promoters of HOXA9 and HOXA10 predicts survival in breast cancer patients. *Clin Epigenetics.* 2017;9:73.
37. Wang K, Jin J, Ma T, Zhai H. MiR-139-5p inhibits the tumorigenesis and progression of oral squamous carcinoma cells by targeting HOXA9. *J Cell Mol Med.* 2017;21(12):3730-40.
38. Kanai M, Hamada J, Takada M, Asano T, Murakawa K, Takahashi Y, et al. Aberrant expressions of HOX genes in colorectal and hepatocellular carcinomas. *Oncol Rep.* 2010;23(3):843-51.
39. Ko SY, Barengo N, Ladanyi A, Lee JS, Marini F, Lengyel E, et al. HOXA9 promotes ovarian cancer growth by stimulating cancer-associated fibroblasts. *J Clin Invest.* 2012;122(10):3603-17.
40. Segditsas S, Sieber O, Deheragoda M, East P, Rowan A, Jeffery R, et al. Putative direct and indirect Wnt targets identified through consistent gene expression changes in APC-mutant intestinal adenomas from humans and mice. *Hum Mol Genet.* 2008;17(24):3864-75.
41. Watanabe Y, Saito M, Saito K, Matsumoto Y, Kanke Y, Onozawa H, et al. Upregulated HOXA9 expression is associated with lymph node metastasis in colorectal cancer. *Oncol Lett.* 2018;15(3):2756-62.
42. van Baal JW, Milano F, Rygiel AM, Bergman JJ, Rosmolen WD, van Deventer SJ, et al. A comparative analysis by SAGE of gene expression profiles of Barrett's esophagus, normal squamous esophagus, and gastric cardia. *Gastroenterology.* 2005;129(4):1274-81.
43. Somasundaram R, Fernandes S, Deuring JJ, de Haar C, Kuipers EJ, Vogelaar L, et al. Analysis of SHIP1 expression and activity in Crohn's disease patients. *PLoS One.* 2017;12(8):e0182308.
44. de Sousa RR, Queiroz KC, Souza AC, Gurgueira SA, Augusto AC, Miranda MA, et al. Phosphoprotein levels, MAPK activities and NFkappaB expression are affected by fisetin. *J Enzyme Inhib Med Chem.* 2007;22(4):439-44.
45. Schindelin J, Rueden CT, Hiner MC, Eliceiri KW. The ImageJ ecosystem: An open platform for biomedical image analysis. *Mol Reprod Dev.* 2015;82(7-8):518-29.
46. van Baal JW, Diks SH, Wanders RJ, Rygiel AM, Milano F, Joore J, et al. Comparison of kinome profiles of Barrett's esophagus with normal squamous esophagus and normal gastric cardia. *Cancer Res.* 2006;66(24):11605-12.
47. Myers TG, Anderson NL, Waltham M, Li G, Buolamwini JK, Scudiero DA, et al. A protein expression database for the molecular pharmacology of cancer. *Electrophoresis.* 1997;18(3-4):647-53.
48. Queiroz KC, Milani R, Ruela-de-Sousa RR, Fuhler GM, Justo GZ, Zambuzzi WF, et al. Violacein induces death of resistant leukaemia cells via kinome reprogramming, endoplasmic reticulum stress and Golgi apparatus collapse. *PLoS One.* 2012;7(10):e45362.
49. Das AM, Eggermont AM, ten Hagen TL. A ring barrier-based migration assay to assess cell migration in vitro. *Nat Protoc.* 2015;10(6):904-15.
50. Gao J, Aksoy BA, Dogrusoz U, Dresdner G, Gross B, Sumer SO, et al. Integrative analysis of complex cancer genomics and clinical profiles using the cBioPortal. *Sci Signal.* 2013;6(269):pl1.

51. Cerami E, Gao J, Dogrusoz U, Gross BE, Sumer SO, Aksoy BA, et al. The cBio cancer genomics portal: an open platform for exploring multidimensional cancer genomics data. *Cancer Discov.* 2012;2(5):401-4.
52. Giannakis M, Mu XJ, Shukla SA, Qian ZR, Cohen O, Nishihara R, et al. Genomic Correlates of Immune-Cell Infiltrates in Colorectal Carcinoma. *Cell Rep.* 2016;15(4):857-65.
53. Seshagiri S, Stawiski EW, Durinck S, Modrusan Z, Storm EE, Conboy CB, et al. Recurrent R-spondin fusions in colon cancer. *Nature.* 2012;488(7413):660-4.
54. Cancer Genome Atlas N. Comprehensive molecular characterization of human colon and rectal cancer. *Nature.* 2012;487(7407):330-7.
55. Brannon AR, Vakiani E, Sylvester BE, Scott SN, McDermott G, Shah RH, et al. Comparative sequencing analysis reveals high genomic concordance between matched primary and metastatic colorectal cancer lesions. *Genome Biol.* 2014;15(8):454.
56. Collins CT, Hess JL. Role of HOXA9 in leukemia: dysregulation, cofactors and essential targets. *Oncogene.* 2016;35(9):1090-8.
57. Bhatlekar S, Viswanathan V, Fields JZ, Boman BM. Overexpression of HOXA4 and HOXA9 genes promotes self-renewal and contributes to colon cancer stem cell overpopulation. *J Cell Physiol.* 2018;233(2):727-35.
58. Borsig L, Wolf MJ, Roblek M, Lorentzen A, Heikenwalder M. Inflammatory chemokines and metastasis--tracing the accessory. *Oncogene.* 2014;33(25):3217-24.
59. Chun E, Lavoie S, Michaud M, Gallini CA, Kim J, Soucy G, et al. CCL2 Promotes Colorectal Carcinogenesis by Enhancing Polymorphonuclear Myeloid-Derived Suppressor Cell Population and Function. *Cell Rep.* 2015;12(2):244-57.
60. Ruan W, Xu E, Xu F, Ma Y, Deng H, Huang Q, et al. IGFBP7 plays a potential tumor suppressor role in colorectal carcinogenesis. *Cancer Biol Ther.* 2007;6(3):354-9.
61. Rupp C, Scherzer M, Rudisch A, Unger C, Haslinger C, Schweifer N, et al. IGFBP7, a novel tumor stroma marker, with growth-promoting effects in colon cancer through a paracrine tumor-stroma interaction. *Oncogene.* 2015;34(7):815-25.
62. Georges RB, Adwan H, Hamdi H, Hielscher T, Linnemann U, Berger MR. The insulin-like growth factor binding proteins 3 and 7 are associated with colorectal cancer and liver metastasis. *Cancer Biol Ther.* 2011;12(1):69-79.
63. Benassi MS, Pazzaglia L, Novello C, Quattrini I, Pollino S, Magagnoli G, et al. Tissue and serum IGFBP7 protein as biomarker in high-grade soft tissue sarcoma. *Am J Cancer Res.* 2015;5(11):3446-54.
64. Bolonsky A, Hose D, Schreder M, Seckinger A, Lipp S, Klein B, et al. Insulin like growth factor binding protein 7 (IGFBP7) expression is linked to poor prognosis but may protect from bone disease in multiple myeloma. *J Hematol Oncol.* 2015;8:10.
65. Mito JK, Conner JR, Hornick JL, Cibas ES, Qian X. SOX10/keratin dual-color immunohistochemistry: An effective first-line test for the workup of epithelioid malignant neoplasms in FNA and small biopsy specimens. *Cancer Cytopathol.* 2018;126(3):179-89.
66. Graf SA, Busch C, Bosserhoff AK, Besch R, Berking C. SOX10 promotes melanoma cell invasion by regulating melanoma inhibitory activity. *J Invest Dermatol.* 2014;134(8):2212-20.
67. Bei L, Lu Y, Eklund EA. HOXA9 activates transcription of the gene encoding gp91Phox during myeloid differentiation. *J Biol Chem.* 2005;280(13):12359-70.
68. Ghannam G, Takeda A, Camarata T, Moore MA, Viale A, Yaseen NR. The oncogene Nup98-HOXA9 induces gene transcription in myeloid cells. *J Biol Chem.* 2004;279(2):866-75.

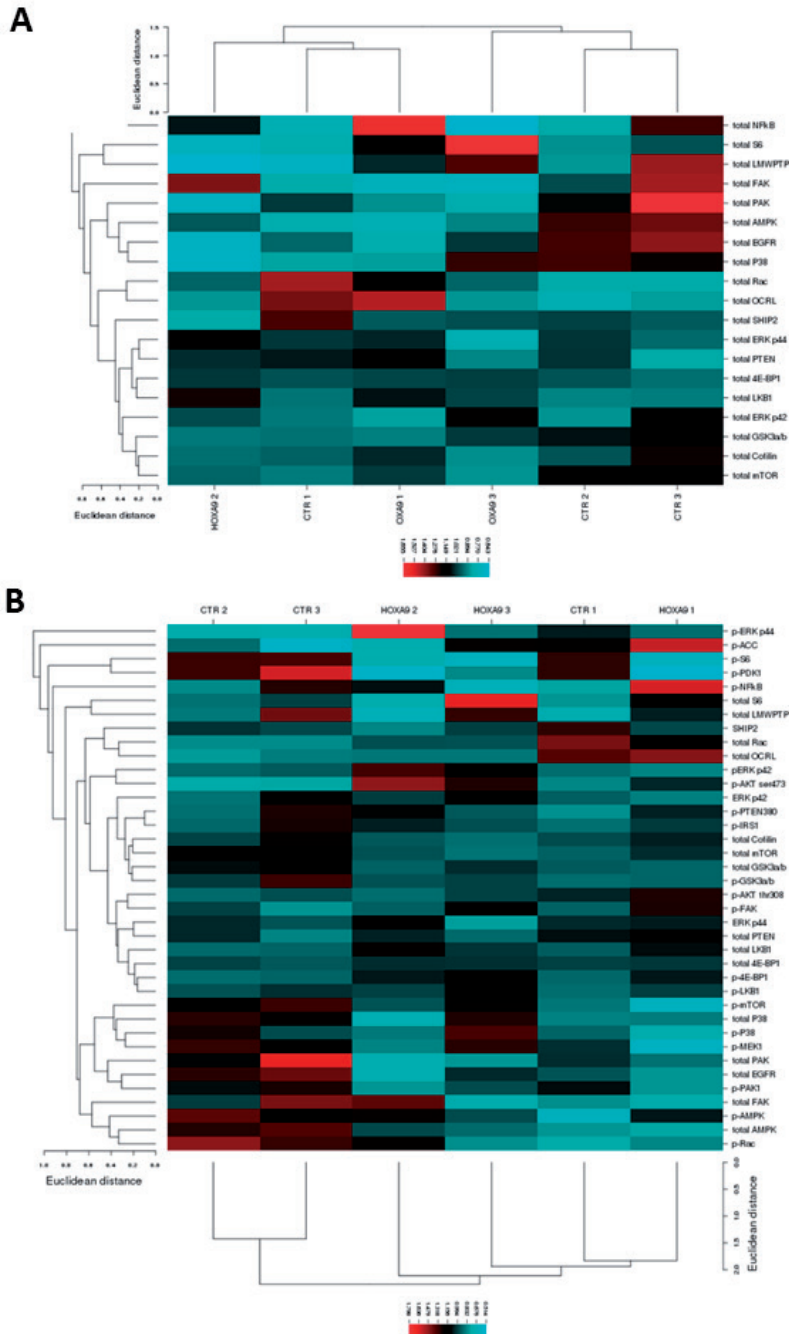
69. Jiang X, Huang H, Li Z, Li Y, Wang X, Gurbuxani S, et al. Blockade of miR-150 maturation by MLL-fusion/MYC/LIN-28 is required for MLL-associated leukemia. *Cancer Cell*. 2012;22(4):524-35.
70. Rossig L, Urbich C, Bruhl T, Dernbach E, Heeschen C, Chavakis E, et al. Histone deacetylase activity is essential for the expression of HoxA9 and for endothelial commitment of progenitor cells. *J Exp Med*. 2005;201(11):1825-35.
71. Shah CA, Bei L, Wang H, Platanias LC, Eklund EA. The leukemia-associated Mll-Ell oncoprotein induces fibroblast growth factor 2 (Fgf2)-dependent cytokine hypersensitivity in myeloid progenitor cells. *J Biol Chem*. 2013;288(45):32490-505.
72. Steger J, Fuller E, Garcia-Cuellar MP, Hetzner K, Slany RK. Insulin-like growth factor 1 is a direct HOXA9 target important for hematopoietic transformation. *Leukemia*. 2015;29(4):901-8.
73. Gupta SD, Das RN, Ghosh R, Sen A, Chatterjee U, Saha K, et al. Expression of COX-2 and p53 in juvenile polyposis coli and its correlation with adenomatous changes. *J Cancer Res Ther*. 2016;12(1):359-63.
74. Baghaei R, Beiraghdar M, Sobhani A, Rafei R, Kolahi L, Foladi L. An investigation of the rate of cyclooxygenase-2 expression on the surface of adenomatous and colorectal adenocarcinoma polyps. *Adv Biomed Res*. 2015;4:200.
75. Banskota S, Regmi SC, Kim JA. NOX1 to NOX2 switch deactivates AMPK and induces invasive phenotype in colon cancer cells through overexpression of MMP-7. *Mol Cancer*. 2015;14:123.
76. Okkenhaug K, Graupera M, Vanhaesebroeck B. Targeting PI3K in Cancer: Impact on Tumor Cells, Their Protective Stroma, Angiogenesis, and Immunotherapy. *Cancer Discov*. 2016;6(10):1090-105.
77. Vanhaesebroeck B, Stephens L, Hawkins P. PI3K signalling: the path to discovery and understanding. *Nat Rev Mol Cell Biol*. 2012;13(3):195-203.
78. Alessi DR, Kozlowski MT, Weng QP, Morrice N, Avruch J. 3-Phosphoinositide-dependent protein kinase 1 (PDK1) phosphorylates and activates the p70 S6 kinase in vivo and in vitro. *Curr Biol*. 1998;8(2):69-81.
79. Zhang Y, Zheng XF. mTOR-independent 4E-BP1 phosphorylation is associated with cancer resistance to mTOR kinase inhibitors. *Cell Cycle*. 2012;11(3):594-603.
80. Fuhler GM, Tyl MR, Olthof SG, Lyndsay Drayer A, Blom N, Vellenga E. Distinct roles of the mTOR components Rictor and Raptor in MO7e megakaryocytic cells. *Eur J Haematol*. 2009;83(3):235-45.
81. Symons M, Segall JE. Rac and Rho driving tumor invasion: who's at the wheel? *Genome Biol*. 2009;10(3):213.
82. Alves MM, Fuhler GM, Queiroz KC, Scholma J, Goorden S, Anink J, et al. PAK2 is an effector of TSC1/2 signaling independent of mTOR and a potential therapeutic target for Tuberous Sclerosis Complex. *Sci Rep*. 2015;5:14534.
83. Gingras AC, Raught B, Sonenberg N. Regulation of translation initiation by FRAP/mTOR. *Genes Dev*. 2001;15(7):807-26.
84. Whale A, Hashim FN, Fram S, Jones GE, Wells CM. Signalling to cancer cell invasion through PAK family kinases. *Front Biosci (Landmark Ed)*. 2011;16:849-64.
85. Foxall E, Pipili A, Jones GE, Wells CM. Significance of kinase activity in the dynamic invadosome. *Eur J Cell Biol*. 2016;95(11):483-92.
86. Ahlquist T, Lind GE, Costa VL, Meling GI, Vatn M, Hoff GS, et al. Gene methylation profiles of normal mucosa, and benign and malignant colorectal tumors identify early onset markers. *Mol Cancer*. 2008;7:94.
87. Ma YY, Zhang Y, Mou XZ, Liu ZC, Ru GQ, Li E. High level of homeobox A9 and PBX homeobox 3 expression in gastric cancer correlates with poor prognosis. *Oncol Lett*. 2017;14(5):5883-9.

88. Wang Y, Krivtsov AV, Sinha AU, North TE, Goessling W, Feng Z, et al. The Wnt/beta-catenin pathway is required for the development of leukemia stem cells in AML. *Science*. 2010;327(5973):1650-3.
89. Segditsas S, Tomlinson I. Colorectal cancer and genetic alterations in the Wnt pathway. *Oncogene*. 2006;25(57):7531-7.

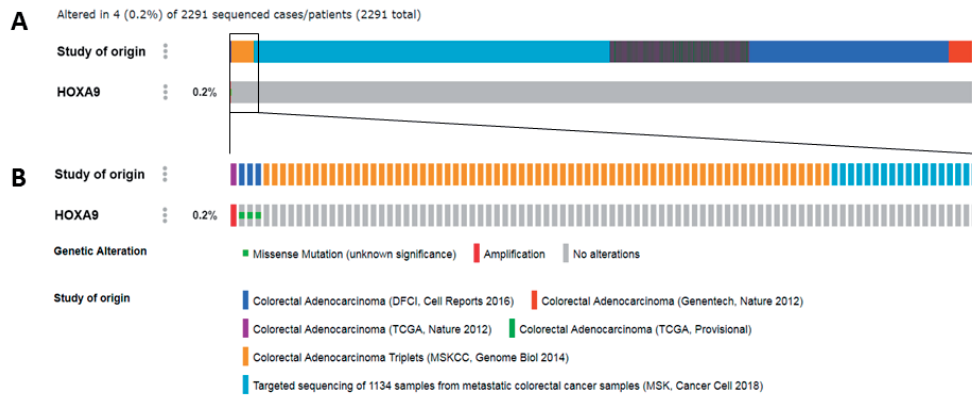
Supplementary information



**Supplementary Figure S1.** Forced *HOXA9* overexpression in Caco-2 cells. *HOXA9* mRNA expression in Caco-2 cell lines after stimulation with decreasing concentrations of doxycycline. Con: control cells, untreated with doxycycline. D: day. Maximal *HOXA9* expression was observed after two days of doxycycline treatment, in order for *HOXA9* to mediate its full effects, all functional experiments were performed after 3 days of doxycycline treatment.



**Supplementary Figure S2.** Heat maps of the protein profile constructed with CIMminer. Increased protein levels or phosphorylation of proteins is depicted in red, conversely decreased phosphorylation is depicted in blue. See scale bar in the top left corner for magnitude of the phosphorylation. Euclidian distance between the samples is depicted on top. For the phosphorylation status of the various signaling proteins Euclidian distance is depicted to the left. **(A)** Total protein levels. **(B)** All total and phosphoprotein levels.



**Supplementary Figure S3.** Visual representation of the cBioportal analysis of potential *HOXA9* mutations, amplifications, and chromosomal translocations. **(A)** All cases visualized with their study of origin, indicated in the legend. **(B)** The magnification shows the individual cases with alterations, indicated in the legend.



Supplementary Table S1. All primers used in this study

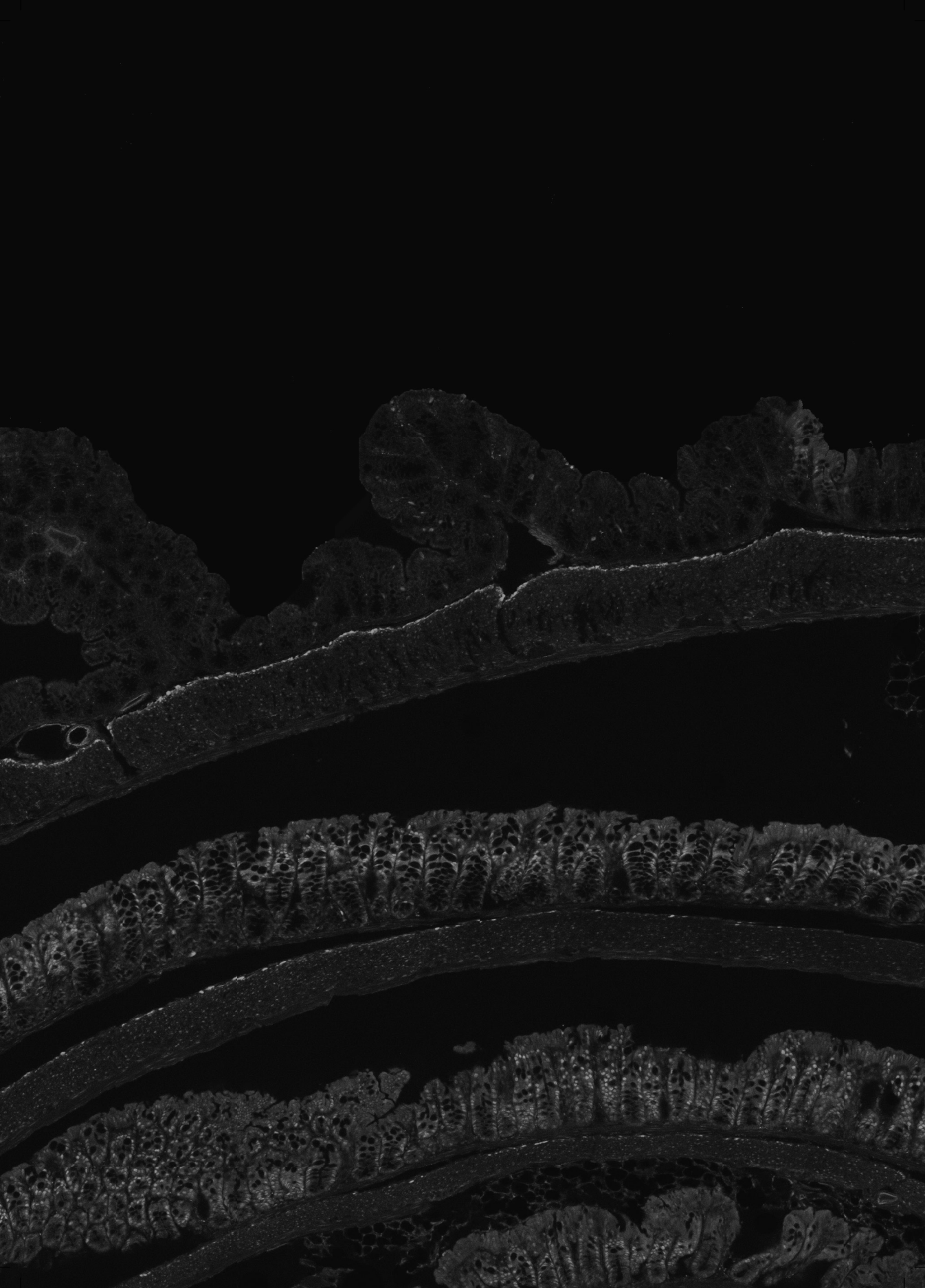
Name gene	Human sequence forward primer	Human sequence reverse primer	Not expressed in Caco-2
<i>ADRB2</i>	GAGCACAAAGCCCTCAAGAC	TCCTGGATCACATGCACAAT	
<i>BMP1</i>	TTCTCTCCCTGAATACCC	GGGACGTGAAGTTCAGGATG	
<i>BMP4</i>	TGAGCCTTTCAGCAAGTTT	GCATTCCGTTACCAGGAATC	
<i>BMPR2</i>	CTACCATGGACCATCTGCT	CCAAGTCTTGCTGATACGG	
<i>BMX</i>	ACGAGCTGAATGAACGAGAGG	TTTCTTGTCCTCCGACGAGATT	X
<i>CCL2</i>	GCCTCCAGCATGAAAGTCTC	AGGTGACTGGGGCATTGAT	
<i>CDH5</i>	AGAGCTCCACTCACGCTCAG	CATCTTCCCAGGAGGAACAG	X
<i>CTNNB1</i>	CTGAGGAGCAGCTTCAGTCC	CGCTGGATTTCAAAACAGT	
<i>CYBB</i>	TCGAAATCTGCTGCTCTCC	AATCATCCATGCCACCAATT	
<i>FGF10</i>	CATGTGCGGAGCTACAATCAC	CAGGATGCTGTACGGGCAG	X
<i>FGF9</i>	ATGGCTCCCTTAGGTGAAGTT	CCCAGGTGGTCACTTAACAAAAC	
<i>FLT3</i>	TGTGAGCAAAAGGICTTGA	TTGGGCATCATCATTTTCTG	
<i>GAPDH</i> (reference gene)	AAGGTGAAGTCCGGAGTCAA	AATGAAGGGGTCAATTGATGG	
<i>HEY1</i>	TGGATCACCTGAAATGCTG	CGAATCCCAAACTCCGATA	
<i>HOXA9</i>	AATGCTGAGAATGAGAGCGG	GTATAGGGGCACCGCTTTT	
<i>IGF1</i>	GCTGTGGATGCTCTTCAGT	ACTCATCCACGATGCCCTGTC	
<i>KRT19</i>	CCGGACTACAGCCACTACT	GTCGATCTGCAGGACAATCC	
<i>MMP9</i>	TGTACCGCTATGGTTACACTGG	GGCAGGACAGTTGCTTCT	
<i>NAT6</i>	AGCTAGGACGGGGAACATC	GGGTCTAGTGTAGGGTCAAG	X
<i>NOS3</i>	TGATGGCGAAGCGAGTGAAG	ACTCATCCATACACAGGACCC	
<i>PSMB9</i>	ACCAACGGGGGACTTACC	ACTCGGAATCAGAACCCAT	
<i>PTGS2</i>	CCGGGTACAATCGCACTTAT	GGCGCTCAGCCATACAG	
<i>SMAD4</i>	GCCTTCCCACTCCCCCTC	GGCGCTCAGCCATACAG	
<i>TPT1</i> (reference gene)	TTCAGCGGAGGCATTTCOC	TTGATCCTTTGGAAACAGTGAA	X
<i>UBC</i> (reference gene)	TGCCCTTGACATCTCGATGGT	GATCGCGGACGGGTGTG	
<i>VIM</i>	CTTCAGAGAGAGGAAGCCGA	GATTTGGGTGCGGTTCTT	
<i>WNT3A</i>	AGCTACCCCGATCTGGTGGTC	ATTCCACTTTGCGTTCAAGG	
<i>WNT3A</i>	GCCAGTATCAATTCCGACATCG	CAAACTCGATGTCCTCGCTAC	X
<i>ZEB1</i>	GATGATGAATGCGAGTCAGATGC	TCACCCGCTATGTGAAGGC	
		ACAGCAGTGTCTTGTGTGTGT	

**Supplementary Table S2.** All antibodies used in this study

Antibody	Dilution	Company	Catalog number
<i>Primary antibodies</i>			
Rabbit-anti-LKB1	1:1000	Cell Signaling Technology	3047
Rabbit-anti-phospho-LKB1 - Ser428	1:1000	Cell Signaling Technology	3482
Rabbit-anti-AMPKa	1:1000	Cell Signaling Technology	2532
Rabbit-anti-phospho-AMPKa - Thr172	1:1000	Cell Signaling Technology	2535
Rabbit-anti-S6K	1:1000	SAB - Signalway Antibody	21225
Rabbit-anti-phospho-S6K - Ser235/236	1:1000	Cell Signaling Technology	4856
Rabbit-anti-PTEN	1:1000	Cell Signaling Technology	9552
Rabbit-anti-phospho-PTEN - Ser380	1:1000	Cell Signaling Technology	9551
Rabbit-anti-mTOR	1:500	Cell Signaling Technology	2972
Rabbit-anti-phospho-mTOR - Ser2448	1:500	Cell Signaling Technology	2971
Mouse-anti-ERK	1:1000	Cell Signaling Technology	4696
Rabbit-anti-phospho-ERK - Thr202/Tyr204	1:1000	Cell Signaling Technology	4370
Rabbit-anti-4E-BP1	1:15000	Cell Signaling Technology	9644
Rabbit-anti-phospho-4E-BP1 - Thr37/46	1:1000	Cell Signaling Technology	2855
Rabbit-anti-GSK3 a/b	1:1000	EPITOMICS	1561-1
Rabbit-anti-phospho-GSK3	1:1000	Upstate (Merck)	05-413
Mouse-anti-p38	1:1000	Cell Signaling Technology	9228
Rabbit-anti-phospho-p38 - Thr180/Tyr182	1:1000	Cell Signaling Technology	4511
Rabbit-anti-RAC1/2/3	1:500	Cell Signaling Technology	2467
Rabbit-anti-phospho-RAC1 - Ser71	1:500	Cell Signaling Technology	2461
Rabbit-anti-PAK1/2/3	1:1000	SAB - Signalway Antibody	21169-1
Rabbit-anti-phospho-PAK1 - Ser199/204	1:1000	Cell Signaling Technology	2605
Rabbit-anti-FAK	1:1000	SAB - Signalway Antibody	11123-2
Rabbit-anti-phospho-FAK - Tyr925	1:1000	SAB - Signalway Antibody	21076-1
Rabbit-anti-AKT	1:1000	Cell Signaling Technology	4691
Rabbit-anti-phospho-AKT - Thr 308	1:1000	SAB - Signalway Antibody	11055-2
Rabbit-anti-phospho-AKT - Ser 473	1:1000	Cell Signaling Technology	4060
Rabbit-anti-EGFR	1:500	SAB - Signalway Antibody	21073-1
Rabbit-anti-cofilin	1:500	SAB - Signalway Antibody	21164-1
Rabbit-anti-phospho-PDK1 - Ser241	1:1000	Cell Signaling Technology	3061
Rabbit-anti-NFkB-p65	1:1000	Cell Signaling Technology	4764
Rabbit-anti-phospho-Acetyl-CoA	1:500	Cell Signaling Technology	3661
Rabbit-anti-MEK1 - Thr292	1:1000	Ustate (Merck)	07-348
Rabbit-anti-phospho-IRS1 - Ser 636/639	1:1000	Cell Signaling Technology	2388
Rabbit-anti-OCRL	1:500	SCBT - Santa Cruz Biotechnology	393577

**Supplementary Table S2.** *Continued*

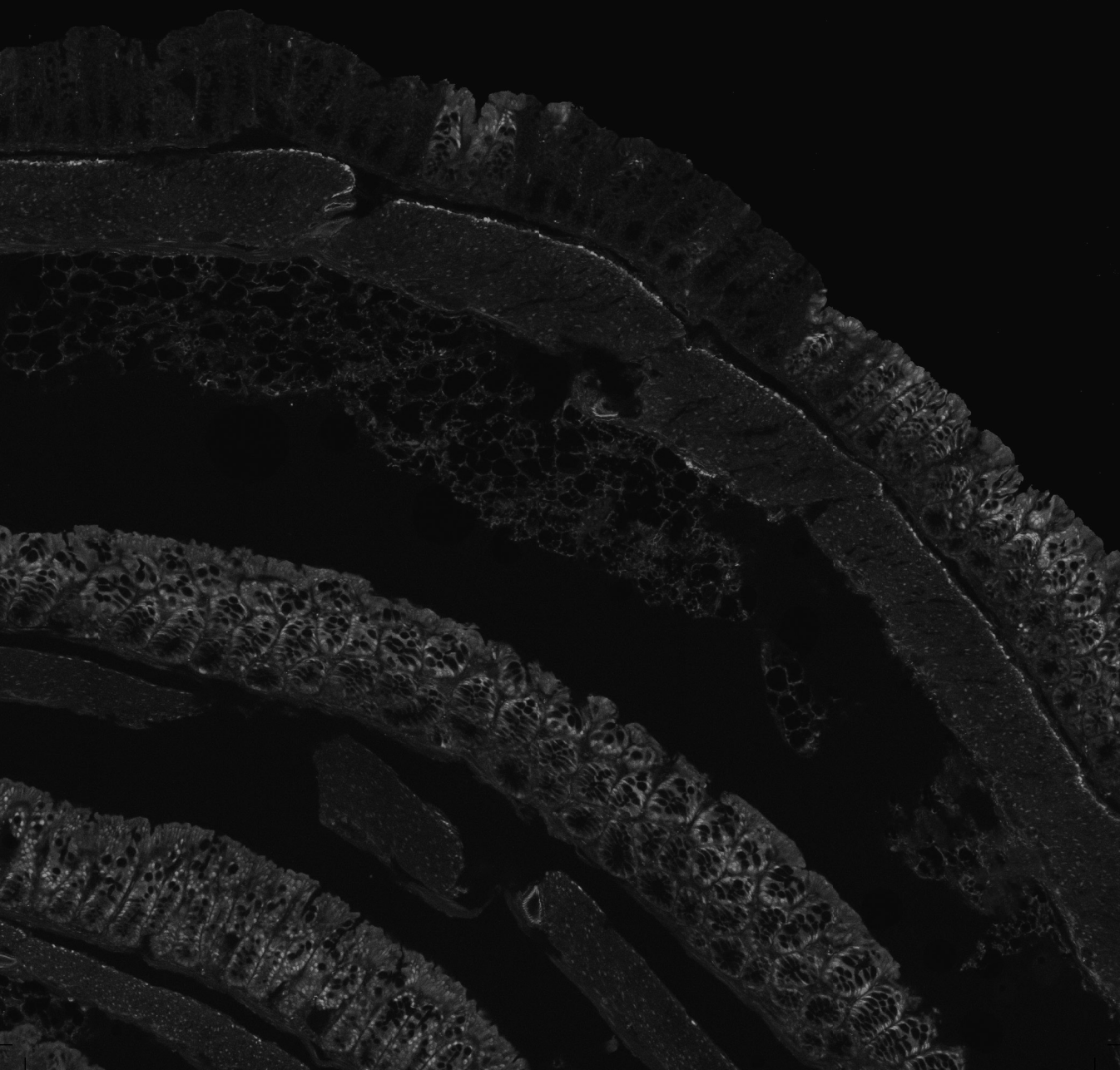
Antibody	Dilution	Company	Catalog number
Rabbit-anti-SHIP2	1:500	SCBT - Santa Cruz Biotechnology	254335
Rabbit-anti-ACP1 (LMWPTP)	1:500	SCBT - Santa Cruz Biotechnology	100343
Mouse-anti- $\beta$ actin	1:1000	SCBT - Santa Cruz Biotechnology	477778
Rabbit-anti-Pan actin	1:1000	Cell Signaling Technology	9228
<i>Secondary antibodies</i>			
Goat-anti-mouse IgG IRDye 680LT	1:5000	LI-COR	926-68020
Goat-anti-rabbit IgG IRDye 800CW	1:5000	LI-COR	926-32211



# Part 3

---

Predicting the development  
of malignant lesions





# Chapter 5

---

Vitamin D receptor polymorphisms  
are associated with reduced esophageal  
vitamin D receptor expression  
and reduced esophageal  
adenocarcinoma risk

Vincent T. Janmaat · Anouk van de Winkel · Maikel P. Peppelenbosch ·  
Manon C. W. Spaander · André G. Uitterlinden · Farzin Pourfarzad ·  
Hugo W. Tilanus · Agnieszka M. Rygiel · Leon M. G. Moons · Pascal P. Arp ·  
Kausilia K. Krishnadath · Ernst J. Kuipers · Luc J.W. van der Laan

*Mol Med. 2015;21:346-54*

## Abstract

Epidemiological studies indicate that vitamin D exerts a protective effect on the development of various solid cancers. However, concerns have been raised regarding the potential deleterious role of high vitamin D levels in the development of esophageal adenocarcinoma (EAC). This study investigated genetic variation in the vitamin D receptor (VDR) in relation to its expression and risk of Barrett esophagus (BE) and EAC. VDR gene regulation was investigated by immunohistochemistry, reverse transcriptase–polymerase chain reaction (RT-PCR) and gel shift assays. Fifteen haplotype tagging single-nucleotide polymorphisms (SNPs) of the VDR gene were analyzed in 858 patients with reflux esophagitis (RE), BE or EAC and 202 healthy controls. VDR mRNA expression was higher in BE compared with squamous epithelium. VDR protein was located in the nucleus in BE. An rs1989969T/rs2238135G haplotype was identified in the 5' regulatory region of the VDR gene. It was associated with an approximately two-fold reduced risk of RE, BE and EAC. Analysis of a replication cohort was done for BE that confirmed this. The rs1989969T allele causes a GATA-1 transcription factor binding site to appear. The signaling of GATA-1, which is regarded as a negative transcriptional regulator, could explain the findings for rs1989969. The rs2238135G allele was associated with a significantly reduced VDR expression in BE; for the rs1989969T allele, a trend in reduced VDR expression was observed. We identified a VDR haplotype associated with reduced esophageal VDR expression and a reduced incidence of RE, BE and EAC. This VDR haplotype could be useful in identifying individuals who benefit most from vitamin D chemoprevention.



## Introduction

The incidence of esophageal adenocarcinoma (EAC) in Western Europe and North America has shown an upward trend for many decades. Despite advances made with respect to its treatment, EAC remains to have a poor prognosis. EAC often arises within Barrett esophagus (BE) (1, 2), a metaplastic condition of the distal esophagus, in which through longstanding gastroesophageal reflux esophagitis (RE), the normal squamous epithelium is replaced by columnar epithelium. In Western countries, the prevalence of BE has increased dramatically since the 1970s (3), which explains the increasing incidence of EAC. BE is likely caused by a combination of genetic and environmental factors (4), but few studies have examined the exact association with dietary components.

Vitamins and antioxidants are believed to be key dietary components, some of which pose anticarcinogenic action (5). Vitamin D is a micronutrient and is the precursor to the steroid hormone calcitriol. It is obtained from dietary sources, but can also be produced endogenously under the influence of solar ultraviolet-B radiation (6). Its main action lies in normal development and mineralization of a healthy skeleton. Despite this, the vitamin D receptor (VDR) is expressed in a variety of tissues that are not involved in calcium or phosphate metabolism. Considerable evidence exists in scientific literature, citing an inverse epidemiological relationship between vitamin D and the incidence of several cancers (5, 7).

The protective properties of vitamin D have been most extensively studied for colorectal cancer. Several meta-analyses reported consistent protective effects of high vitamin D status for colorectal neoplasia (8-11). This could be explained by the finding that the VDR controls nuclear  $\beta$ -catenin levels in colon cancer cells and can thus attenuate the effect of mutations that activate the Wnt/ $\beta$ -catenin pathway (12). Additionally, Hummel et al. (13) showed that increasing dietary vitamin D intake prevents chemically induced preneoplastic lesions in mice colon. However, a large-scale randomized controlled trial, the Women's Health Initiative, found that calcium and vitamin D supplementation had no effect on the incidence of colorectal cancer compared with the placebo arm after a 7-year follow-up; this follow-up period is possibly insufficient for detecting the effect (14). A recent overview of the influence of vitamin D on cause-specific death shows an inverse association with cardiovascular, oncological and other causes of death (15). However, there have been notable exceptions to this protective character, as reported for serum 25-hydroxy vitamin D levels, exposure to vitamin D or increased exposure to sunlight and upper gastrointestinal cancer (16-19). In addition, a significant direct association was observed between the highest tertile versus the lowest tertile of vitamin D intake and EAC, even after adjustment for confounders (20). Similar observations have been made for pancreatic cancer risks (21). The research of Trowbridge et al. (22), although preliminary, suggests that EACs, which do not respond to neoadjuvant therapy, have greater expression of VDR than tumors that do respond completely.

A recent review from this group states that no association can be identified with the current epidemiologic data, but that sun exposure is consistently reported to be inversely associated with EAC (23).

Factors that govern the outcome of vitamin D-mediated chemoprevention may lie in differential expression and/or activity of enzymes responsible for local activation and degradation of vitamin D, or variations in the expression or signaling of the VDR itself. The VDR gene encompasses about 64 kb, consisting of a 5' region containing noncoding exon 1a to 1f, the coding exons 2–9 and a 3' UTR (**Supplementary Figure S1A**) (24–27). It is known that VDR protein is expressed in BE and normal stomach mucosa (28). Additionally, it is present in the normal colon, where it is more abundantly expressed in premalignant and cancerous lesions (29).

At present, little is known about the role of the VDR gene and its single-nucleotide polymorphisms (SNPs) in BE and EAC. Therefore, the aims of this study were to, first, analyze VDR RNA and protein levels in BE. Second, this study aims to analyze 15 haplotype tagging SNPs (htSNPs) with respect to the risk of RE, BE and EAC development. HtSNPs are representative SNPs in a region of the genome with high linkage disequilibrium; each htSNP represents a group of SNPs (that is, a haplotype). The 15 htSNPs chosen are sufficient to cover the common genetic diversity across the VDR gene (24). Thirdly, our study aims to analyze htSNPs that have a different frequency in patients versus controls for VDR expression level. Here, we report two SNPs: 1453C>T (rs1989969) and 1633G>C (rs2238135). The presence of the rs1989969 T/rs2238135 G haplotype was associated with a reduced risk for BE; this finding was confirmed with a replication cohort. The same was found for RE and EAC in a single cohort for each condition. The rs1989969 T allele was found to create a GATA-1 binding site and is associated with a two-fold ( $p=0.11$ ) decrease in VDR expression in BE. The G allele of rs2238135 is associated with a 2.5-fold ( $p=0.01$ ) decrease in VDR expression in BE as well. Potential implications for vitamin D-based chemoprevention will be discussed.

## Materials and methods

### Human patients and healthy controls

The association between VDR alleles and esophageal disease was analyzed in a group of 708 patients with RE, BE or EAC who visited the endoscopy unit of the Erasmus Medical Center Rotterdam or the IJsselland Hospital in Capelle aan den IJssel between November 2002 and February 2005 (30). Additionally, subjects visiting a general practitioner during this period for symptoms unrelated to and without any previous symptoms of gastroesophageal reflux disease (GERD) were asked to participate and served as healthy controls ( $n=202$ ). Patient characteristics are given in **Table 1**. We

**Table 1.** Patient characteristics

	HC	RE	BE	Repl BE	EAC
Number of subjects	202	307	260	150	141
Mean age, y (range)	57 (18-90)	55 (19-88)	61 (33-95)	59 (30-87)	63 (38-87)
Male, %	57	56	69	89	82

HC, healthy controls; RE, reflux esophagitis; BE, Barrett's esophagus; Repl BE, BE replication cohort; EAC, esophageal adenocarcinoma.

attempted to contact all patients and subjects included in the study to collect data regarding their genetic background. In roughly half of the cases, information on ethnic background was obtained. Less than 1% of successfully contacted study participants were of non-Caucasian descent. Subjects included in the RE population had endoscopically confirmed RE (n=307), which was graded according to the Los Angeles (LA) classification (31). Patients were diagnosed endoscopically with BE (n=260) if they had a columnar-lined segment in the esophagus of >2 cm in length with histological signs of specialized intestinal metaplasia. The length of the columnar-lined segment was determined endoscopically by measuring the distance between the squamocolumnar junction (the location at which the light-pink mucosa of the squamous-lined esophagus joined the red mucosa of the columnar-lined epithelium) and the gastroesophageal junction. Endoscopic diagnosis of EAC (n=141) was confirmed by pathologic assessment of the histology of biopsies. An independent BE replication cohort (n=150) was collected from the Academic Medical Center, located in Amsterdam. BE was identified endoscopically by an expert gastroscopist. Random biopsy specimens were taken from each quadrant of the BE at every 2 cm according to standard protocol. The biopsy specimens used in this study were taken from the middle of the BE segment. The random biopsies therefore surround the study biopsies. All random biopsy specimens were analyzed by an expert gastrointestinal pathologist, and the study biopsy specimens were used only when they contained Barrett epithelium. Squamous epithelial biopsies were taken 5 cm above the squamous Barrett junction. This study was approved by the institutional ethics review committees, and all patients gave informed consent before participating in the study.

### Genotyping

Genomic DNA was extracted from 5 mL whole blood by a wizard genomic DNA purification kit (Promega, Madison, WI, USA). Fifteen htSNPs across the VDR gene were genotyped with the use of the high-throughput TaqMan allelic discrimination assays. A random 5% of samples were independently repeated to confirm genotyping results.

**Real-time PCR mRNA quantification from human esophagus samples**

Total RNA was extracted from tissue biopsies by using TriReagent (Sigma-Aldrich, St. Louis, MO, USA) and purified by using an RNeasy micro column kit (Qiagen, Hilden, CA, USA). One-fortieth of a 1 µg cDNA synthesis reaction (iScript cDNA Synthesis Kit; Bio-Rad, Hercules, CA, USA) was used in a 25 µl quantitative reverse transcriptase–polymerase chain reaction (RT-PCR) using SYBR GreenER (Invitrogen (Thermo Fisher Scientific Inc., Waltham, MA, USA)). The following primers were used for VDR gene amplification: 5'-CCGCATCACCAAGGACAAC-3' and 5'-GCTCCCTCCACCATCATTCAC-3'. Duplicate samples were run in independent PCR runs, and the average level of VDR gene expression was normalized to RNA polymerase II and GAPDH gene expression by using the Pfaffl method (32).

**Immunohistochemical staining**

From the formalin-fixed, paraffin-embedded tissue, 5-µm tissue sections were sliced and mounted on adhesive slides (Starfrost, Berlin, Germany). After deparaffinization in xylene and dehydration in alcohol, endogenous peroxidase was inactivated by incubation with 0.5% hydrogen peroxidase in methanol for 15 min. Antigen retrieval was performed by boiling the sections for 10 min in 10 mmol/L citric acid monohydrate buffer (pH 6.0). Sections were blocked with 5% bovine serum albumin. Anti-VDR monoclonal antibody (1:200; clone 9A7, Affinity Bioreagents, Golden, CO, USA) was incubated for 1 h at room temperature, followed by polyclonal biotin–labeled goat anti-rat (1:500; Dako, Denmark). After 45 min of incubation with streptavidin–horseradish peroxidase (HRP) (1:300; Dako, Glostrup, Denmark), VDR was visualized by using 3-amino-9-ethylcarbazole as a substrate and hematoxylin counterstaining. Sections were evaluated by using light microscopy (Axioskop 20; Zeiss, Oberkochen, Germany), and pictures were taken and analyzed by using Nikon software (NisElements 2008; Tokyo, Japan).

**Electrophoretic mobility shift assay**

Oligonucleotides used in electrophoretic mobility shift assay (EMSA) and supershift assays were 5'-CCAGGGTGGTTGTCTACCTGGATGTCACCTCTGACCTCTG-3' (wild-type, representing the rs1989969 C allele) and 5'-CCAGGGTGGTTGTCTATCTGGATGTCACCTCTGACCTCTG-3' (mutant represents the rs1989969 T allele; underlined section represents the GATA binding site, and the bold nucleotide represents the position of the rs1989969 SNP). Probes were 5'-end labeled with (γ-32P)ATP. Nuclear extracts were prepared from murine erythroleukemia (MEL) cells according to the methods used by Wall and coworkers (33). For EMSA experiments, 2.5 µg nuclear extract prepared from MEL cells was incubated for 30 min at 37°C with 1-ng 32P-labeled or 25 ng unlabeled VDR oligonucleotide probe in a binding buffer consisting of 50 mmol/l Tris, pH 8.0, 250 mmol/l NaCl, 5 mmol/l

dithiothreitol, 5 mmol/l ethylenediaminetetraacetic acid and 10% Ficoll in a total volume of 10  $\mu$ l. In competition assays, 25-fold molar excess of unlabeled competitor was included in the binding reaction. For supershift assays, 2  $\mu$ g GATA-1 (N6)X mouse monoclonal antibody (sc-265 X; Santa Cruz Biotechnology, Santa Cruz, CA, USA) was added to reaction mixtures 30 min before addition of the nuclear extract. The protein-DNA complexes were separated from free probes by electrophoresis through a 4% nondenaturing polyacrylamide gel and visualized on a orthochromatic film (Super HR-U30; Fuji Film, Tokyo, Japan) and developed by using a Fuji medical film processor (Model FPM 100A).

### Statistical analyses

Genotype distribution was tested for Hardy-Weinberg equilibrium. The study was powered (80%) to allow detection of a 10% difference in genotype distribution of the VDR SNPs or haplotypes between the groups by performing Pearson  $\chi^2$  analysis. Odds ratio (OR) and 95% confidence interval (CI) were calculated by risk estimate analysis. Logistic regression analysis was applied to establish allele dose effects. Statistical analyses were conducted by using SPSS v11.0 (SPSS (IBM, Armonk, NY, USA)), and two-tailed significance was  $p < 0.05$ . We did not adjust for multiple testing. However, a replication cohort was included for BE. One-tailed  $t$ -tests were performed to test the hypothesis that GG versus CC and TT versus CC genotypes were associated with lower VDR levels.

### *In silico* sequence analysis

The human genomic DNA sequence of the intronic region near the noncoding exon 1c ~1.5 kb upstream of the translation start site was downloaded from the National Center for Biotechnology Information database (<http://www.ncbi.nlm.nih.gov>). The reference sequence used was NC\_018923.2. Transcription factor binding sites were predicted by PROMO (version 3.0.2), which is a virtual laboratory for the identification of putative transcription factor binding sites. PROMO uses the 8.3 version of TRANSFAC (34, 35). The dissimilarity threshold was set at 5%.

## Results

### **BE epithelium has a high expression of VDR compared with squamous epithelium**

We investigated VDR expression in normal squamous epithelium compared with BE tissue in individual BE patients. In the majority of patients (20 of 25, 80%), presence of BE correlated with a two-fold increase in VDR mRNA expression (**Figure 1A**;  $p = 0.002$ ). This result was associated with higher levels of VDR protein in the BE segment, especially in the epithelial compartment, as evident from immunohistochemical staining of

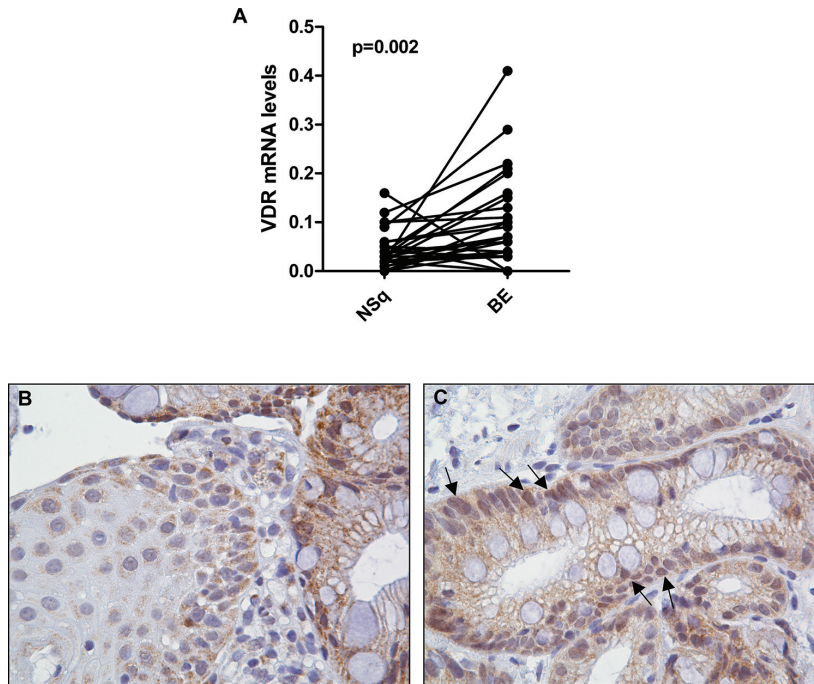


**Figure 1.** Esophageal expression of VDR in BE patients. (A) Relative mRNA levels of VDR in paired squamous and columnar epithelium samples of BE patients. In 20 of 25 patients, VDR mRNA was highest in columnar epithelium samples. Immunohistochemical staining of VDR in squamous (B) and paired columnar epithelium (C) clearly shows a number of VDR-positive nuclei in BE and its mere presence in the cytoplasm of epithelial cells. Arrows indicate some positively stained nuclei.

squamous and BE biopsies from the same patient (Figure 1B). As shown in Figure 1C, in most BE tissue, the VDR protein had a nuclear localization, suggesting activation of the receptor. Thus, VDR mRNA expression is upregulated and VDR protein is activated in BE compared with squamous epithelium.

### **The rs1989969 T/rs2238135 G haplotype is associated with reduced risk for neoplasm-associated esophageal disease**

Genomic DNA was obtained from a group of 708 patients with RE, BE or EAC and compared with a group of 202 healthy controls without any symptoms of esophageal disease. Patient characteristics are given in Table 1. As shown in Table 2, rs1989969 and rs2238135, the two htSNPs in the exon 1c region, were found to be differently distributed in healthy controls versus patients with RE, BE and EAC in this study. Thirteen other VDR htSNPs were found to not be significantly associated with the presence of esophageal disease (data not shown). As shown in Table 3, allele dose

analysis revealed that individuals carrying the rs1989969 T/rs2238135 G haplotype were two-fold less susceptible to RE (OR 0.48, 95% CI 0.28–0.81), BE (OR 0.46, 95% CI 0.26–0.80) and EAC (OR 0.50, 95% CI 0.27–0.96). A BE replication cohort closely mimicked the observations for the rs1989969 T/rs2238135 G haplotype (OR 0.44, 95% CI 0.23–0.85).

**Table 2.** Genotype distribution of *VDR* SNPs rs2238135 and rs1989969 in healthy controls and patients

SNP	Genotype	Genotype, N (frequency)				
		HC N=202	RE N=307	BE N=260	Repl BE N=150	EAC N=141
rs2238135	G/G	127 (0.648)	159 (0.530)	157 (0.625)	72 (0.507)	76 (0.551)
	G/C	58 (0.296)	121 (0.403)	81 (0.323)	65 (0.458)	54 (0.391)
	C/C	11 (0.056)	20 (0.067)	13 (0.052)	5 (0.035)	8 (0.058)
	<i>p</i> value	1	<i>0.03<sup>A</sup></i>	0.83	<i>0.01</i>	0.18
rs1989969	C/C	53 (0.273)	107 (0.357)	85 (0.343)	49 (0.340)	49 (0.360)
	C/T	94 (0.485)	147 (0.490)	128 (0.516)	76 (0.528)	65 (0.478)
	T/T	47 (0.242)	46 (0.153)	35 (0.141)	19 (0.132)	22 (0.162)
	<i>p</i> value	1	<i>0.02</i>	<i>0.02</i>	<i>0.03</i>	0.10

HC, healthy controls; RE, reflux esophagitis; BE, Barrett's esophagus; Repl BE, BE replication cohort; EAC, esophageal adenocarcinoma. <sup>A</sup>Values in *italic* are significant at 95% CI.

**Table 3.** Haplotype-risk analysis of RE, BE and EAC compared to controls

Haplotype	Total alleles (N)	Odds Ratio (95% CI) <sup>A</sup>			
		RE versus HC	BE versus HC	BE Repl versus HC	EAC versus HC
0 GT copies	345	1	1	1	1
1 GT copies	507	0.76 (0.50-1.15)	0.84 (0.54-1.30)	0.88 (0.54-1.43)	0.74 (0.45-1.22)
2 GT copies	169	<i>0.48 (0.28-0.81)</i>	<i>0.46 (0.26-0.80)</i>	<i>0.44 (0.23-0.85)</i>	<i>0.50 (0.27-0.96)</i>
0 GC copies	442	1	1	1	1
1 GC copies	444	1.37 (0.93-2.02)	<i>1.53 (1.02-2.30)</i>	<i>1.64 (1.03-2.61)</i>	1.08 (0.67-1.74)
2 GC copies	125	1.05 (0.57-1.93)	<i>1.84 (1.02-3.32)</i>	0.95 (0.44-2.05)	1.40 (0.71-2.77)
0 CC copies	590	1	1	1	1
1 CC copies	376	<i>1.65 (1.12-2.44)</i>	1.12 (0.74-1.68)	<i>1.98 (1.25-3.12)</i>	1.56 (0.98-2.48)
2 CC copies	57	1.24 (0.68-3.16)	0.96 (0.41-2.21)	0.80 (0.27-2.40)	1.22 (0.47-3.16)

The CT haplotype contained too few alleles for a meaningful comparison. HC, healthy controls; RE, reflux esophagitis; BE, Barrett's esophagus; BE Repl, BE replication cohort; EAC, esophageal adenocarcinoma. <sup>A</sup>The CT haplotype contained too few alleles for a meaningful comparison. <sup>B</sup>Values in *italic* are significant at 95% CI.

### Identification of an rs1989969-dependent GATA-1 binding site in the VDR intronic region near the noncoding exon 1c

With the finding established that carriers of the T allele of rs1989969 and the G allele of rs2238135 are two-fold less susceptible to neoplasm-associated disease, we further analyzed these SNPs. The availability of a multispecies genomic sequence allowed us to examine the sequence conservation across the transcriptional unit and indicated various highly pan-vertebrate conserved regions, especially around the location of rs1989969 and rs2238135, near the non-coding exon 1c ~1.5 kb upstream of the translation start site (**Figure 2**). The strong evolutionary conservation in this region might well be consistent with a role in transcriptional regulation. Interestingly, rs1989969 was found to convert the transcriptionally inert majority allele into a canonical GATA-1 binding site (that is, T/A GATA A/G (36) (**Figure 3, Supplementary Figure S1**). rs1989969 could thus be expected to alter VDR expression in cell types expressing GATA-1 transcription factor. GATA1 expression has been shown in the human stomach and duodenum but not in the small intestine, appendix and colon (37). GATA1/2/3 ortholog expression has been reported in the esophagus of the polychaete annelid, *Capitella* (38). Additionally, *GATA4* and 6 mRNA was found to be expressed highly in the proximal gastrointestinal tract (39, 40). The various GATA transcription factors have closely related and sometimes overlapping binding sites, therefore GATA-4 and 6 could have a similar function to GATA-1 (36).

```

HOM: CTAGCTCTGGACCTGCGTAACTCACTCAGAGT-GCTCT---GAAATTGGCTTTGCTAC---AAGTA---GGACTGCTCCCTGC-CTCA-CAGAACTGTTGTGAG 100%
PAN: CTAGCTCTGGGACCTGCGCAAGTCACTCAGAGT-GCTCT---GAAATTGGCTTTGCTAC---AAGTA---GGACTGCTCCCTGC-CTCA-CAGAACTGTTGTGAG 99%
MAC: CTGGCTCTGGGACCTGCGCAAGTCACTCAGAGT-GCTCT---GAAATTGGCTTTGCTACCTGTAAAGTA---GGACTGCTCCCTGC-CTCA-CAGAACTGTTGTGAG 93%
EQU: -----TGGGACCTGCGCAAGTCACTCAAAGT-GCTCT---GGACTCTGGCTTTGCGCTCTGTGAAGTG---GGACTGCTCCCTGC-CTCA-CAGAACTGTTGTGAG 80%
CAN: CGGGCTCTGGGACCTGCGCAAGTCACTCAAAGT-AGTCT---GGACTCTGGCTTTGCGCTCTGTGAAGTG---GGACTGCTCCCTGC-CTCA-CAGAACTGTTGTGAG 74%
BOS: CTGGCTCTGGGACCTGCGCAAGTCTCAAAGT-GCCCTACCTGGAGTTTGGTTTTCAT---CTGTAAATGGGACTGCTC-TGC-ATCTGCGGGACGTTAGGAG 73%
MUS: ACCGCTCTGGGACCTGCGCAAGTCTCAAAGT-TGGTTTGGGTATCTAT---AAATGAGAGTT-CTCC---CCTTG---CCCCCTCTCCCCGACTCA-AAG-ACTACTGTGAG 66%

```

```

HOM: GGCTAAAT-GAAATAATGTATGCGAGGCTTAGCAGGCTGGCATGTAGTAAAT--ACTCCGGAACA tttttt---TAAGTTCAGGGTGGTGTCTA CTGGAGTCCACC 100%
PAN: GGCTAAAT-GAAATAATGTATGCGAGGCTTAGCAGGCTGGCATGTAGTAAAT--ACTCCGGAACA tttttt---TAAGTTCAGGGTGGTGTCTA CTGGAGTCCACC 99%
MAC: GGCTAAAT-GAAATAATGTATGCGAGGCTTAGCAGGCTGGCATGTAGTAAAT--ACTCCGGAACA tttttt---TAAGTTCAGGGTGGTGTCTA CTGGAGTCCACC 93%
EQU: -----ATGCTGTATGTGGAGCTCAGCAGGCT--GCACACAGTCACT--GCTCCATACAC-CATTTT---GAAGCTCACAGGTGGTGTCTA CTGGAGTCCACC 80%
CAN: GCTCTGTGCGGCGGTACGTAT--AGCGCTGGC-GGCTGGCAGTGTAGAT--ACTCCGGAACGCTTTTCT---TAAGCTCACAGGTGGTGTCTA CTGGAGTCCACC 74%
BOS: GT-TACAT-GAGATCCAGATGGGAAGCTTAGCAGTC-TGGCGCATGTAGAT--ACGC--ACACACTTTTCTC--TGTAAGTTCAGGGATGGTGTCTA CTGGAGTCCACC 73%
MUS: GATTAACTAAAT-AAAGTATGTATGCTTGGCAGTCTAGAAATGTGTATAGATAGACTCCAGCTTTTTTTTTCCTTTTAAGTTCAGGGATGGTGTCTA CTGGAGTCCACC 66%

```

#### Abbreviated name for all mammalian species used:

Hom:	<i>Homo sapiens</i>	(human)
Pan:	<i>Pan troglodytes</i>	(chimpanzee)
Mac:	<i>Macaca mulatta</i>	(rhesus macaque)
Equ:	<i>Equus caballus</i>	(domestic horse)
Can:	<i>Canis familiaris</i>	(domestic dog)
Bos:	<i>Bos taurus</i>	(domestic cow)
Mus:	<i>Mus musculus</i>	(house mouse)

**Figure 2.** Comparative sequence analysis of multi-species alignment of the VDR exon 1c noncoding regulatory region. This region lies near the noncoding exon 1c ~1.5 kb upstream of the translation start site. The regions containing the rs2238135 and rs1989969 SNPs (in boxes) are highly conserved in the human genome and six other mammalian species. The SNPs rs2238135 and rs1989969 are indicated by an “S” and a “Y.” The “S” represents a G or a C, and the “Y” represents a C or a T according to the International Union of Pure and Applied Chemistry (IUPAC) nucleotide base code.



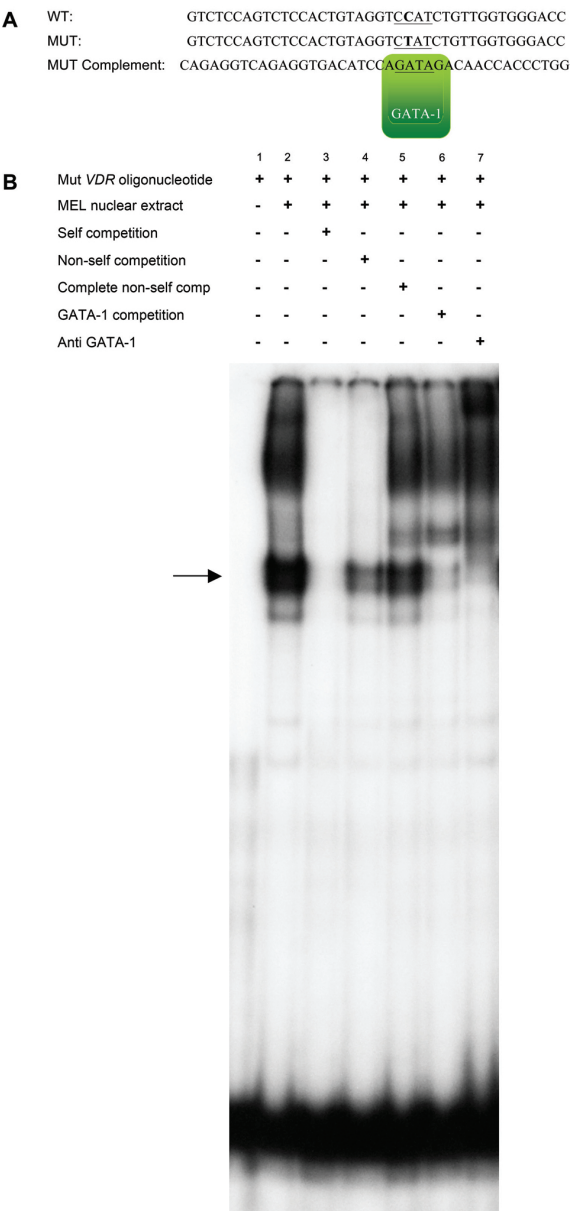


**Figure 3.** The *VDR* rs1989969 T allele causes a functional GATA-1 binding motif to appear. **(A)** A rs1989969-dependent GATA-1 binding site is predicted. **(B)** Gel shift assay using radioactively-labeled oligonucleotides from the rs1989969 region and nuclear extract of MEL cells. The arrow indicates the motility of the oligo–GATA-1 complex. Lane 1, Mut oligo without nuclear extract; lane 2, Mut oligo with nuclear extract; lane 3, with 100× excess of unlabeled Mut oligo (self-competitor); lane 4, with 100× excess of unlabeled WT oligo (non-self-competitor); lane 5, with complete non-self-competitor; lane 6, with 100× excess unlabeled known GATA-1 oligo; lane 7, 1 µg anti–GATA-1 monoclonal antibody. The signal found on the Mut oligo (lane 2) was almost completely eliminated by a 100-fold excess of unlabeled self-competitor and a known GATA-1 oligonucleotide (lanes 3 and 6) but not with WT and complete non-self-oligonucleotides (lanes 4 and 5). Labeled WT oligo did not result in GATA-1 binding (data not shown).

In EMSA, the binding of the GATA-1 transcription factor was tested by using oligonucleotides bearing the C and T allele of rs1989969, together with nuclear extracts and antibodies against GATA-1 (**Figure 3A**). Supershift experiments indicated that GATA-1 transcription factor binds to the oligonucleotide with the rs1989969 T allele, whereas the oligonucleotide bearing the common rs1989969 C allele does not show detectable binding (**Figure 3B**). Thus, the rs1989969 SNP results in a differential binding of GATA-1 to the VDR gene.

### The rs1989969 and rs2238135 SNPs influence esophageal VDR expression

To study the functional consequences of the rs1989969 and rs2238135 SNPs on VDR expression, esophageal biopsies were taken from BE of patients, and VDR expression levels were determined by using quantitative RT-PCR. The expression of VDR in the esophagus was on average 2.5-fold lower in BE patients carrying two copies of the rs2238135 G allele versus subjects carrying two copies of the rs2238135 C allele ( $p=0.01$ ). VDR expression was two-fold lower in BE patients carrying two copies of the rs1989969 T allele versus subjects carrying two copies of the rs1989969 C allele. However, this association did not reach statistical significance ( $p=0.11$ ; **Figure 4**). Thus, the rs2238135 C allele results in 2.5-fold higher esophageal VDR expression. The C allele of rs1989969, in which the GATA-1 binding site is absent, shows a trend in higher esophageal VDR expression.

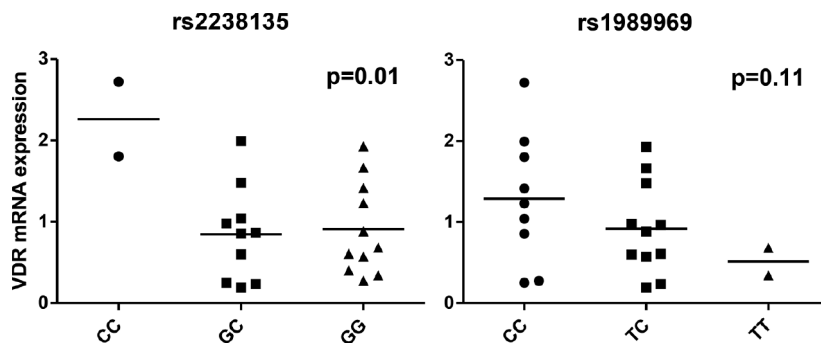


**Figure 4.** Presence of the rs1989969 T or rs2238135 G allele decreases esophageal VDR expression. BE biopsies were analyzed for VDR mRNA levels by quantitative RT-PCR. In the first panel, the esophageal expression of VDR was on average 2.5-fold lower in BE patients carrying two copies of the rs2238135 G allele versus subjects carrying two copies of the rs2238135 C allele ( $p=0.01$ , one-tailed). In the second panel, VDR expression was two-fold lower in BE patients carrying two copies of the T allele of rs1989969 versus subjects carrying two copies of the C allele of rs1989969. However, this association did not reach statistical significance ( $p=0.11$ , one-tailed).

## Discussion

The incidence of EAC rises to date despite surveillance strategies. In many cases, the development of EAC is related to BE. This premalignant stage provides the opportunity to prevent the development of BE-related adenocarcinoma by stratifying BE patients at risk for neoplastic progression. Additionally, it provides the opportunity to identify BE patients who are likely to respond negatively to vitamin D supplementation. Vitamin D supplementation is likely to convey a level of chemopreventive properties against oncogenic transformation in other tissues. Identifying genetic, tissue-specific markers that distinguish individuals on their responsiveness to vitamin D would represent a rationale for detecting groups of patients that could benefit most from vitamin D-based chemoprevention. Obtaining DNA from blood would provide an easy and cheap way to identify patients that have the highest benefit. Therefore, the aim of this study was to investigate the role of VDR in BE; study the consequences of SNPs in the VDR gene on the development of RE, BE and EAC; and elucidate the mechanisms by which these SNPs exert their effect.

We found that BE epithelium has a two-fold higher expression of VDR mRNA compared with squamous epithelium. This result was concomitant with a higher expression of VDR protein detected by immunohistochemistry. In addition, VDR protein was found to predominantly have a nuclear localization, suggesting activation of the receptor. Subsequently, 15 htSNPs of the VDR gene were analyzed with respect to the risk of RE, BE and EAC development. The T allele of rs1989969 was associated with a reduced risk for BE. The same was found for RE in a single cohort. A similar trend was observed for EAC, also in a single cohort. The G allele of rs2238135 was associated with a reduced risk for RE in a single cohort. A similar trend was observed for BE and EAC. The presence of the rs1989969 T/rs2238135 G haplotype was associated with a reduced risk for BE; this finding was confirmed with a replication cohort. The same was found for RE and EAC in a single cohort. The two SNPs were further analyzed to elucidate the mechanisms by which they exert their effect. The rs1989969 minor T allele resulted in a GATA-1 binding site in the VDR intronic region near the noncoding exon 1c. This result was identified *in silico* and was verified by EMSA. Here, oligos containing the T allele of rs1989969 displayed strong GATA-1 transcription factor binding, whereas oligos derived from the major C allele were not capable of doing so. Furthermore, the VDR mRNA level in BE tissue of rs2238135 G allele carriers was found to be lower than the mRNA level in rs2238135 C allele carriers. A trend in the same direction was found for the rs1989969 T versus C allele. This finding resulted in possible vitamin D sensitivity in this organ. This result provides a mechanism that could explain why the rs1989969 T/rs2238135 G haplotype is associated with a reduced risk for neoplasm-associated esophageal disease.

A role of vitamin D in the etiology of BE is expected from the well-known mutual positive interaction between VDR signaling and signaling of bone morphogenetic

proteins. Bone morphogenetic protein-4 expressed in RE induces a columnar phenotype in esophageal squamous cells and is thus possibly important for the precancerous process (41). The present study further supports this concept by establishing the upregulation of VDR signaling during the metaplastic process. GATA factors are well established, mostly negative transcriptional regulators. Accordingly, the rs1989969 T allele, which results in a GATA-1 binding site, reduces expression of the VDR. It was previously shown that IL-4 induces GATA1 expression, which, subsequently, represses VDR expression and enables monocyte-derived dendritic cell differentiation within inflammatory sites (42). This could take place in BE during inflammation, providing additional support for the here-presented findings.

The rs1989969 T/rs2238135 G haplotype was associated with a reduced incidence of RE at a level on par with the reduced incidence in BE and EAC observed in this study. This finding would support the notion that this haplotype exerts its effect on the risk of BE and EAC by reducing the rate of RE instead of reducing the rate of progression from RE to BE and EAC. Both SNPs reported here are haplotype tagging; the association found between the T allele of rs1989969 and a lower incidence of neoplasm-associated esophageal disease and VDR expression levels can in part be due to other genetic variation with which the rs1989969 T allele is associated. The same holds true for rs2238135. Its action could, in part, even be due to an association with rs1989969 by the linkage disequilibrium that exists between the two SNPs. Further research can improve our understanding of the relative importance of individual genetic variations with which the SNPs we report on are associated.

Chang et al. (43) found that rs2238139 (277+2550C>T) and rs2107301 (277+3260C>T) TT homozygotes had a significantly reduced risk of EAC compared with CC homozygotes. Unfortunately, however, we did not analyze the same SNPs and therefore extrapolation is not straightforward. Chang et al. also analyzed SNP rs2238135 for an association with EAC and reported negative results. Our study also reported negative findings for this particular association, but we did observe an association between the G allele of rs2238135 and both RE and reduced VDR expression in this study. An association was also observed in the BE replication cohort but not in the original cohort. The lack of association between rs2238135 and EAC might therefore be a consequence of our study being underpowered for this particular question. Unfortunately, the same reason has probably also prohibited us from being able to draw strong conclusions with regard to the relation between the rs1989969 T allele and reduced VDR mRNA expression in BE. Whereas genetic association studies require replication cohorts, this study did not include replication cohorts for both RE and EAC. Because a BE replication cohort was included and RE, BE and EAC are related conditions, extrapolation of our conclusions with respect to BE to RE and EAC is plausible. However, confirmation of our findings by others, especially with respect to RE and EAC, is necessary. Whereas the ethnic

composition determined from roughly half of the subjects suggests no substantial ethnic admixture of our study group, this notion is uncertain.

Currently, a path between VDR SNPs, probably via influence of VDR expression, and the cancerous process has been established. This association is implied from theoretical (positive interaction with BMP signaling), epidemiological observations (dietary vitamin D intake and UV-B exposure are associated with increased risk for esophageal cancer) as well as the observations made in the present study. GATA transcription factor expression appears to be lower in the distal tract, which has been shown for *GATA-1* (37), *GATA4* and *6* (39). In addition, the vitamin D-based chemopreventive effects in the colon might be transferred through mechanisms other than those involving these VDR SNPs. Therefore, we propose that individuals carrying more rs1989969 T and rs2238135 G alleles will benefit more from vitamin D-based chemopreventive strategies because they are less likely to be confronted with the negative consequences of these strategies, being malignant esophageal disease. Confirmation of this notion obviously requires reevaluation of previous trials involving dietary vitamin D supplementation, assessing the number of rs1989969 T and rs2238135 G alleles in the participants. If confirmed, the rs1989969 and rs2238135 SNPs would represent the first polymorphisms that stratify individuals for the use of a particular chemopreventive strategy.

## Conclusion

This study serves as a proof of principle that SNPs in the VDR gene can modify the risk of RE, BE and EAC, probably through modification of VDR expression. To investigate how serious the impact of vitamin D truly is, additional research is needed into the mechanisms by which vitamin D affects the risk of developing RE, BE and its sequelae EAC. The rs1989969-dependent GATA-1 binding site in the VDR intronic region near the noncoding exon 1c, identified *in silico* and tested in EMSAs, provides a starting point for this. At the same time, evidence from epidemiological studies mimicking the true longlife effects of vitamin D are required to endorse the idea of personalized recommendations for vitamin D supplementation.

## Disclosure

The authors declare they have no competing interests as defined by *Molecular Medicine*, or other interests that might be perceived to influence the results and discussion reported in this paper.

## References

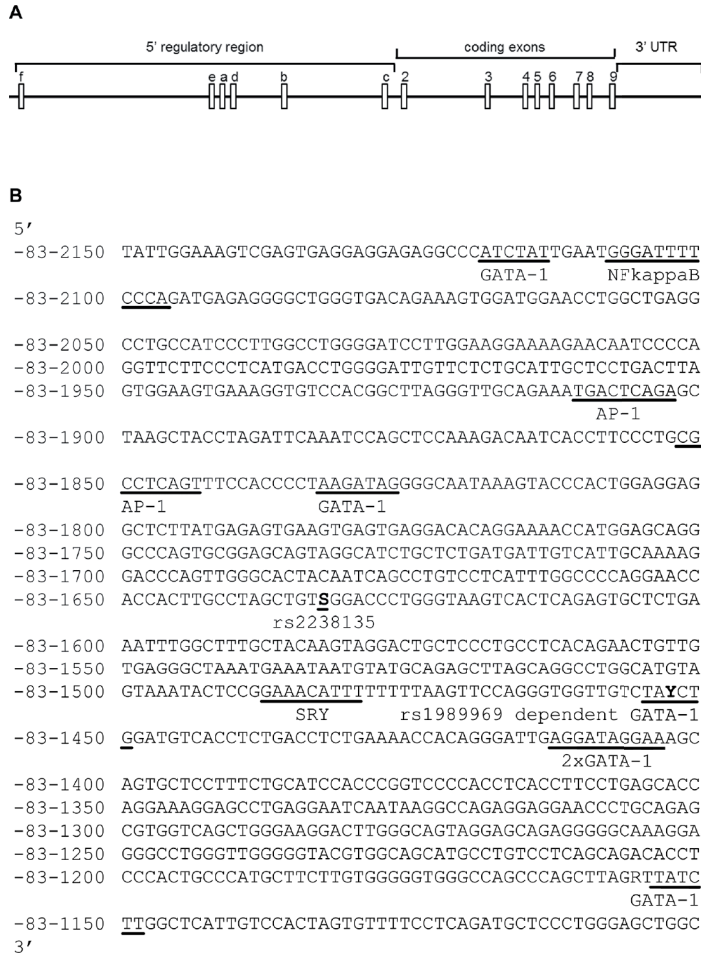
1. Hvid-Jensen F, Pedersen L, Drewes AM, Sorensen HT, Funch-Jensen P. Incidence of adenocarcinoma among patients with Barrett's esophagus. *N Engl J Med*. 2011;365(15):1375-83.
2. Sikkema M, de Jonge PJ, Steyerberg EW, Kuipers EJ. Risk of esophageal adenocarcinoma and mortality in patients with Barrett's esophagus: a systematic review and meta-analysis. *Clin Gastroenterol Hepatol*. 2010;8(3):235-44; quiz e32.
3. Holmes RS, Vaughan TL. Epidemiology and pathogenesis of esophageal cancer. *Semin Radiat Oncol*. 2007;17(1):2-9.
4. Fitzgerald RC. Molecular basis of Barrett's oesophagus and oesophageal adenocarcinoma. *Gut*. 2006;55(12):1810-20.
5. Feldman D, Krishnan AV, Swami S, Giovannucci E, Feldman BJ. The role of vitamin D in reducing cancer risk and progression. *Nat Rev Cancer*. 2014;14(5):342-57.
6. Bogh MK, Schmedes AV, Philipsen PA, Thieden E, Wulf HC. Vitamin D production depends on ultraviolet-B dose but not on dose rate: a randomized controlled trial. *Exp Dermatol*. 2011;20(1):14-8.
7. Giovannucci E. Vitamin D and cancer incidence in the Harvard cohorts. *Ann Epidemiol*. 2009;19(2):84-8.
8. Gorham ED, Garland CF, Garland FC, Grant WB, Mohr SB, Lipkin M, et al. Optimal vitamin D status for colorectal cancer prevention: a quantitative meta analysis. *American Journal of Preventive Medicine*. 2007;32(3):210-6.
9. Wei MY, Garland CF, Gorham ED, Mohr SB, Giovannucci E. Vitamin D and prevention of colorectal adenoma: a meta-analysis. *Cancer Epidemiol Biomarkers Prev*. 2008;17(11):2958-69.
10. Gandini S, Boniol M, Haukka J, Byrnes G, Cox B, Sneyd MJ, et al. Meta-analysis of observational studies of serum 25-hydroxyvitamin D levels and colorectal, breast and prostate cancer and colorectal adenoma. *International Journal of Cancer*. 2011;128(6):1414-24.
11. Yin L, Grandi N, Raum E, Haug U, Arndt V, Brenner H. Meta-analysis: Serum vitamin D and colorectal adenoma risk. *Prev Med*. 2011;53(1-2):10-6.
12. Larriba MJ, Ordonez-Moran P, Chicote I, Martin-Fernandez G, Puig I, Munoz A, et al. Vitamin D receptor deficiency enhances Wnt/beta-catenin signaling and tumor burden in colon cancer. *PLoS One*. 2011;6(8):e23524.
13. Hummel DM, Thiem U, Hobaus J, Mesteri I, Gober L, Stremnitzer C, et al. Prevention of preneoplastic lesions by dietary vitamin D in a mouse model of colorectal carcinogenesis. *J Steroid Biochem Mol Biol*. 2013;136:284-8.
14. Wactawski-Wende J, Kotchen JM, Anderson GL, Assaf AR, Brunner RL, O'Sullivan MJ, et al. Calcium plus vitamin D supplementation and the risk of colorectal cancer. *N Engl J Med*. 2006;354(7):684-96.
15. Chowdhury R, Kunutsor S, Vitezova A, Oliver-Williams C, Chowdhury S, Kieft-de-Jong JC, et al. Vitamin D and risk of cause specific death: systematic review and meta-analysis of observational cohort and randomised intervention studies. *Bmj*. 2014;348:g1903.
16. Abnet CC, Chen Y, Chow WH, Gao YT, Helzlsouer KJ, Le Marchand L, et al. Circulating 25-hydroxyvitamin D and risk of esophageal and gastric cancer: Cohort Consortium Vitamin D Pooling Project of Rarer Cancers. *Am J Epidemiol*. 2010;172(1):94-106.
17. Chen W, Dawsey SM, Qiao YL, Mark SD, Dong ZW, Taylor PR, et al. Prospective study of serum 25(OH)-vitamin D concentration and risk of oesophageal and gastric cancers. *Br J Cancer*. 2007;97(1):123-8.

18. Lipworth L, Rossi M, McLaughlin JK, Negri E, Talamini R, Levi F, et al. Dietary vitamin D and cancers of the oral cavity and esophagus. *Annals of Oncology*. 2009;20(9):1576-81.
19. Toner CD, Davis CD, Milner JA. The vitamin D and cancer conundrum: aiming at a moving target. *J Am Diet Assoc*. 2010;110(10):1492-500.
20. Mulholland HG, Murray LJ, Anderson LA, Cantwell MM. Vitamin D, calcium and dairy intake, and risk of oesophageal adenocarcinoma and its precursor conditions. *Br J Nutr*. 2011;1-10.
21. Stolzenberg-Solomon RZ, Jacobs EJ, Arslan AA, Qi D, Patel AV, Helzlsouer KJ, et al. Circulating 25-hydroxyvitamin D and risk of pancreatic cancer: Cohort Consortium Vitamin D Pooling Project of Rarer Cancers. *Am J Epidemiol*. 2010;172(1):81-93.
22. Trowbridge R, Sharma P, Hunter WJ, Agrawal DK. Vitamin D receptor expression and neoadjuvant therapy in esophageal adenocarcinoma. *Exp Mol Pathol*. 2012;93(1):147-53.
23. Trowbridge R, Mittal SK, Agrawal DK. Vitamin D and the epidemiology of upper gastrointestinal cancers: a critical analysis of the current evidence. *Cancer Epidemiol Biomarkers Prev*. 2013;22(6):1007-14.
24. Fang Y, van Meurs JB, d'Alesio A, Jhamai M, Zhao H, Rivadeneira F, et al. Promoter and 3'-untranslated-region haplotypes in the vitamin d receptor gene predispose to osteoporotic fracture: the rotterdam study. *Am J Hum Genet*. 2005;77(5):807-23.
25. Miyamoto K, Kesterson RA, Yamamoto H, Taketani Y, Nishiwaki E, Tatsumi S, et al. Structural organization of the human vitamin D receptor chromosomal gene and its promoter. *Mol Endocrinol*. 1997;11(8):1165-79.
26. Baker AR, McDonnell DP, Hughes M, Crisp TM, Mangelsdorf DJ, Haussler MR, et al. Cloning and expression of full-length cDNA encoding human vitamin D receptor. *Proc Natl Acad Sci U S A*. 1988;85(10):3294-8.
27. Crofts LA, Hancock MS, Morrison NA, Eisman JA. Multiple promoters direct the tissue-specific expression of novel N-terminal variant human vitamin D receptor gene transcripts. *Proc Natl Acad Sci U S A*. 1998;95(18):10529-34.
28. Trowbridge R, Mittal SK, Sharma P, Hunter WJ, Agrawal DK. Vitamin D receptor expression in the mucosal tissue at the gastroesophageal junction. *Exp Mol Pathol*. 2012;93(2):246-9.
29. Matusiak D, Murillo G, Carroll RE, Mehta RG, Benya RV. Expression of vitamin D receptor and 25-hydroxyvitamin D3-1{alpha}-hydroxylase in normal and malignant human colon. *Cancer Epidemiol Biomarkers Prev*. 2005;14(10):2370-6.
30. Moons LM, Kuipers EJ, Rygiel AM, Groothuismink AZ, Geldof H, Bode WA, et al. COX-2 CA-Haplotype Is a Risk Factor for the Development of Esophageal Adenocarcinoma. *Am J Gastroenterol*. 2007.
31. DiBaise JK. The LA classification for esophagitis: a call for standardization. *Am J Gastroenterol*. 1999;94(12):3403-4.
32. Pfaffl MW. A new mathematical model for relative quantification in real-time RT-PCR. *Nucleic Acids Res*. 2001;29(9):e45.
33. Wall L, deBoer E, Grosveld F. The human beta-globin gene 3' enhancer contains multiple binding sites for an erythroid-specific protein. *Genes Dev*. 1988;2(9):1089-100.
34. Messeguer X, Escudero R, Farre D, Nunez O, Martinez J, Alba MM. PROMO: detection of known transcription regulatory elements using species-tailored searches. *Bioinformatics*. 2002;18(2):333-4.
35. Farre D, Roset R, Huerta M, Aduara JE, Rosello L, Alba MM, et al. Identification of patterns in biological sequences at the ALGGEN server: PROMO and MALGEN. *Nucleic Acids Res*. 2003;31(13):3651-3.
36. Merika M, Orkin SH. DNA-binding specificity of GATA family transcription factors. *Mol Cell Biol*. 1993;13(7):3999-4010.

37. Uhlen M, Oksvold P, Fagerberg L, Lundberg E, Jonasson K, Forsberg M, et al. Towards a knowledge-based Human Protein Atlas. *Nat Biotechnol.* 2010;28(12):1248-50.
38. Boyle MJ, Seaver EC. Developmental expression of foxA and gata genes during gut formation in the polychaete annelid, *Capitella* sp. I. *Evol Dev.* 2008;10(1):89-105.
39. Haveri H, Westerholm-Ormio M, Lindfors K, Maki M, Savilahti E, Andersson LC, et al. Transcription factors GATA-4 and GATA-6 in normal and neoplastic human gastrointestinal mucosa. *BMC Gastroenterol.* 2008;8:9.
40. Hyland PL, Hu N, Rotunno M, Su H, Wang C, Wang L, et al. Global changes in gene expression of Barrett's esophagus compared to normal squamous esophagus and gastric cardia tissues. *PLoS One.* 2014;9(4):e93219.
41. Milano F, van Baal JW, Buttar NS, Rygiel AM, de Kort F, DeMars CJ, et al. Bone morphogenetic protein 4 expressed in esophagitis induces a columnar phenotype in esophageal squamous cells. *Gastroenterology.* 2007;132(7):2412-21.
42. Gobel F, Taschner S, Jurkin J, Konradi S, Vaculik C, Richter S, et al. Reciprocal role of GATA-1 and vitamin D receptor in human myeloid dendritic cell differentiation. *Blood.* 2009;114(18):3813-21.
43. Chang CK, Mulholland HG, Cantwell MM, Anderson LA, Johnston BT, McKnight AJ, et al. Vitamin d receptor gene variants and esophageal adenocarcinoma risk: a population-based case-control study. *J Gastrointest Cancer.* 2012;43(3):512-7.



## Supplementary information



**Supplementary Figure S1.** Genomic structure of the 12q13.1 locus and potential transcription factor binding sites in the exon 1c region of the *VDR* gene. **(A)** Genomic structure of the 12q13.1 locus. The *VDR* gene encompasses about 64,493bp consisting of a 5' region containing non coding exon 1a to 1f, the coding exons 2 to 9, and a 3' UTR (24-27). **(B)** The intronic region near the non-coding exon 1c approximately 1.5 kb upstream of the translation start site contains a number of potential transcription factor binding sites, including for GATA-1, AP-1, SRY and Nf kappaB. Analysis of this region indicated that the rs1989969 T allele causes a GATA-1 binding site to appear. Transcription factor binding sites are indicated by underlining of the sequence and their respective name. Bold bases represent the two htSNPs investigated in this study, rs1989969 and rs2238135. S = G or C, Y = C or T, R = A or G according to The International Union of Pure and Applied Chemistry (IUPAC) nucleotide base code.



# Chapter 6.1

---

Use of immunohistochemical  
biomarkers as independent predictor  
of neoplastic progression in  
Barrett's oesophagus surveillance:  
a systematic review and meta-analysis

Vincent T. Janmaat\* · Sophie H. van Olphen\* · Katharina E. Biermann ·  
Leendert H.J. Looijenga · Marco B. Bruno · Manon C.W. Spaander

\* These authors contributed equally

*PLoS One. 2017;12(10):e0186305*

## Abstract

The low incidence of oesophageal adenocarcinoma (EAC) in Barrett's oesophagus (BE) patients reinforces the need for risk stratification tools to make BE surveillance more effective. Therefore, we have undertaken a systematic review and meta-analysis of published studies on immunohistochemical (IHC) biomarkers in BE to determine the value of IHC biomarkers as neoplastic predictors in BE surveillance. We searched MEDLINE, EMBASE, Web of Science, CENTRAL, Pubmed publisher, and Google scholar. All studies on IHC biomarkers in BE surveillance were included. ORs were extracted and meta-analyses performed with a random effects model. 16 different IHC biomarkers were studied in 36 studies. These studies included 425 cases and 1835 controls. A meta- analysis was performed for p53, aspergillus oryzae lectin (AOL), Cyclin A, Cyclin D and alpha-methylacyl-CoA racemase. Aberrant p53 expression was significantly associated with an increased risk of neoplastic progression with an OR of 3.18 (95% CI 1.68 to 6.03). This association was confirmed for both non-dysplastic BE and BE with low-grade dysplasia (LGD). Another promising biomarker to predict neoplastic progression was AOL, with an OR of 3.04 (95% CI 2.05 to 4.49). In conclusion, the use of p53 IHC staining may improve risk stratification in BE surveillance. Aberrant p53 expression in BE patients appeared to be associated with a significantly increased risk of neoplastic progression for both non-dysplastic and LGD BE patients.

## Introduction

Development of oesophageal adenocarcinoma (EAC) is related to Barrett's oesophagus (BE), a premalignant condition of the distal oesophagus. In BE, the pre-existent squamous epithelium is replaced by columnar epithelium which develops under the influence of chronic acid and bile reflux and frequently contains goblet cells (1-3). The progression from BE to EAC is a gradual process, in which intestinal metaplasia (IM) evolves to low-grade dysplasia (LGD), high-grade dysplasia (HGD) and eventually EAC (4). Therefore, current guidelines recommend endoscopic surveillance in BE patients to detect HGD or EAC at an early stage, with the aim to improve survival rates (5, 6). Several studies have shown that patients diagnosed with EAC during BE surveillance have earlier staged tumors and probably better survival compared to those diagnosed after the onset of symptoms (7-10).

The estimated incidence of EAC in patients with BE was reported to be between 0.5 and 1% per year (11-14). However, more recent population-based studies and two meta-analyses have set this risk around 0.12% to 0.38% per year (15-18). This relatively low annual risk reinforces the need for risk stratification tools to make BE surveillance more effective. BE length, male gender, smoking, and LGD are known risk factors for progression to HGD and EAC (13, 15, 18-20). Two large population studies confirmed that patients with LGD have an approximately five times higher risk of progression compared to patients with non-dysplastic BE (15, 18). Thus, more intensive surveillance is recommended in BE patients with LGD (5, 6). However, the histological diagnosis of LGD is subject to a considerable inter- and intra-observer variation, because of sample error and overlap with features of non-neoplastic regenerative changes (21-24).

Because none of the current clinical and histologic criteria are able to accurately predict which patients are likely to progress to HGD or EAC, there is an increasing interest in (molecular) biomarkers. Many immunohistochemical (IHC) biomarkers have been studied in BE progression, mainly because they can be applied to standard histological samples. In clinical practice, IHC biomarkers are relatively easily applicable compared to other techniques. Currently, the addition of p53 IHC to the histological assessment is recommended in the guideline of the British Society of Gastroenterology as it may improve the diagnostic reproducibility of a histological diagnosis of LGD (5). The use of IHC biomarkers as independent predictor of neoplastic progression is not yet performed in routine clinical care, neither for p53, nor for other IHC biomarkers. Therefore, this study aims to provide a systematic review and meta-analyses of all retrospective case control or cohort studies and prospective cohort studies investigating IHC biomarkers as predictor of neoplastic progression in patients with BE.

## Materials and methods

This review was conducted according to the PRISMA and MOOSE guidelines (**S1 MOOSE checklist**, **S1 PRISMA checklist**) (25, 26).

### Definitions

BE was defined as columnar lined oesophagus (CLE). Neoplastic progression was defined as the development of HGD or EAC during follow up. Patients with neoplastic progression were classified as cases and patients without neoplastic progression as controls.

### Data sources and searches

Records were identified by searching the following electronic databases: 1. EMBASE, 2. MEDLINE, 3. Web of Science, 4. CENTRAL, 5. PubMed Publisher, 6. Google scholar until 09-12-2016 (**S1 Search**). The search strategy was constructed by applying a sensitivity maximizing approach. A combination of MESH subject headings and text words were used related to IHC markers for progression in patients with BE. The search was confined to English language publications. Conference abstracts indexed in Embase from the years 2014 - 2016 were included in order to be able to include new and unpublished papers.

### Study selection

Search results were combined and duplicates removed. Every article was screened on title and abstract level for relevance by a single author (SvO or VJ). Articles were reviewed full text by the same two independent authors and included if they met the following criteria: (1) association between IHC biomarker expression on formalin fixed paraffin embedded material and risk of neoplastic progression was assessed; (2) a cohort or case-control study design; (3) patients with known or newly diagnosed BE with or without LGD at baseline; (4) patients defined as cases had to have progressed to either HGD or EAC during follow-up; (5) mean follow-up of at least one year from the time of initial BE diagnosis; (6) the possibility to extract an OR. Studies were excluded if: (1) BE cohorts included patients with HGD at baseline; (2) endoscopic therapies affecting neoplastic progression were performed during follow-up (**Figure 1**). Some manuscripts studied different biomarkers within the same population, these were considered as individual studies on the level of the individual biomarker.

### Data extraction

For each included study two independent authors extracted data according to a standardized data extraction form and assessed the quality of the eligible studies (**S1**

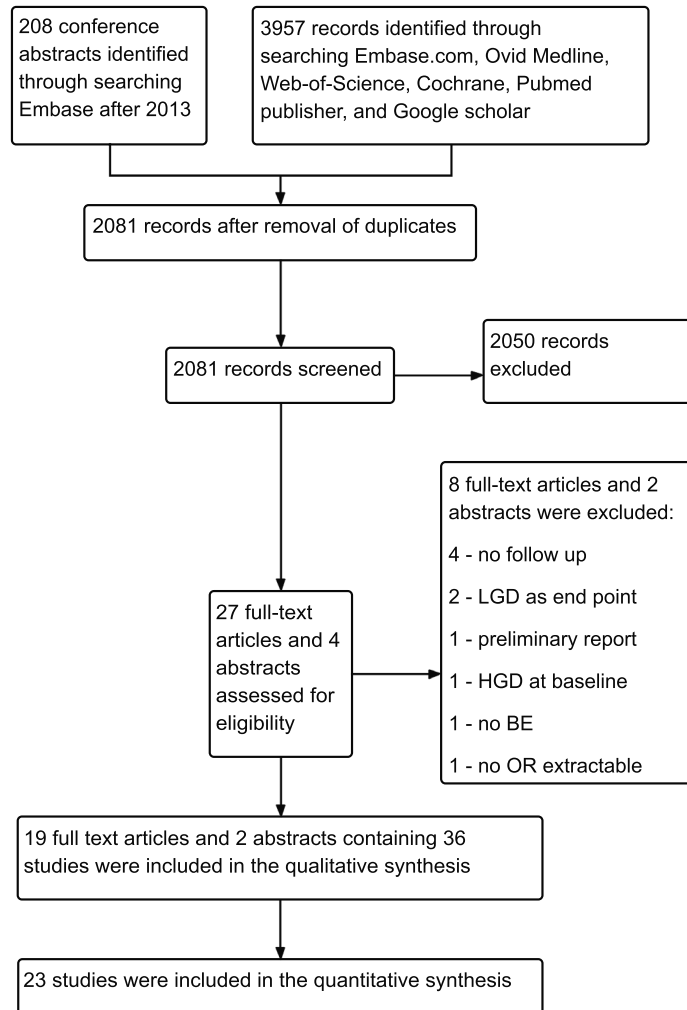


**Figure 1.** Flow chart of the study.

**Standardized data extraction form).** In case of disagreement consensus was reached by consulting a third author (MS). Odds ratio's (OR)s and 95% confidence intervals (CI)s of individual IHC biomarkers were extracted or estimated from the data. If ORs could not be extracted directly from the text or the tables, ORs were calculated indirectly by using the numbers of cases and controls with an aberrant versus a normal IHC biomarker expression from text, tables, or figures.

### Quality assessment

The quality aspects defined were: a difference at baseline between cases and controls of at least 10% (concerning baseline histology, age, sex, length of BE segment, and follow-

up time), adjustments in the form of regression for differences of known predictors of progression (such as baseline histology, age, sex, and length of BE segment), exclusion of prevalent cases, control stainings, number of pathologists, pathologist agreement and pathologist blinding. These aspects were assessed and reported on but not used as exclusion criteria.

### **Data synthesis and analyses**

Meta-analysis were performed if at least two studies were available (27). If multiple studies in a single analysis included the same patients, the oldest study was excluded. An inverse variance random-effect model was used. If data on multiple definitions of aberrant staining were available, definitions were chosen to resemble those from other included studies for that IHC biomarker. If only one study was available, definitions of the authors of that study were used. Pooled estimates of effect, in the form of ORs, were calculated and investigated for statistical heterogeneity by visual inspection and the I-squared test ( $I^2 = ((Q - df) / Q) * 100\%$ , where Q was the chi squared statistic and df was its degree of freedom. Where possible, ORs adjusted for most factors were used in the analysis and unadjusted and adjusted ORs were pooled if necessary. Small study effects such as publication bias were assessed using a funnel plot.

### **Sensitivity and subgroup analyses**

Sensitivity analyses were performed in case of a large standard error (if small study effects were likely present as observed in the funnel plot), if no adjustments were made for known predictors of progression (such as sex, age, histology, i.e. non-dysplastic or LGD, and BE-length), and if only an abstract was available. We excluded individual studies from the most reliable analysis to evaluate the impact of single studies on pooled risk estimates and heterogeneity. Additional analyses were performed to assess if an IHC biomarker can be used as a predictor of neoplastic progression, independent of the presence of dysplasia. Therefore, all studies were summarized which included only non-dysplastic BE patients, only BE with LGD patients, or in which adjustments were made for histology type. Additionally, two subgroup analyses were performed including either non-dysplastic or LGD BE patients.

### **Stringency of the definition for aberrant staining used and its interpretation**

The stringency level of the definition for aberrant staining and its interpretation could lead to variation in the predictive ability of the IHC biomarker investigated. To investigate whether this effect might be present, the proportion of controls deemed positive was plotted against the OR of each study.



## Results

### Included studies

2081 records were retrieved, after removal of duplicates. After excluding 2050 records based on title and abstract, a total of 27 full text articles and four abstracts were assessed in detail (**Figure 1**). Of these, 19 full text articles and two abstracts were included in this review (28-49). These articles contained a total of 36 studies.

### Characteristics

A total of 36 studies were included, containing 2260 patients of which 425 cases, selected from a populations of more than 7000 BE patients. The proportion of male patients ranged from 66% to 100%. Mean duration of follow-up varied from 11.3 months to 120 months. Most studies were retrospective case-control studies (n=33), and three prospective cohort studies. One study defined BE as CLE without IM, other studies defined BE as CLE with IM (n=23), or gave no definition (n=12). Endpoint was EAC in six studies and either HGD or EAC in 30 studies (**Table 1**).

### Dilutions and definitions for aberrant staining used

For p53, the antibody DO-7 (Dako, Glostrup, Denmark) was frequently used with a dilution ranging from 1:20 to 1:1000. The definition for aberrant IHC staining was heterogeneous. Very intense staining was considered aberrant by all studies (being independent of the concentration used). However, intensity of staining was not a prerequisite for considering a staining pattern aberrant in seven studies (29-33, 37, 47). Three more recent studies also considered a total absence of staining as aberrant (35, 36, 39). For aspergillus oryzae lectin (AOL), one study calculated the OR for aberrant AOL IHC staining in 2 or 3 epithelial compartments versus 0 or 1 compartment (34). Another study reported multiple ORs for aberrant AOL in 1, 2, or 3 versus 0 epithelial compartments (39). The OR of aberrant AOL IHC staining in 2 or 3 versus 0 or 1 compartments was extracted from this second study and analyzed together with the data from the first study for the meta-analysis.

### Quality of studies

In 14 of the 36 studies there was at least a 10% difference in baseline histology between cases and controls. In these studies, around 32% of the cases had IND or LGD at baseline, versus 9% in the controls. In five studies an age difference at baseline of at least 5 years was found between cases and controls, in four of these studies the case group was older. In six studies at least 10% more males were included in the case groups, 96% males on average in the cases, versus 73% in controls. Information on length of the BE segment for both cases and controls was provided in 13 studies. In cases a

**Table 1.** Characteristics of included studies

Study	Marker	Design	Patients	Baseline	End-point	DEF BE	Antibody
Younes et al. 1997	p53	Retrospective case-control	25	LGD/ IND	HGD/EAC	BE, IM+	BP-53-12 Bio Genex (m), (not mentioned)
Gimenez 1999	p53	Retrospective case-control	6	LGD	HGD/EAC	NA	Do-7, Dako, (m)(1:50)
Bani-Hani et al. 2000	p53	Retrospective nested case-control	52	IM, non- HGD	EAC	BE, IM+	DO-7-p53, Novocastra (m)(1:100)
Weston et al. 2001	p53	Prospective cohort	48	LGD	HGD/EAC	NA	Zymed, (m) (not mentioned)
Skacel et al. 2002	p53	Retrospective case-control	16	LGD	HGD/EAC	NA	Do-7, Dako, (m)(not mentioned)
Murray et al. 2006 a	p53	Retrospective nested case-control	197	IM	HGD/EAC	BE, IM+	DO-7-p53, Novocastra (m)(1:100)
Brown 2008	p53	Prospective cohort	276	IM, LGD	HGD/EAC	NA	not mentioned
Sikkema et al. 2009 a	p53	Retrospective nested case-control	42	IM, LGD	HGD/EAC	BE, IM+	Do-7, Dako, (m)(1:1000)
Bird-Lieberman et al. 2012 a	p53	Retrospective nested case-control	356	IM,LGD	HGD/EAC	BE, IM+	DO7, Leica, (1:50)
Kastlein et al. 2012 a	p53	Case-control in prospective cohort	635	IM, LGD	HGD/EAC	BE, IM+	Do-7, Dako, (m)(1:25)
Wolf et al. 2014	p53	Retrospective nested case-control	279	IM, IND, LGD	EAC	NA	not mentioned
Davelaar et al. 2015	p53	Prospective cohort	91	IM, IND, LGD	HGD/EAC	BE, IM+	mix of DO-7 and PB53-12, Fisher scientific, (N/A)
Horvath et al. 2016	p53	Retrospective case-control	79	IND	HGD/EAC	NA	Do-7, Dako, (m)(1:20)
Bird-Lieberman et al. 2012 c	AOL	Retrospective nested case-control	321	IM, LGD	HGD/EAC	BE, IM+	AOL 5ug biotinylated lectin, Tokyo chem. Indust.

Table 1. Continued

Study	Marker	Design	Patients	Baseline	End-point	DEF BE	Antibody
Wolf et al. 2014	AOL	Retrospective nested case-control	252	IM, IND, LGD	EAC	NA	not mentioned
Pierre Lao-Sirieix et al. 2007	Cyclin A	Retrospective nested case-control	48	IM	EAC/HGD	BE, IM+	cyclin A, Novocastra (m)(1:20)
Bird-Lieberman et al. 2012 b	Cyclin A	Retrospective nested case-control	323	IM, LGD	HGD/EAC	BE, IM+	Leica (m)(1:50)
Wolf et al. 2014	Cyclin A	Retrospective nested case-control	279	IM, IND, LGD	EAC	NA	not mentioned
Van Olphen et al. 2016	Cyclin A	Case-control in a prospective cohort	625	IM, LGD	HGD/EAC	BE, IM+	Leica (m)(1:200)
Bani-Hani et al. 2000	Cyclin D	Retrospective nested case-control	61	IM	EAC	BE, IM+	NCL-CYCLIN D1, Novocastra (m)(1:30)
Murray et al. 2006 b	Cyclin D	Retrospective nested case-control	197	IM	HGD/EAC	BE, IM+	NCL-L-CYCLIND1-GM, Novocastra, (m)(1:50)
Horvath et al. 2016	Cyclin D	Retrospective case-control	79	IND	HGD/EAC	NA	SP4, ThermoLabVision (m)(1:100)
Kastrelein et al. 2013 b	AMACR	Case-control in prospective cohort	631	IM, LGD	HGD/EAC	BE, IM+	clone 13H4, Thermo Scientific (m)(1:200)
Horvath et al. 2016	AMACR	Retrospective case-control	81	IND	HGD/EAC	NA	13H4, Zeta Corp (m)(1:100)
Lastriaioli et al. 2006	hERG1	Retrospective cohort	23	IM	EAC	BE, IM+	hERG1 alexis corporation (p)(1:200)
Lastriaioli et al. 2016	hERG1	Case-control	94	IM	EAC	NA	hERG1, Dival Toscana Srl (m)(1:200)
Sirieix et al. 2003	MCM2	Retrospective nested case-control	27	IM	HGD/EAC	BE, IM+	Hurchison, Cambridge, (m)(1:10)

Table 1 continues on next page.

**Table 1.** *Continued*

Study	Marker	Design	Patients	Baseline	End-point	DEF BE	Antibody
Capello et al. 2005	CD1a	Retrospective case-control	166	CLE, IM negative	Dysplasia / EAC	BE, IM-	dako clone O10, (m)(1:50)
Murray et al. 2006 d	$\beta$ -catenin	Retrospective nested case-control	194	IM	HGD/EAC	BE, IM+	G10153, Transduction Laboratories, (m)(1:100)
Murray et al. 2006 c	COX-2	Retrospective nested case-control	196	IM	HGD/EAC	BE, IM+	160112, Cayman Chemicals, (m) (1:250)
Sikkema et al. 2009 b	Ki-67	Retrospective case-control	42	IM	HGD/EAC	BE, IM+	Clone MIB-1, Dako (1:100)
Rossi et al. 2009	HER-2	Retrospective case-control	20	IM, LGD	HGD, EAC	NA	Hercept <sup>Test</sup> kit, DAKOCytomation
Bird-Lieberman et al. 2012 e	Sialyl Lewis	Retrospective nested case-control	356	IM, LGD	HGD/EAC	BE, IM+	BOND ready retrieval
Bird-Lieberman et al. 2012 d	WGA	Retrospective nested case-control	331	IM, LGD	HGD/EAC	BE, IM+	Leica BOND-MAX
Bird-Lieberman et al. 2012 f	Lewis	Retrospective nested case-control	350	IM, LGD	HGD/EAC	BE, IM+	CD15, BOND ready, retrieval H2 20 min Leica
Van Olphen et al. 2015	SOX2	Case-control in prospective cohort	635	IM, LGD	HGD/EAC	BE, IM+	AF2018, R&D Systems (p)(1:400)

longer BE segment was present; on average 5.9 cm versus 4.8 cm in the controls. In 17 studies the total follow-up time differed by at least 10% between case and control groups. On average, follow up time was 51 months versus 59 months for cases versus controls, respectively. Seven studies excluded possible prevalent cases (29, 32, 34, 47, 49). Fourteen studies adjusted for known predictors of progression (**Supplementary Table S1**). 16 studies did not describe technical validation of the staining. IHC staining was scored by one observer in 15 studies, by two observers in 13 studies, and by three observers in three studies. Kappa values were mentioned in only eight studies. Whether slides were assessed in a blinded manner was not mentioned in six studies, all other studies reported the use of blinding (**Supplementary Table S1**).

### Meta-analyses

These were possible for p53, AOL, Cyclin A, Cyclin D, and alpha-methylacyl-CoA racemase (AMACR), which were studied 13, 2, 4, 3, and 2 times respectively. Of the 13 studies, two included patients from the same population, which resulted in exclusion of the older study in analyses for which both would have been eligible (32, 34). The most frequent reasons for excluding articles were the absence of follow-up data and LGD being defined as neoplastic progression and end-point of the study (**Figure 1**). Biomarkers studied only once were MCM2, CD1a,  $\beta$ -catenin, COX2, Ki67, HER2, Sialyl Lewis, Wheat germ, Lewis, and SOX2. The same group published two studies on hERG1, both including patients from the same population (46, 48). Therefore, both studies were individually included without summary in a meta-analysis.

### p53

A total of 12 studies were included in the meta-analysis. These contained 1905 patients, of which 342 cases. One study gave multiple ORs for various expression levels of p53 (34). For this study, only the OR for intense overexpression of p53 staining was considered positive. Individual patient data of one study were converted in order to extract an adjusted OR (35). The overall OR for neoplastic progression was 7.04 (95% CI 3.68 to 13.46) for patients with aberrant p53 expression (**Table 2** and **Figure 2**). Aberrant p53 expression, detected in both non-dysplastic BE and LGD patients, was significantly associated with the development of HGD or EAC. Significant heterogeneity ( $I^2=56\%$ ,  $p<0.010$ ) was observed between the included studies, which can be considered a moderate amount of heterogeneity (50). The 12 studies were plotted in a funnel plot which shows that small study effects can be present (**Supplementary Figure S1**). In order to reduce the influence of such effects a sensitivity analysis was performed, which excluded all studies with a standard error above one. Based on this criterion, five studies remained, containing 1413 patients and 289 cases. The overall OR for neoplastic progression was 4.15 (95% CI 1.96 to 8.81) in patients with an aberrant p53 expression (**Table 2**). The use of a more stringent definition of aberrant staining may lead to loss of aberrant

**Table 2.** Summary of meta-analyses of studies investigating p53 IHC as a predictor of neoplastic progression

Analysis	Studies	Cases	Controls	OR	95% CI	I <sup>2</sup>	References
p53 (main)	12 (Figure 2)	342	1563	7.04	3.68-13.46	56%	(28-31, 33-39, 47)
p53 (excluded SE > 1)	5	289	1124	4.15	1.96-8.81	68%	(29, 34-36, 39)
p53 (also excluded unadjusted ORs)	4	278	1044	3.18	1.68-6.03	55%	(29, 34, 35, 39)
p53 (exclude individual study (29) from the above analysis)	3	267	1003	3.20	1.49-6.87	70%	(34, 35, 39)
p53 (exclude individual study (34) from the above analysis)	3	200	766	3.64	1.57-8.41	64%	(29, 35, 39)
p53 (exclude individual study (35) from the above analysis)	3	229	458	2.23	1.37-3.64	0%	(29, 34, 39)
p53 (exclude individual study (39) from the above analysis)	3	138	905	3.78	1.65-8.68	52%	(29, 34, 35)
p53 (also excluded abstracts)	3	138	905	3.78	1.65-8.68	52%	(29, 34, 35)
p53 (only ORs stratified for histology)	6	282	1058	3.86	2.03-7.33	46%	(30, 31, 34, 35, 37, 39)
p53 (only non-dysplastic BE)	2	61	659	6.12	2.99-12.52	0%	(32, 35)
p53 (only LGD)	4	37	145	8.64	3.62-20.62	0%	(30, 31, 35, 37)

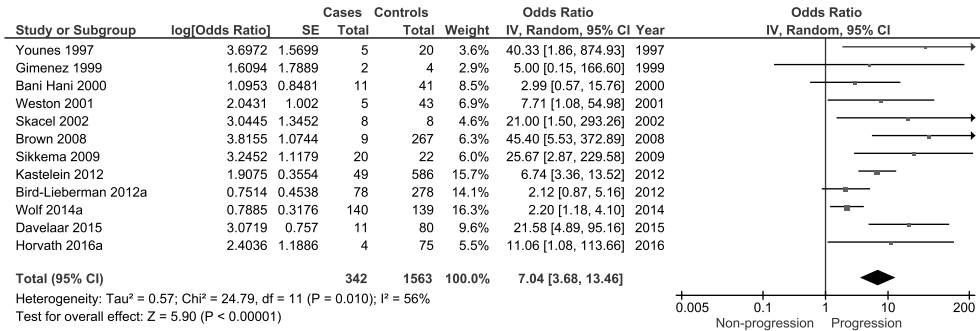


**Figure 2.** Forest plot of studies investigating p53 as a predictor of progression. Twelve studies were included.

expression in cases, in controls, or in both. In order to investigate this, the proportion of controls deemed aberrant was plotted against the OR of each study (**Supplementary Figure S2**). Studies with a higher point estimate of the OR appeared to have had less positive non-progressors. The same is seen if this is analyzed in individual studies where multiple cut-offs for positivity are described (32, 34). Using a more stringent cut off resulted in a higher OR. Further sub sensitivity analyses were performed excluding studies for which no adjusted ORs were available. Four studies remained, containing 1322 patients and 278 cases. The overall OR for neoplastic progression was 3.18 (95% CI 1.68 to 6.03) in patients with an aberrant p53 expression (**Table 2**). Subsequently, individual studies were excluded from this analysis, and finally also studies presented as abstracts. These sensitivity analyses showed similar results with slightly lower point estimates compared to the main analysis (**Table 2**). For three studies both unadjusted and adjusted ORs were available, and all three adjusted ORs had a lower point estimate compared to the unadjusted ones, in line with the outcome of our meta-analyses.

### **p53 as independent predictor of neoplastic progression**

For this analysis studies that did not adjust for histology at baseline were excluded. This led to the inclusion of six studies. These studies contained a total of 1340 BE patients, of which 282 cases. The overall OR, for aberrant p53 IHC on neoplastic progression, after stratification for histology, was 3.86 (95% CI 2.03 to 7.33) (**Table 2**).

### **p53 in non-dysplastic Barrett's oesophagus**

Two studies were included for this analysis. These contained a total of 720 BE patients, of which 61 cases. Individual patient data of one study was re-analyzed to provide an OR for non-dysplastic BE patients only (35). The overall OR for neoplastic progression to HGD or EAC in non-dysplastic BE patients was 6.12 (95% CI 2.99 to 12.52) (**Table 2**).

**p53 in low-grade dysplasia Barrett**

For this analysis four studies were included. These contained a total of 182 BE patients, of which 37 cases. One study was re-analyzed to provide an OR for the LGD subgroup only (35). The overall OR for neoplastic progression to HGD or EAC was 8.64 (95% CI 3.62 to 20.62) (**Table 2**).

**AOL**

Two studies were included in this meta-analysis. These contained 573 BE patients, of which 204 cases. The overall OR for neoplastic progression in BE patients with an aberrant AOL staining in 2 or 3 compartments, versus 0 or 1 compartments of the tissue was 3.04 (95% CI 2.05 to 4.49) (**Table 3** and **Supplementary Figure S3**). Results of the two studies were consistent in their findings ( $I^2=0\%$ ,  $p=0.85$ ).

**Table 3.** Summary of meta-analyses of studies investigating IHC biomarkers other than p53 as a predictor of neoplastic progression

Analysis	Studies	Cases	Controls	OR	95% CI	$I^2$
AOL	2 (Suppl. Fig. S3)	204	369	3.04	2.04-4.49	0%
Cyclin A	4 (Suppl. Fig. S3)	285	990	1.90	0.85-4.22	76%
Cyclin D	3 (Suppl. Fig. S3)	50	287	1.01	0.14-7.03	80%
AMACR	2 (Suppl. Fig. S3)	53	659	4.07	0.66-25.12	53%

**CYCLIN A**

Four studies were included in this meta-analysis. These contained 1275 patients, of which 285 cases. The overall OR for neoplastic progression in BE patients with cyclin A positivity was 1.90 (95% CI 0.85 to 4.22) (**Table 3** and **Supplementary Figure S3**). Results of the three studies were inconsistent in their findings ( $I^2=76\%$ ,  $p=0.005$ ).

**CYCLIN D**

Three studies were included in this meta-analysis. These contained 337 patients, of which 50 cases. The overall OR for neoplastic progression in BE patients with cyclin D positivity was 1.01 (95% CI 0.14 to 7.03) (**Table 3** and **Supplementary Figure S3**). Results of the two studies were inconsistent in their findings ( $I^2=80\%$ ,  $p=0.007$ ).

**Alpha-methylacyl-CoA racemase**

Two studies were included in this meta-analysis. These contained 712 patients, of which 53 cases. The overall OR for neoplastic progression in BE patients with alpha-methylacyl-CoA racemase positivity was 4.07 (95% CI 0.66 to 25.12) (**Table 3** and



**Supplementary Figure S3).** Results of the two studies were moderately consistent in their findings ( $I^2=53\%$ ,  $p=0.14$ ).

### Studies on other IHC biomarkers

The following IHC biomarkers were investigated only once:  $\beta$ -catenin, CD1a, COX2, HER2, Ki67, Lewis, Mcm2, Sialyl Lewis, SOX2, and WGA. The same group published two studies on hERG1, both including patients from the same population (46, 48). Therefore, both studies were individually included without summary in a meta-analysis. In the CD1a study CLE without IM was used as baseline histology (45). When considering study size and point estimate, CD1a, SOX2, and hERG1 appeared most promising (**Supplementary Figure S4**).

## Discussion

This is the first systematic review and meta-analysis to assess if IHC biomarkers can be used as an independent predictor for neoplastic progression in BE surveillance. Sixteen biomarkers have been investigated in this setting, of which five biomarkers have been investigated more than once. The meta-analysis showed that aberrant p53 expression was associated with a significantly increased risk of neoplastic progression. Moreover, aberrant p53 expression predicted neoplastic progression in both non-dysplastic BE patients and BE patients with LGD. Of the other four IHC biomarkers, AOL appeared to be most promising in predicting neoplastic progression, whereas Cyclin A, Cyclin D, and alpha-methylacyl-CoA racemase are still of limited value.

Current use of p53 IHC in BE patients differs in international guidelines. The guideline of the British Society of Gastroenterology recommends the addition of p53 IHC staining for the pathological assessment of BE to improve the diagnostic reproducibility of dysplasia (5). While the American Gastroenterological Association guideline states that: "data supporting the use of biomarkers to confirm the histologic diagnosis of dysplasia must be considered preliminary" (51). No guideline has yet adopted the use of IHC biomarkers to predict neoplastic progression. Two large population based studies confirmed that patients with LGD have an approximately 5 times higher risk of neoplastic progression compared to patients without LGD (15, 18). Our meta-analysis is the first to show that BE patients, independent of the presence of LGD, with aberrant p53 IHC have a similar increased risk to develop cancer compared to patients with LGD. A recent publication claims to have investigated the predictive ability of immunohistochemical biomarkers (52). However, they reported on samples either obtained from a resection specimen or from cases and controls without follow-up. Therefore, based on their current dataset, their current conclusion, i.e. that p53 overexpression predicts malignant progression, is not justified (53).

Although routine p53 IHC will incur higher cost than histological assessment alone, application of this marker has the potential to reduce the overall costs related to BE surveillance by improved risk stratification using expression of p53 IHC in combination with other predictors of progression, such as histology, sex, age, and length of the BE segment. Better risk stratification could result in both earlier detection of lesions in patients at risk, and a reduction in endoscopic and pathology resources for patients that will never develop progression. The disparity in ORs of neoplastic progression found in the various studies may be explained by differences in staining methods, including antibodies used, antigen retrieval methods, definitions, and interpretations of aberrant staining used. Therefore, special consideration should be given to the protocol of staining and the definition and interpretation used for aberrant expression. Some studies did not consider loss of p53 staining aberrant, which might have contributed to the protocol being less predictive compared to other studies. By using a more stringent definition of aberrant expression, cases appeared to remain p53 aberrant, while controls were not considered aberrant (**Supplementary Figure S2**). Therefore, the use of more stringent definitions and interpretations for aberrant staining appears to lead to a higher predictive ability of p53 IHC.

The strength of this paper is the focus on IHC biomarkers as a relatively easy applicable tool to improve risk stratification in BE surveillance. Additionally, we performed a broad search, and the extraction of ORs from text, tables and figures resulted in the inclusion of quite a large number of studies. The inclusion of abstracts results in an up to date overview of this field. Because meta-analysis is the synthesis technique that is most transparent and most likely valid also with small amount of studies included, some of the meta-analysis were performed with only two studies, as no more studies were available (27). This study also has its limitations, such as the confinement to English language publications, the apparent presence of publication bias, differences in baseline comparability within studies, and the various adjustments made for these baseline differences. Therefore, we performed sensitivity analyses of the p53 meta-analyses, these show that the point estimate of the OR decreased from 7.04 to 3.18 when we accounted for these limitations. Because aberrant p53 IHC co-occurs with LGD, separate analyses were performed in which we stratified for dysplastic and non-dysplastic patients. These analyses show that aberrant p53 expression is an independent prognostic factor for neoplastic progression.

In conclusion, we show that sixteen IHC biomarkers in BE surveillance have been studied. Aberrant p53 expression is the most studied IHC biomarker and associated with a significantly increased risk to develop HGD or EAC, this association was independent of the presence of LGD. Consensus amongst pathologists concerning the appropriate staining method, definition, and interpretation of aberrant p53 expression is currently low, and more consensus is required. Other promising biomarkers such as AOL need further investigation.

## Acknowledgements

B.E. Hansen, Department of Gastroenterology and Hepatology, Erasmus University Medical Center Rotterdam, The Netherlands. The biomedical information specialists of the medical library of the Erasmus MC, University Medical Center Rotterdam, The Netherlands for their support with building and running the search.

## References

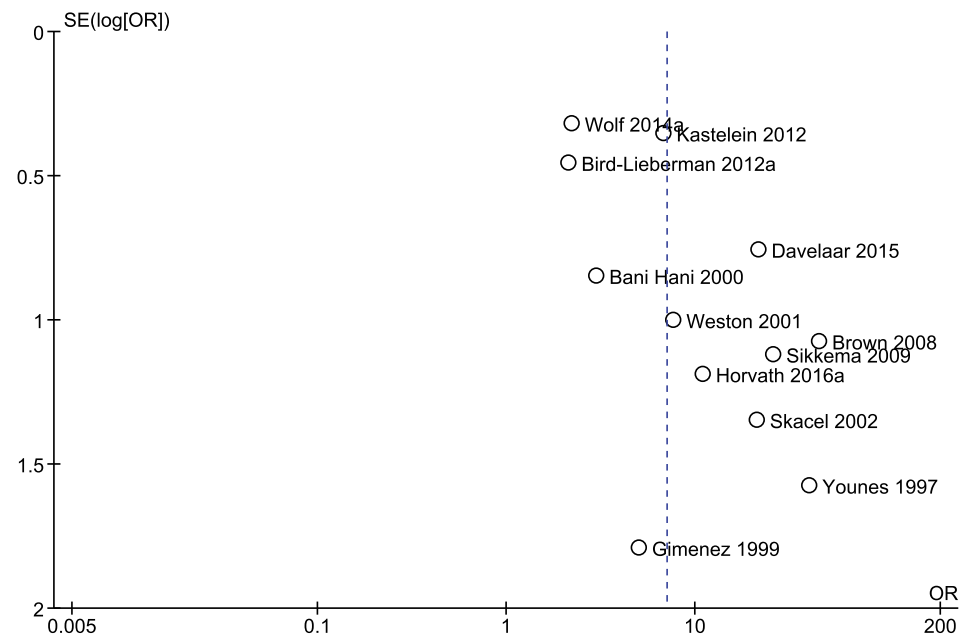
1. American Gastroenterological A, Spechler SJ, Sharma P, Souza RF, Inadomi JM, Shaheen NJ. American Gastroenterological Association medical position statement on the management of Barrett's esophagus. *Gastroenterology*. 2011;140(3):1084-91.
2. Kastelein F, Spaander MC, Biermann K, Vucelic B, Kuipers EJ, Bruno MJ. Role of acid suppression in the development and progression of dysplasia in patients with Barrett's esophagus. *Digestive diseases*. 2011;29(5):499-506.
3. Winters C, Jr., Spurling TJ, Chobanian SJ, Curtis DJ, Esposito RL, Hacker JF, 3rd, et al. Barrett's esophagus. A prevalent, occult complication of gastroesophageal reflux disease. *Gastroenterology*. 1987;92(1):118-24.
4. Buttar NS, Wang KK. Mechanisms of disease: Carcinogenesis in Barrett's esophagus. *Nature clinical practice Gastroenterology & hepatology*. 2004;1(2):106-12.
5. Fitzgerald RC, di Pietro M, Raganath K, Ang Y, Kang JY, Watson P, et al. British Society of Gastroenterology guidelines on the diagnosis and management of Barrett's oesophagus. *Gut*. 2014;63(1):7-42.
6. Wang KK, Sampliner RE, Practice Parameters Committee of the American College of G. Updated guidelines 2008 for the diagnosis, surveillance and therapy of Barrett's esophagus. *The American journal of gastroenterology*. 2008;103(3):788-97.
7. Cooper GS, Kou TD, Chak A. Receipt of previous diagnoses and endoscopy and outcome from esophageal adenocarcinoma: a population-based study with temporal trends. *The American journal of gastroenterology*. 2009;104(6):1356-62.
8. Fountoulakis A, Zafirellis KD, Dolan K, Dexter SP, Martin IG, Sue-Ling HM. Effect of surveillance of Barrett's oesophagus on the clinical outcome of oesophageal cancer. *The British journal of surgery*. 2004;91(8):997-1003.
9. Kastelein F, van Olphen SH, Steyerberg EW, Spaander MC, Bruno MJ, ProBar-study group. Impact of surveillance for Barrett's oesophagus on tumour stage and survival of patients with neoplastic progression. *Gut*. 2016;65(4):548-54.
10. Rubenstein JH, Sonnenberg A, Davis J, McMahon L, Inadomi JM. Effect of a prior endoscopy on outcomes of esophageal adenocarcinoma among United States veterans. *Gastrointestinal endoscopy*. 2008;68(5):849-55.
11. Reid BJ, Levine DS, Longton G, Blount PL, Rabinovitch PS. Predictors of progression to cancer in Barrett's esophagus: baseline histology and flow cytometry identify low- and high-risk patient subsets. *The American journal of gastroenterology*. 2000;95(7):1669-76.
12. Sikkema M, de Jonge PJ, Steyerberg EW, Kuipers EJ. Risk of esophageal adenocarcinoma and mortality in patients with Barrett's esophagus: a systematic review and meta-analysis. *Clinical gastroenterology and hepatology : the official clinical practice journal of the American Gastroenterological Association*. 2010;8(3):235-44; quiz e32.

13. Yousef F, Cardwell C, Cantwell MM, Galway K, Johnston BT, Murray L. The incidence of esophageal cancer and high-grade dysplasia in Barrett's esophagus: a systematic review and meta-analysis. *American journal of epidemiology*. 2008;168(3):237-49.
14. Hage M, Siersema PD, van Dekken H, Steyerberg EW, Dees J, Kuipers EJ. Oesophageal cancer incidence and mortality in patients with long-segment Barrett's oesophagus after a mean follow-up of 12.7 years. *Scandinavian journal of gastroenterology*. 2004;39(12):1175-9.
15. Bhat S, Coleman HG, Yousef F, Johnston BT, McManus DT, Gavin AT, et al. Risk of malignant progression in Barrett's esophagus patients: results from a large population-based study. *J Natl Cancer Inst*. 2011;103(13):1049-57.
16. Desai TK, Krishnan K, Samala N, Singh J, Cluley J, Perla S, et al. The incidence of oesophageal adenocarcinoma in non-dysplastic Barrett's oesophagus: a meta-analysis. *Gut*. 2012;61(7):970-6.
17. Desai TK, Singh J, Samala N, Subbiah P. The incidence of esophageal adenocarcinoma in Barrett's esophagus has been overestimated. *The American journal of gastroenterology*. 2011;106(7):1364-5; author reply 5-6.
18. Hvid-Jensen F, Pedersen L, Drewes AM, Sorensen HT, Funch-Jensen P. Incidence of adenocarcinoma among patients with Barrett's esophagus. *N Engl J Med*. 2011;365(15):1375-83.
19. Wani S, Falk G, Hall M, Gaddam S, Wang A, Gupta N, et al. Patients with nondysplastic Barrett's esophagus have low risks for developing dysplasia or esophageal adenocarcinoma. *Clin Gastroenterol Hepatol*. 2011;9(3):220-7; quiz e6.
20. Coleman HG, Bhat S, Johnston BT, McManus D, Gavin AT, Murray LJ. Tobacco smoking increases the risk of high-grade dysplasia and cancer among patients with Barrett's esophagus. *Gastroenterology*. 2012;142(2):233-40.
21. Curvers WL, ten Kate FJ, Krishnadath KK, Visser M, Elzer B, Baak LC, et al. Low-grade dysplasia in Barrett's esophagus: overdiagnosed and underestimated. *The American journal of gastroenterology*. 2010;105(7):1523-30.
22. Kerkhof M, van Dekken H, Steyerberg EW, Meijer GA, Mulder AH, de Bruine A, et al. Grading of dysplasia in Barrett's oesophagus: substantial interobserver variation between general and gastrointestinal pathologists. *Histopathology*. 2007;50(7):920-7.
23. Cameron AJ, Carpenter HA. Barrett's esophagus, high-grade dysplasia, and early adenocarcinoma: a pathological study. *The American journal of gastroenterology*. 1997;92(4):586-91.
24. Levine DS, Haggitt RC, Blount PL, Rabinovitch PS, Rusch VW, Reid BJ. An endoscopic biopsy protocol can differentiate high-grade dysplasia from early adenocarcinoma in Barrett's esophagus. *Gastroenterology*. 1993;105(1):40-50.
25. Moher D, Liberati A, Tetzlaff J, Altman DG, Group P. Preferred reporting items for systematic reviews and meta-analyses: the PRISMA statement. *J Clin Epidemiol*. 2009;62(10):1006-12.
26. Stroup DF, Berlin JA, Morton SC, Olkin I, Williamson GD, Rennie D, et al. Meta-analysis of observational studies in epidemiology: a proposal for reporting. Meta-analysis Of Observational Studies in Epidemiology (MOOSE) group. *Jama*. 2000;283(15):2008-12.
27. Valentine JC, Pigott TD, Rothstein HR. How Many Studies Do You Need? A Primer on Statistical Power for Meta-Analysis. *Journal of Educational and Behavioral Statistics*. 2010;Vol. 35(No. 2):pp. 215-47.
28. Younes M, Ertan A, Lechago LV, Somoano JR, Lechago J. p53 Protein accumulation is a specific marker of malignant potential in Barrett's metaplasia. *Digestive diseases and sciences*. 1997;42(4):697-701.
29. Bani-Hani K, Martin IG, Hardie LJ, Mapstone N, Briggs JA, Forman D, et al. Prospective study of cyclin D1 overexpression in Barrett's esophagus: association with increased risk of adenocarcinoma. *Journal of the National Cancer Institute*. 2000;92(16):1316-21.

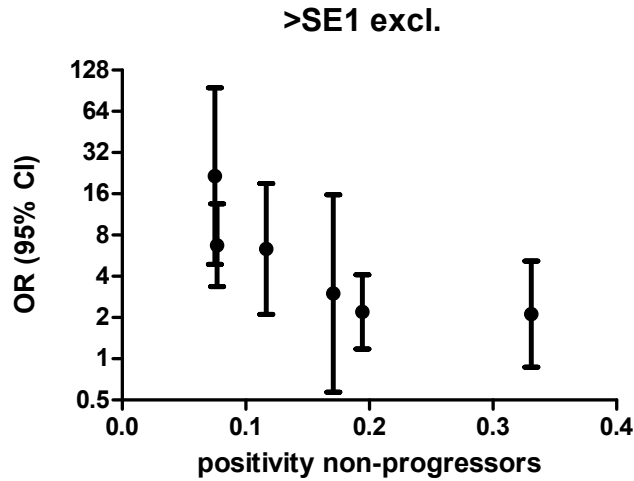
30. Weston AP, Banerjee SK, Sharma P, Tran TM, Richards R, Cherian R. p53 protein overexpression in low grade dysplasia (LGD) in Barrett's esophagus: immunohistochemical marker predictive of progression. *The American journal of gastroenterology*. 2001;96(5):1355-62.
31. Skacel M, Petras RE, Rybicki LA, Gramlich TL, Richter JE, Falk GW, et al. p53 expression in low grade dysplasia in Barrett's esophagus: correlation with interobserver agreement and disease progression. *The American journal of gastroenterology*. 2002;97(10):2508-13.
32. Murray L, Sedo A, Scott M, McManus D, Sloan JM, Hardie LJ, et al. TP53 and progression from Barrett's metaplasia to oesophageal adenocarcinoma in a UK population cohort. *Gut*. 2006;55(10):1390-7.
33. Sikkema M, Kerkhof M, Steyerberg EW, Kusters JG, van Strien PM, Looman CW, et al. Aneuploidy and overexpression of Ki67 and p53 as markers for neoplastic progression in Barrett's esophagus: a case-control study. *The American journal of gastroenterology*. 2009;104(11):2673-80.
34. Bird-Lieberman EL, Dunn JM, Coleman HG, Lao-Sirieix P, Oukrif D, Moore CE, et al. Population-based study reveals new risk-stratification biomarker panel for Barrett's esophagus. *Gastroenterology*. 2012;143(4):927-35 e3.
35. Kastelein F, Biermann K, Steyerberg EW, Verheij J, Kalisvaart M, Looijenga LH, et al. Aberrant p53 protein expression is associated with an increased risk of neoplastic progression in patients with Barrett's oesophagus. *Gut*. 2013;62(12):1676-83.
36. Davelaar AL, Calpe S, Lau L, Timmer MR, Visser M, Ten Kate FJ et al. Aberrant TP53 detected by combining immunohistochemistry and DNA-FISH improves Barrett's esophagus progression prediction: a prospective follow-up study. 2015;54(2):82-90.
37. Gimenez A, de Haro LM, Parrilla P, Bermejo J, Perez-Guillermo M, Ortiz MA. Immunohistochemical detection of p53 protein could improve the management of some patients with Barrett esophagus and mild histologic alterations. *Arch Pathol Lab Med*. 1999;123(12):1260-3.
38. Brown K, Younes M, Ertan A, Verm R, Meriano FV. M1928 P53 Immunostaining Predicts Malignant Progression in Barrett's Metaplasia: WB Saunders; 2008.
39. Wolf WA, Lao-Sirieix P, Duits LC, Chak A, Shaheen NJ, Fitzgerald R, et al. Utility of a biomarker panel to predict progression to esophageal adenocarcinoma in barrett's esophagus. *Gastroenterology*. 2014;146(5):S-330.
40. Lao-Sirieix P, Lovat L, Fitzgerald RC. Cyclin A immunocytochemistry as a risk stratification tool for Barrett's esophagus surveillance. *Clinical cancer research : an official journal of the American Association for Cancer Research*. 2007;13(2 Pt 1):659-65.
41. Sirieix PS, O'Donovan M, Brown J, Save V, Coleman N, Fitzgerald RC. Surface expression of minichromosome maintenance proteins provides a novel method for detecting patients at risk for developing adenocarcinoma in Barrett's esophagus. *Clinical cancer research : an official journal of the American Association for Cancer Research*. 2003;9(7):2560-6.
42. Kastelein F, Biermann K, Steyerberg EW, Verheij J, Kalisvaart M, Looijenga LH, et al. Value of alpha-methylacyl-CoA racemase immunochemistry for predicting neoplastic progression in Barrett's oesophagus. *Histopathology*. 2013;63(5):630-9.
43. van Olphen S, Biermann K, Spaander MC, Kastelein F, Steyerberg EW, Stoop HA, et al. SOX2 as a Novel Marker to Predict Neoplastic Progression in Barrett's Esophagus. *The American journal of gastroenterology*. 2015;110(10):1420-8.
44. Rossi E, Grisanti S, Villanacci V, Della Casa D, Cengia P, Missale G, et al. HER-2 overexpression/ amplification in Barrett's oesophagus predicts early transition from dysplasia to adenocarcinoma: a clinico-pathologic study. 2009;13(9B):3826-33.
45. Cappello F, Rappa F, Anzalone R, La Rocca G, Zummo G. CD1a expression by Barrett's metaplasia of gastric type may help to predict its evolution towards cancer. 2005;92(5):888-90.

46. Lastraioli E, Taddei A, Messerini L, Comin CE, Festini M, Giannelli M, et al. hERG1 channels in human esophagus: evidence for their aberrant expression in the malignant progression of Barrett's esophagus. *J Cell Physiol.* 2006;209(2):398-404.
47. Horvath B, Singh P, Xie H, Thota PN, Sun X, Liu X. Expression of p53 predicts risk of prevalent and incident advanced neoplasia in patients with Barrett's esophagus and epithelial changes indefinite for dysplasia. *Gastroenterol Rep (Oxf).* 2016;4(4):304-9.
48. Lastraioli E, Lottini T, Iorio J, Freschi G, Fazi M, Duranti C, et al. hERG1 behaves as biomarker of progression to adenocarcinoma in Barrett's esophagus and can be exploited for a novel endoscopic surveillance. *Oncotarget.* 2016;7(37):59535-47.
49. van Olphen SH, Ten Kate FJ, Doukas M, Kastelein F, Steyerberg EW, Stoop HA, et al. Value of cyclin A immunohistochemistry for cancer risk stratification in Barrett esophagus surveillance: A multicenter case-control study. *Medicine (Baltimore).* 2016;95(47):e5402.
50. Higgins JP, Thompson SG, Deeks JJ, Altman DG. Measuring inconsistency in meta-analyses. *Bmj.* 2003;327(7414):557-60.
51. Spechler SJ, Sharma P, Souza RF, Inadomi JM, Shaheen NJ. American gastroenterological association technical review on the management of Barrett's esophagus. *Gastroenterology.* 2011;140(3):e18-e52.
52. Altaf K, Xiong JJ, la Iglesia D, Hickey L, Kaul A. Meta-analysis of biomarkers predicting risk of malignant progression in Barrett's oesophagus. *The British journal of surgery.* 2017;104(5):493-502.
53. Janmaat VT, Peppelenbosch MP, Bruno MJ, Spaander MCW. Comment on: 'Meta-analysis of biomarkers predicting risk of malignant progression in Barrett's oesophagus' (*Br J Surg* 2017; 104: 493-502). *British Journal of Surgery*; 2017 [updated 14-06-2017. Available from: <https://www.bjs.co.uk/article/meta-analysis-of-biomarkers-predicting-risk-of-malignant-progression-in-barretts-oesophagus/>.

Supplementary information

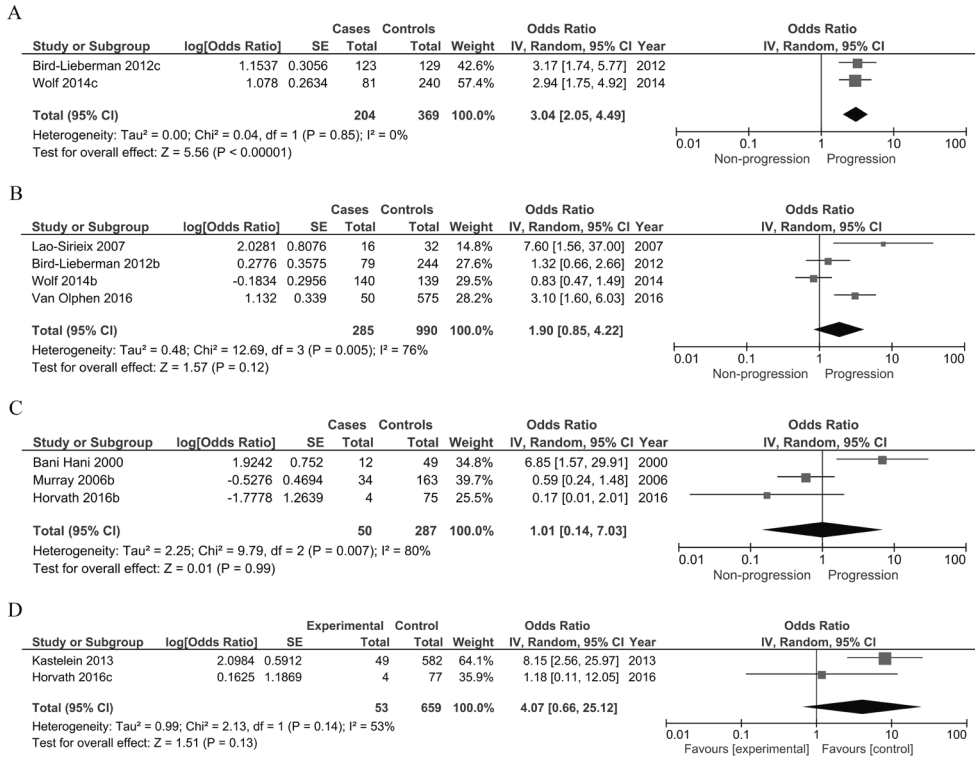


**Supplementary Figure S1.** Funnel plot of all studies investigating p53 IHC as a predictor of progression. The exact patient numbers and the SE of these studies can be found in Figure 2.

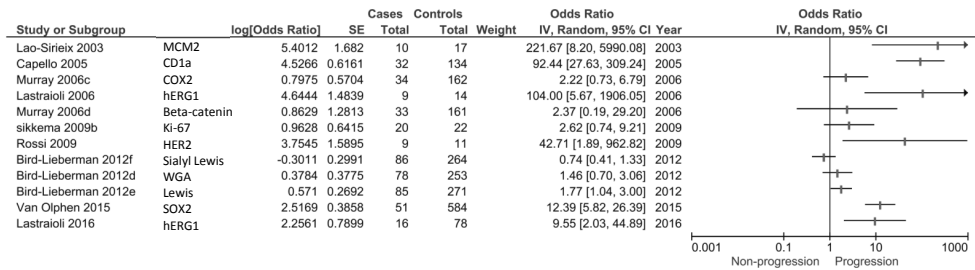


**Supplementary Figure S2.** Stringency of the definition and interpretation of aberrant p53 IHC. A more stringent definition of aberrant staining, and interpretation of that definition, may lead to loss of aberrant expression in cases, in controls, or in both. In order to investigate this, the proportion of controls deemed aberrant was plotted against the OR of each study with a standard error below 1. The use of a more stringent definition and interpretation for aberrant p53 staining appeared to result in a bigger reduction in the number of controls considered to have aberrant staining, compared to cases. Thus, by applying a more stringent definition and interpretation, the predictive value of p53 for neoplastic progression appears to increase. Formal statistical tests were not performed due to the limited number of data points and the post hoc nature of this analysis.





**Supplementary Figure S3.** Forest plot of all studies investigating AOL, Cyclin A, Cyclin D, and AMACR as a predictor of progression. (A) Two studies were included in the forest plot for AOL. (B) Four studies were included in the forest plot for Cyclin A. (C) Three studies were included in the forest plot for Cyclin D. (D) Two studies were included in the forest plot for AMACR.



**Supplementary Figure S4.** Forest plot, without meta-analysis, of all studies investigating IHC biomarkers which have been studied only once. 12 studies were included in this forest plot.

**Supplementary Table S1.** Additional characteristics of included studies

Study	Marker	Data adjusted for:	Follow up time (mean in months unless otherwise specified)	Age (mean in years)	Proportion male (%)	# pathologists	Blind assessment
Younes et al. 1997	p53	unadjusted	22 months for p53+, 25 months for p53-	not mentioned	not mentioned	1	Yes
Gimenez 1999	p53	unadjusted	84 cases and 40.8 controls	62.3 all patients	66% all patients	1	Yes
Bani-Hani et al. 2000	p53	sex, age, follow-up, BE length, # of biopsy specimens	52.0 cases and 56.5 controls	60.3 cases and 61.5 controls	92% cases and 94% controls	1	Yes
Weston et al. 2001	p53	unadjusted	41.2 all patients	61.9 all patients	100% all patients	3	N/A
Skacel et al. 2002	p53	unadjusted	11.3 cases and 35.4 controls	62 cases and 67.4 controls	100% cases and 62.5% controls	3	Yes
Murray et al. 2006 a	p53	pathology laboratory	27.6 cases and 46.8 controls	68 cases and 67.1 controls	77.1% all patients	2	Yes
Brown 2008	p53	unadjusted	41 months all patients	not mentioned	not mentioned	N/A	N/A
Sikkema et al. 2009 a	p53	unadjusted	82.8 cases and 94.8 controls	58.8 cases and 56.2 controls	89% cases and 74% controls	2	Yes
Bird-Lieberman et al. 2012 a	p53	age, sex, year of diagnosis, histology	80.4 all patients	63.8 cases and 63.8 controls	75% cases and 75% controls	10% had 2 <sup>nd</sup> observer	Yes
Kasrelein et al. 2012 a	p53	age, sex, BE length, and esophagitis, after re-analysis adjusted for age, sex, BE length, and histology	median 81.6 controls and 36 cases	median 60 controls and 65	82% cases and 73% controls	2	Yes

Supplementary Table S1. Continued

Study	Marker	Data adjusted for:	Follow up time (mean in months unless otherwise specified)	Age (mean in years)	Proportion male (%)	# pathologists	Blind assessment
Wolf et al. 2014	p53	age, BE length, time in study, and histology	46.8 cases and 38.4 controls	60 cases and 60 controls	82% cases and 81% non-cases	N/A	Yes
Davelaar et al. 2015	p53	age, sex, BE length, after extracting the OR no adjustment could be made	median 71 all patients	62 all patients	85% all patients	1	Yes
Horvath et al. 2016	P53	unadjusted	median 59 months	60.5 cases and 63 controls	100% cases and 76% controls	1	Yes
Bird-Lieberman et al. 2012 c	AOL	age, sex, year of diagnosis, histology	80.4 all patients	63.8 cases and 63.8 controls	75% cases and 75% controls	10% had 2 <sup>nd</sup> observer	Yes
Wolf et al. 2014	AOL	unadjusted	46.8 cases and 38.4 controls	60 cases and 60 controls	82% cases and 81% non-cases	N/A	Yes
Pierre Lao-Siriex et al. 2007	Cyclin A	age, gender, length of follow-up	78 cases and 66 controls	62.2 cases and 56.7 controls	87.5% cases and 72.2% controls	1	Yes
Bird-Lieberman et al. 2012 b	Cyclin A	age, sex, year of diagnosis, histology	80.4 all patients	63.8 cases and 63.8 controls	75% cases and 75% controls	10% had 2 <sup>nd</sup> observer	Yes
Wolf et al. 2014	Cyclin A	unadjusted	46.8 cases and 38.4 controls	60 cases and 60 controls	82% cases and 81% non-cases	N/A	Yes
Van Olphen et al. 2016	Cyclin A	age, sex, BE length, and histology	median 80.4 months	65 cases and 60 controls	82% cases and 73% controls	2	Yes
Bani-Hani et al. 2000	Cyclin D	sex, age, follow-up, BE length, # of biopsy specimens	52.0 cases and 56.5 controls	60.3 cases and 61.5 controls	92% cases and 94% controls	1	Yes

Supplementary Table S1 continues on next page.

Supplementary Table S1. *Continued*

Study	Marker	Data adjusted for:	Follow up time (mean in months unless otherwise specified)	Age (mean in years)	Proportion male (%)	# pathologists	Blind assessment
Murray et al. 2006 b	Cyclin D	pathology laboratory	27.6 cases and 46.8 controls	68 cases and 67.1 controls	77.1% all patients	2	Yes
Horvath et al. 2016	Cyclin D	unadjusted	median 59 months	60.5 cases and 63 controls	100% cases and 76% controls	1	Yes
Kastelein et al. 2013 b	AMACR	unadjusted	median 36 cases and 81.6 controls	median 60 controls and 65 cases	82% cases and 73% controls	2	Yes
Horvath et al. 2016	AMACR	unadjusted	median 59 months	60.5 cases and 63 controls	100% cases and 76% controls	1	Yes
Sirieux et al. 2003	MCM2	unadjusted	72 cases and controls 60	not mentioned	not mentioned	N/A	N/A
Capello et al. 2005	CD1a	unadjusted	12-36 all patients	not mentioned	not mentioned	2	N/A
Murray et al. 2006 d	$\beta$ -catenin	pathology laboratory	27.6 cases and 46.8 controls	68 cases and 67.1 controls	77.1% all patients	2	Yes
Lastrioli et al. 2006	hERG1	unadjusted	at least 5 years	not mentioned	not mentioned	2	N/A
Murray et al. 2006 c	COX-2	pathology laboratory	27.6 cases and 46.8 controls	68 cases and 67.1 controls	77.1% all patients	2	Yes
Sikkema et al. 2009 b	Ki-67	unadjusted	82.8 cases and 94.8 controls	58.8 cases and 56.2 controls	89% cases and 74% controls	2	Yes

Supplementary Table S1. Continued

Study	Marker	Data adjusted for:	Follow up time (mean in months unless otherwise specified)	Age (mean in years)	Proportion male (%)	# pathologists	Blind assessment
Rossi et al. 2009	HER-2	unadjusted	45.8 cases and 54.7 controls	63 years	76% all patients	2	N/A
Bird-Lieberman et al. 2012 e	Sialyl Lewis	age, sex, year of diagnosis, higtology	80.4 all patients	63.8 cases and 63.8 controls	75% cases and 75% controls	10% had 2 <sup>nd</sup> observer	Yes
Bird-Lieberman et al. 2012 d	wheat germ agglutinin	age, sex, year of diagnosis, higtology	80.4 all patients	63.8 cases and 63.8 controls	75% cases and 75% controls	10% had 2 <sup>nd</sup> observer	Yes
Bird-Lieberman et al. 2012 f	Lewis	age, sex, year of diagnosis, higtology	80.4 all patients	63.8 cases and 63.8 controls	75% cases and 75% controls	10% had 2 <sup>nd</sup> observer	Yes
Van Olphen et al. 2015	SOX2	unadjusted	median 39.6 cases and 78 controls	median 60 controls and 65 cases	82% cases and 73% controls	2	Yes
Lastraoli et al. 2016	hERG1	age and sex	at least 120	not mentioned	not mentioned	3	N/A

## Supplementary information search

### Appendix 1: EMBASE search

(immunohistochemistry/exp OR Immunocytochemistry/exp OR histochemistry/de OR 'biological marker'/exp OR 'disease marker'/de OR 'tumor marker'/de OR 'molecular marker'/de OR marker/de OR staining/de OR 'antibody labeling'/exp OR (immunohistochem\* OR Immunocytochemistr\* OR Immunohistocytochemis\* OR immunostain\* OR stain\* OR histochemist\* OR Histocytochemist\* OR marker\* OR biomarker\* OR (marking NEAR/3 agent\*) OR ((antibod\* OR immun\*) NEAR/3 label\*) OR immunolabel\*):ab,ti) AND ('oncogenesis and malignant transformation'/exp OR 'cancer risk'/de OR 'disease course'/de OR ('esophageal adenocarcinoma'/exp AND 'risk assessment'/exp) OR (((malign\* OR metasta\* OR cancer\* OR adenocarcinom\* OR tumo\* OR ac OR eac OR high-grade OR hgd OR neoplas\*) NEAR/10 (potential\* OR transformat\* OR predict\* OR progress\* OR develop\* OR risk OR growth OR progress\*)) OR (risk NEAR/3 progress\*) OR carcinogene\* OR oncogene\* OR (tumo\* NEAR/3 promot\*)):ab,ti) AND ('Barrett esophagus'/exp OR (Barret\*):ab,ti) AND [english]/lim NOT ([animals]/lim NOT [humans]/lim) NOT ([Conference Abstract]/lim OR [Letter]/lim OR [Note]/lim OR [Editorial]/lim)

### Appendix 2: MEDLINE search

(exp immunohistochemistry/ OR Histocytochemistry/ OR "Biological Markers"/ OR "disease marker"/ OR exp "Tumor Markers, Biological"/ OR exp "Staining and Labeling"/ OR (immunohistochem\* OR Immunocytochemistr\* OR Immunohistocytochemis\* OR immunostain\* OR stain\* OR histochemist\* OR Histocytochemist\* OR marker\* OR biomarker\* OR (marking ADJ3 agent\*) OR ((antibod\* OR immun\*) ADJ3 label\*) OR immunolabel\*).ab,ti.) AND (exp "Carcinogenesis"/ OR "Disease Progression"/ OR ("Esophageal Neoplasms"/ AND "Risk Assessment"/) OR (((malign\* OR metasta\* OR cancer\* OR adenocarcinom\* OR tumo\* OR ac OR eac OR high-grade OR hgd OR neoplas\*) ADJ10 (potential\* OR transformat\* OR predict\* OR progress\* OR develop\* OR risk OR growth OR progress\*)) OR (risk ADJ3 progress\*) OR carcinogene\* OR oncogene\* OR (tumo\* ADJ3 promot\*)):ab,ti.) AND ("Barrett Esophagus"/ OR (Barret\*).ab,ti.) AND english.la. NOT (exp animals/ NOT humans/) NOT (letter OR news OR comment OR editorial OR congresses OR abstracts).pt.

### Appendix 3: Web of Science search

((immunohistochem\* OR Immunocytochemistr\* OR Immunohistocytochemis\* OR immunostain\* OR stain\* OR histochemist\* OR Histocytochemist\* OR marker\* OR biomarker\* OR (marking NEAR/3 agent\*) OR ((antibod\* OR immun\*) NEAR/3 label\*) OR immunolabel\*):ab,ti) AND (((((malign\* OR metasta\* OR cancer\* OR adenocarcinom\* OR tumo\* OR ac OR eac OR high-grade OR hgd OR neoplas\*)

NEAR/10 (potential\* OR transformat\* OR predict\* OR progress\* OR develop\* OR risk OR growth OR progress\*)) OR (risk NEAR/3 progress\*) OR carcinogene\* OR oncogene\* OR (tumo\* NEAR/3 promot\*)):ab,ti) AND ((Barret\*):ab,ti)

#### Appendix 4: CENTRAL search

TS=(((immunohistochem\* OR Immunocytochemistr\* OR Immunohistocytochemis\* OR immunostain\* OR stain\* OR histochemist\* OR Histocytochemist\* OR marker\* OR biomarker\* OR (marking NEAR/2 agent\*) OR ((antibod\* OR immun\*) NEAR/2 label\*) OR immunolabel\*)) AND (((malign\* OR metasta\* OR cancer\* OR adenocarcinom\* OR tumo\* OR ac OR eac OR high-grade OR hgd OR neoplas\*) NEAR/10 (potential\* OR transformat\* OR predict\* OR progress\* OR develop\* OR risk OR growth OR progress\*)) OR (risk NEAR/2 progress\*) OR carcinogene\* OR oncogene\* OR (tumo\* NEAR/2 promot\*))) AND ((Barret\*)) NOT ((animal\* OR rat OR rats OR mouse OR mice OR murine) NOT (human\* OR patient\*))) AND dt=(article)

#### Appendix 5: Pubmed publisher search

(immunohistochemistry[mh] OR Histocytochemistry[mh] OR "Biological Markers"[mh] OR "disease marker"[mh] OR "Tumor Markers, Biological"[mh] OR "Staining and Labeling"[mh] OR (immunohistochem\*[tiab] OR Immunocytochemistr\*[tiab] OR Immunohistocytochemis\*[tiab] OR immunostain\*[tiab] OR stain\*[tiab] OR histochemist\*[tiab] OR Histocytochemist\*[tiab] OR marker\*[tiab] OR biomarker\*[tiab] OR (marking AND agent\*[tiab]) OR ((antibod\*[tiab] OR immun\*[tiab] OR immuni\*[tiab]) AND label\*[tiab]) OR immunolabel\*[tiab])) AND ("Carcinogenesis"[mh] OR "Disease Progression"[mh] OR ("Esophageal Neoplasms"[mh] AND "Risk Assessment"[mh]) OR (((malign\*[tiab] OR metasta\*[tiab] OR cancer\*[tiab] OR adenocarcinom\*[tiab] OR tumor\*[tiab] OR tumour\*[tiab] OR ac OR eac OR high-grade OR hgd OR neoplas\*[tiab]) AND0 (potential\*[tiab] OR transformat\*[tiab] OR predict\*[tiab] OR progress\*[tiab] OR develop\*[tiab] OR risk OR growth OR progress\*[tiab])) OR (risk AND progress\*[tiab]) OR carcinogene\*[tiab] OR oncogene\*[tiab] OR ((tumor\*[tiab] OR tumour\*[tiab]) AND promot\*[tiab]))) AND ("Barrett Esophagus"[mh] OR (Barret\*[tiab])) AND english[la] NOT (animals[mh] NOT humans[mh]) NOT (letter[pt] OR news[pt] OR comment[pt] OR editorial[pt] OR congresses[pt] OR abstracts[pt]) AND publisher[sb])

#### Appendix 6: Google scholar search

immunohistochemistry|Immunocytochemistristry|immunostaining|histochemististry|immunolabeling "Barrett esophagus|oesophagus" malignant|metastatic|cancer|tumor potential|transformation|progression|progression|carcinogenesis|oncogenesis

## **S1 Standardized data extraction form**

### **Appendix 7: standardized data extraction form**

A standardized data extraction form was used, which contained the following items:

- General information: title, authors, source, contact address, country, published/unpublished, full paper / abstract, language, and year of publication.
- Study design.
- Quality assessment: a difference at baseline between cases and controls of at least 10% (concerning baseline histology, age, sex, length of BE segment, and follow-up time), adjustments in the form of regression for differences of known predictors of progression (such as baseline histology, age, sex, and length of BE segment), exclusion of prevalent cases, control stainings, number of pathologists, pathologist agreement and pathologist blinding.
- Patients: baseline histology, end-point histology, definition of BE used, age of the patients, proportion of male patients.
- Staining characteristics: IHC biomarker studied, antibody used and dilution, cutoff value of IHC biomarker expression used, positive/negative control used.
- Outcomes: Numbers of IHC biomarker positive cases and controls and IHC biomarker negative cases and controls. ORs and the factors that were adjusted for.

With regard to the MOOSE and PRISMA checklists, these can be accessed through PLoS One.







# Chapter 6.2

---

Letter to the editor in response to:  
Meta-analysis of biomarkers predicting  
risk of malignant progression in  
Barrett's oesophagus

Vincent T. Janmaat · Maikel P. Peppelenbosch · Marco B. Bruno ·  
Manon C.W. Spaander

*British Journal of Surgery, 2017*



## To the editor,

Altaf and colleagues present an interesting systematic review and meta-analysis on the ability of biomarkers to predict the risk of malignant progression in Barrett's oesophagus (1). This is particularly interesting as endoscopic interventions for Barrett's oesophagus are widely available and increasingly being adopted (2). Some concerns however, arise about the methodology used in this meta-analysis (3). To assess the predictive ability of a biomarker, the biomarker status must have been established in tissue taken before the occurrence of the event. Therefore, prospective studies or case control studies, in which controls are representative for the population from which the cases are derived, are required (4). Most of the 40 studies that were included comparing P53 biomarker status in adenocarcinoma versus Barrett's, reported on samples either obtained from a resection specimen or from cases and controls without follow-up. These studies should have been excluded from the analysis. Based on the current dataset, therefore, the current conclusion that p53 overexpression predicts malignant progression is not justified. Additionally, the paper included a series of funnel plots which showed the presence of small study effects, such as publication bias. The authors considered it unlikely that these effects would change the magnitude of the pooled estimates in prediction of the progression to OAC. However, this was not analyzed nor were efforts made to reduce the influence of small study effects. This may have led to an overestimation of the prognostic ability of the biomarkers investigated. We feel that the role of p53 as a biomarker of progression needs further investigation.

## References

1. Altaf K, Xiong JJ, la Iglesia D, Hickey L, Kaul A. Meta-analysis of biomarkers predicting risk of malignant progression in Barrett's oesophagus. *The British journal of surgery*. 2017;104(5):493-502.
2. Alderson D, Wijnhoven BP. Interventions for Barrett's oesophagus and early cancer. *The British journal of surgery*. 2016;103(5):475-6.
3. Stroup DF, Berlin JA, Morton SC, Olkin I, Williamson GD, Rennie D, et al. Meta-analysis of observational studies in epidemiology: a proposal for reporting. Meta-analysis Of Observational Studies in Epidemiology (MOOSE) group. *Jama*. 2000;283(15):2008-12.
4. Lewington S, Bragg F, Clarke R. A review on metaanalysis of biomarkers: promises and pitfalls. *Clin Chem*. 2012;58(8):1192-204.



# Chapter 7

---

## DNA integrity as biomarker in pancreatic cyst fluid

Wesley K. Utomo · Vincent T. Janmaat · Auke P. Verhaar · Jérôme Cros · Philippe  
Lévy · Philippe Ruszniewski · Mirella S. Vredenburg-van den Berg · Guido Jenster ·  
Marco J. Bruno · Henri Braat · Gwenny M. Fuhler · Maikel P. Peppelenbosch

*Am J Cancer Res.* 2016;6(8):1837-41

## Abstract

Identification of pancreatic cysts with malignant potential is important to prevent pancreatic cancer development. Integrity of cell free DNA (cfDNA) has been described as tumor biomarker, but its potential for pancreatic cancer is unclear. While normal apoptotic cells release uniformly truncated DNA, malignant tissues release long fragments of cell free DNA (cfDNA). We measured 247 base pair (bp) and 115 bp DNA fragments of ALU repeats by qPCR in serum from healthy controls and pancreatic cancer patients, and in cyst fluid from pancreatic cyst patients. No differences in total cfDNA (ALU115) and cfDNA integrity (ALU247/115) were observed between sera from healthy controls (n=19) and pancreatic cancer patients (n=19). Although elevated as compared to serum, but no differences in cfDNA were found in cyst fluid from high risk (n=10) and low risk (n=20) cyst patients. We conclude that cfDNA integrity is not a useful marker to identify (pre)malignant pancreatic lesions.



## Introduction

Pancreatic cystic neoplasms (PCN) can give rise to pancreatic cancer, with intraductal papillary mucinous neoplasms (IPMN) and mucinous cystic neoplasms (MCN) showing a high malignant potential, whereas serous cystic adenomas and solid pseudopapillary neoplasms have a more favorable prognosis (1). Development of pancreatic cancer may be prevented by resection of the cysts with high risk malignant potential. Unfortunately, current imaging and diagnostic techniques have difficulty distinguishing low risk cysts from high risk and transformed cysts, which in some cases leads to unnecessary surgery (2). Thus, better diagnostic tools are urgently needed. Patients with neoplastic diseases often have an increased amount of free circulating, cell-free DNA (cfDNA) in their peripheral blood, which originates from the tumor (3–5). This cfDNA is not all of an equal length. While apoptotic cells release small, ~180 base pair (bp) DNA fragments, necrotic cells release larger fragments of irregular size (6). Whereas apoptosis is a normal physiological process occurring in all cells that need to be cleared from the body, necrosis is a potentially harmful form of cell death, which occurs under pathological conditions, including cancer. Thus, the presence of longer DNA fragments in serum is taken as a sign of enhanced necrosis taking place in the body and is thought to be indicative of disease (7). In order to reliably measure such DNA fragments, researchers have employed the abundant presence in the human genome of DNA ALU repeats - repetitive ~300 bp sequences of retrotransposon origin found in genomic introns (8). Using different primers, fragments of these ALU repeats can be detected of either >200 bp (indicative of necrotic DNA), or of <200 bp (detecting both necrotic and apoptotic DNA). Detection of these longer cfDNA fragments and their relative abundance compared to short cfDNA fragments in sera appears to be a promising tool for diagnosis and prognostic prediction of malignancies (9,10). However, the percentage of cfDNA originating from tumor cells has been estimated to range from 10% to 90% of total cfDNA, and applicability of measuring cfDNA length (i.e. DNA integrity) in serum may therefore depend on the type of disease (6). Thus, while ALU-repeat measurements have been shown to adequately predict colorectal and breast cancer, the presence of pancreatic cancer could not be diagnosed by high length cfDNA fragments in serum (11). We speculated that pancreatic cyst fluid, coming from a small and enclosed environment, would provide a more suitable biological fluid in which to search for tumor markers. Therefore we compared DNA integrity in fluid from high risk and low risk cysts.

## Material and methods

### Pancreatic cyst fluid acquirement

Pancreatic cyst fluid of patients undergoing surgery was collected from two separate biobanks (Erasmus MC Rotterdam, the Netherlands, MEC-2008-233 and MEC-2012-

107, and Hôpital Beaujon, Clichy France; DEC-2009-938). Fluid was obtained by endoscopic ultrasound-fine needle aspiration (EUS-FNA) or post-resection and stored sterile at -80°C until analysis. Samples were selected so as to represent the different groups of pancreatic cyst based on malignant potential. Cysts with histologically confirmed low grade and intermediate dysplasia were grouped under 'low grade dysplasia', and cysts with high grade dysplasia or invasive carcinoma were considered 'high grade dysplasia'.

### **Serum acquirement**

Patients with pancreatic adenocarcinoma who were eligible for surgery were included at the EMC. Healthy controls (mean age 60±4 years) were collected from the biorepository of the Rotterdam arm of the ERSPC (12,13) (MEC 138.741/1994/152). Serum was obtained by whole blood centrifugation in serum separator tubes (BD-Vacutainer), aliquoted and stored at -80°C until analysis.

### **Sample preparation and qPCR**

To digest proteins that might confound results, both cyst fluid and serum were mixed with a buffer containing 25 ml/l Tween 20, 50 mmol/l Tris, 1 mmol/l EDTA, and 0.8 mg/ml proteinase K in a 1:1 ratio. Subsequently, the mix was incubated at 50°C for 20 minutes, followed by heat inactivation at 95°C for 5 minutes. Next, the samples were centrifuged at 10,000g for 5 minutes and 0.2 µl of the supernatant was used in the qPCR reaction. This protocol was also described earlier (14). After preparation of samples, DNA integrity was determined by measuring the presence of ALU repeat fragments of 115 bp size and of 247 bp size, using previously described primers (15). The ALU115 primers are designed to amplify both the shorter and the longer fragments, and are therefore indicative of total circulating cfDNA (including DNA released from both apoptotic and necrotic cells) whereas the ALU247 primers only amplify the longer DNA fragments, and thus detect of tumor DNA. To measure the absolute concentration of DNA in the samples, we constructed a calibration curve using genomic DNA derived from Huh7 cell lines at a concentration ranging from 2.97 pg/µl up to 297 ng/µl. The absolute concentration was measured (in the most concentrated sample) using the Nanodrop (Thermo Scientific). This was subsequently used in a serial dilution and used as a template in triplicate on each qPCR-plate measured. The same serial dilutions were used to produce standard curves for all qPCR runs.

For the qPCR reaction of the ALU repeats, previously published primers were used: ALU115 forward, CCTGAGGTCAGGAGTTCGAG; ALU115 reverse, CCCGAGTAGCTGGGATTACA; ALU247 forward, GTGGCTCACGCCTGTAATC; ALU247 reverse CAGGCTGGAGTGCAGTGG. The total volume of the qPCR reaction mix was 25 µl, consisting of 12.5 µl SYBR Green (Life technologies), 2.5 µl 10 µM forward and reverse primer, 9.8 µl Microbial DNA-Free Water (Qiagen), and 0.2 µl template.

The qPCR was run at 95°C for 10 minutes, and subsequently at 95°C for 30 seconds, 64°C for 30 seconds and 72°C for 30 seconds for 40 cycles using the StepOnePlus™ Real-Time PCR System (Life technologies). ALU repeat expression levels were measured in duplicate. The genomic DNA used for the calibration curve and negative controls were measured in triplicate.

### Analysis

Using the data obtained from the serial diluted genomic DNA, we constructed a calibration curve on each plate measured using the Graphpad Prism 5. From this, we derived the intercept and slope of the curve using a nonlinear regression model and recalculated the absolute concentration of the samples from measured Ct values using the following formula: Absolute concentration =  $10^{((Ct-intercept)/slope)}$ . Finally, to obtain ALU247/115 ratios, the absolute concentration of ALU247 was divided by the absolute concentration ALU115 measured in the samples. Mean differences were analysed using Mann-Whitney *U* test. A *p* value of <0.05 was considered statistically significant.

## Results

While previous reports were unable to find a relationship between pancreatic cancer and cfDNA length in serum, we wanted to verify this in our own cohort (see **Table 1**). The mean total circulating cfDNA, as represented by ALU115-qPCR values, was  $20 \pm 3$  pg/μl in control sera (n=19) vs  $36 \pm 14$  pg/μl in sera from pancreatic cancer patients (n=19) (*p*=0.559) (**Figure 1A**), whereas the mean amount of circulating tumor

**Table 1.** Patient characteristics of the serum samples

Number of patients	19
Age, years	
Range	24-82
Mean (SD)	65 (13)
Gender, n (%)	
Male	11 (57.9)
Female	8 (42.1)
Disease location (%)	
Pancreas corpus	3 (15.8)
Pancreas head/uncinate	5 (26.3)
Pancreas head	7 (36.9)
Bile duct	3 (15.8)
Papilla	1 (5.2)

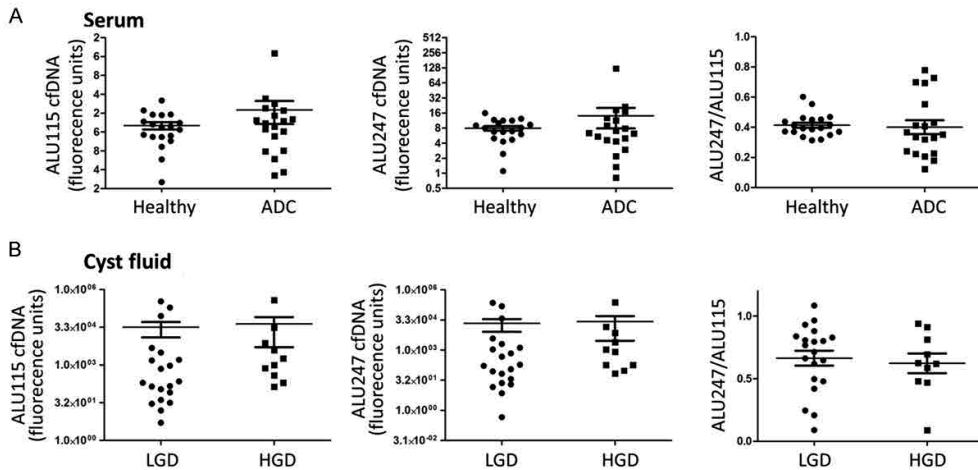


**Figure 1.** Levels of cfDNA in serum or pancreatic cyst fluid do not identify high risk/adenocarcinoma patients. PCRs detecting short, apoptotic cell-derived cfDNA (ALU115) and longer cfDNA fragments (ALU247) were performed on **(A)** serum from healthy donors ( $n=19$ ) and patients with pancreatic adenocarcinoma (ADC,  $n=19$ ) and **(B)** pancreatic cyst fluid from patients with low grade dysplasia (LGD,  $n=20$ ) and high grade dysplasia (HGD and ADC,  $n=10$ ). cfDNA was detected by ALU115 and ALU247, and DNA integrity was calculated (ALU247/ALU115). No differences in cfDNA levels and cfDNA integrity were observed.

DNA, as determined by ALU247-qPCR values, was  $8 \pm 1$  and  $14 \pm 6$  pg/ $\mu$ l ( $p=0.793$ ). The ratio of ALU247/ALU115, allowing quantification of the integrity of the cfDNA, was  $0.41 \pm 0.02$  and  $0.40 \pm 0.05$  for healthy controls and pancreatic cancer patients, respectively ( $p=0.267$ ). Thus, no increased total cfDNA or tumor-associated DNA was detected in sera from pancreatic cancer patients.

Next, we analysed cyst fluid obtained from 40 pancreatic cyst patients, 23 of which had low risk cysts, and 17 had high risk cysts. In 10 of these samples, we were unable to perform a reliable analysis due to the mucinous nature of the fluid. In the remaining samples (**Table 2**), we observed drastically higher levels of cfDNA as compared to sera, presumably due to the enclosed nature of these cysts. However, the mean amount of total and tumor circulating cfDNA did not differ between the high risk ( $n=10$ ) and low risk ( $n=20$ ) samples:  $44,463 \pm 39,228$  vs  $33,021 \pm 20,004$  pg/ $\mu$ l for ALU115 ( $p=0.10$ ) and  $27,254 \pm 24,268$  vs  $22,118 \pm 13,774$  pg/ $\mu$ l for ALU247 ( $p=0.18$ ), respectively (**Figure 1B**). Furthermore, no significant differences in ALU247/ALU115 ratio between high risk and low risk cysts ( $0.63 \pm 0.07$  vs  $0.66 \pm 0.06$ ,  $p=0.34$ ) was seen. Overall, ratios were higher than in serum, with some samples reaching almost 1. Thus, the nature of cyst fluid makes it a less suitable compartment to determine necrotic/apoptotic cfDNA ratios.

**Table 2.** Patient characteristics of the cyst fluid samples

	Total	LGD	HGD
Number of patients	30	20	10
Age, years			
Range	19-85	19-79	52-85
Mean (SD)	59.5 (15.3)	54.7 (15.4)	69.2 (10)
Gender			
Male	10 (33.3%)	3 (15%)	7 (70%)
Female	20 (66.7%)	17 (85%)	3 (30%)
Diagnosis			
IPMN	17 (56.7%)	8 (40%)	9 (90%)
MCN	13 (43.3%)	12 (60%)	1 (10%)
Disease location (%)			
Pancreas head	6 (20%)	2 (10%)	4 (40%)
Pancreas corpus	5 (16.7%)	3 (15%)	2 (20%)
Pancreas tail	18 (60%)	15 (75%)	3 (30%)
Unknown	1 (3.3)	0 (0%)	1 (10%)

## Discussion

Measurement of necrotic cell-derived long cfDNA fragments in serum has been suggested for the early detection of tumors. However, usefulness of this tool in pancreatic diseases has so far not been shown, and we were unable to find increased levels of necrotic cell-derived cfDNA in sera from pancreatic cancer patients. As pancreatic cancer can derive from PCN, we speculated that cyst fluid would present the ideal biological fluid to detect premalignant lesions. Indeed, total levels of cfDNA observed in cyst fluid were almost 1000 fold higher as compared to sera. Nevertheless, we did not observe differences in cfDNA length between high risk and low risk cysts. While the apoptotic process reduces DNA to 180-200 bp fragments, incomplete cleaving of the DNA may result of the presence of multimers of these fragments, which can subsequently also be detected by ALU247 primers. This background ‘noise’ of 180 bp multimers accounts for the fact that a signal is detected in the ALU247 PCR in samples where no necrotic cfDNA is expected (i.e. healthy serum), and detection of tumor-derived, necrotic DNA depends on a relative increase in the abundance of long cfDNA, and hence a shift in DNA integrity (ALU247/ALU115 ratio). It is conceivable that pancreatic tumor cells produce too little necrotic cfDNA to be detected above background levels. Additionally, in cyst fluid, high levels of total cfDNA levels present may preclude detection of additional long cfDNA fragments.

We acknowledge several limitations to our study. Of the cystic fluid samples selected for this pilot study, 15 of 30 were obtained after resection, with ischemic damage potentially

causing necrosis. However, subanalysis of the re-resection and post-resection obtained samples did not show significant differences in total cfDNA levels or ALU247/ALU115 ratios (not shown).

A second limitation is the low number of high risk cyst fluid samples in our analysis. The mucinous nature of the fluid prevented accurate analysis in ~25% of cases. As mucinous cysts show a higher malignant potential, it is not surprising that many of the excluded samples were high risk. This means that the intrinsic nature of high risk cyst fluid makes them less suitable for this type of analysis.

In conclusion, our data suggest that the use of cfDNA integrity in pancreatic cyst fluid is not suitable to distinguish low risk from high risk cysts.

## Acknowledgements

Gweny M Fuhler is financially supported by the Dutch Cancer Society (EMCR 2010-4737). Maikel P Peppelenbosch is supported by NWO-ALW (840.12.001). Authors declare no conflict of interest, all authors have read the journal's policy on disclosure of potential conflicts of interest.

## References

1. Hamilton SR, Aaltonen (Eds.) LA. World Health Organization Classification of Tumours. Pathology and Genetics of Tumours of the Digestive System. IARC Press: Lyon. 2000.
2. Utomo WK, Braat H, Bruno MJ, van Eijck CHJ, Koerkamp BG, Krak NC, van de Vreede A, Fuhler GM, Peppelenbosch MP, Blermann K. Cytopathological Analysis of Cyst Fluid Enhances Diagnostic Accuracy of Mucinous Pancreatic Cystic Neoplasms. *Medicine (Baltimore)*. 2015;94(24):e988.
3. Shapiro B, Chakrabarty M, Cohn EM, Leon SA. Determination of circulating DNA levels in patients with benign or malignant gastrointestinal disease. *Cancer*. 1983;51(11):2116–20.
4. Sorenson GD, Pribish DM, Valone FH, Memoli VA, Bzik DJ, Yao SL. Soluble normal and mutated DNA sequences from single-copy genes in human blood. *Cancer Epidemiol Biomarkers Prev* 2013;3(1):67–71.
5. Spindler KLG, Pallisaard N, Andersen RE, Brandslund I, Jakobsen A. Circulating free DNA as biomarker and source for mutation detection in metastatic colorectal cancer. *PLoS One* 2015;10(4):e0108247.
6. Jahr S, Hentze H, Englisch S, Hardt D, Fackelmayer FO, Hesch RD, Knippers R. DNA fragments in the blood plasma of cancer patients: quantitations and evidence for their origin from apoptotic and necrotic cells. *Cancer Res*. 2001;61(4):1659–65.
7. Giacona MB, Ruben GC, Iczkowski KA, Roos TB, Porter DM, Sorenson GD. Cell-free DNA in human blood plasma: length measurements in patients with pancreatic cancer and healthy controls. *Pancreas*. 1998;17(1):89–97.

8. Hormozdiari F, Alkan C, Ventura M, Hajirasouliha I, Malig M, Hach F, Yorukoglu D, Dao P, Bakhshi M, Sahinalp SC, Eichler EE. Alu repeat discovery and characterization within human genomes. *Genome Res.* 2011;21(6):840–9.
9. Agostini M, Enzo M V, Bedin C, Belardinelli V, Goldin E, Del Bianco P, Maschietto E, D'Ángelo E, Izzi L, Saccani A, Zavagno G, Nitti D. Circulating cell-free DNA: a promising marker of regional lymphonode metastasis in breast cancer patients. *Cancer Biomark.* 2012;11(2-3):89–98.
10. da Silva Filho BF, GurgelAP, Neto MA, de Azevedo DA, de Freitas AC, Silva Neto Jda C, Silva LAl. Circulating cell-free DNA in serum as a biomarker of colorectal cancer. *J Clin Pathol.* 2013;66(9):775–8.
11. Sikora K, Bedin C, Vicentini C, Malpeli G, D'Angelo E, Sperandio N, Laelor RT, Bassi C, Tortora G, Niti D, Agostini M, Fassan M, Scarpa A. Evaluation of cell-free DNA as a biomarker for pancreatic malignancies. *Int J Biol Markers*;30(1):e136–41.
12. Roobol MJ, Kranse R, Bangma CH, van Leenders AGJLH, Blijenberg BG, van Schaik RHN, Kirkels WJ, Otto SJ, van der Kwast TH, de Koning HJ, Schroder FH; ECRPC Rotterdam Study Group. Screening for prostate cancer: results of the Rotterdam section of the European randomized study of screening for prostate cancer. *Eur Urol.* 2013 Oct;64(4):530–9.
13. Roobol MJ, Schröder FH. European Randomized Study of Screening for Prostate Cancer: achievements and presentation. *BJU Int* [Internet]. 2003 Dec;92 Suppl 2:117–22.
14. Umetani N, Kim J, Hiramatsu S, Reber HA, Hines OJ, Bilchik AJ, Hoon DS. Increased integrity of free circulating DNA in sera of patients with colorectal or periampullary cancer: Direct quantitative PCR for ALU repeats. *Clin Chem.* 2006;52(6):1062–9.
15. Iqbal S, Vishnubhatla S, Raina V, Sharma S, Gogia A, Deo SS, Mathur S, Shukla NK. Circulating cell-free DNA and its integrity as a prognostic marker for breast cancer. *Springerplus* [Internet]. 2015 Jan [cited 2015 Sep 18];4:265.





# Chapter 8

---

## Molecular profile of Barrett's esophagus and gastroesophageal reflux disease in the development of translational physiological and pharmacological studies

Edyta Korbut · Vincent T. Janmaat · Mateusz Wierdak · Jerzy Hankus ·  
Dagmara Wójcik · Marcin Surmiak · Katarzyna Magierowska · Tomasz Brzozowski ·  
Maikel P. Peppelenbosch · Marcin Magierowski

## Abstract

Barrett's esophagus (BE) is a premalignant condition caused by gastroesophageal reflux disease (GERD) where physiological squamous epithelium is replaced by columnar epithelium. Several *in vivo* and *in vitro* BE models were developed with questionable translational relevance when implemented separately. Therefore, we aimed to screen Gene Expression Omnibus 2R (GEO2R) databases to establish clinical BE molecular profile being comparable with animal and optimized human esophageal squamous cell lines-based *in vitro* models. The GEO2R tool and selected databases were used to establish human BE molecular profile. BE-specific mRNAs in human esophageal cell lines (Het-1A and EPC2) were determined after 1, 3 and/or 6-days treatment with acidified medium (pH 5.0) and/or 50 and 100  $\mu$ M bile mixture (BM). Wistar rats underwent microsurgical procedures to generate esophagogastrroduodenal anastomosis (EGDA) leading to BE. BE-specific genes (keratin (*KRT*)1, *KRT*4, *KRT*5, *KRT*6A, *KRT*13, *KRT*14, *KRT*15, *KRT*16, *KRT*23, *KRT*24, *KRT*7, *KRT*8, *KRT*18, *KRT*20, trefoil factor (*TFF*)1, *TFF*2, *TFF*3, villin (*VIL*)1, mucin (*MUC*)2, *MUC*3A/B, *MUC*5B, *MUC*6, and *MUC*13) mRNA expression was assessed by real-time PCR. Pro/anti-inflammatory factors (interleukin (IL)-1 $\beta$ , IL-2, IL-4, IL-5, IL-6, IL-10, IL-12, IL-13, tumor necrosis factor  $\alpha$ , interferon  $\gamma$ , granulocyte-macrophage colony-stimulating factor) serum concentration was assessed by Luminex assay. Expression profile *in vivo* reflected about 45% of clinical BE with accompanied inflammatory response. 6-day treatment with 100  $\mu$ M BM (pH 5.0) altered gene expression *in vitro* reflecting in 73% human BE profile and making this the most reliable *in vitro* tool taking into account two tested cell lines. Our optimized and established combined *in vitro* and *in vivo* BE models can improve further physiological and pharmacological studies testing pathomechanisms and novel therapeutic targets of this disorder.

## Introduction

Barrett's esophagus (BE) is a complex, genetically predisposed, premalignant condition of the distal esophagus characterized as replacement of the esophageal squamous epithelium into an intestinal-type columnar epithelium with a crypt-like architecture (1-3). Epithelium in BE is usually composed of mucous-producing cells which aids in the protection of the esophagus from the constant insult of acid and bile (2). BE affects 2% of the adult population in the Western world (4, 5). It has been confirmed that chronic gastroesophageal reflux disease (GERD) is one of the most important etiological component of BE (4, 5).

Importantly, BE and GERD are closely associated with a high risk of developing esophageal adenocarcinoma (EAC). EAC has a very poor prognosis with a 9-15% 5-year survival rate (4). The pattern of reflux is a significant factor that may influence the progression of BE towards advanced precancerous changes (6, 7). In contrast to the physiological esophageal epithelium, the BE development results in alternation of several individual molecular markers and signaling pathways. These changes include variety of mucins (MUC), mucin-associated trefoil factor family (TFF) peptides, and villin (VIL) (8-10). However, the physiological and pathophysiological aspects still require further investigation, especially in the context of the implementation of novel non-invasive methods of treatment of this disorder.

Both BE and GERD are related to inflammation of the esophageal epithelium. Chronic inflammation in BE has been linked to DNA damage, leading to mutations and genomic instability, and altered expression of genes that are involved in cellular proliferation and programmed cell death (11). The inflammatory response also includes increased oxidative stress, activation of several signaling pathways, and release of inflammatory cytokines (11). Moreover, chronic inflammation can lead to a higher rate of cellular turnover, which is typical for BE and can alter the pattern of gene expression in epithelial cells (11). For example, an analysis of keratin (KRT), a major constituent of the esophageal epithelium, revealed significant changes from those keratins normally expressed in squamous epithelia to those expressed in columnar epithelium (8, 12, 13).

The diagnostic criteria for BE phenotype requires endoscopic identification of columnar mucosa and microscopic appearance of columnar epithelium with presence of goblet cells within the esophageal mucosa (3). The basic therapeutic options for patients with BE include pharmacological treatment with proton pump inhibitors or endoscopic procedures with surgical resection, and chemo- and radiotherapy (14). However, the evidence from randomized controlled trial shows that pharmacological and surgical therapies do not completely prevent or eliminate BE and existing dysplasia (14). Therefore, development of novel or alternative pharmacological therapeutic interventions seems to be justified, also taking into account recently published evidence (5). Current advances

in the understanding of the complex molecular mechanisms of BE development which came from experimental models of BE include overexpression of cyclooxygenase-2 (COX-2) (15, 16), epidermal growth factor EGF (17-19), or mitogen-activated protein kinase (MAPK) and the protein kinase phosphorylation (PI3K) pathways (20, 21), as well as increased secretion of gastrin due to achlorhydria as complication of prolonged proton pump inhibitors (PPI) therapy (22). However, many ongoing controversies and challenges and potential mediators responsible for the development of BE still remain unsolved. Additionally, the conversion process of normal squamous epithelium towards Barrett's metaplasia is difficult to monitor directly under clinical conditions (23). Thus, over the last few years, several experimental models using various types of cell cultures and animal models have been published to investigate the mechanisms of bile and/or acid exposure in BE pathogenesis (1, 23). However, the relevance of each of the models implemented separately is considered to be questionable.

Therefore, this study was designed to establish relevant experimental models for further studies underlying the effectiveness of possible protective treatment of BE esophageal metaplasia with pharmacological agents. Thus, we selected appropriate translational molecular markers such as *KRT*, *MUC*, *TFF* and *VIL* genes to compare expression profiles in clinical biopsies derived from BE patients with the animal surgical model and an *in vitro* model of BE involving two human derived primary immortalized esophageal cell lines. We put special emphasis on the optimization of this *in vitro* model with the aim to reflect the molecular events observed clinically as closely as possible.

## Material and methods

### Analysis of BE expression profile for selected genes in human biopsies based on GSE datasets

Expression profiles from human biopsies derived from patients with normal esophageal epithelium and with diagnosed BE epithelium were obtained from Gene Expression Omnibus datasets GSE13083 (7 patients with normal vs 7 patients with BE) (8), GSE34619 (8 patients with normal vs 10 patients with BE) (9) and GSE1420 (8 patients with normal vs 8 patients with BE) (24). The results demonstrated on Table 1 are shown based on the analysis of the part of the data derived from the previously published databases (8, 9, 24). Analyses were performed *in silico* using the NCBI Gene Expression Omnibus (GEO) database and the GEO2R tool ([www.ncbi.nlm.nih.gov/geo/geo2r/](http://www.ncbi.nlm.nih.gov/geo/geo2r/)). The results were represented as a log<sub>2</sub>-fold change (logFC) in BE samples vs normal esophageal epithelium. For each logFC, an empirical Bayes moderated t-statistic was calculated by the software. Adjusted *p* values, corrected for multiple testing using the Benjamini & Hochberg false discovery rate method were taken for the results interpretation. *P*<0.05 was interpreted as statistically significant and marked in the

table with asterisk (\*) for the genes with logFC values higher than 2 or lower than -2, which was considered as biologically significant up- or downregulation, respectively. Additionally, we further analyzed genes that were included in all three GSE datasets and were significantly up-/downregulated in at least one database.

### Cell cultures

The human SV40-immortalized esophageal squamous (Het-1A) epithelial cell line was a gift of J. W. P. M. van Baal (Utrecht University, The Netherlands). Het-1A cells were cultured in serum-free EPM2 medium (AthenaES, Baltimore, Maryland, USA). Het-1A cells were grown on FNC Coating Mix® (AthenaES, Baltimore, MD, USA) containing fibronectin, collagen and albumin. The primary human telomerase reverse transcriptase (hTERT) immortalized esophageal epithelial (EPC2) cell line was a gift of K. K. Krishnadath (University of Amsterdam, Amsterdam, The Netherlands). EPC2 cells were cultured in Keratinocyte-SFM (Life Technologies, Paisley, UK) medium supplemented with 50 µg/ml Bovine Pituitary Extract (BPE) (Life Technologies, Paisley, UK) and 1.0 ng/ml human recombinant Epidermal Growth Factor (EGF) (Life Technologies, Paisley, UK). Both culture media were supplemented with 100 U/ml penicillin and 50 mg/ml streptomycin (Sigma-Aldrich, Saint Louis, MO, USA). Cells were maintained at 37°C and 5% CO<sub>2</sub> and detached from the flasks prior to subculturing by the removal of the medium and the addition of 0.25% trypsin (Sigma-Aldrich, Saint Louis, MO, USA) for 1 to 5 minutes. These cell lines were selected as the most appropriate to be tested in experimental model of BE as described previously (1, 25, 26).

### Acid/bile mixture (BM) treatment

Het-1A and EPC2 epithelial cell lines were used to reflect the response of normal human esophageal epithelium to low pH and/or BM exposure. Both cell lines were seeded at a density of 10<sup>5</sup> cells/well in 6-well plates. The cells were cultured until they reached approximately 40–50% confluence. At this stage, the cells were subjected to 1, 3 and 6 days of acid and/or BM treatment, with a 30-min period of exposure per day. The BM contained 25% deoxycholic acid, 45% sodium glycocholate hydrate and 30% sodium taurochenodeoxycholate (Sigma-Aldrich, Saint Louis, MO, USA); total BM concentration used in final experiments was 50 and 100 µM. The acidified medium consisted of appropriate culture medium adjusted to pH 5.0 in which pH was adjusted with 5 M HCl. Cells were also cultured in regular medium (pH 7.3 for EPM2 medium; pH 7.2 for Keratinocyte-SFM medium) with/or without co-incubation with BM. After acid/BM exposure, the cells were rinsed with PBS, and then regular medium was added. After the last day of exposure, cells were left for 24 h and then lysed for RNA extraction. Cells were approximately 90% confluent at this time. The type and the molar ratio of bile salts in the BM have been based on studies analyzing gastroesophageal refluxate of patients with erosive esophagitis and BE (27, 28). Daily exposure time to BM and

BM concentrations were selected based on cell viability assays data, cell morphology observations and previously published data (27).

### **Cell viability assays**

Cell viability was evaluated by MTT colorimetric assay using thiazolyl blue tetrazolium bromide (MTT) (Sigma-Aldrich, St. Louis, MO, USA). Het-1A and EPC2 cells were plated in 5 replicates in 96-well plates at a density of  $10^4$  cells/well in a final volume of 100  $\mu$ l medium. After overnight incubation at 37°C, 5% CO<sub>2</sub>, dilutions of BM in acidified (pH 5.0) or regular medium were added in 5 replicates for 30 minutes. Untreated cells (appropriate volumes of medium added) served as controls. After 24 h, 50  $\mu$ l of the MTT solution was added to each well and incubated for 4 h at 37°C. Medium was removed and the formazan product of MTT reduction was dissolved in 75  $\mu$ l of DMSO per well. The optical density was measured at 550 nm.

### **Analysis of mRNA expression by real-time polymerase chain reaction (PCR)**

Total RNA was isolated using commercially available kit with spin-columns (Universal RNA/miRNA Purification Kit, EURx, Gdansk, Poland) according to manufacturer protocol. RNA concentration was measured using Qubit 4 Fluorometer (Thermo Fisher Scientific, Waltham, MA, USA). Reversed transcription to cDNA was performed using the High-Capacity cDNA Reverse Transcription Kit (Applied Biosystems, Foster City, CA, USA) using 1.8  $\mu$ g of RNA for each reaction well.

Relative gene expression was determined by real-time PCR according to the MIQE guidelines. All reactions were performed in 96-well reaction plates in duplicates or triplicates via the Quant Studio 3 system (Applied Biosystems, Foster City, CA). 2X TaqMan Fast Advanced Master Mix (Thermo Fisher Scientific, Waltham, MA, USA) and 20X TaqMan gene expression assays (Thermo Fisher Scientific, Waltham, MA, USA) were used according to the manufacturers protocol (see gene IDs in **Supplementary Tables S1** and **S2**). PCR reaction conditions were as follows: i) an initial incubation at 50°C for 2 min, ii) denaturation at 95°C for 2 min, iii) 40 cycles of 95°C for 1 sec and 60°C for 20 sec. The relative quantitation of gene expression was performed using the  $2^{-\Delta\Delta CT}$  method with cDNA derived from untreated cells or physiological esophageal epithelium of rat as reference samples.  $P < 0.05$  was interpreted as statistically significant for at least a two-fold up/downregulation in relative expression which was considered as biologically relevant. Barrett's like samples were selected in the no of 5 for gene expression analysis in animal biopsies.

**Animal model of BE**

The study was approved by the I Local Animal Care and Use Ethical Committee held on Jagiellonian University Medical College in Cracow and were run in compliance with the European Union regulations, ARRIVE guidelines and with implications for replacement, refinement or reduction (the 3Rs) principle regarding handling of experimental animals (Approval no 89/2017, permission date: 22 November 2017 and Approval no 23/2016, permission date: 20 July 2016).

Male Wistar rats (*Rattus norvegicus*) in the total number of 15 were used in the experiments. Animals were fasted for 24 h before surgery with free access to drinking water. An anastomosis between the gastroesophageal junction (GEJ) and the duodenum (esophagogastrroduodenal anastomosis, EGDA) on its anterior mesenteric border was created to induce mixed duodenogastroesophageal reflux according to the method introduced by Nishijima et al. (29) and based on generation of a shortcut for the chronic mixed gastroduodenal contents reflux through the damaged lower esophageal sphincter (15). This surgical model with slight modifications has been widely described in scientific literature (30, 31). Briefly, under general isoflurane (2-4%) anesthesia, midline laparotomy was performed and followed by the longitudinal incision extending approximately 5 mm along the lower part of anterior esophagus wall, including GEJ area. Next, the second incision of 5 mm in length was generated 4 cm distally from Treitz ligament on the anterior mesenteric border of the duodenum. These incisions were side to side anastomosed using 7-0 silk sutures. The abdomen muscles and skin were closed separately with 4-0 silk sutures. After surgical procedure during recovery phase, rats were infused s.c. with 5-10 ml of isotonic sodium chloride. For the next 10 weeks, animals were fed standard diet with free access to the drinking water. After that period animals were sacrificed by i.p. administration of lethal dose of pentobarbital (Biowet, Pulawy, Poland).

The esophagus and stomach were removed and opened longitudinally for macroscopic examination. For microscopic evaluation biopsies containing esophagus, GEJ and forestomach were sectioned. These segments were embedded in paraffin, cut into 4 µm sections and stained by haematoxylin/eosin (H&E) and alcian blue/periodic acid-Schiff (AB/PAS) for microscopic evaluation. Samples were evaluated using a light microscope (AxioVert A1, Carl Zeiss, Oberkochen, Germany). Digital documentation of histological slides was obtained using above mentioned microscope equipped with automatic scanning table and ZEN Pro 2.3 software (Carl Zeiss, Oberkochen, Germany) to collect multiple photographs of each histological sample and to stitch them into one picture; to obtain better quality of each picture, the background was subtracted and unified as white (32). Esophageal mucosal samples were collected for biochemical and molecular assessments on ice, snap-frozen in liquid nitrogen and stored at -80°C until further analysis (32). Blood samples were collected from vena cava and serum was stored at -80°C until further analysis (32).

Macroscopic degree of the esophageal mucosa injury and disease progression was assessed based on following criteria (lesion score):

- 0 physiological normal esophageal mucosa with squamous epithelium,
- 1 inflammation without ulcers reaching up to 1.5 cm of the esophagus as measured from GEJ,
- 2 inflammation without ulcers reaching beyond 1.5 cm of the esophagus as measured from GEJ,
- 3 inflammation with macroscopic ulceration and papillomatosis of the esophageal mucosa surface reaching up to 1.5 cm of the esophagus as measured from GEJ,
- 4 inflammation with macroscopic ulceration and papillomatosis of the esophageal mucosa surface reaching beyond 1.5 cm of the esophagus as measured from GEJ.

Presence or absence of the following criteria was included in microscopic and histological analysis of the disease progression within esophageal mucosa:

1. hyperplasia of squamous epithelium,
2. fibrosis of lamina propria,
3. esophagitis: 1- thickening of squamous epithelium with basal cell layer occupying up to 30% of its height; elongation of connective tissue papillae, 2- regeneration layer occupying 50% of the epithelium thickness; hyperemia and scanty inflammatory infiltrate are present in connective tissue papillae, 3- expansion of the regeneration zone to 75% of the epithelial height; moderate inflammatory infiltrate in connective tissue papillae, 4- ulceration or massive inflammatory infiltrate,
4. Barrett's-like lesion with the presence of goblet cells.

#### **Determination of serum content of pro- and anti-inflammatory factors by Luminex microbeads fluorescent assays**

Serum concentration of IL-1 $\beta$ , IL-2, IL-4, IL-5, IL-6, IL-10, IL-12, IL-13, TNF- $\alpha$ , IFN- $\gamma$ , GM-CSF was assessed using Luminex microbeads fluorescent assays (Bio-Rad, Hercules, CA, USA) and Luminex MAGPIX System (Luminex Corp., Austin, TX, USA). Results were calculated from calibration curves and expressed in pg/ml, according to the manufacturers protocol, as described previously (32).

#### **Statistical analysis**

Analyses were performed using GraphPad Prism 5 (GraphPad Prism Software Inc., San Diego, CA, USA). Results are presented as mean  $\pm$  SEM. Statistical analysis was performed with Student's *t*-test or ANOVA with Dunnett's multiple comparison if more than two experimental groups were compared. For all statistical analyses, the level of significance was set as  $p < 0.05$ .



## Results

### Analysis of BE expression profile for selected genes in human biopsies based on GSE datasets

Expression of mRNA for squamous epithelium-specific genes such as *KRT1*, *KRT4*, *KRT5*, *KRT6A-C*, *KRT13*, *KRT14*, *KRT15*, *KRT16*, *KRT23*, and *KRT24* was significantly decreased in human Barrett's esophagus biopsies as compared with expression of these specific genes in samples collected from normal squamous epithelium and observed in at least one out of three analyzed databases ( $p < 0.05$ , **Table 1**). Expression of mRNA for columnar and intestinal epithelium-specific genes such as *KRT7*, *KRT8*, *KRT18*, *KRT20*, *TFF1*, *TFF2*, *TFF3*, *VIL1*, *MUC2*, *MUC3A/B*, *MUC5B*, *MUC6*, and *MUC13* was significantly upregulated in human BE biopsies as compared with gene expression in samples collected from normal squamous epithelium in at least one out of three analyzed databases ( $p < 0.05$ , **Table 1**). Genes such as *KRT10*, *KRT17*, *KRT19*, *MUC1*, *MUC5ac*, *MUC12*, *MUC15*, *MUC17*, and *MUC21* did not fulfil our selection criteria and were not interpreted (**Table 1**).

### The effect of exposition to various bile mixture (BM) concentrations and pH values on the viability of esophageal epithelial cell lines

To determine the effect of the exposure to BM on cell viability, cells were incubated for 30 min with various BM concentrations (0–800  $\mu\text{M}$ ) in regular or low pH (pH 5.0) cell culture medium (**Figure 1A** and **1B**). **Figures 1A–B** show no significant changes in cell viability when BM (0–800  $\mu\text{M}$ ) was applied in regular medium in both cell lines as compared with control cells not exposed to BM. In contrast, when Het-1A and EPC2 cells were incubated with BM in the concentrations  $\geq 200$   $\mu\text{M}$  and at low pH, a dose-dependent and significant decrease in cell viability was observed in comparison to the respective doses of BM applied in regular medium ( $p < 0.05$ , **Figure 1A** and **1B**).

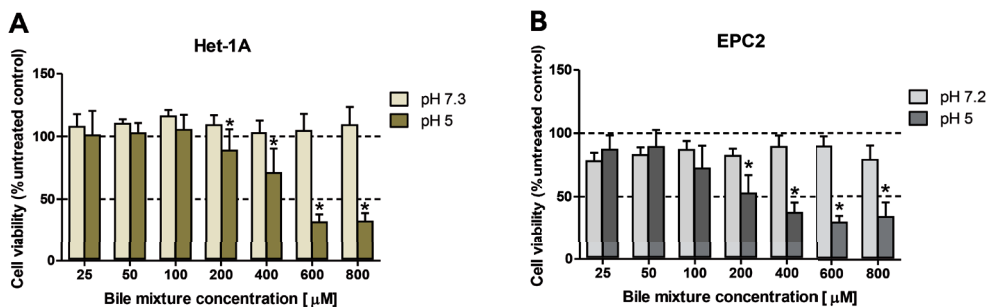


**Figure 1.** The effect of exposure to various concentrations of bile mixture (BM) and different pH on the viability of esophageal epithelial cell lines. Het-1A (A) and EPC2 (B) cells were treated for 30 min with BM at concentrations ranging from 0 to 800  $\mu\text{M}$ . After 24 h, MTT assay was used to determine cell viability. Significant changes ( $p < 0.05$ ) in cell viability after BM treatment at pH 5.0 as compared to the treatment with BM in regular medium were indicated by asterisk (\*).

**Table 1.** Alterations in selected genes expression in human biopsies derived from patients with Barrett's metaplasia as compared with normal squamous epithelium, based on analysis of the database no GSE13083 (8), GSE34619 (9) and GSE1420 (24). Asterisk (\*) indicates statistically significant difference with  $p < 0.05$  in parallel with logFC values lower than -2 or higher than 2.

Gene symbol	Predicted type of epithelium	Database no GSE13083 (N=7):				Database no GSE34619 (N=18):				Database no GSE1420 (N=16):			
		Gene ID	logFC	p value		Gene ID	logFC	p value		Gene ID	logFC	p value	
<i>KRT1</i>	squamous (esophageal)	205900_at	-7.49126	1.11e-05*		7963491	-3.3024845	1.10e-03*		205900_at	-2.217323	0.277797	
<i>KRT4</i>	squamous (esophageal)	213240_s_at	-4.6401743	5.80e-02		7963534	-5.428193	2.16e-05*		214399_s_at	0.9627934	0.291337	
<i>KRT5</i>	squamous (esophageal)	201820_at	-6.9473657	1.02e-02*		7963427	-5.19733	1.27e-05*		201820_at	0.2659335	0.939807	
<i>KRT6A, 6B, 6C</i>	squamous (esophageal)	214580_x_at	-5.0172743	3.66e-02*		7963410	-4.5273685	7.31e-05*		214580_x_at	0.3930203	0.885997	
<i>KRT10</i>	squamous (esophageal)	207023_x_at	-1.9265443	4.80e-03*		8015104	-1.9039765	1.43e-02*		207023_x_at	0.0731168	0.925068	
<i>KRT13</i>	squamous (esophageal)	207935_s_at	-5.3344986	4.04e-02*		8015323	-5.5419725	5.55e-05*		207935_s_at	0.4701058	0.861817	
<i>KRT14</i>	squamous (esophageal)	209351_at	-4.0982471	1.17e-01		8015366	-2.2296553	1.88e-03*		209351_at	1.928972	0.499067	
<i>KRT15</i>	squamous (esophageal)	204734_at	-6.05938	2.09e-03*		8015337	-4.686177	2.79e-10*		204734_at	-0.327417	0.941066	
<i>KRT16</i>	squamous (esophageal)	209800_at	-5.0731586	5.63e-03*		8015376	-3.5205307	2.61e-05*		209800_at	1.16582	0.682918	
<i>KRT17</i>	squamous (esophageal)	212236_x_at	-2.6745814	8.21e-02		8005449	-1.7824035	1.42e-03*		205157_s_at	2.6061311	0.297826	

Table 1. Continued.

Gene symbol	Predicted type of epithelium	Database no GSE13083 (N=7): Barrett's metaplasia (7 samples) vs normal squamous epithelium (7 samples)			Database no GSE34619 (N=18): Barrett's metaplasia (N=10) vs normal squamous epithelium (N=8)			Database no GSE1420 (N=16): Barrett's metaplasia (N=8) vs normal squamous epithelium (N=8)		
		Gene ID	logFC	p value	Gene ID	logFC	p value	Gene ID	logFC	p value
<i>KRT23</i>	squamous (esophageal)	218963_s_at	-2.0889186	3.74e-02*	8015133	-1.2800192	7.70e-02	218963_s_at	0.0060589	0.997257
<i>KRT24</i>	squamous (esophageal)	220267_at	-4.4806771	2.26e-03*	8015060	-2.905637	7.73e-05*	220267_at	-0.676433	0.81305
<i>KRT7</i>	columnar (intestinal)	209016_s_at	2.2155471	4.07e-02*	7955613	1.9065172	5.46e-06*	209016_s_at	1.6998427	0.204673
<i>KRT8</i>	columnar (intestinal)	209008_x_at	6.4172871	2.18e-09*	7963567	4.0091988	3.50e-11*	209008_x_at	2.6806701	0.027973*
<i>KRT18</i>	columnar (intestinal)	201596_x_at	3.4490243	5.03e-06*	8154725	2.024285	2.16e-06*	201596_x_at	1.9282774	0.082523
<i>KRT19</i>	columnar (intestinal)	201650_at	1.7536714	1.01e-03*	8015349	0.759105	3.08e-02	201650_at	1.2141959	0.658343
<i>KRT20</i>	columnar (intestinal)	213953_at	8.5259443	3.44e-09*	8015124	4.374532	2.00e-04*	213953_at	4.8072071	0.037302*
<i>TFF1</i>	columnar (intestinal)	205009_at	8.2017486	1.75e-05*	8070579	6.4595337	1.46e-12*	205009_at	5.6843253	0.010407*
<i>TFF2</i>	columnar (intestinal)	214476_at	7.6665729	4.86e-05*	8070574	5.2354248	1.23e-08*	214476_at	5.8714482	0.006909*
<i>TFF3</i>	columnar (intestinal)	204623_at	8.9897857	9.11e-08*	8070567	2.2346355	2.20e-04*	204623_at	3.3738183	0.110978

Table 1 continues on next page.

Table 1. Continued.

Gene symbol	Predicted type of epithelium	Database no GSE13083 (N=7): Barrett's metaplasia (7 samples) vs normal squamous epithelium (7 samples)				Database no GSE34619 (N=18): Barrett's metaplasia (N=10) vs normal squamous epithelium (N=8)				Database no GSE1420 (N=16): Barrett's metaplasia (N=8) vs normal squamous epithelium (N=8)			
		Gene ID	logFC	p value		Gene ID	logFC	p value		Gene ID	logFC	p value	
<i>VILI</i>	columnar (intestinal)	209950_s_at	5.8340643	8.63e-09*		8078665	2.2711873	1.88e-08*		209950_s_at	2.5215122	0.025483*	
<i>MUC1</i>	columnar (intestinal)	213693_s_at	1.5493643	1.21e-01		7920642	1.9449625	1.69e-05*		213693_s_at	1.1435938	0.427828	
<i>MUC2</i>	columnar (intestinal)	204673_at	6.7226214	3.16e-06*		7937560	2.1981597	2.77e-03*		204673_at	2.9508572	0.271622	
<i>MUC3A/B</i>	columnar (intestinal)	217117_x_at	0.7757457	9.80e-02		8135015	4.3127432	6.68e-09*		217117_x_at	0.9212935	0.225325	
<i>MUC4</i>	columnar (intestinal)	217109_at	-1.07354	1.13e-01		8092978	0.1271057	8.92e-01		204895_x_at	1.903752	0.360547	
<i>MUC5ac</i>	columnar (intestinal)	214385_s_at	8.1766871	8.25e-07*		not included in the database				214385_s_at	7.1466461	0.005318*	
<i>MUC5B</i>	columnar (intestinal)	213432_at	2.7593857	4.75e-02*		7937612	1.6075105	2.00e-03*		213432_at	2.3107749	0.510519	
<i>MUC6</i>	columnar (intestinal)	214133_at	3.1026371	7.45e-03*		7945595	5.9384813	1.46e-11*		214133_at	3.4098322	0.017934*	
<i>MUC12</i>	columnar (intestinal)	not included in the database				8135033	2.2172345	1.33e-03*		not included in the database			

Table 1. Continued.

Gene symbol	Predicted type of epithelium	Database no GSE13083 (N=7): Barrett's metaplasia (7 samples) vs normal squamous epithelium (7 samples)				Database no GSE34619 (N=18): Barrett's metaplasia (N=10) vs normal squamous epithelium (N=8)				Database no GSE1420 (N=16): Barrett's metaplasia (N=8) vs normal squamous epithelium (N=8)			
		Gene ID	logFC	p value		Gene ID	logFC	p value		Gene ID	logFC	p value	
<i>MUC13</i>	columnar (intestinal)	218687_s_at	7.3541829	5.65e-10*		8090180	7.3474513	1.87e-11*		218687_s_at	3.6273263	0.031468*	
<i>MUC15</i>	columnar (intestinal)	not included in the database				7947156	-4.7653307	4.28e-10*		not included in the database			
<i>MUC17</i>	columnar (intestinal)	not included in the database				8135048	5.953779	6.32e-08*		not included in the database			
<i>MUC21</i>	columnar (intestinal)	not included in the database				8177931	-5.732196	5.46e-07*		not included in the database			

### Optimization of the experimental procedure duration

To identify the optimal duration of acidic BM treatment in the establishment of an *in vitro* model of BE type molecular profile development, based on the analysis of GSE datasets, two squamous (*KRT4*, *KRT15*) and two columnar (*KRT8*, *KRT18*) epithelium-specific genes were randomly selected. For this purpose, Het-1A (Figure 2, A-D) and EPC2 (Figure 3, A-D) cell lines were daily exposed for 30 min to acidified medium (pH 5.0) and/or 100  $\mu$ M of bile mixture (BM) for 1, 3 or 6 consecutive days. The concentration of 100  $\mu$ M of BM (pH 5.0) was selected based on previous experiments documenting that this concentration was the highest concentration at which the cells viability was not significantly affected (Figure 1A and 1B).

No amplification of *KRT4* gene was observed in Het-1A cell line (Figure 2A) but Figure 3A shows that at 100  $\mu$ M BM in acidified medium, a significant downregulation of the

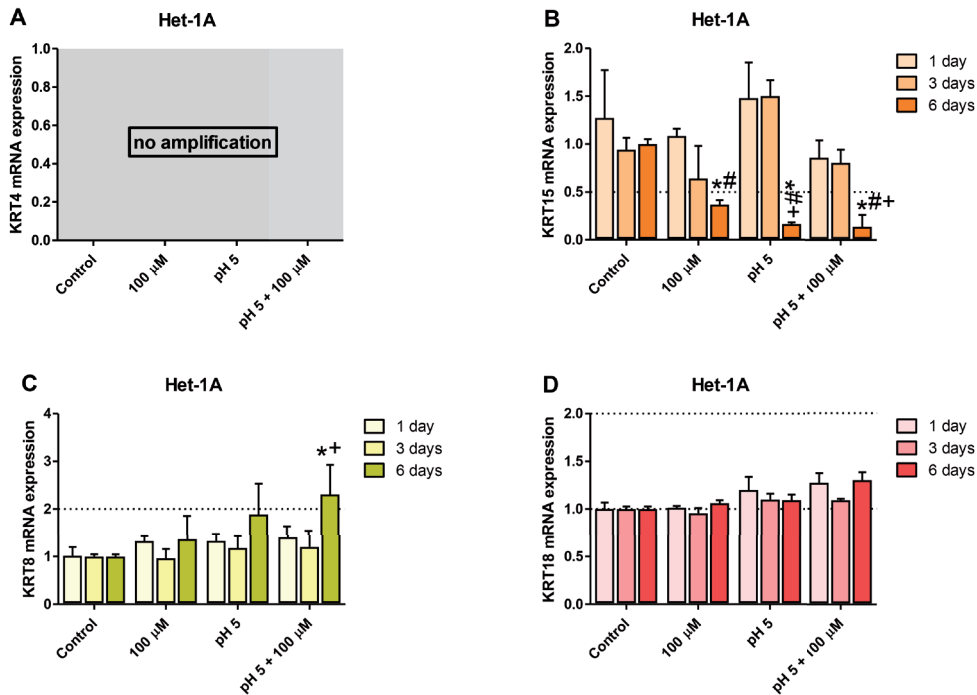


**Figure 2.** The effect of treatment with bile mixture (BM), acidified medium alone or acidic BM for 1, 3 and 6 consecutive days on *KRT4*, 15, 8 and 18 mRNA expression in Het-1A cell line. Het-1A cell line underwent 30 min of daily incubation with BM at concentration of 100  $\mu$ M, acidified medium to pH 5.0 alone or BM (100  $\mu$ M) in acidified medium (pH 5.0) for 1, 3 or 6 consecutive days and expression of *KRT4*, *KRT15*, *KRT8* and *KRT18* mRNA was analyzed by real-time PCR (A-D). PCR reaction was performed in duplicates and quantified using ACTB/GAPDH as reference genes. Data from three independent experiments are shown as the mean  $\pm$  SEM. An asterisk (\*) indicates a significant change as compared with untreated control cells ( $p < 0.05$ ). Significant change ( $p < 0.05$ ) in gene expression as compared with 1 day exposure to respective treatment regime is indicated by a hash (#). A cross (+) indicates a significant change as compared with cells after 3 days of treatment for respective treatment regime ( $p < 0.05$ ).

expression of squamous epithelium-specific *KRT4* mRNA in EPC2 cells was observed after 1, 3 and 6 days of treatment in comparison to untreated control cells ( $p<0.05$ ). Moreover, *KRT4* mRNA level in EPC2 cells was significantly decreased after 6 days in comparison to 1 and 3 days of treatment ( $p<0.05$ ; **Figure 3A**). Additionally, the low pH and 100  $\mu$ M BM applied separately to EPC2 cells for 6 but not 3 days significantly inhibited *KRT4* mRNA expression in comparison to untreated control cells and to respective experimental group after 1 day treatment ( $p<0.05$ ; **Figure 3A**).

**Figure 2B** and **Figure 3B** show significant downregulation of *KRT15* mRNA expression in both cell lines after 6 days as compared to untreated control cells and to 1 and 3 days of treatment with BM at pH 5.0 ( $p<0.05$ ). Additionally, in Het-1A cells low pH alone decreased level of *KRT15* mRNA after 6 days in comparison to untreated control cells and to cells after 1 and 3 days of treatment ( $p<0.05$ ; **Figure 2B**). Moreover, we

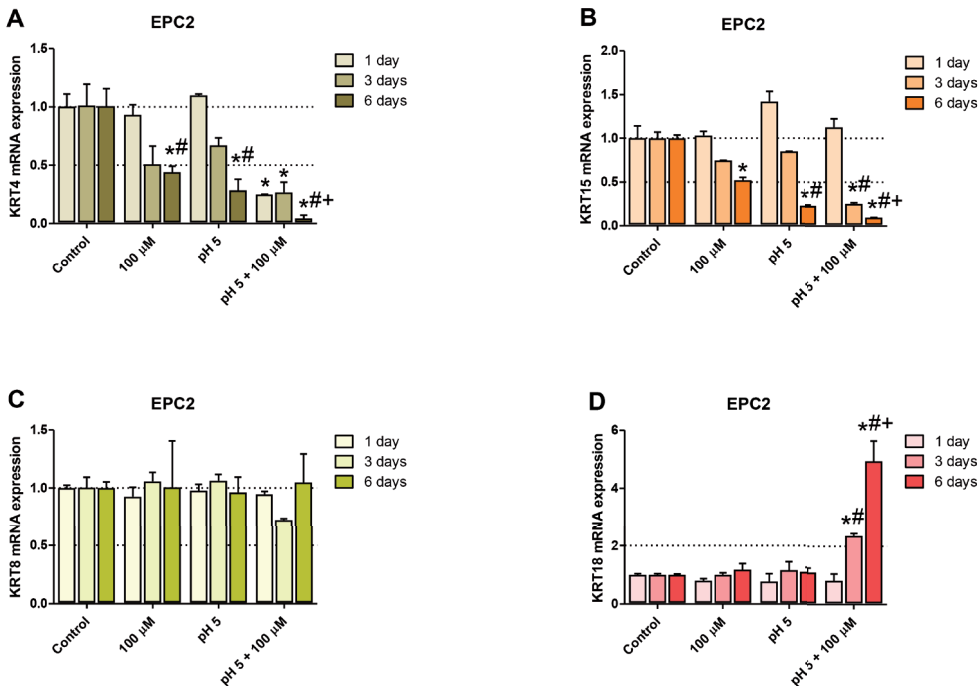


**Figure 3.** The effect of treatment with bile mixture (BM), acidified medium alone or acidic BM for 1, 3 and 6 consecutive days on *KRT4*, 15, 8 and 18 mRNA expression in EPC2 cell line. EPC2 cell line underwent 30 min of daily incubation with BM at concentration of 100  $\mu$ M, acidified medium to pH 5.0 alone or BM (100  $\mu$ M) in acidified medium (pH 5.0) for 1, 3 or 6 consecutive days and expression of *KRT4*, *KRT15*, *KRT8* and *KRT18* mRNA was analyzed by real-time PCR (**A-D**). PCR reaction was performed in duplicates and quantified using ACTB/GAPDH as reference genes. Data from three independent experiments are shown as the mean  $\pm$  SEM. An asterisk (\*) indicates a significant change as compared with untreated control cells ( $p<0.05$ ). Significant change ( $p<0.05$ ) in gene expression as compared with 1 day exposure for respective treatment regime is indicated by hash (#). A cross (+) indicates a significant change as compared with cells after 3 days of treatment ( $p<0.05$ ).

have noticed that 100  $\mu$ M BM applied at regular medium to Het-1A cells for 6 days significantly downregulated *KRT15* mRNA expression in comparison to untreated control cells and to cells after 1 day of treatment ( $p < 0.05$ ; **Figure 2B**). In EPC2 cells low pH alone inhibited *KRT15* mRNA expression after 6 days in comparison to untreated control cells and to cells after 1 day of treatment ( $p < 0.05$ ; **Figure 3B**). BM applied in concentration 100  $\mu$ M (regular pH 7.2) for 6 days significantly decreased *KRT15* mRNA level in EPC2 cells in comparison to respective untreated control cells ( $p < 0.05$ ; **Figure 3B**).

Our time sequence determination revealed that a significant upregulation of *KRT8* mRNA was observed exclusively in Het-1A but not in EPC2 cells after 6 days as compared with 1 and 3 days of treatments or with untreated control cells ( $p < 0.05$ ; **Figure 2C** and **3C**). *KRT18* mRNA was significantly upregulated in EPC2 but not in Het-1A cell line after 3 and 6 days as compared with 1 day of treatment or with untreated control cells ( $p < 0.05$ ; **Figure 2D** and **3D**).

To summarize two out of three and three out of four genes from the BE molecular profile, in Het-1A and EPC2 respectively, show a significantly higher fold change after 6 days of acidic BM treatment, compared to 1 or 3 days of treatment. As the fold change in expression between BE and squamous epithelium is most resembled by the model using 6 days of acidic BM treatment, this condition was selected for further study.

### **Squamous and columnar epithelium-specific genes expression in *in vitro* model**

**Figures 4A-J** show changes in mRNA expression for squamous epithelium-specific genes selected based on **Table 1** analysis as characteristic for human BE biopsies, determined in Het-1A and EPC2 cells treated for 30 minutes per day with 0  $\mu$ M, 50  $\mu$ M, and 100  $\mu$ M BM at either pH 7.2/3 or pH 5.0, for 6 consecutive days. Incubation of EPC2 cells with 100  $\mu$ M BM at pH 5.0 resulted in a significant decrease in expression of all investigated squamous epithelium-specific *KRT* (*KRT1*, *KRT4*, *KRT5*, *KRT6*, *KRT13*, *KRT14*, *KRT15*, *KRT16*, *KRT23*, *KRT24*) genes as compared to untreated control cells ( $p < 0.05$ ; **Figure 4, A-J**). Significant downregulation of *KRT1* (4A), *KRT4* (4B), *KRT5* (4C), *KRT6* (4D), *KRT14* (4F), *KRT16* (4H) and *KRT24* (4J) mRNA as compared to EPC2 cells incubated with low pH alone was observed ( $p < 0.05$ ). Incubation of EPC2 cells with lower concentration of BM (50  $\mu$ M) at pH 5.0 significantly downregulated mRNA expression of *KRT1* (4A), *KRT4* (4B), *KRT6* (4D), *KRT13* (4E), *KRT15* (4G), *KRT23* (4I) and *KRT24* (4J) in comparison to untreated control cells ( $p < 0.05$ ). Exposure of EPC2 cells to 100  $\mu$ M of BM at regular medium resulted in a significant decrease of *KRT1* (4A), *KRT4* (4B), *KRT15* (4G) and *KRT23* (4I) mRNA levels as compared to untreated control cells ( $p < 0.05$ ). In turn, 50  $\mu$ M of BM applied alone inhibited mRNA expression of *KRT1* (4A) and *KRT4* (4B) in comparison to untreated control EPC2 cells ( $p < 0.05$ ). The mRNA expression of *KRT1* (4A), *KRT4* (4B), *KRT13* (4E), *KRT15*



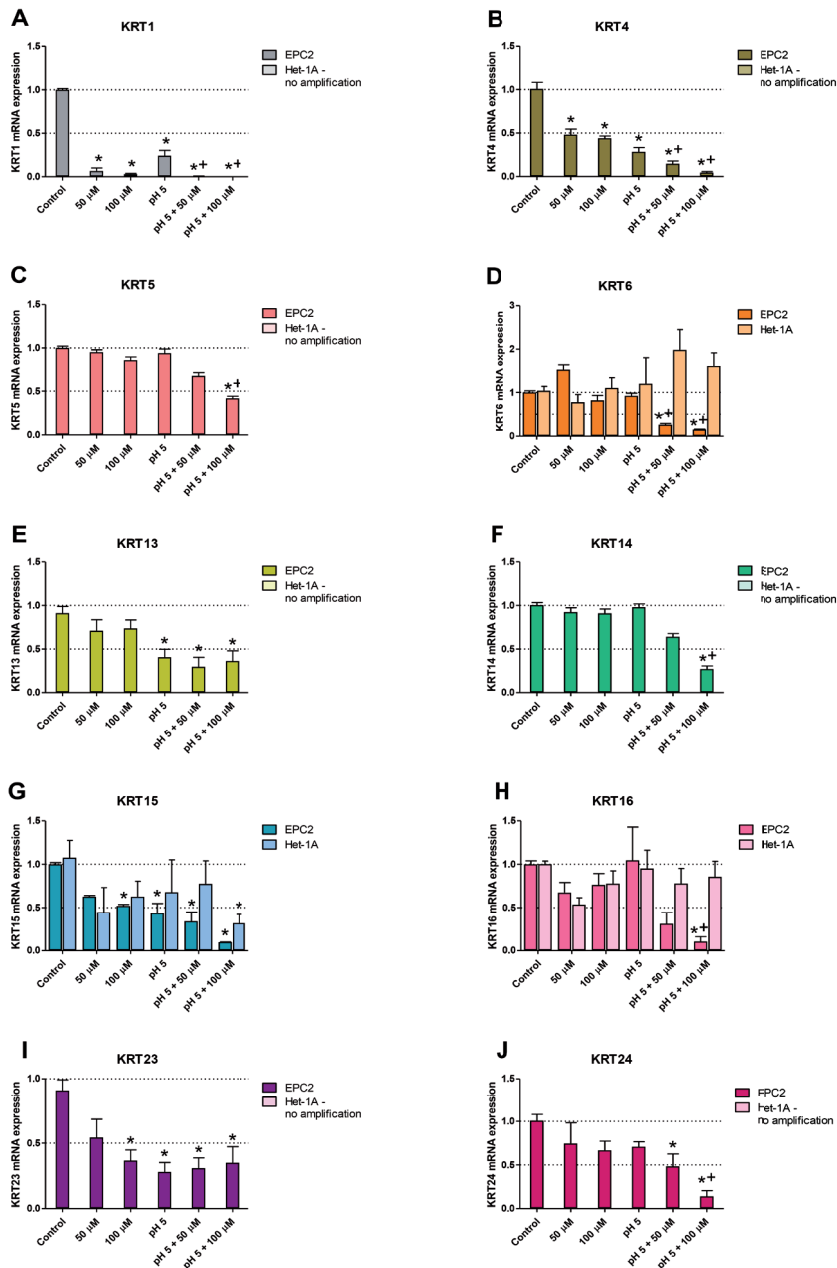


**Figure 4.** Squamous epithelium-specific mRNA expression upon incubation of Het-1A and EPC2 cells with bile mixture (BM) at pH 5.0. Het-1A and EPC2 cell lines were incubated with BM (50  $\mu$ M and 100  $\mu$ M) in acidified medium (pH 5.0) or regular medium for 6 consecutive days and squamous epithelium-specific mRNA expression was analyzed by real-time PCR (A-J). PCR reaction was performed in duplicates and quantified using ACTB/GAPDH as reference genes. Data from three independent experiments are shown as the mean  $\pm$  SEM. Significant change in gene expression after 6 days treatment as compared with untreated control cells is indicated by an asterisk (\*) ( $p < 0.05$ ). A cross (+) indicates a significant change as compared with cells incubated with pH 5.0 alone ( $p < 0.05$ ).

(4G) and *KRT23* (4I) in EPC2 cells cultured in acidified medium (pH 5.0) without BM was significantly inhibited as compared to untreated control cells ( $p<0.05$ ). In Het-1A cells, no mRNA amplification of *KRT1* (4A), *KRT4* (4B), *KRT5* (4C), *KRT13* (4E), *KRT14* (4F), *KRT23* (4I) and *KRT24* (4J) and no changes in mRNA expression of *KRT6* (4D) and *KRT16* (4H) was observed in all experimental groups. Only *KRT15* mRNA expression was significantly downregulated in Het-1A cells after the treatment with BM (100  $\mu$ M) at pH 5.0, as compared to untreated control cells ( $p<0.05$ ; **Figure 4G**).

**Figures 5A-G** show mRNA expression of columnar epithelium-specific genes, selected based on **Table 1** analysis, altered in patients with BE, and determined in Het-1A and EPC2 cells. In EPC2 cells treated with 100  $\mu$ M BM at pH 5.0, significant upregulation of *KRT7* (5A), *KRT18* (5C) and *TFF3* (5D) mRNA expression in comparison to untreated control cells and cells treated with low pH alone was observed ( $p<0.05$ ). In contrast, exposure to 50  $\mu$ M BM at pH 5.0 significantly elevated only *TFF3* mRNA expression in EPC2 cells ( $p<0.05$ ; **Figure 5D**). When BM (100  $\mu$ M) at pH 5.0 was co-incubated with Het-1A cells, the upregulation of *KRT8* (5B), *TFF3* (5D), *MUC2* (5E), *MUC13* (5F) and *VIL1* (5G) mRNA was detected as compared to untreated control cells ( $p<0.05$ ). In turn, BM applied at the concentration of 50  $\mu$ M at pH 5.0 significantly elevated only *TFF3* (5D) and *MUC13* (5F) mRNA expression over the mRNA expression levels obtained in untreated control Het-1A cells ( $p<0.05$ ). Likewise, BM (100  $\mu$ M) applied at regular medium significantly increased mRNA expression of *TFF3* as compared to untreated control Het-1A cells ( $p<0.05$ ; **Figure 5D**). In Het-1A cells cultured in acidified medium (pH 5.0) without BM significant upregulation of *KRT8* (5B), *TFF3* (5D), *MUC2* (5E), *MUC13* (5F) and *VIL1* (5G) mRNA was determined as compared to untreated control cells ( $p<0.05$ ). No amplification was observed for either *KRT20*, *TFF1*, *TFF2*, *MUC6*, *MUC5B* and *MUC3A/B* mRNA in all experimental groups for both cell lines (data not shown).

### **Morphology of esophageal mucosa, gastroesophageal junction (GEJ), and gastric cardia in rats with esophagogastrroduodenal anastomosis (EGDA)**

**Table 2** shows that in rats with 10 weeks of EGDA, the lesion score assessed macroscopically reached 3 in 70% of cases (7 out of 10 animals). In 20% of rats, disease progression reached score 4 and only 10% of animals reached lesion score 2 (**Table 2**).

**Table 2.** Incidence of the particular macroscopic lesion score in esophageal mucosa of rats 10 weeks after esophagogastrroduodenal anastomosis (EGDA)-inducing surgery

Macroscopic lesion score	Number of animals with EGDA (%) (N=10)
2	1 (10%)
3	7 (70%)
4	2 (20%)

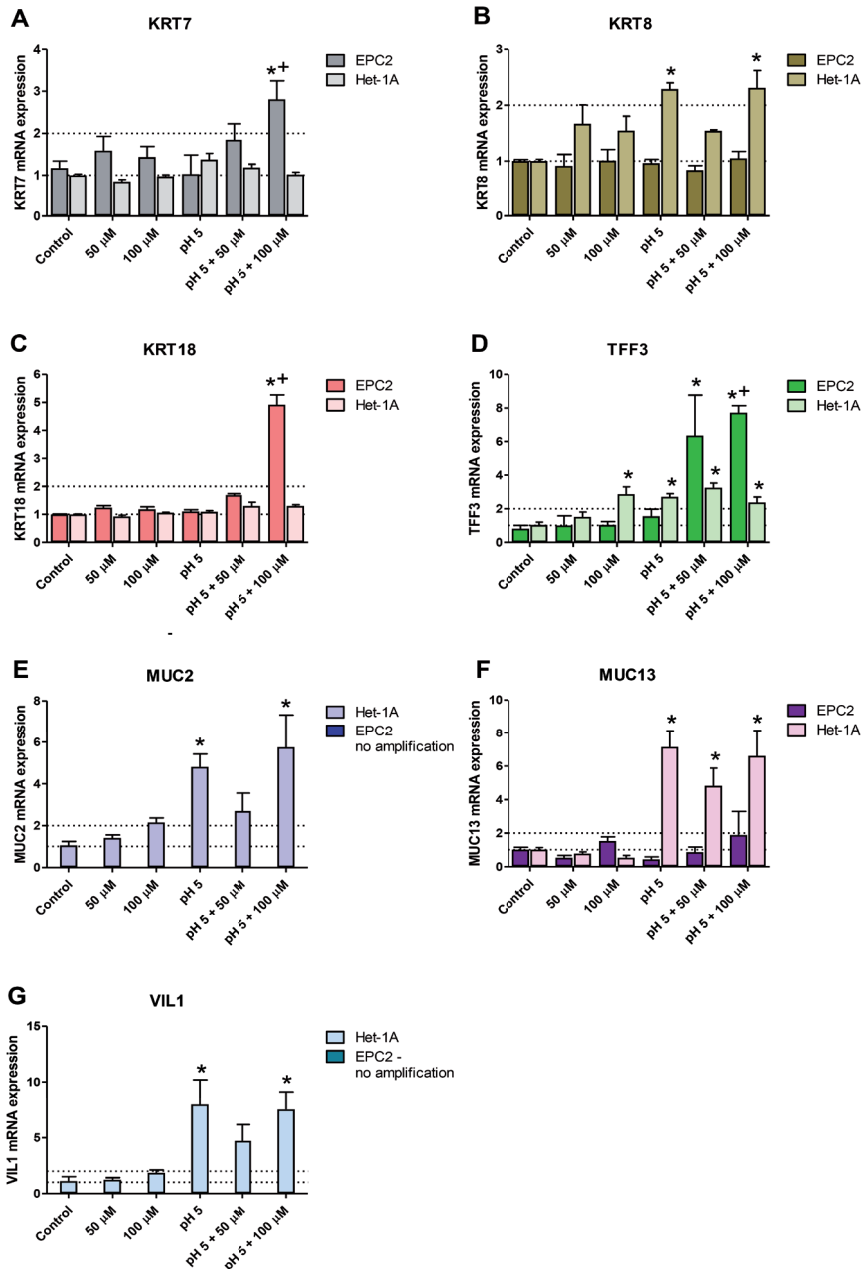


**Figure 5.** Columnar epithelium-specific mRNA expression upon incubation of Het-1A and EPC2 cells with bile mixture (BM) at pH 5.0. Het-1A and EPC2 cell lines were incubated with BM (50  $\mu$ M and 100  $\mu$ M) in acidified medium (pH 5.0) or regular medium for 6 consecutive days and squamous epithelium-specific mRNA expression was analyzed by real-time PCR (A-G). PCR reaction was performed in duplicates and quantified using ACTB/GAPDH as reference genes. Data from representative three independent experiments are shown as the mean  $\pm$  SEM. Significant change in gene expression after 6 days treatment as compared with untreated control cells is indicated by an asterisk (\*) ( $p < 0.05$ ). A cross (+) indicates a significant change as compared with cells incubated with pH 5.0 alone ( $p < 0.05$ ).

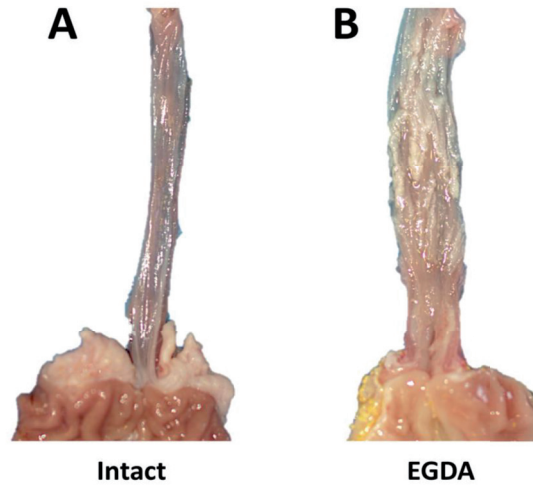


**Figure 6.** Macroscopic appearance of esophageal mucosa, gastroesophageal junction and gastric cardia in representative rats without (Intact, **A**) or with esophagogastrroduodenal anastomosis (EGDA, **B**). Table 3 shows that all 10 animals with EGDA developed hyperplasia of squamous epithelium and fibrosis of the lamina propria at 10 weeks after surgery. In 80% of the rats esophagitis with ulceration was observed (Table 3). Barrett's metaplasia was present in 60% of the rats (Table 3).

**Table 3.** Incidence of the selected microscopic criteria in esophageal mucosa of rats 10 weeks after esophagogastrroduodenal anastomosis (EGDA)-inducing surgery

Assessed microscopic criteria	Number of animals with EGDA with presence of the criteria (%) (N=10)
Hyperplasia of squamous epithelium	10 (100%)
Fibrosis of lamina propria	10 (100%)
Barrett's metaplasia	6 (60%)
Esophagitis with ulceration	8 (80%)

**Figure 6** shows the macroscopic appearance of esophageal mucosa, GEJ, and gastric cardia of representative rats with or without EGDA (**Figure 6A** and **6B**, respectively). After exposure to chronic reflux due to EGDA, thickening of esophageal wall with ulceration and papillomatosis of the esophageal mucosa surface was observed (**Figure 6B**).

**Figure 7A1** and **7A2** shows the microscopic appearance of the esophageal mucosa, GEJ, and gastric mucosa obtained from representative intact rats. The typical morphology manifestation of hyperplasia, fibrosis or inflammation of experimental BE was not observed in esophageal epithelium and submucosa attached to the GEJ of intact rats (**Figure 7A1**) and the AB/PAS staining did not show any pathological changes within the tissue of these rats (**Figure 7A2**). In contrasts, **Figure 7B1** and **7B2** show that in rats with EGDA, the GEJ architecture is altered. Esophageal mucosa is characterized by

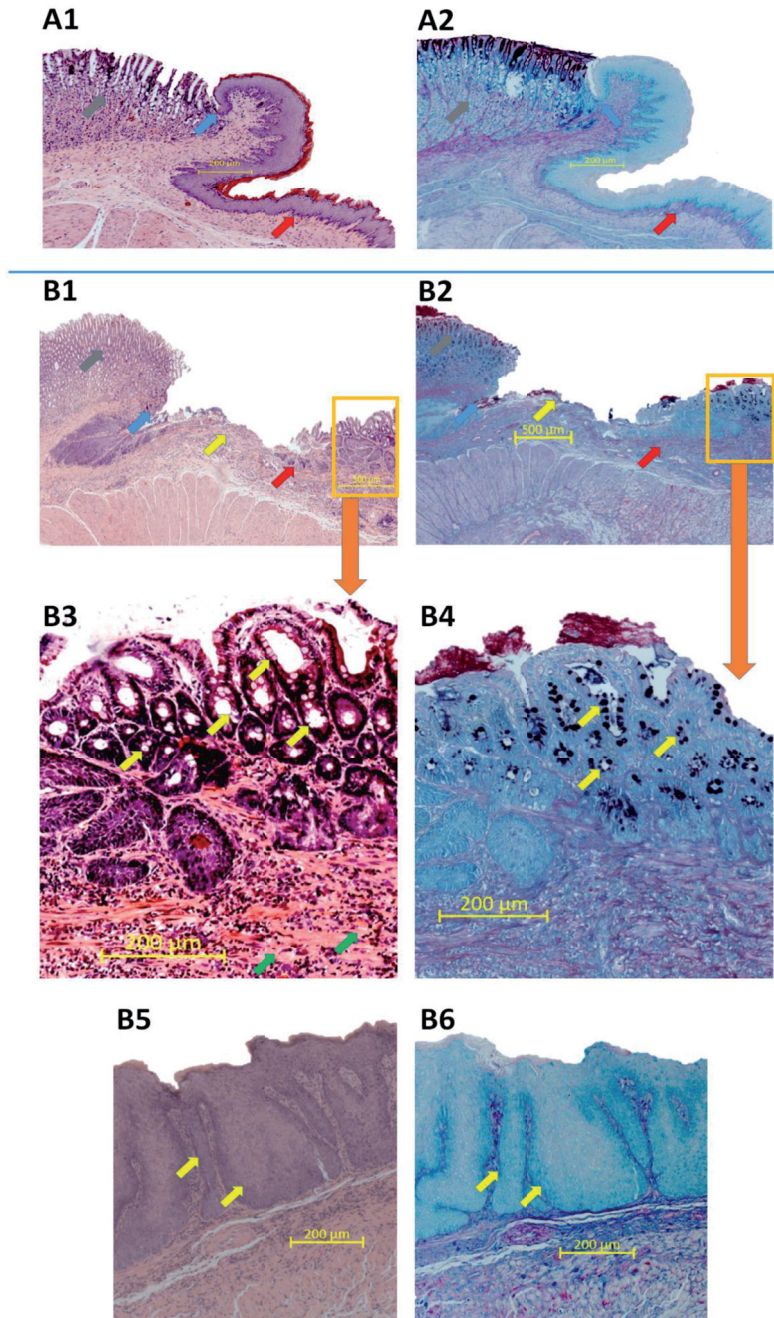


**Figure 7.** Microscopic appearance of esophageal mucosa, gastroesophageal junction (GEJ) and gastric cardia stained with H&E or AB/PAS in representative rats without (A1, A2) or with an esophagogastrroduodenal anastomosis (B1-B6). Grey arrow points out gastric mucosa, blue arrow points out GEJ, red arrow indicates esophageal mucosa, yellow arrow indicates esophageal ulceration, orange frame shows Barrett's-like lesions (A1, A2, B1, B2). (B3, B4) show high resolution images of Barrett's-like lesions where yellow arrows indicate goblet cells and green arrows indicate fibrosis. Yellow arrows indicate epithelial hyperplasia (B5, B6).

evident ulceration and fibrosis as demonstrated at high resolution image (**Figure 7B3**). Moreover, Barrett's-like lesions metaplasia with presence of AB-positive goblet cells is observed proximally from the GEJ (**Figure 7B3** and **7B4**). **Figure 7B5** and **7B6** present photomicrographs of esophageal tissue section collected separately from the same rate as shown in **Figure 7B3** and **7B4**. In animals with EGDA, the esophageal squamous mucosa shows pronounced epithelial hyperplasia (**Figure 7B5** and **7B6**).

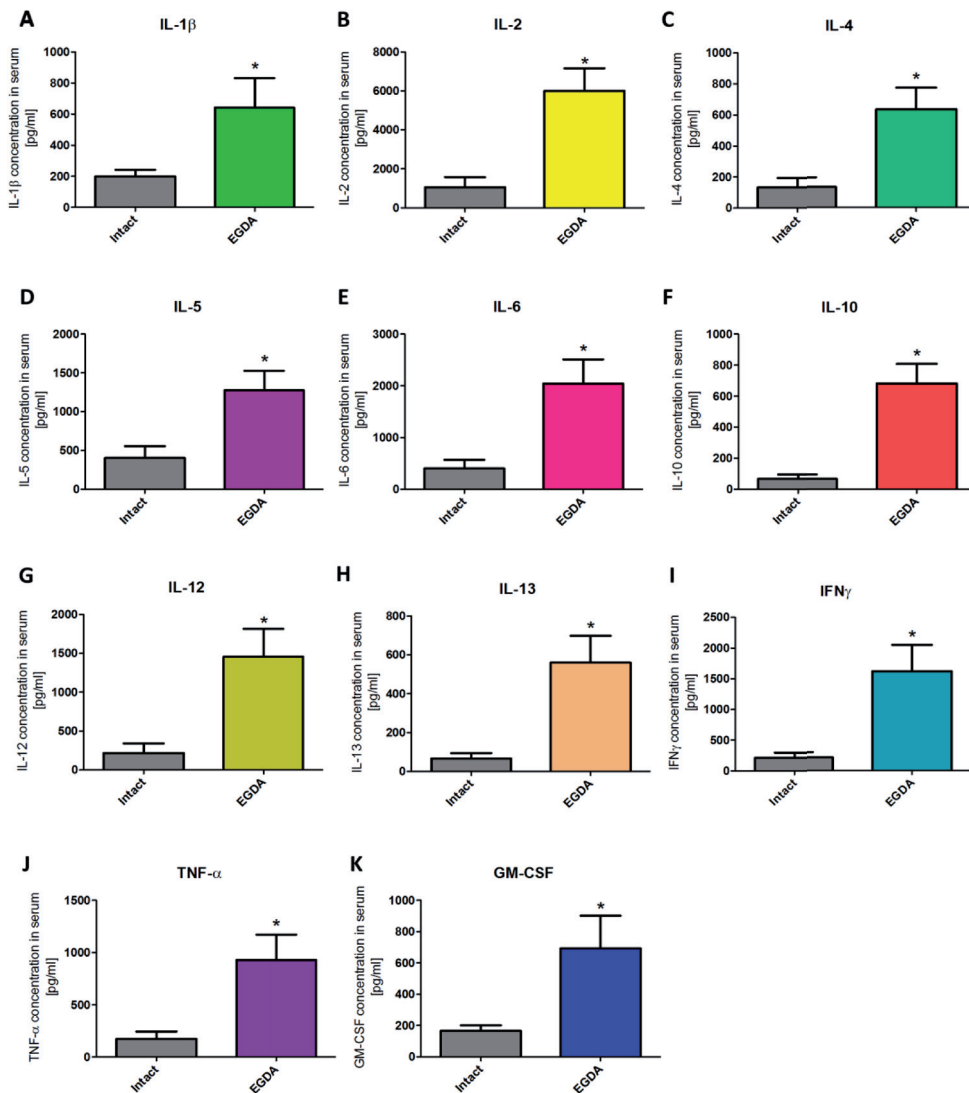


**Figure 8.** Serum concentration of interleukin (IL)-1 $\beta$  (A), IL-2 (B), IL-4 (C), IL-5 (D), IL-6 (E), IL-10 (F), IL-12 (G), IL-13 (H), interferon (IFN)- $\gamma$  (I), tumor necrosis factor (TNF)- $\alpha$  (J), and granulocyte-macrophage colony-stimulating factor GM-CSF (K) in rats without (intact) and with esophagogastrroduodenal anastomosis (EGDA). Results are mean  $\pm$  SEM of five samples per each experimental group. Asterisk (\*) indicates a significant change as compared with respective values obtained in rats without EGDA ( $p < 0.05$ ).

### Alterations in serum content of pro- and anti-inflammatory cytokines in rats with EGDA

**Figures 8A-K** show that serum contents of interleukin (IL)-1 $\beta$  (8A), IL-2 (8B), IL-4 (8C), IL-5 (8D), IL-6 (8E), IL-10 (8F), IL-12 (8G), IL-13 (8H), interferon (IFN)- $\gamma$  (8I), tumor necrosis factor (TNF)- $\alpha$  (8J), and granulocyte-macrophage colony-stimulating factor (GM-CSF) (8K), respectively, were significantly increased in rats with EGDA as compared with intact animals ( $p < 0.05$ ).

### Squamous and columnar epithelium-specific mRNA expression in esophageal mucosa of rats with EGDA

**Figure 9** shows expression of squamous epithelium-specific (A-G) genes in esophageal mucosa of rats with EGDA. In esophageal mucosa of rats with EGDA, *KRT4* (9A), *KRT13* (9D) and *KRT15* (9F) mRNA expression was significant downregulated in line with *in vitro* model and *KRT1* (9A), *KRT5* (9C) and *KRT14* (9E) mRNA fold changes were significantly increased not in line with *in vitro* model as compared to intact rats ( $p < 0.05$ ). EGDA did not significantly affect mRNA expression of *KRT23* (9G).

**Figure 10** shows that the mRNA expression of columnar epithelium-specific genes *KRT7* (10A), *KRT8* (10B), *KRT18* (10C), *KRT20* (10D), *TFF3* (10F), *MUC2* (10H) and *MUC13* (10I) was significantly upregulated in rats with EGDA in comparison to intact rats ( $p < 0.05$ ). Only *TFF1* (10E) mRNA was downregulated after EGDA. EGDA *did not* lead to any significant *changes* in *VIL1* (10G) mRNA expression. No amplification was observed for *KRT6*, *KRT16*, *KRT24*, *TFF2*, *MUC3A*, *MUC5B* and *MUC6* mRNA in rats (data not shown).

## Discussion

Human BE is a pathological condition associated with longstanding GERD and is defined as metaplasia of the flat, layered esophageal squamous epithelium into a tall intestinal columnar epithelial cells (23, 33). It is important to highlight that Barrett's metaplasia may originate from GEJ stem cells (34, 35).

In our study, we have aimed to establish an appropriate experimental model which enables the evaluation of the effectiveness of novel pharmacological tools in the pathophysiology of Barrett's metaplasia development at the microscopic, systemic, and especially molecular levels. For this purpose, we have chosen three datasets GSE13083 (8), GSE34619 (9) and GSE1420 (24) from Gene Expression Omnibus (GEO) and applied them for GEO2R online tool to select the commonly expressed genes in BE epithelium. We observed significant downregulation in mRNA expression for squamous epithelium-specific genes such as *KRT1*, *KRT4*, *KRT5*, *KRT6A-C*, *KRT13*, *KRT14*,

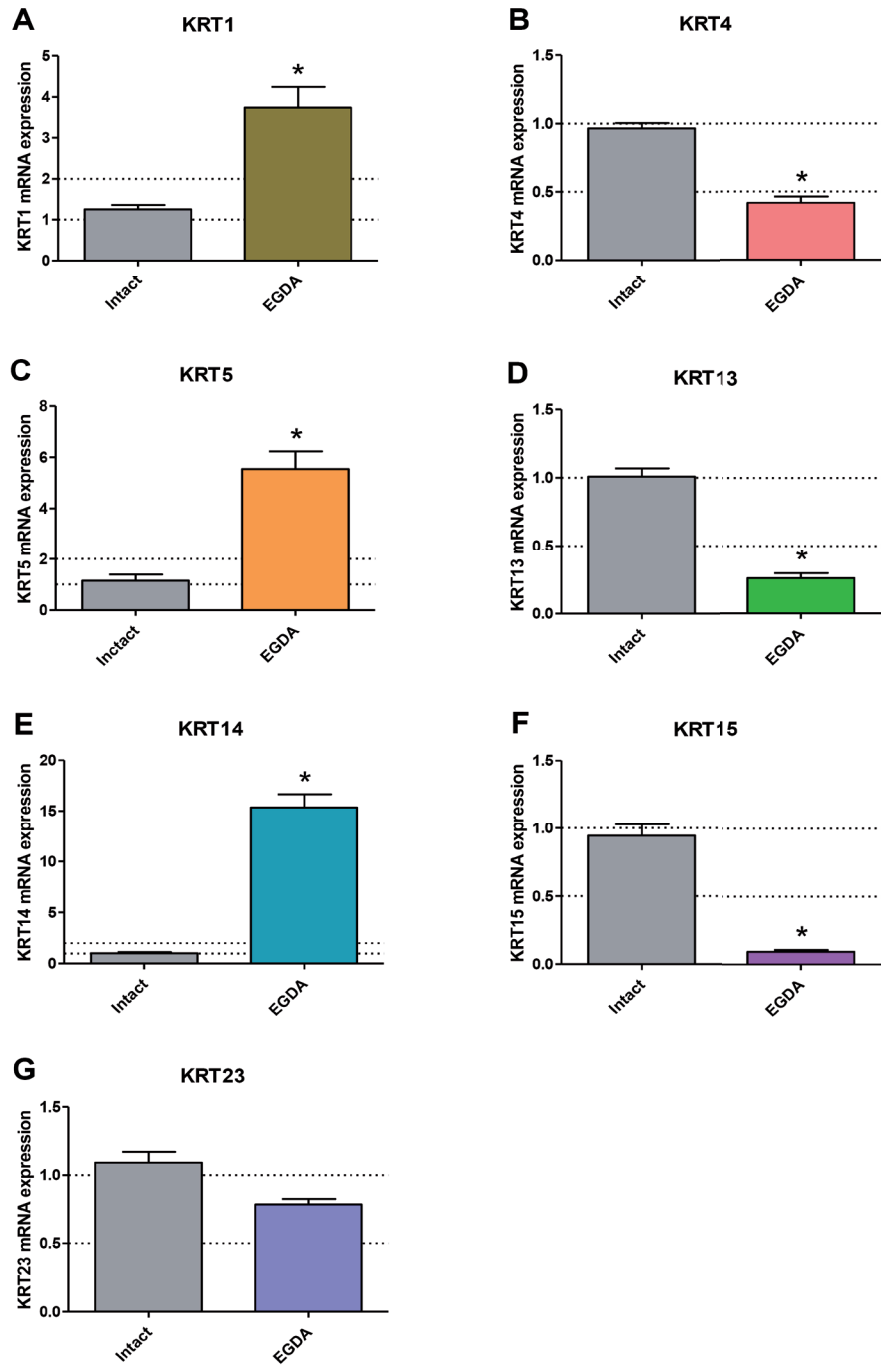


**Figure 9.** Expression of mRNA for squamous epithelium-specific genes in rats without (intact) and with esophagogastrroduodenal anastomosis (EGDA). Results are expressed as mRNA expression of squamous epithelium-specific genes (A-G) normalized to ACTB/GAPDH expression and are mean  $\pm$  SEM for n=5 samples per each experimental group. Asterisk (\*) indicates a significant change as compared with respective values obtained in rats without EGDA ( $p < 0.05$ ).



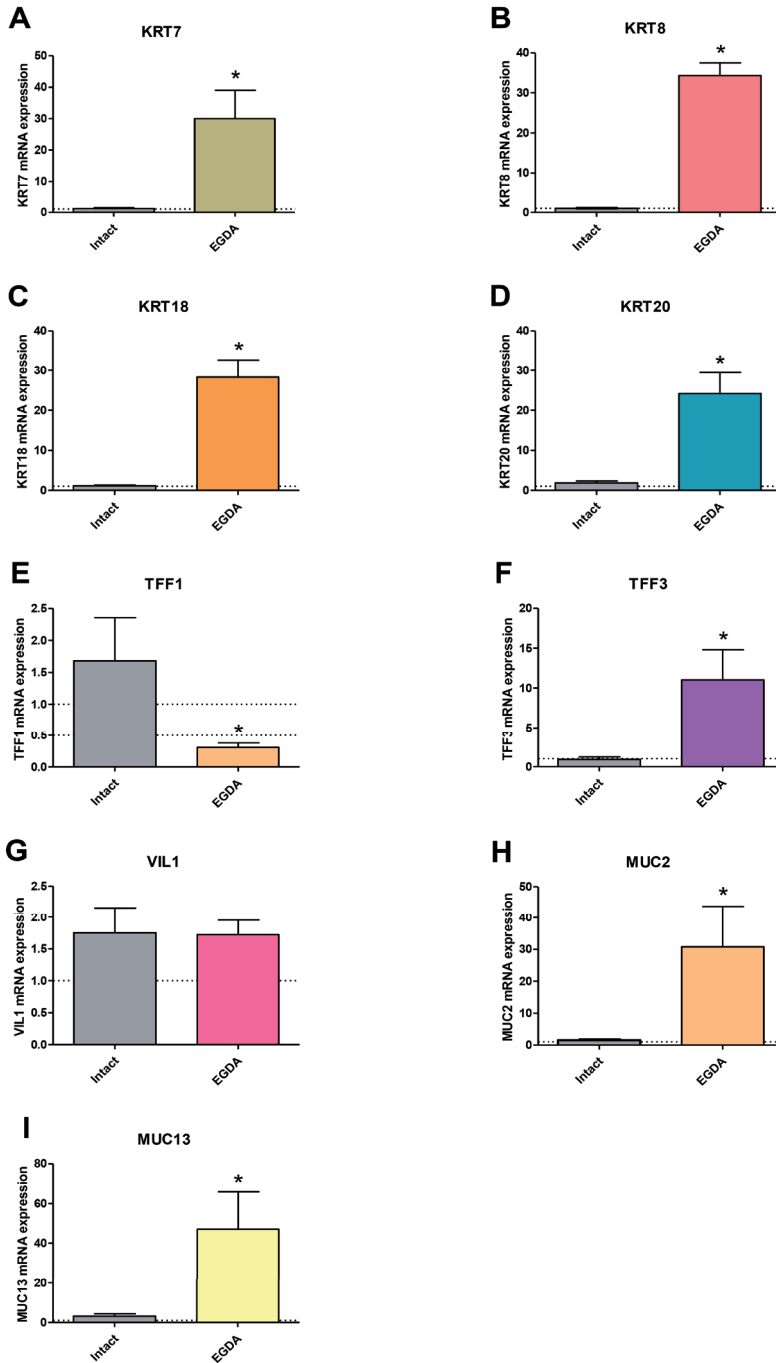


**Figure 10.** Expression of mRNA for columnar epithelium-specific genes in rats without (intact) and with esophagogastrroduodenal anastomosis (EGDA). The results are expressed as mRNA expression of columnar epithelium-specific genes (A-I) normalized to ACTB/GAPDH expression and are the mean  $\pm$  SEM for  $n=5$  Barrett's-like samples per experimental group. Asterisk (\*) indicates a significant change as compared with respective values obtained in rats without EGDA ( $p < 0.05$ ).

*KRT15*, *KRT16*, *KRT23* and *KRT24* in human BE biopsies as compared with samples collected from normal squamous esophageal epithelium. In turn, expression of mRNA for columnar and intestinal epithelium-specific genes such as *KRT7*, *KRT8*, *KRT18*, *KRT20*, *TFF1*, *TFF2*, *TFF3*, *VIL1*, *MUC2*, *MUC3A/B*, *MUC5B*, *MUC6* and *MUC13* was significantly upregulated. We assume that the alterations in the mRNA expression of above mentioned specific genes reflect the development of metaplasia within the epithelium on molecular level.

There have been several attempts to develop experimental *in vivo* models of GERD leading to BE and/or EAC which attempt to mimic the clinical course of this disorder. The most widely described model in literature is the surgical animal model with rats (36). Attwood et al. divided existing reflux models into three categories depending on the production of esophagitis alone (rat pyloric ligation, Wendel esophagogastroplasty, or external esophageal perfusion), esophagitis and BE but not EAC (total gastrectomy or mucosal excision with hiatal hernia creation), and esophagitis, BE, and EAC (esophagojejunostomy, esophagoduodenal anastomosis, or esophagogastrroduodenal anastomosis) (37). Interestingly, Quante et al. demonstrated that genetically modified mice overexpressing IL-1 $\beta$  also develop Barrett's-like lesions (34).

We have selected and implemented the well-known surgical rat model based on generation of an appropriate anastomosis between the GE and EGDA according to the method described previously by Nishijima et al. (29). Microscopic and histological analysis confirmed BE metaplasia with the presence of goblet cells in 60% of rats with 10 weeks of EGDA.

Additionally, we have demonstrated an evident increase in expression of pro/anti-inflammatory cytokines in rats with experimental gastroduodenoesophageal reflux. This is corroborative with previous findings that chronic inflammation of esophageal mucosa may occur as the secondary consequence of multiple exposures of esophageal structure to the acidic and alkaline content. Thus, there is no doubt that this gastroduodenal content may represent a common risk factors in the BE pathogenesis and its further progression (7, 15, 29, 30, 38).

Moreover, based on the analysis of the BE expression profile in human biopsies, we sought to identify alterations in mRNA expression of selected genes including squamous epithelium-specific (*KRT1*, *KRT4*, *KRT5*, *KRT6*, *KRT13*, *KRT14*, *KRT15*, *KRT16*, *KRT23*, *KRT24*) and columnar epithelium-specific (*KRT7*, *KRT8*, *KRT18*, *KRT20*) keratins together with secretory (*MUC2*, *MUC5B*, *MUC6*) and epithelial membrane-bound (*MUC3A/B*) mucins, trefoil factor family (*TFF1*, *TFF2*, *TFF3*) and villin (*VIL1*) genes in the esophageal mucosa of rats with EGDA in comparison to intact rats without EGDA. We found that expression of squamous epithelium-specific *KRT4*, *KRT13* and *KRT15* mRNA was significantly downregulated in esophageal mucosa of rats with

**Table 4.** Major differences between human and rat esophagus physiology and Barrett's esophagus (BE) pathophysiology

	Human	Rat
Esophageal epithelium	Non-keratinized	Keratinized
Esophageal submucosal glands and papillae	Present	Absent
Stratum corneum	Absent	Present
Squamocolumnar transition at GEJ	Yes	No
Natural reflux	Yes	No
Natural BE to EAC progression	Yes	No
<i>Compartmentalized stomach</i> (forestomach and distal stomach)	No	Yes
BE progression time	10 years	Around 2-3 months

EGDA. These findings seem to closely correlate with changes in mRNA expression as demonstrated in mucosal biopsies collected from patients with BE. In addition, among investigated columnar epithelium-specific genes *KRT7*, *KRT8*, *KRT18*, *KRT20*, *TFF3*, *MUC2* and *MUC13* mRNA expression was significantly upregulated reflecting changes observed in BE patients (**Table 5**). In contrary, *KRT1*, *KRT5*, *KRT14*, *TFF1* and *VIL1* mRNA expression was increased in animal biopsies which is not in line with these genes expression observed in human BE biopsies. This phenomenon can be explained by species-specific discrepancy between humans and rodents, especially taking into account that *KRT1*, *KRT5* and *KRT14* are expressed in human squamous epithelium. The direct translational character of the scientific data derived from animal studies related to BE and compared with human BE can be doubtful when considering e.g. the variability in the structure and physiology between the rodent and human esophagus (**Table 4**) (26, 39).

Our data accumulated in this study may support the notion proposed by Attwood et al. that results from animal models cannot be always translated to clinical settings [35]. Thus, if the results are achieved without the solid pathology background, experimental as well as molecular evidences, the results of subsequent work must be interpreted carefully (37). Therefore, there is a great need for alternative methods that will be more available, will not depend on the presence of BE patients, and strive to mimic the human *in vivo* microenvironments in an *in vitro* setting (40). For instance, Bus et al. reviewed a large variety of *in vitro* models and incubation conditions for studying BE development (1). In their *in vitro* studies, bile salts at either a low or neutral pH were required to induce expression of BE-specific factors (1). Moreover, they proposed that the esophageal squamous epithelium cell lines, such as the Het-1A cells appear to be the most appropriate models for studying of BE pathogenesis (1). In contrary, according to Underwood et al., Het-1A cell line does not possess the characteristics of normal

esophageal squamous cells and should be studied with caution in translational research on BE (41). Thus, besides commonly used Het-1A cell line, we have implemented human esophageal keratinocytes EPC2 cell line to investigate their molecular response to acid and/or BM exposures.

Since the major constituent of the esophageal epithelium are the keratins (40, 42), we chose them as a focal point to investigate the molecular pattern of Barrett's metaplasia and to identify the optimal duration of acid and/or BM treatment to establish an *in vitro* model of BE development. Based on cell viability analysis we have selected BM at the concentration of 100  $\mu$ M applied in medium adjusted to pH 5.0 as the highest concentration, which did not affect esophageal cell lines survival. We have further assessed possible time-dependent alterations in the expression of two squamous (*KRT4*, *KRT15*) and two columnar (*KRT8*, *KRT18*) epithelium-specific KRT genes in Het-1A and EPC2 cell lines after exposing the cells for 30 min per day to desired BM (100  $\mu$ M) at pH 5.0 for 1, 3 and 6 consecutive days. In majority of cases investigated KRT genes revealed the most efficient changes in mRNA expression reflecting these observed in human biopsies only when treatment was repeated for 6 consecutive days in contrast to those recorded at 1 or 3 days. Thus, we conclude that six days of treatment seems to be the most optimal for both tested cell-lines to induce a specific BE molecular pattern and these conditions have been chosen for further analysis of a broader spectrum of genes. Interestingly, for EPC2 cells three days of treatments were sufficient to induce this molecular pattern. Thus, to determine whether and how low pH and/or BM exposure can affect mRNA expression of squamous and columnar epithelium-specific genes observed in humans (**Table 2**), both Het-1A and EPC2 cells were exposed for 30 minutes daily in 6 consecutive days with BM (50  $\mu$ M and 100  $\mu$ M) at pH 5.0, or with BM (50  $\mu$ M and 100  $\mu$ M) and medium adjusted to pH 5.0 applied separately. We found that in EPC2 and Het-1A cells, BM at the concentration 50  $\mu$ M at pH 5.0, as well as BM and acidified medium (pH 5.0) applied separately were less effective in induction of gene expression changes characteristic for BE patients in comparison to the experiments in which BM in higher concentration of 100  $\mu$ M has been applied at pH 5.0. This clearly indicates that changes in the specific gene expression are dependent on bile concentration and acidic environment. Moreover, we observed that incubation of EPC2 cells with 100  $\mu$ M of BM at pH 5.0 downregulated mRNA expression of all investigated squamous epithelium-specific KRT genes as compared to untreated control cells. Interestingly, in Het-1A cells only *KRT15* mRNA expression was significantly downregulated. This is in accordance with observation by Mari et al. (25), who claimed that Het-1A cells lacked the expression of majority of squamous epithelium-specific KRT genes, confirming that this cell line has an incomplete squamous phenotype. In addition, in our study, more columnar epithelium-specific genes were upregulated in Het-1A in comparison to EPC2 under optimized experimental conditions. For instance, when Het-1A cells were treated with 100  $\mu$ M BM at pH 5.0, the expression of

columnar epithelium-specific *KRT8*, *TFF3*, *VIL1*, *MUC2* and *MUC13* was upregulated in comparison to untreated control cells. The same experimental conditions in EPC2 cells provoked upregulation of columnar epithelium-specific *KRT7*, *KRT18* and *TFF3* mRNA as compared to untreated control cells.

Summarized, alterations in BE-specific gene expression observed in human biopsies and *in vitro* and *in vivo* models were presented in **Table 5**.

**Table 5.** Summary of alterations in expression of squamous and columnar epithelium-specific genes observed in human biopsies and *in vitro* using Het-1A and EPC2 cells and *in vivo* EGDA rat model. A vertical up arrow (↑) indicates upregulation of mRNA expression in Barrett's metaplasia as compared with samples without Barrett's metaplasia/untreated control cells/intact rats; a vertical down arrow (↓) indicates downregulation of mRNA expression in Barrett's metaplasia as compared with samples without Barrett's metaplasia/untreated control cells/intact rats; a horizontal left right arrow (↔) indicates no changes in mRNA expression; n.a. indicates no amplification; n.d. not determined.

Gene symbol	Type of epithelium	<i>In vitro</i> models		<i>In vivo</i> model	Human biopsies
		Het-1A	EPC2		
KRT1	squamous	n.a.	↓	↑	↓
KRT4	squamous	n.a.	↓	↓	↓
KRT5	squamous	n.a.	↓	↑	↓
KRT6	squamous	↔	↓	n.d.	↓
KRT13	squamous	n.a.	↓	↓	↓
KRT14	squamous	n.a.	↓	↑	↓
KRT15	squamous	↓	↓	↓	↓
KRT16	squamous	↔	↓	n.a.	↓
KRT23	squamous	n.a.	↓	↔	↓
KRT24	squamous	n.a.	↓	n.a.	↓
KRT7	columnar	↔	↑	↑	↑
KRT8	columnar	↑	↔	↑	↑
KRT18	columnar	↔	↑	↑	↑
KRT20	columnar	n.a.	n.a.	↑	↑
TFF1	columnar	n.a.	n.a.	↓	↑
TFF2	columnar	n.a.	n.a.	n.a.	↑
TFF3	columnar	↑	↑	↑	↑
VIL1	columnar	↑	n.a.	↔	↑
MUC2	columnar	↑	n.a.	↑	↑
MUC3	columnar	n.a.	n.a.	n.a.	↑
MUC5B	columnar	n.a.	n.a.	n.a.	↑
MUC6	columnar	n.a.	n.a.	n.a.	↑
MUC13	columnar	↑	↔	↑	↑

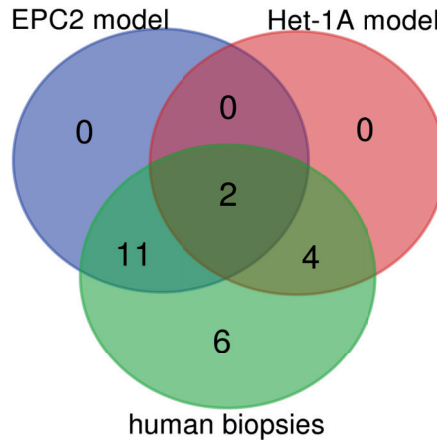


**Figure 11.** Venn diagram displaying numbers of up/downregulated genes in human biopsies derived from patients with Barrett's metaplasia as compared with *in vitro* Het-1A and EPC2 model of Barrett's esophagus. Overlap area shows the number of the same up/downregulated genes in the appropriate groups. Graphs were obtained through Venn diagrams software (available online: <http://bioinformatics.psb.ugent.be/webtools/Venn/>). Different color meant different datasets.

Based on our data, EPC2 and Het-1A cells react differently to the implemented chronic mixed acid and bile treatment. Interestingly, when we took a deeper look into the outcome of our investigations *in vitro*, we find that the expression pattern of analyzed genes demonstrated around 57% of similarities between the human biopsies and the EPC2 cells treated with acidic BM (**Figure 11, Table 5**). In turn, in Het-1A model only 26% of genes reflected the expression pattern similar to that obtained in biopsies from BE patients (**Figure 11, Table 5**).

Additionally, we have found that in animal BE model 45% of assessed genes were expressed in a pattern characteristic for human BE metaplasia (**Figure 12, Table 5**). In turn, when expression profile of both cell lines within the optimized *in vitro* BE model were analyzed together, 73% of genes reflected alterations observed in human biopsies (**Figure 12, Table 5**).

Taken together, we conclude that our optimized *in vitro* model based on two primary immortalized human esophageal squamous cell lines is suitable to observe an efficient induction markers specific for human BE epithelium. However, it is worth to mention that cell cultures apparently lack of systemic inflammatory response, the influence of esophageal microcirculation, microenvironmental factors, neural components, neuropeptides and cellular interactions characteristic for esophageal cells functioning *in vivo* (26, 43). Therefore, these doubts could be, at least in part, solved by studies in animal models of BE *in vivo* providing additional information about macroscopic, microscopic, functional and biochemical alterations. The animal model, applied

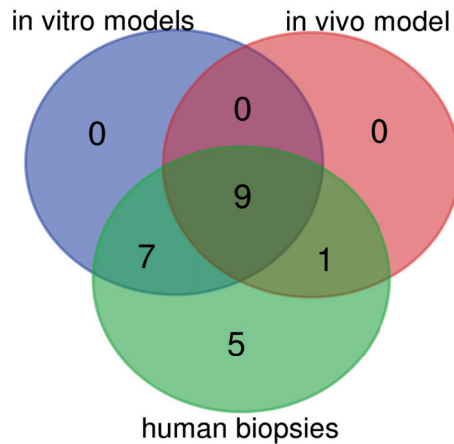


**Figure 12.** Venn diagram displaying numbers of up/downregulated genes in human biopsies derived from patients with Barrett's metaplasia as compared with *in vitro* (Het-1A and EPC2) models and surgical animal model of Barrett's esophagus. Overlap area shows the number of the same up/downregulated genes in the appropriate groups. Graphs were obtained through Venn diagrams software (available online: <http://bioinformatics.psb.ugent.be/webtools/Venn/>). Different color meant different datasets.

simultaneously with the optimized *in vitro* model could offer the opportunity to the evaluation of the molecular response and the effectiveness of possible drugs candidates targeting BE prevention and/or treatment.

## Acknowledgments

We would like to acknowledge Anna Chmura, MSc for her input related to the technical preparation of histological slides. This study was supported by research grant for M.M. received from National Science Centre Poland (UMO-2016/23/D/NZ4/01913) and from the National Centre for Research and Development, Poland (LIDER/9/0055/L-8/16/NCBR/2017).

## References

1. Bus P, Siersema PD, van Baal JW. Cell culture models for studying the development of Barrett's esophagus: a systematic review. *Cell Oncol (Dordr)*. 2012;35(3):149-61.
2. Kosoff RE, Gardiner KL, Merlo LM, Pavlov K, Rustgi AK, Maley CC. Development and characterization of an organotypic model of Barrett's esophagus. *J Cell Physiol*. 2012;227(6):2654-9.
3. Naini BV, Souza RF, Odze RD. Barrett's Esophagus: A Comprehensive and Contemporary Review for Pathologists. *The American journal of surgical pathology*. 2016;40(5):e45-66.

4. Su Z, Gay LJ, Strange A, Palles C, Band G, Whiteman DC, et al. Common variants at the MHC locus and at chromosome 16q24.1 predispose to Barrett's esophagus. *Nat Genet.* 2012;44(10):1131-6.
5. Jankowski JAZ, de Caestecker J, Love SB, Reilly G, Watson P, Sanders S, et al. Esomeprazole and aspirin in Barrett's oesophagus (AspECT): a randomised factorial trial. *Lancet.* 2018;392(10145):400-8.
6. Savarino E, Zentilin P, Frazzoni M, Cuoco DL, Pohl D, Dulbecco P, et al. Characteristics of gastro-esophageal reflux episodes in Barrett's esophagus, erosive esophagitis and healthy volunteers. *Neurogastroenterol Motil.* 2010;22(10):1061-e280.
7. Tolone S, Limongelli P, Romano M, Federico A, Docimo G, Ruggiero R, et al. The patterns of reflux can affect regression of non-dysplastic and low-grade dysplastic Barrett's esophagus after medical and surgical treatment: a prospective case-control study. *Surg Endosc.* 2015;29(3):648-57.
8. Stairs DB, Nakagawa H, Klein-Szanto A, Mitchell SD, Silberg DG, Tobias JW, et al. Cdx1 and c-Myc foster the initiation of transdifferentiation of the normal esophageal squamous epithelium toward Barrett's esophagus. *PLoS One.* 2008;3(10):e3534.
9. di Pietro M, Lao-Sirieix P, Boyle S, Cassidy A, Castillo D, Saadi A, et al. Evidence for a functional role of epigenetically regulated midcluster HOXB genes in the development of Barrett esophagus. *Proceedings of the National Academy of Sciences of the United States of America.* 2012;109(23):9077-82.
10. Van De Bovenkamp JH, Korteland-Van Male AM, Warson C, Buller HA, Einerhand AW, Ectors NL, et al. Gastric-type mucin and TFF-peptide expression in Barrett's oesophagus is disturbed during increased expression of MUC2. *Histopathology.* 2003;42(6):555-65.
11. Poehlmann A, Kuester D, Malfertheiner P, Guenther T, Roessner A. Inflammation and Barrett's carcinogenesis. *Pathol Res Pract.* 2012;208(5):269-80.
12. Squier CA, Kremer MJ. Biology of oral mucosa and esophagus. *Journal of the National Cancer Institute Monographs.* 2001(29):7-15.
13. Flejou JF. Barrett's oesophagus: from metaplasia to dysplasia and cancer. *Gut.* 2005;54 Suppl 1:i6-12.
14. Rees JR, Lao-Sirieix P, Wong A, Fitzgerald RC. Treatment for Barrett's oesophagus. *The Cochrane database of systematic reviews.* 2010(1):CD004060.
15. Majka J, Rembiasz K, Migaczewski M, Budzynski A, Ptak-Belowska A, Pabianczyk R, et al. Cyclooxygenase-2 (COX-2) is the key event in pathophysiology of barrett's esophagus. lesson from experimental animal model and human subjects. *Journal of Physiology and Pharmacology.* 2010;61(4):409-18.
16. Lagorce C, Paraf F, Vidaud D, Couvelard A, Wendum D, Martin A, et al. Cyclooxygenase-2 is expressed frequently and early in Barrett's oesophagus and associated adenocarcinoma. *Histopathology.* 2003;42(5):457-65.
17. Menke V, Pot RG, Moons LM, van Zoest KP, Hansen B, van Dekken H, et al. Functional single-nucleotide polymorphism of epidermal growth factor is associated with the development of Barrett's esophagus and esophageal adenocarcinoma. *Journal of human genetics.* 2012;57(1):26-32.
18. Jankowski J, Coghill G, Tregaskis B, Hopwood D, Wormsley KG. Epidermal growth factor in the oesophagus. *Gut.* 1992;33(11):1448-53.
19. Majka J, Wierdak M, Szlachcic A, Magierowski M, Targosz A, Urbanczyk K, et al. Interaction of epidermal growth factor with COX-2 products and peroxisome proliferator-activated receptor gamma system in experimental rat Barrett's esophagus. *Am J Physiol Gastrointest Liver Physiol.* 2020;318(3):G375-89.



20. Vona-Davis L, Frankenberry K, Cunningham C, Riggs DR, Jackson BJ, Szwerc MF, et al. MAPK and PI3K inhibition reduces proliferation of Barrett's adenocarcinoma in vitro. *The Journal of surgical research*. 2005;127(1):53-8.
21. Sarosi GA, Jr., Jaiswal K, Herndon E, Lopez-Guzman C, Spechler SJ, Souza RF. Acid increases MAPK-mediated proliferation in Barrett's esophageal adenocarcinoma cells via intracellular acidification through a Cl-/HCO<sub>3</sub>- exchanger. *Am J Physiol Gastrointest Liver Physiol*. 2005;289(6):G991-7.
22. Han YM, Park JM, Kangwan N, Jeong M, Lee S, Cho JY, et al. Role of proton pump inhibitors in preventing hypergastrinemia-associated carcinogenesis and in antagonizing the trophic effect of gastrin. *Journal of Physiology and Pharmacology*. 2015;66(2):159-67.
23. Ahrens TD, Lutz L, Lassmann S, Werner M. Turning Skyscrapers into Town Houses: Insights into Barrett's Esophagus. *Pathobiology*. 2017;84(2):87-98.
24. Kimchi ET, Posner MC, Park JO, Darga TE, Kocherginsky M, Karrison T, et al. Progression of Barrett's metaplasia to adenocarcinoma is associated with the suppression of the transcriptional programs of epidermal differentiation. *Cancer Res*. 2005;65(8):3146-54.
25. Mari L, Milano F, Parikh K, Straub D, Everts V, Hoebe KK, et al. A pSMAD/CDX2 complex is essential for the intestinalization of epithelial metaplasia. *Cell Rep*. 2014;7(4):1197-210.
26. Whelan KA, Muir AB, Nakagawa H. Esophageal 3D Culture Systems as Modeling Tools in Esophageal Epithelial Pathobiology and Personalized Medicine. *Cell Mol Gastroenterol Hepatol*. 2018;5(4):461-78.
27. Bus P, Siersema PD, Verbeek RE, van Baal JWPM. Upregulation of miRNA-143,-145,-192, and-194 in esophageal epithelial cells upon acidic bile salt stimulation. *Diseases of the Esophagus*. 2014;27(6):591-600.
28. Nehra D, Howell P, Williams CP, Pye JK, Beynon J. Toxic bile acids in gastro-oesophageal reflux disease: influence of gastric acidity. *Gut*. 1999;44(5):598-602.
29. Nishijima K, Miwa K, Miyashita T, Kinami S, Ninomiya I, Fushida S, et al. Impact of the biliary diversion procedure on carcinogenesis in Barrett's esophagus surgically induced by duodenoesophageal reflux in rats. *Ann Surg*. 2004;240(1):57-67.
30. Kohata Y, Fujiwara Y, Machida H, Okazaki H, Yamagami H, Tanigawa T, et al. Role of Th-2 cytokines in the development of Barrett's esophagus in rats. *Journal of Gastroenterology*. 2011;46(7):883-93.
31. Pera M, Brito MJ, Poulson R, Riera E, Grande L, Hanby A, et al. Duodenal-content reflux esophagitis induces the development of glandular metaplasia and adenosquamous carcinoma in rats. *Carcinogenesis*. 2000;21(8):1587-91.
32. Magierowska K, Korbut E, Hubalewska-Mazgaj M, Surmiak M, Chmura A, Bakalarz D, et al. Oxidative gastric mucosal damage induced by ischemia/reperfusion and the mechanisms of its prevention by carbon monoxide-releasing tricarbonyldichlororuthenium (II) dimer. *Free radical biology & medicine*. 2019;145:198-208.
33. Buskens CJ, Hulscher JB, van Gulik TM, Ten Kate FJ, van Lanschot JJ. Histopathologic evaluation of an animal model for Barrett's esophagus and adenocarcinoma of the distal esophagus. *The Journal of surgical research*. 2006;135(2):337-44.
34. Quante M, Abrams JA, Lee Y, Wang TC. Barrett esophagus: what a mouse model can teach us about human disease. *Cell Cycle*. 2012;11(23):4328-38.
35. Sayin SI, Baumeister T, Wang TC, Quante M. Origins of Metaplasia in the Esophagus: Is This a GE Junction Stem Cell Disease? *Dig Dis Sci*. 2018;63(8):2013-21.
36. Pavlov K, Maley CC. New models of neoplastic progression in Barrett's oesophagus. *Biochem Soc Trans*. 2010;38(2):331-6.
37. Attwood SE, Harrison LA, Preston SL, Jankowski JA. Esophageal adenocarcinoma in "mice and men": back to basics! *Am J Gastroenterol*. 2008;103(9):2367-72.

38. Wang RH. From reflux esophagitis to Barrett's esophagus and esophageal adenocarcinoma. *World J Gastroenterol*. 2015;21(17):5210-9.
39. Kapoor H, Lohani KR, Lee TH, Agrawal DK, Mittal SK. Animal Models of Barrett's Esophagus and Esophageal Adenocarcinoma-Past, Present, and Future. *Clinical and translational science*. 2015;8(6):841-7.
40. Nakagawa H, Whelan K, Lynch JP. Mechanisms of Barrett's oesophagus: intestinal differentiation, stem cells, and tissue models. *Best practice & research Clinical gastroenterology*. 2015;29(1):3-16.
41. Underwood TJ, Derouet MF, White MJ, Noble F, Moutasim KA, Smith E, et al. A comparison of primary oesophageal squamous epithelial cells with HET-1A in organotypic culture. *Biology of the cell*. 2010;102(12):635-44.
42. Sun TT, Shih C, Green H. Keratin cytoskeletons in epithelial cells of internal organs. *Proc Natl Acad Sci U S A*. 1979;76(6):2813-7.
43. Samarasena JB, Ahluwalia A, Tarnawski AS, Shinoura S, Choi KD, Lee JG, et al. Expression of Nerve Growth Factor, Its Trka Receptor, and Several Neuropeptides in Porcine Esophagus. Implications for Interactions between Neural, Vascular and Epithelial Components of the Esophagus. *Journal of Physiology and Pharmacology*. 2015;66(3):415-20.

## Supplementary information

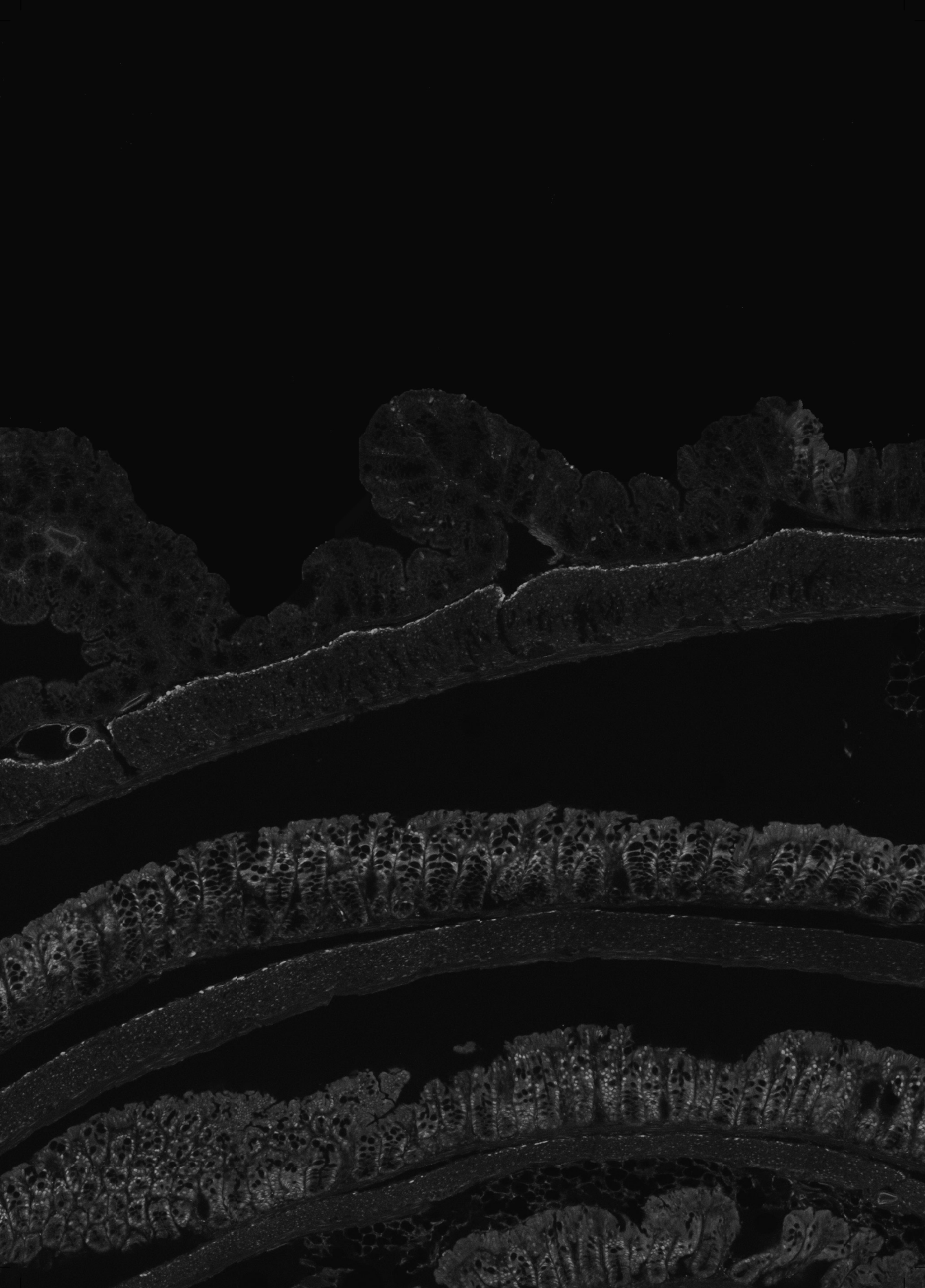
**Supplementary Table S1.** The list of selected human genes (and reference genes) and the corresponding TaqMan assays

No.	Gene name and symbol	Assay ID	NCBI gene reference
1	$\beta$ -actin, <i>ACTB</i>	Hs99999903_m1	NM_001101.3
2	Glyceraldehyde-3-phosphate dehydrogenase, <i>GAPDH</i>	Hs99999905_m1	NM_002046.5
3	Keratin 1, <i>KRT1</i>	Hs00196158_m1	NM_006121.3
4	Keratin 4, <i>KRT4</i>	Hs00361611_m1	NM_002272.3
5	Keratin 5, <i>KRT5</i>	Hs00361185_m1	NM_000424.3
6	Keratin 6A, <i>KRT6A</i>	Hs01699178_g1	NM_005554.3
7	Keratin 7, <i>KRT7</i>	Hs00559840_m1	NM_005556.3
8	Keratin 8, <i>KRT8</i>	Hs01670053_m1	NM_001256282.1
9	Keratin 13, <i>KRT13</i>	Hs00999762_m1	NM_153490.2
10	Keratin 14, <i>KRT14</i>	Hs00265033_m1	NM_000526.4
11	Keratin 15, <i>KRT15</i>	Hs00267035_m1	NM_002275.3
12	Keratin 16, <i>KRT16</i>	Hs00373910_g1	NM_005557.3
13	Keratin 18, <i>KRT18</i>	Hs02827483_g1	NM_000224.2
14	Keratin 20, <i>KRT20</i>	Hs00300643_m1	NM_019010.2
15	Keratin 23, <i>KRT23</i>	Hs01119992_m1	NM_015515.4
16	Keratin 24, <i>KRT24</i>	Hs00962561_m1	NM_019016.2
17	Mucin 2, oligomeric mucus/gel-forming, <i>MUC2</i>	Hs00159374_m1	NM_002457.3
18	Mucin 3A/B, cell surface associated, <i>MUC3A/B</i>	Hs03649367_mH	NM_005960.1
19	Mucin 6, oligomeric mucus/gel-forming, <i>MUC6</i>	Hs01674026_g1	NM_005961.2
20	Mucin 5B, oligomeric mucus/gel-forming, <i>MUC5B</i>	Hs00861588_m1	NM_002458.2
21	Mucin 13, cell surface associated, <i>MUC13</i>	Hs00217230_m1	NM_033049.3
22	Trefoil factor 1, <i>TFF1</i>	Hs00170216_m1	NM_003225.2
23	Trefoil factor 2, <i>TFF2</i>	Hs00193719_m1	NM_005423.4
24	Trefoil factor 3, <i>TFF3</i>	Hs00173625_m1	NM_003226.3
25	Villin 1, <i>VIL1</i>	Hs00200229_m1	NM_007127.2

**Supplementary Table S2.** The list of selected rat genes (and reference genes) and the corresponding TaqMan assays

No.	Gene name and symbol	Assay ID	NCBI gene reference
1	$\beta$ -actin, <i>ACTB</i>	Rn00667869_m1	NM_031144
2	Glyceraldehyde-3-phosphate dehydrogenase, <i>GAPDH</i>	Rn01462662_g1	NM_017008
3	Keratin 1, <i>KRT1</i>	Rn02346048_m1	NM_001008802
4	Keratin 4, <i>KRT4</i>	Rn02346072_m1	NM_001008806
5	Keratin 5, <i>KRT5</i>	Rn01533116_gH	NM_183333
6	Keratin 6, <i>KRT6</i>	not available	
7	Keratin 7, <i>KRT7</i>	Rn01533141_m1	XM_003750407
8	Keratin 8, <i>KRT8</i>	Rn01532759_g1	NM_199370
9	Keratin 13, <i>KRT13</i>	Rn01464231_m1	NM_001004021
10	Keratin 14, <i>KRT14</i>	Rn01467684_m1	NM_001008751
11	Keratin 15, <i>KRT15</i>	Rn01460389_m1	NM_001004022
12	Keratin 16, <i>KRT16</i>	Rn02345941_g1	NM_001008752
13	Keratin 18, <i>KRT18</i>	Rn01533362_g1	NM_053976
14	Keratin 20, <i>KRT20</i>	Rn00687576_m1	NM_173128
15	Keratin 23, <i>KRT23</i>	Rn01773106_m1	NM_001008753
16	Keratin 24, <i>KRT24</i>	Rn01471287_m1	NM_001004131
17	Mucin 2, oligomeric mucus/gel-forming, <i>MUC2</i>	Rn01498197_m1	XM_008760048
18	Mucin 3A, intestinal, <i>MUC3a</i>	Rn01481134_m1	XM_008769185
19	Mucin 5B, oligomeric mucus/gel-forming, <i>MUC5B</i>	Rn01502008_m1	XM_006230608
20	Mucin 6, oligomeric mucus/gel-forming, <i>MUC6</i>	Rn01759814_m1	XM_008760036
21	Mucin 13, cell surface associated, <i>MUC13</i>	Rn01647776_g1	XM_008768788
22	Trefoil factor 1, <i>TFF1</i>	Rn01428805_m1	NM_057129
23	Trefoil factor 2, <i>TFF2</i>	Rn00587721_m1	NM_053844
24	Trefoil factor 3, <i>TFF3</i>	Rn00564851_m1	NM_013042
25	Villin 1, <i>VIL1</i>	Rn01400773_g1	NM_001108224

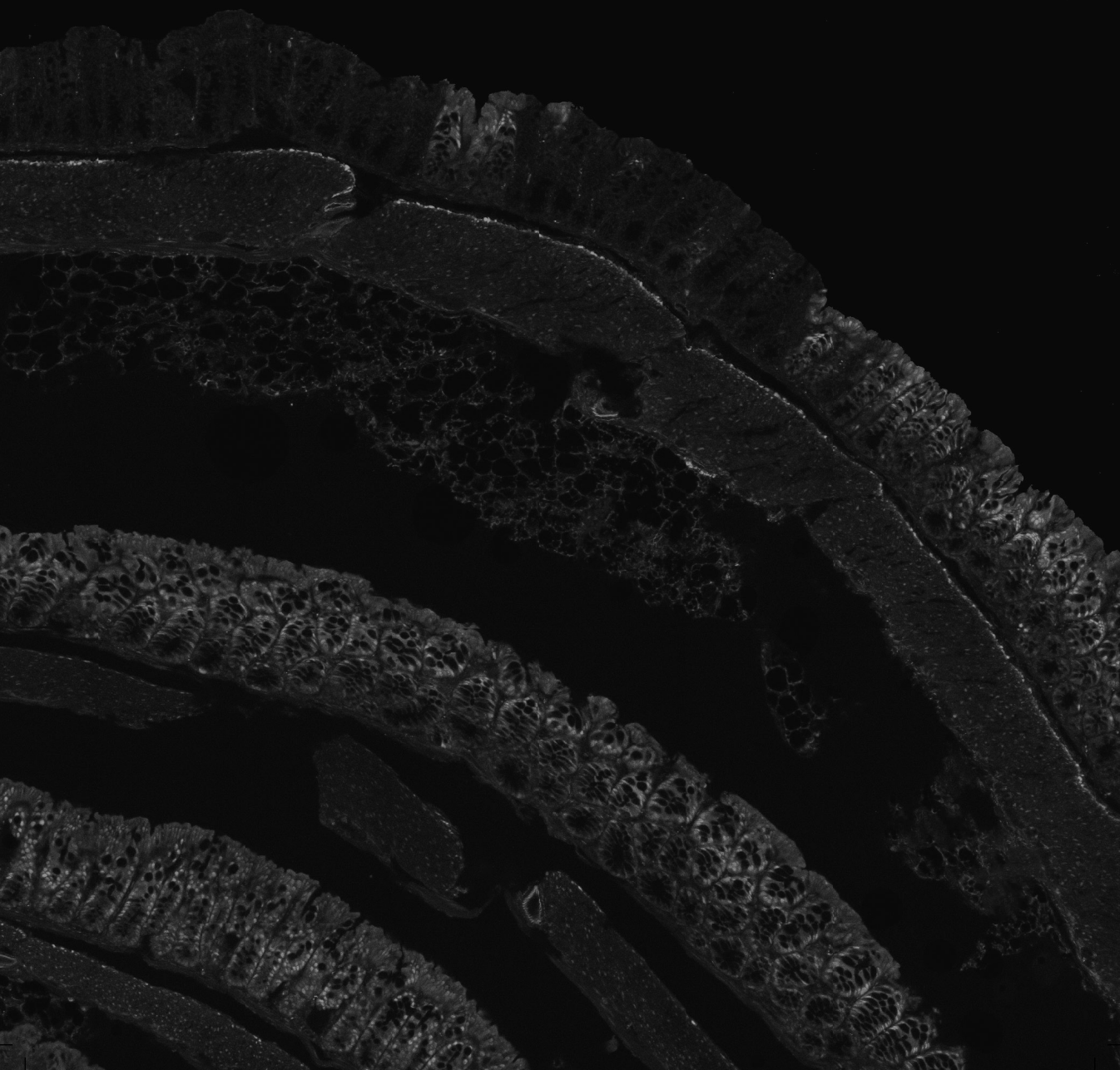




# Part 4

---

## Palliative treatment of esophageal cancer







# Chapter 9

---

## Palliative chemotherapy and targeted therapies for esophageal and gastroesophageal junction cancer

Vincent T. Janmaat · Ewout W. Steyerberg · Ate van der Gaast · Ron H.J. Mathijssen ·  
Marco J. Bruno · Maikel P. Peppelenbosch · Ernst J. Kuipers · Manon C.W. Spaander

## Abstract

Almost half of people with esophageal or gastroesophageal junction cancer have metastatic disease at the time of diagnosis. Chemotherapy and targeted therapies are increasingly used with a palliative intent to control tumor growth, improve quality of life, and prolong survival. To date, and with the exception of ramucirumab, evidence for the efficacy of palliative treatments for esophageal and gastroesophageal cancer is lacking. Our objective was to assess the effects of cytostatic or targeted therapy for treating esophageal or gastroesophageal junction cancer with palliative intent. We searched the Cochrane Central Register of Controlled Trials (CENTRAL), MEDLINE, Embase, the Web of Science, PubMed Publisher, Google Scholar, and trial registries up to 13 May 2015, and we hand searched the reference lists of studies. We did not restrict the search to publications in English. Additional searches were run in September 2017 prior to publication, and they are listed in the ‘Studies awaiting assessment’ section. We included randomized controlled trials (RCTs) on palliative chemotherapy and/or targeted therapy versus best supportive care or control in people with esophageal or gastroesophageal junction cancer. Two authors independently extracted data. We assessed the quality and risk of bias of eligible studies according to the Cochrane Handbook for Systematic Reviews of Interventions. We calculated pooled estimates of effect using an inverse variance random-effects model for meta-analysis. We identified 41 RCTs with 11,853 participants for inclusion in the review as well as 49 ongoing studies. For the main comparison of adding a cytostatic and/or targeted agent to a control arm, we included 11 studies with 1347 participants. This analysis demonstrated an increase in overall survival in favor of the arm with an additional cytostatic or targeted therapeutic agent with a hazard ratio (HR) of 0.75 (95% confidence interval (CI) 0.68 to 0.84, high-quality evidence). The median increased survival time was one month. Five studies in 750 participants contributed data to the comparison of palliative therapy versus best supportive care. We found a benefit in overall survival in favor of the group receiving palliative chemotherapy and/or targeted therapy compared to best supportive care (HR 0.81, 95% CI 0.71 to 0.92, high-quality evidence). Subcomparisons including only people receiving second-line therapies, chemotherapies, targeted therapies, adenocarcinomas, and squamous cell carcinomas all showed a similar benefit. The only individual agent that more than one study found to improve both overall survival and progression-free survival was ramucirumab. Palliative chemotherapy and/or targeted therapy increased the frequency of grade 3 or higher treatment-related toxicity. However, treatment-related deaths did not occur more frequently. Quality of life often improved in the arm with an additional agent. In conclusion, people who receive more chemotherapeutic or targeted therapeutic agents have an increased overall survival compared to people who receive less. These agents, administered as both first-line or second-line treatments, also led to better overall survival than best supportive care. With the exception of ramucirumab, it remains unclear which other individual agents cause the survival benefit. Although treatment associated toxicities of grade 3 or more occurred more frequently in arms with an additional chemotherapy or targeted therapy agent, there is no evidence that palliative chemotherapy and/or targeted therapy decrease quality of life. Based on this meta-analysis, palliative chemotherapy and/or targeted therapy can be considered standard care for esophageal and gastroesophageal junction carcinoma.

## Plain language summary

This review aimed to investigate the effectiveness of adding cytostatic or targeted therapy to supportive care in people with esophageal or gastroesophageal junction cancer. Esophageal cancer is the eighth most common cancer in the world. Many people are diagnosed only after the disease has spread to other parts of the body, when cure is rarely possible. These people can be treated with palliative chemotherapy or targeted therapy (a drug directed against a specific component of the tumor). The aim of this treatment is to control tumor growth and increase survival, without a significant decrease in quality of life. We searched reference lists, biomedical databases (Cochrane Central Register of Controlled Trials (CENTRAL), MEDLINE, Embase, the Web of Science, PubMed Publisher, and Google Scholar), and trial registries up to 13 May 2015. Additional searches were run in September 2017 prior to publication, and they are listed in the 'Studies awaiting assessment' section. We identified 41 randomized controlled trials (RCTs) that met our inclusion criteria for inclusion in the review, as well as 49 ongoing studies. This review and meta-analysis shows that people who receive more chemotherapeutic or targeted therapeutic agents live longer and with less disease progression than people who receive best supportive care or less therapy. The only individual agent that more than one study found to improve survival was ramucirumab. We found severe treatment-associated toxicities (grade 3 or above) more frequently in the arms with an additional chemotherapy or targeted therapy agent. However, there is no evidence that palliative chemotherapy and/ or targeted therapy decreases quality of life. Our meta-analysis indicates that chemotherapy and targeted therapy are effective palliative treatments for people with esophageal and gastroesophageal junction cancer. The evidence that more chemotherapeutic or targeted therapeutic agents increase survival is of high quality, as is the evidence for improved survival compared to best supportive care. The evidence for the increased occurrence of severe treatment-related toxicities is of very low quality, while the evidence showing no decrease in quality of life is also low quality.

## Introduction

See Appendix 1 for a glossary of key terms.

### Description of the condition

#### *Epidemiology*

Esophageal cancer is the eighth most common cancer worldwide (Arnold 2015), with approximately 398,000 people diagnosed with squamous cell carcinoma (SCC) and 52,000 with adenocarcinoma in 2012. This corresponds with incidence rates of 5.2 and 0.7 per 100,000 population, respectively. Adenocarcinomas develop from metaplastic Barrett mucosa located in the lower esophagus, while SCC develops from the squamous epithelium (Enzinger 2003). Both histological types have dysplasia as their precursor. Recent epidemiological data indicate that 79% of SCCs worldwide occur in Southeastern and Central Asia, whereas 46% of people with adenocarcinomas are diagnosed in Northern and Western Europe, North America, and Oceania. In general, incidence of esophageal cancer is higher in men than in women, especially in adenocarcinoma, for which the male to female ratio is 4.4:1, compared to 2.7:1 for SCC (Arnold 2015). In the past few decades, developed countries have seen an increase in the incidence of adenocarcinoma (Edgren 2013), attributed to the higher prevalence of obesity. On the other hand, the decreasing incidence of SCC in these contexts correlates with the decline in smoking (Cook 2009). SCC remains most common in low- and middle-income countries, including in Africa and Eastern Asia (Lin 2013, Ocamo 2008, Somdyala 2010, White 2009). Almost half of people with esophageal carcinoma have distant disease at the time of diagnosis (Howlader 2014).

#### *Prognosis and management options*

Endoscopic therapy may be an option for early oesophageal cancers, but a Cochrane Review found no randomized controlled trials (RCTs) comparing management options for this early stage (Bennett 2012). Surgical resection is the potentially curative treatment for esophageal cancer, but it is only feasible in people who are fit for surgery, have locally resectable disease, and show no signs of distant metastases. Unfortunately, most people develop recurrent tumor growth within the first few years after surgery. Palliative care is the only option for metastatic disease, with a five year survival rate of less than three per cent (Hur 2013). Palliative therapy aims to control tumor growth and increase survival without significantly decreasing quality of life.

### Description of the intervention

In daily practice, clinicians often offer palliative chemotherapy to control tumor growth, increase quality of life, and increase life expectancy. Clinicians have the option

to choose from cytostatic therapy, which is directed at fast dividing cells in general, or from targeted therapies directed against specific molecules needed for carcinogenesis and tumor growth. The most extensively used agents for this disease are 5-fluorouracil (5-FU) and cisplatin, which are included in most combination chemotherapy regimens. However, the chemotherapy agents used in RCTs are very heterogeneous. Researchers have examined targeted therapies as palliative treatment for a decade (Lorenzen 2009). People treated with these anti-neoplastic agents experience fewer side effects compared to people treated with classic cytotoxic chemotherapies. The most common targets studied are the epidermal growth factor receptor (EGFR) and the vascular endothelial growth factor receptor two (VEGFR2). Most targeted therapies studied are monoclonal antibodies, except for the tyrosine kinase inhibitor, gefitinib (Dutton 2014).

### **Why it is important to do this review**

Palliative chemotherapy and/or targeted therapies are widely accepted treatment options. However, except for ramucirumab, evidence for the efficacy of palliative treatment for esophageal and gastroesophageal cancer is lacking. To assess whether a benefit exists, there is a need for large randomized studies assessing the effects of chemotherapy or targeted therapy for treating people with esophageal and GE-junction cancer with palliative intent. In a randomized gastric cancer study, (Thuss-Patience 2011) reported that accrual for first-line studies is very difficult because most people refuse randomization, so new data from large randomized studies investigating first-line chemotherapy or targeted therapy versus best supportive care (BSC) will probably not become available. On the other hand, interesting new data have become available regarding targeted therapies and second line therapies. Due to the limited availability of relevant data, summarizing the available evidence could increase insight into whether chemotherapy and targeted therapies are justifiably being prescribed to people with advanced or metastatic esophageal or gastroesophageal (GE)-junction cancer.

We have chosen to construct the main meta-analysis in a way that summarizes the largest number of studies. The downside of this approach is the heterogeneity of the included studies in terms of intervention and participant groups. Because this approach complicates the straightforward translation of results to individuals, we performed subgroup analyses wherever possible to investigate whether the overall result was consistent across subsets of treatments and participants.

### **Objectives**

To assess the effects of cytostatic or targeted therapy for treating esophageal or gastroesophageal junction cancer with palliative intent.

## Methods

### Criteria for considering studies for this review

#### *Types of studies*

We included RCTs with or without blinding. We included abstracts that met the inclusion criteria and that reported data on review outcomes as studies awaiting classification. If the abstract was a study protocol, we included it as an ongoing study.

We excluded all non-randomized and quasi-randomized studies, as we considered they did not provide sufficiently high-quality evidence.

#### *Types of participants*

People with advanced (T3-T4NxM0 non-resectable; and all TxNxM1), recurrent, or metastatic carcinoma of the esophagus and GE-junction. We included only studies involving participants with advanced or non-resectable disease who received chemotherapy with palliative intent. We did not consider studies including participants receiving chemotherapy for locally advanced cancer in order to assess resectability. We included people with both SCC and adenocarcinoma, as well as people who had received prior chemotherapy.

We included in the qualitative synthesis studies involving only a subset of eligible participants, for instance studies including participants with both GE-junction cancer and gastric cancer, if they described the results for GE-junction cancer separately and included at least 15 eligible participants. We evaluated these studies for inclusion in the quantitative synthesis under certain circumstances (see Sensitivity analysis).

#### *Types of interventions*

We included treatments with systemic intravenous and single oral chemotherapy or targeted therapy, as well as combination regimens in all doses and schedules. We defined 'control arm' as BSC or treatment with at least one chemotherapy agent whose composition, dose, and schedule were equal in both arms. Dose defining RCTs were not eligible for this review. Chemotherapy encompassed all cytotoxic and anti-neoplastic drug treatment, and targeted therapy encompasses all anti-neoplastic drug treatment targeting a specific protein or small group of proteins. We did not consider combined radiochemotherapy or radio-targeted therapy interventions for this review.

Our main comparison was chemotherapy or targeted therapy agent(s) plus any control intervention versus control intervention alone. We also performed a sensitivity analysis to assess the effect of the intervention in people with esophageal and GE-junction cancer versus gastric cancer.

Finally, we performed several subgroup analyses.

- a. Chemotherapy or targeted therapy plus BSC versus BSC.
- b. Effect of intervention in participants who had received previous chemotherapy (versus control intervention alone).
- c. Chemotherapeutic agent plus control intervention versus control intervention alone.
- d. Targeted therapeutic agent plus control intervention versus control intervention alone.
  - i. Epidermal growth factor receptor (EGFR)-targeting agent plus control intervention versus control intervention alone.
  - ii. Cetuximab plus control intervention versus control intervention alone.
  - iii. Ramucirumab plus control intervention versus control intervention alone.
- e. Chemotherapy or targeted therapy agent(s) plus control intervention versus control intervention alone in people with adenocarcinoma of the esophagus.
- f. Chemotherapy or targeted therapy agent(s) plus control intervention versus control intervention alone in people with SCC of the esophagus.

#### ***Types of outcome measures***

We did not use the outcome measures mentioned below as inclusion criteria but as a list of outcome measures of interest to this review.

#### ***Primary outcomes***

Median overall survival (OS) (time to death) and hazard ratio (HR) with 95% confidence interval (CI).

#### ***Secondary outcomes***

- Median progression-free survival (PFS) (time to disease progression and/or death) and HR with 95% CI.
- Toxicity (type, severity, and percentage of acute and chronic toxic effect, including toxic death), classified according to World Health Organization (WHO) or National Cancer Institute Common Toxicity Criteria (NCI-CTC). The focus was on toxicities of grade 3 or higher. Grade 3 toxicities are described in the Common Terminology Criteria for Adverse Events (CTCAE) Version 4.0 as “severe or medically significant but not immediately life-threatening; hospitalization or prolongation of hospitalization indicated; disabling; limiting self-care activities of daily living” (Common Toxicity Criteria 4.0).
- Quality of life (including all validated outcome measures).

## **Search methods for identification of studies**

### ***Electronic searches***

We identified records by searching the following electronic databases using the search strategies detailed in the appendices.

1. Cochrane Central Register of Controlled Trials (CENTRAL; 2017, Issue 9) in the Cochrane Library (searched 19 September 2017; Appendix 2).
2. MEDLINE (1950 to 19 September 2017; Appendix 3).
3. Embase (1980 to 19 September 2017; Appendix 4).
4. Web of Science (1900 to 19 September 2017; Appendix 5).
5. Pubmed Publisher (1950 to 19 September 2017; Appendix 6).
6. Google Scholar (1592 to 19 September 2017; Appendix 7).
7. Clinicaltrials.gov (searched 19 September 2017; Appendix 8).
8. WHO International Clinical Trials Registry Platform (ICTRP) (searched 19 September 2017; Appendix 9).

We constructed the search strategy by applying a sensitivity maximizing approach, using a combination of MeSH subject headings and text words related to chemotherapy or targeted therapy with a palliative intent for cancer of the esophagus and GE-junction. We adapted the MEDLINE search strategy for use in the other databases. We did not confine the search to English-language publications. We placed studies identified after the search of 13 May 2015 in ‘Studies awaiting classification’ or ‘Ongoing studies’. In the next version of the review, we will screen these and incorporate them as appropriate.

### ***Searching other resources***

We hand-searched reference lists from studies included in the qualitative assessment to identify further relevant studies. Additionally, within the retrieved records, we identified and selected reviews based on title and abstract, extracting relevant references and including them as retrieved records.

## **Data collection and analysis**

### ***Selection of studies***

Two review authors (VJ, MS) independently scanned the title and abstract of every record retrieved during the search. If the information given suggested that the RCT included participants with advanced (T3-T4NxM0 non-resectable; and all TxNxM1), recurrent, or metastatic carcinoma of the esophagus or GE-junction and used random allocation to generate the comparison groups, or if there was any doubt regarding these criteria, we retrieved the full text for detailed assessment. We resolved differences in data extraction through discussion.



**Data extraction and management**

Two review authors (VJ, MS) independently extracted details on study population, interventions, and outcomes by using a standardized data extraction form, which included the following items.

- General information: title, authors, source, contact address, country, publication status, full paper/abstract, language, and year of publication.
- Study characteristics: design, allocation concealment, blinding, number of arms, phase, and duration of follow-up.
- Participants: inclusion and exclusion criteria, sample size, baseline characteristics, similarity of groups at baseline, dropouts described, and ITT performed.
- Intervention: which comparison was performed, type, dose, route, and schedule of drug administration.
- Outcomes: as specified above: median OS and PFS, HRs and their 95% CIs, toxicity, and quality of life.

We contacted authors of all eligible studies to provide us with individual participant data.

**Assessment of risk of bias in included studies**

Two review authors (VJ, MS) independently assessed the risk of bias and the quality of the eligible studies according to the Cochrane Handbook for Systematic Reviews of Interventions (Higgins). In case of disagreements, they consulted a third review author to reach consensus. We extracted data using the assessment form designed for this review.

We assessed each study taking into account the following points (Higgins); (Jadad 1996).

- Was the allocation random?
- Was the concealment of treatment allocation adequate?
- Was the study blinded?
- Was there selective reporting?
- Were the groups similar at baseline?
- Were the number of withdrawals, dropouts, and losses to follow-up described?
- Was intention-to-treat analysis performed?

We rated each study as being at low, high, or unclear risk of bias for these domains.

We defined baseline comparability as follows: we considered the most important prognostic factors to be tumor stage (advanced versus metastatic disease), performance index (Eastern Cooperative Oncology Group (ECOG) status 0 to 1 versus 2 to 3), and the number of organs involved in metastatic disease (one versus more than one). We considered a difference of more than 15% between study arms to be clinically relevant. For the median age of participants in treatment arms, we considered baseline differences of five years to be clinically relevant.

We defined intention-to-treat analysis as either randomized analysis restricted to participants who received at least one cycle of chemotherapy or targeted therapy and for which survival data were available, or methodologies that included all participants at randomization in the analysis.

### ***Measures of treatment effect***

We extracted or directly or indirectly estimated HRs and 95% CIs from the given data in each included study (Altman 2001). If we could not extract the data directly from the text, we determined them indirectly. For example, we estimated HRs from ratios of median survival times, from observed to expected event ratios and from time point survival ratios (Machin 1997); (Parmar 1998). Sometimes, we had to read these ratios from a Kaplan-Meier graph provided in the paper. We extracted median overall and progression-free survival times if available.

### ***Dealing with missing data***

Where studies did not report outcomes directly, we calculated them if possible (see Measures of treatment effect) and reported them narratively if not.

### ***Assessment of heterogeneity***

For each data synthesis, we calculated pooled estimates of effect and investigated results for statistical heterogeneity. We assessed forest plots for heterogeneity by visual inspection. To quantify inconsistency across studies, we calculated the  $I^2$  statistic as  $((Q - df)/Q) \times 100\%$ , where  $Q$  is the  $\text{Chi}^2$  statistic and  $df$  its degrees of freedom. See also Sensitivity analysis.

### ***Assessment of reporting biases***

We assessed small study effects such as publication bias in a qualitative manner using a funnel plot if enough studies were present (i.e. at least 10).

### ***Data synthesis***

In the meta-analyses, we aimed to combine data from different RCTs reporting similar comparisons. Therefore, only RCTs in which treatments were added to BSC or a control arm were included. Given the amount of variation in the interventions studied in the included studies, we calculated pooled estimates of effect using an inverse variance random-effects model for the meta-analyses. We did not include all studies in the quantitative synthesis. Under Included studies, subheading 'Interventions', we give a summary of which agents are included in the analyses.

We synthesized data on OS and PFS in meta-analyses, and we summarized data on toxicity and quality of life. We present the results on toxicity and quality of life narratively for the main comparison but not for the subcomparisons.

**Subgroup analysis and investigation of heterogeneity**

For the main objective, we identified six subcomparisons. In subcomparison 1, we investigated chemotherapy or targeted therapy plus BSC versus BSC alone. In subcomparison 2, we investigated the effect of the intervention for second-line chemotherapy or targeted therapy. For subcomparison 3, we included only interventions with a chemotherapy drug. For subcomparison 4, we included only interventions with a targeted therapy agent. For subcomparison four, we identified three further subgroups. The first subgroup, 4a, consisted of studies that investigated regimens containing EGFR-targeting agents versus those containing a non-EGFR-targeting agent. The second subgroup, 4b, consisted of studies that investigated cetuximab versus non-cetuximab containing regimens. The third subgroup, 4c, consisted of studies that investigated regimens that contained ramucirumab versus those that did not. In subcomparison 5, we investigated chemotherapy or targeted therapy agent(s) plus control intervention versus control intervention alone in people with adenocarcinoma of the esophagus. In subcomparison 6, we assessed the same comparison for people with SCC of the esophagus.

**Sensitivity analysis**

A potential effect modifier in the meta-analyses was the inclusion of studies that included participants with gastric cancer. If the effect of the interventions investigated in the included studies were similar for both participants with esophageal or GE-junction cancer versus participants with gastric cancer, it would have been reasonable to include studies involving participants with any of these cancers and which did not report results separately for these groups. Thereto, we investigated eligibility for inclusion into the quantitative synthesis by assessing the effect of the interventions on both the esophageal and GE-junction versus the gastric cancer subgroups. We compared all studies included in the meta-analysis of the main comparison for OS (including only esophageal and GE-junction) to a group of studies that had included participants with esophageal, GE-junction, and gastric cancer, through a random-effects meta-regression analysis using the R statistical computing software (R 2014). In this meta-regression analysis, the interventions in both groups of studies were not similar. Therefore, we performed a second meta-regression analysis that focused on studies reporting the effect of the intervention on OS for esophageal and GE-junction cancer groups and gastric cancer groups separately. If non-significant heterogeneity existed between the two groups of participants, we included studies containing a subset of eligible participants for the main analysis.

**Summary of findings tables**

We used the GRADE system to assess the quality of evidence for each analysis (Guyatt 2008), presenting our assessments in 'Summary of findings' tables using Review Manager 5 (RevMan 2014). The GRADE system describes the quality of evidence based on how

confident the authors are that an estimate of effect reflects the comparison being assessed. The quality of evidence considers study limitations, inconsistent results, indirectness of evidence, imprecision, and publication bias. We present the synthesized data and these assessments in 'Summary of findings' tables, using Review Manager 5 (RevMan 2014).

## Results

### Description of studies

See: Characteristics of included studies; Characteristics of excluded studies; Characteristics of studies awaiting classification; Characteristics of ongoing studies.

### Results of the search

We retrieved 5786 unique records and excluded 5571 after screening title and abstract. We excluded 69 (see Excluded studies and **Figure 1**). The quantitative synthesis includes 41 studies. We added a total of 46 and 49 potential new studies of interest to a list of 'Studies awaiting classifications' and 'Ongoing studies', respectively. We will assess these and incorporate as appropriate in the next version of this review.

### Included studies

Eleven studies in 1347 participants contributed data to the meta-analysis of the main comparison: chemotherapy or targeted therapy agent(s) plus control intervention versus control intervention alone. For more details about the included studies, see Characteristics of included studies. We performed six subcomparisons, described below.

### Participants

The median age of participants in the population included in the meta-analyses was 60 years (range 53 to 72 years). The proportion of participants reported as having metastatic disease ranged from 69% in (Al-Batran 2013) to 100% in (Nicolaou 1982). We could not extract the percentage of people with metastasis in 5 out of 19 studies included in the meta-regression analyses. For information on individual studies, see Characteristics of included studies.

With regard to baseline differences, we saw a five-year difference in median age between the study arms in one trial (Rao 2010). In another, the proportion of the metastatic sites involved per participant was not similar at baseline: 29% of participants in the intervention group had one site involved, compared to 58% in the BSC group (Thuss-Patience 2011). Performance status was well balanced in all studies, with no differences greater than 15% between study arms. The percentage of participants with ECOG-2 or -3 was in the range of 0% to 35%.

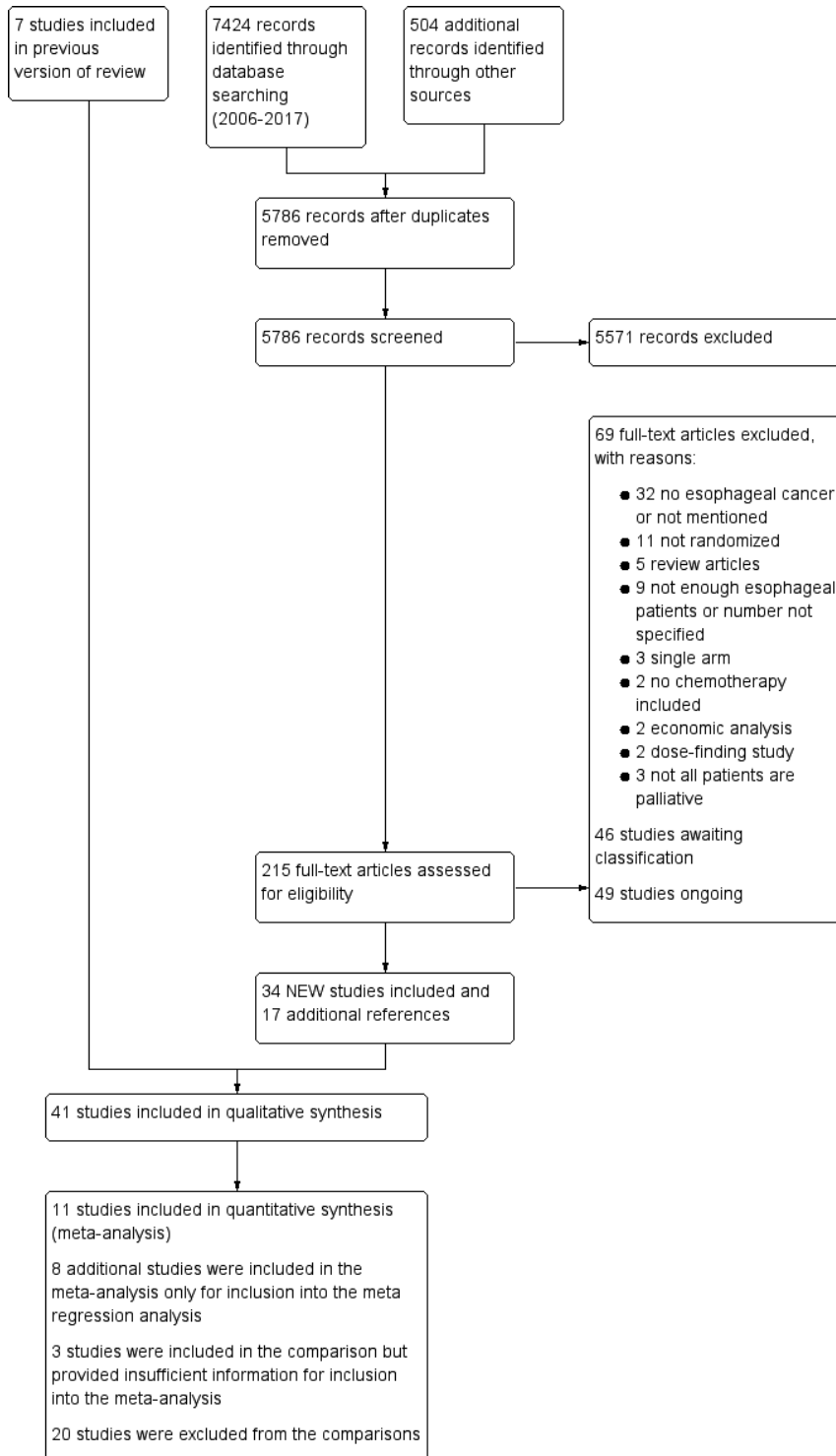


**Figure 1.** Study flow diagram: review update.

Seven studies included in the meta-analyses took place completely or partially in Asia (Bang 2010); (Fuchs 2014); (Huang 2009); (Lordick 2013); (Ohtsu 2011); (Shen 2014); (Wilke 2014), (Xu 2013). One study was translated from Chinese (Huang 2009).

Two studies selected participants based on biomarker expression. The effect of a targeted therapeutic can be expected to depend on the presence of the target in the tumor. The first included only EGFR-positive participants (Lorenzen 2009). The second included only participants that were eligible if their tumor samples, stained with HER2, were scored as 3 or more on immunohistochemistry or if they tested positive using fluorescent in situ hybridization (FISH) analysis (HER2:CEP17 ratio X 2) (Bang 2010). The results of these studies cannot be extrapolated to people that do not have biomarker expression as defined by these studies.

## Comparisons

### *Main comparison*

Eleven studies contributed data to the meta-analysis for the main comparison: chemotherapy or targeted therapy agent(s) plus control intervention versus control intervention alone in people with esophageal and GE-junction cancer. Trials used the following agents: 5-FU (Bleiberg 1997), 5-FU and cisplatin (Levard 1998), cetuximab (Lordick 2013); (Lorenzen 2009), cyclophosphamide and doxorubicin (Nicolaou 1982), docetaxel (Ford 2014), gefitinib (Dutton 2014), ramucirumab (Fuchs 2014); (Wilke 2014), Shenyi Capsule (Huang 2009), and trastuzumab (Bang 2010). Six studies were first-line therapy regimens (Bang 2010); (Bleiberg 1997); (Levard 1998); (Lordick 2013); (Lorenzen 2009); (Nicolaou 1982), one was a mixed therapy (Huang 2009), and the others were second-line treatments. Three studies were included in the main comparison but did not provide enough detail for inclusion in the meta-analysis (Eatock 2013); (Wilkes 2011); (Xu 2013).

### *Sensitivity analysis*

We compared the effect of the intervention in the studies of the main comparison to the effect of intervention in the studies that also included gastric cancer participants. These studies investigated: bevacizumab (Ohtsu 2011); (Shen 2014), cetuximab (Richards 2013), docetaxel (Al-Batran 2013), irinotecan (Thuss-Patience 2011), matuzumab (Rao 2010), mitomycin (Tebbutt 2002), and rilotumumab (Iveson 2014). Six studies were first-line therapies (Al-Batran 2013); (Iveson 2014); (Ohtsu 2011), (Rao 2010); (Shen 2014); (Tebbutt 2002), and two were mixed or unclear (Richards 2013); (Thuss-Patience 2011). The subsequent meta-regression analysis focused on studies that reported the effectiveness of the intervention for GE-junction and gastric cancer participants separately. We made a direct comparison with regard to the effectiveness of treatment on these two subgroups in five studies: (Bang 2010) (trastuzumab), (Ford

2014) (docetaxel), (Fuchs 2014) (ramucirumab), (Lordick 2013) (cetuximab), and (Wilke 2014) (ramucirumab). Two studies focused on first-line therapy regimens (Bang 2010); (Lordick 2013), and three used second-line therapies (Ford 2014); (Fuchs 2014); (Wilke 2014). SCCs were not included in any of these studies.

#### *Subcomparison 1*

Five studies investigated chemotherapy or targeted therapy plus BSC versus BSC, using the following agents: cyclophosphamide plus doxorubicin (Nicolaou 1982), 5-FU plus cisplatin (Levard 1998), docetaxel (Ford 2014), ramucirumab (Fuchs 2014), and gefitinib (Dutton 2014). Two studies were first-line therapy regimens (Nicolaou 1982); (Levard 1998), and the others were second-line regimens.

#### *Subcomparison 2*

Four studies investigated second-line therapy regimens. (Dutton 2014) investigated gefitinib in participants with progression after chemotherapy and excluded participants receiving either cytotoxic chemotherapy, immunotherapy, hormonal therapy, or radiotherapy to the site of measurable or evaluable disease within the four weeks prior to inclusion. (Ford 2014) investigated docetaxel in a participant population with documented disease progression during or within six months of treatment with platinum and fluoropyrimidine-based treatment. These participants were not allowed to have had previous chemotherapy with a taxane. (Fuchs 2014) investigated ramucirumab in a participant population with disease progression either within four months of the last dose of first-line platinum-containing or fluoropyrimidine-containing chemotherapy for metastatic disease, or within six months of the last dose of platinum-containing or fluoropyrimidine-containing adjuvant treatment. (Wilke 2014) investigated ramucirumab with participants that had disease progression during or within four months of the last dose of first-line platinum and fluoropyrimidine doublet.

#### *Subcomparison 3*

Five studies compared a chemotherapy agent(s) plus control intervention versus control intervention, using the following agents: 5-FU (Bleiberg 1997), 5-FU plus cisplatin (Levard 1998), docetaxel (Ford 2014), cyclophosphamide plus doxorubicin (Nicolaou 1982), and Shenyi Capsule (Huang 2009). Three studies were first-line therapy regimens (Bleiberg 1997); (Levard 1998); (Nicolaou 1982), one used mixed therapies (Huang 2009), and one a second-line regimen (Ford 2014). One study included in the subcomparison did not provide enough detail for inclusion in the meta-analysis (Wilkes 2011).

#### *Subcomparison 4*

Six studies compared a targeted therapeutic agent plus control intervention versus control intervention alone, testing the following agents: cetuximab (EGFR) (Lordick

2013); (Lorenzen 2009), gefitinib (tyrosine kinase inhibitor for EGFR) (Dutton 2014), ramucirumab (VEGFR2) (Fuchs 2014); (Wilke 2014), and trastuzumab (HER2) (Bang 2010). Three studies focused on first-line regimens (Bang 2010); (Lordick 2013); (Lorenzen 2009), and the others used second-line therapies. One study was included in the subcomparison but did not provide enough detail for inclusion in the meta-analysis (Xu 2013).

Subgroup 4a. Three studies investigated EGFR-targeting agents plus control intervention versus control intervention alone (Dutton 2014); (Lordick 2013); (Lorenzen 2009). Two studies were first-line therapies (Lordick 2013); (Lorenzen 2009), and one was a second-line regimen (Dutton 2014). One study was included in the subgroup but did not provide enough detail for inclusion in the meta-analysis (Xu 2013).

Subgroup 4b. Two studies investigated the EGFR-targeting agent cetuximab plus control intervention versus control intervention alone, both with first-line therapy regimens (Lordick 2013); (Lorenzen 2009).

Subgroup 4c. Two studies compared VEGFR2-targeting agent ramucirumab plus control intervention versus control intervention alone, both with second-line therapies (Fuchs 2014); (Wilke 2014).

#### *Subcomparison 5*

Five studies investigated chemotherapy or targeted therapy agent(s) plus control intervention versus control intervention alone in participants with adenocarcinoma of the esophagus, using the following agents: trastuzumab (Bang 2010), docetaxel (Ford 2014), ramucirumab (Fuchs 2014), cetuximab (Lordick 2013), and ramucirumab (Wilke 2014). Two studies were first-line therapy regimens (Bang 2010); (Lordick 2013), and three were second-line therapies (Ford 2014); (Fuchs 2014); (Wilke 2014). One study was included in the subcomparison but did not provide enough detail for inclusion in the meta-analysis (Eatock 2013).

#### *Subcomparison 6*

Five studies investigated chemotherapy or targeted therapy agent(s) plus control intervention versus control intervention alone in participants with SCC of the esophagus, using 5-FU (Bleiberg 1997), 5-FU and cisplatin (Levard 1998), cetuximab (Lorenzen 2009), doxorubicin (Nicolaou 1982), and gefitinib (Dutton 2014). Four studies were first-line therapy regimens (Bleiberg 1997); (Levard 1998); (Lorenzen 2009), (Nicolaou 1982), and one was a second-line therapy (Dutton 2014). One study was included in the subcomparison but did not provide enough detail for inclusion in the meta-analysis (Xu 2013).



We describe all interventions in detail, along with the type and location of the tumors, in the Characteristics of included studies. We defined second-line therapy studies as including only participants that had received previous chemotherapy or targeted therapy within six months of starting the study regimen, including adjuvant therapy.

#### Studies excluded from the comparisons

Five studies included only eligible participants, however, these studies were not eligible for inclusion in any of our comparisons. (Waddell 2013) studied panitumumab and adjusted the control regimen of epirubicin, oxaliplatin, and capecitabine in the experimental arm. One study was not eligible because it compared leucovorin and 5-FU versus S-1 on a background of cisplatin (Pang 2014). Three studies used an equal number of agents in each arm. These studies compared: atofluding versus Morafur on a background of either mitomycin C plus etoposide, cisplatin plus hydroxycamptothecin, cisplatin plus vindesine, or mitomycin C plus adriamycin (Li 2002), epirubicin versus mitomycin on a background of cisplatin plus 5-FU (Ross 2002), and adriamycin versus methotrexate or 5-FU (Ezdinli 1980).

There were 15 studies that also included participants with gastric cancer that we excluded from the comparisons because they did not compare the addition of an agent to an unaltered control regimen. These studies compared: S1 versus 5-FU on a background of cisplatin (Ajani 2010); oxaliplatin versus cisplatin on a background of 5-FU plus leucovorin (Al-Batran 2013); cisplatin versus oxaliplatin on a background of epirubicin plus 5-FU or capecitabine, and 5-FU versus capecitabine on a background of epirubicin plus cisplatin or oxaliplatin (Cunningham 2008); irinotecan plus folinic acid versus cisplatin on a background of 5-FU (Dank 2008); continuous 5-FU plus cisplatin versus bolus 5-FU plus leucovorin (Duffour 2006); irinotecan versus cisplatin on a background of capecitabine (Moehler 2010); 5-FU versus cisplatin on a background of irinotecan (Pozzo 2004); irinotecan versus 5-FU on a background of docetaxel (Roy 2012); and epirubicin plus cisplatin versus doxorubicin plus methotrexate on a background of 5-FU (Waters 1999). Five studies did add an agent to a control regimen but adjusted their control regimens in the experimental arm. They investigated docetaxel plus cisplatin (Ajani 2005); docetaxel plus oxaliplatin, either with or without 5-FU (Van Cutsem 2015); lapatinib (Lorenzen 2009); docetaxel plus oxaliplatin with or without capecitabine (Van Cutsem 2015); or cisplatin and 5-FU with or without docetaxel (Van Cutsem 2006). One study was not eligible for inclusion because it tested two agents (cisplatin, 5-FU) versus one agent (capecitabine) (Tebbutt 2010).

In order to analyze the data from studies with a mixed participant population, including both eligible and ineligible participants, we requested individual participant data from authors of studies that we included after the search round of 3 October 2013. Only one author responded and provided individual participant data. Subsequently, we decided

to investigate the information from the studies that included both esophageal and/or GE-junction, mixed with gastric cancer participants, in a sensitivity analysis to assess the influence of gastric cancer participants on the outcome of the individual studies.

### **Outcomes**

OS and toxicity were the most commonly described outcomes, followed by PFS, time to progression (TTP), and objective response rate. Studies did not always classify toxicity according to NCI-CTC or WHO. Studies published before 2010 did not report quality of life with validated methods, and where reported, authors did not always report this outcome separately for esophageal and GE-junction cancer subgroups.

### **Excluded studies**

See Characteristics of excluded studies. We updated and revised the search for this version of the review. We excluded 5571 records based on their title and abstract as well as another 69 articles after reading the full text. The most frequent reason for exclusion was because the study turned out not to involve esophageal or GE-junction cancer participants. The reasons for exclusion are further specified in **Figure 1** according to the recommendations of the PRISMA statement (Moher 2009). We included studies that contained non-eligible participants as well as eligible participants. However, we excluded two studies that contained only nine and four eligible participants (Cascinu 2011); (Li 2011), respectively), as they did not provide sufficient data. We also excluded (Koizumi 2014) because authors did not specify the number of participants with GE-junction cancer. Additionally, we excluded several studies currently published as abstracts only, because full information on risk of bias and/or data on the esophageal and GE-junction cancer subgroup were unavailable. We classified these as ‘Studies awaiting classification’.

### **Risk of bias in included studies**

For details on the included studies see Characteristics of included studies and the summary figure of the quality assessment (**Figure 2**). Investigators performed and described blinding in 8 out of 41 studies. This poses a certain risk of bias in many of the included studies.

### **Allocation**

Studies frequently failed to describe allocation concealment, and six studies did not describe the method of random sequence generation.

### **Blinding**

Two studies evaluated progression using a blinded independent review board (Lordick 2013); (Rao 2010). We did not downgrade the GRADE level of evidence for the primary

	Random sequence generation (selection bias)	Allocation concealment (selection bias)	Blinding (performance bias and detection bias)	Selective reporting (reporting bias)	Similar at baseline for most prognostic factors (selection bias)	Complete description of the number of withdrawals, dropouts and losses to follow-up in each group. (selection bias)	Intention-to-treat analysis performed (selection bias)
Ajani 2005	?	?	?	?	?	?	?
Ajani 2010	?	?	?	?	?	?	?
Al-Batran 2008	?	?	?	?	?	?	?
Al-Batran 2013	?	?	?	?	?	?	?
Bang 2010	?	?	?	?	?	?	?
Bleiberg 1997	?	?	?	?	?	?	?
Cunningham 2008	?	?	?	?	?	?	?
Dank 2008	?	?	?	?	?	?	?
Duffour 2006	?	?	?	?	?	?	?
Dutton 2014	?	?	?	?	?	?	?
Eatock 2013	?	?	?	?	?	?	?
Ezdini 1980	?	?	?	?	?	?	?
Ford 2014	?	?	?	?	?	?	?
Fuchs 2014	?	?	?	?	?	?	?
Huang 2009	?	?	?	?	?	?	?
Iveson 2014	?	?	?	?	?	?	?
Levard 1998	?	?	?	?	?	?	?
Li 2002	?	?	?	?	?	?	?
Lordick 2013	?	?	?	?	?	?	?
Lorenzen 2009	?	?	?	?	?	?	?
Lorenzen 2015	?	?	?	?	?	?	?
Moehler 2010	?	?	?	?	?	?	?
Nicolaou 1982	?	?	?	?	?	?	?
Ohtsu 2011	?	?	?	?	?	?	?
Pang 2014	?	?	?	?	?	?	?
Pozzo 2004	?	?	?	?	?	?	?
Rao 2010	?	?	?	?	?	?	?
Richards 2013	?	?	?	?	?	?	?
Ross 2002	?	?	?	?	?	?	?
Roy 2012	?	?	?	?	?	?	?
Shen 2014	?	?	?	?	?	?	?
Tebbutt 2002	?	?	?	?	?	?	?
Tebbutt 2010	?	?	?	?	?	?	?
Thuss-Patience 2011	?	?	?	?	?	?	?
Van Cutsem 2006	?	?	?	?	?	?	?
Van Cutsem 2015	?	?	?	?	?	?	?
Waddell 2013	?	?	?	?	?	?	?
Waters 1999	?	?	?	?	?	?	?
Wilke 2014	?	?	?	?	?	?	?
Wilkes 2011	?	?	?	?	?	?	?
Xu 2013a	?	?	?	?	?	?	?

**Figure 2.** Risk of bias summary: review authors' judgements about each risk of bias item for each included study.

outcome, OS, due to lack of binding or mentioning of blinding in the study report. This because we assume knowledge of allocation has limited effect on survival and the detection of survival and would, thus, not induce performance or detection bias. Seven studies described use of an external review board but did not describe blinding (Ajani 2005); (Ajani 2010); (Duffour 2006); (Pozzo 2004); (Roy 2012); (Tebbutt 2010); (Van Cutsem 2006).

#### ***Incomplete outcome data***

Incomplete outcome data with risk of attrition bias was present in a few included studies, either because there was no intention to- treat analysis (Li 2002); (Moehler 2010); (Pang 2014); (Pozzo 2004); (Van Cutsem 2006); (Xu 2013), or because authors did not describe dropouts (Li 2002); (Xu 2013).

#### ***Selective reporting***

Risk of reporting bias was present in one study (Ross 2002), where authors reported the data in esophageal participants separately for overall response rate but not for other outcomes. We did not consider studies that reported overall survival for esophageal participants separately and did not report on other outcome measures to be at high risk of reporting bias, as overall survival was the primary endpoint of analysis in this review.

#### ***Other potential sources of bias***

We considered that four studies had groups that were not similar at baseline. This was due to age difference (Rao 2010), number of organs involved in metastatic disease (Lorenzen 2009, Thuss-Patience 2011), or both (Ezdinli 1980). We assessed small study effects, such as publication bias, in a qualitative manner using a funnel plot for the main analysis, but we found no evidence that these effects were present.

#### **Effects of interventions**

See: Summary of findings for the main comparison Summary of findings table: chemotherapy or targeted therapy agent(s) plus control intervention versus control intervention alone for palliative treatment of esophageal and GE-junction carcinoma; Summary of findings 2 Summary of findings table (sensitivity analysis): interventions esophageal and GE-junction carcinoma versus gastric carcinoma; Summary of findings 3 Summary of findings table (subcomparison 1): chemotherapy or targeted therapy plus best supportive care (BSC) versus BSC for palliative treatment of esophageal and GE-junction carcinoma; Summary of findings 4 Summary of findings table (subcomparison 2): second-line chemotherapy or targeted therapy agent(s) plus control intervention versus control intervention alone for palliative treatment of esophageal and GE-junction carcinoma; Summary of findings 5 Summary of findings table (subcomparison

3): chemotherapy agent(s) plus control intervention versus control intervention alone for palliative treatment of esophageal and GE-junction carcinoma; Summary of findings 6 Summary of findings table (subcomparison 4): targeted therapy agent plus control intervention versus control intervention alone for palliative treatment of esophageal and GE-junction carcinoma; Summary of findings 7 Summary of findings table (subcomparison 5): chemotherapy or targeted therapy agent(s) plus control intervention versus control intervention alone in participants with AC of the esophagus; Summary of findings 8 Summary of findings table (subcomparison 6): chemotherapy or targeted therapy agent(s) plus control intervention versus control intervention alone in participants with SCC of the esophagus

### Main analysis: chemotherapy or targeted therapy agent(s) plus control intervention versus control intervention alone

#### Overall survival

Eleven studies in 1347 participants contributed data to this meta-analysis (Bang 2010); (Bleiberg 1997); (Dutton 2014); (Ford 2014); (Fuchs 2014); (Huang 2009); (Levard 1998); (Lordick 2013); (Lorenzen 2009); (Nicolau 1982); (Wilke 2014). These studies included only people with esophageal and/or GE-junction cancer, or they reported the results separately for this group. The overall HR in favor of the arm with the additional agent was 0.75 (95% CI 0.68 to 0.84, high-quality evidence), showing an OS benefit (Analysis 1.1; **Figure 3**). On average, participants in the arm with the additional chemotherapy or targeted therapy agent received 2.1 chemotherapy or targeted therapy

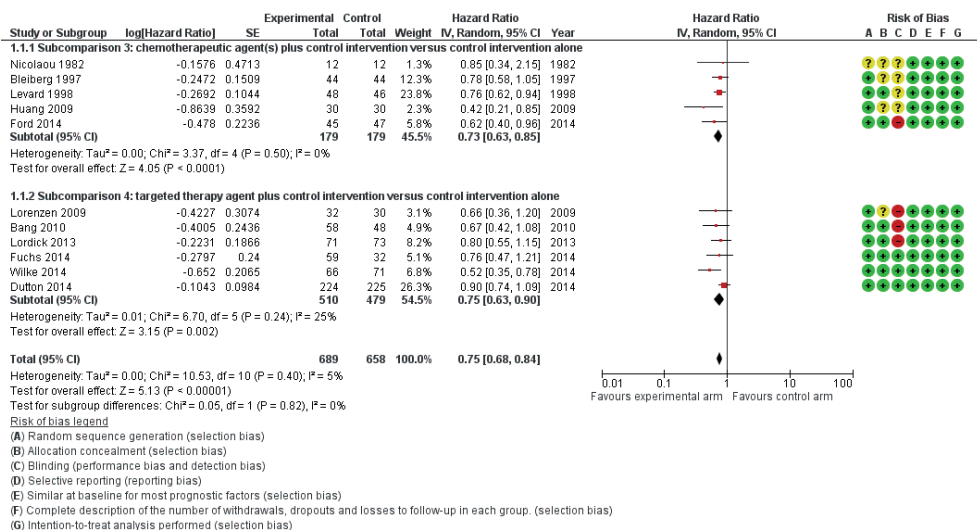


**Figure 3.** Forest plot of the main analysis: chemotherapy or targeted therapy agent(s) plus control arm versus control arm, outcome: 1.1 Overall survival.

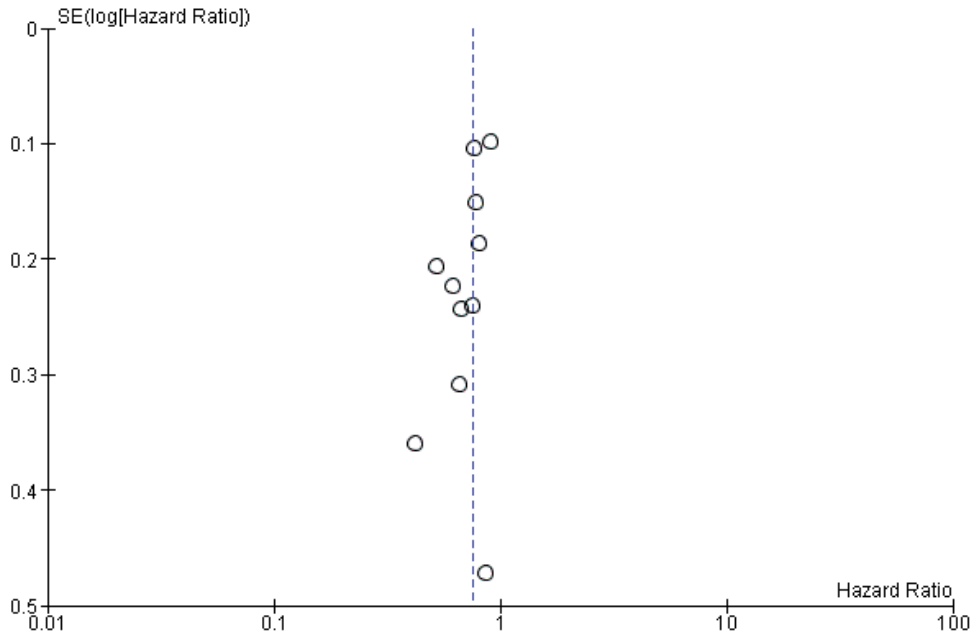


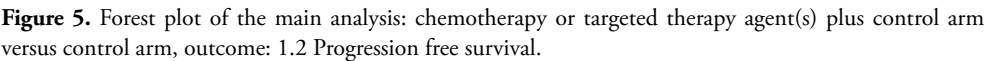
**Figure 4.** Funnel plot of the main comparison: chemotherapy or targeted therapy agent(s) plus control arm versus control arm, outcome: 1.1 Overall survival.

agents, versus an average of 1.0 agents in the control arms. Median OS, weighted for study size, in the arm with the additional agent was 6.7 months versus 5.7 months in the control arm. We could not include two studies because they did not report median overall survival data (Bang 2010); (Huang 2009). Cochrane's  $Q$  test for heterogeneity showed a non-significant amount of heterogeneity ( $I^2=5\%$ ,  $p=0.40$ ), which indicated that results of the different studies were consistent in their findings. We did not note any small study effects such as publication bias (**Figure 4**).

Two studies included in the meta-analysis selected participants based on biomarker expression (Lorenzen 2009, Bang 2010). We could not include three studies under this comparison in the meta-analysis because of insufficient information. (Eatock 2013) investigated trebananib. Median OS times at the time of analysis were 9.1 months, 9.4 months, and 12.8 months for the 10.0 mg/ kg, 3.0 mg/kg, and control arms, respectively. (Wilkes 2011) studied thalidomide and reported that survival was not affected by group allocation. (Xu 2013) found higher, statistically significant ( $p<0.05$ ) OS in the nimotuzumab group relative to the control group.

#### Progression-free survival

Of all studies included in this comparison, only studies that investigated a targeted therapy agent reported PFS. Therefore, we describe the results of this analysis in more



## Toxicity

In (Bang 2010), the most common grade 3 and 4 adverse events reported with trastuzumab plus chemotherapy versus chemotherapy alone were neutropenia (27% versus 30%), anemia (12% versus 10%), and diarrhea (9% versus 4%). Treatment-related mortality was 3% in the trastuzumab plus chemotherapy arm, versus 1% in the chemotherapy alone arm. (Bleiberg 1997) reported that grade 3 and 4 adverse events occurred most frequently in the 5-FU cisplatin arm versus the cisplatin alone arm. These were nausea or vomiting (27% versus 11%) and leukocytopenia and thrombocytopenia (both 12% versus 0%). Seven (16%) treatment related deaths occurred in the treatment arm. (Dutton 2014) reported that any grade 3, 4, or 5 toxicities occurred in 45% of

participants in the gefitinib plus control arm versus 39% of participants in the control arm. Two treatment-related deaths occurred in the placebo group and one in the gefitinib group. (Ford 2014) found that grade 4 toxicities occurred more frequently in participants treated with docetaxel compared to participants in the control arm (21% versus 4%). Neutropenia, infections, and febrile neutropenia were the toxicities that differed most between the study arms. None of the deaths were attributed to the treatment. In both arms of (Fuchs 2014), 2% of the participants died due to drug-related toxicity. Ramucirumab was not associated with increased rates of fatigue, decreased appetite, vomiting, anemia, or other notable toxic effects. (Huang 2009) used WHO guideline classifications but did not specify the grade of the side effects that occurred. In (Lordick 2013), any grade 3 or 4 adverse events occurred in 83% of participants in the cetuximab plus control arm versus 77% in the control arm. Nine per cent of participants in the chemotherapy plus cetuximab arm and eight per cent of participants in the control arm had an adverse event leading to death. (Lorenzen 2009) reported that grade 3 and 4 adverse events, which occurred more frequently in the cetuximab group, were diarrhea (16% versus 0%), neutropenia (22% versus 13%), and rash (6% versus 0%). Additionally, they reported one (3%) treatment related death in the control arm and none in the experimental arm. (Wilke 2014) found that the most frequently occurring grade 3, 4, and 5 adverse events in the ramucirumab arm versus the control arm were neutropenia (41% versus 19%), leukopenia (18% versus 7%), and hypertension (15% versus 3%). In both arms, 2% of participants had adverse events leading to death with a causal relation to the study drugs.

Overall, palliative chemotherapy and/or targeted therapy appears to increase the frequency of treatment-related toxicity of at least grade 3. Treatment-related deaths were rare in most studies, and there is no clear evidence that treatment-related deaths occur more frequently in the study arms with an additional chemotherapy or targeted therapy agent.

### **Quality of life**

Five studies included in the main analysis did not report on quality of life (Bleiberg 1997); (Lordick 2013); (Lorenzen 2009); (Nicolaou 1982); (Wilkes 2011). Four studies did not report quality of life separately for the esophageal and GE-junction cancer subgroup (Bang 2010); (Ford 2014); (Fuchs 2014); (Wilke 2014). Two studies reported on quality of life but did not use validated methods (Huang 2009); (Levard 1998). (Huang 2009) used improvement after treatment in the treatment arm versus the control arm for the Karnofsky score (33% versus 10%) and body weight (27% versus 6.7%). (Levard 1998) studied dysphagia in order to judge the quality of life during the survival of their participants. (Bang 2010), see (Satoh 2014) reported that trastuzumab plus chemotherapy versus chemotherapy alone prolonged time to 10% definitive deterioration in all QLQ-C30 and QLQ-STO22 scores (Aronson 1993);



(Blazeby 2004), including QLQ-C30 global quality of life score, from 6.4 months to 10.2 months. (Dutton 2014) reported no differences between the gefitinib and placebo groups in global quality of life measured with QLQ-C30. However, odynophagia worsened for participants on placebo and improved significantly for participants on gefitinib. (Ford 2014) reported that the mean quality-adjusted life weeks (QLQ-C30) were 12.1 weeks (standard deviation (SD) 0.84) for the docetaxel group and 9.3 weeks (SD 0.73) for the control group. (Fuchs 2014) reported a trend toward better quality of life (QLQ-C30) at six weeks for participants in the ramucirumab group compared to those in the placebo group ( $p=0.23$ ). Median time of deterioration to a score of 2 or worse in ECOG performance status was 2.4 months (95% CI 1.3 to not reached) in the placebo group and 5.1 months (95% CI 1.9 to 16.8) in the ramucirumab group. (Wilke 2014) reported that baseline and end-of-treatment results for global quality of life from the QLQ-C30 and index scores from the EQ-5D-3L were similar in the treatment groups (EuroQol 1990). Overall, the studies reporting quality of life did so in different ways. Although recent studies often use the QLQ-C30, the outcomes were reported in the form of either mean values with SD, change from the baseline, proportions improved, or mean area under the curve. This prohibited a meta-analysis of quality of life outcomes. The five studies were not representative for all the studies in this analysis, as four of them tested a targeted agent, and four did not report data separately for the esophageal and GE-junction cancer subgroup. However, the quality of life improved in the arms with the additional agent.

#### ***Sensitivity analysis: effect of the intervention in participants with esophageal and GE-junction cancer versus gastric cancer***

We conducted this sensitivity analysis to investigate whether there was a significant difference in the effect of the intervention between both the participants with esophageal and GE-junction cancer and the participants with gastric cancer. The sensitivity analysis consisted of two parts, both regarding OS. Firstly, we compared the group of studies that included participants with both esophageal/GE-junction and gastric cancer to the group of studies that included only participants with esophageal and GE-junction cancer through a meta-regression analysis. In this meta-regression analysis, the interventions between groups of studies were not similar, making the comparison indirect. Therefore, we performed a second sensitivity analysis, also by meta-regression, which focused on five studies that reported the effect of the intervention on OS for participant groups with both GE-junction and gastric cancer separately.

For the first part of the sensitivity analysis, we meta-analyzed the group of studies that included participants with both esophageal/ GE-junction and gastric cancer. This group contained eight studies and 1755 participants, 459 of whom had esophageal or GE-junction cancer (Al-Batran 2013); (Iveson 2014); (Ohtsu 2011); (Rao 2010); (Richards 2013); (Shen 2014); (Tebbutt 2002); (Thuss-Patience 2011). (Iveson 2014) investigated

rilotumumab at two concentrations, 7.5 mg/kg and 15 mg/kg. The HR that we used in the meta-analysis was derived from both groups versus the control arm. In this analysis, the overall HR, in favor of the arm with the additional agent was 0.94 (95% CI 0.83 to 1.05), showing a trend toward a survival benefit in the arm with the additional agent versus the control arm (Analysis 2.1). Cochrane's  $Q$  test for heterogeneity showed a considerable amount of heterogeneity ( $I^2=54\%$ ,  $p=0.03$ ), which indicated that results of the different studies were somewhat inconsistent in their findings.

We performed a meta-regression analysis to compare the effect of the intervention in studies involving participants with esophageal and GE-junction cancer (main analysis group, HR 0.75, 95% CI 0.68 to 0.84, high-quality evidence), versus studies in participants with both gastric and esophageal/GE-junction cancer (HR 0.94, 95% CI 0.83 to 1.05). This meta-regression analysis showed that there was a difference in the effect of intervention between the two groups of studies ( $p=0.004$ ).

For the second part of the sensitivity analysis, we assessed the group of studies reporting the effect of the intervention on OS for participants with both GE-junction and gastric cancer separately in two meta-analyses, each containing five studies (Bang 2010); (Ford 2014); (Fuchs 2014); (Lordick 2013); (Wilke 2014). The meta-analysis of the participant subgroups with GE-junction cancer contained 538 participants. The meta-analysis of the participant subgroups with gastric cancer contained 2093 participants. The effect of adding a chemotherapeutic or targeted therapeutic agent in the participant subgroups with GE-junction cancer on OS in these studies was HR 0.66 (95% CI 0.54 to 0.81; Analysis 3.1). The effect of adding a chemotherapeutic or targeted therapeutic agent to the participant subgroups with gastric cancer in these studies was HR 0.89 (95% CI 0.76 to 1.04; Analysis 3.2). That said, this was a selected group of participants with gastric cancer, so this meta-analysis might not accurately reflect the effect of adding a chemotherapeutic or targeted agent to the control regimen of participants with gastric cancer in general. This meta-analysis was not meant to be exhaustive with regard to the effect of chemotherapy or targeted therapy in people with gastric cancer. For more information, see Wagner 2010. We performed a meta-regression analysis between these groups, which indicated that both participant subgroups responded significantly differently to the investigated interventions ( $p=0.03$ ), in line with the first part of the sensitivity analysis. This meta-regression analysis indicated that the studied interventions appeared to result in an increased beneficial effect on OS in participants with GE-junction cancer compared to participants with gastric cancer. Therefore, we excluded the studies that also included participants with gastric cancer and did not report outcomes separately from the meta-analyses of this review.

### Subcomparison 1: chemotherapy or targeted therapy plus BSC versus BSC

#### Overall survival

Five studies in 750 participants contributed data to this meta-analysis (Dutton 2014); (Ford 2014); (Fuchs 2014); (Levard 1998); (Nicolaou 1982). For overall survival, we found an HR of 0.81 (95% CI 0.71 to 0.92, high-quality evidence; Analysis 4.1; **Figure 6**) in favor of the chemotherapy or targeted therapy arm. Median OS, weighted for study size, in the chemotherapy arm was 4.7 months versus 4.2 months in the BSC arm. Only two studies used first-line therapies (Levard 1998); (Nicolaou 1982), while the others used second-line. Cochrane's *Q* test for heterogeneity was non-significant ( $I^2=0\%$ ,  $p=0.56$ ), which indicated that results of the five studies were consistent in their findings.

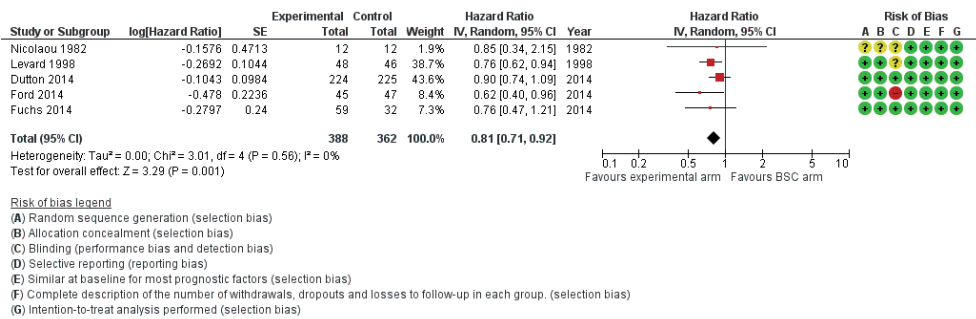


**Figure 6.** Forest plot of subcomparison 1: chemotherapy or targeted therapy agent(s) plus BSC versus BSC, outcome 4.1: overall survival.

#### Progression-free survival

Two studies in 540 participants contributed data to this meta-analysis (Dutton 2014); (Fuchs 2014)). Both studies assessed a targeted therapeutic agent. The other three studies did not report on PFS. The overall HR of 0.58 (95% CI 0.28 to 1.18, very low quality evidence; Analysis 4.2; **Figure 7**) in favor of targeted therapy demonstrated that there was a larger, non-significant effect estimate toward a PFS benefit when participants received targeted therapy; however, we are uncertain of these findings due to the very low quality of evidence. Median progression-free survival was only available from (Dutton 2014) and was 1.6 months in the targeted therapy arm versus 1.2 months in the BSC arm. Cochrane's *Q* test for heterogeneity showed significant heterogeneity ( $I^2=85\%$ ,  $p=0.01$ ), which indicated that results of the two studies were not consistent.

### Subcomparison 2: participants who had received previous chemotherapy

We intended for this subcomparison to investigate whether chemotherapy or targeted therapy for participants that had previously received chemotherapy resulted in a benefit

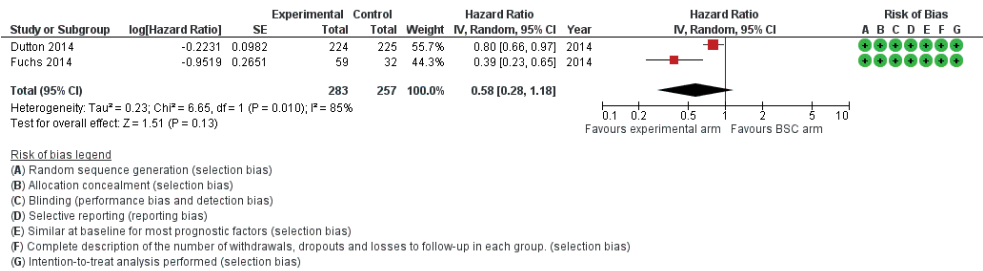


**Figure 7.** Forest plot of subcomparison 1: chemotherapy or targeted therapy agent(s) plus BSC versus BSC, outcome 4.1: progression free survival.

for overall survival, progression-free survival, or both. We did not include studies if only some of the participants had received previous chemotherapy. For a description of criteria used for including studies with regard to previous chemotherapy, see Characteristics of included studies, ‘Participants’ section.

Overall survival

This meta-analysis included four studies in 769 participants (Dutton 2014); (Ford 2014); (Fuchs 2014); (Wilke 2014). Three studies included participants with GE-junction cancer only. In (Dutton 2014), 24% of the esophageal cancers were SCC. Two studies investigated ramucirumab (Fuchs 2014); (Wilke 2014), which we analyzed separately in subgroup analysis 4b. The overall HR of 0.71 (95% CI 0.54 to 0.94, moderate-quality evidence; Analysis 5.1) in favor of the arm with the additional agent demonstrated that an additional chemotherapeutic or targeted agent leads to a survival benefit. Median OS, weighted for study size, was 5.1 months in the chemotherapy arm versus 4.4 months in the BSC arm. Cochrane’s *Q* test for heterogeneity showed significant heterogeneity ( $I^2=57\%$ ,  $p=0.07$ ), indicating that results of the three included studies were quite inconsistent in their findings.

Progression-free survival

Three studies in 677 participants contributed data to this meta-analysis (Dutton 2014); (Fuchs 2014); (Wilke 2014). All three studies investigated targeted agents. Two studies (both of ramucirumab) included participants with GE-junction cancer only. In the third study, 24% of the esophageal cancers were SCC. The overall HR of 0.51 (95% CI 0.29 to 0.90, low-quality evidence; Analysis 5.2) in favor of the targeted therapy arms demonstrated that there may be a PFS benefit for people receiving targeted therapy agents. Cochrane’s *Q* test for heterogeneity showed substantial heterogeneity ( $I^2=83\%$ ,  $p<0.001$ ), which indicated that results of the three studies were inconsistent in their findings.

**Subcomparison 3: chemotherapy agent(s) plus control intervention versus control intervention alone****Overall survival**

Five studies in 358 participants contributed data to this meta-analysis (Bleiberg 1997); (Ford 2014); (Huang 2009); (Levard 1998); (Nicolaou 1982). The overall HR of 0.73 (95% CI 0.63 to 0.85, moderate-quality evidence; Analysis 1.1; **Figure 3**, subcomparison 3) in favor of the arm with the additional chemotherapy agent demonstrates that there is probably a significant survival benefit in people receiving an additional chemotherapy agent. Median survival time, weighted for study size, was 6.9 months in the chemotherapy arm versus 5.8 months in the control arm. We could not include (Huang 2009) in the median OS analysis because it did not report this outcome. Cochrane's *Q* test for heterogeneity showed non-significant heterogeneity ( $I^2=0\%$ ,  $p=0.50$ ), which indicated that results of the five studies were consistent in their findings. Considering the limited number of studies and the low heterogeneity in the model, we consider that the quality of evidence is moderate.

One study included in the comparison did not contribute to the meta-analysis for subcomparison 3 for OS because the publication did not provide enough information. (Wilkes 2011) only reported that survival was not affected by group allocation or whether the participant was able to complete the protocol.

**Progression-free survival**

None of the four studies reported on PFS.

**Subcomparison 4: targeted agent plus control intervention versus control intervention alone****Overall survival**

Six studies with 989 participants contributed to this meta-analysis (Bang 2010); (Dutton 2014); (Fuchs 2014); (Lordick 2013); (Lorenzen 2009); (Wilke 2014). The overall HR in favor of the arm containing a targeted agent was 0.75 (95% CI 0.63 to 0.90, high-quality evidence. This analysis demonstrated a survival benefit for participants randomized to the arm with the additional targeted agents (Analysis 1.1; **Figure 3**, subcomparison 4). Median OS in the arm with the additional targeted agent, weighted for study size, was 6.7 months versus 5.7 months in the control arm. We could not include (Bang 2010) because it did not report median OS data. Cochrane's *Q* test for heterogeneity showed low heterogeneity ( $I^2=24\%$ ,  $p=0.25$ ), indicating that results of the different studies were quite consistent in their findings.

Two studies included in the meta-analysis selected participants based on biomarker expression (Lorenzen 2009, Bang 2010). (Xu 2013) found higher PFS and OS in the nimotuzumab group. However, the study did not provide enough information to extract HRs, so we could not include it in the analyses.

***Subgroup analysis 4a: EGFR-targeting agent plus control intervention versus control intervention alone***

Three studies in 655 participants contributed data to this meta-analysis (Dutton 2014); (Lordick 2013); (Lorenzen 2009). The overall HR of 0.86 (95% CI 0.73 to 1.01, moderate-quality evidence; Analysis 6.1) in favor of the arms that contained an EGFR-targeting agent showed that there is probably a survival benefit in the arm with the additional EGFR-targeting agent. Cochrane's *Q* test for heterogeneity showed no significant heterogeneity ( $I^2=0\%$ ,  $p=0.56$ ), which indicated that results of the four studies were very consistent in their findings. Median OS, weighted for study size, was 6.4 months in the treatment arm containing an EGFR-targeting agent versus 5.5 months in the control arm.

One study included in the meta-analysis selected participants based on biomarker expression (Lorenzen 2009). (Xu 2013) found higher PFS and the OS in the nimotuzumab group. However, the study did not provide enough information to extract HRs, so we could not include it in the meta-analysis.

(Waddell 2013) investigated panitumumab. We could not formally include this study in the comparison because the control regimen was adjusted in the arm with the additional EGFR-targeting agent. This study found that the addition of panitumumab resulted in an HR for OS of 1.37 (95% CI 1.07 to 1.76), but readers should interpret these results with caution.

***Subgroup analysis 4b: cetuximab plus control intervention versus control intervention alone***

Two studies in 206 participants contributed data to this meta-analysis (Lordick 2013); (Lorenzen 2009). (Lordick 2013) investigated the addition of cetuximab to a control arm of capecitabine plus cisplatin; (Lorenzen 2009) used cisplatin plus 5-FU as a control regimen. The overall HR of 0.76 (95% CI 0.55 to 1.04, low-quality evidence; Analysis 7.1) in favor of the cetuximab arm showed that there may be a non-significant survival benefit for participants randomized to receive cetuximab. Median OS, weighted for study size, was 12.2 months in the cetuximab arm versus 9.4 months in the control arm. Cochrane's *Q* test for heterogeneity showed nonsignificant heterogeneity ( $I^2=0\%$ ,  $p=0.58$ ), which indicated that results of the two studies were consistent in their findings. One study included in the meta-analysis selected participants based on biomarker expression (Lorenzen 2009).

***Subgroup analysis 4c: ramucirumab plus control intervention versus control intervention alone***

Two studies in 228 participants contributed data to this meta-analysis (Fuchs 2014); (Wilke 2014). (Fuchs 2014) investigated ramucirumab versus BSC, while (Wilke 2014) added ramucirumab to paclitaxel. The two studies included only people with GE-junction cancer who had previously received chemotherapy, so the results of this meta-

analysis are not generalizable to other patient populations. The overall HR of 0.62 (95% CI 0.43 to 0.88, moderate quality evidence; Analysis 8.1) in favor of the ramucirumab arm showed that there is probably an overall survival benefit. Median OS, weighted for study size, was 7.5 months in the ramucirumab arm versus 6.3 months in the control arm. Cochrane's  $Q$  test for heterogeneity showed non-significant heterogeneity ( $I^2=28\%$ ,  $p=0.24$ ), which indicated that results of the two studies were consistent in their findings.

### Progression-free survival

Five studies in 883 participants contributed data to this meta-analysis (Dutton 2014); (Fuchs 2014); (Lordick 2013); (Lorenzen 2009); (Wilke 2014). The five studies investigated targeted therapies. In this analysis, the overall HR, in favor of the treatment arm that contained a targeted therapy agent, was 0.64 (95% CI 0.45 to 0.92, moderate-quality evidence). This showed that there is probably a PFS benefit for people treated with the targeted therapy agent (Analysis 1.2; **Figure 5**). Median progression-free survival, weighted for study size, was 2.9 months in the arm with the additional targeted therapy agent versus 2.4 months in the control arm. We could not include two studies in the analysis because they did not report median PFS data (Fuchs 2014); (Wilke 2014). Cochrane's  $Q$  test for heterogeneity showed substantial heterogeneity ( $I^2=79\%$ ,  $p<0.001$ ), which indicated that results of the individual studies were quite inconsistent in their findings. One study included in the meta-analysis selected participants based on biomarker expression (Lorenzen 2009).

### *Subgroup analysis 4a: EGFR-targeting agent plus control intervention versus control intervention alone*

Three studies in 655 participants contributed data to this meta-analysis (Dutton 2014); (Lordick 2013); (Lorenzen 2009). The overall HR of 0.85 (95% CI 0.73 to 1.00, low-quality evidence; Analysis 6.2) in favor of the arm with the EGFR-targeting agent demonstrated that there may be a non-significant PFS benefit in the arms with the EGFR-targeting agents. Cochrane's  $Q$  test for heterogeneity showed non-significant results ( $I^2=2\%$ ,  $p=0.36$ ), which indicated that results of the three studies were consistent in their findings. Median progression-free survival, weighted for study size, was 2.9 months in the treatment arm that contained an EGFR-targeting agent versus 2.4 months in the control arm.

One study included in the meta-analysis selected participants based on biomarker expression (Lorenzen 2009). (Waddell 2013) investigated panitumumab, but we could not formally include it in the comparison because the control regimen was adjusted in the panitumumab arm. The addition of panitumumab resulted in an HR for PFS of 1.22 (95% CI 0.98 to 1.52), but readers should interpret these results with caution.

***Subgroup analysis 4b: cetuximab plus control intervention versus control intervention alone***

Two studies in 206 participants contributed data to this meta-analysis (Lordick 2013); (Lorenzen 2009). The overall HR of 0.90 (95% CI 0.59 to 1.37, very low-quality evidence; Analysis 7.2) shows a small and very uncertain PFS benefit in favor of the cetuximab arm. Median progression-free survival, weighted for study size, was 5.7 months in the cetuximab arms versus 5.0 months in the control arms. Cochrane's *Q* test for heterogeneity showed a considerable amount of heterogeneity ( $I^2=53\%$ ,  $p=0.14$ ), which indicated that results of the two studies were not very consistent in their findings. One study included in the meta-analysis selected participants based on biomarker expression (Lorenzen 2009).

***Subgroup analysis 4c: ramucirumab plus control intervention versus control intervention alone***

Two studies in 228 participants contributed data to this meta-analysis (Fuchs 2014); (Wilke 2014). This meta-analysis only applies to GE-junction participants, the only participants included. The overall HR of 0.39 (95% CI 0.28 to 0.54, moderate-quality evidence; Analysis 8.2) in favor of the ramucirumab arm demonstrated that there was probably a PFS benefit in the ramucirumab group. We could not determine median PFS, as neither study reported this outcome. Cochrane's *Q* test for heterogeneity showed nonsignificant heterogeneity ( $I^2=0\%$ ,  $p=0.99$ ), which indicated that results of the two studies were very consistent in their findings.

***Subcomparison 5: chemotherapy or targeted therapy agent(s) plus control intervention versus control intervention alone in participants with adenocarcinoma of the esophagus*****Overall survival**

Five studies in 538 participants contributed data to this meta-analysis (Bang 2010); (Ford 2014); (Fuchs 2014); (Lordick 2013); (Wilke 2014). For overall survival, we found an HR of 0.66 (95% CI 0.54 to 0.81, high-quality evidence; Analysis 9.1) in favor of the experimental arm. Median OS, weighted for study size, was 7.1 months in the added agent arm versus 6.0 months in the control arm. We could not include (Bang 2010) because it did not report median overall survival data. Two studies were first-line therapy regimens (Bang 2010); (Lordick 2013), and three were second-line therapies (Ford 2014); (Fuchs 2014); (Wilke 2014). Cochrane's *Q* test for heterogeneity was non-significant ( $I^2=0\%$ ,  $p=0.55$ ), which indicated that results from the five studies were consistent in their findings. (Eatock 2013) investigated trebananib in participants with esophageal adenocarcinoma but did not provide enough detail for inclusion in the meta-analysis. Median OS at the time of analysis were 9.1 months, 9.4 months, and 12.8 months for the 10.0 mg/kg, 3.0 mg/kg, and control arms, respectively.



**Progression-free survival**

Four studies in 713 participants contributed data to this meta-analysis (Dutton 2014); (Fuchs 2014); (Lordick 2013); (Wilke 2014). For progression-free survival, we found an HR of 0.62 (95% CI 0.38 to 1.00, very low-quality evidence; Analysis 9.2) in favor of the experimental arm; however, we are uncertain of these results due to the low-quality evidence. Median OS, weighted for study size, was 1.8 months in the added agent arm versus 1.7 months in the control arm. We could not include two studies in the analysis because they did not report median PFS data (Fuchs 2014); (Wilke 2014). One study was on first-line therapy regimens (Lordick 2013), and three were second-line therapies (Dutton 2014); (Fuchs 2014); (Wilke 2014). Cochrane's *Q* test for heterogeneity was non-significant ( $I^2=84\%$ ,  $p<0.001$ ), which indicated that results of the four studies were very inconsistent in their findings. (Eatock 2013) investigated trebananib in participants with esophageal adenocarcinoma but did not provide enough detail for inclusion in the meta-analysis. Median PFS times at the time of analysis were 4.2 months, 4.9 months, and 5.2 months for the 10.0 mg/kg, 3.0 mg/kg, and control arms, respectively.

***Subcomparison 6: chemotherapy or targeted therapy agent(s) plus control intervention versus control intervention alone in participants with SCC of the esophagus***

**Overall survival**

Four studies in 268 participants contributed data to this meta-analysis (Bleiberg 1997); (Levard 1998); (Lorenzen 2009); (Nicolaou 1982). For overall survival, we found an HR of 0.76 (95% CI 0.65 to 0.90, high-quality evidence; Analysis 10.1) in favor of the experimental arm. Median OS, weighted for study size, was 8.0 months in the added agent arm versus 6.5 months in the control arm. All studies were first-line therapy regimens. Cochrane's *Q* test for heterogeneity was non-significant ( $I^2=0\%$ ,  $p=0.95$ ), which indicated that results of the four studies were consistent in their findings. (Xu 2013) found that the OS of the nimotuzumab group was increased relative to the control group.

**Progression-free survival**

Two studies in 168 participants contributed data to this meta-analysis (Dutton 2014); (Lorenzen 2009). For overall survival, an HR of 0.72 (95% CI 0.55 to 0.96, low-quality evidence; Analysis 10.2) showed that there may be a benefit in favor of the experimental arm. Median OS, weighted for study size, was 1.7 months in the added agent arm versus 1.2 months in the control arm. All studies were first-line therapy regimens. Cochrane's *Q* test for heterogeneity was non-significant ( $I^2=0\%$ ,  $p=0.97$ ), which indicated that results of the four studies were consistent in their findings. (Xu 2013) found that the PFS of the nimotuzumab group was higher than in the control group.

***Studies excluded from the meta-analysis***

(Li 2002) did not detect a difference between the response rates of participants with esophageal cancer who received atofludung (20.0%) versus Morafur (24.6%). (Ross 2002) reported that the overall response rate with epirubicin, cisplatin, and 5-FU was 37.5% for participants with esophageal cancer and 54.8% for participants with GE-junction cancer versus an overall response rate with mitomycin, cisplatin, and 5-FU of 49.5% for participants with esophageal cancer and 41.5% for participants with GE-junction cancer. (Ezdinli 1980) reported median overall survival of 8.1 months for the adriamycin arm, 13.7 months for the methotrexate arm, and 15.4 months for the 5-FU arm. (Pang 2014) reported that the median OS of the intervention (leucovorin, 5-FU, and cisplatin) was 12 months versus 9 months in the control group (cisplatin and S-1) ( $p=0.045$ ). (Waddell 2013) found that the addition of panitumumab resulted in an HR for OS of 1.37 (95% CI 1.07 to 1.76) and an HR for PFS of 1.22 (95% CI 0.98 to 1.52). This study adjusted the dose of the control regimen in the experimental arm. Our analysis did not include the information from studies that contain participants with esophageal and/or GE-junction cancer alongside that from participants with gastric cancer. A meaningful sensitivity analysis was not possible, and we could not quantify the influence of the participants with gastric cancer on the outcome of the individual studies.

**Discussion****Summary of main results**

This review and meta-analysis included only RCTs. Eight of the included studies reported details on adequate blinding. Apart from blinding, the most common methodological weakness in the included studies was the lack of description regarding allocation concealment. Palliative chemotherapy and/or targeted therapy significantly increased OS compared to BSC in participants with esophageal or GE-junction carcinoma. Additionally, participants who received multiple chemotherapeutic or targeted therapeutic agents had an increased OS and PFS. Although treatment associated toxicities of at least grade 3 occurred more frequently in the arms with an additional chemotherapy or targeted therapy agent, there was no evidence that palliative chemotherapy and/or targeted therapy decreased quality of life.

***Main comparison: chemotherapy or targeted therapy agent(s) plus control intervention versus control intervention alone***

The meta-analysis focused on the addition of a chemotherapeutic or targeted agent to the regimen or BSC treatment provided in the control arm. This meta-analysis provided evidence of an OS benefit for participants treated with an additional chemotherapy or

targeted therapy agent (Analysis 1.1; **Figure 3**). Results of the different studies were consistent in their findings. Median OS, weighted for study size, was longer in the arm with the additional agent versus the control arm, and we did not find small study effects.

The meta-analysis for PFS provided evidence of a benefit for participants who had received an additional targeted agent (Analysis 1.2; **Figure 5**). Median progression-free survival, weighted for study size, was longer in the arm with the additional agent versus in the control arm. Palliative chemotherapy and/or targeted therapy appears to increase the frequency of treatment-related toxicity of at least grade 3. However, treatment-related deaths did not appear to occur more frequently. Five studies included in this analysis measured quality of life with validated methods. Although the five studies were not representative of all the studies in this analysis, as four out of five tested a targeted agent and four did not report data separately for the esophageal and GE-junction cancer subgroup, the quality of life improved in the arms with the additional agent.

***Sensitivity analysis: effect of the intervention in participants with esophageal and GE-junction cancer versus gastric cancer***

We included the group of studies that also included gastric cancer participants in a separate meta-analysis. Subsequently, we performed a meta-regression analysis between these studies and those including only esophageal and GE-junction cancer participants. This analysis showed significant heterogeneity between groups of studies. Studies that included participants with esophageal or GE-junction cancer only showed a larger OS risk reduction compared to studies that also included participants with gastric cancer. In this sensitivity analysis, the interventions between the groups of studies were not similar, complicating a straightforward comparison. Therefore, we performed a second sensitivity analysis that focused on five studies reporting the effect of the intervention on OS for participants with GE-junction and gastric cancer separately. This meta-regression analysis indicated that the studied interventions appeared to result in an increased beneficial effect on OS in participants with GE-junction cancer compared to participants with gastric cancer. Therefore, we excluded the studies involving participants with gastric cancer from the meta-analyses of this review. We did not perform any further meta-regression analyses because a comparison between participant groups exposed to the same intervention was not possible. Additionally, the sample size was too small for meta-regression analyses of responses in different participant groups across interventions.

***Subcomparison 1: chemotherapy or targeted therapy plus BSC versus BSC***

This analysis showed that palliative chemotherapy or targeted therapy for participants with esophageal or GE-junction cancer in the palliative setting increased OS (Analysis 4.1; **Figure 6**). We are uncertain whether PFS increased when participants with esophageal or GE-junction cancer received chemotherapy or targeted therapy in the palliative setting

(Analysis 4.2; **Figure 7**). Considering the data available, toxicity levels were similar in both arms of the studies, except for in (Levard 1998). Only (Dutton 2014) described quality of life, showing a trend toward improvement for the chemotherapy arm for one domain.

***Subcomparison 2: participants who had received previous chemotherapy***

In the main analysis, we analyzed first- and second-line palliative chemotherapy together. In subcomparison 2, we investigated the effect of the intervention in participants who had received previous chemotherapy, i.e. second-line palliative therapy studies. This subanalysis showed a probable OS benefit even in participants with prior chemotherapy who received additional chemotherapy or targeted therapy (i.e. second-line therapy). Regarding PFS, there may be a benefit for participants treated with an additional targeted therapy agent.

***Subcomparison 3: chemotherapy agent(s) plus control intervention versus control intervention alone***

The meta-analyses of subcomparison 3 on OS demonstrated that there is probably an effect with regard to OS in favor of the arm with the additional chemotherapy agent, (Analysis 1.1; **Figure 3**, subcomparison 3). Median OS in the arm with the additional chemotherapy agent, weighted for study size, was longer than in the control arm.

***Subcomparison 4: targeted therapy agent plus control intervention versus control intervention alone***

The meta-analyses of subcomparison 4 regarding OS demonstrated the presence of an effect with regard to OS in favor of the arm with the additional targeted agent (Analysis 1.1; **Figure 3**, subcomparison 4). Median overall survival in the arm with the additional targeted agent, weighted for study size, was longer than in the control arm. We performed a subgroup analysis with three studies investigating agents targeting EGFR signaling, finding that these agents probably prolong OS. Subsequently, cetuximab, an EGFR-targeting agent, may decrease the hazard of death. We performed another subgroup analysis that focused on studies investigating ramucirumab and found that this agent also probably decreases the hazard of death. The two studies included only GE-junction participants. The meta-analyses of subcomparison 4 regarding PFS was identical to the meta-analysis of comparison one for PFS as described above. We performed a subgroup analysis investigating EGFR-targeting agents plus control intervention versus control intervention alone, finding a possible reduction of the HR of PFS. Subsequently, we analyzed cetuximab plus control intervention versus control intervention alone; results showed uncertainty with regard to whether this agent reduces the HR for PFS. We performed a third subgroup analysis that focused on studies investigating ramucirumab plus control intervention versus control intervention alone. This resulted in a probable reduction of the HR in favor of the ramucirumab arm, indicating a probable PFS benefit in the ramucirumab group. This meta-analysis only applied to participants with GE-

junction cancer. Regarding quality of life, (Wilke 2014) and (Dutton 2014) reported no differences between groups. Furthermore, (Fuchs 2014) reported a trend toward better quality of life for the arm with the addition of the targeted therapy, ramucirumab in this case.

***Subcomparison 5: chemotherapy or targeted therapy agent(s) plus control intervention versus control intervention alone in participants with adenocarcinoma of the esophagus***

The meta-analyses of subcomparison 5 regarding OS demonstrated the presence of an effect in favor of the arm with the additional chemotherapy or targeted therapy agent (Analysis 9.1). Median OS in the arm with the additional chemotherapy agent, weighted for study size, was longer than in the control arm.

***Subcomparison 6: chemotherapy or targeted therapy agent(s) plus control intervention versus control intervention alone in participants with SCC of the esophagus***

The meta-analyses of subcomparison 6 regarding OS demonstrated the presence of an effect with regard to OS in favor of the arm with the additional chemotherapy or targeted therapy agent (Analysis 10.1). Median OS in the arm with the additional chemotherapy agent, weighted for study size, was longer than in the control arm.

**Overall completeness and applicability of evidence**

In most of the included studies, the participants were only partially representative of all people with esophageal and GE-junction cancer. For instance, they were generally younger, with a median age of 60 years, compared to the overall population of people with esophageal and GE-junction cancer. The proportion of participants with metastatic disease was 69% to 100%, which is roughly comparable to the population normally seen in the clinic. The percentage of participants with ECOG-2 or -3 was in the range of 0% to 35% in the included studies. Two studies selected participants based on tumor biomarker expression, and their results cannot be extrapolated to people that do not have biomarker expression as defined by these studies. The effect of a targeted therapeutic can be expected to depend on the presence of the target in the tumor. (Lorenzen 2009) included only people with EGFR-positive cancer, and (Bang 2010) included only people with HER2-positive cancer. It is therefore not possible to apply these studies' findings to all people, and it is unclear whether they are equally generalizable to everyone with both esophageal and GE-junction cancer. Furthermore, it was not feasible to differentiate between participants with esophageal SCC and adenocarcinoma or investigate their response to various treatments individually because of insufficient availability of data.

Palliative therapy that shows increased survival but without evidence of its effect on quality of life has unclear applicability. Therefore, the preservation of quality of life is an important goal and should be an outcome measure in clinical studies of palliative

treatment modalities (Blazeby 2001). Because not all included studies reported on quality of life in a validated manner, we can only conclude that there is no evidence that palliative chemotherapy and/or targeted therapy decreases quality of life. Various validated measures are available to assess generic as well as disease-specific quality of life. The most commonly used measure for esophageal cancer is the EORTC QLQ-C30 (Aaronson 1993). This measure is specifically designed to measure quality of life in people diagnosed with cancer. A worthwhile addition to this questionnaire is the EORTC QLQ-OES18, a measure specifically designed for people with esophageal cancer that contains more specific questions on dysphagia, chest pain, and reflux symptoms (Blazeby 2003). Only (Rao 2010) used this last measure. More recent studies often use the QLQ-C30 to measure quality of life.

The median absolute survival gain found in the above described analyses, weighted for study size, is limited. For the main analysis, this survival gain applies to the addition of 1.1 agents on average. Adding three agents to BSC, for instance, will likely increase the absolute survival gain. In addition, this analysis also included second-line studies for which the potential survival gain is likely less in absolute terms when compared to first-line palliative care regimens. Except for these limitations, readers may consider the evidence cited above as complete and applicable.

### **Quality of the evidence**

We generally considered the analyzed RCTs to be at low risk of bias in most domains. However, studies were frequently at unclear or high risk of bias with regard to blinding and allocation concealment. More recent RCTs often contained more useful information for determining risk of bias in their descriptions of methodology when compared to older RCTs. For more details about risk of bias, see Risk of bias in included studies.

Various chemotherapy and targeted therapy regimens have been applied for esophageal and GE-junction cancer in a palliative setting. As the regimens in the included RCTs of this review are very heterogeneous, it was often not feasible to make a direct comparison between the various chemotherapeutic agents. The only agents that more than one trial investigated by adding them individually to a control regimen were cetuximab and ramucirumab. Because of the heterogeneity of the agents used, most information can be extracted from an analysis in the form of the main comparison. However, it remains largely unclear which agents lead to a survival benefit. Moderate-quality evidence supports the effectiveness of ramucirumab, and targeting EGFR signaling appears promising. The same heterogeneity is present in the agents that make up the control arms of the studies. Today, some of these agents are no longer or rarely used. Studies testing agents on a background of more popular regimens, for instance containing platinum-based agents and 5-FU, could influence the added effect of the tested agent on survival.

**Potential biases in the review process**

One significant threat to the validity of the review was the possibility of publication bias, that is, studies that did not find the treatments to have been effective may not have been published. We investigated small study effects such as publication bias in a qualitative manner using a funnel plot (**Figure 4**) but found no evidence of its presence.

**Agreements and disagreements with other studies or reviews**

(Mohammad 2015) investigated whether a triplet regimen was superior to a doublet regimen in terms of overall survival, progression-free survival, and objective response rate in participants receiving first-line chemotherapy for advanced or metastatic esophagogastric carcinoma. They found a significant improvement in OS in favor of a triplet regimen (HR 0.90, 95% CI 0.83 to 0.97). Additionally, they found that toxicity grades 3 and 4 were significantly higher in the triplet regimens. Both of these conclusions are in line with our findings.

(Amdal 2013) investigated the effect of palliative radiotherapy and/ or chemotherapy on symptoms and quality of life, as assessed by person-reported outcomes and measurement of toxicity for people with esophageal cancer. They had included mixed populations, including those with gastric, GE-junction, or esophageal cancer. They found no clear association between quality of life and treatment toxicity. Interestingly, two of the RCTs included in our review, which investigated chemotherapy, reported better quality of life despite more treatment toxicity in the experimental arm versus the standard arm (Van Cutsem 2006); (Waters 1999).

Differences in risk factors, gene expression, and tumor biology exist between adenocarcinoma of the stomach, GE-junction, and esophagus (Marsman 2005); (Shah 2011). In this review, we found a difference in chemotherapy and targeted therapy efficacy between GE-junction adenocarcinoma and gastric adenocarcinoma. We found a similar trend in a study by (Chau 2009) using individual participant data from four studies (Cunningham 2008); (Ross 2002); (Tebbutt 2002); (Waters 1999). They concluded that response rates in participants were 44.1% in esophageal, 41.1% in GE-junction, and 35.6% in gastric cancer. Regarding chemotherapeutic treatment of advanced gastric carcinoma, a Cochrane Review has been published (Wagner 2010).

**Authors' conclusions****Implications for practice**

Palliative chemotherapy and targeted therapy increase overall survival in people with esophageal or GE-junction carcinoma compared to BSC. With regard to PFS, we saw a probable trend in the same direction. Additionally, adding chemotherapeutic or targeted

agents increases OS, and adding a targeted agents lengthens PFS. However, the median survival benefit is limited. Of all the individual chemotherapeutic and targeted agents studied, only cetuximab and ramucirumab were investigated more than once. Only ramucirumab significantly prolonged OS and PFS in people with GE-junction cancer that had previously been treated with chemotherapy. Palliative chemotherapy and/or targeted therapy appear to increase the frequency of treatment-related toxicity of at least grade 3. However, treatment-related deaths did not occur more frequently. Five studies measured quality of life with validated methods in this analysis. Although they were not perfectly representative of all the studies in this analysis, they did show that quality of life improved in the arms with the additional agent. Overall, palliative chemotherapy and/or targeted therapy can be considered as standard care for esophageal and GE-junction carcinoma.

### **Implications for research**

There is a need for well-designed, adequately powered, phase III studies on chemotherapy and targeted therapy for metastatic esophageal and GE-junction carcinoma. The main objective should be increased survival, with an additional emphasis on quality of life. These future studies comparing palliative treatment modalities should assess quality of life with validated measures. Studies should be designed in such a way that they enable the comparison of different individual agents on a meta-analysis level. Our results suggest that the participants with GE-junction cancer respond differently to chemotherapy and targeted therapy when compared to the participants with gastric cancer. We do not suggest excluding either group from studies. However, it is advisable to report outcomes separately for these and other subgroups of participants. Additionally, studies pooling these plausibly differently reacting populations might underestimate the number of participants necessary to reach definitive conclusions for each subgroup. Separate reporting for SCC, adenocarcinoma of the esophagus, and adenocarcinoma of the GE-junction would further increase the understanding of the effectiveness of chemotherapies and targeted therapies in these groups.

### **Acknowledgements**

The authors would like to thank the Cochrane Upper Gastrointestinal and Pancreatic Group for their critical review, support and advice. Additionally, the authors would like to thank the biomedical information specialists of the medical library of the Erasmus MC, University Medical Center Rotterdam, The Netherlands for their support with building the search. Finally, we thank the previous authors of this review who paved the way for this updated version.



## References

1. Aaronson NK, Ahmedzai S, Bergman B, Bullinger M, Cull A, Duez NJ, et al. The European Organization for Research and Treatment of Cancer QLQ-C30: a quality-of-life instrument for use in international clinical trials in oncology. *J Natl Cancer Inst.* 1993;85(5):365-76.
2. Ajani JA, Fodor MB, Tjulandin SA, Moiseyenko VM, Chao Y, Cabral Filho S, et al. Phase II multi-institutional randomized trial of docetaxel plus cisplatin with or without fluorouracil in patients with untreated, advanced gastric, or gastroesophageal adenocarcinoma. *J Clin Oncol.* 2005;23(24):5660-7.
3. Ajani JA, Rodriguez W, Bodoky G, Moiseyenko V, Lichinitser M, Gorbunova V, et al. Multicenter phase III comparison of cisplatin/S-1 with cisplatin/infusional fluorouracil in advanced gastric or gastroesophageal adenocarcinoma study: The FLAGS trial. *J Clin Oncol.* 2010;28(9):1547-53.
4. Al-Batran SE, Pauligk C, Homann N, Hartmann JT, Moehler M, Probst S, et al. The feasibility of triple-drug chemotherapy combination in older adult patients with oesophagogastric cancer: A randomised trial of the Arbeitsgemeinschaft Internistische Onkologie (FLOT65+). *Eur J Cancer.* 2013;49(4):835-42.
5. Altman DG. Systematic reviews of evaluations of prognostic variables. *Bmj.* 2001;323(7306):224-8.
6. Amdal CD, Jacobsen AB, Guren MG, Bjordal K. Patient-reported outcomes evaluating palliative radiotherapy and chemotherapy in patients with oesophageal cancer: a systematic review. *Acta Oncol.* 2013;52(4):679-90.
7. Arnold M, Soerjomataram I, Ferlay J, Forman D. Global incidence of oesophageal cancer by histological subtype in 2012. *Gut.* 2015;64(3):381-7.
8. Bang YJ, Van Cutsem E, Feyereislova A, Chung HC, Shen L, Sawaki A, et al. Trastuzumab in combination with chemotherapy versus chemotherapy alone for treatment of HER2-positive advanced gastric or gastro-oesophageal junction cancer (ToGA): A phase 3, open-label, randomised controlled trial. *Lancet.* 2010;376(9742):687-97.
9. Bennett C, Green S, DeCaestecker J, Almond M, Barr H, Bhandari P, et al. Surgery versus radical endotherapies for early cancer and high-grade dysplasia in Barrett's oesophagus. *Cochrane Db Syst Rev.* 2012(11).
10. Blazeby JM. Measurement of outcome. *Surg Oncol.* 2001;10(3):127-33.
11. Blazeby JM, Conroy T, Bottomley A, Vickery C, Arraras J, Sezer O, et al. Clinical and psychometric validation of a questionnaire module, the EORTC QLQ-STO 22, to assess quality of life in patients with gastric cancer. *Eur J Cancer.* 2004;40(15):2260-8.
12. Blazeby JM, Conroy T, Hammerlid E, Fayers P, Sezer O, Koller M, et al. Clinical and psychometric validation of an EORTC questionnaire module, the EORTC QLQ-OES18, to assess quality of life in patients with oesophageal cancer. *Eur J Cancer.* 2003;39(10):1384-94.
13. Bleiberg H, Conroy T, Paillot B, Lacave AJ, Blijham G, Jacob JH, et al. Randomised phase II study of cisplatin and 5-fluorouracil (5-FU) versus cisplatin alone in advanced squamous cell oesophageal cancer. *EUR J CANCER PART A.* 1997;33(8):1216-20.
14. Cascinu S, Galizia E, Labianca R, Ferrau F, Pucci F, Silva RR, et al. Pegylated liposomal doxorubicin, 5-fluorouracil and cisplatin versus mitomycin-C, 5-fluorouracil and cisplatin for advanced gastric cancer: a randomized phase II trial. *Cancer Chemother Pharmacol.* 2011;68(1):37-43.
15. Chau I, Norman AR, Cunningham D, Oates J, Hawkins R, Iveson T, et al. The impact of primary tumour origins in patients with advanced oesophageal, oesophago-gastric junction and gastric adenocarcinoma-025EFindividual patient data from 1775 patients in four randomised controlled trials. *Ann Oncol.* 2009;20(5):885-91.

16. Cook MB, Chow WH, Devesa SS. Oesophageal cancer incidence in the United States by race, sex, and histologic type, 1977-2005. *Brit J Cancer*. 2009;101(5):855-9.
17. Cunningham D, Starling N, Rao S, Iveson T, Nicolson M, Coxon F, et al. Capecitabine and oxaliplatin for advanced esophagogastric cancer. *New Engl J Med*. 2008;358(1):36-46.
18. Dank M, Zaluski J, Barone C, Valvere V, Yalcin S, Peschel C, et al. Randomized phase III study comparing irinotecan combined with 5-fluorouracil and folinic acid to cisplatin combined with 5-fluorouracil in chemotherapy naive patients with advanced adenocarcinoma of the stomach or esophagogastric junction. *Ann Oncol*. 2008;19(8):1450-7.
19. Duffour J, Bouche O, Rougier P, Milan C, Bedenne L, Seitz JF, et al. Safety of cisplatin combined with continuous 5-FU versus bolus 5-FU and leucovorin, in metastatic gastrointestinal cancer (FFCD 9404 randomised trial). *Anticancer Res*. 2006;26(5B):3877-83.
20. Dutton SJ, Ferry DR, Blazeby JM, Abbas H, Dahle-Smith A, Mansoor W, et al. Gefitinib for oesophageal cancer progressing after chemotherapy (COG): A phase 3, multicentre, double-blind, placebo-controlled randomised trial. *Lancet Oncol*. 2014;15(8):894-904.
21. Eatock MM, Tebbutt NC, Bampton CL, Strickland AH, Valladares-Ayerbes M, Swieboda-Sadlej A, et al. Phase II randomized, double-blind, placebo-controlled study of AMG 386 (trebananib) in combination with cisplatin and capecitabine in patients with metastatic gastro-oesophageal cancer. *Annals of Oncology*. 2013;24(3):710-8.
22. Edgren G, Adami HO, Vainio EW, Nyren O. A global assessment of the oesophageal adenocarcinoma epidemic. *Gut*. 2013;62(10):1406-14.
23. Enzinger PC, Mayer RJ. Medical progress - Esophageal cancer. *New Engl J Med*. 2003;349(23):2241-52.
24. Ezdinli EZ, Gelber R, Desai DV, Falkson G, Moertel CG, Hahn RG. Chemotherapy of advanced esophageal carcinoma: Eastern Cooperative Oncology Group experience. *Cancer-Am Cancer Soc*. 1980;46(10):2149-53.
25. Ford HER, Marshall A, Bridgewater JA, Janowitz T, Coxon FY, Wadsley J, et al. Docetaxel versus active symptom control for refractory oesophagogastric adenocarcinoma (COUGAR-02): An open-label, phase 3 randomised controlled trial. *Lancet Oncol*. 2014;15(1):78-86.
26. Fuchs CS, Tomasek J, Yong CJ, Dumitru F, Passalacqua R, Goswami C, et al. Ramucirumab monotherapy for previously treated advanced gastric or gastro-oesophageal junction adenocarcinoma (REGARD): an international, randomised, multicentre, placebo-controlled, phase 3 trial. *Lancet*. 2014;383(9911):31-9.
27. Guyatt GH, Oxman AD, Kunz R, Vist GE, Falck-Ytter Y, Schunemann HJ, et al. What is "quality of evidence" and why is it important to clinicians? *Bmj*. 2008;336(7651):995-8.
28. Higgins JPT, Green S. *Cochrane Handbook for Systematic Reviews of Interventions* Version 5.1.0 The Cochrane Collaboration, 2011.; [Available from: [www.handbook.cochrane.org](http://www.handbook.cochrane.org).
29. Howlader N, Noone AM, Krapcho M, Garshell J, Miller D, Altekruse SF, et al. SEER Cancer Statistics Review, 1975-2011: National Cancer Institute. Bethesda, MD 2014 [Based on November 2013 SEER data submission, posted to the SEER web site, April 2014.:[Available from: [https://seer.cancer.gov/archive/csr/1975\\_2011/](https://seer.cancer.gov/archive/csr/1975_2011/).
30. Huang JY, Sun Y, Fan QX, Zhang YQ. Efficacy of Shenyi Capsule combined with gemcitabine plus cisplatin in treatment of advanced esophageal cancer: A randomized controlled trial. *J Chin Integr Med*. 2009;7(11):1047-51.
31. Hur C, Miller M, Kong CY, Dowling EC, Nattinger KJ, Dunn M, et al. Trends in esophageal adenocarcinoma incidence and mortality. *Cancer*. 2013;119(6):1149-58.

32. Iveson T, Donehower RC, Davidenko I, Tjulandin S, Deptala A, Harrison M, et al. Rilotumumab in combination with epirubicin, cisplatin, and capecitabine as first-line treatment for gastric or oesophagogastric junction adenocarcinoma: an open-label, dose de-escalation phase 1b study and a double-blind, randomised phase 2 study. *Lancet Oncol.* 2014;15(9):1007-18.
33. Jadad AR, Moore RA, Carroll D, Jenkinson C, Reynolds DJ, Gavaghan DJ, et al. Assessing the quality of reports of randomized clinical trials: is blinding necessary? *Control Clin Trials.* 1996;17(1):1-12.
34. Koizumi W, Kim YH, Fujii M, Kim HK, Imamura H, Lee KH, et al. Addition of docetaxel to S-1 without platinum prolongs survival of patients with advanced gastric cancer: a randomized study (START). *J Cancer Res Clin Oncol.* 2014;140(2):319-28.
35. Levard H, Pouliquen X, Hay JM, Fingerhut A, Langlois Zantain O, Huguier M, et al. 5-fluorouracil and cisplatin as palliative treatment of advanced oesophageal squamous cell carcinoma: A multicentre randomised controlled. *European-Journal-of-Surgery.* 1998;164:849-57.
36. Li Q, Feng FY, Han J, Sui GJ, Zhu YG, Zhang Y, et al. [Phase III clinical study of a new anticancer drug atofluding]. *Ai Zheng.* 2002;21(12):1350-3.
37. Li XD, Shen H, Jiang JT, Zhang HZ, Zheng X, Shu YQ, et al. Paclitaxel based vs oxaliplatin based regimens for advanced gastric cancer. *World J Gastroenterol.* 2011;17(8):1082-7.
38. Lin YS, Totsuka Y, He YT, Kikuchi S, Qiao YL, Ueda JK, et al. Epidemiology of Esophageal Cancer in Japan and China. *J Epidemiol.* 2013;23(4):233-42.
39. Lordick F, Kang YK, Chung HC, Salman P, Oh SC, Bodoky G, et al. Capecitabine and cisplatin with or without cetuximab for patients with previously untreated advanced gastric cancer (EXPAND): A randomised, open-label phase 3 trial. *Lancet Oncol.* 2013;14(6):490-9.
40. Lorenzen S, Schuster T, Porschen R, Al-Batran SE, Hofheinz R, Thuss-Patience P, et al. Cetuximab plus cisplatin-5-fluorouracil versus cisplatin-5-fluorouracil alone in first-line metastatic squamous cell carcinoma of the esophagus: a randomized phase II study of the Arbeitsgemeinschaft Internistische Onkologie. *Ann Oncol.* 2009;20(10):1667-73.
41. Machin D, Stenning SP, Parmar MK, Fayers PM, Girling DJ, Stephens RJ, et al. Thirty years of Medical Research Council randomized trials in solid tumours. *Clin Oncol (R Coll Radiol).* 1997;9(2):100-14.
42. Marsman WA, Tytgat GNJ, Ten Kate FJW, Van Lanschot JJB. Differences and similarities of adenocarcinomas of the esophagus and Esophagogastric junction. *J Surg Oncol.* 2005;92(3):160-8.
43. Moehler M, Kanzler S, Geissler M, Raedle J, Ebert MP, Daum S, et al. A randomized multicenter phase II study comparing capecitabine with irinotecan or cisplatin in metastatic adenocarcinoma of the stomach or esophagogastric junction. *Ann Oncol.* 2010;21(1):71-7.
44. Mohammad NH, ter Veer E, Ngai L, Mali R, van Oijen MG, van Laarhoven HW. Optimal first-line chemotherapeutic treatment in patients with locally advanced or metastatic esophagogastric carcinoma: triplet versus doublet chemotherapy: a systematic literature review and meta-analysis. *Cancer Metastasis Rev.* 2015;34(3):429-41.
45. Moher D, Liberati A, Tetzlaff J, Altman DG, Grp P. Preferred Reporting Items for Systematic Reviews and Meta-Analyses: The PRISMA Statement. *J Clin Epidemiol.* 2009;62(10):1006-12.
46. Nicolaou N, Conlan AA. Cyclophosphamide, doxorubicin and celestin intubation for inoperable oesophageal carcinoma. *S AFR MED J.* 1982;61(12):428-31.
47. Ocamo P, Kagimu MM, Odida M, Wabinga H, Opio CK, Colebunders B, et al. Factors associated with carcinoma of the oesophagus at Mulago Hospital, Uganda. *Afr Health Sci.* 2008;8(2):80-4.
48. Ohtsu A, Shah MA, Van Cutsem E, Rha SY, Sawaki A, Park SR, et al. Bevacizumab in combination with chemotherapy as first-line therapy in advanced gastric cancer: a randomized, double-blind, placebo-controlled phase III study. *Journal of Clinical Oncology.* 2011;29(30):3968-76.

49. Pang LN, Wang F, He W, Zhou R, Cao L, Fan QX. Efficacy and safety of S-1 or fluorouracil combined with cisplatin in treatment of advanced esophagus cancer. *World Chin J Dig.* 2014;22(3):383-8.
50. Parmar MKB, Torri V, Steward L. Extracting summary statistics to perform meta-analysis of the published literature for survival endpoints. *Statistics in Medicine* 1998;17:15-34.
51. Pozzo C, Barone C, Szanto J, Padi E, Peschel C, Bukki J, et al. Irinotecan in combination with 5-fluorouracil and folinic acid or with cisplatin in patients with advanced gastric or esophageal-gastric junction adenocarcinoma: Results of a randomized phase II study. *Ann Oncol.* 2004;15(12):1773-81.
52. Rao S, Starling N, Cunningham D, Sumpter K, Gilligan D, Ruhstaller T, et al. Matuzumab plus epirubicin, cisplatin and capecitabine (ECX) compared with epirubicin, cisplatin and capecitabine alone as first-line treatment in patients with advanced oesophago-gastric cancer: A randomised, multicentre open-label phase II study. *Ann Oncol.* 2010;21(11):2213-9.
53. Richards D, Kocs DM, Spira AI, David McCollum A, Diab S, Hecker LI, et al. Results of docetaxel plus oxaliplatin (DOCOX) (plus or minus) cetuximab in patients with metastatic gastric and/or gastroesophageal junction adenocarcinoma: Results of a randomised Phase 2 study. *Eur J Cancer.* 2013;49(13):2823-31.
54. Ross P, Nicolson M, Cunningham D, Valle J, Seymour M, Harper P, et al. Prospective randomized trial comparing mitomycin, cisplatin, and protracted venous-infusion fluorouracil (PVI 5-FU) With epirubicin, cisplatin, and PVI 5-FU in advanced esophagogastric cancer. *J Clin Oncol.* 2002;20(8):1996-2004.
55. Roy A, Cunningham D, Hawkins R, Sorbye H, Adenis A, Barcelo JR, et al. Docetaxel combined with irinotecan or 5-fluorouracil in patients with advanced oesophago-gastric cancer: A randomised phase II study. *Br J Cancer.* 2012;107(3):435-41.
56. Satoh T, Xu RH, Chung HC, Sun GP, Doi T, Xu JM, et al. Lapatinib plus paclitaxel versus paclitaxel alone in the second-line treatment of HER2-amplified advanced gastric cancer in Asian populations: TyTAN--a randomized, phase III study. *J Clin Oncol.* 2014;32(19):2039-49.
57. Shah MA, Khanin R, Tang L, Janjigian YY, Klimstra DS, Gerdes H, et al. Molecular Classification of Gastric Cancer: A New Paradigm. *Clin Cancer Res.* 2011;17(9):2693-701.
58. Shen L, Li J, Xu J, Pan H, Dai G, Qin S, et al. Bevacizumab plus capecitabine and cisplatin in Chinese patients with inoperable locally advanced or metastatic gastric or gastroesophageal junction cancer: randomized, double-blind, phase III study (AVATAR study). *Gastric Cancer.* 2014;18(1):168-76.
59. Somdyala NIM, Bradshaw D, Gelderblom WCA, Parkin DM. Cancer incidence in a rural population of South Africa, 1998-2002. *Int J Cancer.* 2010;127(10):2420-9.
60. Tebbutt NC, Cummins MM, Sourjina T, Strickland A, Van Hazel G, Ganju V, et al. Randomised, non-comparative phase II study of weekly docetaxel with cisplatin and 5-fluorouracil or with capecitabine in oesophagogastric cancer: The AGITG ATTAX trial. *Br J Cancer.* 2010;102(3):475-81.
61. Tebbutt NC, Norman A, Cunningham D, Iveson T, Seymour M, Hickish T, et al. A multicentre, randomised phase III trial comparing protracted venous infusion (PVI) 5-fluorouracil (5-FU) with PVI 5-FU plus mitomycin C in patients with inoperable oesophago-gastric cancer. *Ann Oncol.* 2002;13(10):1568-75.
62. Thuss-Patience PC, Kretzschmar A, Dogan Y, Rothmann F, Blau I, Schwaner I, et al. Docetaxel and capecitabine for advanced gastric cancer: Investigating dose-dependent efficacy in two patient cohorts. *Br J Cancer.* 2011;105(4):505-12.
63. Van Cutsem E, Boni C, Tabernero J, Massuti B, Middleton G, Dane F, et al. Docetaxel plus oxaliplatin with or without fluorouracil or capecitabine in metastatic or locally recurrent gastric cancer: a randomized phase II study. *Ann Oncol.* 2015;26(1):149-56.

64. Van Cutsem E, Moiseyenko VM, Tjulandin S, Majlis A, Constenla M, Boni C, et al. Phase III study of docetaxel and cisplatin plus fluorouracil compared with cisplatin and fluorouracil as first-line therapy for advanced gastric cancer: A report of the V325 study group. *Journal of Clinical Oncology*. 2006;24(31):4991-7.
65. Waddell T, Chau I, Cunningham D, Gonzalez D, Frances A, Okines C, et al. Epirubicin, oxaliplatin, and capecitabine with or without panitumumab for patients with previously untreated advanced oesophagogastric cancer (REAL3): a randomised, open-label phase 3 trial. *The lancet oncology*. 2013;14(6):481-9.
66. Wagner AD, Unerzagt S, Grothe W, Kleber G, Grothey A, Haerting J, et al. Novel Chemotherapy Combinations in Advanced Gastric Cancer: An Updated Meta-Analysis. *Ann Oncol*. 2010;21:226-.
67. Waters JS, Norman A, Cunningham D, Scarffe JH, Webb A, Harper P, et al. Long-term survival after epirubicin, cisplatin and fluorouracil for gastric cancer: results of a randomized trial. *Br J Cancer*. 1999;80(1-2):269-72.
68. White RE, Parker RK, Fitzwater JW, Kasepoi Z, Topazian M. Stents as sole therapy for oesophageal cancer: a prospective analysis of outcomes after placement. *Lancet Oncol*. 2009;10(3):240-6.
69. Wilke H, Muro K, Van Cutsem E, Oh SC, Bodoky G, Shimada Y, et al. Ramucirumab plus paclitaxel versus placebo plus paclitaxel in patients with previously treated advanced gastric or gastro-oesophageal junction adenocarcinoma (RAINBOW): A double-blind, randomised phase 3 trial. *Lancet Oncol*. 2014;15(11):1224-35.
70. Wilkes EA, Selby AL, Cole AT, Freeman JG, Rennie MJ, Khan ZH. Poor tolerability of thalidomide in end-stage oesophageal cancer. *Eur J Cancer Care (Engl)*. 2011;20(5):593-600.
71. Xu Z, Chen J, Tao M. Nimotuzumab combined with cisplatin and 5-FU in treatment of patients with advanced esophageal squamous cell carcinoma. *J Pract Oncol*. 2013;28(6):650-3.

**Summary of findings table for the main comparison.** Chemotherapy or targeted therapy agent(s) plus control intervention versus control intervention alone for palliative treatment of esophageal and GE-junction carcinoma.

Outcome	Relative effect (95% CI)	No. of participants (studies)	Quality of the evidence (GRADE)	Comments
Overall survival	<b>HR 0.75</b> (0.68 to 0.84) Median OS 6.7 months in the chemotherapy or targeted therapy agent(s) + control arm versus 5.7 months in the control arm	1347 participants (11 RCTs)	⊕⊕⊕⊕ High	Quality not downgraded. Although participant populations and agents used differ between studies, there is low imprecision and low inconsistency. Cochrane's <i>Q</i> test for heterogeneity showed almost no heterogeneity ( $I^2=5\%$ , $p=0.50$ )
Progression-free survival	<b>HR 0.64</b> (0.45 to 0.92)	883 participants (5 RCTs)	⊕⊕⊕⊕ Moderate <sup>a</sup>	Cochrane's <i>Q</i> test for heterogeneity showed considerable heterogeneity ( $I^2=79\%$ , $p<0.001$ )
Toxicity	Palliative chemotherapy and/or targeted therapy appear to increase the frequency of treatment-related toxicity of at least grade 3. However, treatment-related deaths did not occur more frequently.	For 3296 participants with esophageal, GE-junction, and gastric cancer (9 RCTs) information was provided on toxicity according to WHO or NCI-CTC guidelines. For at least 1189 participants with esophageal and GE-junction cancer from these trials, toxicity was reported.	⊕⊕⊕⊕ Very low <sup>b</sup>	Small sample size of studies reporting toxicity for the esophageal and GE-junction cancer subgroup separately, for both arms, and with validated methods. Heterogeneity in the relative frequency of toxicities due to palliative chemotherapy and/or targeted therapy.

Summary of findings table for the main comparison. *Continued*

Outcome	Relative effect (95% CI)	No. of participants (studies)	Quality of the evidence (GRADE)	Comments
Quality of life	Quality of life was measured with validated methods in 5 studies included in this analysis. Although the 5 studies were not representative of all the studies in this analysis, as 4 tested a targeted agent, the quality of life reported improved in the arms with the additional agent.	For 1870 participants with esophageal, GE- junction, and gastric cancer (5 RCTs), information was provided on quality of life. For at least 823 participants with esophageal and GE-junction cancer, quality of life was reported.	⊕⊕⊕⊕ Very low <sup>c</sup>	Small sample size of studies reporting data for the esophageal and GE-junction cancer subgroup separately whilst using validated methods.

CI: confidence interval; GE: gastroesophageal; HR: hazard ratio; NCI-CTC: National Cancer Institute Common Toxicity Criteria; OS: overall survival; RCT: randomized controlled trial; WHO: World Health Organization.

GRADE Working Group grades of evidence:

High quality: further research is very unlikely to change our confidence in the estimate of effect.

Moderate quality: further research is likely to have an important impact on our confidence in the estimate of effect and may change the estimate. Low quality: further research is very likely to have an important impact on our confidence in the estimate of effect and is likely to change the estimate. Very low quality: we are very uncertain about the estimate.

<sup>a</sup>Downgraded by one level due to inconsistency.

<sup>b</sup>Downgraded by three levels due to small sample size of studies reporting toxicity for the esophageal and GE-junction cancer subgroup separately, for both arms, and with validated methods. Additionally, some studies in general, or for specific toxicities, reported no difference in toxicity, which indicates possible inconsistency.

<sup>c</sup>Downgraded by three levels due to lack of studies reporting data for the esophageal and GE-junction cancer subgroup separately whilst using validated methods.

**Summary of findings table 2.** Sensitivity analysis: chemotherapy or targeted therapy agent(s) plus control intervention versus control intervention alone for palliating esophageal and GE-junction carcinoma versus gastric carcinoma.

Comparison	Outcome	Relative effect (95% CI)	No. of participants (studies)	Quality of the evidence (GRADE)	Comments
Studies with gastric cancer participants in addition to eligible participants	Overall survival	<b>HR 0.94</b> (0.83 to 1.05)	1755 participants (8 RCTs)	It should not be judged in- dependently as it is not meant to be an exhaustive summary of either esophageal, GE-junction, or gastric cancer participant data.	Cochrane's <i>Q</i> test for heterogeneity showed considerable heterogeneity ( $I^2=54\%$ , $p=0.03$ ).
Sensitivity analysis, meta-regression analysis, first part	Overall survival	<b>HR 0.75</b> (0.68 to 0.84) versus <b>HR 0.94</b> (0.83 to 1.05), <b><i>p</i>=0.004</b> (treatment has a significantly different effect)	1347 participants (11 RCTs) versus 1755 participants (8 RCTs)	⊕⊕⊕⊕ Very low <sup>b</sup>	Cochrane's <i>Q</i> test for heterogeneity showed almost no heterogeneity ( $I^2=5\%$ , $p=0.50$ ) in the arm with esophageal and GE-junction cancer participants. Cochrane's <i>Q</i> test for heterogeneity showed considerable heterogeneity ( $I^2=54\%$ , $p=0.03$ ) in the arm that included also gastric cancer participants.
Sensitivity analysis, only esophageal and GE-junction cancer participants	Overall survival	<b>HR 0.66</b> (0.54 to 0.81)	538 participants (5 RCTs)	It should not be judged in- dependently as it is not meant to be an exhaustive summary of either esophageal and GE-junction participant data.	Cochrane's <i>Q</i> test for heterogeneity showed no heterogeneity ( $I^2=0\%$ , $p=0.56$ ). This meta-analysis was not meant to be exhaustive with regard to the effect of chemotherapy or targeted therapy in people with esophageal and GE-junction cancer.



Summary of findings table 2. *Continued*

Comparison	Outcome	Relative effect (95% CI)	No. of participants (studies)	Quality of the evidence (GRADE)	Comments
Sensitivity analysis, only gastric cancer participants	Overall survival	<b>HR 0.89</b> (0.76 to 1.04)	2093 participants (5 RCTs)	It should not be judged in- dependently as it is not meant to be an exhaustive summary of gastric cancer participant data.	Cochrane's <i>Q</i> test for heterogeneity showed heterogeneity ( $I^2=52\%$ , $p=0.08$ ). This meta-analysis was not meant to be exhaustive with regard to the effect of chemotherapy or targeted therapy in people with gastric cancer.
Sensitivity analysis, meta-regression analysis, second part	Overall survival	HR 0.66 (0.54 to 0.81) versus <b>HR 0.89</b> (0.76 to 1.04), $p=0.03$ (treatment has a significantly different effect)	538 participants (5 RCTs) versus 2093 participants (5 RCTs)	⊕⊕⊕⊕ Moderate <sup>b</sup>	Cochrane's <i>Q</i> test for heterogeneity showed no heterogeneity ( $I^2=0\%$ , $p=0.56$ ) in the arm with only GE-junction cancer participants and heterogeneity ( $I^2=52\%$ , $p=0.08$ ) in the arm with only gastric cancer participants. This result applies only to GE-junction versus gastric cancer.

CI: confidence interval; GE: gastroesophageal; HR: hazard ratio; OS: overall survival; RCT: randomized controlled trial.

GRADE Working Group grades of evidence:

High quality: further research is very unlikely to change our confidence in the estimate of effect.

Moderate quality: further research is likely to have an important impact on our confidence in the estimate of effect and is likely to change the estimate. Low quality: further research is very likely to have an important impact on our confidence in the estimate of effect and is likely to change the estimate. Very low quality: we are very uncertain about the estimate.

<sup>a</sup>Downgraded by three levels due to inconsistency in the group of studies with gastric cancer participants besides eligible participants. Additionally, quality was downgraded because the interventions in both groups of studies were not similar, making the comparison indirect.

<sup>b</sup>Downgraded by one level due to small sample size (for a meta-regression analysis) and inconsistency of the arm of the meta-regression analysis that contains gastric cancer participants.

**Summary of findings table 3.** Subcomparison 1: chemotherapy or targeted therapy plus best supportive care (BSC) versus BSC for palliative treatment of esophageal and GE-junction carcinoma.

Outcomes	Relative effect (95% CI)	No. of participants (studies)	Quality of the evidence (GRADE)	Comments
Overall survival	<b>HR 0.81</b> (0.71 to 0.92) Median OS 4.7 months in the chemotherapy or targeted therapy arm versus 4.2 months in the BSC arm	750 (5 RCTs)	⊕⊕⊕⊕ High	Quality not downgraded. Participant populations and agents used differ between studies. However, there is low imprecision and low in- consistency. Cochrane's <i>Q</i> test for heterogeneity showed almost no heterogeneity ( $I^2=0\%$ , $p=0.57$ ), indicating that results of the studies were consistent.
Progression-free survival	<b>HR 0.58</b> (0.28 to 1.18)	540 (2 RCTs)	⊕⊕⊕⊕ Very low <sup>a</sup>	95% CI includes benefit and harm. Cochrane's <i>Q</i> test for heterogeneity showed considerable heterogeneity ( $I^2=85\%$ , $p=0.01$ ).
Toxicity	Palliative chemotherapy and/or targeted therapy appear to increase the frequency of treatment-related toxicity of at least grade 3. However, treatment-related deaths did not occur more frequently.	For 972 participants with esophageal, GE- junction, and gastric cancer (3 RCTs) information was provided on toxicity according to WHO or NCI-CTC guidelines. For at least 632 participants with esophageal and GE- junction cancer from these trials, toxicity was reported.	⊕⊕⊕⊕ Very low <sup>b</sup>	3/5 studies reported on toxicities with validated methods. 1/3 studies reporting on toxicity, reported it for the esophageal and GE-junction cancer subgroup separately, for both arms and with validated methods.

Summary of findings table 3. *Continued*

Outcomes	Relative effect (95% CI)	No. of participants (studies)	Quality of the evidence (GRADE)	Comments
Quality of life	On average, the quality of life reported improved in the arms with the additional agent.	For 1129 participants with esophageal, GE-junction, and gastric cancer (4 RCTs) information was provided on quality of life. For at least 789 participants with esophageal and GE-junction cancer, quality of life was reported.	⊕⊕⊕⊕ Very low <sup>c</sup>	4/5 studies reported on quality of life. 2/4 studies reported quality of life separately for the esophageal and GE-junction cancer subgroup.

BSC: best supportive care; CI: confidence interval; GE: gastroesophageal; HR: hazard ratio; NCI-CTC: National Cancer Institute Common Toxicity Criteria; OS: overall survival; RCT: randomized controlled trial; WHO: World Health Organization.

GRADE Working Group grades of evidence:

High quality: further research is very unlikely to change our confidence in the estimate of effect.

Moderate quality: further research is likely to have an important impact on our confidence in the estimate of effect and may change the estimate. Low quality: further research is very likely to have an important impact on our confidence in the estimate of effect and is likely to change the estimate. Very low quality: we are very uncertain about the estimate.

<sup>a</sup>Downgraded by three levels due to very serious imprecision (small sample size, 95% CI includes appreciable benefit and harm) and serious inconsistency.

<sup>b</sup>Downgraded by three levels due to non-validated methods used and failure to report toxicities specifically for esophageal and GE-junction cancer patient group.

<sup>c</sup>Downgraded by three levels because not all studies reported on quality of life, and not all studies reported quality of life specifically for esophageal and GE-junction cancer patients.

**Summary of findings table 4.** Subcomparison 2: second-line chemotherapy or targeted therapy agent(s) plus control intervention versus control intervention alone for palliative treatment of esophageal and GE-junction carcinoma.

Outcomes	Relative effect (95% CI)	No. of participants (studies)	Quality of the evidence (GRADE)	Comments
Overall survival	<b>HR 0.71</b> (0.54 to 0.94) Median OS 5.1 months in the chemotherapy or targeted therapy arm versus 4.4 months in the BSC arm	769 participants (4 RCTs)	⊕⊕⊕⊕ Moderate <sup>a</sup>	2 studies investigated the same agent. Cochrane's <i>Q</i> test for heterogeneity showed considerable heterogeneity ( $I^2=57\%$ , $p=0.07$ )
Progression-free survival	<b>HR 0.51</b> (0.29 to 0.90)	677 participants (3 RCTs)	⊕⊕⊕⊕ Low <sup>b</sup>	2 studies investigated the same agent. Cochrane's <i>Q</i> test for heterogeneity showed considerable heterogeneity ( $I^2=86\%$ , $p<0.001$ )
Toxicity	Palliative chemotherapy and/or targeted therapy appear to increase the frequency of treatment-related toxicity of at least grade 3. However, treatment-related deaths did not occur more frequently.	For 1638 participants with esophageal, GE-junction, and gastric cancer (4 RCTs) information was provided on toxicity according to WHO or NCI-CTC guidelines. For at least 769 participants with esophageal and GE-junction cancer from these trials toxicity was reported.	⊕⊕⊕⊕ Very low <sup>c</sup>	1/4 studies reported toxicity for the esophageal and GE-junction cancer subgroup separately, for both arms, and with validated methods.

Summary of findings table 4. *Continued*

Outcomes	Relative effect (95% CI)	No. of participants (studies)	Quality of the evidence (GRADE)	Comments
Quality of life	On average, the quality of life reported improved in the arms with the additional agent.	For 1638 participants with esophageal, GE-junction, and gastric cancer (4 RCTs) information was provided on quality of life. For at least 769 participants with esophageal and GE-junction cancer, quality of life was reported.	⊕⊕⊕⊕ Very low <sup>d</sup>	1/4 studies reported quality of life separately for the esophageal and GE-junction cancer sub-group.

CI: confidence interval; GE: gastroesophageal; HR: hazard ratio; NCI-CTC: National Cancer Institute Common Toxicity Criteria; OS: overall survival; RCT: randomized con- trolled trial; WHO: World Health Organization.

GRADE Working Group grades of evidence:

High quality: further research is very unlikely to change our confidence in the estimate of effect.  
Moderate quality: further research is likely to have an important impact on our confidence in the estimate of effect and may change the estimate. Low quality: further research is very likely to have an important impact on our confidence in the estimate of effect and is likely to change the estimate. Very low quality: we are very uncertain about the estimate.

<sup>a</sup>Downgraded by one level due to small sample size and inconsistency.

<sup>b</sup>Downgraded by two levels due to small sample size and inconsistency.

<sup>c</sup>Downgraded by three levels due to the use of non-validated methods and failure to report toxicities specifically for esophageal and GE-junction cancer patient group.

<sup>d</sup>Downgraded by three levels because not all studies reported on quality of life, and not all studies reported quality of life specifically for esophageal and GE-junction cancer patients.

**Summary of findings table 5.** Subcomparison 3: chemotherapy agent(s) plus control intervention versus control intervention alone for palliative treatment of esophageal and GE-junction carcinoma.

Outcome	Relative effect (95% CI)	No. of participants (studies)	Quality of the evidence (GRADE)	Comments
Overall survival	<b>HR 0.73</b> (0.63 to 0.85) Median OS 6.9 months in the chemotherapy + control arm versus 5.8 months in the control arm.	358 participants (5 RCTs)	⊕⊕⊕⊕ Moderate <sup>a</sup>	There is low imprecision and low inconsistency. Cochrane's <i>Q</i> test for heterogeneity showed low heterogeneity ( $I^2=0\%$ , $p=0.50$ ).
Progression-free survival	No data on progression-free survival was available for this comparison.			
Toxicity	Palliative chemotherapy and/or targeted therapy appear to increase the frequency of treatment-related toxicity of at least grade 3. However, treatment-related deaths did not occur more frequently.	For 1638 participants with esophageal, GE- junction, and gastric cancer (4 RCTs) information was provided on toxicity according to WHO or NCI-CTC guidelines. For at least 769 participants with esophageal and GE-junction cancer from these trials toxicity was reported.	⊕⊕⊕⊕ Very low <sup>b</sup>	1/4 studies reported toxicity for the esophageal and GE-junction cancer sub-group separately, for both arms, and with validated methods.

Summary of findings table 5. *Continued*

Outcome	Relative effect (95% CI)	No. of participants (studies)	Quality of the evidence (GRADE)	Comments
Quality of life	On average, the quality of life reported improved in the arms with the additional agent.	For 450 participants with esophageal and GE- junction cancer, quality of life was reported.	⊕⊕⊕⊕ Very low <sup>c</sup>	4/5 studies reported on quality of life. 1/4 studies reported quality of life separately for the esophageal and GE-junction cancer subgroup.

CI: confidence interval; GE: gastroesophageal; HR: hazard ratio; NCI-CTC: National Cancer Institute Common Toxicity Criteria; OS: overall survival; RCT: randomized con- trolled trial; WHO: World Health Organization.

GRADE Working Group grades of evidence:

High quality: further research is very unlikely to change our confidence in the estimate of effect.

Moderate quality: further research is likely to have an important impact on our confidence in the estimate of effect and may change the estimate. Low quality: further research is very likely to have an important impact on our confidence in the estimate of effect and is likely to change the estimate. Very low quality: we are very uncertain about the estimate.

<sup>a</sup>Downgraded by one level due to small sample size.

<sup>b</sup>Downgraded by three levels due to the use of non-validated methods and failure to report toxicities specifically for esophageal and GE-junction cancer patient group.

<sup>c</sup>Downgraded by three levels because not all studies reported on quality of life, and not all studies reported quality of life specifically for esophageal and GE-junction cancer patients.

**Summary of findings table 6.** Subcomparison 4: targeted therapy agent plus control intervention versus control intervention alone for palliative treatment of esophageal and GE-junction carcinoma.

Outcome	Comparison	Relative effect (95% CI)	No. of participants (studies)	Quality of the evidence (GRADE)	Comments
Overall survival	Subcomparison 4, targeted therapy	<b>HR 0.75</b> (0.63 to 0.90) Median OS 6.7 months in the targeted therapy agent- t(s) + control arm versus 5.7 months in the control arm	989 participants (6 RCTs)	⊕⊕⊕⊕ High	Quality not downgraded. Participant populations and agents used differ between studies. However, there is low imprecision and low inconsistency. Cochrane's <i>Q</i> test for heterogeneity showed low heterogeneity ( $I^2=24\%$ , $p=0.25$ ).
	Subcomparison 4a, EGFR-targeting agents	<b>HR 0.86</b> (95% CI 0.73 to 1.01)	655 participants (3 RCTs)	⊕⊕⊕⊕ Moderate <sup>a</sup>	Cochrane's <i>Q</i> test for heterogeneity showed low heterogeneity ( $I^2=0\%$ , $p=0.56$ ).
	Subcomparison 4b, cetuximab	<b>HR 0.76</b> (95% CI 0.55 to 1.04)	206 participants (2 RCTs)	⊕⊕⊕⊕ Low <sup>b</sup>	95% CI includes benefit and harm. Cochrane's <i>Q</i> test for heterogeneity showed low heterogeneity ( $I^2=0\%$ , $p=0.58$ ).
	Subcomparison 4c, ramucirumab	<b>HR 0.62</b> (0.43 to 0.88)	228 participants (2 RCTs)	⊕⊕⊕⊕ Moderate <sup>a</sup>	Cochrane's <i>Q</i> test for heterogeneity showed low heterogeneity ( $I^2=28\%$ , $p=0.24$ ).



Summary of findings table 6. *Continued*

Outcome	Comparison	Relative effect (95% CI)	No. of participants (studies)	Quality of the evidence (GRADE)	Comments
Progression-free survival	Subcomparison 4, targeted therapy	<b>HR 0.64</b> (0.45 to 0.92)	883 participants (5 RCTs)	⊕⊕⊕⊕ Moderate <sup>c</sup>	Cochrane's <i>Q</i> test for heterogeneity showed low heterogeneity ( $I^2=79\%$ , $p<0.001$ ).
	Subcomparison 4a, EGFR-targeting agents	<b>HR 0.85</b> (0.73 to 1.00)	655 participants (3 RCTs)	⊕⊕⊕⊕ Low <sup>b</sup>	95% CI includes benefit and lack of effect. Cochrane's <i>Q</i> test for heterogeneity showed low heterogeneity ( $I^2=2\%$ , $p=0.36$ ).
	Subcomparison 4b, cetuximab	<b>HR 0.90</b> (0.59 to 1.37)	206 participants (2 RCTs)	⊕⊕⊕⊕ Very low <sup>d</sup>	95% CI includes benefit and harm. Cochrane's <i>Q</i> test for heterogeneity showed a moderate amount of heterogeneity ( $I^2=53\%$ , $p=0.14$ ). One of the two studies was not blinded and did not use an independent review board.
	Subcomparison 4c, ramucirumab	<b>HR 0.39</b> (0.28 to 0.54)	228 participants (2 RCTs)	⊕⊕⊕⊕ Moderate <sup>a</sup>	Cochrane's <i>Q</i> test for heterogeneity showed low heterogeneity ( $I^2=0\%$ , $p=0.99$ ).
Toxicity	Subcomparison 4, targeted therapy	Palliative chemotherapy and/or targeted therapy appear to increase the frequency of treatment-related toxicity of at least grade 3. However, treatment-related deaths did not occur more frequently.	For 3020 participants with esophageal, GE-junction, and gastric cancer (6 RCTs) information was provided on toxicity according to WHO or NCI-CTC guidelines. For at least 990 participants with esophageal and GE-junction cancer from these trials toxicity was reported.	⊕⊕⊕⊕ Very low <sup>e</sup>	2/6 studies reported toxicity for the esophageal and GE-junction cancer subgroup separately, for both arms and with validated methods.

*Summary of findings table 6 continues on next page.*

Summary of findings table 6. *Continued*

Outcome	Comparison	Relative effect (95% CI)	No. of participants (studies)	Quality of the evidence (GRADE)	Comments
Quality of life	Subcomparison 4, targeted therapy	On average, the quality of life reported improved in the arms with the additional agent.	For 2054 participants with esophageal, GE-junction, and gastric cancer (4 RCTs) information was provided on quality of life. For at least 784 participants with esophageal and GE-junction cancer, quality of life was reported.	⊕⊕⊕⊕ Very low <sup>f</sup>	4/6 studies reported on quality of life. 1/4 studies reported quality of life separately for the esophageal and GE-junction cancer subgroup.

CI: confidence interval; EGFR: epidermal growth factor receptor; GE: gastroesophageal; HR: hazard ratio; NCI-CTC: National Cancer Institute Common Toxicity Criteria; OS: overall survival; RCT: randomized controlled trial; WHO: World Health Organization.

GRADE Working Group grades of evidence:

High quality: further research is very unlikely to change our confidence in the estimate of effect.

Moderate quality: further research is likely to have an important impact on our confidence in the estimate of effect and may change the estimate. Low quality: further research is very likely to have an important impact on our confidence in the estimate of effect and is likely to change the estimate. Very low quality: we are very uncertain about the estimate.

<sup>a</sup>Downgraded by one level due to small sample size.

<sup>b</sup>Downgraded by two levels due to small sample size and imprecision.

<sup>c</sup>Downgraded by one level due to inconsistency.

<sup>d</sup>Downgraded by three levels due to small sample size and imprecision.

<sup>e</sup>Downgraded by three levels due to use of non-validated methods and failure to report toxicities specifically for esophageal and GE-junction cancer patient group.

<sup>f</sup>Downgraded by three levels because not all studies reported on quality of life, and not all studies reported quality of life specifically for esophageal and GE-junction cancer patients.

**Summary of findings table 7.** Subcomparison 5: chemotherapy or targeted therapy agent(s) plus control intervention versus control intervention alone in participants with AC of the esophagus.

Outcomes	Relative effect (95% CI)	No of participants (studies)	Quality of the evidence (GRADE)	Comments
Overall survival	<b>HR 0.66</b> (0.54 to 0.81) Median OS 7.1 months in the chemotherapy or targeted therapy arm versus 6.0 months in the BSC arm	538 (5 RCTs)	⊕⊕⊕⊕ High	Quality not downgraded. Participant populations and agents used differ between studies. However, there is low imprecision and low inconsistency. Cochran's <i>Q</i> test for heterogeneity showed almost no heterogeneity ( $I^2=0\%$ , $p=0.55$ ), indicating that results of the studies were consistent.
Progression-free survival	<b>HR 0.62</b> (0.38 to 1.00)	713 (4 RCTs)	⊕⊕⊕⊕ Very low <sup>a</sup>	95% CI includes benefit and no effect. Cochran's <i>Q</i> test for heterogeneity showed considerable heterogeneity ( $I^2=84\%$ , $p<0.001$ ).
Toxicity	Palliative chemotherapy and/or targeted therapy appear to increase the frequency of treatment-related toxicity of at least grade 3. However, treatment-related deaths did not occur more frequently.	For 2676 participants with esophageal, GE- junction, and gastric cancer (5 RCTs) information was provided on toxicity according to WHO or NCI-CTC guidelines. For at least 570 participants with esophageal and GE-junction cancer from these trials, toxicity was reported.	⊕⊕⊕⊕ Very low <sup>b</sup>	0/5 studies reported toxicity for the esophageal and GE-junction cancer subgroup separately, for both arms, and with validated methods.

*Summary of findings table 7 continues on next page.*

Summary of findings table 7. *Continued*

Outcomes	Relative effect (95% CI)	No of participants (studies)	Quality of the evidence (GRADE)	Comments
Quality of life	On average, the quality of life reported improved in the arms with the additional agent.	For 1772 participants with esophageal, GE-junction, and gastric cancer (4 RCTs) information was provided on quality of life. For at least 426 participants with esophageal and GE-junction cancer, quality of life was reported.	⊕⊕⊕⊕ Very low <sup>c</sup>	4/5 studies reported on quality of life. 0/4 studies reported quality of life separately for the esophageal and GE-junction cancer subgroup.

AC: adenocarcinoma; BSC: best supportive care; CI: confidence interval; HR: hazard ratio; NCI-CTC: National Cancer Institute Common Toxicity Criteria; OS: overall survival; RCT: randomized controlled trial; WHO: World Health Organization.

GRADE Working Group grades of evidence:

High quality: further research is very unlikely to change our confidence in the estimate of effect.

Moderate quality: further research is likely to have an important impact on our confidence in the estimate of effect and may change the estimate. Low quality: further research is very likely to have an important impact on our confidence in the estimate of effect and is likely to change the estimate. Very low quality: we are very uncertain about the estimate.

<sup>a</sup>Downgraded three levels due to very serious imprecision (95% CI includes appreciable benefit and no effect) and serious inconsistency.

<sup>b</sup>Downgraded by three levels due to use of non-validated methods and failure to report toxicities, specifically for esophageal and GE-junction cancer patient group.

<sup>c</sup>Downgraded by three levels because not all studies reported on quality of life, and not all studies reported quality of life specifically for esophageal and GE-junction cancer patients.

**Summary of findings table 8.** Subcomparison 6: chemotherapy or targeted therapy agent(s) plus control intervention versus control intervention alone in participants with SCC of the esophagus.

Outcomes	Relative effect (95% CI)	No. of participants (studies)	Quality of the evidence (GRADE)	Comments
Overall survival	HR 0.76 (95% CI 0.65 to 0.90) Median OS 8.0 months in the chemotherapy or targeted therapy arm versus 6.5 months in the BSC arm.	268 (4 RCTs)	⊕⊕⊕⊕ High	Quality not downgraded. Participant populations and agents used differ between studies. However, there is low imprecision and low inconsistency. Cochrane's <i>Q</i> test for heterogeneity showed almost no heterogeneity ( $I^2=0\%$ , $p=0.95$ ), indicating that results of the studies were consistent.
Progression-free survival	HR 0.72 (95% CI 0.55 to 0.96)	168 (2 RCTs)	⊕⊕⊕⊕ Very low <sup>a</sup>	Cochrane's <i>Q</i> test for heterogeneity showed significant heterogeneity ( $I^2=0\%$ , $p=0.97$ ), indicating that results of the 2 studies were not consistent. One of the 2 studies was not blinded and did not use an independent review board.
Toxicity	Palliative chemotherapy and/or targeted therapy appear to increase the frequency of treatment- related toxicity of at least grade 3. However, treatment-related deaths did not occur more frequently.	For 150 participants with esophageal and GE-junction cancer (2 RCTs) information was provided on toxicity according to WHO or NCI- CTC guidelines.	⊕⊕⊕⊕ Very low <sup>b</sup>	2/4 studies reported on toxicities with validated methods. 2/2 studies reporting toxicity for the esophageal and GE-junction cancer subgroup separately, for both arms, and with validated methods.

*Summary of findings table 8 continues on next page.*

**Summary of findings table 8.** *Continued*

Outcomes	Relative effect (95% CI)	No. of participants (studies)	Quality of the evidence (GRADE)	Comments
Quality of life	On average, the quality of life reported improved in the arms with the additional agent.	For 156 participants with esophageal and GE-junction cancer (1 RCT) information was provided on quality of life.	⊕⊕⊕⊕ Very low <sup>c</sup>	1/4 studies reported on quality of life.

BSC: best supportive care; CI: confidence interval; GE: gastro-esophageal; HR: hazard ratio; NCI-CTC: National Cancer Institute Common Toxicity Criteria; OS: overall survival; RCT: randomized controlled trial; SCC: squamous cell carcinoma; WHO: World Health Organization.

GRADE Working Group grades of evidence:

High quality: further research is very unlikely to change our confidence in the estimate of effect.

Moderate quality: further research is likely to have an important impact on our confidence in the estimate of effect and may change the estimate. Low quality: further research is very likely to have an important impact on our confidence in the estimate of effect and is likely to change the estimate. Very low quality: we are very uncertain about the estimate.

<sup>a</sup>Downgraded by two levels due to small sample size, and one level due lack of blinding or use of an independent review board.

<sup>b</sup>Downgraded by three levels due to use of non-validated methods and failure to report toxicities specifically for esophageal and GE-junction cancer patient group.

<sup>c</sup>Downgraded by three levels because not all studies reported on quality of life, and not all studies reported quality of life specifically for esophageal and GE-junction cancer patients.

## Supplementary information

With regard to the characteristics of the excluded studies, studies awaiting assessment, and ongoing studies, these can be accessed through the Cochrane Library.

With regard to the comparisons and analyses, these can be accessed through the Cochrane Library.

### Appendix 1. Glossary

- Chemotherapy: a drug treatment that uses chemicals to kill fast-growing cells in the body in a fairly aspecific manner.
- Dysphagia: the symptom of difficulty in swallowing.
- Metastatic: the spread of cancer from one part of the body to another without being directly connected to it.
- Non-resectable: not able to be removed by surgery. This can have multiple possible causes, for instance, the cancer has grown into a vital organ which cannot be removed, or the removal of the cancer would not cure the person because metastases are present, or the person is in such physical condition that exposure to surgery would cause a significant risk of dying.
- Palliative care: treatment that reduces the effects or symptoms of a medical condition without curing it.
- Cytostatic therapy: a drug treatment that is directed at fast-dividing cells in general.
- Targeted therapy: a drug treatment, often a monoclonal antibody or a small molecule, to block the growth and spread of cancer by interfering with specific molecules.
- Toxicity: any unfavourable event, symptom, or disease associated with the use of a treatment that may or may not be considered related to the treatment.

### Appendix 2. CENTRAL search strategy

```
((esophag* OR oesophag* OR gastroesophag* OR gastrooesophag* OR junction*)
NEAR/6 (neoplas* OR cancer* OR tumo* OR metasta* OR meta-stasis OR meta-
static OR malign* OR carcinom* OR adenocarcinom*)):ab,ti)AND ((chemotherap*
OR chemoradi* OR radiochemo* OR photochemo* OR ((drug* OR chemo*)
NEAR/6 (radi* OR therap*)):ab,ti) AND ((palliat* OR unresect* OR irresect* OR
nonresect* OR inopera* OR unopera* OR nonopera* OR advanced OR (non NEAR/1
(opera* OR resect*)):ab,ti)) NOT ((preopera* OR ((pre OR post) NEAR/1 opera*) OR
postopera*)):ab,ti)
```

### Appendix 3. MEDLINE OvidSP

```
("Esophageal Neoplasms"/ OR (exp "Esophagogastric Junction"/ AND exp "Digestive
System Neoplasms"/) OR ((esophag* OR oesophag*OR gastroesophag* OR
```

gastroesophag\* OR junction\* ) ADJ6 (neoplas\* OR cancer\* OR tumo\* OR metasta\* OR meta-stasis OR meta-static OR malign\* OR carcinom\* OR adenocarcinom\*)).ab,ti.) AND (exp “drug therapy”/ OR exp “digestive systemcancer”/dt OR (chemotherap\* OR chemoradi\* OR radiochemo\* OR photochemo\* OR ((drug\* OR chemo\*) ADJ6 (radi\* OR therap\*))).ab,ti.) AND (“PalliativeCare”/ OR (palliat\* OR unresect\* OR irresect\* OR nonresect\* OR inopera\* OR unopera\* OR nonopera\* OR advanced OR (non ADJ1 (opera\* OR resect\*)).ab,ti.)) AND (“randomized controlled trial”.pt. OR “evaluation studies”.pt. OR “comparative study”.pt. OR “ Follow-Up Studies”/ OR “Prospective Studies”/ OR (random\* OR factorial\* OR crossover\* OR (cross ADJ over\*) OR placebo\* OR ((doubl\* OR singl\* OR tripl\*) ADJ (mesk\* OR blind\*)) OR assign\* OR allocat\* OR volunteer\* OR comparat\* OR evaluat\* OR follow-up OR followup OR prospectiv\* OR control\*).ab,ti.) NOT (“preoperative period”/ OR exp “postoperative period”/ OR (preopera\* OR ((pre OR post) ADJ1 opera\*) OR postopera\*).ab,ti.)

#### Appendix 4. Embase search strategy

('esophagus cancer'/exp OR ('lower esophagus sphincter'/de AND 'digestive system cancer'/exp) OR ((esophag\* OR oesophag\* OR gastroesophag\* OR gastrooesophag\* OR junction\*) NEAR/6 (neoplas\* OR cancer\* OR tumo\* OR metasta\* OR meta-stasis OR meta-static OR malign\* OR carcinom\* OR adenocarcinom\*)):ab,ti) AND ('drug therapy'/exp OR 'digestive system cancer'/exp/dm`dt OR (chemotherap\* OR chemoradi\* OR radiochemo\* OR photochemo\* OR ((drug\* OR chemo\*) NEAR/6 (radi\* OR therap\*)):ab,ti) AND ('advanced cancer'/de OR 'palliative therapy'/exp OR (palliat\* OR unresect\* OR irresect\* OR nonresect\* OR inopera\* OR unopera\* OR nonopera\* OR advanced OR (non NEAR/1 (opera\* OR resect\*)):ab,ti)) AND ('crossover procedure'/de OR 'doubleblind procedure'/de OR 'randomized controlled trial'/de OR 'single-blind procedure'/de OR evaluation/de OR 'comparative study'/ exp OR 'follow up'/de OR 'prospective study'/de OR (random\* OR factorial\* OR crossover\* OR (cross NEXT/1 over\*) OR placebo\* OR ((doubl\* OR singl\* OR tripl\*) NEXT/1 (mesk\* OR blind\*)) OR assign\* OR allocat\* OR volunteer\* OR comparat\* OR evaluat\* OR follow-up OR followup OR prospectiv\* OR control\*):ab,ti) NOT ('preoperative period'/exp OR 'postoperative period'/exp OR (preopera\* OR ((pre OR post) NEAR/1 opera\*) OR postopera\*):ab,ti)

#### Appendix 5. Web of Science

TS=(((esophag\* OR oesophag\* OR gastroesophag\* OR gastrooesophag\* OR junction\*) NEAR/6 (neoplas\* OR cancer\* OR tumo\* OR metasta\* OR meta-stasis OR meta-static OR malign\* OR carcinom\* OR adenocarcinom\*))) AND ((chemotherap\* OR chemoradi\* OR radiochemo\* OR photochemo\* OR ((drug\* OR chemo\*) NEAR/6 (radi\* OR therap\*))) AND ((palliat\* OR unresect\* OR irresect\* OR nonresect\* OR inopera\* OR unopera\* OR nonopera\* OR advanced OR (non NEAR/1 (opera\* OR resect\*)))) NOT ((preopera\* OR ((pre OR post) NEAR/1 opera\*) OR postopera\*)) AND (random\* OR factorial\* OR



crossover\* OR (cross NEAR/ 1 over\*) OR placebo\* OR ((doubl\* OR singl\* OR tripl\*) NEAR/1 (mesk\* OR blind\*)) OR assign\* OR allocat\* OR volunteer\* OR comparat\* OR evaluat\* OR follow-up OR followup OR prospectiv\* OR control\*)) Appendix 6. PubMed publisher (((esophag\*[tiab] OR oesophag\*[tiab] OR gastroesophag\*[tiab] OR gastrooesophag\*[tiab] OR junction\*[tiab] ) AND (neoplas\*[tiab] OR cancer[tiab] OR cancers[tiab] OR tumor[tiab] OR tumors[tiab] OR tumor\*[tiab] OR metasta\*[tiab] OR meta-sta\*[tiab] OR malign\*[ tiab] OR carcinom\*[tiab] OR adenocarcinom\*[tiab])))) AND ((chemotherap\*[tiab] OR chemoradi\*[tiab] OR radiochemo\*[tiab] OR photochemo\*[tiab] OR ((drug[tiab] OR drugs[tiab] OR chemo[tiab]) AND (radio[tiab] OR radiother[tiab] OR therapy[tiab] OR therapies[tiab])))) AND ((palliat\*[tiab] OR unresect\*[tiab] OR irresect\*[tiab] OR nonresect\*[tiab] OR inopera\*[tiab] OR unopera\*[ tiab] OR nonopera\*[tiab] OR advanced OR non opera\*[tiab] OR non resect\*[tiab])) AND ((random\*[tiab] OR factorial\*[tiab] OR crossover\*[tiab] OR cross over\*[tiab]OR placebo\*[tiab] OR ((doubl\*[tiab] OR singl\*[tiab] OR tripl\*[tiab]) AND (mesk\*[tiab]OR blind\*[tiab])) OR assign\*[tiab] OR allocat\*[tiab] OR volunteer\*[tiab] OR comparat\*[tiab] OR evaluat\*[tiab] OR follow-up OR followup OR prospectiv\*[tiab] OR control[tiab] OR controlled[tiab])) NOT ((preopera\*[tiab] OR pre opera\*[tiab] OR post opera\*[tiab] OR postopera\*[tiab])) AND publisher[sb]

## Appendix 6. Google scholar

“(esophagus|esophageal|oesophagus|esophageal|junction) (neoplasm|neoplasms|cancer| malignant|carcinoma)” (chemotherapy|chemoradiotherapy|radiochemotherapy)

## Appendix 7. Clinicaltrials.gov

(esophageal OR esophagus OR gastresophageal) AND (neoplasm OR neoplasms OR cancer OR tumors) AND (chemotherapy OR chemoradiotherapy OR radiochemotherapy) AND (palliative OR unresectable OR irresectable OR nonresectable OR inoperable OR advanced)

## Appendix 8.WHO International Clinical Trials Registry Platform (ICTRP) search strategy

Esophag\* AND neoplas\* AND palliat\* OR Oesophag\* AND neoplas\* AND palliat\* OR Esophag\* AND cancer\* AND palliat\* OR Oesophag\* AND cancer\* AND palliat\* OR Esophag\* AND neoplas\* AND unresectable\* OR Oesophag\* AND neoplas\* AND unresectable\* OR Esophag\* AND cancer\* AND unresectable\* OR Oesophag\* AND cancer\* AND unresectable\*

The sections: what's new, history, contributions of authors, declarations of interest, sources of support, differences between protocol and review, and index terms can be accessed through the Cochrane Library.



# Chapter 10

---

## Cost-effectiveness of cetuximab for advanced esophageal squamous cell carcinoma

Vincent T. Janmaat · Marco J. Bruno · Suzanne Polinder · Sylvie Lorenzen ·  
Florian Lordick · Maikel P. Peppelenbosch · Manon C.W. Spaander

*PLoS One. 2016;11(4):e0153943*

## Abstract

Costly biologicals in palliative oncology are emerging at a rapid pace. For example, in patients with advanced esophageal squamous cell carcinoma addition of cetuximab to a palliative chemotherapy regimen appears to improve survival. However, it simultaneously results in higher costs. We aimed to determine the incremental cost-effectiveness ratio of adding cetuximab to first-line chemotherapeutic treatment of patients with advanced esophageal squamous cell carcinoma, based on data from a randomized controlled phase II trial. A cost effectiveness analysis model was applied based on individual patient data. It included only direct medical costs from the health-care perspective. Quality-adjusted life-years and incremental cost-effectiveness ratios were calculated. Sensitivity analysis was performed by a Monte Carlo analysis. Adding cetuximab to a cisplatin-5-fluorouracil first-line regimen for advanced esophageal squamous cell carcinoma resulted in an incremental cost-effectiveness ratio of €252,203 per quality-adjusted life-year. Sensitivity analysis shows that there is a chance of less than 0.001 that the incremental cost-effectiveness ratio will be less than a maximum willingness to pay threshold of €40,000 per quality-adjusted life-year, which is representative for the threshold used in The Netherlands and other developed countries. In conclusion, the addition of cetuximab to a cisplatin-5-fluorouracil first-line regimen for advanced esophageal squamous cell carcinoma is not cost-effective when appraised according to currently accepted criteria. Cost-effectiveness analyses using outcome data from early clinical trials (*i.e.* a phase II trial) enable pharmaceutical companies and policy makers to gain early insight into whether a new drug meets the current eligibility standards for reimbursement and thereby potential admittance for use in regular clinical practice.

## Introduction

The use of biologicals in palliative oncology is expanding at a rapid pace. These new therapeutic agents may improve patients' survival and quality of life. However, the money spend on biologicals is expected to increase at a faster rate than the overall spending growth on pharmaceuticals and is projected to represent roughly one fifth of the total costs by 2017 (1). It would be beneficial for drug companies, policy makers, physicians and patients alike when the cost-effectiveness of these biologicals would become apparent at an early stage of development.

A good example of a carcinoma for which biologicals are being studied in palliative phase II trials is esophageal squamous cell carcinoma (ESCC). ESCC is the predominant form of esophageal carcinoma worldwide, and most patients are diagnosed in advanced stages not amenable to curative treatment (2-4). Palliative therapy consists of chemotherapy or (chemo-)radiation therapy, management of pain, and achieving optimal nutrition. Currently survival in these patients receiving palliative care remains poor.

Lorenzen et al. conducted a phase II trial in 62 patients with non-resectable epidermal growth factor receptor (EGFR)-expressing ESCC (5). This trial showed that addition of cetuximab (Erbix, Merck Serono, Geneva, Switzerland) in palliative treatment of ESCC is likely to prolong survival. The median progression-free survival increased from 3.6 months (95% confidence interval (CI) 1.0-6.2) to 5.9 months (95% CI 3.8-8.0). The median overall survival increased from 5.5 months (95% CI 1.9-9.1) to 9.5 months (95% CI 8.4-10.6). The three adverse events that occurred more often in the cetuximab arm were neutropenia (22% vs 13%), diarrhea (16% vs 0%), and nausea (13% vs 3%), while fatigue decreased (3% vs 10%) (5).

The cost-effectiveness of cetuximab as palliative treatment has not been investigated in ESCC, but has been assessed for other malignancies. Hannouf et al. (6) estimated that adding cetuximab to platinum-based chemotherapy for squamous cell carcinoma of the head and neck (SCCHN) resulted in a cost-utility ratio of €249,888 per quality adjusted life year (QALY). In addition an incremental cost-effectiveness ratio (ICER) of €242,494 per QALY was reported by the National Institute for Care and health Excellence (NICE) after exploratory analysis using alternative assumptions and parameters in the economic model of the treatment of SCCHN with cetuximab (7). In metastasized KRAS wild type colorectal carcinomas, an ICER of €112,707 per QALY was reported (8). All these studies with incurable patients receiving cetuximab show ICERs above a maximum willingness to pay threshold of €40,000. This threshold is representative for The Netherlands and other developed countries (9-14).

Phase III trials investigating the effectiveness of adding cetuximab to palliative therapy of ESCC were started after the publication of Lorenzen et al. (15). Although the addition of cetuximab seems to offer a health benefit, it might have an ICER above the current

maximum willingness to pay threshold. Early estimation of the ICER would give early insight into the costs of the therapy regimen and hence the probability that the drug will be reimbursed. If there is too much of a gap between effectiveness and costs, informed decision-making could question the costly development of a drug that will have a hard time to be commercially viable and, importantly, early information sharing would spare the public from developing false expectations.

This paper aims to calculate the expected mean ICER of adding cetuximab to the standard palliative treatment of ESCC in a Dutch health-care setting, based on published data from a phase II trial (5). It shows that the addition of cetuximab is not cost-effective.

## Methods

### Framework of cost-effectiveness analysis

The cost-effectiveness analysis was based on data from the study performed by Lorenzen et al. (5). A linear model was used. Two clinical outcome measures, namely mean progression free survival (PFS) and mean overall survival (OS), were used in addition to an approximation of overall costs, in order to calculate ICERs. The cost-effectiveness analysis assumed the health-care perspective, including only direct medical costs. Modelling was done using Microsoft Excel (Microsoft Corporation, Redmond, WA).

### One-way sensitivity analysis

A one-way sensitivity analysis was conducted by taking all input variables of the model and varying them by 10% in both directions. When varying one input variable, other input variables were kept constant.

### Probabilistic sensitivity analysis

The probabilistic sensitivity analysis was performed using a Monte Carlo simulation using Microsoft Excel (Microsoft Corporation, Redmond, WA). For this analysis, 1000 simulated trials were run, where the values for the OS and PFS of both arms were sampled at random from normalized probability distributions based on the trial sample means and their standard deviation. By using the standard deviation of the mean values the variation of the sample means estimate of the population mean was taken into account. Other parameters of the model were kept constant. This generated the mean costs and mean survival benefit for 1000 simulated trials.

### Patients

In the study of Lorenzen et al. (5), 62 patients were randomly assigned to the cetuximab, cisplatin, and fluorouracil arm (n=32) or to the cisplatin and fluorouracil arm (n=30). The

protocol of the study of Lorenzen et al. was approved by the ethics committee for human research at the Technische Universität München, Munich, Germany, and conformed to the principles of the Declaration of Helsinki and its subsequent amendments. The analyses presented in this study fall under the same protocol. All patients gave written informed consent. Patient records/information was anonymized and de-identified prior to analysis. The patients were at least 18 years of age, had histologically confirmed and EGFR-expressing advanced non-resectable ESCC. They had not received (neo)adjuvant chemotherapy within six months of enrollment into the study and had not had prior chemotherapy for recurrent or metastatic disease. Their Eastern Cooperative Oncology Group performance status (ECOG PS) had to be one or less, creatinine clearance had to be above 70 ml/min. They had to have adequate hepatic function, bone marrow function, and a lesion measurable in one dimension of at least one cm in diameter detected by computed tomography (CT) scan was required. Exclusion criteria were a second malignancy, uncontrolled infection, a neuropathy grade more than one, and pregnancy or lactation. Median follow-up time was 21.5 months. Both groups were well balanced with respect to age, tumor differentiation, and intensity of EGFR staining. However, there was a marked difference in the gender balance between the arms with the cetuximab arm containing more female patients. More than 30% of patients in each arm had either prior surgery, radiotherapy, or both. In contrast, only 13% of patients in each arm had received prior systemic chemotherapy (5).

### Therapy regimen

For a maximum of six 29-day cycles, patients received cisplatin 100 mg/m<sup>2</sup>, day 1, plus fluorouracil 1000 mg/m<sup>2</sup>, days 1-5, either alone or in combination with cetuximab. Cetuximab was initially dosed at 400 mg/m<sup>2</sup>, followed by 250 mg/m<sup>2</sup> weekly thereafter (5). The modelled therapy regimen was constructed to take treatment discontinuation into account, the level of treatment discontinuation was chosen so as to assume a mean cetuximab use equal to that calculated for the phase II trial (see results section).

### Determination of QALYs

PFS and OS figures were used from the study of Lorenzen et al. The authors reported median OS and PFS times. Using individual patient data, mean OS and PFS times were calculated, as these data were necessary to calculate the ICER of the proposed therapy regimen. The utility score during PFS was calculated. Asymptomatic adenocarcinoma of the esophagus was associated with a utility score of 0.77, symptomatic adenocarcinoma of the esophagus was associated with a utility score of 0.675 (16, 17). Since most patients were diagnosed because they presented themselves with symptoms, the utility score of symptomatic disease was used, i.e. 0.675. The utility score during disease progression was defined as the average of the utility score at death, which is zero, and the utility score during PFS. This approach reflects the assumption that the utility score linearly declines

from the point of progression to the point of passing away, see **Figure 1** for a schematic representation of the assumptions used. QALYs were calculated by:  $PFS \times \text{utility score during PFS} + (OS - PFS) \times \text{utility score during disease progression}$ :  $PFS \times 0.675 + (OS - PFS) \times 0.675$ . The amount of QALYs gained was calculated by taking the amount of QALYs calculated for the intervention group minus the amount of QALYs calculated for the control group.

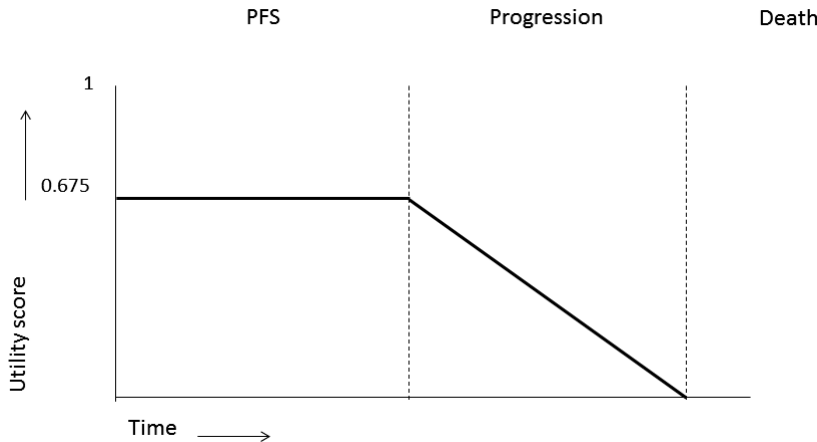


**Figure 1.** Schematic representation of the health states and utility scores used in the linear model. At diagnosis a utility score of 0.675 was assumed. This utility score remains stable during progression free survival. During progressive disease, it was assumed that the utility score declines linearly from 0.675 to 0 at the time of death.

### Determination of costs

An estimate was made of the medical resource usage that resulted from the incremental cost of adding cetuximab to the standard treatment. Unless otherwise specified, unit costs were obtained from the Dutch manual for cost-effectiveness research 2010 (18). The cost of cetuximab for an average patient was calculated. The cost of cetuximab in 2007 was €207 per 100 mg in the Netherlands, and €237.20 in 2009 (19). The model accounted for: value attributed tax, duration of treatment, the increased dose for the first treatment (400 versus 250 mg), the male female difference in dosage, the relative proportion of both sexes affected by ESCC, and the amount of treatment discontinuation. The cost of an outpatient visit was estimated to be €251 (18). The number of outpatient clinic visits was calculated. Duration of therapy and the number of outpatient visits that can be combined with visits for chemotherapy were accounted for. The incremental cost of these combined visits was estimated. Lorenzen et al. screened for EGFR expressing tumor patients (5). Screening for a subset of eligible patients significantly contributes to therapy cost, increasing with decreasing biomarker frequencies (16). The cost of



evaluation of EGFR expression (€750) was based on the reimbursement for such a test in the Dutch healthcare system. It was assumed that 60% of patients have EGFR expressing tumors (20-22). Although all patients have to be screened. Incremental cost for housing and depreciation of goods (6.5%) and overhead (35.5%) were accounted for. Possible costs associated with an increase in adverse events were not accounted for. All costs and effects were converted to the price level of 2009 according to the general Dutch consumer price index (23). Results of other studies, reported in CAD and Pound Sterling, were converted to euros using the purchasing power parity index of the year closest to the year in which the study outcome was reported (24). A cost-effectiveness ratio below €40,000 per gained QALY was assumed to be acceptable. This threshold is representative for the willingness to pay threshold in The Netherlands and other developed countries (9-14). The time horizon of the base case model was 0.9 years. Because of this short time horizon, neither costs nor clinical outcomes were discounted.

## Results

Lorenzen et al. reported a median OS of 5.5 and a median PFS of 3.6 months for the CF arm as well as a median OS of 9.5 and a median PFS of 5.9 months for the CET CF arm. This translates into a mean OS of 8.6 and a mean PFS of 5.6 months for the CF arm as well as a mean OS of 10.8 and a mean PFS of 7.1 for the CET CF arm. The median cumulative dose of cetuximab per patient was reported to be 8 690mg. The mean cumulative dose of cetuximab per patient was recalculated. This resulted in a mean cumulative dose of 6,443mg cetuximab per patient. Subsequently, the level of treatment discontinuation was chosen so as to assume a mean cetuximab use of 6,444 mg.

The mean survival gained by the addition of cetuximab to standard chemotherapy was 0.187 life years and 0.105 QALYs. The mean incremental cost was calculated to be €26,459 per treated patient. The incremental costs included the costs of cetuximab, additional day treatment facilities, and the cost of evaluation EGFR status, in order of impact. Adding cetuximab to a cisplatin-5-fluorouracil first-line regimen for advanced ESCC resulted in a mean ICER of €252,203 per QALY.

A one-way sensitivity analysis was conducted by taking all input variables of the model and varying them by 10% in both directions. The resulting ICERs were depicted in a tornado plot, see **Figure 2**. The input extracted from the phase II trial, had most effect on the determination of the ICER. Other factors of influence were the quality of life assumption used, the amount of cetuximab used, and the price of cetuximab.

A probabilistic sensitivity analysis was performed by conducting a Monte Carlo analysis, results are shown in **Figure 3**. Each point represents one of the 1000 trials runs. The data

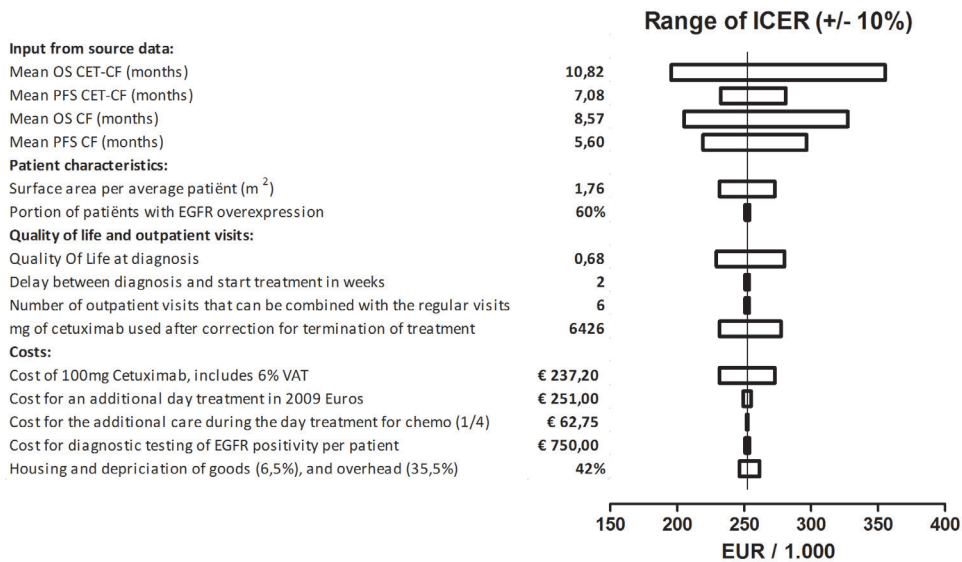


**Figure 2.** Tornado plot of a one-way sensitivity analysis. Input variables were tested in a one-way sensitivity analysis. These variables were either decreased by 10% of the value used in the base case model, or increased 10% from their original value. The bars represent the range of the ICER if the variable lies between -10% and +10% of its assumed value in the base case model. The ICER from the base case model was indicated by the vertical dotted line.

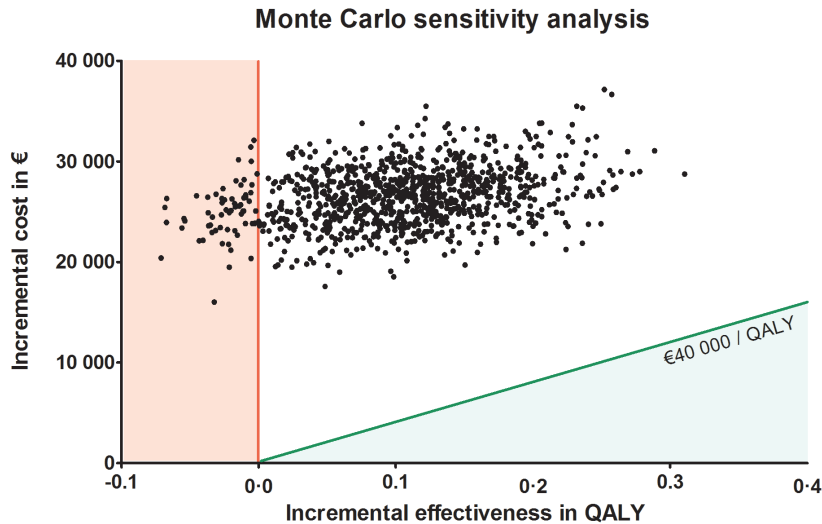


**Figure 3.** Scatter plot of Monte Carlo sensitivity analysis. One thousand repeated random samplings from the model described are depicted in the figure. Each sampling is depicted by one dot and represents the average QALY gained and the incremental cost of that sampling from the model. The vertical line separates the plane (to the left), for which the intervention is not effective. With the plane to the right for which the intervention is effective. The inclining line depicts the maximum willingness to pay threshold at an ICER of €40,000 per QALY gained. This line separates the plane above it, for which the intervention is effective but not cost effective, with the plane below, for which the intervention is effective and cost effective.

extracted from the phase II trial had most influence on the determination of the ICER in the one-way sensitivity analysis. Therefore, with respect to the input data for the OS and PFS of both arms, each input was assigned a random value. This was based on the mean and standard deviation extracted from the individual patient data. Other input data was kept constant. The solid diagonal line indicates the €40,000 per QALY gained willingness to pay threshold. Trial points that fall to the left and above this diagonal line indicate a cost-effectiveness of that trial run above the given maximum willingness to pay threshold level. This analysis shows that  $p < 0.001$  of the ICER being below a maximum willingness to pay threshold of €40,000.

## Discussion

The mean ICER of adding cetuximab to a cisplatin-5-fluorouracil first-line palliative regimen for ESCC, is €252,203 per QALY gained. By performing a Monte Carlo analysis we showed that there's a chance of less than 0.001 that the ICER would be below a threshold of acceptable cost per QALY of €40,000. This threshold is representative for the willingness to pay threshold in the Netherlands. Thus, the therapy regimen will at present not be considered cost-effective by decision makers and, in all probability, will not be reimbursed within the regulated Dutch health insurance system.

In the United Kingdom, the NICE uses an unpublished threshold of £30,000 (€36,997) in 2012 (12, 13). In Japan the willingness to pay threshold is 5,000,000 JPY (€43,014) in 2010. In the United States of America the threshold is US\$ 62,000 (€46,617) in 2010 (14). This indicates the threshold used, of €40,000, is representative for a willingness to pay threshold used in many developed countries (9, 10). The price of cetuximab is the dominant driver of the overall costs. Although biosimilars are expected to become available at a 15% to 30% lower prices, substitution of cetuximab with a biosimilar would not make the therapy regimen cost effective (25). In fact, due to testing of EGFR overexpression and the need for additional day treatments, the ICER was modelled to become €45,907 if cetuximab would be available for free. The ICER that we calculated is in line with previous findings for SCCHN, which has similarities in etiology and pathology (6, 7, 26), and for KRAS wild type colorectal carcinomas (8, 27). Cost-effectiveness studies after phase II trials have been previously performed (28). This method has been discussed related to the topic of streamlining the drug development process and early estimation and decision making for reimbursement in 2001 and 2003 (29, 30). However, no widespread adaptation has taken place.

This study has certain limitations. Quality of life of the patients receiving cetuximab could be affected negatively by side effects. This has not been accounted for in the model. Other limitations of this study are the lack of data on utility scores, both during PFS and after progression of ESCC, therefore data for adenocarcinoma of the esophagus

was used. Vial wastage and possible discounts negotiated by hospitals have not been accounted for. Since we did not have access to actual cost data from patient enrolled in this phase II study, another limitation is the use of costs that were taken from a manual for cost-effectiveness.

The results of the phase II trial remain promising despite the considered lack in cost effectiveness. Selecting patients for whom the drug has the most effect will increase treatment effectiveness and remove the burden of side effects from unselected patients. The EGFR staining pattern could be used as a criterion for selection. It has been correlated with poor prognosis in ESCC in a western European population (20). Tumor specific EGFR downstream signaling mutations in *KRAS* (8, 31), *BRAF* (31, 32), *PTEN* (33), and *PIK3CA* (31, 34) cause reduced benefit of cetuximab therapy in colon carcinoma patients. Germ line polymorphisms could also predict response to treatment, as has been studied in colorectal cancer (35-38). These options for selection of patients are still speculative and should be investigated further.

## Conclusions

Addition of cetuximab to a cisplatin-5-fluorouracil first-line regimen for advanced ESCC is not cost-effective when appraised according to currently accepted criteria. Cost-effectiveness analyses using outcome data from early clinical trials (*i.e.* a phase II trial) enable pharmaceutical companies and policy makers to gain early insights into whether a new drug meets the current eligibility standards for reimbursement and thereby potential allowance for use in clinical practice.

## References

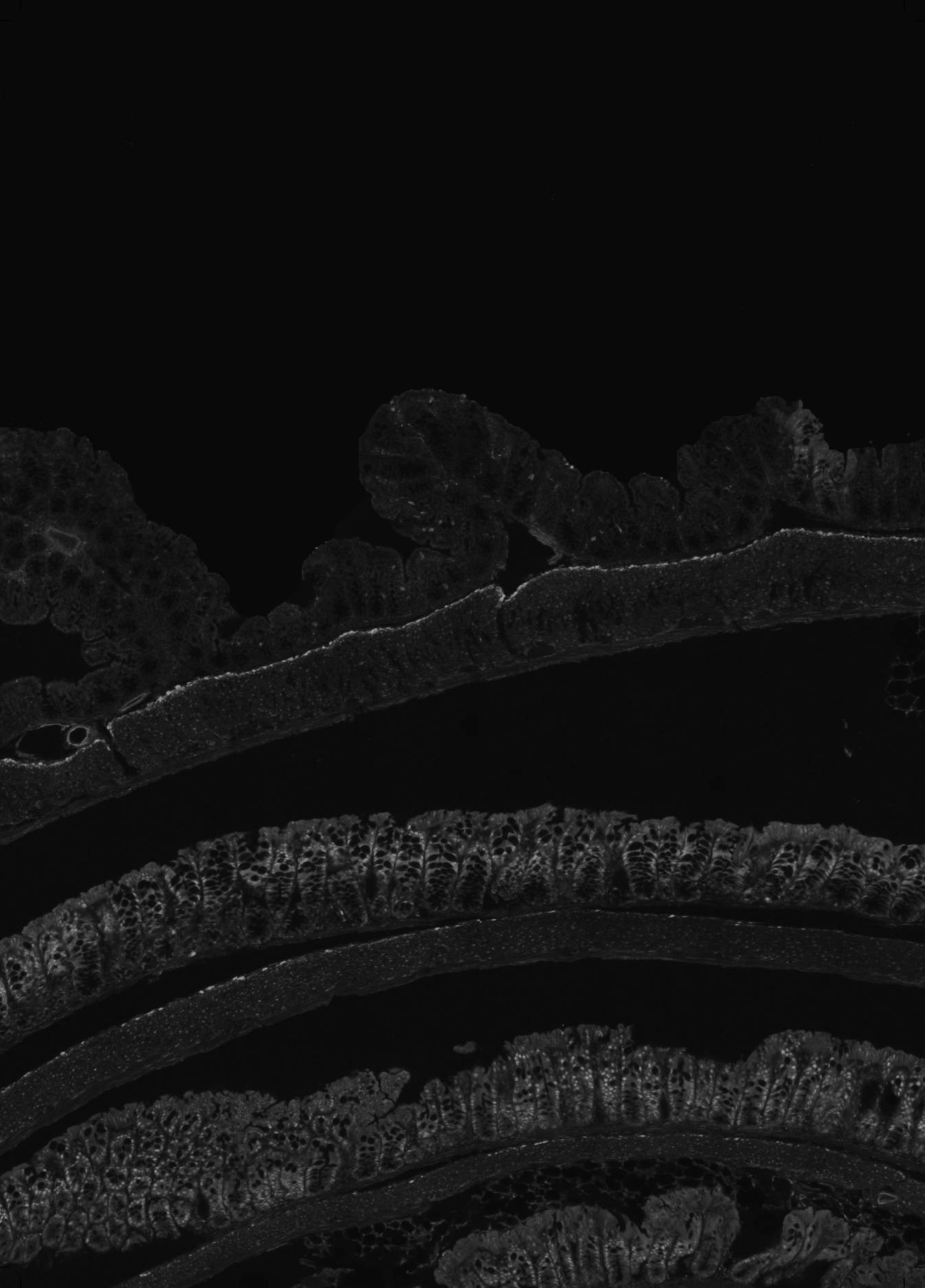
1. Rickwood S, Kleinrock M, Núñez-Gaviria, IMS Institute for Healthcare Informatics. The Global Use of Medicines: Outlook through 2017. <http://www.imshealth.com/2013>.
2. Enzinger PC, Mayer RJ. Esophageal cancer. *N Engl J Med*. 2003;349(23):2241-52.
3. Jemal A, Siegel R, Ward E, Hao Y, Xu J, Thun MJ. Cancer statistics, 2009. *CA Cancer J Clin*. 2009;59(4):225-49.
4. Polednak AP. Trends in survival for both histologic types of esophageal cancer in US surveillance, epidemiology and end results areas. *Int J Cancer*. 2003;105(1):98-100.
5. Lorenzen S, Schuster T, Porschen R, Al-Batran SE, Hofheinz R, Thuss-Patience P, et al. Cetuximab plus cisplatin-5-fluorouracil versus cisplatin-5-fluorouracil alone in first-line metastatic squamous cell carcinoma of the esophagus: a randomized phase II study of the Arbeitsgemeinschaft Internistische Onkologie. *Ann Oncol*. 2009;20(10):1667-73.
6. Hannouf MB, Sehgal C, Cao JQ, Mocanu JD, Winquist E, Zaric GS. Cost-effectiveness of adding cetuximab to platinum-based chemotherapy for first-line treatment of recurrent or metastatic head and neck cancer. *PLoS One*. 2012;7(6):e38557.

7. National Institute for Care and health Excellence (NICE). Cetuximab for the treatment of recurrent and/or metastatic squamous cell cancer of the head and neck. June 2009.
8. Mittmann N, Au HJ, Tu D, O'Callaghan CJ, Isogai PK, Karapetis CS, et al. Prospective cost-effectiveness analysis of cetuximab in metastatic colorectal cancer: evaluation of National Cancer Institute of Canada Clinical Trials Group CO.17 trial. *J Natl Cancer Inst.* 2009;101(17):1182-92.
9. Smulders YM, Thijs A. [The cost per year of life gained: trends and internal contradictions] *Kostprijzen per gewonnen levensjaar: trends en tegenstrijdigheden.* *Ned Tijdschr Geneesk.* 2006;150(45):2467-70.
10. Council for Public Health and Health Care (RVZ). *Sensible and Sustainable Care.* 2006.
11. Thijssen J, van den Akker van Marle ME, Borleffs CJ, van Rees JB, de Bie MK, van der Velde ET, et al. Cost-effectiveness of primary prevention implantable cardioverter defibrillator treatment: data from a large clinical registry. *Pacing Clin Electrophysiol.* 2014;37(1):25-34.
12. Martin S, Rice N, Smith PC. Comparing costs and outcomes across programmes of health care. *Health Econ.* 2012;21(3):316-37.
13. Appleby J, Devlin N, Parkin D, Buxton M, Chalkidou K. Searching for cost effectiveness thresholds in the NHS. *Health Policy.* 2009;91(3):239-45.
14. Shiroiwa T, Sung YK, Fukuda T, Lang HC, Bae SC, Tsutani K. International survey on willingness-to-pay (WTP) for one additional QALY gained: what is the threshold of cost effectiveness? *Health Econ.* 2010;19(4):422-37.
15. Hurt CN, Nixon LS, Griffiths GO, Al-Mokhtar R, Gollins S, Staffurth JN, et al. SCOPE1: a randomised phase II/III multicentre clinical trial of definitive chemoradiation, with or without cetuximab, in carcinoma of the oesophagus. *BMC Cancer.* 2011;11:466.
16. National Institute for Health and Clinical Excellence. *Barrett's Oesophagus: Ablative Therapy for the Treatment of Barrett's Oesophagus.* London: National Institute for Health and Clinical Excellence; 2010.
17. Garside R, Pitt M, Somerville M, Stein K, Price A, Gilbert N. Surveillance of Barrett's oesophagus: exploring the uncertainty through systematic review, expert workshop and economic modelling. *Health Technol Assess.* 2006;10(8):1-142, iii-iv.
18. L. Hakkaart- van Roijen, S.S. Tan, C.A.M. Bouwmans. *Handleiding voor kostenonderzoek, Methoden en standaard kostprijzen voor economische evaluaties in de gezondheidszorg: Instituut voor Medical Technology Assessment Erasmus Universiteit Rotterdam;* 2010.
19. Hulp CF. *Farmacotherapeutisch rapport Cetuximab.* 22 oktober 2007.
20. Gibault L, Metges JP, Conan-Charlet V, Lozac'h P, Robaszkiewicz M, Bessaguet C, et al. Diffuse EGFR staining is associated with reduced overall survival in locally advanced oesophageal squamous cell cancer. *Br J Cancer.* 2005;93(1):107-15.
21. Hanawa M, Suzuki S, Dobashi Y, Yamane T, Kono K, Enomoto N, et al. EGFR protein overexpression and gene amplification in squamous cell carcinomas of the esophagus. *Int J Cancer.* 2006;118(5):1173-80.
22. Itakura Y, Sasano H, Shiga C, Furukawa Y, Shiga K, Mori S, et al. Epidermal growth factor receptor overexpression in esophageal carcinoma. An immunohistochemical study correlated with clinicopathologic findings and DNA amplification. *Cancer.* 1994;74(3):795-804.
23. Marsman WA, van Sandick JW, Tytgat GNJ, ten Kate FJW, van Lanschot JJB. The presence and mucin histochemistry of cardiac type mucosa at the esophagogastric junction. *Am J Gastroenterol.* 2004;99(2):212-7.
24. Wagner AD, Unverzagt S, Grothe W, Kleber G, Grothey A, Haerting J, et al. Chemotherapy for advanced gastric cancer. *Cochrane Db Syst Rev.* 2010(3).
25. Simoons S. Biosimilar medicines and cost-effectiveness. *Clinicoecon Outcomes Res.* 2011;3:29-36.

26. Greenhalgh J, Bagust A, Boland A, Fleeman N, McLeod C, Dundar Y, et al. Cetuximab for the treatment of recurrent and/or metastatic squamous cell carcinoma of the head and neck. *Health Technol Assess.* 2009;13 Suppl 3:49-54.
27. Hoyle M, Crathorne L, Peters J, Jones-Hughes T, Cooper C, Napier M, et al. The clinical effectiveness and cost-effectiveness of cetuximab (mono- or combination chemotherapy), bevacizumab (combination with non-oxaliplatin chemotherapy) and panitumumab (monotherapy) for the treatment of metastatic colorectal cancer after first-line chemotherapy (review of technology appraisal No.150 and part review of technology appraisal No. 118): a systematic review and economic model. *Health Technol Assess.* 2013;17(14):1-237.
28. Higginson IJ, McCrone P, Hart SR, Burman R, Silber E, Edmonds PM. Is short-term palliative care cost-effective in multiple sclerosis? A randomized phase II trial. *J Pain Symptom Manage.* 2009;38(6):816-26.
29. Hill S, Freemantle N. A role for two-stage pharmacoeconomic appraisal? Is there a role for interim approval of a drug for reimbursement based on modelling studies with subsequent full approval using phase III data? *Pharmacoeconomics.* 2003;21(11):761-7.
30. Hughes DA, Walley T. Economic evaluations during early (phase II) drug development: a role for clinical trial simulations? *Pharmacoeconomics.* 2001;19(11):1069-77.
31. De Roock W, Claes B, Bernasconi D, De Schutter J, Biesmans B, Fountzilias G, et al. Effects of KRAS, BRAF, NRAS, and PIK3CA mutations on the efficacy of cetuximab plus chemotherapy in chemotherapy-refractory metastatic colorectal cancer: a retrospective consortium analysis. *Lancet Oncol.* 2010;11(8):753-62.
32. Di Nicolantonio F, Martini M, Molinari F, Sartore-Bianchi A, Arena S, Saletti P, et al. Wild-type BRAF is required for response to panitumumab or cetuximab in metastatic colorectal cancer. *J Clin Oncol.* 2008;26(35):5705-12.
33. Frattini M, Saletti P, Romagnani E, Martin V, Molinari F, Ghisletta M, et al. PTEN loss of expression predicts cetuximab efficacy in metastatic colorectal cancer patients. *Br J Cancer.* 2007;97(8):1139-45.
34. Sartore-Bianchi A, Martini M, Molinari F, Veronese S, Nichelatti M, Artale S, et al. PIK3CA mutations in colorectal cancer are associated with clinical resistance to EGFR-targeted monoclonal antibodies. *Cancer Res.* 2009;69(5):1851-7.
35. Graziano F, Ruzzo A, Loupakis F, Canestrari E, Santini D, Catalano V, et al. Pharmacogenetic profiling for cetuximab plus irinotecan therapy in patients with refractory advanced colorectal cancer. *J Clin Oncol.* 2008;26(9):1427-34.
36. Lurje G, Nagashima F, Zhang W, Yang D, Chang HM, Gordon MA, et al. Polymorphisms in cyclooxygenase-2 and epidermal growth factor receptor are associated with progression-free survival independent of K-ras in metastatic colorectal cancer patients treated with single-agent cetuximab. *Clin Cancer Res.* 2008;14(23):7884-95.
37. Pander J, Gelderblom H, Antonini NF, Tol J, van Krieken JH, van der Straaten T, et al. Correlation of FCGR3A and EGFR germline polymorphisms with the efficacy of cetuximab in KRAS wild-type metastatic colorectal cancer. *Eur J Cancer.* 2010;46(10):1829-34.
38. Zhang W, Gordon M, Press OA, Rhodes K, Vallbohmer D, Yang DY, et al. Cyclin D1 and epidermal growth factor polymorphisms associated with survival in patients with advanced colorectal cancer treated with Cetuximab. *Pharmacogenet Genomics.* 2006;16(7):475-83.

## Supplementary information

**S1 Model.** Cost effectiveness model as described in the manuscript. This model can be found at <https://journals.plos.org/plosone>.

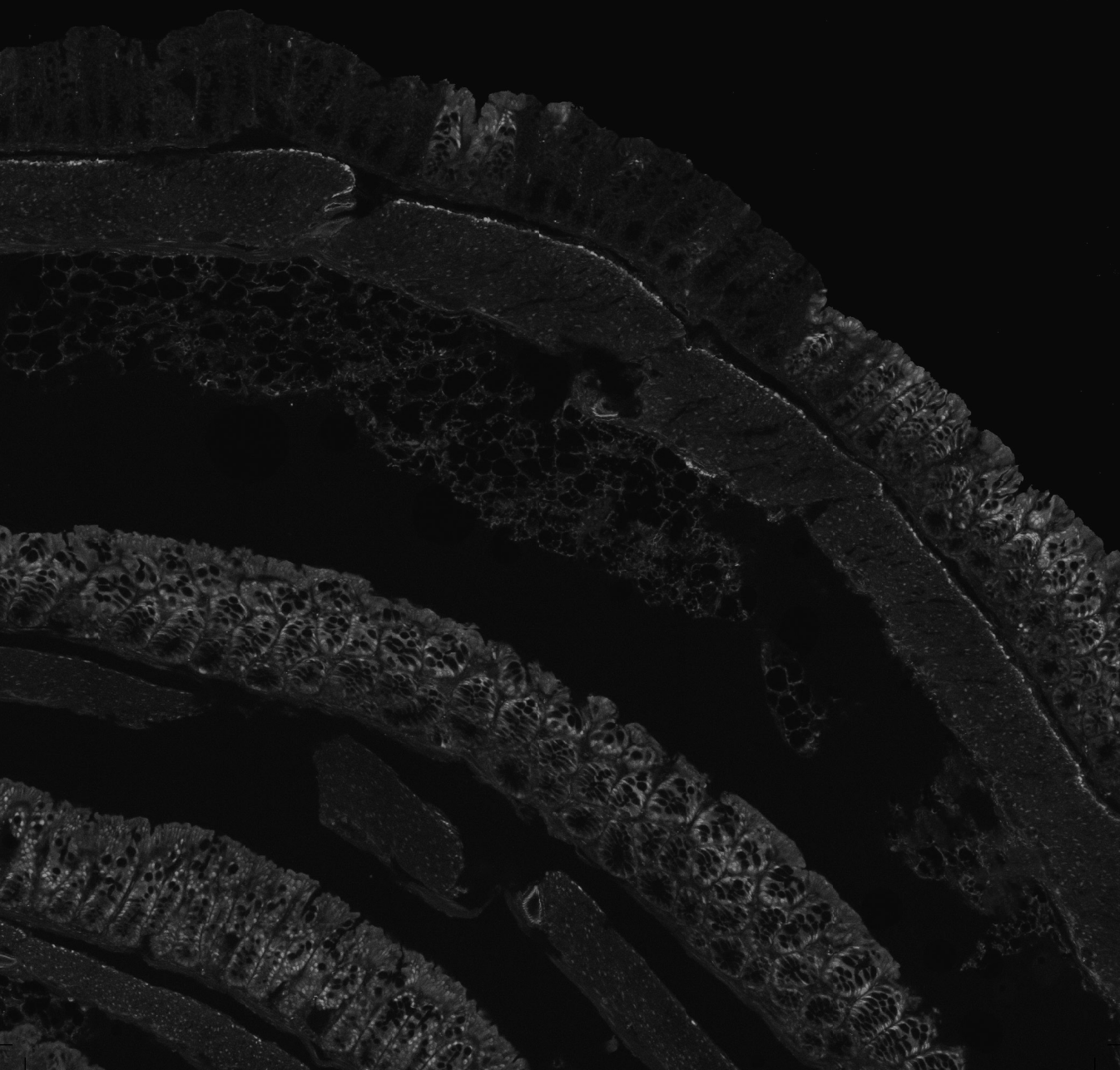




# Part 5

---

Summary, discussion,  
and appendices





# Chapter 11

---

Summary and general discussion



## Summary

The overall aim of this thesis is to gain better understanding of the etiology, the detection, and the palliative treatment of gastrointestinal (GI) cancer. This thesis is divided into five parts.

**Part 1** contains the introduction to this thesis. In **Chapter 1.1**, GI is described as a type of disease characterized by increased cell growth combined with the ability of these cells to spread to or invade other parts of the body. GI is one of the leading causes of morbidity and mortality worldwide. Esophageal cancer is the eighth most common cancer worldwide, with approximately 398,000 people diagnosed with esophageal squamous cell carcinoma (ESCC) and 52,000 with esophageal adenocarcinoma (EAC) in 2012. Barrett's esophagus (BE) is an intestinal metaplasia of the esophagus and can give rise to EAC. In the past few decades, developed countries have seen an increase in the incidence of BE and EAC, attributed to the higher prevalence of obesity. As various infectious diseases can be treated, or managed, better than before and the patient population is aging, oncological conditions become more and more prevalent in the gastroenterological patient population. Without profound understanding of the causes of cancer of the GI-tract, prevention, detection, and treatment are impossible. **Chapter 1.2** describes the outline of this thesis.

In **Part 2** of this thesis, we aim to increase our fundamental understanding on oncogenesis in the GI-tract through study of *HOX* gene signaling in (pre)malignant lesions of the GI tract. In **Part 3**, we investigate several approaches to improve the prediction of the development of malignant lesions and develop models for translational studies. In **Part 4**, we study the palliative treatment of esophageal cancer. Our findings will be summarized in this chapter. **Part 5** consists out of the summary, discussion, and appendices.

### **Part 2: *HOX* genes in (pre)malignant lesions of the GI-tract**

In **Chapter 2**, *HOXA13* was studied in esophageal carcinogenesis, because the biology and early events of metaplasias in the GI tract remain elusive. Here, we showed that *HOX* gene collinearity exists in great detail in the GI tract of adult humans and mice. In metaplasias, EAC, and heterotopias of the upper GI tract, a colon-like *HOX* gene expression was observed, with marked upregulation of the, in physiology, classically thought of as distally expressed *HOXA13*. ISH of *HOXA13* showed it was expressed mainly epithelial and confirmed its expression in metaplasia of the upper GI tract and its sequela. These *HOX* gene aberrations are paralleled in the stem cell component of the GI epithelium and BE. This supports a role for *HOX* gene expression in stem cells in the development of metaplasia. Data from a mouse model showed physiological *Hoxa13* expression was crypt clonal and expression along the baso-luminal axis was location specific. The proximal expression border was located between the proximal and distal

colon, this was conserved in humans. Strikingly, physiological *HOX* collinearity was interrupted by expression of the distal *HOXA13* in the upper GI-tract. This was detected just distally from the gastroesophageal junction and in the esophageal submucosal glands of adult humans and in the glandular stomach epithelium of adult mice. In fetal humans, high and specific *HOXA13* expression was observed at the gastric cardia, while more distal stomach and epithelium of esophagus were less positive. In a gut progenitor cell model, *HOXA13* reduced differentiation efficiency and, consequently, increased proliferation. In definitive endoderm, *HOXA13* supports caudal epithelial functions and appears to promote proliferation. Thus, *HOXA13*-positive cells at the gastroesophageal junction may outcompete other cell clones through a reduction in differentiation and an increase in proliferation. *HOXA13* downregulates the epidermal differentiation complex, which is an example of the capacity of a clustered multigene family member to regulate other clustered multigene families. In a BE cell culture model, *HOXA13* downregulates the epidermal differentiation complex and increases proliferation. In an *in vivo* tissue reconstitution model, parental cells of a BE cell line produce both intestinal-type columnar epithelium and stratified squamous epithelium from the same clone, suggesting this cell line has dual potential. In this model, *HOXA13* knock-out impaired epithelial proliferation and counteracted formation of the intestinal-type columnar epithelium. Thus, *HOXA13* emerges as a critical gene mediating BE pathophysiology.

In **Chapter 3**, the oncogenic hallmarks which *HOXA13* confers to esophageal keratinocytes were studied. To this end, *HOXA13* was overexpressed in a non-transformed human esophageal cell line EPC2-hTERT, gene expression profiling was performed to identify key processes and functions, and functional experiments were performed. We found that *HOXA13* expression confers oncogenic hallmarks to esophageal keratinocytes. It provides proliferation advantage to keratinocytes, reduces sensitivity to chemical agents, downregulates MHC class I expression, alters differentiation status, and promotes cellular migration. Our data indicate a crucial role of *HOXA13* in early stages of esophageal carcinogenesis.

In **Chapter 4**, *HOXA9* overexpression in premalignant colonic lesions was studied. Colorectal cancer is an important contributor to cancer deaths worldwide. It follows an adenoma-to-carcinoma sequence. Thus, identifying the molecular aberrations at the premalignant adenoma stage may help to understand its malignant potential. *HOXA9* acts as an oncogene in the hematopoietic system. However, its role in the colonic adenoma is unknown. Therefore, the aim of this study was to assess the expression of *HOXA9* in colonic adenoma tissue and its involvement in carcinogenesis. *HOXA9* mRNA levels are increased in colonic adenomas compared to location matched healthy tissue ( $p < 0.0001$ ). It inhibits cellular migration, which appears to be mediated by decreased PAK activity. This is the first mechanistic study into the effect of *HOXA9* in a premalignant solid lesion. Strikingly, the pro-oncogenic phenotype of *HOXA9* alteration in hematologic

malignancies was also found in this study as *HOXA9* stimulates cell growth. This phenotype appears to be mediated through increased *IGF1*, *FLT3*, *PTGS2*, p-4E-BP1, and p-ERK1/2. In conclusion, *HOXA9* has a pro-oncogenic effect on colon adenomas suggesting its importance for the adenoma-to-carcinoma sequence in particular and solid tumors in general.

### Part 3: predicting the development of malignant lesions

If the progression of BE to EAC could be predicted, therapies are available to effectively and safely remove the BE. Therefore, good screening and surveillance have the potential to reduce the disease burden for EAC significantly.

In **Chapter 5**, vitamin D receptor (VDR) polymorphisms were studied in relation to esophageal VDR expression and EAC risk. Epidemiological studies indicate that vitamin D exerts a protective effect on the development of various solid cancers. However, concerns have been raised regarding the potential deleterious role of high vitamin D levels in the development of EAC. This study investigated genetic variation in the VDR in relation to its expression and risk of BE and EAC. *VDR* mRNA expression was higher in BE compared with squamous epithelium. VDR protein was located in the nucleus in BE. A rs1989969T/rs2238135G haplotype was identified in the 5' regulatory region of the *VDR* gene. It was associated with an approximately halved risk of RE, BE, and EAC. Analysis of a replication cohort was done for BE which confirmed this. Rs1989969T causes a GATA-1 transcription factor binding site to appear. The signaling of GATA-1, which is regarded as a negative transcriptional regulator, could explain the findings for rs1989969. Rs2238135G was associated with a significantly reduced *VDR* expression in BE, for the rs1989969T allele a trend in reduced *VDR* expression was observed. We identified a *VDR* haplotype associated with reduced esophageal *VDR* expression and a reduced incidence of RE, BE, and EAC. This *VDR* haplotype could be useful to identify individuals who benefit most from vitamin D chemoprevention.

In **Chapter 6.1**, immunohistochemical (IHC) biomarkers for risk stratification of neoplastic progression in BE were systematically reviewed and a meta-analysis was performed. The low incidence of EAC in BE patients reinforces the need for risk stratification tools to make BE surveillance more effective. Therefore, we have undertaken a systematic review and meta-analysis of published studies on IHC biomarkers in BE to determine the value of IHC biomarkers as neoplastic predictors in BE surveillance. Sixteen different IHC biomarkers were studied in 36 studies. These studies included 425 cases and 1835 controls. A meta-analysis was performed for p53, aspergillus oryzae lectin (AOL), Cyclin A, Cyclin D and alpha-methylacyl-CoA racemase. Aberrant p53 expression was significantly associated with an increased risk of neoplastic progression with an odds ratio of 3.18 (95% CI 1.68 to 6.03). This association was confirmed for both non-dysplastic BE and BE with low-grade dysplasia. Another promising biomarker

to predict neoplastic progression was AOL, with an odds ratio of 3.04 (95% CI 2.05 to 4.49). Use of p53 IHC staining may improve risk stratification in BE surveillance.

In **Chapter 6.2**, we responded to a review and meta-analysis in which studies were included without follow-up. However, these studies were used to assess the value of p53 as a predictor of malignant progression.

In **Chapter 7**, DNA integrity was investigated as a biomarker in pancreatic cyst fluid. Identification of pancreatic cysts with malignant potential is important to prevent pancreatic cancer development. Integrity of cell free DNA (cfDNA) has been described as a tumor biomarker, but its potential for pancreatic cancer is unclear. Normal apoptotic cells release uniformly truncated DNA, whereas malignant tissues release long fragments of cell free DNA. We measured 247 base pair and 115 base pair DNA fragments of ALU repeats by qPCR in serum from healthy controls and pancreatic cancer patients, and in cyst fluid from pancreatic cyst patients. No differences in total cfDNA (ALU115) and cfDNA integrity (ALU247/115) were observed between sera from healthy controls (n=19) and pancreatic cancer patients (n=19). Though elevated as compared to serum, no differences in cfDNA were found in cyst fluid between high risk (n=10) and low risk (n=20) cyst patients.

In **Chapter 8**, we studied and optimized BE models. The formation of a Barrett's esophagus is difficult to monitor directly under clinical conditions. Thereto, experimental models have been published to investigate the mechanisms of BE pathogenesis. However, either the technical possibilities or the translational relevance of these models, or both, is limited. We analyzed Gene Expression Omnibus 2R (GEO2R) databases to establish a clinical BE molecular profile. Subsequently, by using keratin markers we were able to optimize an *in vitro* BE model based upon two immortalized squamous esophageal epithelial cell lines. Finally, we compared this optimized model and a rat surgical model to the BE molecular profile. The *in vitro* model reflected 73% of the human BE profile while the *in vivo* model reflected about 45% of the human BE profile.

#### **Part 4: Palliative treatment of esophageal cancer**

Despite increasing understanding of the biology of GI-tract cancer and efforts to prevent cancer the incidence of EAC has been rising in Western countries. Despite efforts to detect cancer at an early stage almost half of patients are diagnosed with esophageal cancer at a palliative stage. However, it was unclear whether palliative chemotherapy or targeted therapies are effective for esophageal cancer.

In **Chapter 9**, palliative chemotherapy and targeted therapies for esophageal and GEJ cancer were systematically reviewed and a meta-analysis was performed. Chemotherapy and targeted therapies are increasingly used with a palliative intent to control tumor growth, improve quality of life, and prolong survival. Our aim was to assess the effects of cytostatic or targeted therapy for treating esophageal or GEJ cancer with palliative



intent. We identified 41 randomized controlled trials with 11,853 participants for inclusion in the review. We demonstrated an increase in overall survival in favor of the arm with an additional cytostatic or targeted therapeutic agent with a hazard ratio (HR) of 0.75 (95% confidence interval (CI) 0.68 to 0.84, high-quality evidence). The median increased survival time was one month. We found a benefit in overall survival in favor of the group receiving palliative chemotherapy and/or targeted therapy compared to best supportive care (HR 0.81, 95% CI 0.71 to 0.92, high-quality evidence). Subcomparisons including only people receiving second-line therapies, chemotherapies, targeted therapies, EAC, and SCC all showed a similar benefit. Palliative chemotherapy and/or targeted therapy increased the frequency of grade 3 or higher treatment-related toxicity. However, treatment-related deaths did not occur more frequently. Quality of life often improved in the arm with an additional agent. In conclusion, people who receive more chemotherapeutic or targeted therapeutic agents have an increased overall survival compared to people who receive less, which appeared not to negatively affect quality of life in the studies included.

In **Chapter 10**, the cost-effectiveness of giving cetuximab for advanced esophageal SCC, based on phase II trial data was investigated. In patients with advanced esophageal SCC, the addition of cetuximab to a cisplatin-5-fluorouracil first-line palliative chemotherapy regimen appears to improve survival. However, it results in an incremental cost-effectiveness ratio of €252,203 per quality-adjusted life-year. Sensitivity analysis shows that there is a chance of less than 0.001 to one that the incremental cost-effectiveness ratio will be less than a maximum willingness to pay threshold of €40,000 per quality-adjusted life-year. Adding cetuximab to palliative regimen for advanced esophageal SCC is not cost-effective. Cost-effectiveness analyses using outcome data from early clinical trials (i.e. a phase II trial) enable pharmaceutical companies and policy makers to gain early insight into whether a new drug meets the current eligibility standards for reimbursement and thereby potential admittance for use in regular clinical practice.

In **Part 5**, we summarize and discuss of the main findings of this thesis in **Chapter 11**. **Chapter 12** contains a Dutch summary and **Chapter 13** consists out of the appendices.

## General discussion

In this general discussion we aim to discuss the research firstly per chapter and secondly for the thesis as a whole.

### **Part 1: *HOX* genes in (pre)malignant lesions of the gastrointestinal tract**

Metaplasia is a common occurrence in the adult gut. Metaplasia acquires a caudal phenotype in a rostral location, and can thus be termed a homeotic transformation.

Therefore, positional misspecification is likely involved. Regulation of rostral-caudal patterning of specialized tissue in embryology and adulthood is largely dependent on the concerted action of two evolutionary highly conserved gene systems, the Caudal-related Homeobox (*CDX*) transcription factor gene family and the genes of the Homeobox (*HOX*) cluster. The function of *CDX* genes has been studied extensively (1, 2), but *HOX* genes less so in this context. *HOX* genes are linked to homeotic transformations and neoplasia (3, 4).

### ***Chapter 2 HOXA13 in etiology and oncogenic potential of Barrett's esophagus***

We have shown the adult gut is characterized by *HOX* collinearity. In Barrett's esophagus (BE) *HOX* expression is reprogrammed to a distal pattern in stem and differentiated cells, with prominent *HOXA13* expression. *HOXA13* expression appears mediated by lncRNA *HOTTIP*. Strikingly, *HOXA13* was found to be expressed in the gastroesophageal junction. In a model of the cell of origin of BE, *HOXA13* confers a relative competitive advantage and a pro-oncogenic expression profile. In BE models, *HOXA13* downregulates the epidermal differentiation complex, increases proliferation, and conveys phenotypical aspects of BE. Recently, the thesis that the origin of BE lies in the GEJ has been gaining influence. Jiang et al. describes p63<sup>+</sup>KRT5<sup>+</sup>KRT7<sup>+</sup> basal cells at the murine GEJ as the origin of a BE-like lesion while a similar human basal cell population has also been postulated (5). In apparent agreement, murine Lgr5<sup>+</sup> gastric cardia stem cells that lineage trace into an early BE-like lesion have been described (6). Furthermore, Wang et al. show that a discrete population of embryonic cells persists in adult mice and humans at the SCJ. These embryonic cells migrate upwards and form a BE-like lesion upon epithelial damage (7). We could learn more from attempting to lineage trace *HOXA13*-positive cells to a Barrett's (like) lesion in a mouse, rat, or naturally occurring human model. On the other hand, in esophagogastrostomy patients BE can reoccur, proving the involvement of the GEJ is not a prerequisite for the development of BE (8). In the latter study submucosal glands of the esophagus were hypothesized to contain a BE progenitor cell. This fits with our analysis of single cell RNA-seq data published by Owen et al. (44). This analysis shows a small population of *HOXA13*-positive cells is present in the normal squamous esophagus of BE patients. These *HOXA13*-positive cells express designated esophageal submucosal gland markers indicating that the small population of *HOXA13*-positive cells resides in the submucosal glands in the physiological adult human squamous esophageal epithelium. The submucosal gland as a potential origin of Barrett's esophagus is also supported by the canine study of Gillen et al. (9). In this study, squamous barriers were employed to prevent proximal migration of columnar epithelium from the stomach to the mucosal defect. Despite this barrier, the regenerated epithelium was frequently found to have a columnar morphology. In another canine study performed by Li et al. (10) acid suppression resulted in squamous islands to appear in the epithelium that would otherwise regenerate in a columnar

morphology. This aligns with the potential cell of origin model, which we illustrated in figure 6E. This model of cellular identity in BE suggest that *HOXA13* expressing clones in the GEJ may outcompete clones with another positional identity, depending on local circumstances. When taking into account our finding of *HOXA13*-positive gastric inlet patches this is in line with an hypothesis postulated in 1923 by Nicholson (11) whom proposes that local differentiation of existing pluripotent cells might result in heterotopic gastric mucosa. He describes this as an example of a heteromorphosis. A later hypothesis, which aligns with this thought, states that esophageal submucosal glands might become clogged, form cysts and finally erupt to form a gastric inlet patch. As gastric IM expresses *HOXA13*, positive cells at the GEJ are insufficient explanation for the existence of gastric IM in other parts of the stomach. One explanation might be the presence, potentially dependent on developmental stage, of multiple positional misspecified microcompartments, or single *HOXA13*-positive cells, throughout the GI tract. Our immunohistochemical data of mouse glandular stomach tissue shows dispersed *HOXA13*-positive cells in the stomach of that species. It would be interesting to attempt a more detailed characterization of cell populations based on their positional identity in various parts of the GI tract. This study could have translational meaning if areas of the gut were chosen with a higher cancer risk. Additionally, studying junction areas between gut segments would be interesting, for instance the junction between the proximal and distal ileum, regardless of the presence of a Meckels diverticulum. The 4 cells depicted on the Y-Z plane in figure 6E represent multiple potential cells of origin of metaplasia or rather heteromorphosis of the GI tract. The thought that multiple potential origins might exist is recognized in the literature (12). While evidence for some of the, above mentioned, previously proposed model appears convincing, none of these proposed model can explain the formation of BE in all circumstances. Often, these models do not clearly show a link between the proposed cell of origin and the characteristic morphology of BE. Additionally, some models depend almost solely on evidence from mouse models, while the mouse models have translational issues in the case of BE research.

Only one previous study has been published on *HOX* genes in BE. In this study *HOXA* cluster gene expression partially contrasts with our findings (13). Employing the Affymetrix HuGene-1\_0-st-v1 microarray, this study describes *HOXA6* and *11* upregulation in BE. Our study, however, documents modest upregulation of *HOXA11* but strong *HOXA13* expression in BE. This discrepancy may be due to the highly homologous nature of different *HOX* genes, thus probe-based array technology might not be ideally suited. We do confirm their qPCR based findings regarding *HOXB6* and *7*, show their involvement in IM of the stomach, and the establishment of deregulation in the deep stem cell in BE. A second study shows a germline variant of Msh homeobox 1 (*MSX1*) in a Dutch family with clustering of BE and EAC. Loss of the wild type allele was found in the tumor DNAs of the affected family members. This shows the relevance

of homeobox genes in this disease characterized by homeotic transformation (14). Germline variants of *HOXA13* have been described, but not for BE or EAC. The pro-oncogenic characteristics of *HOXA13* have been shown before in different contexts (15). Decreased wild type Hoxa13 protein in the early developing chick caudal endoderm results in endoderm-specific atresia of the hindgut rostral to the cloaca in line with our observations (16). In pancreatic cancer, it was shown by *in vitro* assays that *HOTTIP* alterations affected stemness, tumorigenesis, and levels of stemness related genes *LIN28*, *NANOG*, *OCT4*, and *SOX2* in pancreatic stem cells. *HOTTIP* regulating *HOXA13* levels is supported by our data. Knowing this, our observation that *HOXA13* increased *NANOG* signaling in the definitive endoderm context is in line with these findings. The present study highlights the importance of regional patterning by *HOX* genes in gut epithelium. It would be interesting to perform functional experiments with other *HOX* paralogues potentially involved in BE pathophysiology, candidates would be *HOXA10*, *11*, *B13*, and *C10*. *GATA* genes could be of interest as well as *GATA4* was found to be involved in establishing jejunal versus ileal identity (17).

### **Chapter 3 Forced expression of *HOXA13* confers oncogenic hallmarks to esophageal keratinocytes**

The disease etiology of esophageal squamous cell carcinoma (ESCC) is still poorly understood. *HOXA13* appears to be involved as it is overexpressed, high protein expression is correlated with a shorter median survival time, and poor clinicopathological characteristics in ESCC (18-20). How these effects are exerted was largely unclear. We overexpressed *HOXA13* in a squamous esophageal cell line and performed functional experiments. Our data show that *HOXA13* expression confers oncogenic hallmarks to esophageal keratinocytes. It provides proliferation advantage to keratinocytes, reduces sensitivity to chemical agents, regulates MHC class I expression and differentiation status, and promotes cellular migration. The down-regulated expressions of HLA class I in ESCC is correlated with tumor grade and lymph node status (60). Our results indicate that *HOXA13* expression may drive the immune escape of neoantigen-bearing transformed keratinocytes. Whether the correlation found is an effect of immune escape, which allows for local and distant spread is unclear. Possibly, more advanced malignancies have had more and longer immune pressure under which the clones with more immune escape are selected for. In this second case immune escape also appears to provide the lesion with more opportunity to progress, but might not be obligatory for this process. Reduced HLA class I expression makes cells vulnerable for NK cell-mediated killing. Multiple malignancies are associated with reduced HLA class I expression (21). It appears likely that there is an optimum in the amount of HLA class I expression which provides immune escape but avoids NK cell-mediated killing. In a series of 143 cases of ESCC 36.4% were found to be negative for HLA class I by immunohistochemistry (60). This indicates that NK-escape mechanisms are more complex than just expression levels of this complex (22). In this study, we

found *HOXA13* overexpression did not significantly affect 2D growth of esophageal cells as measured with an MTT assay, although a trend towards increased cell pool growth was seen. However, when assessed as growth in spheroid form the *HOXA13* overexpression does increase the size of spheroids. This points to the importance of being conservative in interpreting the results of a single model system. Our model shows *HOXA13* overexpression makes these cells more resistant to paclitaxel-induced death. Previously, high *HOXA13* expression was found to be associated with inferior tumor regression grade and poor overall survival in 131 ESCC patients treated with cisplatin and paclitaxel. Caution is warranted while interpreting this result as the *HOXA13* expression was assessed by immunohistochemistry (32). *HOXB7* has recently also been found to mediate Cisplatin resistance in ESCC by mechanism of DNA damage repair (23).

#### ***Chapter 4 HOXA9 mediates and marks premalignant compartment size expansion in colonic adenomas***

Our data shows *HOXA9* mRNA levels are increased in colonic adenomas compared to location matched healthy tissue. *HOXA9* inhibits cellular migration, which appears to be mediated by decreased PAK activity. This is the first mechanistic study into the effect of *HOXA9* in a premalignant solid lesion. Strikingly, the pro-oncogenic phenotype of *HOXA9* alterations in hematologic malignancies was also found in this study as *HOXA9* stimulates cell growth. This phenotype appears to be mediated through increased *IGF1*, *FLT3*, *PTGS2*, p-4E-BP1, and p-ERK1/2. Forced *HOXA9* expression upregulates *IGF1* and *FLT3*, this stimulates cell proliferation and inhibit apoptosis (24, 25). *PTGS2* was overexpressed while it is known that inhibition of *PTGS2* with nonsteroidal anti-inflammatory drugs (NSAIDs), decreases the risk of developing adenomas and colorectal carcinoma (CRC) (26-29). *CYBB* was downregulated in line with *CYBB* levels in stomach cancer (30). It is known that *HOXA10*, which is closely related to *HOXA9*, represses *CYBB* during inflammation (31). *CYBB* forms reactive oxygen species, which are important for death receptor activation and induction of apoptosis (32-34). *CYBB* downregulation is in line with an increase in cell pool size. In acute myeloid leukemia, *HOXA9* upregulates *FGF2*, in contrast to our findings (35). Increased *WNT5a* is in line with its levels in colonic adenomas and CRC (36). In CRC it acts as a tumor suppressor and attenuates EMT (37). Wnt genes have, apart from a role in oncogenesis, also a role in cell fate and patterning during embryogenesis, related to the role of HOX genes (38). Interestingly, *Wnt5a* and its target gene *CCND2*, both upregulated, have a higher expression in the proximal colon versus the distal colon (39). *HOXA9* might thus affect positional identity of the colon epithelium. A recent study reports *HOXA9* overexpression in CRC with a similar fold change, their main message is that *HOXA9* expression level in CRC is associated with the presence of lymph node metastasis (40). These authors could not find a relation to overall survival (OS) which might have been

due to differences in tumor stage, as the population studied contained mostly stage 2 and 3 patients. In contrast to our findings, *HOXA9* knock down with a siRNA, after which cells were counted after 24 and 48 hours, did not reveal a statistically significant effect of *HOXA9* expression on the cell pool size. Based on data from the publically available cBioPortal database, gene amplification appears not to be involved in the increase of *HOXA9* levels in CRC. Assuming that gene amplifications are rare in colonic adenomas, this is in line with our findings. Another study reports overexpression of nucleus accumbens-associated protein 1 confers chemotherapy resistance via *HOXA9* in CRC cells (41). Bhatlekar et al. found *HOXA4* and *HOXA9* are up-regulated in CRC stem cells (42). Their data indicate that *HOXA9* aids self-renewal and overpopulation of stem cells in CRC. Multiple reports have described *HOXA9* as a pro-oncogenic factor in other solid tumors (43-50). *HOXA9* was not differentially methylated in CRC (51). Recently, it was suggested that hsa\_circ\_0079662, as a covalently closed circular RNA, might be a hsa-mir-324-5p sponge, and it was suggested that *HOXA9* is a direct target of has-mir-324-5p. High *HOXA9* contributed to chemotherapy drug oxaliplatin resistance in CRC through the TNF- $\alpha$  pathway in human colon cancer (52).

## **Part 2: predicting the development of malignant lesions**

The incidence of esophageal adeno carcinoma (EAC) rises to date despite screening and surveillance strategies. BE provides the opportunity to prevent the development of BE related adenocarcinoma (AC) by stratifying BE patients at risk for neoplastic progression.

### ***Chapter 5 Vitamin D receptor polymorphisms are associated with reduced esophageal vitamin D receptor expression and reduced esophageal adenocarcinoma risk***

Vitamin D supplementation is likely to convey a level of chemo preventive properties against oncogenic transformation in for instance the colon. However, there is evidence some BE patients are likely to respond negatively to vitamin D. We identified a rs1989969T/rs2238135G haplotype in the 5' regulatory region of the vitamin D receptor (VDR) gene which is associated with a lower VDR expression and an approximately halved risk of reflux esophagitis, BE, and EAC. Since then, a nonrandomized interventional study assessed the effects of vitamin D supplementation in BE. However, despite improved vitamin D status with supplementation, no significant alterations in gene expression profiles were noted (53). This is in contrast with other cancers (54, 55). Obviously, a longer duration or higher dose of supplementation might be able to show an effect. Evidence from epidemiological studies mimicking true long-life effects of vitamin D are required to endorse the idea of personalized recommendations for vitamin D supplementation. A recent study concluded that population-wide screening for vitamin D deficiency and supplementation should not be recommended for cancer prevention (56). For CRC they found an odds ratio of 0.92 (95% confidence interval 0.76 to 1.10)

per 25 nmol/l increase in genetically determined 25(OH)D concentrations. This might indicate a modest protective effect with respect to CRC. A Mendelian randomization study found no association with BE or EAC and low genetically estimated 25(OH)D concentrations (57). Unfortunately, both alleles studied in our paper were not included.

***Chapter 6 Use of immunohistochemical biomarkers as independent predictor of neoplastic progression in Barrett's oesophagus surveillance: a systematic review and meta-analysis***

We show that sixteen immunohistochemical (IHC) biomarkers in BE surveillance have been studied. Aberrant p53 expression is the most studied IHC biomarker and associated with a significantly increased risk to develop high grade dysplasia (HGD) or EAC, this association was independent of the presence of low grade dysplasia (LGD). There has been a case published in which a p53 mutation was shown to have occurred in cardia type metaplastic tissue, thus without goblet cells (58). Therefore, although difficult to study, it is plausible that p53 is a more biologically relevant identifier of progression risk compared to the better known risk factor, being the presence of goblet cells. More consensus is required amongst pathologists concerning the appropriate staining method, definition, and interpretation of aberrant p53 expression. Our research group previously reported in a large case-control study that aberrant p53 expression was significantly associated with an increased risk of neoplastic progression in BE. However, only 40% of the BE patients with progression to HGD or EAC showed an aberrant p53 protein expression during surveillance, indicating that additional biomarkers are needed (59). One such promising biomarker is aspergillus oryzae lectin. Other types of biomarkers could also contribute, an interesting protocol has appeared investigating DNA methylation, histone modification, chromatin remodeling, micro and non-coding RNAs of all types for their value of predicting progression from BE to EAC (60). A recently published study claimed to have investigated the predictive ability of IHC biomarkers (61). However, they reported on samples obtained either from a resection specimen or from cases and controls without follow-up. Therefore, based on their current dataset, their current conclusion, i.e. that p53 overexpression predicts malignant progression, is not justified (62). This case shows the fragility of the current peer review system and emphasizes caution is warranted when interpreting conclusions from published studies. Although routine p53 and other IHC biomarker staining incur higher costs, application of a panel of biomarkers has the potential to reduce the overall costs of BE surveillance. Patients at low-risk of neoplastic progression, i.e. the majority of the patients with LGD, might be followed-up less intensively. A recent study into the "Use of Ancillary Stains in the Diagnosis of BE and BE-associated LGD and HGD on p53 IHC" concluded: "Although p53 is a promising marker for identifying high-risk BE patients, it is not recommended for routine use at present; additional studies are needed to address questions regarding case selection, interpretation, integration with morphologic diagnosis, and impact on clinical outcome" (63). Recently, Snyder

et al. (64) performed a separate meta-analysis of case-control and cohort studies. They expressed the results of their meta-analysis as RRs instead of ORs, deeming this easier to compare with other studies of risk stratification techniques. Their results are similar to ours as they found an OR of 4 to 6 for case-control studies and a RR of 14 to 17 for cohort studies. They align with the BSG recommendations, as do we, and state that IHC assessment of p53 in BE should be investigated as a risk stratification tool (65). The next step would be a randomized controlled trial (RCT) with implementation of p53 IHC in a risk stratification tool which also contains simple clinical parameters (66), randomizing patients to both ways of surveillance, i.e. with or without the risk stratification tool. Knowledge on rs1989969 and rs2238135 as well as knowledge from genome wide association studies could contribute to this risk stratification tool. After sufficient time, clinical, social, and economic outcomes of the intervention could be investigated. Such a trial would provide the level of evidence and practical tools necessary for widespread implementation.

#### ***Chapter 7 DNA integrity as biomarker in pancreatic cyst fluid***

The integrity of cell free DNA (cfDNA) was studied in serum of patients with pancreatic carcinoma and controls. We did not observe any significant differences between patients and controls. Previous studies were also unable to show cfDNA fragments in serum from pancreatic cancer patient. We analyzed pancreatic cyst fluids and found DNA levels are roughly a thousand fold higher in cyst fluids. However, no differences in DNA integrity were found in high versus low risk cysts. As tumor size determines the amount of necrosis, the size of these premalignant lesions might be too small for this assay. Extrapolating these findings to BE it seems unlikely that integrity of cfDNA in serum will provide enough information for risk stratification. However, a recent study has shown loss of heterozygosity analysis in cfDNA could be valuable in BE (67). Receiver operating characteristic curve analysis showed an area under the curve of 0.79. Interestingly, loss of heterozygosity (LOH) frequencies near or within TP53 showed a trend towards discrimination between BE and dysplastic samples. This shows interesting markers from LOH studies and IHC studies could be valuable in the other modality as well. IHC markers have the advantage that they can be performed and analyzed concurrently with the histological analysis. LOH markers, if multiple would be found with additional predictive power, could (partially) obviate the need for surveillance endoscopies. A question that remains is if other lesions would not interfere with this analysis as surveillance is often done in an older patient group. Analysis of biopsy specimens is not subject to this uncertainty.



**Chapter 8 Molecular profile of Barrett's esophagus and gastroesophageal reflux disease in the development of translational physiological and pharmacological studies**

The process of conversion of normal squamous epithelium towards Barrett's metaplasia is difficult to monitor directly under clinical conditions. This has impeded the progress of the field. Thus, over the years, several experimental models have been published to investigate the mechanisms of BE pathogenesis. However, either the technical possibilities or the translational relevance of these models, or both, is limited. Animal models generally do not offer a good representation of the situation in humans. The most used animal models are variants of surgical rat models, which are physiologically not similar to humans and require long time periods to develop BE and EAC. The benefit of the rat models is the relative ease of performing surgical procedures on rats when compared to mice. Mice have the advantage of being much easier to manipulate genetically. Anatomic differences, i.e. the presence of a squamous forestomach, the lack of esophageal submucosal glands, and the fact that BE or reflux does not occur naturally in rodents are also important drawbacks. Higher order animals such as dogs, pigs, and primates do offer a similar anatomy compared to humans. However, the development of BE takes very long, due to their size these animals are difficult to handle in a laboratory setting, and, in general, the use mammals for these experiments is increasingly seen as unethical which is especially the case for higher animals (68). Our data appears to suggest that results from animal models should be interpreted carefully when clinical translation is sought (36). The observation that the proximal expression border of *HOXA13* and the presence of *HOXA13*-positive cells at the upper GI tract were made in both mice and humans, leads us to conclude that mice appear a reasonable *in vivo* model for studies into the role of *HOX* genes in the GI tract. Given the downsides of these animal models, the development of suitable *in vitro* models is important. Downsides of these models are that these cell lines are usually transformed in order to keep the cells continuously growing. These models lack a microenvironment consisting out of immune cells and stroma and the factors that these cell secrete (69). We found 57% similarity between the human biopsies and the EPC2 cell model and only 26% similarity for the Het-1A model. This indicates a lot of heterogeneity, which is surprising as both cell lines are derived from the squamous esophageal epithelium. Combining both expression profiles resulted in 73% overlap with the human biopsy data. This indicates the importance of combining multiple model systems to study a research question especially in the setting of BE. The development of organotypic culture models using spheroids or differentiated embryonic stem cells could offer model systems that offer possibilities not met with either cell line models or animal models alone. These models would offer a higher throughput and less ethical constraints compared to animal models. While offering more of the microenvironment lacking in the cell line models. Finally, given the debate on the cell of origin of Barrett's esophagus, the choice for the correct model system is not always straightforward. Whether a cell line, organotypic culture, or animal model is

chosen adequately does not only depend on the research question but will often depend on the theoretical framework with which the researcher(s) are aligned.

### **Part 3: Palliative treatment of esophageal cancer**

Almost half of patients with esophageal cancer present themselves in the palliative stage. This emphasizes the need for screening and surveillance. However, this is hindered by the high incidence of BE, the low progression rates from BE to EAC, and the invasive procedures necessary for surveillance. As these obstacles will not be easy to overcome, improvement of palliative therapy remains an important research goal.

#### ***Chapter 9 Palliative chemotherapy and targeted therapies for esophageal and gastroesophageal junction cancer***

We have shown that people who receive more chemotherapeutic or targeted therapeutic agents live longer compared to people who receive less therapy or best supportive care. There was no evidence that palliative chemotherapy and targeted therapy decreased quality of life (QoL). A triplet regimen was superior to a doublet regimen with regard to OS in participants receiving first-line chemotherapy for advanced or metastatic esophagogastric carcinoma (70). This is in line with our findings. We did not expect to find an increase in toxicities without a decrease in QoL. Interestingly, two included RCTs reported better QoL despite more toxicity in the experimental arm versus the control arm (71, 72). A previous study also found no clear association between QoL and toxicity (73). Differences in risk factors, gene expression, and tumor biology exist between AC of the stomach, the GE-junction, and EAC (74, 75). In this chapter, we found a difference in efficacy of chemotherapy and targeted therapy between gastro esophageal (GE)-junction AC and gastric AC. We found a similar trend in a previous study (76). This study used individual participant data from four studies (72, 77-79). They concluded that response rates in participants were 44.1% in esophageal, 41.1% in GE-junction, and 35.6% in gastric cancer. We included studies awaiting classification to update our search but did not include these in the analysis. There were several studies eligible for inclusion identified amongst these studies. Most study targeted therapeutic agents and most of them present results in line with our current main conclusion. In this chapter, we used the GRADE approach to assess the quality of the evidence per analysis. Recently, a new tool has been developed to quantify the magnitude of clinical benefit of anti-cancer therapies. This tool is called the European Society for Medical Oncology Magnitude of Clinical Benefit Scale (ESMO-MCBS) (80). The aim of this tool is to assign grades to trials based on adequate power for a relevant magnitude of clinical benefit. The magnitude of effect in our main analysis is only one month of additional OS for the addition of one agent. The mean OS of this patient group is about half a year. Even though we have shown a statistically significant difference in survival, the magnitude of effect is limited. Future use of the ESMO-MCBS might reflect this

more accurately compared to the reporting of mean OS times as we did in this chapter. It also emphasizes the search for adequate therapies is long from over. Recently a quality of life study was performed in Denmark by interviewing patients with oesophageal cancer. Their conclusions are that the main issues these patients face are loneliness and lack of continuity. Patients feel banished from their normal lives (81). This provides an important perspective on the palliative phase of treatment for esophageal cancer patients.

#### **Chapter 10 Cost-effectiveness of cetuximab for advanced esophageal squamous cell carcinoma**

We found the mean incremental cost effectiveness ratio (ICER) of adding cetuximab to a cisplatin-5-fluorouracil (5-FU) first-line palliative regimen for esophageal squamous cell carcinoma (ESCC), is €252,203 per QALY gained. By performing a Monte Carlo analysis, we showed that there is a chance of less than 0.001 that the ICER could be below a threshold of acceptable cost per QALY of €40,000. The ICER that we calculated is in line with previous findings for squamous cell carcinoma of the head and neck (SCCHN), which has similarities in etiology and pathology, (82-84) and for *KRAS* wild type CRC (85, 86). A study showed prolonged OS (49.0 vs. 29.3 months) for patients who receive cetuximab added to the comparator radiotherapy for locally advanced SCCHN (87). A recent cost-effectiveness study based on that dataset showed probabilities between 0.76 and 0.87 of radiotherapy with cetuximab being cost-effective compared to radiotherapy alone (88). This indicates that for other indications, where more clinical effectiveness is observed, cetuximab does seem to be cost effective. Cost-effectiveness studies after phase II trials have been previously performed (89). This method has been discussed related to the topic of streamlining the drug development process and early estimation and decision making for reimbursement in 2001 and 2003 (90, 91). However, no widespread adaptation has taken place. The reluctance of adopting these methodologies by pharmaceutical companies can be explained, as they know decision makers do not base themselves solely on cost effectiveness studies. Many see these studies as controversial and using them to make policy decisions is seen as a form of health care rationing. These concerns have affected policy makers in the United States to such an extent that the Senate Finance Committee in writing The Patient Protection and Affordable Care Act of 2010 forbade the newly created Patient-Centered Outcomes Research Institute from using “dollars-per-quality adjusted life year (or similar measure that discounts the value of a life because of an individual’s disability) as a threshold to establish what type of health care is cost effective or recommended”. However controversial, cost effectiveness will have to be assessed as unlimited access to all therapies cannot be afforded by society. The NICE is the most progressive institute in the world in this regard and their policies could serve as an example for other societies. Classic chemotherapeutic agents do not appear to be less effective for esophageal cancer compared to targeted agents and do not seem to reduce QoL. As targeted agents are

more expensive, chemotherapeutic agents are probably the more sensible class to use from a cost effectiveness perspective. A higher level of clinical benefit might reasonably be expected for targeted agents before choosing to prescribe them.

## Discussion

Considering the data on VDR polymorphisms, weight loss in palliative esophageal cancer patients may cause fast liberation of excessive amounts of vitamin D from its adipose storage. This might contribute to the dismal prognosis of these patients and stresses the need for optimal nutritional support. Endocrine regulation of *HOX* genes is known. The regulatory region of *HOXA10* is known to contain a vitamin D responsive element and has been shown to be regulated by 1,25-dihydroxycholecalciferol in both hematopoietic and endometrial cells (92). *Hoxa13* is not regulated by the sex steroids *in vivo* (92-94). Estrogens regulate expression of the 5' *Hox* paralogs such as *Hoxa9*, *Hoxa10*, and *Hoxa11*, in posterior and distal domains of the body axis (94). Additionally, retinoic acid treatment also up-regulates expression of *Hoxa1* and *Hoxb1* (95).

In our studies of *HOXA13* EPC2-hTERT and HET-1A were used alongside each other for bile and acid exposure experiments. In these experiments a one time exposure of a bile and acid mixture was chosen, the results of Chapter 8 suggest that 6 consecutive days of exposure results in an effect, or a larger effect, with regard to the expression of keratins, which alters in parallel with their expression in BE. For our overexpression experiments with esophageal keratinocytes EPC2-hTERT was chosen, as this cell line was immortalized using hTERT whereas the HET-1A cell line was immortalized using the SV40 large T antigen. The latter was deemed more likely to influence the biology of the cell line. The results of Chapter 8 show that exposure of a bile and acid mixture induced a gene expression profile in EPC2-hTERT which was more comparable with a BE gene signature, when compared with the gene expression profile that was induced in HET-1A.

There are several reports of *HOXA13* expression as a predictor of survival in gastric cancer (96), HCC (97-99), ESCC (44, 100), and pancreatic cancer (101). Outside of the GI tract similar results have been found in cervical cancer, ovarian cancer, and prostate carcinoma (102-104). Some of these studies are based on IHC which we deem not to be very trustworthy. To our knowledge, it has never been shown that *HOXA13* is also useful as a predictor of survival in EAC. We inspected the data available through the cBioPortal database ([www.cbioportal.org](http://www.cbioportal.org)) in 2015. Using a linear regression approach no correlation was seen between mRNA expression of *HOXA13* and survival. Repeating the analysis using the online tool on the website provided the same results. Experimentally, we performed RNA-ISH for *HOXA13* on roughly 20 patients. No correlation between *HOXA13* and survival was found for the whole group. However, there was a correlation

if all patients surviving beyond 1.5 years were excluded under the assumption these patients were not palliative, leaving only ten patients in the analysis. We were able to confirm previous reports that *HOXA13* expression in HCC negatively correlates with survival as we found a correlation in the same direction with recurrence of HCC in a patient group that was resected with curative intention (98, 99). This opens up the possibility for improving the determination of the prognosis of individual patients based on their *HOXA13* status, amongst other factors.

In pancreatic ductal AC (PDAC) *HOTTIP* was shown to be one of the most significantly upregulated lncRNAs. Knockdown of *HOXA13* showed *HOTTIP* promoted proliferation, invasion, and resistance to gemcitabine of PDAC cells, at least partly through regulating *HOXA13*. High *HOXA13* expression was correlated with lymph node metastasis, poor histological differentiation, and decreased OS in PDAC patients. (101). Inhibition of *HOTTIP* potentiated the antitumor effects of gemcitabine *in vitro* and *in vivo*. In CRC overexpression of nucleus accumbens-associated protein 1 confers chemotherapy resistance via *HOXA9* (41). This shows *HOX* gene signaling appears capable of interfering with chemotherapy response. A role for *HOTTIP* and *HOXA13* as markers for chemotherapy resistance in EAC is conceivable. As both gemcitabine and 5-FU are nucleoside analogues, response to 5-FU might also be predicted by *HOXA13* and *HOTTIP* status in the esophagus. This could be very relevant, particularly for ESCC chemotherapy where 5-FU is one of the primary building blocks of therapy. In ESCC *HOXA13* was shown to have tumorigenic effects *in vivo*. A significant association between *HOXA13* and OS was described (44). Co-expression of *HOXA13* with annexinA2 and SOD was shown to be significantly associated with poor prognosis (105). In gastric cancer *HOXA1*, 4, 10, and 13, and *HOXB7*, and *HOXC10* were previously found to be overexpressed. *HOXA13* overexpression was associated with T stage, M stage, histologic differentiation, relapse, and a decrease in OS (106). Concerning *HOXB7*, *in vitro* studies have shown overexpression of *HOXB7* in gastric cancer cells promotes cellular invasion and migration, and inhibited apoptosis, whereas silencing *HOXB7* showed the opposite effects (107, 108).

Although we have shown a decrease in methylation and an increase in hydroxymethylation of the *HOXA9* promotor in BE versus squamous esophagus, in CRC *HOXA9* was not found to be differentially methylated (51).

In conclusion, this thesis has shown *HOX* genes play an important role in (pre)malignant lesions of the-GI tract. Vitamin D receptor polymorphisms and p53 IHC can predict progression from BE to EAC. Palliative chemotherapy and targeted therapies increase the survival of esophageal and gastroesophageal junction cancer patients and cost effectiveness analysis of phase II trial data is feasible.

## References

1. Mari L, Milano F, Parikh K, Straub D, Everts V, Hoebe KK, et al. A pSMAD/CDX2 complex is essential for the intestinalization of epithelial metaplasia. *Cell Rep*. 2014;7(4):1197-210.
2. Silberg DG, Sullivan J, Kang E, Swain GP, Moffett J, Sund NJ, et al. Cdx2 ectopic expression induces gastric intestinal metaplasia in transgenic mice. *Gastroenterology*. 2002;122(3):689-96.
3. Pearson JC, Lemons D, McGinnis W. Modulating Hox gene functions during animal body patterning. *Nat Rev Genet*. 2005;6(12):893-904.
4. Shah N, Sukumar S. The Hox genes and their roles in oncogenesis. *Nat Rev Cancer*. 2010;10(5):361-71.
5. Jiang M, Li H, Zhang Y, Yang Y, Lu R, Liu K, et al. Transitional basal cells at the squamous-columnar junction generate Barrett's oesophagus. *Nature*. 2017;550(7677):529-33.
6. Quante M, Bhagat G, Abrams JA, Marache F, Good P, Lee MD, et al. Bile acid and inflammation activate gastric cardia stem cells in a mouse model of Barrett-like metaplasia. *Cancer Cell*. 2012;21(1):36-51.
7. Wang X, Ouyang H, Yamamoto Y, Kumar PA, Wei TS, Dagher R, et al. Residual embryonic cells as precursors of a Barrett's-like metaplasia. *Cell*. 2011;145(7):1023-35.
8. Hamilton SR, Yardley JH. Regenerative of cardiac type mucosa and acquisition of Barrett mucosa after esophagogastrostomy. *Gastroenterology*. 1977;72(4 Pt 1):669-75.
9. Gillen P, Keeling P, Byrne PJ, West AB, Hennessy TP. Experimental columnar metaplasia in the canine oesophagus. *Br J Surg*. 1988;75(2):113-5.
10. Li H, Walsh TN, O'Dowd G, Gillen P, Byrne PJ, Hennessy TP. Mechanisms of columnar metaplasia and squamous regeneration in experimental Barrett's esophagus. *Surgery*. 1994;115(2):176-81.
11. Nicholson GW. Heteromorphoses (metaplasia) of the alimentary tract. *The Journal of Pathology and Bacteriology*. 1926.
12. Rhee H, Wang DH. Cellular Origins of Barrett's Esophagus: the Search Continues. *Curr Gastroenterol Rep*. 2018;20(11):51.
13. Di Pietro M, Lao-Sirieix P, Boyle S, Cassidy A, Castillo D, Saadi A, et al. Evidence for a functional role of epigenetically regulated midcluster HOXB genes in the development of Barrett esophagus. *Proceedings of the National Academy of Sciences of the United States of America*. 2012;109(23):9077-82.
14. van Nistelrooij AMJ, van Marion R, van Ijcken WFJ, de Klein A, Wagner A, Biermann K, et al. Germline variant in MSX1 identified in a Dutch family with clustering of Barrett's esophagus and esophageal adenocarcinoma. *Fam Cancer*. 2018;17(3):435-40.
15. Joo MK, Park JJ, Chun HJ. Impact of homeobox genes in gastrointestinal cancer. *World Journal of Gastroenterology*. 2016;22(37):8247-56.
16. de Santa Barbara P, Roberts DJ. Tail gut endoderm and gut/genitourinary/tail development: a new tissue-specific role for Hoxa13. *Development*. 2002;129(3):551-61.
17. Thompson CA, Wojta K, Pulakanti K, Rao S, Dawson P, Battle MA. GATA4 Is Sufficient to Establish Jejunal Versus Ileal Identity in the Small Intestine. *Cell Mol Gastroenterol Hepatol*. 2017;3(3):422-46.
18. Chen K-N, Gu Z-D, Ke Y, Li J-Y, Shi X-T, Xu G-W. Expression of 11 HOX Genes Is Deregulated in Esophageal Squamous Cell Carcinoma. *Clinical Cancer Research*. 2005;11(3):1044.
19. Lin C, Wang Y, Wang Y, Zhang S, Yu L, Guo C, et al. Transcriptional and posttranscriptional regulation of HOXA13 by lncRNA HOTTIP facilitates tumorigenesis and metastasis in esophageal squamous carcinoma cells. *Oncogene*. 2017;36(38):5392-406.

20. Gu Z-D, Shen L-Y, Wang H, Chen X-M, Li Y, Ning T, et al. HOXA13 Promotes Cancer Cell Growth and Predicts Poor Survival of Patients with Esophageal Squamous Cell Carcinoma. *Cancer Research*. 2009;69(12):4969.
21. Sandel MH, Speetjens FM, Menon AG, Albertsson PA, Basse PH, Hokland M, et al. Natural killer cells infiltrating colorectal cancer and MHC class I expression. *Mol Immunol*. 2005;42(4):541-6.
22. Garrido F, Aptsiauri N. Cancer immune escape: MHC expression in primary tumours versus metastases. *Immunology*. 2019;158(4):255-66.
23. Zhou T, Fu H, Dong B, Dai L, Yang Y, Yan W, et al. HOXB7 mediates cisplatin resistance in esophageal squamous cell carcinoma through involvement of DNA damage repair. *Thorac Cancer*. 2019.
24. Samani AA, Yakar S, LeRoith D, Brodt P. The role of the IGF system in cancer growth and metastasis: overview and recent insights. *Endocr Rev*. 2007;28(1):20-47.
25. Masson K, Ronnstrand L. Oncogenic signaling from the hematopoietic growth factor receptors c-Kit and Flt3. *Cell Signal*. 2009;21(12):1717-26.
26. Wang D, Dubois RN. The role of COX-2 in intestinal inflammation and colorectal cancer. *Oncogene*. 2010;29(6):781-8.
27. Harris RE. Cyclooxygenase-2 (cox-2) blockade in the chemoprevention of cancers of the colon, breast, prostate, and lung. *Inflammopharmacology*. 2009;17(2):55-67.
28. Takkouche B, Regueira-Mendez C, Etminan M. Breast cancer and use of nonsteroidal anti-inflammatory drugs: a meta-analysis. *J Natl Cancer Inst*. 2008;100(20):1439-47.
29. Cole BF, Logan RF, Halabi S, Benamouzig R, Sandler RS, Grainge MJ, et al. Aspirin for the chemoprevention of colorectal adenomas: meta-analysis of the randomized trials. *J Natl Cancer Inst*. 2009;101(4):256-66.
30. Montalvo-Jave EE, Olguin-Martinez M, Hernandez-Espinosa DR, Sanchez-Sevilla L, Mendieta-Condado E, Contreras-Zentella ML, et al. Role of NADPH oxidases in inducing a selective increase of oxidant stress and cyclin D1 and checkpoint 1 over-expression during progression to human gastric adenocarcinoma. *Eur J Cancer*. 2016;57:50-7.
31. Lindsey S, Zhu C, Lu YF, Eklund EA. HoxA10 represses transcription of the gene encoding p67phox in phagocytic cells. *J Immunol*. 2005;175(8):5269-79.
32. Zhang AY, Yi F, Zhang G, Gulbins E, Li PL. Lipid raft clustering and redox signaling platform formation in coronary arterial endothelial cells. *Hypertension*. 2006;47(1):74-80.
33. Zhang AY, Yi F, Jin S, Xia M, Chen QZ, Gulbins E, et al. Acid sphingomyelinase and its redox amplification in formation of lipid raft redox signaling platforms in endothelial cells. *Antioxid Redox Signal*. 2007;9(7):817-28.
34. Circu ML, Aw TY. Reactive oxygen species, cellular redox systems, and apoptosis. *Free Radic Biol Med*. 2010;48(6):749-62.
35. Shah CA, Bei L, Wang H, Platanias LC, Eklund EA. The leukemia-associated Mll-Ell oncoprotein induces fibroblast growth factor 2 (Fgf2)-dependent cytokine hypersensitivity in myeloid progenitor cells. *J Biol Chem*. 2013;288(45):32490-505.
36. Smith K, Bui TD, Poulosom R, Kaklamanis L, Williams G, Harris AL. Up-regulation of macrophage wnt gene expression in adenoma-carcinoma progression of human colorectal cancer. *Br J Cancer*. 1999;81(3):496-502.
37. Cheng R, Sun B, Liu Z, Zhao X, Qi L, Li Y, et al. Wnt5a suppresses colon cancer by inhibiting cell proliferation and epithelial-mesenchymal transition. *J Cell Physiol*. 2014;229(12):1908-17.
38. Gregorieff A, Pinto D, Begthel H, Destree O, Kielman M, Clevers H. Expression pattern of Wnt signaling components in the adult intestine. *Gastroenterology*. 2005;129(2):626-38.

39. Neumann PA, Koch S, Hilgarth RS, Perez-Chanona E, Denning P, Jobin C, et al. Gut commensal bacteria and regional Wnt gene expression in the proximal versus distal colon. *Am J Pathol.* 2014;184(3):592-9.
40. Watanabe Y, Saito M, Saito K, Matsumoto Y, Kanke Y, Onozawa H, et al. Upregulated HOXA9 expression is associated with lymph node metastasis in colorectal cancer. *Oncol Lett.* 2018;15(3):2756-62.
41. Ju T, Jin H, Ying R, Xie Q, Zhou C, Gao D. Overexpression of NAC1 confers drug resistance via HOXA9 in colorectal carcinoma cells. *Mol Med Rep.* 2017;16(3):3194-200.
42. Bhatlekar S, Viswanathan V, Fields JZ, Boman BM. Overexpression of HOXA4 and HOXA9 genes promotes self-renewal and contributes to colon cancer stem cell overpopulation. *J Cell Physiol.* 2018;233(2):727-35.
43. Ma YY, Zhang Y, Mou XZ, Liu ZC, Ru GQ, Li E. High level of homeobox A9 and PBX homeobox 3 expression in gastric cancer correlates with poor prognosis. *Oncol Lett.* 2017;14(5):5883-9.
44. Gu ZD, Shen LY, Wang H, Chen XM, Li Y, Ning T, et al. HOXA13 promotes cancer cell growth and predicts poor survival of patients with esophageal squamous cell carcinoma. *Cancer Res.* 2009;69(12):4969-73.
45. Zhang ZF, Wang YJ, Fan SH, Du SX, Li XD, Wu DM, et al. MicroRNA-182 downregulates Wnt/beta-catenin signaling, inhibits proliferation, and promotes apoptosis in human osteosarcoma cells by targeting HOXA9. *Oncotarget.* 2017;8(60):101345-61.
46. Park SM, Choi EY, Bae M, Choi JK, Kim YJ. A long-range interactive DNA methylation marker panel for the promoters of HOXA9 and HOXA10 predicts survival in breast cancer patients. *Clin Epigenetics.* 2017;9:73.
47. Wang K, Jin J, Ma T, Zhai H. MiR-139-5p inhibits the tumorigenesis and progression of oral squamous carcinoma cells by targeting HOXA9. *J Cell Mol Med.* 2017;21(12):3730-40.
48. Ko SY, Barengo N, Ladanyi A, Lee JS, Marini F, Lengyel E, et al. HOXA9 promotes ovarian cancer growth by stimulating cancer-associated fibroblasts. *J Clin Invest.* 2012;122(10):3603-17.
49. Kanai M, Hamada J, Takada M, Asano T, Murakawa K, Takahashi Y, et al. Aberrant expressions of HOX genes in colorectal and hepatocellular carcinomas. *Oncol Rep.* 2010;23(3):843-51.
50. Segditsas S, Sieber O, Deheragoda M, East P, Rowan A, Jeffery R, et al. Putative direct and indirect Wnt targets identified through consistent gene expression changes in APC-mutant intestinal adenomas from humans and mice. *Hum Mol Genet.* 2008;17(24):3864-75.
51. Ahlquist T, Lind GE, Costa VL, Meling GI, Vatn M, Hoff GS, et al. Gene methylation profiles of normal mucosa, and benign and malignant colorectal tumors identify early onset markers. *Mol Cancer.* 2008;7:94.
52. Lai M, Liu G, Li R, Bai H, Zhao J, Xiao P, et al. Hsa\_circ\_0079662 induces the resistance mechanism of the chemotherapy drug oxaliplatin through the TNF- $\alpha$  pathway in human colon cancer. *J Cell Mol Med.* 2020;24(9):5021-7.
53. Cummings LC, Thota PN, Willis JE, Chen Y, Cooper GS, Furey N, et al. A nonrandomized trial of vitamin D supplementation for Barrett's esophagus. *PLoS One.* 2017;12(9):e0184928.
54. Moreno J, Krishnan AV, Swami S, Nonn L, Peehl DM, Feldman D. Regulation of prostaglandin metabolism by calcitriol attenuates growth stimulation in prostate cancer cells. *Cancer Res.* 2005;65(17):7917-25.
55. Krishnan AV, Swami S, Peng L, Wang J, Moreno J, Feldman D. Tissue-selective regulation of aromatase expression by calcitriol: implications for breast cancer therapy. *Endocrinology.* 2010;151(1):32-42.
56. Dimitrakopoulou VI, Tsilidis KK, Haycock PC, Dimou NL, Al-Dabhani K, Martin RM, et al. Circulating vitamin D concentration and risk of seven cancers: Mendelian randomisation study. *Bmj.* 2017;359:j4761.



57. Dong J, Gharahkhani P, Chow WH, Gammon MD, Liu G, Caldas C, et al. No Association Between Vitamin D Status and Risk of Barrett's Esophagus or Esophageal Adenocarcinoma: A Mendelian Randomization Study. *Clin Gastroenterol Hepatol*. 2019;17(11):2227-35 e1.
58. Lavery DL, Martinez P, Gay LJ, Cereser B, Novelli MR, Rodriguez-Justo M, et al. Evolution of oesophageal adenocarcinoma from metaplastic columnar epithelium without goblet cells in Barrett's oesophagus. *Gut*. 2016;65(6):907-13.
59. Kastelein F, Biermann K, Steyerberg EW, Verheij J, Kalisvaart M, Looijenga LHJ, et al. Aberrant p53 protein expression is associated with an increased risk of neoplastic progression in patients with Barrett's oesophagus. *Gut*. 2013;62(12):1676-83.
60. Nieto T, Tomlinson CL, Dretzke J, Bayliss S, Dilworth M, Beggs AD, et al. Epigenetic biomarkers in progression from non-dysplastic Barrett's oesophagus to oesophageal adenocarcinoma: a systematic review protocol. *BMJ Open*. 2016;6(12):e013361.
61. Altaf K, Xiong JJ, la Iglesia D, Hickey L, Kaul A. Meta-analysis of biomarkers predicting risk of malignant progression in Barrett's oesophagus. *The British journal of surgery*. 2017;104(5):493-502.
62. Janmaat VT, Peppelenbosch MP, Bruno MJ, Spaander MCW. Comment on: 'Meta-analysis of biomarkers predicting risk of malignant progression in Barrett's oesophagus' (Br J Surg 2017; 104: 493-502). *British Journal of Surgery*; 2017 [updated 14-06-2017. Available from: <https://www.bjs.co.uk/article/meta-analysis-of-biomarkers-predicting-risk-of-malignant-progression-in-barretts-oesophagus/>.
63. Srivastava A, Appelman H, Goldsmith JD, Davison JM, Hart J, Krasinskas AM. The Use of Ancillary Stains in the Diagnosis of Barrett Esophagus and Barrett Esophagus-associated Dysplasia: Recommendations From the Rodger C. Haggitt Gastrointestinal Pathology Society. *Am J Surg Pathol*. 2017;41(5):e8-e21.
64. Snyder P, Dunbar K, Cipher DJ, Souza RF, Spechler SJ, Konda VJA. Aberrant p53 Immunostaining in Barrett's Esophagus Predicts Neoplastic Progression: Systematic Review and Meta-Analyses. *Dig Dis Sci*. 2019;64(5):1089-97.
65. Fitzgerald RC, di Pietro M, Ragunath K, Ang Y, Kang JY, Watson P, et al. British Society of Gastroenterology guidelines on the diagnosis and management of Barrett's oesophagus. *Gut*. 2014;63(1):7-42.
66. Holmberg D, Ness-Jensen E, Mattsson F, Lagergren J. Clinical prediction model for tumor progression in Barrett's esophagus. *Surg Endosc*. 2019;33(9):2901-8.
67. Rumiato E, Boldrin E, Malacrida S, Realdon S, Fassan M, Morbin T, et al. Detection of genetic alterations in cfDNA as a possible strategy to monitor the neoplastic progression of Barrett's esophagus. *Transl Res*. 2017;190:16-24 e1.
68. Kapoor H, Lohani KR, Lee TH, Agrawal DK, Mittal SK. Animal Models of Barrett's Esophagus and Esophageal Adenocarcinoma-Past, Present, and Future. *Clinical and translational science*. 2015;8(6):841-7.
69. Bus P, Siersema PD, van Baal JWPM. Cell culture models for studying the development of Barrett's esophagus: a systematic review. *Cellular oncology (Dordrecht)*. 2012;35(3):149-61.
70. Mohammad NH, ter Veer E, Ngai L, Mali R, van Oijen MG, van Laarhoven HW. Optimal first-line chemotherapeutic treatment in patients with locally advanced or metastatic esophagogastric carcinoma: triplet versus doublet chemotherapy: a systematic literature review and meta-analysis. *Cancer Metastasis Rev*. 2015;34(3):429-41.
71. Van Cutsem E, Boni C, Tabernero J, Massuti B, Middleton G, Dane F, et al. Docetaxel plus oxaliplatin with or without fluorouracil or capecitabine in metastatic or locally recurrent gastric cancer: a randomized phase II study. *Ann Oncol*. 2015;26(1):149-56.

72. Waters JS, Norman A, Cunningham D, Scarffe JH, Webb A, Harper P, et al. Long-term survival after epirubicin, cisplatin and fluorouracil for gastric cancer: results of a randomized trial. *Br J Cancer*. 1999;80(1-2):269-72.
73. Amdal CD, Jacobsen AB, Guren MG, Bjordal K. Patient-reported outcomes evaluating palliative radiotherapy and chemotherapy in patients with oesophageal cancer: a systematic review. *Acta Oncol*. 2013;52(4):679-90.
74. Marsman WA, Tytgat GN, ten Kate FJ, van Lanschot JJ. Differences and similarities of adenocarcinomas of the esophagus and esophagogastric junction. *J Surg Oncol*. 2005;92(3):160-8.
75. Shah MA, Khanin R, Tang L, Janjigian YY, Klimstra DS, Gerdes H, et al. Molecular classification of gastric cancer: a new paradigm. *Clin Cancer Res*. 2011;17(9):2693-701.
76. Chau I, Norman AR, Cunningham D, Oates J, Hawkins R, Iveson T, et al. The impact of primary tumour origins in patients with advanced oesophageal, oesophago-gastric junction and gastric adenocarcinoma--individual patient data from 1775 patients in four randomised controlled trials. *Ann Oncol*. 2009;20(5):885-91.
77. Ross P, Nicolson M, Cunningham D, Valle J, Seymour M, Harper P, et al. Prospective randomized trial comparing mitomycin, cisplatin, and protracted venous-infusion fluorouracil (PVI 5-FU) With epirubicin, cisplatin, and PVI 5-FU in advanced esophagogastric cancer. *J Clin Oncol*. 2002;20(8):1996-2004.
78. Tebbutt NC, Norman A, Cunningham D, Iveson T, Seymour M, Hickish T, et al. A multicentre, randomised phase III trial comparing protracted venous infusion (PVI) 5-fluorouracil (5-FU) with PVI 5-FU plus mitomycin C in patients with inoperable oesophago-gastric cancer. *Ann Oncol*. 2002;13(10):1568-75.
79. Cunningham D, Starling N, Rao S, Iveson T, Nicolson M, Coxon F, et al. Capecitabine and oxaliplatin for advanced esophagogastric cancer. *N Engl J Med*. 2008;358(1):36-46.
80. Cherny NI, Sullivan R, Dafni U, Kerst JM, Sobrero A, Zielinski C, et al. A standardised, generic, validated approach to stratify the magnitude of clinical benefit that can be anticipated from anti-cancer therapies: the European Society for Medical Oncology Magnitude of Clinical Benefit Scale (ESMO-MCBS). *Ann Oncol*. 2015;26(8):1547-73.
81. Laursen L, Schønau MN, Bergenholtz HM, Siemsen M, Christensen M, Missel M. Table in the corner: a qualitative study of life situation and perspectives of the everyday lives of oesophageal cancer patients in palliative care. *BMC Palliat Care*. 2019;18(1):60.
82. Greenhalgh J, Bagust A, Boland A, Fleeman N, McLeod C, Dundar Y, et al. Cetuximab for the treatment of recurrent and/or metastatic squamous cell carcinoma of the head and neck. *Health Technol Assess*. 2009;13 Suppl 3:49-54.
83. Hannouf MB, Sehgal C, Cao JQ, Mocanu JD, Winkquist E, Zaric GS. Cost-effectiveness of adding cetuximab to platinum-based chemotherapy for first-line treatment of recurrent or metastatic head and neck cancer. *PLoS One*. 2012;7(6):e38557.
84. National Institute for Care and health Excellence (NICE). Cetuximab for the treatment of recurrent and/or metastatic squamous cell cancer of the head and neck. June 2009.
85. Hoyle M, Crathorne L, Peters J, Jones-Hughes T, Cooper C, Napier M, et al. The clinical effectiveness and cost-effectiveness of cetuximab (mono- or combination chemotherapy), bevacizumab (combination with non-oxaliplatin chemotherapy) and panitumumab (monotherapy) for the treatment of metastatic colorectal cancer after first-line chemotherapy (review of technology appraisal No.150 and part review of technology appraisal No. 118): a systematic review and economic model. *Health Technol Assess*. 2013;17(14):1-237.

86. Mittmann N, Au HJ, Tu D, O'Callaghan CJ, Isogai PK, Karapetis CS, et al. Prospective cost-effectiveness analysis of cetuximab in metastatic colorectal cancer: evaluation of National Cancer Institute of Canada Clinical Trials Group CO.17 trial. *J Natl Cancer Inst.* 2009;101(17):1182-92.
87. Bonner JA, Harari PM, Giralt J, Cohen RB, Jones CU, Sur RK, et al. Radiotherapy plus cetuximab for locoregionally advanced head and neck cancer: 5-year survival data from a phase 3 randomised trial, and relation between cetuximab-induced rash and survival. *Lancet Oncol.* 2010;11(1):21-8.
88. van der Linden N, van Gils CW, Pescott CP, Buter J, Vergeer MR, Groot CA. Real-world cost-effectiveness of cetuximab in locally advanced squamous cell carcinoma of the head and neck. *Eur Arch Otorhinolaryngol.* 2015;272(8):2007-16.
89. Higginson IJ, McCrone P, Hart SR, Burman R, Silber E, Edmonds PM. Is short-term palliative care cost-effective in multiple sclerosis? A randomized phase II trial. *J Pain Symptom Manage.* 2009;38(6):816-26.
90. Hill S, Freemantle N. A role for two-stage pharmacoeconomic appraisal? Is there a role for interim approval of a drug for reimbursement based on modelling studies with subsequent full approval using phase III data? *Pharmacoeconomics.* 2003;21(11):761-7.
91. Hughes DA, Walley T. Economic evaluations during early (phase II) drug development: a role for clinical trial simulations? *Pharmacoeconomics.* 2001;19(11):1069-77.
92. Du H, Daftary GS, Lalwani SI, Taylor HS. Direct regulation of HOXA10 by 1,25-(OH)2D3 in human myelomonocytic cells and human endometrial stromal cells. *Mol Endocrinol.* 2005;19(9):2222-33.
93. Ma L, Benson GV, Lim H, Dey SK, Maas RL. Abdominal B (AbdB) Hoxa genes: regulation in adult uterus by estrogen and progesterone and repression in müllerian duct by the synthetic estrogen diethylstilbestrol (DES). *Dev Biol.* 1998;197(2):141-54.
94. Block K, Kardana A, Igarashi P, Taylor HS. In utero diethylstilbestrol (DES) exposure alters Hox gene expression in the developing müllerian system. *FASEB J.* 2000;14(9):1101-8.
95. Conlon RA, Rossant J. Exogenous retinoic acid rapidly induces anterior ectopic expression of murine Hox-2 genes in vivo. *Development.* 1992;116(2):357-68.
96. Han Y, Tu WW, Wen YG, Li DP, Qiu GQ, Tang HM, et al. Identification and validation that up-expression of HOXA13 is a novel independent prognostic marker of a worse outcome in gastric cancer based on immunohistochemistry. *Medical Oncology.* 2013;30(2).
97. Cillo C, Schiavo G, Cantile M, Bihl MP, Sorrentino P, Carafa V, et al. The HOX gene network in hepatocellular carcinoma. *Int J Cancer.* 2011;129(11):2577-87.
98. Pan TT, Jia WD, Yao QY, Sun QK, Ren WH, Huang M, et al. Overexpression of HOXA13 as a potential marker for diagnosis and poor prognosis of hepatocellular carcinoma. *Tohoku J Exp Med.* 2014;234(3):209-19.
99. Quagliata L, Matter MS, Piscuoglio S, Arabi L, Ruiz C, Procino A, et al. Long noncoding RNA HOTTIP/HOXA13 expression is associated with disease progression and predicts outcome in hepatocellular carcinoma patients. *Hepatology.* 2014;59(3):911-23.
100. Ma RL, Shen LY, Chen KN. Coexpression of ANXA2, SOD2 and HOXA13 predicts poor prognosis of esophageal squamous cell carcinoma. *Oncology Reports.* 2014;31(5):2157-64.
101. Li Z, Zhao X, Zhou Y, Liu Y, Zhou Q, Ye H, et al. The long non-coding RNA HOTTIP promotes progression and gemcitabine resistance by regulating HOXA13 in pancreatic cancer. *Journal of translational medicine.* 2015;13(1):442-.
102. Liu C, Tian X, Zhang J, Jiang L. Long Non-coding RNA DLEU1 Promotes Proliferation and Invasion by Interacting With miR-381 and Enhancing HOXA13 Expression in Cervical Cancer. *Front Genet.* 2018;9:629.

103. Yu H, Xu Y, Zhang D, Liu G. Long noncoding RNA LUCAT1 promotes malignancy of ovarian cancer through regulation of miR-612/HOXA13 pathway. *Biochem Biophys Res Commun.* 2018;503(3):2095-100.
104. Dong Y, Cai Y, Liu B, Jiao X, Li ZT, Guo DY, et al. HOXA13 is associated with unfavorable survival and acts as a novel oncogene in prostate carcinoma. *Future Oncol.* 2017;13(17):1505-16.
105. Ma RL, Shen LY, Chen KN. Coexpression of ANXA2, SOD2 and HOXA13 predicts poor prognosis of esophageal squamous cell carcinoma. *Oncol Rep.* 2014;31(5):2157-64.
106. Han Y, Tu WW, Wen YG, Li DP, Qiu GQ, Tang HM, et al. Identification and validation that up-expression of HOXA13 is a novel independent prognostic marker of a worse outcome in gastric cancer based on immunohistochemistry. *Med Oncol.* 2013;30(2):564.
107. Joo MK, Park JJ, Yoo HS, Lee BJ, Chun HJ, Lee SW, et al. The roles of HOXB7 in promoting migration, invasion, and anti-apoptosis in gastric cancer. *J Gastroenterol Hepatol.* 2016;31(10):1717-26.
108. Cai JQ, Xu XW, Mou YP, Chen K, Pan Y, Wu D. Upregulation of HOXB7 promotes the tumorigenesis and progression of gastric cancer and correlates with clinical characteristics. *Tumour Biol.* 2016;37(2):1641-50.





# Chapter 12

---

Nederlandse samenvatting





Het doel van dit proefschrift is het verkrijgen van een beter begrip van de etiologie, de detectie en de palliatieve behandeling van gastro-intestinale kanker. Dit proefschrift is onderverdeeld in vijf delen.

**Deel 1** bevat de introductie van het proefschrift. In **Hoofdstuk 1.1** wordt gastro-intestinale kanker beschreven. Deze ziekte kenmerkt zich door een toename van celgroei in het maagdarmkanaal gecombineerd met het vermogen van deze cellen om zich te verspreiden buiten het weefsel van origine. Gastro-intestinale kanker is één van de hoofdoorzaken van morbiditeit en mortaliteit in de wereld. Slokdarmkanker is de op zeven na meest voorkomende vorm van kanker ter wereld. In 2012 werden ongeveer 398.000 patiënten gediagnosticeerd met plaveiselcelkanker van de slokdarm en 52.000 met kliercelkanker van de slokdarm. Barrett slokdarm is een intestinale metaplasie van de slokdarm en deze aandoening kan aanleiding geven tot kliercelkanker van de slokdarm. In de afgelopen decennia hebben ontwikkelde landen een toename gezien van de incidentie van zowel Barrett slokdarm als kliercelkanker van de slokdarm. Deze toename van Barrett slokdarm wordt toegeschreven aan de toenemende prevalentie van obesitas. Met een diepgaand inzicht in de mechanismen van het ontstaan van kanker in het maagdarmkanaal zijn preventie, detectie en behandeling effectiever toe te passen. **Hoofdstuk 1.2** beschrijft de opbouw van dit proefschrift.

In **Deel 2** van dit proefschrift proberen we het fundamentele inzicht in het mechanisme van het ontstaan van kanker in het maagdarmkanaal te vergroten. Hiervoor bestuderen we *HOX*-gen signalering in (pre)maligne laesies van het maagdarmkanaal. In **Deel 3** bestuderen we verschillende methodieken om te voorspellen welke afwijkingen maligne zullen ontaarden en bestuderen we modellen om het mechanisme van het ontstaan van kanker te kunnen onderzoeken. In **Deel 4** bestuderen we de palliatieve behandeling van slokdarmkanker. **Deel 5** bestaat uit de samenvatting, discussie en appendices. Hieronder zullen we dit proefschrift in het Nederlands samenvatten.

## **Deel 2: *HOX*-genen in (pre)maligne laesies van het maagdarmkanaal**

In **Hoofdstuk 2** werd de rol van *HOXA13* in de vorming van Barrett slokdarm en uiteindelijk de ontaarding in kliercelkanker van de slokdarm bestudeerd. De biologie van Barrett slokdarm en meer algemeen, metaplasie in het maagdarmkanaal, is namelijk nog slechts beperkt bekend. We hebben aangetoond dat de volgorde waarin *HOX*-genen gecodeerd zijn in het genoom parallel loopt met de volgorde waarin zij tot expressie komen langs de lengteas van het maagdarmkanaal van volwassen mensen en muizen. Bij Barrett slokdarm, kliercelkanker van de slokdarm, heterotopie van de slokdarm, metaplasie van de maag, en het Meckels divertikel werd een *HOX*-gen expressiepatroon waargenomen dat vergelijkbaar is met het patroon dat werd waargenomen in de dikke darm en afwijkt van het patroon dat kenmerkend is voor de proximale gastro-intestinale tractus. Dit patroon wordt gekenmerkt door een sterk verhoogde expressie van *HOXA13* ten opzichte

van het omliggende weefsel. In de embryologische ontwikkeling komt *HOXA13* distaal in orgaansystemen tot expressie. RNA *In situ* hybridisatie van *HOXA13* toont aan dat het voornamelijk epitheliaal tot expressie komt en bevestigde de expressie van *HOXA13* in Barrett slokdarm en de overige metaplastische en heterotopische weefsels van het bovenste gedeelte van het maagdarmkanaal. Deze afwijkende expressie van *HOX*-genen wordt ook gezien in de stamcellen van zowel fysiologisch slijmvlies van het maagdarmkanaal alsook in Barrett slokdarm. Dit wijst op betrokkenheid van zowel epitheliale stamcellen als *HOX*-genen tijdens de ontwikkeling van metaplasie. Bevindingen afkomstig van een muismodel lieten zien dat *Hoxa13* expressie in de fysiologie nauwkeurig gereguleerd is. De proximale expressiegrens bevond zich tussen het proximale en het distale colon van de muis. Deze expressiegrens is op dezelfde locatie aanwezig bij mensen. Opvallend was dat het expressiepatroon van *HOX*-genen werd onderbroken door expressie van *HOXA13* in de proximale gastro-intestinale tractus. *HOXA13* werd gedetecteerd net distaal van de overgang van de slokdarm naar de maag en in submucosale klieren van de slokdarm in volwassen mensen, en in het klierepitheel van de maag van volwassen muizen. In humane foetussen werd veel *HOXA13*-expressie gezien in de proximale maag en minder expressie in de slokdarm en de distale maag. In een model van maagdarmkanaal voorlopercellen, zijnde definitief endoderm, verminderde *HOXA13* de differentiatie efficiëntie van deze cellen. Een remmende werking op de differentiatie zou kunnen verklaren hoe een *HOXA13*-positieve klonale populatie van cellen sneller zou kunnen uitgroeien na beschadiging van het slokdarmslijmvlies in vergelijking met andere klonale populaties van cellen aanwezig op dezelfde locatie. Kunstmatige toename van *HOXA13*-expressie zorgt voor toename van expressie van genen in de Nanog-sigtaaltransductieroute. Dit verklaart het mechanisme waarop *HOXA13* de differentiatie remt. In de definitieve endoderm cellen bevordert *HOXA13* de expressie van genen kenmerkend voor distaal darmepitheel en stimuleert het de groeisnelheid van de celpopulatie. *HOXA13* onderdrukt de expressie van het epidermale differentiatiecomplex dat tot expressie komt vanaf chromosoom 1q21.3 en stimuleert de groeisnelheid van de celpopulatie in een Barrett celmodel en een celmodel van plaveiselcellen van de slokdarm. In een levend model waarin door cellijnen een slijmvlies kan worden gevormd, produceert een normale Barrett cellijn zowel kliertype slijmvlies met kolomvormige cellen alsook plaveiseltype slijmvlies. Dit laat zien dat een enkele cellijn zich kan ontwikkelen in twee typen epitheel. Het uitschakelen van *HOXA13* in deze cellijn zorgt voor een afname van de ontwikkeling van het kliertype epitheel. Concluderend, kennis van de expressie en functie van *HOXA13* geeft informatie over de oorsprong, het uiterlijk en het risico op progressie van Barrett slokdarm tot slokdarmkanker.

In **Hoofdstuk 3** werden de oncogene kenmerken bestudeerd die *HOXA13* geeft aan slokdarmkeratinocyten. *HOXA13* werd verhoogd tot expressie gebracht in een celmodel van plaveiselcellen van de slokdarm. Genexpressieprofielen werden vervaardigd en functionele experimenten werden uitgevoerd. De expressie van *HOXA13* in het celmodel

bleek oncogene kenmerken over te brengen op de cellen. *HOXA13* zorgt voor een toename van de groeisnelheid van de celpopulatie, het vermindert de gevoeligheid voor chemische stoffen, het vermindert de expressie van het MHC-klasse 1 eiwitcomplex, het verandert de mate van differentiatie en het bevordert de migratie van cellen. Deze data wijst op een cruciale rol van *HOXA13* in een vroeg stadium van maligne ontaarding van het plaveiselcelepitheel van de slokdarm.

In **Hoofdstuk 4** wordt de verhoogde expressie van *HOXA9* in poliepen van het colon bestudeerd. Kanker van de dikke darm komt relatief vaak voor. Deze kanker ontstaat uit een poliep. Meer kennis over afwijkingen in signaaloverdrachtketens die in cellen van deze poliepen plaatsvinden, kan helpen bij het begrijpen welke personen risico lopen op het krijgen van dikke darmkanker. *HOXA9* gedraagt zich als een oncogen in het bloedvormend orgaansysteem. De expressie van *HOXA9* in poliepen van de dikke darm en de rol van *HOXA9* bij de ontwikkeling van poliepen naar dikke darmkanker waren tot op heden onbekend en werden bestudeerd. *HOXA9*-expressie blijkt hoger te zijn in poliepen van de dikke darm in vergelijking met naastgelegen controle slijmvlies. *HOXA9* vermindert celmigratie wat wordt gemedieerd door PAK. *HOXA9* bevordert de groei van de celpopulatie in parallel met de rol van *HOXA9* in het bloedvormend orgaansysteem. Hierbij vindt een toename plaats van expressie van de genen *IGF1*, *FLT3*, *PTGS2*, p-4E-BP1 en p-ERK1/2. Concluderend kunnen we stellen dat *HOXA9* verhoogd tot expressie komt in poliepen van de dikke darm en groei van de celpopulatie stimuleert voordat maligne ontaarding optreedt.

### Deel 3: Voorspellen van de ontwikkeling van kwaadaardige laesies

Als de progressie van Barrett slokdarm naar slokdarm kliercelkanker kon worden voorspeld, zouden we weten welke patiënten actiever moeten worden vervolgd of zelfs preventief moeten worden behandeld. Een goede voorspelling van het risico op maligne ontaarding van Barrett slokdarm heeft daarom het potentieel om de ziektelast door slokdarm kliercelkanker aanzienlijk te verminderen.

In **Hoofdstuk 5** werden vitamine D-receptor (*VDR*) polymorfismen bestudeerd in relatie tot *VDR* expressie in de slokdarm. Daarnaast werd de invloed van *VDR* polymorfismen op het risico op het ontwikkelen van slokdarm kliercelkanker onderzocht. Epidemiologische studies hebben laten zien dat vitamine D de kans vermindert dat bepaalde vormen van kanker zich ontwikkelen. Er zijn echter aanwijzingen dat hoge vitamine D-spiegels bij de ontwikkeling van slokdarm kliercelkanker een schadelijke rol kunnen spelen. Deze studie onderzocht genetische variatie in het gen dat codeert voor de *VDR* in relatie tot de expressie van dit gen en het risico op de ontwikkeling van Barrett slokdarm en slokdarm kliercelkanker. *VDR*-mRNA kwam verhoogd tot expressie in Barrett slokdarm slijmvlies in vergelijking met plaveiselcel slijmvlies van de slokdarm. *VDR*-eiwit bevond zich in de kern van de cellen in het Barrett slokdarm slijmvlies.

Een rs1989969 T/rs2238135 G haplotype werd geïdentificeerd in het 5' regulerende gebied van het *VDR* gen. Dit haplotype ging gepaard met een ongeveer tweevoudige verlaging van het risico op de aanwezigheid van reflux oesofagitis, een Barrett slokdarm en/of slokdarm kliercelkanker. Analyse van een replicatiecohort werd uitgevoerd voor Barrett slokdarm en deze analyse bevestigde bovenstaande bevinding. Het Rs1989969 T polymorfisme zorgt voor het verschijnen van een GATA-1 transcriptiefactor bindingsplaats. GATA-1 wordt beschouwd als een negatieve regulator van transcriptie. Dit zou de bevindingen voor rs1989969 kunnen verklaren. Het allel Rs2238135 G was geassocieerd met een significant verminderde *VDR*-expressie in Barrett slokdarm. Voor het allel rs1989969 T werd een trend in verminderde *VDR*-expressie waargenomen. Concluderend identificeerden we een *VDR*-haplotype dat is geassocieerd met een verminderde *VDR*-expressie in de slokdarm en een verminderde incidentie van reflux oesofagitis, Barrett slokdarm en slokdarm kliercelkanker. Dit *VDR*-haplotype kan nuttig zijn om individuen te identificeren die het meest baat hebben bij vitamine D-chemopreventie.

In **Hoofdstuk 6.1** werden immunohistochemische biomarkers voor risicostratificatie van maligne progressie in de Barrett slokdarm systematisch beoordeeld en werd een meta-analyse uitgevoerd. De kans is klein dat een patiënt slokdarm kliercelkanker ontwikkelt vanuit een Barrett slokdarm. Daarom is er behoefte aan methoden om het risico op het ontstaan van slokdarm kliercelkanker te kunnen bepalen. Zo zouden patiënten met een hoger risico vaker kunnen worden gesurveilleerd en patiënten met een lager risico minder vaak. Daarom hebben we een systematische review en meta-analyse uitgevoerd van gepubliceerde studies over immunohistochemische biomarkers die zijn toegepast op bipten uit Barrett slokdarm slijmvlies. 16 verschillende immunohistochemische biomarkers uit 36 studies werden bestudeerd. Deze studies bevatten samen 425 patiënten die slokdarm kliercelkanker of hooggradige dysplasie ontwikkelden en 1835 patiënten waarbij geen sprake was van maligne progressie. Meta-analyses werden uitgevoerd voor de immunohistochemische biomarkers p53, aspergillus oryzae lectine, cycline A, cycline D en alfa-methylacyl-CoA racemase. Afwijkende p53-expressie was significant geassocieerd met een verhoogd risico op het ontwikkelen van kanker. Deze associatie werd bevestigd voor zowel niet-dysplastische Barrett slokdarm als Barrett slokdarm met laaggradige dysplasie. Een andere veelbelovende biomarker om maligne ontaarding te voorspellen was aspergillus oryzae lectine. Gebruik van p53 immunohistochemische kleuring, op bipten afgenomen tijdens controle endoscopische onderzoeken, kan de risico-inschatting op maligne ontaarding van een Barrett slokdarm verbeteren.

In **Hoofdstuk 6.2** hebben we een reactie geschreven op een review en meta-analyse waarin tevens studies werden geïnccludeerd zonder follow-up. Deze studies werden wel gebruikt om uitspraken te doen over de waarde van p53 als een voorspeller van maligne ontaarding van Barrett slokdarm.

In **Hoofdstuk 7** werd DNA-integriteit afkomstig uit cysten van de alvleesklier onderzocht als mogelijke voorspeller van het risico op maligne ontaarding van deze cysten. Identificatie van cysten in de alvleesklier met een hoge kans om zich te ontwikkelen tot kanker is belangrijk om de cysten goed te kunnen vervolgen en op tijd in te grijpen indien noodzakelijk. Cellen die op een gecontroleerde manier sterven geven uniform in stukken gebroken DNA af, terwijl bij sterfte van kwaadaardige cellen langere fragmenten DNA vrijkomen. We maten de hoeveelheid van beide DNA-fragmenten van ALU-herhalingen, één van 247 en één van 115 basenparen. Dit deden we door middel van een kwantitatieve polymerase kettingreactie. Als monsters gebruikten we het serum van gezonde controle patiënten en patiënten met alvleesklierkanker, en vloeistof uit cysten in de alvleesklier. Er werden geen verschillen in totaal cel vrij DNA (ALU115) of cel vrij DNA integriteit (ALU247 / 115) waargenomen tussen sera van gezonde controle patiënten (n=19) en patiënten met alvleesklierkanker (n=19). De hoeveelheid cel vrij DNA was verhoogd in cysten van de alvleesklier. Er werd geen verschil in cel vrij DNA-integriteit gevonden tussen vloeistof uit cysten van de alvleesklier van hoog risico patiënten (n=10) versus laag risico patiënten (n=20). Concluderend blijkt uit onze data dat cel vrij DNA-integriteit in cyste vloeistof niet geschikt is om laag versus hoog risico cystes van elkaar te onderscheiden.

In **Hoofdstuk 8** hebben we Barrett slokdarm modellen bestudeerd en geoptimaliseerd. De reden hiervoor was dat de formatie van een Barrett slokdarm moeilijk is om direct te monitoren in de kliniek. Derhalve zijn er experimentele modellen gepubliceerd om het mechanisme van Barrett slokdarm pathogenese te bestuderen. Echter zijn ofwel de technische mogelijkheden ofwel de vertaalbaarheid naar de klinische situatie, of beiden, beperkt. We hebben genexpressie gegevensbestanden geanalyseerd om een klinisch moleculair profiel van Barrett slokdarm vast te kunnen stellen. Vervolgens hebben we een *in vivo* model geoptimaliseerd door gebruik te maken van keratine markers. Dit model was gebaseerd op twee geïmmortaliseerde cellijnen. Tenslotte hebben we dit model en het chirurgische ratten model vergeleken met het klinische moleculaire profiel van Barrett slokdarm. Het *in vitro* model kwam overeen met 73% van het moleculaire profiel terwijl het *in vivo* model overeenkwam met 45% van het moleculaire profiel.

#### **Deel 4: Palliatieve behandeling van slokdarmkanker**

Ondanks het toenemende begrip van de biologie van kanker van het maagdarmkanaal en de inspanningen om kanker te voorkomen, is de incidentie van slokdarm kliercelkanker in westerse landen toegenomen over de laatste decennia. Ondanks pogingen om kanker in een vroeg stadium op te sporen, wordt bijna de helft van de patiënten met slokdarmkanker in een palliatieve fase gediagnosticeerd. Het was voorheen echter onduidelijk of chemotherapieën of gerichte therapieën effectief zijn tegen slokdarmkanker in de palliatieve fase.

In **Hoofdstuk 9** werden palliatieve chemotherapie en gerichte therapieën voor slokdarmkanker en kanker van de overgang van slokdarm naar maag systematisch beoordeeld en werd een meta-analyse uitgevoerd. Chemotherapie en gerichte therapieën worden steeds meer gebruikt met als doel controle van de tumorgroei, verbetering van de kwaliteit van leven en verlenging van het leven. We identificeerden 41 gerandomiseerde studies met controlegroepen. Deze studies bevatten samen 11.853 deelnemers die konden worden opgenomen in de beoordeling. We hebben een toename van de totale overleving aangetoond ten gunste van de arm met een extra cytostatisch of gericht therapeutisch agens met een risicofactor ratio van 0,75 (95% betrouwbaarheidsinterval 0,68 tot 0,84). De mediaan van de toename in overlevingstijd was één maand. We vonden een voordeel in overleving ten gunste van de groep die palliatieve chemotherapie en/of gerichte therapie kreeg in vergelijking met patiënten die ondersteunende zorg ontvingen met een risicofactor ratio van 0,81 (95% betrouwbaarheidsinterval 0,71 tot 0,92). Deel analyses, die alleen deelnemers bevatten die tweedelijns therapieën, chemotherapie, of gerichte therapieën kregen, en slokdarm kliercelkanker ofwel plaveiselcel kanker van de slokdarm hadden, lieten allemaal een vergelijkbaar voordeel zien. Palliatieve chemotherapie en/of gerichte therapie verhoogden de frequentie van aan de behandeling gerelateerde toxiciteit van graad drie of hoger. Aan de behandeling gerelateerde sterfgevallen kwamen echter niet vaker voor. De kwaliteit van leven was vaak verbeterd in de arm met een extra middel. Concluderend, deelnemers die meer chemotherapeutische of gerichte therapeutische middelen krijgen, hebben een verhoogde algehele overleving in vergelijking met deelnemers die minder middelen krijgen, wat de kwaliteit van leven van de deelnemers in de opgenomen studies niet negatief leek te beïnvloeden.

In **Hoofdstuk 10** werd de kosteneffectiviteit van het geven van cetuximab voor gevorderde plaveiselcel kanker van de slokdarm onderzocht op basis van een fase twee studie. Bij patiënten met gevorderde plaveiselcel kanker van de slokdarm lijkt de toevoeging van cetuximab aan een cisplatinum 5-fluorouracil, eerstelijns, palliatief chemotherapie regime de overleving te verbeteren. Het resulteert echter in een incrementele kosteneffectiviteitsratio van € 252.203 per voor kwaliteit gecorrigeerd levensjaar. Een gevoeligheidsanalyse toont aan dat er een kans van minder dan 0,001 op 1 is dat de incrementele kosteneffectiviteitsratio voor deze therapie lager zal zijn dan € 40.000 per voor kwaliteit gecorrigeerd levensjaar. Dit is de maximale drempel voor betalingsbereidheid per voor kwaliteit gecorrigeerd levensjaar. Het is dus niet kosteneffectief om cetuximab toe te voegen aan een palliatieve behandeling voor gevorderde plaveiselcel kanker van de slokdarm. Uit deze studie blijkt dat kosteneffectiviteitsanalyses met behulp van gegevens uit fase twee studies farmaceutische bedrijven en beleidsmakers in staat kunnen stellen om vroegtijdig inzicht te krijgen in de vraag of een nieuw geneesmiddel voldoet aan de huidige standaarden voor vergoeding. Daarmee kan worden afgewogen of er een redelijke kans bestaat dat het middel zal worden toegelaten voor gebruik in de reguliere klinische praktijk.

In **Deel 5** vatten we de belangrijkste bevindingen van dit proefschrift samen. We bediscussiëren deze bevindingen in **Hoofdstuk 11**. **Hoofdstuk 12** bevat een Nederlandse samenvatting. **Hoofdstuk 13** bestaat uit meerdere bijlagen, te weten, het dankwoord, de publicatielijst, het PhD portfolio en het curriculum vitae.





# Chapter 13

---

Appendices



## Dankwoord

Dit proefschrift was niet tot stand gekomen zonder de hulp, inzet en aanmoedigingen van vele collega's, vrienden en familie. De volgende personen wil ik graag in het bijzonder bedanken.

Als eerst dank ik graag de promotiecommissie voor hun bereidheid zitting te nemen in de commissie.

Prof. Peppelenbosch, beste **Maikel**, dank voor de steun en de vrijheid het onderzoek deels zelf vorm te geven. Dit heeft ertoe geleid dat we veel interessante experimenten hebben kunnen doen, waarvan sommigen met interessante en onverwachte resultaten. Onze gesprekken onttaarden vaak in politieke, biologische, geografische en geschiedkundige chaos maar bleven altijd van hoog niveau.

Prof. Bruno, beste **Marco** jij hebt me vaak voorgehouden: "in der beschränkung zeigt sich erst der meister". Ondanks dat het me niet altijd gelukt is, heeft de geachte hieraan me wel geholpen om de projecten af te ronden. Veel dank voor je steun en begeleiding.

Prof. Spaander, beste **Manon**, dank voor je bereidheid om mij aan te nemen op een grotendeels experimenteel onderzoek. Je hebt me altijd welkom laten voelen in de klinische wereld en in de persoonlijke sfeer. Hieruit ontstond een unieke kans om het basale onderzoek te combineren met mooie klinische projecten.

Dr. Fuhler, beste **Gweny**, dank voor je kritische blik en je passie voor basaal onderzoek. Je hebt me altijd scherp weten te houden en ik ben blij dat ik veel van je heb mogen leren.

**Anouk**, jij bent begonnen met het *HOX* onderzoek op de afdeling. Het heeft mij een aantal jaar van de straat gehouden en ik denk dat er nog veel meer in het vat zit. Zeker met betrekking tot het hoofdstuk over vitamine D receptor polymorfismen heb je zeer genereus het stokje overgedragen.

Prof. Kuipers, beste **Ernst**, dank voor jouw tomeloze energie en enthousiasme bij de initiatie van drie hoofdstukken. Het was een voorrecht om elkaar in Chicago te ontmoeten tijdens het James W. Freston conference on metaplasia.

**Kateryna**, I take off my hat to you for completing some of our complex projects. You are conscientious and have your priorities straight. It has been inspiring to see your development into a great researcher and I am very happy you are my paranimf.

**Auke**, dank voor al je hulp en natuurlijk de samenwerking bij de begeleiding van studenten. Onze discussies over het onderzoek hielden mij scherp en ik heb daarnaast veel praktische kennis van je mogen overnemen. Je hebt me welkom geheten op het laboratorium en gevormd als onderzoeker.

**Ron**, te pas en te onpas liep ik bij je binnen, jij kan diep en kritisch op de theorie ingaan en hebt tegelijkertijd veel praktische kennis. Dank dat je bleef aandringen op het gebruik van een tweede techniek die mij naar Dresden heeft gebracht. Met jouw hulp heb ik mooie experimenten kunnen uitvoeren onder andere resulterend in de cover van dit boekje.

Prof van der Laan, beste **Luc**, dank dat je me de ruimte hebt gegeven om door te bouwen op het werk van Anouk en voor al jouw hulp om verder te komen.

**André** en **Jun**, dank, specifiek voor de hulp met de verwerking van de RNA-Seq data.

**Hanneke**, dank dat je alle biobanken bijhoudt, ik heb een paar keer juweeltjes van materiaal kunnen gebruiken.

**Leendert**, **Katharina**, **Arjun**, **Jan**, **Bas**, **Sjoerd** en **Fiebo**, de Barrett club stafleden, dank voor jullie feedback en inspiratie. Leendert en Katharina daarnaast ook veel dank voor jullie hulp bij het verkrijgen van weefsels en het doen van kleuringen.

Dr. **Ewout** Steyerberg, dr. **Ate** van der Gaast en dr. **Ron** Mathijssen dank voor de hulp en het advies omtrent de Cochrane review over palliatieve chemotherapie voor slokdarm en slokdarm maag overgangs tumoren.

**Sophie**, het was erg leuk om te kunnen samenwerken en van elkaar te leren, zeker omdat ons studieonderwerp klinisch toepasbaar is. Veel succes in Utrecht.

Dr. **Cros**, dr. **Lévy**, dr. **Ruszniewski**, dr. **van den Berg**, dr. **Jenster** en dr. **Braat** thank you for collaborating on the pancreatic cyst and cancer biomarker study. A special thanks for dr. **Utomo**, it was really nice to work together!

Dr. **Lorenzen** and prof. dr. **Lordick**, your generosity to share the individual patient data on cetuximab from the phase II trial enabled us to publish a paper with firm conclusions. Ook dr. **Polinder** erg bedankt voor de hulp bij het schrijven van deze paper. Het was erg leerzaam voor mij.

Dr. **Uitterlinden**, dr. **Pourfarzad**, dr. **Tilanus**, dr. **Rygiel**, dr. **Moons**, dr. **Arp** en dr. **Krishnadath**, veel dank van al jullie bijdragen aan de paper over vitamine D receptor polymorfismen.

Prof. dr. **Wayne** Phillips and dr. **Nick** Clemons, thank you so much, firstly for the discussions we had in San Diego, later in Chicago and finally for performing the experiments in your unique model system. You are an inspiration and your willingness to collaborate is an example for all.

Dr. **Stadler** and dr. **Sandoval-Guzmán**, many thanks for the opportunity to work with the *Hoxa13*-GFP mouse model. Our collaboration has provided us with beautiful illustrations and new insights that could otherwise not have been obtained.

**Hui** and **Timo**, your assays have provided relevant insight into the biology of *HOXA9* and *HOXA13*. Thank you for all your efforts and interesting discussions.

**Rodrigo**, your unstoppable energy was of great benefit to our projects but also an inspiration to be around. Knowing your positive nature, I am sure you will overcome all obstacles on your path and have a bright future. **Karla**, thank you for all your efforts with regard to the *HOXA9* project. It was a very positive experience.

**Marcin**, it has been a lot of fun to collaborate with such an ambitious researcher. The cell models we made have already resulted in a nice paper. I am looking forward to celebrating with you in The Netherlands, Poland or beyond. I hope to continue our collaboration in the future.

**Marieke**, zonder al jouw hulp met de FACS zouden we onze cel modellen niet kunnen hebben gemaakt.

**Max, Pamela, Ilona, Mark, Chantal, Pieter, Eveline, Wendy, Eva** en **Jessica**, zonder jullie hulp was het onderzoek nooit zover gekomen en was het bovendien een stuk minder leuk geweest. Heel veel dank voor al jullie inzet en doorzettingsvermogen.

**Leonie**, het is niet verantwoord om je ooit met pensioen te laten gaan.

**Rik, Wesley, Martijn, Evelyn, Michelle** en **Elmer**, team BOTM, ik was laat van de partij maar kwam binnen in een rijdende trein die bestond uit borrels, strandweekenden, kamperen, themafeesten en meer. Dank voor een heerlijke tijd!

**Lauke**, wat heb ik genoten van onze discussies, juist omdat we het meestal niet met elkaar eens zijn. Ik hoop dat we dit in de toekomst kunnen voortzetten, al dan niet tijdens het vissen.

**Michiel**, prachtig hoe jij mensen op het verkeerde been kan zetten met een subtiele vorm van sarcasme. Jouw ambitieuze verbouwing heeft me geïnspireerd en Ivonne is je dankbaar.

**Wen, Hakim, Thijmen, Suk-Yi, Yingying, Pauline, Adriaan, Sunrui, Rachid, Ruby, Jorke**, my roommates, I had a wonderful time with you and a special thanks for organizing the goodbye lunch!

**Maren, Evelien** en **Daphne**, het was geweldig om de “diamond edition” skireis met jullie te mogen organiseren.

Alle collega's van het lab: **Hugo, Andrea, Thomas, Wanlue, Kan, Hester, Juan, Pengyu, Xiaolei, Eelke, Wenhui, Wenshi, Estella, Yijin, Lei, Yuebang, Guoying, Xinying, Paula, Aniek, Frances, Jan, Anthonie, Kim, Shanta, Gertine, Martine, Buddy, Petra, Lianne, Patrick, Jaap, Marcel, Abdullah, Sonja, Lucia, Jun, Noe, Diahann, Qiuwei, Henk, Monique V, Yik, Floris, Emmeloes, Renee, Cynthia, Ishaku, Monique de B,**

**Wouter, Sunrui, Aafke, Yingying, Janine, Gijs, Gülce, Yunlong, Meng, Shan, Yiaye, Pengyu, Buyun, Xmin, Changbo, Shaojun, Ling, Qin, Shaoshi, Kelly, Sharida, Effie, Cindy, Amy, Natascha** en alle collega's van het vroegere dak en uit de kliniek: **Heng, Anniek, Willem Pieter, Margo, Anne, Esmee, Jihan, Shannon, Ingrid, Joany, Mitchell, Wim, Alison, Gwen, Raoel, Lisanne, Priscilla, Eline, Kostas, Loes, Evelien, Louisa, Jorn, Stella, Rosalie, Kasper, Renske, Arjan, Carlijn, Marjolein, Fanny, Sophia, Alison, Ad, Jerome, Angela**, en **Vera**, wat hebben jullie de afgelopen jaren tot een onvergetelijke tijd gemaakt!

Prof. **van der Woude** dank voor het in mij gestelde vertrouwen door mij op te leiden tot Maag-, Darm-, en Leverarts. Dr. **Schrama**, en alle collega **arts-assistenten** en **medisch specialisten** van het Franciscus Gasthuis en Vlietland, mede door het hechte team heb ik een mooie tijd gehad. Tegen mijn verwachting in waren de nefrologie stage en de coronatijd hoogtepunten van mijn vooropleiding.

Veel dank aan **Dencher, Sluijsmans, Franzen, van der Kemp, Rauwé, van Lidth de Jeude, Spaan, Vink**, en **Siregar**, mijn clubgenoten. **Van der Torren**, het is al even geleden dat je me het goede voorbeeld gaf. **Hafkamp**, ik hoop je weer te zien. **Van Dullemen**, het was bijzonder om samen op het lab te kunnen werken, ik ben blij dat jij druk bent met je opleiding en gezin en trots dat je mijn paranimf wil zijn! Bij jullie is het echt thuiskomen, ik vraag me af of we ooit helemaal op zullen groeien en een deel van mij hoopt van niet.

**Marja**, dank je voor al je initiatieven. Ik hoop er ook in de toekomst deelgenoot van te zijn, ga zo door. **Eduard**, ik hoop dat je op je ouders gaat lijken.

**Jan, Gijs** en **Sander** wat een mooie wedstrijden, tochten en hachelijke momenten hebben we meegemaakt. Ik hoop dat er nog vele zullen volgen.

**Navin, Marthe, Nadia**, LIMSCers, wat mooi om te zien hoe jullie gegroeid zijn in jullie carrières en wat fijn om contact te kunnen houden na ons geweldige avontuur.

**Jack** en **Kate**, mijn schoonouders, dank dat jullie me altijd hebben verwelkomd en in slechte tijden voor een slaapplek en lekker eten hebben gezorgd.

**Theo** en **Cobie**, mijn ouders, zonder jullie was ik nooit zover gekomen. Cobie, dank dat je altijd vertrouwen in me had en me hebt gesteund toen ik dat nodig had. Theo, we lijken meer op elkaar dan goed voor ons is. Dank voor al je hulp en in het bijzonder de laatste jaren, ik heb ontzettend veel van je geleerd. **Cynthia** en **Simone**, mijn zussen, ik ben ontzettend trots op jullie, hetgeen jullie nu al hebben bereikt en hoop dat ik in de toekomst meer rust kan vinden om jullie vaker te zien. **Kevin**, ik haal veel steun uit het feit dat we hetzelfde doormaken en hoop dat ook jij na jouw promotie meer tijd krijgt voor ontspanning. **Lune**, blijf vrolijk, niet te veel naar je ouders luisteren en ik ben ervan overtuigd dat je ooit zult leren lopen.

Fantastische **Ivonne**, mijn verloofde, jij hebt veel met mij te stellen gehad de afgelopen jaren. Initieel vooral omdat de cellen verzorgd moesten worden en jouw weekenden daarvan het slachtoffer werden. Vervolgens omdat we een paar jaar zijn gaan verbouwen. Je hebt mijn afwezigheid, vermoeidheid, stof en kabaal moeten verwerken. Door jouw eigen grenzeloze ambitie en het vertrouwen dat we samen altijd een weg zullen vinden, was het allemaal mogelijk. Dank je voor de ruimte die je me hebt gegeven. Wat hebben we het toch fijn samen. Ik hou van je en je weet dat je nooit van me af zult komen!

## List of publications

1. Gurnani N, van Deurzen DF, Janmaat VT, van den Bekerom MP. Tenotomy or tenodesis for pathology of the long head of the biceps brachii: a systematic review and meta-analysis. *Knee Surg Sports Traumatol Arthrosc.* 2016;24(12):3765-71.
2. Janmaat VT, Bruno MJ, Polinder S, Lorenzen S, Lordick F, Peppelenbosch MP, et al. Cost-Effectiveness of Cetuximab for Advanced Esophageal Squamous Cell Carcinoma. *PLoS One.* 2016;11(4):e0153943.
3. Janmaat VT, Steyerberg EW, van der Gaast A, Mathijssen RH, Bruno MJ, Peppelenbosch MP, et al. Palliative chemotherapy and targeted therapies for esophageal and gastroesophageal junction cancer. *Cochrane Database Syst Rev.* 2017;11:CD004063.
4. Janmaat VT, Van De Winkel A, Peppelenbosch MP, Spaander MC, Uitterlinden AG, Pourfarzad F, et al. Vitamin D Receptor Polymorphisms Are Associated with Reduced Esophageal Vitamin D Receptor Expression and Reduced Esophageal Adenocarcinoma Risk. *Mol Med.* 2015;21:346-54.
5. Janmaat VT, van Olphen SH, Biermann KE, Looijenga LHJ, Bruno MB, Spaander MCW. Use of immunohistochemical biomarkers as independent predictor of neoplastic progression in Barrett's oesophagus surveillance: A systematic review and meta-analysis. *PLoS One.* 2017;12(10):e0186305.
6. Utomo WK, Janmaat VT, Verhaar AP, Cros J, Levy P, Ruszniewski P, et al. DNA integrity as biomarker in pancreatic cyst fluid. *Am J Cancer Res.* 2016;6(8):1837-41.
7. Janmaat VT, Kortekaas KE, Moerland TM, Vereijken MWC, Schoones JW, van Hylckama Vlieg A, et al. Research-Tutored Learning: An Effective Way for Students to Benefit Research by Critical Appraisal. *Medical Science Educator.* 2013;23(2):269-77.
8. da Silva RA, Fuhler GM, Janmaat VT, da C Fernandes CJ, da Silva Feltran G, Oliveira FA, et al. HOXA cluster gene expression during osteoblast differentiation involves epigenetic control. *Bone.* 2019;125:74-86.
9. Janmaat VT, Liu H, da Silva RA, Wisse PHA, Spaander MCW, Ten Hagen TLM, et al. HOXA9 mediates and marks premalignant compartment size expansion in colonic adenomas. *Carcinogenesis.* 2019;40(12):1514-24.
10. Keijser WA, Handgraaf HJM, Isfordink LM, Janmaat VT, Vergroesen PA, Verkade J, et al. Development of a national medical leadership competency framework: the Dutch approach. *BMC Med Educ.* 2019;19(1):441.
11. Nesteruk K, Janmaat VT, Liu H, Ten Hagen TLM, Peppelenbosch MP, Fuhler GM. Forced expression of HOXA13 confers oncogenic hallmarks to esophageal keratinocytes. *Biochim Biophys Acta Mol Basis Dis.* 2020;1866(8):165776.



12. Korbut E, Janmaat VT, Wierdak M, Hankus J, Wójcik D, Surmiak M, Magierowska K, et. al. Molecular profile of Barrett's esophagus and gastroesophageal reflux disease in the development of translational physiological and pharmacological studies. *Int J Mol Sci* 2020;21:6436.
13. Janmaat VT, Nesteruk K, Spaander MCW, Verhaar AP, Yu B, Silva RA, Phillips WA, et. al. HOXA13 in etiology and oncogenic potential of Barrett's esophagus. In revision.

## PhD portfolio

General description	Description	Workload (ECTS)
<i>General courses</i>		
31-03/04-04-2014	BROK course	1.5
27-02-2014	The Workshop on Microsoft Excel 2010: Advanced. 27-02-2014/ 27-02-2014	0.4
25-03/27-05-2014	The course on Biomedical English Writing Course for MSc and PhD-students	1.3
14-01-2014	Scientific integrity course	0.3
15-10/29-10-2013	Workshops Systematic Literature Retrieval and EndNote. (Grade 8.0)	2.0
30-06/ 02-07-2016	UEGW basic science course with travel grant	0.7
<i>Oral presentations at attended conferences</i>		
20/21-03-2014	Overexpression of <i>HOXA13</i> in Barrett's esophagus is a potential mediator of its posterior phenotype. Spring meeting of the Dutch Society for Gastroenterology (NVGE), Veldhoven, The Netherlands.	1.0
17/18-03-2016	<i>HOX</i> gene expression in Barrett's esophagus resembles that of the colon, can be modulated by acid and bile exposure, and induces Barrett's specific gene products. Day of the Molecular Medicine Postgraduate School, Rotterdam, The Netherlands.	1.0
17/18-03-2016	Palliative chemotherapy and targeted therapies for esophageal and gastroesophageal junction cancer. Spring meeting of the Dutch Society for Gastroenterology (NVGE), Veldhoven, The Netherlands.	1.0
17/18-03-2016	Cost-effectiveness of Cetuximab for advanced esophageal squamous cell carcinoma. Spring meeting of the Dutch Society for Gastroenterology (NVGE), Veldhoven, The Netherlands.	1.0
21/24-04-2016	<i>HOX</i> Gene Expression in Barrett's Esophagus Resembles That of the Colon, Can Be Modulated by Acid and Bile Exposure, and Induces Barrett's Specific Gene Products. Digestive Diseases Week, San Diego, USA.	1.0
15/19-10-2016	Palliative chemotherapy and targeted therapies for esophageal and gastroesophageal junction cancer. United European Gastroenterology Week, Vienna, Austria.	1.0
20/24-10-2018	Barrett's metaplasia originates from <i>HOXA13</i> -positive cells in the gastroesophageal junction. United European Gastroenterology Week, Vienna, Austria.	1.0

General description	Description	Workload (ECTS)
<i>Poster presentations at attended conferences</i>		
04/06-04-2014	Hoxa Cluster Expression along the Gastrointestinal Tract. Digestive Diseases Week, Chicago, USA.	1.0
18/22-10-2014	<i>HOXA13</i> overexpression in Barrett's esophagus is a potential mediator of its posterior phenotype. United European Gastroenterology Week, Vienna, Austria.	1.0
21/24-04-2016	Palliative Chemotherapy and Targeted Therapies for Esophageal and Gastroesophageal Junction Cancer. Digestive Diseases Week, San Diego, USA.	1.0
19/20-08-2016	<i>HOX</i> gene expression in Barrett's esophagus resembles that of the colon, can be modulated by acid and bile exposure, and induces Barrett's specific gene products. James W. Freston conference on intestinal metaplasia, Chicago, USA.	1.0
07/11-10-2016	Immunohistochemical biomarkers for risk stratification of neoplastic progression in Barrett esophagus. European Society for Medical Oncology, Copenhagen, Denmark	1.0
15/19-10-2016	<i>HOX</i> gene expression in Barrett's esophagus resembles that of the colon, can be modulated by acid and bile exposure, and induces Barrett's specific gene products. United European Gastroenterology Week, Vienna, Austria.	1.0
28-10/01-11-2017	Gastric cardia glands manifest apparent broad differentiation potential, as evidenced by <i>HOXA13</i> expression, implications for the origin of Barrett's esophagus. United European Gastroenterology Week, Barcelona, Spain.	1.0
<i>Attended conferences</i>		
2014	Daniel den Hoed symposium	0.4
2016	Sattelite symposium Amsterdam	1.0
2017	Spring meeting of the Dutch Society for Gastroenterology (NVGE), Veldhoven, The Netherlands.	0.5
<i>Scientific awards and grants</i>		
2014	<i>HOXA13</i> overexpression in Barrett's esophagus is a potential mediator of its posterior phenotype. United European Gastroenterology Week, Vienna, Austria, Poster of excellence.	
2014	Dutch Society for Gastroenterology (NVGE) "Gastrostart" grant	
2014	UEGW travel grant	
2016	UEGW travel grant	
2016	ESMO travel grant	
2016	AGA travel grant	

General description	Description	Workload (ECTS)
2016	NVGE travel grant	
2016	Erasmus Trustfonds travel grant	
2016	Immunohistochemical biomarkers for risk stratification of neoplastic progression in Barrett esophagus. European Society for Medical Oncology, Copenhagen, Denmark, best poster prize.	
2016	<i>HOX</i> gene expression in Barrett's esophagus resembles that of the colon, can be modulated by acid and bile exposure, and induces Barrett's specific gene products. United European Gastroenterology Week, Vienna, Austria, best poster prize	
2016	<i>HOX</i> Gene Expression in Barrett's Esophagus Resembles That of the Colon, Can Be Modulated by Acid and Bile Exposure, and Induces Barrett's Specific Gene Products. Digestive Diseases Week, San Diego, USA, Acknowledgement for achievements as a young researcher.	
2017	Erasmus Trustfonds travel grant	
2017	"Meer Kennis met Minder Dieren - module Maatschappelijke partners" grant	
<i>Seminars</i>		
2014-2018	Weekly MDL seminar program in experimental gastroenterology and hepatology (attending)	9.0
2014-2018	Weekly MDL seminar program in experimental gastroenterology and hepatology (presenting)	2.25
2014-2018	Weekly research group education (attending)	9.0
2014-2018	Weekly research group education (presenting)	9.0
2014-2018	Weekly Gastroenterology and Hepatology journal club	4.5
<i>Teaching activities</i>		
2014	Chantal Govaart, 3 <sup>rd</sup> year MLO student.	5.7
2015	Max van Dullemen, 4 <sup>th</sup> year medical student.	2.1
2015	Pieter Wisse, 4 <sup>th</sup> year medical student.	2.8
2015	Mark van der Lee, 2 <sup>nd</sup> year HBO student.	2.8
2016	Ilona Edelijn, 2 <sup>nd</sup> year HBO student.	3.6
2016	Eveline Zwalua, 2 <sup>nd</sup> year HBO student.	3.6
2016	Wendy van Dam, 2 <sup>nd</sup> year HBO student.	2.8
2017	Pamela Vasic, 2 <sup>nd</sup> year HBO student.	3.2
2017	Eva Zielhuis, 3 <sup>rd</sup> year Biomedical Sciences student.	4.4
2018	Jessica Knoop, 4 <sup>th</sup> year HBO student.	3.0

General description	Description	Workload (ECTS)
<i>Memberships</i>		
2014 - current	Dutch society of gastroenterology	
2016 - current	American Gastroenterology Association	

## Curriculum vitae

Vincent T. Janmaat was born June 20<sup>th</sup> 1988 in Woerden, The Netherlands. Raised by his beloved parents Theo and Cobie Janmaat, he grew up together with his younger sisters Cynthia and Simone Janmaat. In 2006, he finished secondary school (VWO-gymnasium) and started studying Medicine at Leiden University. In 2008, he enrolled in the pre-Master Biomedical Sciences and followed a master Biomedical Sciences from 2010 onwards. In 2011, he performed his graduation research for his doctoral thesis in Medicine at the laboratory of molecular cell biology at Leiden University under supervision of prof. dr. Rob Hoeben. This graduation research was entitled “Beta-cell protection against the recurrence of autoimmunity”. In 2014, he performed his graduation research for his Master of Science degree in Biomedical Sciences at the laboratory of Gastroenterology and Hepatology under supervision of prof. dr. Maikel Peppelenbosch and dr. Manon Spaander. His research was entitled “*HOXA13* expression in Barrett’s could mediate its posterior phenotype”. After obtaining his Medical and Biomedical Sciences degrees in 2014, he started a PhD project at the department of Gastroenterology and Hepatology, Erasmus University Medical Center, Rotterdam. This work was done under supervision of prof. dr. Maikel Peppelenbosch, prof. dr. Marco Bruno, prof. dr. Manon Spaander, and dr. Gwenny Fuhler, ultimately resulting in this thesis. In May 2018, he started his Internal Medicine residency in the Franciscus Gasthuis & Vlietland hospital (program director dr. Y.C. Schrama). In May 2020, he started his training in Gastroenterology and Hepatology at the Erasmus University Medical Center (program director prof. dr. C.J. van der Woude). Vincent lives in Rotterdam, together with his fiancée Ivonne.